UNIVERSITÉ LILLE 1 - SCIENCES ET TECHNOLOGIES

ÉCOLE DOCTORALE SCIENCES DE LA MATIÉRE DU RAYONNEMENT ET DE L'ENVIRONNEMENT

THÈSE

pour obtenir le grade de

DOCTEUR DE L'UNIVERSITE LILLE 1 SCIENCES ET TECHNOLOGIES

Spécialité: Molécules et Matière Condensée

Soutenance publique prévue le 21 décembre 2012 par

Ionut MIHALCEA

Crystal Chemistry of Coordination Polymers Based on Uranyl and Mixed Uranyl / Lanthanide Carboxylates

These dirigée par Mr. Thierry LOISEAU et co-encadrée par Mme. Natacha HENRY

Composition de la commission d'examen :

Nicolas DACHEUX (Professeur des Universités, Montpellier II)	*rapporteur*
Michel EPHRITIKHINE (Directeur de Recherche CNRS, SIS2M, Saclay)	*rapporteur*
Gérard FÉREY (Membre de l'Institut, Professeur Émérite, Versailles)	*membre*
Dermot O'HARE (Professeur, Oxford, Angleterre)	*membre*
Natacha HENRY (Maitre de Conférences, Lille 1)	*membre*
Thierry LOISEAU (Directeur de Recherche CNRS, Lille 1)	*membre*

Contents

Table of contents

General introduction

The team "Solid State Chemistry and Nuclear Materials" belonging to the "Catalysis and Solid state Chemistry Unit (UCCS – University of Lille Nord de France)" laboratory has focused its research axes on investigations dealing with the chemistry of light actinide elements (thorium, uranium) in association with lanthanide ones. Considering the nuclear industry background, the 4f block elements are of potential interest since they are found as fission products following the nuclear reactions or can be used a surrogate metals for mimicking the chemical reactivity of heavier actinides such as plutonium, americium, … which exhibit highly radiotoxic radiations. The manipulation of the so-called 'hot' actinides implies the use of specific laboratory facilities, which are available only at the French Nuclear Agency (CEA; see for instance ATALANTE lab at the Marcoule site). Our researches deal with different aspects of the nuclear fuel. It concerns its treatment for the fabrication of the uranium oxide, from mines up to the UO_2 ceramic, through the fluorination processes involving the UF_4 and UF_6 intermediates. The second activity is related to the recycling process of the spent nuclear fuel, involving the oxalate precipitation route in order to recover uranium and/or plutonium elements.

The main goals of this thesis work is to improve the basic knowledge of the synthesis and characterization of new U^{VI} or mixed U^{VI}/Ln^{III} based coordination complexes followed by their thermal degradation under different conditions. The analysis of the degradation products for possible applications as fuels in the nuclear energy industry is then investigated and would bring some highlights about the synthesis under mild conditions of uranium oxides, mixed uranium / lanthanide oxides or carbides.

From the endless list of possible organic ligands we have decided to work with the class of carboxylic acids for their good complexating properties, partial water solubility and previous reported results on the uranyl oxalates in our laboratory[3]. Considering the class of carboxylic acids we have arbitrarily chosen to work with the aromatic ones due to their high carbon content per molecule,

which could favor the obtaining of carbides. Here the carbon source would come from the organic part itself, without adding any graphite component. Also the field of uranyl aromatic carboxylates is less explored, in comparison with the aliphatic ones, since fewer complexes of this type have been reported. These different compounds will be further mentioned and detailed in this chapter.

This thesis work is structured on six chapters: first chapter is a very brief introduction describing the nuclear energy context and is mainly focused on the state of the art concerning carboxylate coordination complex bearing uranyl cation.

The next three chapters are focused on the work conducted on three aromatic carboxylic acids: phthalic, isophthalic and pyromellitic acid respectively. The fifth chapter describes a family of complexes containing discrete six-fold coordinated uranium polyhedra. The last chapter, followed by the general conclusions describes a few cases of mixed uranyl / lanthanide carboxylates, still involving aromatic polycarboxylate ligands.

Chapter I
The world of uranyl carboxylates

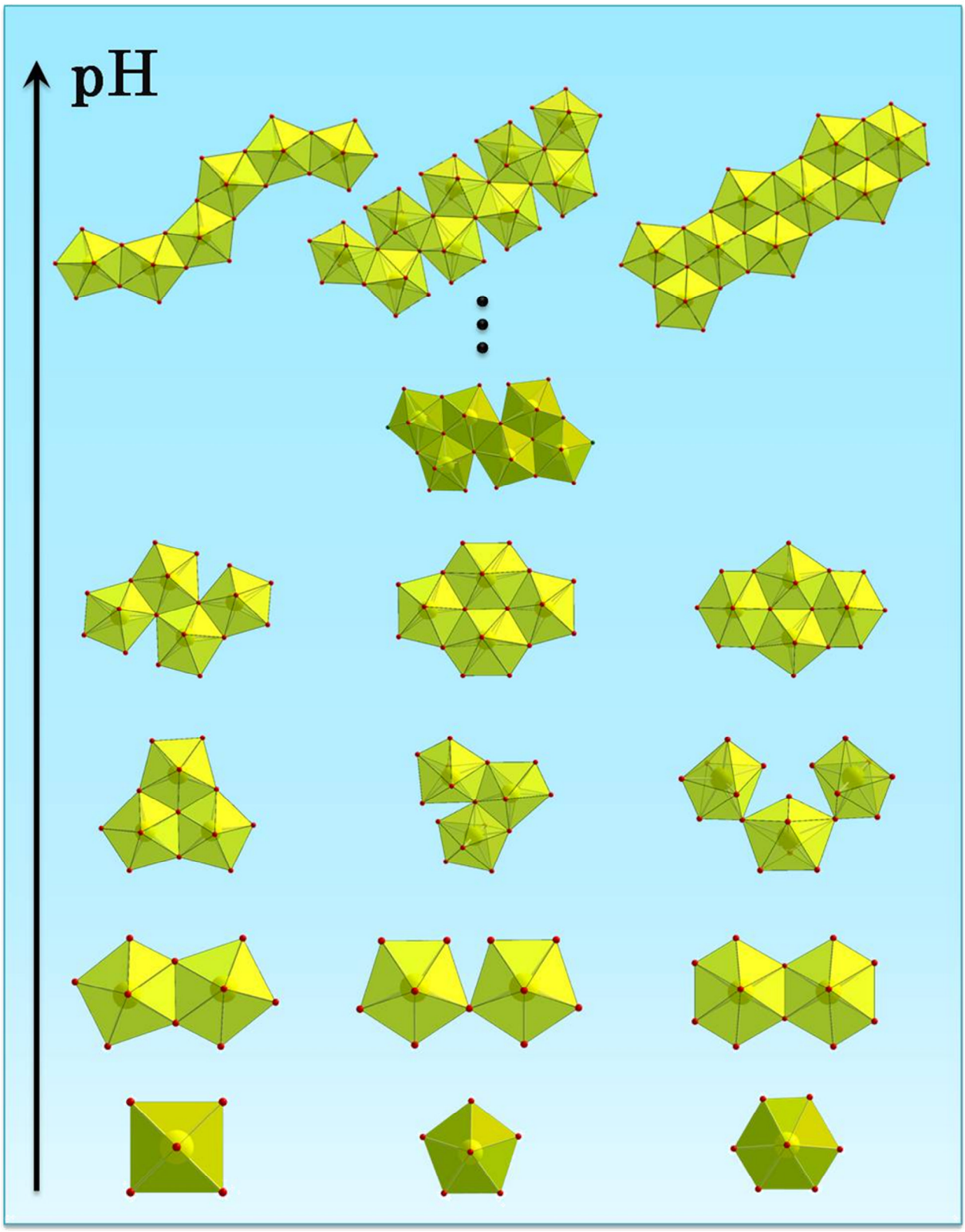

Chapter I The world of uranyl carboxylates

I.1 . The context of nuclear reactors

Because of the continuous population expansion, which has reached over seven billion people (it is expected to reach 10 billion in 2050), the energy demand increases each year. This fact, combined with the exhaustion of the non renewable resources conducts to one single conclusion: for the Earth to support its growing population, the use of the so-called sustainable or green energy supplies needs to be increased. Although the nuclear energy is not as sustainable as the wind, solar, hydro, tide or wave energy, it is a non-greenhouse-gas-emitting source of electricity and production of co-products (hydrogen for instance) could be envisaged. Around the world, there are about 400 nuclear reactors covering about 16% of the world electricity production. The main drawback of this energy source is the long-life radionuclides production found in the spent nuclear fuel. In order to overcome this problem and to avoid the storage of large quantities of radioactive material, a new generation of nuclear reactors has been planned to have an enhanced consumption of recycled fuel and a diminished consumption of traditional fuel. Also they are designed to use the ^{238}U isotope (fast neutron reactor), not only the fissile ^{235}U isotope which has an abundance of only 0.7% in natural uranium. There are six designs of nuclear systems of the so-called generation IV which would be deployed from 2030-40. Most of the six systems employ a closed fuel cycle to maximize the resource base and minimize high-level wastes. Three of the six are fast neutron reactors (FNR), one is described as epithermal, and only two operate with thermal neutrons like today's plants. Only one of the reactors, the supercritical water cooled reactor (SCWR), is cooled by light water, two are helium-cooled, the gas-cooled fast reactor (GFR) and the very high-temperature gas reactors (VHTR) and the others have lead-bismuth, sodium or fluoride salt coolant, the lead-cooled fast reactor (LFR), the sodium-cooled fast reactor (SFR) and respectively the molten salt reactors (MSR). The latter three operate at low pressure, with significant safety advantages. The last has the uranium fuel dissolved in the circulating coolant.

Temperatures range from 510°C to 1000°C, compared with less than 330°C for today's light water reactors; this means that four of them can be used for thermochemical hydrogen production. The powers range from 150 to 1500 MWe. The specifications for each reactor design are presented in Table I.1.1.

Most of these new generation nuclear reactors could or will employ mixed types fuels such as mixed (U,Pu) oxides (MOX), carbides or nitrides. The fabrication of these types of fuels implies different preparation techniques but also the reprocessing of the spent fuel is considered.

Table I.1.1 Design parameters for the generation IV nuclear reactors.

	Neutron spectrum	Power (MWe)	Coolant	Temp. (°C)	Pressure (bar)	Fuel	Fuel cycle
GFR*	fast	1200	helium	850	90	(U,Pu)C/SiC (70/30%) with 20% Pu	closed, on site
LFR*	fast	300-1200	Pb or Pb/Bi	550-800	~1	U,Pu alloy or U,Pu nitride	closed
MSR*	fast thermal	1000 1000-1500	fluoride salts	700-800 750-1000	~1	U fluoride in salt UO_2 particle in prism	closed open
SFR	fast	300-2000	sodium	530-550	~1	$(U,Pu)O_2$ or U, Pu alloy	closed
SCWR	fast thermal	1000-1500 1000-1700	water	510-625	250	UO_2, or Ni-alloy cladding	closed open
VHTR*	thermal	250-300	helium	900-1000	70-150	ZrC-coated UO_2 particles in blocks	open

* reactor capable of thermochemical hydrogen production.

I.2 . Recycling the spent nuclear fuel. Reprocessing techniques.

Originally the reprocessing was used only to separate and recover fissionable plutonium from the irradiated nuclear fuel in order to serve different purposes, initially for nuclear weapons and later to be used as MOX in thermal reactors. Throughout history several separation techniques have been developed and applied but one of the most efficient of them is the class of solvent extraction separation techniques. First of its class is the PUREX (Plutonium and Uranium REcovery by Extraction) technique, which involves dissolving the fuel elements in concentrated nitric acid and a multistep extracting process in order to separate uranium and plutonium, independent to each other. This is the most developed and widely used process in the industry at present but it has one major

disadvantage; it implies the production of plutonium with high enough purity to be used in nuclear weapons production. A modified version of PUREX, in order to provide greater proliferation resistance is UREX (URanium EXtraction). This method involves the addition in the extraction process of acetohydroxamic acid which diminishes the extractability of plutonium and neptunium, providing only the uranium and technetium extraction and separation from each other and from the other fission products and actinides. Another PUREX derivate technique is TRUEX (Trans Uranic EXtraction), a process that involves the use of octyl(phenyl)-N,N-dibutyl carbamoylmethyl phosphine oxide in combination with tributylphosphate as extracting agents. This technique is designed to remove the transuranic metals (Am/Cm) from waste lowering its alpha activity. With this way the waste can be disposed easier and safer. A similar TRUEX technique is DIAMEX (DIAMide EXtraction). The difference between them is that the DIAMEX, using as extracting agent a malondiamide, avoids the formation of organic waste containing sulfur, which by incineration will conduct to acid gases, contributing to the acid rains. A new technique, which is still being worked, is SANEX (Selective ActiNide EXtraction). Once defined, this technique will allow the actinides such as americium to be either reused as industrial sources or as fuel, by permitting their separation from lanthanides, which by their large neutron cross sections are poisoning the neutron driven nuclear reactions. Another technique developed in Czech Republic and Russian Federation, designed to completely remove the most undesired radioisotopes (Sr, Cs and minor actinides) from the waste remaining after the extraction of uranium and plutonium from used nuclear fuel, is the UNEX (UNiversal EXtraction). The chemistry of this process is complex and it involves the use of several extracting agents and diluents.

The methods that attracted our interest are GANEX (Grouped Actinide EXtraction) and COEX. The two methods are developed and tested by CEA and AREVA at Atalante center, Marcoule and La Hague reprocessing plant. Both routes involve the co-extraction and co-precipitation of uranium and plutonium (and usually neptunium) together, eliminating any separation of plutonium on its own. The GANEX process implies one supplementary step of separating the

minor actinides and some lanthanides from the short-lived fission products. The uranium, plutonium and minor actinides together would become fuel in Generation IV fast neutron reactors and the lanthanides become waste. These two methods use as extracting agents different organic compounds, capable of selectively complexating the actinide atoms, like tributyl phosphate (TBP), tetramethylmalonamide (TMMA) and studies are conducted on different, more branched versions of the previously mentioned.

Both methods (GANEX and COEX) use in at least one of the processing steps the oxalic acid (noted H_2ox) as a precipitation agent. This is the reason why a large number of studies has been devoted to the identification and structural characterization of the different actinide or/and lanthanide oxalates in order to understand the crystal growth processes occurring during the reprocessing. One study that caught our attention, conducted by Pr. F. Abraham in our laboratory, implied the use of oxalic acid as precipitating organic ligand. In this study it has been shown that the oxalic acid, possessing two coordinating carboxylate functions, is capable of co-precipitating the U^{IV} and Pu^{III} in solution, forming two types of coordination polymeric complexes, each exhibiting within the structure a unique U^{IV}/Pu^{III} mixed crystallographic site. By filtration and thermal calcinations, this compound will give the MOX type fuel with enhanced homogeneity and possessing the initial U/Pu ratio. This study began in our group, in 2005 with the syntheses and structure solving of two types of mixed U^{IV}/Ln^{III} oxalates (Figure I.2.1). First class $(NH_4)_{1-x}[Ln_{1-x}U_x(ox)_2(H_2O)]$ where Ln = Pr, Nd, Sm, Gd, Tb and x varies between 0.25 and 0.6, crystallizes in the tetragonal crystal system and the second one $(N_2H_5)_{2.6}[U_{1.4}Ln_{0.6}(ox)_5]\cdot xH_2O$ where Ln = Nd, Sm in hexagonal crystal system. The metal valence difference between the parent compounds, $(NH_4)[Ln^{III}(ox)_2(H_2O)]$ & $(NH_4)_2[U^{IV}_2(ox)_5]\cdot 0.7H_2O$, and the substituted ones is compensated by the single-charge ions (ammonium or hydrazinium) present in both types of structures.[1] Also in this study, a third mixed U^{IV}/Ln^{III} oxalate has been obtained, but having the two metals in different crystallographic sites. The research has been continued in 2007, replacing in both classes of compounds Ln^{III} with An^{III} and creating two original series of mixed An^{IV}/An^{III} oxalate compounds where An^{IV} = Th, Np, U or

Pu and An^{III} = Pu or Am. The originality of these two series resides in the An^{IV}/An^{III} mixed crystallographic sites, inducing local homogeneity at a molecular level.[2]

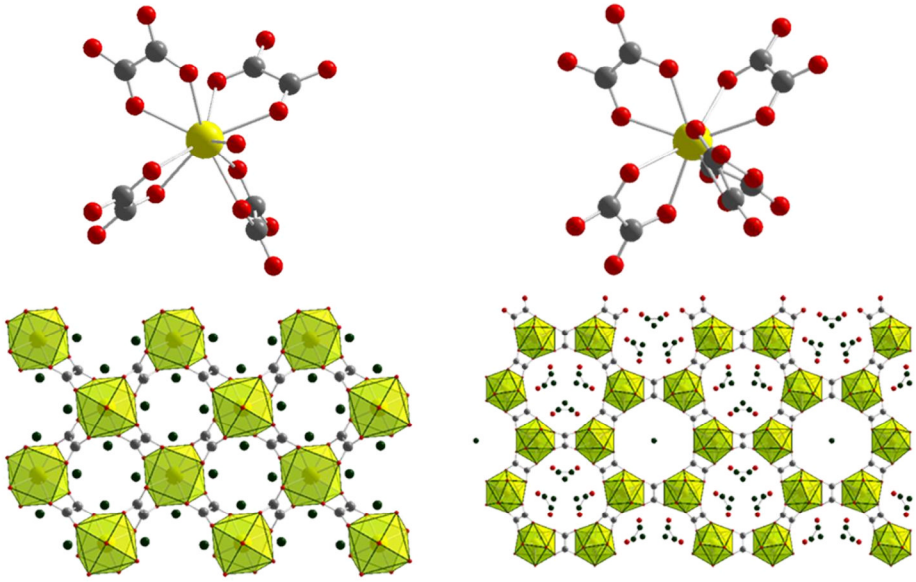

Figure I.2.1 Environment of $An^{IV/III}$ mixed crystallographic site up, and structural arrangement down for the tetragonal mixed oxalate (left) and the hexagonal one (right)[2].

In this thesis work we have decided to follow a closely related study by replacing the oxalic acid as a ligand by other poly-carboxylates with an increased number of carbon atoms in molecule. The aim is then to examine the thermal decomposition of the resulting coordination polymers, in order to characterize the different formation of oxides as a function of the nature of hybrid organic-inorganic precursor. The formation possibility of metallic carbides is also envisaged from the decomposition of the organic part (as carbon source) of the precursor. However, the crystallization of actinide carboxylates is not new and has been subject to many reports in literature. In our work, we paid a specific attention to the study of aromatic multidentate carboxylates such as phthalic acid and their derived molecules (isopthalate, terephthalate, pyromellitate …) in association with the uranyl cation, UO_2^{2+}.

I.3 . State of the art

From the literature, (*CSD - The Cambridge Structural Database and Web of Knowledge)* there have been investigated 322 uranyl carboxylate compounds, which have been previously identified. A first attempt of classification could lie on the nature and nuclearity of the uranyl motif and this will the subject and the guiding line of the bibliographic presentation. Thus, 225 (69.9%) of them possess monomeric units, 44 (13.7%) have dimeric Secondary Building Units (SBUs), 25 (7.7%) have tetrameric SBUs, 23 (7.1%) polymeric SBUs and only three possessing trimeric SBUs. There have been found two special cases, one of a hexameric SBU and the other a mixed valence (U^{IV}/U^{VI}) monomeric unit. It is related that the SBU type of an uranyl carboxylate compound could be dictated by the concentration of the OH^- species (hydrolysis rate) present in the system, implicitly by the pH of the reaction medium (in the case of aqueous systems). This dependence is given by the type of anionic bridge in the SBU, which usually are oxo or/and hydroxo bridges. Basically, the higher the pH, the more bridges can be created between the polyhedra, the larger the SBU will be. This fact is also confirmed by some studies on the uranyl ion hydrolysis.

$$p(UO_2)^{2+} + q\ H_2O = [(UO_2)_p(OH)q]^{(2p-q)} + qH^+ \quad (1)$$

From the hydrolysis equation (1) it can be observed that the equilibrium constant, implicitly the stability of hydrolytic species depends mainly on the solution pH but also is strongly on the initial concentration of the $(UO_2)^{2+}$ ions in solution. In general, at low concentration (< 1 mmol/L) the mononuclear species are predominant, while polynuclear complexes are formed at higher concentration. Another important factor that influences the stability of the hydrolytic complexes is the temperature, the solution ionic strength and pH being dependent of this factor. Using analytical techniques such as potentiometry, UV/vis spectrometry, luminescence spectrometry and different calculation methods, there have been obtained the equilibrium constants for the various species obtained by the uranyl ions hydrolysis. Also it has been established an uranyl pH dependent speciation diagram at 25°C, in a 0.1 mol/L

potassium nitrate solution using a uranyl concentration of 1 mmol/L.[3] The results are illustrated in Figure I.3.1.

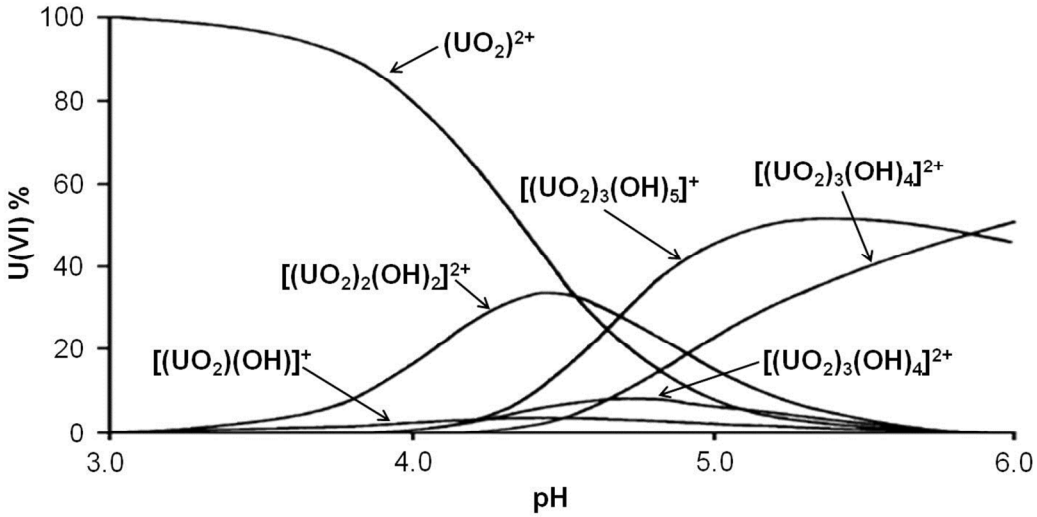

Figure I.3.1 U(VI) various species distribution as a function of pH at 25°C.

From the structural study it can be observed that almost 70% of the compounds are monomeric, implicitly they have been synthesized at a low pH. Although it seems to be simple to obtain large SBU just by increasing the pH, this also increases the number of phases that could be stable in those conditions and the separation of these phases could prove a challenge. Also, increasing the pH, the crystallinity of the obtained phases begins to decrease, making difficult the job of finding a crystal suitable for single crystal XRD analysis, implicitly the structure determination of the phase being hampered, if not impossible. This could be explained that only 30% of the investigated complexes have superior SBUs.

Different review articles have been published so far for the uranyl carboxylates family, which are sometimes referred as Uranyl-Organic Framework (UOF), following the terminology used for the crystalline porous hybrid organic-inorganic compounds named Metal-Organic Framework (MOF).[4] Uranyl carboxylates related literature is quite rich and will be described as a function of the nuclearity of the uranyl cations. Also some rare cases of mixed 4f-5f carboxylate complexes illustrations have been added at the end of our review. Abbreviations of the organic ligands are reported at the end of the chapter I.

Mononuclear type uranyl carboxylate complexes

Uranium (VI) usually exhibits three types of coordination sphere (Figure I.3.2). They are commonly encountered, with two typical short linear uranyl bonds (U=O), having an average length of 1.79(3) Å in the hexa-coordinated state (**T**etragonal bipyramid), 1.79(4) Å in the hepta-coordinated case (**H**exagonal bipyramid) and 1.78(3) Å in the octa-coordinated one (**P**entagonal bipyramid), being situated in the apical position. Usually these bonds are chemically inert, not participating to any other chemical bonding, excepting the rare cases of cation-cation interaction, when a uranyl oxygen atom also coordinates a second metal atom (see page - 39 -). The uranium coordination sphere is completed by other four to six longer bonds (U—O) in the equatorial plane, having the average length of 2.28(5) Å for the hexa-coordinated uranium polyhedra, 2.37(9) Å for the hepta-coordinated ones and 2.47(12) Å for the octa-coordinated ones. The latter form the equatorial base of the bipyramid.[5] Nevertheless, a fourth type of coordination could be observed, being represented in the field of carboxylate coordination complexes by only one structure[6], having instead of two, four short bonds of 1.88 to 2.03 Å and four long bonds of 2.41 to 2.55 Å.

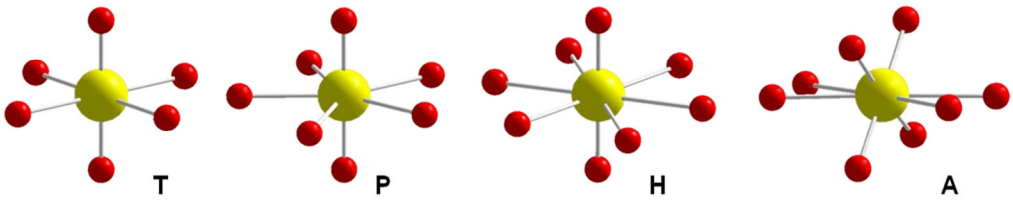

Figure I.3.2 Three typical coordination types for hexavalent uranium: tetragonal bipyramid (T), pentagonal bipyramid (P), Hexagonal bipyramid (H) and one case,[11] of a distinct octa-coordinated uranium (VI) environment (A).

So far, there have been found in the literature, 255 uranium carboxylate monomeric type coordination complexes from which 107 (47.6%) contain type H (hexagonal) polyhedra, 104 (46.2%) contain type P (pentagonal) polyhedra, 11 (4.9%) contain mixed type of polyhedra, from which, one structure contains also the type A (eight-fold coordination) polyhedron and, only three structures (1.3%) contain the T (tetragonal) type coordination sphere. In the same class of compounds 103 (45.8%) structures are zero-dimensional, 58 (25.8%) are one-

dimensional, 49 (21.8%) are bi-dimensional and only 15 (6.6%) are tri-dimensional.

In the field of monomeric SBUs the largest number of structures, obtained using the same ligand is described with the oxalates (ox) linkers. There have been found 32 uranyl oxalates (listed in Table I.3.1) having dimensionalities ranging from 0D to 3D and having coordination spheres of type P, H or P + H.

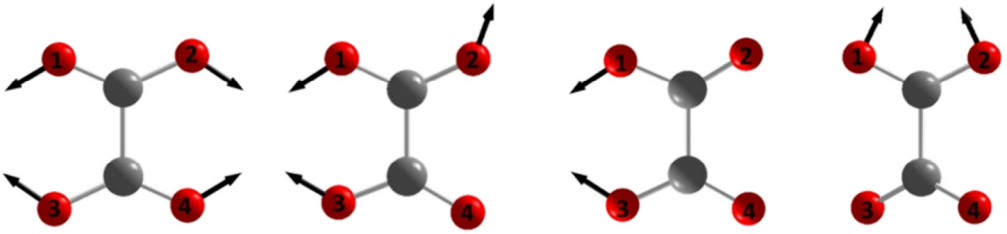

Figure I.3.3 Coordination possibilities for the oxalic acid molecule.

The oxalic acid has proven a versatile ligand, due to the different coordination possibilities. In most of the cases the oxalate chelates the metal with two oxygen atoms (Figure I.3.3) belonging to the two distinct carboxylate groups. The free rotation around the C-C bond is fixed, making the ligand a planar one and reducing the dimensionality of the structures to maximum 2D (Figure I.3.4).

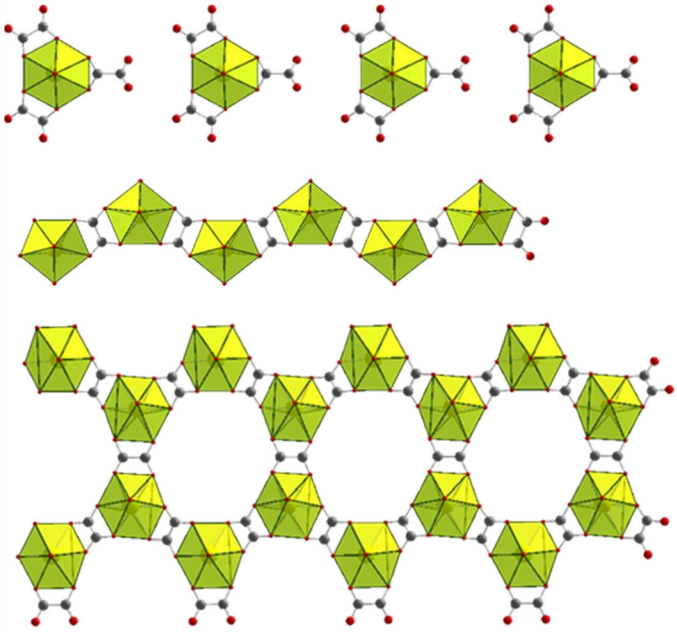

Figure I.3.4 Most common coordination types in uranyl oxalate field for zero-dimensional structures (top)[7], one-dimensional structures (middle)[8], and bidimensional structures (bottom)[9].

In the cases of tri-dimensional uranyl oxalate structures, the third dimension is usually ensured by an additional coordinated cation or organic ligand.

Table I.3.1 List of the monomeric type uranyl oxalates.

Compound	Pattern	Coordination type	Reference
$(NH_4)_4[UO_2(ox)_3]$	0D	H	7
$(NH_4)_2[(UO_2)_2(ox)_3]$	1D	P	10
$Na_2[(UO_2)_4(ox)_5(H_2O)_2]\cdot 8H_2O$	2D	P	11
$[UO_2(ox)(H_2O)]\cdot H_2O$	1D	P	8
$K_2[(UO_2)_2(ox)_3]\cdot 4H_2O$	2D	H	9
$(NH_4)_2[UO_2(ox)_2]$	1D	P	12
$[UO_2(ox)(H_2O)]\cdot 2H_2O$	1D	P	9, 13, 14
$(NH_4)_2[(UO_2)_2(ox)_3]\cdot 3H_2O$	2D	H	15
$[UO_2(ox)(H_2O)]$	0D	H	16
$[UO_2(ox)]$	0D	H	16
$(NH_4)(Hhyd)[(UO_2)_2(ox)_3]\cdot 3H_2O$	2D	H	15
$(Hhyd)_2[UO_2(ox)_2(H_2O)]$	0D	P	17
$(Hhyd)_6[(UO_2)_2(ox)_5]\cdot 2H_2O$	0D	P	18
$(NH_4)_4[(UO_2)_2(ox)_3(scn)_2]\cdot H_2O$	0D	P	19
$(NH_4)[UO_2(ox)(scn)]\cdot 2H_2O$	1D	P	20
$[Htea]_4[(UO_2)_2(ox)(scn)_6]\cdot H_2O$	0D	P	21
$K_4[(UO_2)_2(ox)_3(scn)_2]\cdot 4H_2O$	0D	P	22
$Rb_2[UO_2(ox)(scn)]_2\cdot H_2O$	1D	P	23
$Cs_2[UO_2(ox)(scn)]_2\cdot H_2O$	1D	P	23
$(NH_4)(Hgu)_2[(UO_2)(ox)_2(scn)]\cdot 2H_2O$	0D	P	24
$(H_2eda)[UO_2(ox)_2(hpa)_2]\cdot H_2O$	0D	P	25
$[(UO_2)_2(ox)_2(dmh)_2]\cdot gu\cdot H_2O$	1D	P	25
$[(UO_2)_2(pca)_2(ox)]$	3D	P	26
$[UO_2(ox)(Hgpi)]$	1D	H	27
$(Hdea)[UO_2(ac)_2(ox)]\cdot H_2O$	0D	H	28
$[UO_2(ox)(dmu)_2]$	1D	P	29
$[(UO_2)_2(H_2dota)(ox)(H_2O)_2]\cdot 6H_2O$	2D	P	30
$(NH_4)_2[(UO_2)_2(ox)(ac)_4]\cdot 2H_2O$	0D	H	31
$[(UO_2)_2(pic)_2(ox)]$	2D	P	32
$[(UO_2)_2(poa)_2(ox)]\cdot H_2O$	2D	P	32
$[(UO_2)_4(ox)_3(NO_3)_2(H_2O)_6]\cdot cb6\cdot 6H_2O$	0D	P + H	33
$[(UO_2)_2(H_2teta)(ox)(H_2O)_2]$	3D	P	34

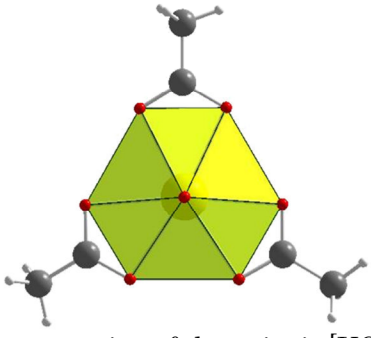

Figure I.3.5 Representation of the anionic $[UO_2(ac)_3]^-$ unit[35-43].

Acetic acid is another ligand that has been extensively studied. There have been found 29 compounds of the uranyl acetate (ac) type (Table I.3.2) from which 2 are mixed oxalate acetate ligands (see previous oxalate section).

Table I.3.2 List of the monomeric type uranyl acetates.

Compound	Pattern	Coordination type	Reference
$H_3O^+[UO_2(ac)_3]$	0D	H	35
(Htea) $[UO_2(ac)_3]$	0D	H	35
$Na[UO_2(ac)_3]$	0D	H	36,37
(Hmz)$[UO_2(ac)_3]$	0D	H	38
(Hpz)$[UO_2(ac)_3]$	0D	H	38
$K[UO_2(ac)_3]$	0D	H	39
$Tl[UO_2(ac)_3]$	0D	H	40
$NH_4[UO_2(ac)_3]$	0D	H	41
$Cs[UO_2(ac)_3]$	0D	H	42
(Htea)$[(UO_2)_2(ac)_3]$	0D	H	35
(Hhyd)$[UO_2(ac)_3)]$	0D	H	43
$(NH_4)_3[(UO_2)_2(ac)_6]\cdot scn$	0D	H	44
$(H_2arg)[UO_2(ac)_3]\cdot Hac\cdot H_2O$	0D	H	45
$K_2[UO_2(ac)_3]_2\cdot H_2O$	0D	H	46
$[UO_2(ac)(gpi)]$	0D	H	47
$[UO_2(ac)_2(dmac)]$	0D	P	48
$[(UO_2)_2(ac)_4(urea)_3]$	0D	P + H	49
$[UO_2(ac)(odpy)]$	0D	H	50
$(NH_4)_3[(UO_2)_3(ac)_7(scn)_2(H_2O)]$	0D	H + P	44
(eotp)$[(UO_2)_5(ac)_3]$	0D	H	51
$[UO_2(sbh)(ac)]$	0D	P	52
$[UO_2(ac)_2(apy)]$	0D	P	53
$[UO_2(ac)_2(H_2O)_2]\cdot Hac$	0D	H	54
$[UO_2(ac)_2(H_2O)_2]\cdot 18c6\cdot 2H_2O$	0D	H	55
$[(UO_2)(Hac)_2(ac)_2]$	0D	P	56, 57
$[UO_2(ac)_2(mz)_2]$	0D	H	58
$[UO_2(ac)_2(H_2O)]\cdot H_2O$	1D	P	59
(Hdea)$[UO_2(ac)_2(ox)]\cdot H_2O$	0D	H	28
$(NH_4)_2[(UO_2)_2(ox)(ac)_4]\cdot 2H_2O$	0D	H	31

Eleven of the compounds have the formula $[B]^+[UO_2(ac)_3]^-$ where B is a metallic or organic single charge counter-cation. The negative central ion is represented in Figure I.3.5. Other three compounds are derivatives of this formula, containing also neutral molecules or hydration water trapped in the

crystalline structure. All of the compounds, except one, exhibit zero-dimensional molecular structures, involving chelating acetate groups. The only one-dimensional structure is a special case where one acetate molecule does not chelate the metal, but bridges in a bidentate fashion, two uranyl ions in order to create a 1D infinite chain (Figure I.3.6).

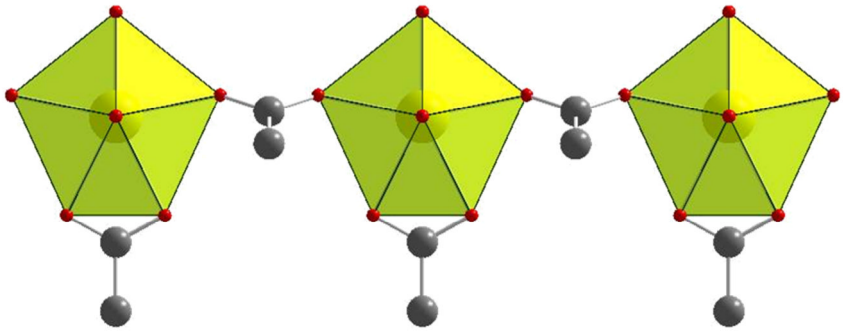

Figure I.3.6 Structure representation of bridging coordination type in the acetate case ($[UO_2(ac)_2(H_2O)]\cdot H_2O$)[59].

The next class of compounds corresponds to uranyl aromatic carboxylates. The most common and simple aromatic carboxylate is the benzoic acid. There have been found in the literature eight uranyl benzoate (box) structures[60-67] and other 13 structures[68-77] having a benzoate derivative linker (Table I.3.3). The majority of these structures (18) are zero-dimensional due to the preference of the mono-dentate carboxylate group, as in the case of the acetic acid, to chelate the uranium metal instead of bridging two uranyl centers.

Table I.3.3 List of uranyl aromatic carboxylates.

Compound	Pattern	Coordination type	Reference
$[UO_2(box)_2]$	1D	T	60
$K_{11}[(UO_2)_{23}(box)_{57}(H_2O)_{18}]\cdot 7H_2O$	0D	P + H	61
$Na[UO_2(box)_3]\cdot 2H_2O$	0D	H	62, 63
$Na[UO_2(box)_3]$	0D	H	62
$Na[UO_2(C_7H_5O_2)_3]\cdot Hbox\cdot H_2O$	0D	H	64
$[UO_2(box)_2(dmf)]$	0D	P	65
$[UO_2(box)_2(py)_2]$	0D	H	66
$[UO_2(box)_2(H_2O)]\cdot EtOH$	1D	P	67
$[UO_2(pbba)_2(H_2O)]$	0D	P	68, 69
$[UO_2(mbba)_2]$	1D	T	68
$[UO_2(ahba)_2(Hahba)]\cdot 3cb6\cdot 16H_2O$	0D	H	70
$[UO_2(pcba)_2(H_2O)]$	0D	P	69
$[UO_2(piba)_2(H_2O)]$	0D	P	69
$Na[UO_2(pasa)_3]$	0D	H	71

Compound	Pattern	Coordination type	Reference
$[UO_2(dmb)_2(H_2O)_2]\cdot H_2O$	0D	H	72
$[UO_2(dmb)_2(H_2O)_2]\cdot 8H_2O$	0D	H	72
$[UO_2(pdab)(EtOH)(phen)]$	0D	P	73
$(H_3O)[UO_2(ohb)_3]\cdot 5H_2O$	0D	H	74
$(H_3O)[UO_2(oab)_3]\cdot H_2O$	0D	H	75
$[(UO_2(gre)_2(H_2O)_2]\cdot 8H_2O$	0D	H	76
$[UO_2(odpy)(pfb)_2]$	0D	H	77
$[(UO_2)_2(pht)_2(urea)_2]\cdot H_2O$	1D	P	78
$[UO_2(pht)(H_2O)]\cdot H_2O$	1D	P	79
$(NH_4)_2[(UO_2)_2(tpa)_3]\cdot 5H_2O$	2D	H	80
$[UO_2(Hobtp)_2]$	2D	H	80
$(Hdmf)[(UO_2)_3(ipa)_4]\cdot H_2O$	1D	H	81
$[UO_2(Htms)(H_2O)]\cdot H_2O$	1D	P	82
$[(UO_2)_3(hmm)_2(H_2O)_4]$	3D	P + H	83
$[UO_2(H_2btec)(H_2O)_2]\cdot H_2O$	1D	H	84
$[(UO_2)_2(btec)(phen)_2]$	2D	H	85
$[(UO_2)_3(H_2O)_6(mel)]_2\cdot 23H_2O$	2D	H	86
$[UO_2(bndc)(H_2O)]$	1D	P	87
$[UO_2(dda)(H_2O)]\cdot H_2O$	1D	P	88
$[(UO_2)_2(mddb)_3](H_2O)$*	2D	H	89
$[(UO_2)_4(H_2pddb)_2(pddb)]$*	2D	P	89
$[(UO_2)_2(mddb)_4]$*	1D	T	89
$[UO_2(anca)_2(H_2O)_2]\cdot 3dox$	0D	H	90
$(H_2pdpy)(Hpdpy)_2[(UO_2)_4(pndc)_6]$	2D	P	91
$[UO_2(pndc)(odpy)]$	1D	H	91
$[UO_2(pndc)]\cdot eg$	1D	H	92
$[UO_2(podb)(H_2O)]$	1D	P	93, 94
$(Htea)[UO_2(tob)_3]\cdot 2dcm$	0D	H	95
$(Hdiea)[UO_2(phtob)_3]\cdot diea$	0D	H	95
$[(UO_2)_2(onppc)_2(H_2O)][(U(onppc)(H_2O)_4]\cdot 5H_2O$*	2D	T + P + A	6
$K_2[(UO_2)_2(pndc)_3]\cdot 2H_2O$	2D	H	80
$(Hgu)_2[(UO_2)_2(pndc)_3](H_2O)_2$	2D	H	80
$[UO_2(ptpb)(dmf)]\cdot H_2O$	1D	P	96
$[UO_2(H_2bptc)(H_2O)_2]\cdot 2H_2O$	1D	H	97
$[(UO_2)_3(Hbpnt)_2(H_2O)]\cdot 3H_2O$	2D	P	98

*- the structure formula is presented as it has been reported by the authors, although the compound's electro-neutrality is not respected.

With this type of ligands there are only three chain-like unidimensional structures (Figure I.3.7), two of them almost similar with benzoic and 3-bromobenzoic acids, having a very rare T uranyl coordination type, and one with a more common P uranyl coordination type.

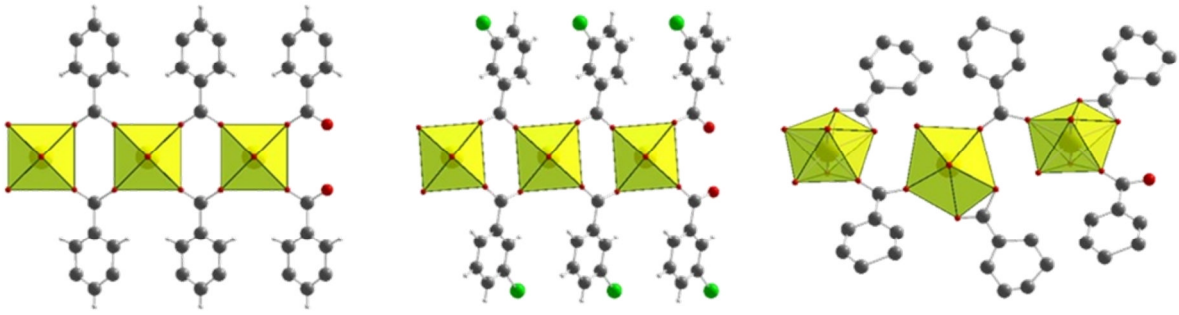

Figure I.3.7 Representation of three unidimensional benzoate and benzoate-derived structures (left)[60], (middle)[68], (right)[67].

The most interesting uranyl benzoate has been obtained using KOH as a pH moderator. The resulting structure (Figure I.3.8) contains K^+ as a counter-cation and combines in the same crystal two types of discrete entities. In the first one, the benzoate molecule coordinates the uranyl ion exactly as in the case of Figure I.3.7 (right) but the infinite chain is interrupted in order to form a six-member ring. The second entity is commonly encountered, being formed by three ligand molecules chelating a uranyl hexagonal bipyramid. Both entities have nothing unseen before, but the combination of the two in the same crystal structure gives a very interesting and complex compound obtained with a common and previously studied ligand[61].

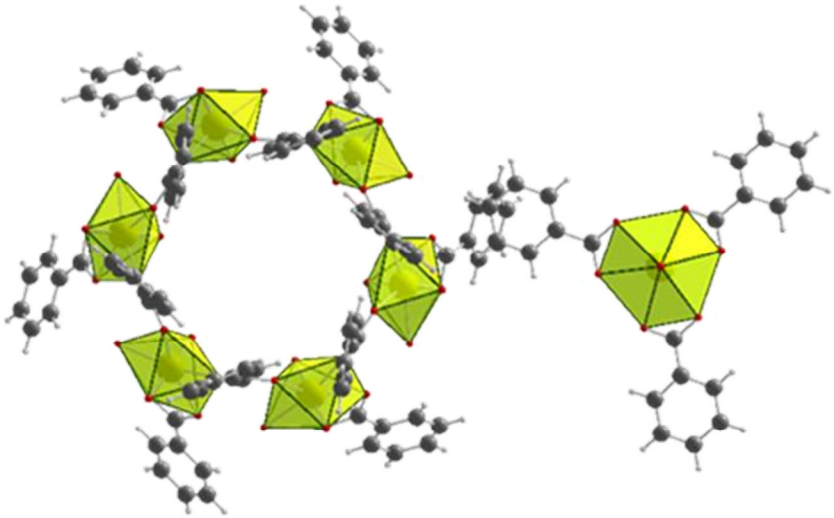

Figure I.3.8 Occurrence of two molecular entities in the same crystal structure $(K_{11}[(UO_2)_{23}(box)_{57}(H_2O)_{18}]\cdot 7H_2O)$[61].

A little bit more complicated is the case of benzene di- and poly-carboxylates, where the presence of at least two carboxylate groups and the free rotation of these groups around the C-C bond give rise to the formation of at least

one-dimensional structures. Although this class is a prolific one due to the diversity of the possibilities of multidentate connection modes of carboxylates functions, it contained only ten structures referenced in litterature[78-86]. This observation incited us to examine the different structural topology networks resulting from the combination of such benzene-based poly-carboxylates molecules with uranyl entities, which was the subject area of this thesis. The complexes of this class will be discussed comparatively in the next chapters.

Another targeted category of ligands are the aromatic mono- or poly-carboxylates possessing at least two benzene rings, condensed (ex. naphthalene derivatives) or not (ex. biphenyl derivatives). In this category, also partially debated in the further chapters of this work, the coordination possibilities are various increasing the number of different phases obtained with a given ligand. This is due to the high complexity of the ligands backbone and also due to the relatively large number of carboxylate groups. With this type of ligands, there have been found reported in the literature 18 compounds[6, 80, 87-98]. None of these compounds possess a tridimensional structure mainly due to the ligands preference to planar conformations. But one of the compounds ($[(UO_2)_2(onppc)_2(H_2O)][(U(onppc)(H_2O)_4]\cdot 5H_2O$)[6] raises interest due to the presence of three types of U(VI) coordination, the common P, the rare T, and the unique A, all occurring in the same crystalline structure (Figure I.3.9). The six-fold coordination sphere is ensured by four carboxylate groups of four different ligand molecules, all bridging the T sphere to other two uranyl ions. The seven-fold sphere is completed by two bridging units, similar to the T case, one chelating carboxylate group of the ligand and one coordinating water molecule. The A type coordination sphere is unique and formed by four coordinating water molecules (U—O bond of 1.88 to 2.03 Å), and two chelating carboxylate groups of the ligand (U—O bond of 2.41 to 2.55 Å). The complexity of the structure is possibly given by the geometry of the ligand; the two nitro groups being close to each other determine an increased dihedral angle between the two benzene rings, changing the planar typical conformation of the biphenyl type ligands, inducing elements of asymmetry in structure, all conducting to the multiple coordination types present in the structure of $[(UO_2)_2(onppc)_2(H_2O)][(U(onppc)(H_2O)_4]\cdot 5H_2O$.

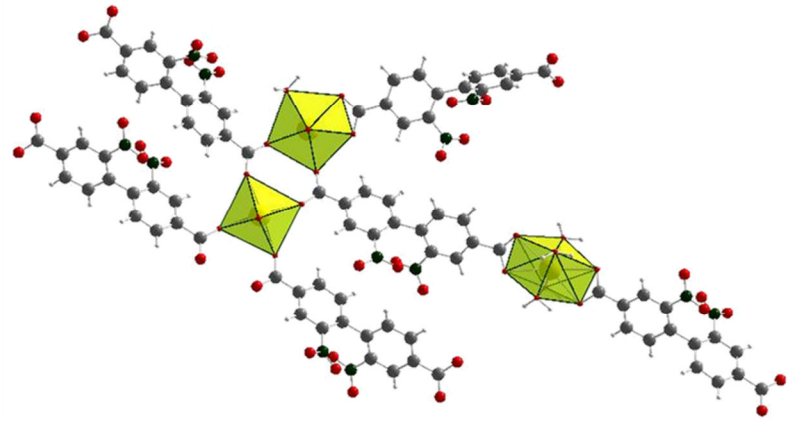

Figure I.3.9 Structure representation of a uranyl aromatic nitro-carboxylate possessing three types of coordination environments in $[(UO_2)_2(onppc)_2(H_2O)][(U(onppc)(H_2O)_4]\cdot 5H_2O$[6].

The next largest category of monomeric uranyl carboxylates is the one of aromatic heterocycles with N- or S-donor (Table I.3.4).

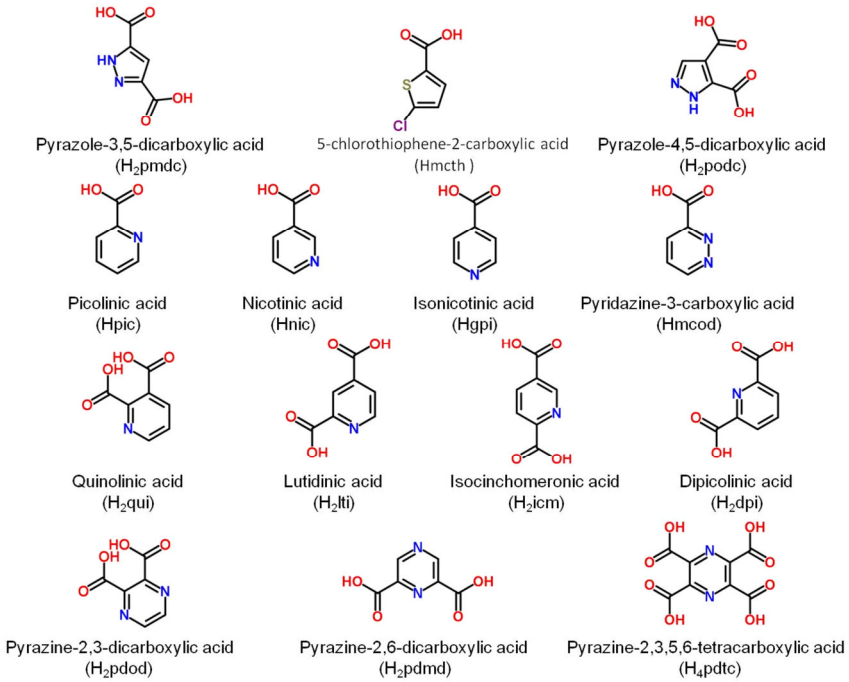

Figure I.3.10 Classes of heterocyclic carboxylate ligands and their representatives.

In this category of ligands are included carboxylate derivative of five member aromatic heterocycles of the thiophene and pyrazole type and six member aromatic rings of the pyridine, pyrazine and pyridazine types (Figure I.3.10). Also in this class, there have been introduced compounds having as a ligand complex molecules with more than one heterocycle, condensed or not, but having the carboxylate group directly linked to the aromatic ring.

The main characteristic of this class of ligands is the coordination capacity of the heteroatom from the cycle. When this happens, usually, the carboxylate

groups are constrained, if they are close enough to the heteroatom (α and β positions), to be coplanar with the aromatic ring, giving structures with a maximum bi-dimensional pattern.

Table I.3.4 List of uranyl heterocyclic aromatic carboxylates.

Compound	Pattern	Coordination type	Ref
$[UO_2(podc)]$	2D	P	101
$[UO_2(pmdc)(H_2O)]$	2D	H	102
$(H_2pdpy)[(UO_2)_2(mcth)_6]\cdot 2H_2O$	0D	H	103
$(H_2edpy)[(UO_2)_2(mcth)_6]\cdot 2H_2O$	0D	H	103
$[UO_2(gpi)_2]$	2D	P	104
$(H_3O)[UO_2(pnmi)_3]\cdot 4H_2O$	0D	H	94
$[UO_2(pic)_2]$	1D	P	105
$[UO_2(nic)_2(H_2O)_2]$	0D	H	106
$[(UO_2)_3(pic)_4(NO_3)_2]$	2D	P + H	107
$[UO_2(meni)_2]$	2D	H	108
$[UO_2(mcod)_2(H_2O)]\cdot H_2O$	0D	P	109
$[UO_2(icm)]$	3D	P	99
$(H_3O)_2[(UO_2)_3(dpi)_4]\cdot 2H_2O$	2D	P + H	110
$[UO_2(dpi)(H_2O)]$	1D	P	111, 112
$[UO_2(qui)]$	2D	P	100
$[UO_2(lti)]$	3D	P	100
$[UO_2(dpi)]$	3D	P	100
$(Hacr)_2[UO_2(dpi)_2]$	0D	H	113
$(Htea)_2[UO_2(dpi)_2]\cdot 2H_2O$	0D	H	114
$[UO_2(Hdpi)_2]\cdot 4H_2O$	0D	H	112
$Rb_2[UO_2(dpi)_2]\cdot 3H_2O$	0D	H	112
$Cs_2[UO_2(dpi)_2]\cdot 4H_2O$	0D	H	112
$[UO_2(Hdpi)_2]\cdot Hpic\cdot 6H_2O$	0D	H	115
$[UO_2(pdod)(H_2O)_2]$	1D	P	116
$[UO_2(pdod)(H_2O)]$	1D	P	116
$[UO_2(pdmd)(H_2O)]$	1D	P	117
$[(UO_2)_2(pdtc)(H_2O)]\cdot 2H_2O$	2D	H	117
$[(UO_2Na_2(pdtc)(H_2O)_4]$	1D	H	117
$[(UO_2K_2(pdtc)(H_2O)_2]\cdot 2H_2O$	0D	H	117
$K_2[(UO_2(H_2pdtc)_2]\cdot 4H_2O$	0D	H	117
$Rb_2[UO_2(H_2pdtc)_2]\cdot 4H_2O$	0D	H	117
$[(UO_2)_2(pdtc)(cb6)(H_2O)_2]\cdot 12H_2O$	0D	P	33
$[UO_2(ptcp)_2(H_2O)_2]$	0D	H	105
$[UO_2(phndc)]$	1D	P	118
$[UO_2(odpydc)(H_2O)]\cdot 3H_2O$	1D	P	97
$[UO_2(odpydc)(dmf)]\cdot 3H_2O$	1D	P	97
$[UO_2(odpydc)(H_2odpydc)](H_2O)$	1D	P	97

There are three exceptions of this rule[99, 100], where even though the carboxylates groups are constrained, the equatorial plane of the uranyl ion is not in the same plane with the aromatic ring, giving the third dimension. Moreover, only one of the carboxylate groups can be constrained and the other has a high torsion angle from the ring, the result being the same: the propagation of the structure to the third direction. Other examples of tridimensional structures containing this type of ligands appear, but in mixed ligands systems, where the co-ligand plays an important role in establishing the dimensionality of the structure.

Another rich category concerns the use of linear aliphatic dicarboxylates associated with uranyl cations.

Table I.3.5 List of linear uranyl aliphatic dicarboxylates.

Compound	Pattern	Coordination type	Ref
$[UO_2(adp)(H_2O)_2]$	1D	H	119
$[UO_2(fmr)(H_2O)_2]$	1D	H	120
$[UO_2(mln)(H_2O)]\cdot 2H_2O$	2D	P	121
$[UO_2(suc)(H_2O)]$	3D	P	81, 122
$K(H_3O)[UO_2(act)_2(H_2O)]\cdot 3H_2O$	1D	P	123
$Cs_2[UO_2(act)_2(H_2O)]\cdot 2H_2O$	1D	P	123
$Li[(UO_2)(glt)(Hglt)]\cdot 4H_2O$	1D	H	124
$(H_2pdpy)[UO_2(mln)_2]\cdot 4H_2O$	0D	P	125
$(H_2pdpy)[(UO_2)_2(glt)_3]\cdot 2H_2O$	2D	H	126
$[UO_2(pdpy)(adp)]$	2D	H	126
$(H_2pdpy)[(UO_2)_2(pml)_2(Hpml)_2]\cdot pdpy\cdot 2H_2O$	1D	H	126
$[(UO_2)_2(sbc)(pdpy)_2]$	2D	P	126
$(H_2edpy)[(UO_2)_2(adp)_3]$	1D	H	126
$(H_2edpy)[(UO_2)_2(pml)_3]$	2D	H	126
$[(UO_2)_2(azl)_2(edpy)]$	2D	P	126
$(H_2lptz)[UO_2(mln)_2(H_2O)]\cdot 2H_2O$	0D	P	127
$[(UO_2)_2(sbc)_2(edpy)(H_2O)]$	3D	P	128
$(H_2edpy)[(UO_2)_2(sbr)_3]$	1D	H	128
$[(UO_2)_2(azl)_2(edpy)]$	2D	P	128
$(Hedpy)_2[(UO_2)_2(azl)_3]\cdot 2H_2O$	1D	H	128
$[(UO_2)_6(sbc)_2(cb6)_3(H_2O)_6(NO_3)_8]\cdot cb6\cdot 8H_2O$	0D	P + H	129
$(H_2eda)[UO_2(dmmln)_2(H_2O)]$	0D	P	130
$(H_2ppz)_2[(UO_2)_2(mml)_4(H_2O)_2]\cdot 3H_2O$	0D	P	131
$(H_2dmeda)[UO_2(mml)_2(H_2O)]\cdot H_2O$	0D	P	131
$(H_2ppz)[UO_2(demln)_2(H_2O)]\cdot H_2O$	0D	P	131
$(H_2teda)[UO_2(demln)_2(H_2O)]\cdot H_2O$	0D	P	131
$(Hdma)_4[(UO_2)_4(sbc)_6]\cdot cb6\cdot H_2O$	1D	H	132
$[UO_2(phscc)(H_2O)]$	2D	P	98

The ligands included in this category are basically more or less long saturated hydrocarbon chains being capped at each end by a carboxylate group capable of coordinating, usually chelating, the uranyl ion. Due to the flexibility of the organic backbone, the conformations that could be adopted in the crystalline structure are endless. The dimensionality of the obtained structures varies from 0D to 3D, but the most common one being 1D. Concerning the coordination sphere around the uranyl ion, with this type of ligands there are no case of type T or A polyhedra. In the literature there have been found 27 compounds (Table I.3.5) with this type of linkers from which 4 are simple metal-ligand structure. The rest is negatively charged entities and having as counter-ion metallic cations or protonated organic bases or is neutral entities but containing some neutral organic molecules trapped inside the crystal structure.

The last and the most prolific category contains aliphatic linear or cyclic, mono- or polycarboxylates. Without counting the oxalate and acetate structures previously discussed, so far there have been found 51 reported compounds (Table I.3.6). The simplest aliphatic carboxylic acid is the formic acid. Used as a ligand, it has been reported in four uranyl complexes. The structures exhibit type P coordination spheres around the uranyl ion and the following patterns: one of the structures is zero-dimensional, two are one-dimensional and the fourth one is tri-dimensional. From this it can be observed that this ligand has no preference neither for chelating nor bridging the metal coordination spheres. Due to its reduced molecular volume, together with the oxalic and acetic acid, the formic acid is a good choice for synthesizing mixed ligands coordination polymers with original structures.

Table I.3.6 List of aliphatic, linear and cyclic carboxylates and their derivatives.

Compound	Pattern	Coordination type	Ref
$(NH_4)_2[UO_2(fa)_4]$	0D	P	133
$[UO_2(fa)_2(H_2O)]$	1D	P	134
$Na[UO_2(fa)_3]\cdot H_2O$	1D	P	135
$[UO_2(fa)_2(H_2O)]$	3D	P	136
$[UO_2(Hgly)_4](NO_3)_2$	0D	H	137
$[UO_2(Hhaa)_2]$	2D	P	138
$[UO_2(mlm)_2(H_2O)]\cdot 2H_2O$	0D	P	127

Compound	Pattern	Coordination type	Ref
$NH_4[UO_2(paa)]\cdot H_2O$	2D	P	139
$[UO_2(Hpaa)(H_2O)]\cdot H_2O$	1D	P	140
$Na[UO_2(pha)_3]$	0D	H	141
$[(UO_2)_2(ppi)_4(urea)_3]$	0D	P + H	142
$Ca[(UO_2)_2(ppi)_6(H_2O)_5]\cdot H_2O$	0D	H	124
$Cs[(UO_2)(ppi)_3]$	0D	H	143
$K[UO_2(ppi)_3]$	0D	H	144
$NH_4[UO_2(ppi)_3]$	0D	H	144
$[UO_2(isb)_2(H_2O)_2]$	0D	H	145
$[UO_2(lac)_2]$	2D	P	104
$[UO_2(hmpa)_2)]$	2D	P	146
$K[UO_2(bua)_3]$	0D	H	144
$[UO_2(gaba)_3](ClO_4)$	0D	H	147
$[UO_2(gaba)_3](NO_3)_2\cdot H_2O$	0D	H	148
$[UO_2(beo)_2(H_2O)_2]$	0D	H	149
$[UO_2(eta)_2]$	2D	P	150
$(H_2deda)[UO_2(oda)_2]$	0D	H	151
$(H_2tmeda)[UO_2(oda)_2]$	0D	H	151
$[UO_2(oda)]$	3D	P	152
$[UO_2(Hida)_2]$	1D	H	153
$[UO_2(ida)]$	2D	P	154
$[UO_2(ta)(H_2O)]$	2D	P	155
$[UO_2(Hcrm)]$	2D	P	156
$Na[UO_2(trc)]\cdot 4H_2O$	2D	H	157
$[(UO_2)_3(Hcit)_2(H_2O)_3]\cdot 2H_2O$	3D	P	157
$[(UO_2)_2(btca)(H_2O)_4]\cdot 4H_2O$	2D	H	158
$(H_3O)_2[(UO_2)_5(btca)_3(H_2O)_6]$	3D	H	158
$[(UO_2(Hnta)(H_2O)_2]\cdot 3H_2O$	1D	P	159, 160
$[UO_2(boda)(H_2O)]$	1D	P	161
$(H_2dabco)_2[(UO_2)_4(boda)_6](H_2O)_3$	1D	H	161
$[UO_2Na(Hdcta)(H_2O)]$	2D	P	161
$[(UO_2)_3(bta)_2(H_2O)_5]\cdot 5H_2O$	2D	P + H	98
$[(UO_2(Httpa)](H_2O)(imd)$	2D	H	162
$[(UO_2)_2(cbtc)(H_2O)_2]\cdot 2H_2O$	3D	P	158
$[(UO_2)_2(cbtc)(H_2O)_2]\cdot 3H_2O$	3D	P	158
$[UO_2(cmpr)(py)_2]\cdot py$	1D	H	163
$[UO_2(cmpr)(Hmoh)]\cdot Hmoh$	2D	P	163
$[(UO_2)_2(cmpr)(Hcmpr)_2]\cdot 3H_2O$	0D	H	164
$[UO_2(chdc)(H_2O)]$	2D	P	165
$[(UO_2)_2(chdc)_2(H_2O)_3]\cdot H_2O\cdot 15c5$	1D	P	165
$[UO_2(madc)(H_2O)]\cdot H_2O$	1D	P	166
$[(UO_2)_3(Hbota)_2(H_2O)_6]\cdot 10H_2O$	2D	H	97
$(Hpy)[UO_2(beica)]\cdot py$	0D	H	167

Increasing the size of the ligand (excluding acetates and oxalates), the next group of linear aliphatic carboxylates is formed by the acetic acid derivatives. There have been found 4 complexes possessing this type of linker. One with aminoacetic acid, where the amino group of the ligand is protonated, gives neutral charge on the ligand molecule. This is a specific property for the amino acids, where the obtained complexes require this time a counter-anion in order to compensate the positive charge of the uranyl ion. The second is hydroxiacetic acid, where the coordinating capacity of the hydroxo group gives a bi-dimensional structure. The third is malonamic acid, where the oxy group also coordinates the metal, but the amino group limits the dimensionality of the structure at zero. The fourth is phenylacetic acid, obtaining a zero-dimensional structure similar to the one of acetates. Additionally, other derivates is phosphoacetic acid, where the phosphonic group has a tridentate coordination capacity giving mono- and bi-dimensional structures.

Increasing further the size of the ligand, the next group corresponds to propionic acid and its derivatives. There have been found 5 uranyl propionates. They all exhibit zero-dimensional structures due to the same chelating preference encountered in the acetates cases and three propionate derivates, where the methyl substituted one behaves similarly to the parent compound and the two hydroxo substituted ones are giving bidimensional structures.

With butyric acid and its derivatives there have been found four compounds. There are one phase with the parent ligand and the second one with the α,β-unsaturated derivative (crotonic acid), both giving the same type of chelating mode in zero-dimensional structures. The last two compounds are with the γ-amino butyric acid, also giving zero-dimensional structures but having the typical amino-acid behavior, requiring a counter anion in the structure.

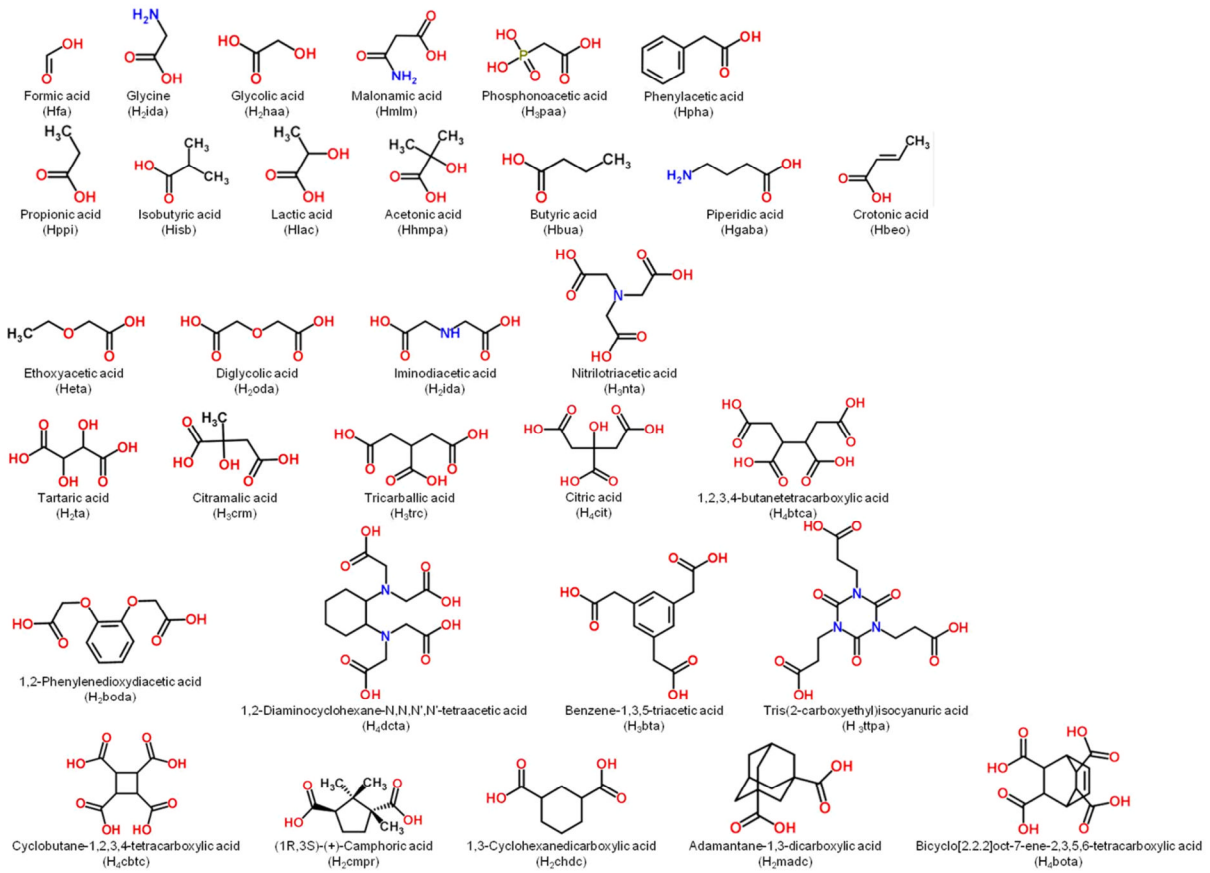

Figure I.3.11 Subclasses of ligands and their representatives: molecular structure representation.

In the same class of linear uranyl aliphatic carboxylates there have been found another 18 members where the ligands possess multiple coordinating groups and complex architectures giving rise to interesting high dimensionality structures. The subclass of cyclic aliphatic carboxylates bearing uranyl has ten representatives. Two of them are based on cyclobutanetetracarboxylic acid, giving two tridimensional structures, other three are with camphoric acid, a versatile ligand, giving structures with 0-, 1- or 2-dimensionalities, two are with cyclohexanedicarboxylic acid and the last three are with polycyclic carboxylates. A list of the encountered aliphatic ligands is presented in Figure I.3.11.

One of the most interesting complex in this category contains 3,3',3''-((2,4,6-triethylbenzene-1,3,5-triyl)tris((1-oxoethane-2,1-diyl)imino))tris(1,5,7-trimethyl-2,4-dioxo-3-azabicyclo[3.3.1]nonane-7-carboxylic acid.[167] (Figure I.3.12) The ligand is a high complexity organic molecule specific designed to perfectly encapsulate by coordination a single uranyl ion with type H coordination sphere.

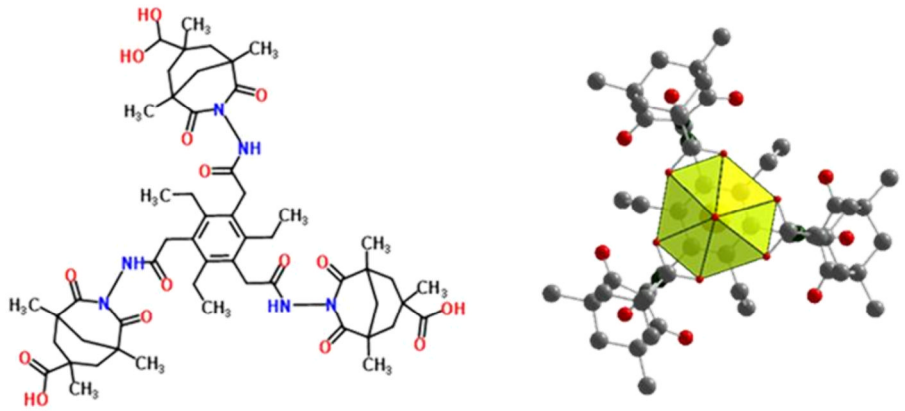

Figure I.3.12 Molecular structural representation of the ligand (left) and the complex (right) for the uranyl 3,3',3''-((2,4,6-triethylbenzene-1,3,5-triyl)tris((1-oxoethane-2,1-diyl)imino))tris(1,5,7-trimethyl-2,4-dioxo-3-azabicyclo[3.3.1]nonane-7-carboxylate[167].

The most interesting monomeric uranyl carboxylate complex has been obtained using as ligand the dipicolinic acid and contains U^{VI}/U^{IV} mixed valence cations. The compound with the formula $K(H_2py)[UO_2(H_2O)U(dpi)_4]\cdot 2H_2O$[168] has a zero-dimensional structure (Figure I.3.13) and a common P type monomeric unit for the hexavalent uranium atom in a unique combination with a nine-fold coordinated monomeric species for the tetravalent uranium atom. Although the intention of the authors was to obtain a pure tetravalent uranium complex, this result is unique.

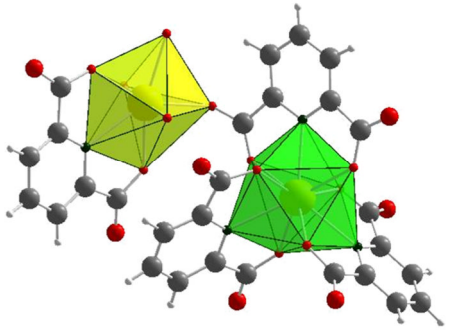

Figure I.3.13 Representation of the uranium-centered polyhedra of the unique mixed valence U^{IV}(green)/U^{VI}(yellow) carboxylate framework[168].

Dinuclear type uranyl carboxylate complexes

Based on the geometry of the SBU and uranyl coordination state, the dimeric structures can be classified into 3 large classes presented in the Figure I.3.14. So far there have been found 44 from which 8 are type H edge sharing

polyhedra, 4 are type P corner sharing, 24 are type P edge sharing and 8 are mixed dimeric, monomeric moieties.

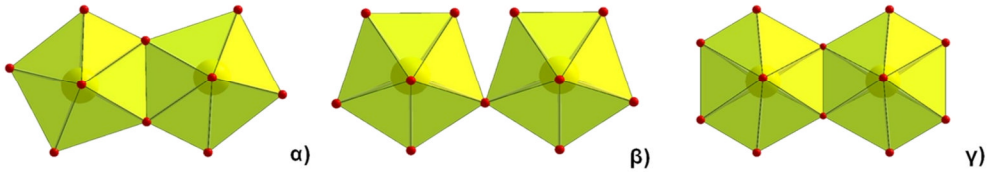

Figure I.3.14 Connection modes and coordination geometries for carboxylates bearing dinuclear uranyl units.

In the class of P type edge-sharing dimers (Figure I.3.14-α), the interesting feature is the chemical nature of bridging oxygen atom between the uranyl-centered polyhedra. From the investigated 22 compounds of this type (Table I.3.7), the inter-polyhedra bridge is formed by the coordinating oxygen carboxylate groups (μ_3-Oc) of the ligand in 11 cases, the other 11 having a hydroxo bridge (μ_2-OH). In this class there are no oxo bridge cases.

Table I.3.7 Dinuclear uranyl carboxylate edge-sharing P polyhedra type complexes.

Compound	CNB*	Pattern	Ref
$[UO_2(glt)]$	μ_2-Oc	2D	169
$[UO_2(pml)]$	μ_2-Oc	2D	170
$[UO_2(adp)]$	μ_2-Oc	3D	119
$[UO_2(sbc)]$	μ_2-Oc	2D	170
$(Htea)_2[(UO_2)_2(dpi)_2(moh)_2]\cdot H_2O\cdot Hmoh$	μ_2-Oc	0D	114
$(H_2dabco)[UO_2(Hcit)(H_2O)]_2\cdot 2H_2O$	μ_2-Oc	0D	171
$(H_2dabco)[UO_2(crm)]_2$	μ_2-Oc	1D	171
$(H_2pdpy)[UO_2(Hcit)]_2$	μ_2-Oc	1D	171
$(H_2pdpy)[UO_2(crm)(H_2O)]_2\cdot H_2O$	μ_2-Oc	0D	171
$(H_2odpy)_2[UO_2(Hcit)]_2\cdot 5H_2O$	μ_2-Oc	1D	171
$(H_2cry)[UO_2(Hcit)]_2\cdot 4H_2O$	μ_2-Oc	1D	171
$[UO_2(fa)(HO)(H_2O)]$	μ_2-OH	2D	172
$[(UO_2)_2(ac)_3(HO)_2(H_2O)_2]\cdot{}_{18}c_6$	μ_2-OH	0D	55
$[UO_2(OH)(pic)]$	μ_2-OH	1D	32
$[UO_2(OH)(cpym)]$	μ_2-OH	1D	32
$(Htea)_2[(UO_2)_2(dpi)_2(OH)_2]\cdot 2H_2O$	μ_2-OH	0D	114
$(Htmeda)(Htea)[(UO_2)_2(dpi)_2(OH)_2]\cdot 2H_2O$	μ_2-OH	0D	114
$[(UO_2)_2(ox)(OH)_2(H_2O)_2]$	μ_2-OH	1D	173
$[(UO_2)_2(cb7)(OH)_2(fa)_2(H_2O)_3]\cdot 8H_2O$	μ_2-OH	0D	174
$(Hpy)_2[(UO_2)_3(OH)(cit)(Hcit)]$	μ_2-OH	2D	156
$[UO_2(pyac)(OH)]$	μ_2-OH	1D	175
$(H_2ppz)[(UO_2)_2(ida)_2(OH)_2]\cdot 8H_2O$	μ_2-OH	0D	151
$(H_2hmta)_2[UO_2(oda)_2(OH)_2]\cdot 2H_2O$	μ_2-OH	0D	151
$[UO_2(Hpamb)(OH)(fa)(H_2O)]\cdot cb6\cdot dmf\cdot 7H_2O$	μ_2-OH	0D	70

* Chemical nature of the inter-polyhedra bridge

In the case of corner sharing pentagonal dimeric units (Figure I.3.14-β), there are no oxo bridges, all 4 compounds (Table I.3.8) of this class having a shared μ_2-hydroxo group. In none of these cases the ligand cannot ensure the corner shared link.

Table I.3.8 Dinuclear uranyl carboxylate corner-sharing polyhedra type complexes.

Compound	CNB*	Pattern	Ref
$[(UO_2)_2(apa)_3(HO)(H_2O)_2]\cdot H_2O$	μ_2-OH	1D	176
$NH_4[(UO_2)_2(OH)(sq)(ox)]\cdot H_2O$	μ_2-OH	2D	177
$Na[(UO_2)_2(ox)_2(OH)]\cdot 2H_2O$	μ_2-OH	2D	155
$Cs[(UO_2)_2(pzdc)_2(OH)(H_2O)]$	μ_2-OH	3D	116

* Chemical nature of the inter-polyhedra bridge

In the case of dimeric H type SBUs (Figure I.3.14-γ), the situation slightly differs from that one of P type dimers. In 3 of the compounds (Table I.3.9) the connection is ensured by a μ_2-hydroxo bridge in the first[178], by an μ_2-oxo one in the second[114] and by a μ_2-fluoro in the third.[81] In the other 5 remaining cases[130, 163, 179-181], the bridge being formed by the ligand (Oc) through a special μ_2-η_1:η_1:η_2 carboxylate group bonding (Figure I.3.15-left).

Table I.3.9 Dinuclear uranyl carboxylate edge-sharing H polyhedra type complexes.

Compound	CNB*	Pattern	Ref
$[UO_2(OH)(ac)(phen)]$	μ_2-OH	0D	178
$(Htea)_2[(UO_2)_2O_2(dpi)_2(H_2O)_2]\cdot 2H_2O$	μ_2-O	0D	114
$[UO_2F(Hglt)]\cdot 2H_2O$	μ_2-F	1D	81
$[UO_2(ohb)(NO_3)]\cdot$tea	μ_2-Oc	0D	179
$[UO_2(ohb)(NO_3)]\cdot$dmap	μ_2-Oc	0D	180
$[UO_2(hpm)(ac)]\cdot$Hmoh	μ_2-Oc	0D	181
$(Hpy)[UO_2(cbdc)(NO_3)]$	μ_2-Oc	0D	163
$(H_2teeda)[(UO_2)_2(dmmln)_3]$	μ_2-Oc	1D	130

* Chemical nature of the inter-polyhedra bridge

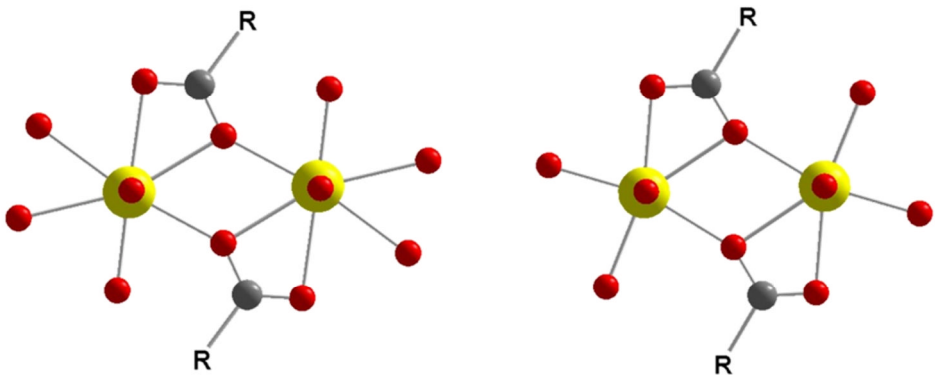

Figure I.3.15 Representation of μ_2-η_1:η_1:η_2 ligand coordination in the γ type dimeric units (left) and α type dimeric units (right).

One interesting class of compounds is formed by the mixed dimeric - monomeric phases. There have been found 8 structures of this type (Table I.3.10), all having high dimensionalities and also high structural complexity. The chemical process route for the formation of these structures could be the synthesis pH, permitting the hydrolysis reaction leading to chemical equilibrium stabilizing the formation of the dimeric unit together with the monomeric one.

Table I.3.10 Uranyl carboxylate complexes mixed dimer-monomer SBU type.

Compound	CNB*	Pattern	Linkage**	Ref
$(teea)_2[(UO_2)_3(cit)_2(H_2O)_2]\cdot 2H_2O$	μ_2-Oc	2D	α + H	156
$(H_2pdpy)[(UO_2)_3(paa)_2(Hpaa)(H_2O)]\cdot 3H_2O$	μ_2-Oc	2D	β + P	182
$(H_2etdpy)[(UO_2)_3(paa)_2(Hpaa)(H_2O)]\cdot 2H_2O$	μ_2-Oc	2D	β + P	182
$(H_2edpy)[(UO_2)_3(paa)_2(Hpaa)(H_2O)]\cdot 2H_2O$	μ_2-Oc	2D	β + P	182
$[(UO_2)_4(paa)_2(Hpaa)(H_2O)_4]\cdot 3H_2O$	μ_2-Oc	2D	β + P	139
$(H_2teeda)_2[(UO_2)_3(demln)_5]\cdot H_2O$	μ_2-Oc	1D	γ + P	131
$(dmppz)[(UO_2)_3(dmmln)_4(H_2O)_2]\cdot 4H_2O$	μ_2-Oc	1D	γ + H	130
$[(UO_2)_5(cit)_2(cb6)(NO_3)_2(H_2O)_6]\cdot 7H_2O$	μ_2-Oc	3D	α + P	33

* Chemical nature of the inter-polyhedra bridge

**- with greek small letters (α, β, γ) there have been noted the type of dimeric unit as it is presented in Figure I.3.14 and with capital latin letters the type of monomeric units as described in Figure I.3.2

Trinuclear type uranyl carboxylate complexes

For this class, there are only 3 representatives (Table I.3.11) each of them exhibiting a different type of linkage between P type polyhedra (Figure I.3.16).

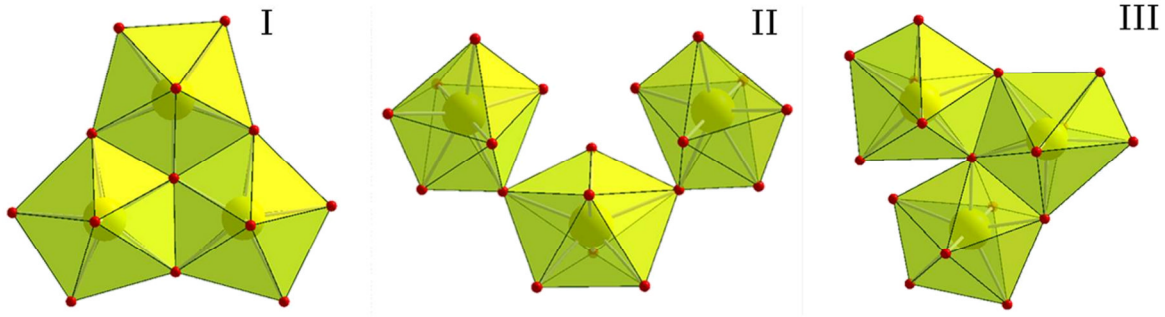

Figure I.3.16 Representation of the three types of trinuclear uranyl centered SBU I[183], II[139] and III[132].

The first compound crystallized with the formic acid as a ligand and the cucurbit[6]uril (cb6) as template, and presents the most condensed building unit.[183] Each of the uranyl-centered polyhedra shares two edges with the other two neighbors through one tri-coordinating, centered μ_3-oxo group and two other

external bi-coordinating μ_2-hydroxo groups, in order to create the three shared edges. The trinuclear unit has a total negative charge of two, being compensated by the potassium cations also present in the structure.

The second compound[139] has been synthesized using the methyl-phosphonoacetic acid as ligand. This structure has the less condensed SBU, since the three uranyl-centered polyhedra are linked by corner sharing mode only. The interesting fact about this structure is that there is no μ_2-oxo or μ_2-hydroxo bridge, the ligand's conformation being able to ensure the linkage (Oc) between the polyhedra. This is a very rare case where one oxygen atom belonging to a carboxylate group of the ligand is able to ensure a corner sharing linkage between the polyhedra.

Table I.3.11 list of trinuclear uranyl building blocks in carboxylate complexes.

Compound	CNB*	Pattern	Linkage type	Ref
$K_2[(UO_2)_2O(OH)_2(H_2O)_2(fa)_2]\cdot 2cb6\cdot 2dmf\cdot 4H_2O$	μ_3-O, μ_2-OH	0D	I	183
$(NH_4)_2[(UO_2)_3(mpaa)_2(Hmpaa)]\cdot 2H_2O$	μ_2-O_C	2D	II	139
$(Hdma)_2[(UO_2)_6O_2(OH)_4(pml)_2(Hpml)_2(H_2O)]\cdot 2cb6\cdot 8H_2O$	μ_3-O, μ_2-OH	1D	III	132

* Chemical nature of the inter-polyhedra bridge

The structure of the third compound[132] has the SBU's compactness somewhere in between the first two cases. The complex has been created using the pimelic acid as ligand, cb6 as organic template and dimethylamine as pH moderator. The SBU is formed by one pentagonal bipyramid sharing in the equatorial plane two edges with two neighboring polyhedra, each of the two also sharing a corner to each other. The edges are formed by a central μ_3-oxo group and two external μ_2-hydroxo groups. The coordination sphere is completed by the ligand's carboxylate coordinating groups.

Tetranuclear and hexanuclear type uranyl carboxylate complexes

An important group of compounds is described from tetranuclear SBUs. Although there are many cases of tetrameric units reported in literature, there have been found only five types for the restrained class of uranyl carboxylates

(Figure I.3.17), for which the most common and frequently encountered is the type (i). From the 26 tetrameric studied complexes (Table I.3.12) 14 possess this type of coordination. The (i) type SBU is formed by four pentagonal bipyramids, two of them sharing two edges and one corner with the adjacent neighbors and the other two having one edge and one corner in common with the first two. Because all the connection nodes between the polyhedra take place in the equatorial plane and all of the bipyramids share at least one edge, all four uranium atoms are nearly coplanar. Regardless the existence of planar SBU, the compounds of this type may exhibit different dimensionalities. The decisive factor in this matter is the geometry of the ligand. The next type of SBU, following the number of members, is the (ii) type, having three representatives[184]. All 3 compounds contain the same phthalic acid as ligand and have similar structures, but differing by the nature of counter-cation. The structures are zero-dimensional and have the SBU formed by two type P polyhedra and two H type. The hexagonal ones share three edges, two with the P polyhedra and one with the other H type, each the pentagonal units sharing two edges, both with the H type ones.

An even smaller group of tetramers possess the (iii) type tetrameric unit. The two compounds[126] are closely related having same ligand (suberic acid), and the same 2D dimensionality, the structural difference being made by the nature of the utilized organic template (4,4'-ethylenedipyridine and 4,4'-dipyridine). The SBU unit of these compounds resembles with the (ii) type, and differs by the replacement of the P type polyhedra with the H type ones and vice versa.

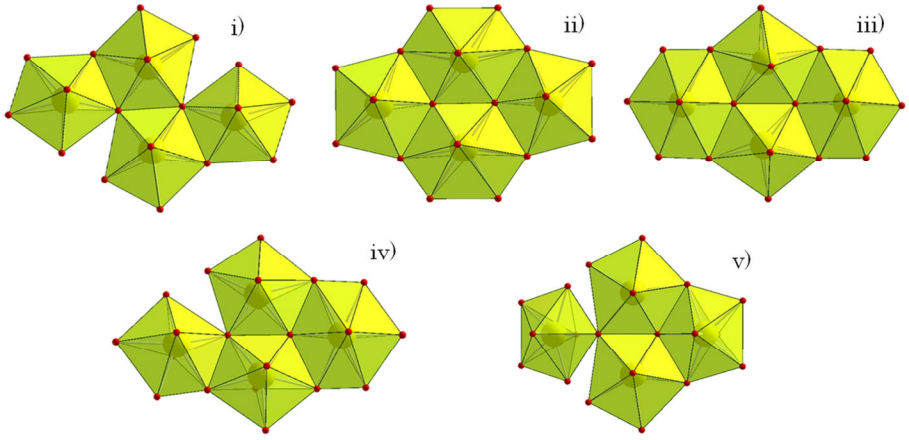

Figure I.3.17 Representation of the five connection modes of tetranuclear uranyl SBU in carboxylate complexes.

Only one compound from the tetramers list has the (iv) type SBU[126]. It has been synthesized using the pimelic acid ligand and has the same 2D dimensionality as the previous structures, probably due to the same type of dipyridine organic template used in all three cases. The tetrameric unit is formed from three pentagonal bipyramids and one hexagonal bipyramid. It seems to be a combination of type (iii) and type (i) units, by replacing in (iii) one H polyhedra with a P one.

Interesting cases are the ones of mixed tetramer - monomer or tetramer - dimer SBUs. There have been found four tetramer-dimer cases, all having H type uranyl-centered polyhedra combined with different types of tetrameric units. In one case, the tetrameric unit is a type (v) one[83]. This SBU is formed by four pentagonal bipyramids, three of them interconnected by edge sharing mode and the fourth being corner linked. The fourth uranium atom has a deviation from the other three's plane which together with the complexity of the trimellitic acid used as ligand gives the tridimensional structure of this compound. Also there has been reported a case of mixed (i) type tetramer with an (α) type dimer[181]. The structure is zero-dimensional and contains both deprotonated and protonated forms of methanol, acetic acid and hydroxy-di-(2-pyridyl)methoxide as linkers.

Table I.3.12 Tetranuclear uranyl units in carboxylate complexes.

Compound	CNB*	Pattern	Linkage type**	Ref
$(Hdma)_2[(UO_2)_4O_2(tma)_2]\cdot H_2O$	μ_3-O, μ_2-Oc	3D	i	83
$(dma)_2[(UO_2)_4O_2(adp)_3]\cdot cb8\cdot 8H_2O$	μ_3-O, μ_2-Oc	2D	i	132
$Ca_2[(UO_2)_8O_4(sbr)_6(H_2O)]\cdot 13H_2O\cdot cb6\cdot dmf$	μ_3-O, μ_2-Oc	2D	i	132
$[(UO_2)_2O(ac)_2(dmso)_2]$	μ_3-O, μ_2-Oc	0D	i	185
$[(UO_2)_4(azl)_2O_2(H_2O)_2(pdpy)]$	μ_3-O, μ_2-Oc	1D	i	126
$(H_2dmae)_2[(UO_2)_4O_2(ac)_4(dmae)_2]$	μ_3-O, μ_2-Oc	0D	i	186
$Sr_2[(UO_2)_8O_4(sbc)_6]\cdot 8H_2O\cdot cb6\cdot 2dmf$	μ_3-O, μ_2-Oc	2D	i	132
$(Hdma)_2[(UO_2)_2(paba)_2O(OH)(H_2O)]_2\cdot cb6\cdot 15H_2O$	μ_3-O, μ_2-OH	0D	i	70

Compound	CNB*	Pattern	Linkage type**	Ref
$(Hdma)_2[(UO_2)_2(mpaba)_2O(OH)(H_2O)]_2 \cdot cb6 \cdot 17H_2O$	μ_3-O, μ_2-OH	0D	i	70
$(Hdma)_2[(UO_2)_4O_2(OH)_2(sbr)_2(cb6)] \cdot 8H_2O$	μ_3-O, μ_2-OH	2D	i	132
$(Hdma)_2[(UO_2)_4O_2(OH)_2(azl)_2(cb6)] \cdot 5H_2O$	μ_3-O, μ_2-OH	2D	i	132
$(Hdma)_2[(UO_2)_4O_2(OH)_2(azl)_2(cb6)] \cdot 8H_2O$	μ_3-O, μ_2-OH	3D	i	132
$K_2[(UO_2)_4(ac)_2(ox)(HO)_2O_2(H_2O)_2] \cdot 2H_2O$	μ_3-O, μ_2-OH	1D	i	187
$[(UO_2)_4(Hpmb)_2(pmb)(OH)_2O_2(H_2O)_4]_2$- $\cdot 4cb6 \cdot cb8 \cdot Hpmb \cdot NO_3 \cdot 20H_2O$	μ_3-O, μ_2-OH	0D	i	70
$K_4[(UO_2)_4O_2(pht)_4] \cdot 3H_2O$	μ_3-O, μ_2-Oc	0D	ii	184
$Cs_4[(UO_2)_4O_2(pht)_4] \cdot 3H_2O$	μ_3-O, μ_2-Oc	0D	ii	184
$(NH_4)_4[(UO_2)_4O_2(pht)_4] \cdot 3H_2O$	μ_3-O, μ_2-Oc	0D	ii	184
$[(UO_2)_2O(sbr)(edpy)_2]$	μ_3-O, μ_2-Oc	2D	iii	126
$[(UO_2)_2O(sbr)(H_2O)(pdpy)]$	μ_3-O, μ_2-Oc	2D	iii	126
$[(UO_2)_4(pml)_2O_2(H_2O)_2(pdpy)] \cdot H_2O$	μ_3-O, μ_2-Oc	2D	iv	126
$Sr_2[(UO_2)_6O_2(sbr)_6] \cdot 9H_2O \cdot cb6 \cdot 3dmf$	μ_3-O, μ_2-Oc	2D	i + H	132
$(NH_4)_2[(UO_2)_5O_2(ac)_8]$	μ_3-O, μ_2-Oc	1D	ii + H	57
$[(UO_2)_5O_2(sbc)_3(edpy)_2(H_2O)_2]$	μ_3-O, μ_2-Oc	3D	iii + H	128
$[(UO_2)_6(HO)_2(tma)_2(Htma)_2(H_2O)_2] \cdot 6H_2O$	μ_3-OH, μ_2-Oc	3D	v + H	83
$[(UO_2)_6(hpm)_4O_2(ac)_2(moh)_2(Hmoh)_2] \cdot H_2O$	μ_3-O, μ_2-Oc, μ_2-Oc	0D	i + α	181

* - Chemical Nature of the inter-polyhedra Bridge

** - with small latin digits (i, ii, iii) have been marked the tetranuclear SBUs as shown in Figure I.3.17; with capital latin letters (T, P, H) have been marked the monomeric SBUs as shown in Figure I.3.2 and with small greek letters(α, ß, γ) have been marked the dinuclear units, as shown in Figure I.3.14

The most uncommon uranyl carboxylate with tetrameric motif is based on the oxalate linker, having the formula $[(UO_2)_2(ox)(OH)_2(H_2O)_2] \cdot H_2O$[173]. The SBU of this complex is formed by four P type polyhedra interconnected by corner sharing in order to form a four-member cycle, without any edge-sharing

connection (Figure I.3.18). The corner sharing interactions take place through μ2-hydroxo bridges; each tetrameric unit is connected to four others through the ligand's molecule and the coordination sphere is completed by one coordinating water molecule for each uranium atom.

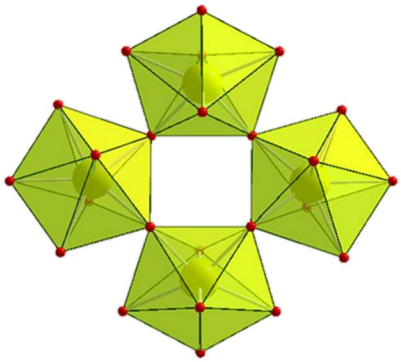

Figure I.3.18 A unique case of tetranuclear SBU in uranyl oxalate $[(UO_2)_2(ox)(OH)_2(H_2O)_2]\cdot H_2O$[173].

There have not been found any pentanuclear SBUs for the class of uranyl carboxylates, but the largest reported discrete motif is a hexanuclear one (Figure I.3.19). This complex, with formula $[(UO_2)_3(HO)_2O(cm)(H_2O)_2]\cdot nH_2O$[188] has been synthesized using as ligand the cinchomeronic acid and has the SBU formed by six interconnected pentagonal bipyramids. Each SBU is connected through the ligand with four others in order to form a bidimensional structure.

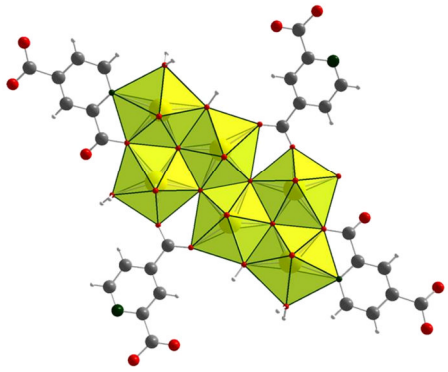

Figure I.3.19 Representation of a hexanuclear uranyl-centered SBU, the largest one, so far reported [188].

Infinite polynuclear motifs in uranyl carboxylate complexes

In the field of purely inorganic chemistry, the class of extended networks from condensed SBUs is very rich (oxides, silicates, phosphates…), but in the

case of uranyl carboxylates field, there are only 22 representatives (Table I.3.13). They are all described as infinite ribbons of corner- or edge-sharing uranyl centered polyhedra and are represented in Figure I.3.20

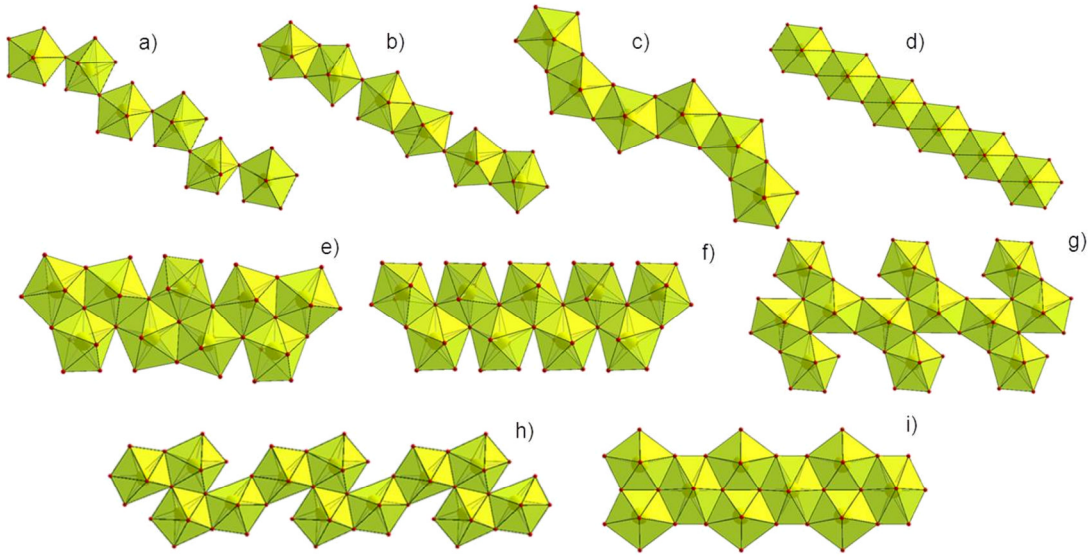

Figure I.3.20 Types of infinite ribbons of uranyl centered polyhedra encountered in the field of uranyl carboxylates.

A first type of infinite SBU (Figure I.3.20-a) is formed by pentagonal bipyramids, interconnected to each other by corner sharing in order to form a continuous simple *trans* chain. The linkage between the polyhedra is ensured by μ_2-hydroxo groups. There have been found 3 complexes having this type of SBU. [105, 128, 173] All three being bidimensional, the chains being interconnected through the different used ligands.

Only one complex is reported with the second type of SBU showing an alternation of edge- and corner-sharing connection sequence (Figure I.3.20-b)[189]. It has been synthesized using the acetic acid and the structure contains Na^+ as counter cation. The SBU can be viewed as type α dimeric units with corner sharing interconnection in order to form an infinite chain of type P polyhedra. The structure is 1D and the polymeric chains are kept together only by ionic interactions.

The third type of continuous polymeric SBUs (Figure I.3.20-c) is also an infinite simple chain of interconnected P type polyhedra, but this time all of bipyramids are edge sharing interconnected in the 1-3 position, resulting in a sinusoidal chain. From the 3 compounds[47, 190] possessing this type of SBU, two

are isostructures and have the chains interconnected through the organic ligands, generating bidimensional network and the third has the chains free, generating unidimensional expansion.

There is only one case of infinite interconnected H type bipyramids (Figure I.3.20-d). Here the linkage takes place by edge-sharing in *trans* connection fashion resulting in a straight chain, which is encountered in two compounds[170]. For both phases the linkage is ensured by the ligands bonding the uranyl polyhedra within the chains but also between the chains, thus generating 2D structures.

The last type of simple chain contains interconnected type P polyhedra SBU (Figure I.3.20-h) and resembles with the (g) type. All the polyhedra are edge sharing interconnected and the infinite ribbon can be viewed as the connection of linear four uranyl blocks, which are linked *via* edge-sharing to each other with the external polyhedra in position 1-4. For (g), the connection occurs *via* the polyhedra in position 2-3. The only compound possessing this type of SBU has been synthesized using the dipicolinic acid as ligand[100]; the bridges between the polyhedra are ensured by the carboxylate groups of the ligand and by μ_3-oxo groups. There is no chemical interconnection between the chains, the dimensionality of the structure being one.

The double chains of P type polyhedra are more commonly encountered. There are three types of this SBU (Figure I.3.20-e, -f, -g), from which the (e) type is the most frequently found.

Table I.3.13 Infinite polynuclear uranyl chains in carboxylate complexes.

Compound	CNB*	Pattern	Linkage type**	Ref
$[(UO_2)_2(sbc)(HO)_2(edpy)]$	μ_2-OH	2D	a	128
$[UO_2(OH)(poa)]$	μ_2-OH	2D	a	105
$[(UO_2)_2(ox)(OH)_2(H_2O)_2]$	μ_2-OH	2D	a	173
$Na[(UO_2)_2(ac)_2(OH)_3]$	μ_2-OH	1D	b	189
$K_2[(UO_2)_2(fa)(OH)_4]_2{\cdot}7H_2O{\cdot}cb5$	μ_2-OH	2D	c	190
$Cs_2[(UO_2)_2(fa)(OH)_4]_2{\cdot}5H_2O{\cdot}cb5$	μ_2-OH	2D	c	190
$[UO_2F_2(Hgpi)]$	μ_2-F	1D	c	47
$[UO_2(sbr)]$	μ_2-Oc	2D	d	170
$[UO_2(azl)]$	μ_2-Oc	2D	d	170

Compound	CNB*	Pattern	Linkage type**	Ref
$[(UO_2)_6O_2(OH)_4(Hcm)_2(cm)]$	μ_3-O, μ_3-OH, μ_2-Oc	2D	e	188
$K[(UO_2)_3(OH)_4(pnba)_2]OH$	μ_3-OH, μ_2-OH	1D	e	191
$Na_3[(UO_2)_{12}O_4(OH)_{12}(fa)_7(H_2O)_2]\cdot 16H_2O\cdot 2cb6$	μ_3-O, μ_3-OH, μ_2-OH	1D	e	183
$(H_3O)[(UO_2)_3(Hnic)_2O(OH)_3]$	μ_3-O, μ_3-OH, μ_2-OH	1D	e	85
$[(UO_2)_6(glt)_3O_2(HO)_4]\cdot edpy\cdot 9H_2O$*	μ_3-O, μ_3-OH, μ_2-Oc	2D	e	128
$K[(UO_2)_3O(pnba)_2(OH)_3](H_2O)$	μ_3-O, μ_3-OH, μ_2-OH	1D	e	192
$(Hdabco)[(UO_2)_3(HO)_3O(fa)_2]\cdot 4H_2O$	μ_3-O, μ_3-OH, μ_2-OH	1D	e	134
$[(UO_2)_2(OH)_2(pypa)_2]$	μ_3-OH	1D	f	94
$(teea)_2[(UO_2)_4O_2(ox)(haa)_2]$	μ_3-O, μ_2-Oc	2D	g	193
$[(UO_2)_2(dpi)O(H_2O)]$	μ_3-O, μ_2-Oc	1D	h	100
$[(UO_2)_3(ac)_2O_2(H_2O)_2]$	μ_3-O, μ_2-Oc	1D	i	194

* - Chemical nature of the inter-polyhedra bridge

** - with small latin letters (a, b, c) have been marked the infinite polynuclear SBUs as shown in Figure I.3.20

The dimensionality of the structures containing this type of SBU varies from one to two, depending on the presence of inter-chain chemical interactions.

One interesting infinite ribbon is the (i) type, being formed by alternating dimeric units of P polyhedra with hexagonal bipyramidal (H) monomeric units. There is only one compound containing this type of SBU. It's being synthesized using acetic acid and the linkage between the polyhedra is ensured by the ligand and by μ_3-oxo groups in the center of the chain. The low dimensionality of the structure is due to the lack of interactions between the chains.

A case of uranyl carboxylate possessing unique SBU has been reported in the compound, with formula $[(UO_2)_2F_4(gpi)]\cdot H_2O$[47]. It presents an infinite layered

SBU, defining the dimensionality of the structure (Figure I.3.21). In this case the SBU is being formed by parallel infinite type (a) chains (Figure I.3.20) of polyhedra interconnected by type (α) dimeric unit (Figure I.3.14) through corner sharing linkage. The links between the polyhedra are ensured by μ_2-fluoride anions and the rest of the coordination sphere is completed by the carboxylate groups of the isonicotinic acid used as ligand[47].

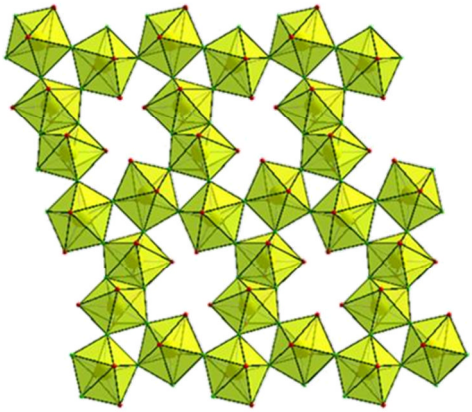

Figure I.3.21 A rare case of 2D inorganic layer bearing uranyl centers[47].

Rare cases of cation-cation interaction occurring in uranyl carboxylates

The main characteristics of the uranyl ion (UO_2^{2+}) are the short uranyl (U=O) bond lengths defined by the O=U=O linear geometry, the chemical inertia of the uranyl type oxygen atoms and the restricted position of the co-ligands to an equatorial plane perpendicular to the uranyl direction. Perturbations of this geometry are usually small, and do require special conditions, such as the presence of bulky ligand, which are not so frequently reported. One of these perturbations is the so-called Cation-Cation Interaction (CCI). This type of bonding is more common to the U(V) oxidation state but examples of compounds possessing U(VI) involved in a CCI also exist. The cation-cation interaction appears whenever an uranyl type oxygen atom becomes chemically active and also coordinates in the equatorial plane another uranyl ion. Another type of perturbation in the uranyl coordination sphere is the uranyl-heterocation interaction. It resembles with the CCI, the uranyl oxygen atom involved in this bonding coordinating this time not another uranyl ion but a heteroatom (usually an alkaline atom, copper…).

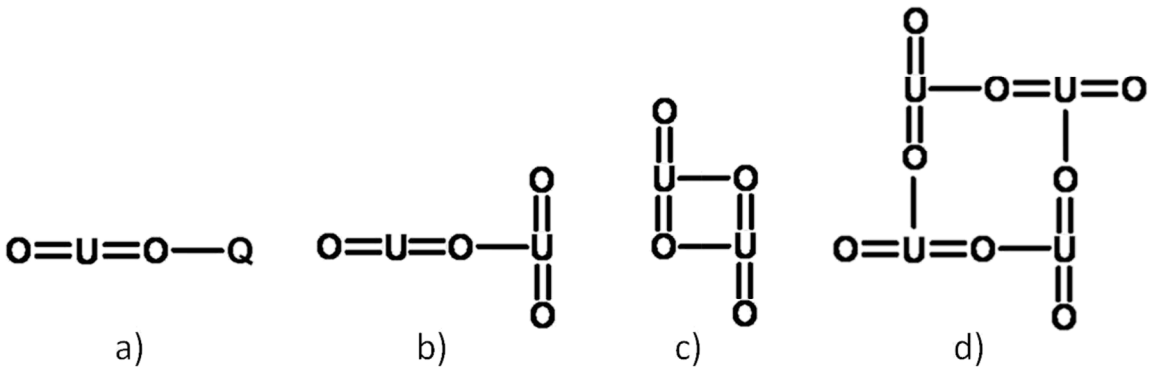

Figure I.3.22 Diagram of uranium-cation interaction a)[14, 155, 157, 195] and uranium cation-cation interaction: *T*-shaped model b)[196, 197], parallel model c)[198] and square model d)[198]

The uranyl-cation interaction with alkaline metals (Figure I.3.22-a) is more commonly encountered in the U(VI) chemistry, lesser being the cases of uranyl (VI) cation-cation interaction, appearing only as *T*-shaped models (Figure I.3.22-b). The other two models of CCI (Figure I.3.22-c, -d) are specific to the U(V) compounds.

In the field of uranyl carboxylates, two compounds have been reported in literature so far. A first complex[199] has the formula $[(UO_2)_2(ontp)_2(H_2O)]$ (Figure I.3.23) and exhibits a tri-dimensional structure. This dimensionality is ensured by two factors: the conformation adopted by the ligand, the two carboxylate groups forming a torsion angle of 81.637(3)°between each other; and the CCI between the two uranyl centers forming the dimeric SBU. Both uranyl centers are type P polyhedra. The coordination sphere is ensured completely by the carboxylate groups of the ligand for the first and by the uranyl type oxygen atom from the first uranyl, one coordinating water molecule and three bidentate bridging carboxylate groups of the ligand for the second (figure I.2.23).

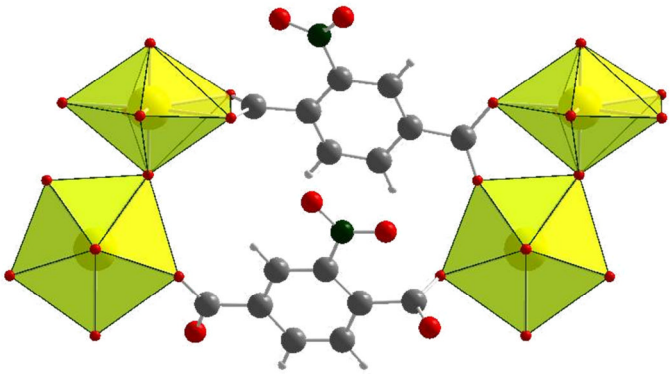

Figure I.3.23 Representation of complex $[(UO_2)_2(ontp)_2(H_2O)]$. A rare case of tridimensional framework possessing dinuclear SBU involving CCI.

The second complex, having the formula $[(UO_2)_4O(OH)_2(H_2O)_2(cit)]\cdot 2H_2O$ exhibits a 2D SBU being formed by parallel type (f) infinite double chains (Figure I.3.20) interconnected by type (d) tetrameric units (Figure I.3.17) through corner sharing cation-cation interactions (Figure I.3.24). The structure expansion to the third dimension is ensured by the citrate linker.[197]

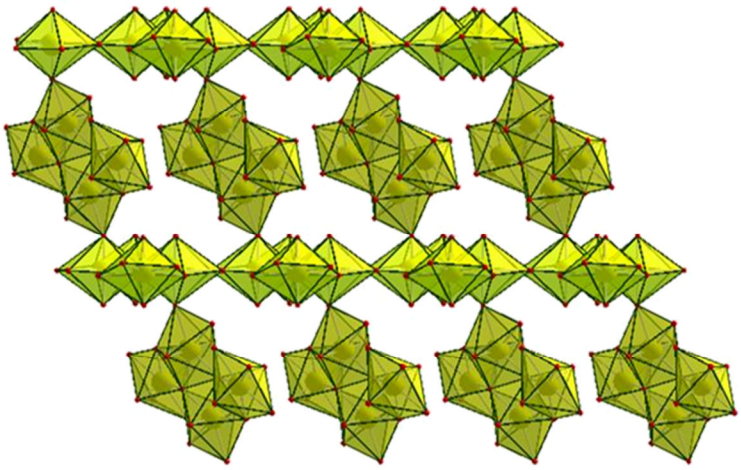

Figure I.3.24 A unique case of 3D UOF exhibiting unusual cation - cation interactions[197].

Mixed uranyl – lanthanide (III) carboxylate complexes

In this thesis work, it has been also attempted the synthesis of heterometallic uranyl-lanthanide carboxylates. Beside the general interest of lanthanides for their optical properties, the *4f* elements could also be used as surrogate simulating the chemical reactivity of the highly radiotoxic actinides such as plutonium or other minor actinides (americium, curium…). In this context, the chemical combination of some lanthanides (cerium, neodymium…) with uranium could be of great interest for the understanding of the crystal chemistry involving 4f-5f metals.

In this field very few structural data are presented in literature and most of the reported complexes are obtained using organic ligands with different functionalities, where the lanthanide ion may interact with the N-donor organic functions and the uranyl ion is preferentially bound by the O-donor groups.

Because of the reduced number of mixed uranyl-lanthanide carboxylates and the complexity of these types of structures, the data of these phases will not

be structured in tables as previously but will be discussed separately. Only 7 structural types of complexes have been isolated up to now.

$[(UO_2)_2Ln(dota)(ox)(OH)(H_2O)]\cdot 3H_2O$ (**A**) compounds (Figure I.3.25), where Ln = Gd or Eu, are formed by infinite chains of dinuclear μ_2-hydroxo corner shared uranyl units bridged by oxalate ligand. The chains are interconnected by the second ligand (dota) in order to construct the final layered edifice. The isolated lanthanide cation (nine-fold coordination) is trapped inside the ligand cycle and is also coordinated by the oxygen atom of one water molecule[200].

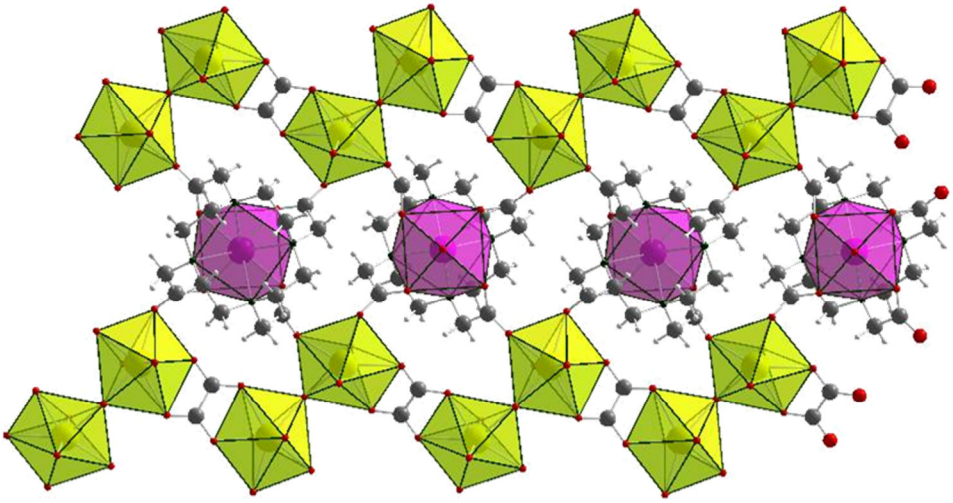

Figure I.3.25 Structure representation of the complex **A** $[(UO_2)_2Ln(dota)(ox)(OH)(H_2O)]\cdot 3H_2O$.

In the same oxalate-dota system, the $[(UO_2)_2Gd(dota)(ox)(OH)]\cdot H_2O$ (**B**) complex has been isolated. The differences between this phase and **A** are the number of hydration water molecules and the coordination number of the lanthanide atoms; the coordinating water molecule from the previous case does not exist, decreasing the coordination number of Gd to eight.

As in the two previous complexes also in the case of $[(UO_2)_2Ln(dota)_2(ox)]$ (**C**), where Ln = Sm or Eu, the lanthanide atom is fully coordinated by the ligand (Figure I.3.26). In this case two pentacoordinated uranyl ions bridged by one oxalate ligand are also coordinated monodentate by six dota molecules. Each macrocycle is coordinating monodentate one lanthanide belonging to a second macrocycle, forming the complex 3D edifice.

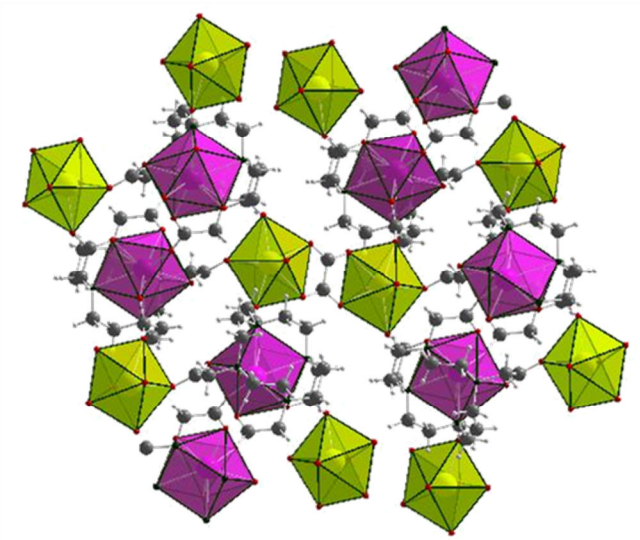

Figure I.3.26 Structure representation of complex **C** $[(UO_2)_2Ln(dota)_2(ox)]$.

The last term in the oxalate-dota series is $[(UO_2)_4Gd_2(dota)_2(ox)_3(H_2O)_6]\cdot 2H_2O$ (**D**). The dimensionality of this structure is only two, due to the lack of interaction between the macrocycles. Each dota ligand coordinates one Gd and two uranyl cations[201]. (Figure I.3.27)

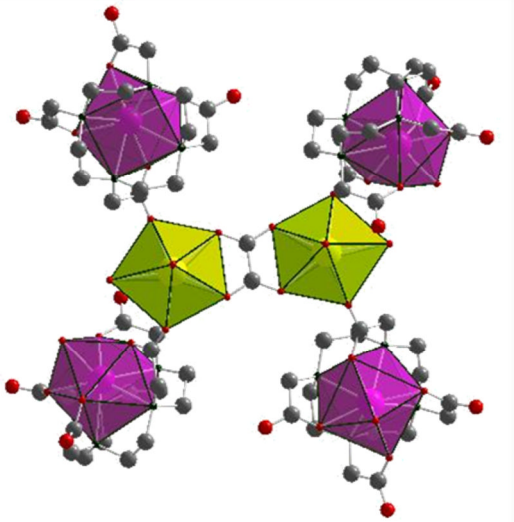

Figure I.3.27 Structure representation of complex **D** $[(UO_2)_4Gd_2(dota)_2(ox)_3(H_2O)_6]\cdot 2H_2O$.

With another ligand involving combination of phosphonate and acetate functionalities, the $[(UO_2)_2(paa)(Hpaa)_2Sm(H_2O)]\cdot 2H_2O$ (**E**) complex has been very recently reported. The structure of this compound possesses infinite chains as secondary building blocks composed of intercalated dimeric penta- and hexa-coordinated uranyl units edge-sharing monomeric octa-coordinated Sm units (Figure I.3.28). The polynuclear chains are bound by the pentadentate ligand in order to create the final 2D structure[202]. Here the uranyl cations are linked to the samarium atoms via tridentate phosphonate groups belonging to the ligand.

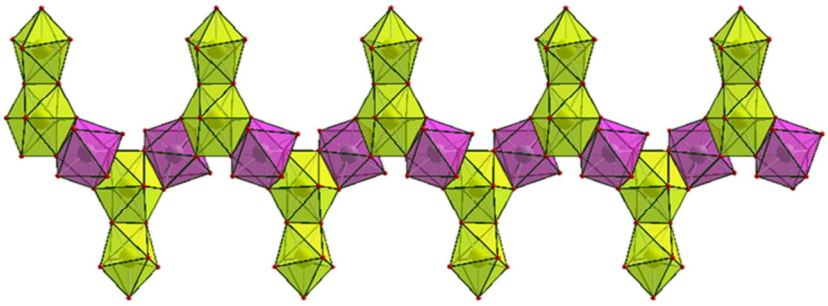

Figure I.3.28 Complex's **E** $[(UO_2)_2(paa)(Hpaa)_2Sm(H_2O)]\cdot 2H_2O$ SBU structural representation (for clarity the ligand's molecules have been removed).

Another molecular complex $[La_2(ppi)_4(H_2O)_6][UO_2(ppi)_3UO_2(ppi)_{2.5}(ac)_{0.5}]$ (**F**) possesses discrete type H monomeric units as inorganic building units (Figure I.3.29 (left), surrounding the infinite chains formed by edge sharing between lanthanum polyhedra (Figure I.3.29 right). The uranyl ion is coordinated in the equatorial plane by acetate and propionate ligands, each of the ligands chelating the metal. The lanthanum cation is coordinated only by the propionate ligand and by coordinating water molecule. In this case the ligand ensures the bridge between the lanthanum polyhedra by a μ_3-η_1:η_1:η_2 coordination configuration[203].

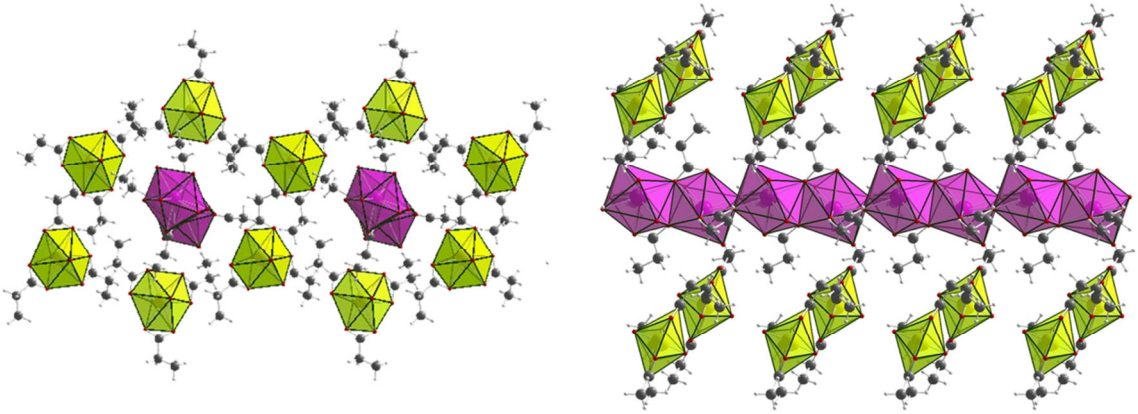

Figure I.3.29 Structure representation of complex **F** $[La_2(ppi)_4(H_2O)_6][UO_2(ppi)_3$-$UO_2(ppi)_{2.5}(ac)_{0.5}]$[203] view along the [100] (left) and [010] (right) directions.

The $[(UO_2)Ln(Hhmel)(H_2O)_7]\cdot H_2O$[204] (**G**) (where Ln = Pr, Eu, Tb and Er) coordination polymer (Figure I.3.30) exhibits two distinct crystallographic sites for the metal atoms. First belongs to the uranium atom which is eight-fold coordinated and possesses a typical hexagonal bipyramidal shaped polyhedron. In the equatorial plane, this polyhedron is exclusively coordinated by the carboxylate arms of the ligand. The second site belongs to the lanthanide atom which is nine-fold coordinated; twice by carboxyl oxygen atoms and seven times

by aquo type oxygen atoms belonging to coordinating water molecules. The organic ligand (hexahydromellitic acid) interlinks the metal-centered polyhedra into a bidimensional edifice developing in the [011] plane and presenting a pavement in which inorganic and organic rows are alternating along the [001] direction and uranyl/lanthanide polyhedra are alternating along the [010] axis. Only one free water molecule per formula unit is present intercalated between the polymer layers.

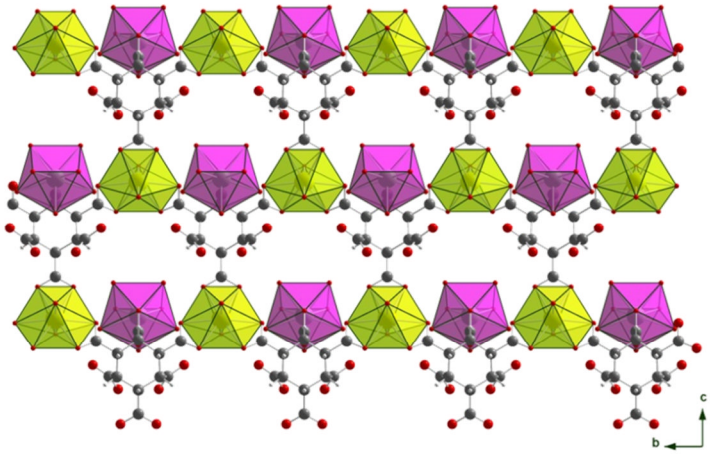

Figure I.3.30 Structure representation of complex **G** $[(UO_2)Ln(Hhmel)(H_2O)_7]\cdot H_2O$[204]. View along the [100] direction.

The complex $[(UO_2)_2Ln(OH)(H_2O)_3(mel)]_2\cdot 5H_2O$[86] (**H**) (where Ln = Nd or Ce) has been described by our group, using the mellitic acid (1,2,3,4,5,6-benzenehexacarboxylic acid) as ligand. The obtained mixed complex possesses as SBUs one T type uranyl monomeric unit and a discrete heteronuclear U(VI)/Ln(III) dimeric unit (Figure I.3.31. left).

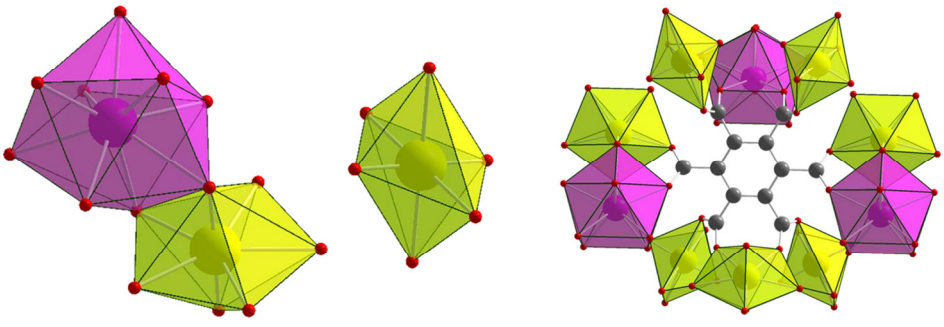

Figure I.3.31 Structural representation of the complex **H** $[(UO_2)_2Ln(OH)(H_2O)_3(mel)]_2\cdot 5H_2O$[86]: the two types of SBU (left) and the ligand coordination μ_{10} configuration (right)

The dimeric unit is formed by the condensation of a type P uranyl polyhedron with a nine-fold coordinated lanthanide center. The link between the

two polyhedra is an edge sharing type and is ensured by a hydroxo group and one uranyl type oxygen atom. This atom also involves the uranium atom in a uranyl-cation interaction making this complex the first reported in literature possessing a uranyl/lanthanide heterometallic CCI and the second possessing an edge sharing CCI. The two SBUs are interconnected by the numerous μ_2-bridging carboxylate groups of the ligand in order to create the final 3D edifice (Figure I.3.31).

In the next chapters of this thesis there will be discussed the properties of the obtained complexes. The structuring of the next three chapters will be based on the utilized ligands (Figure I.3.32). Chapter II will describe the work conducted on the phthalate complexes; chapter III will describe uranyl isophthalates and chapter IV will be focused on the pyromellitate system. Chapter V will concern the family of carboxylates containing six-fold coordinated uranium and chapter VI will describe a family of mixed uranyl / lanthanide carboxylates.

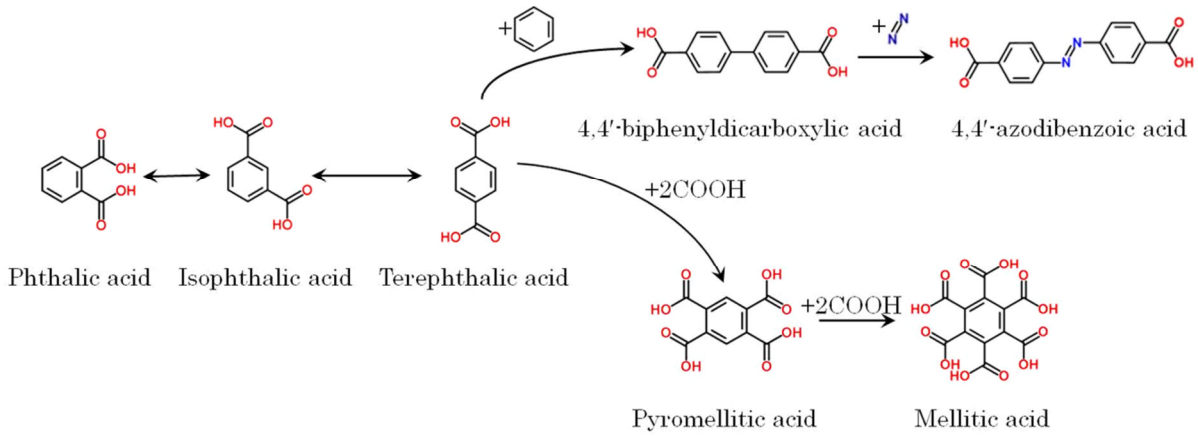

Figure I.3.32 Aromatic di- and policarboxylic acids used in the synthesis of the coordination polymers presented in this thesis work

Abbreviations list:

15c5 - 15-crown-5;
18c6 - 18-crown-6;
acr - acridine;
apy - antipyrine, 1,5-dimethyl-2-phenyl-1,2-dihydro-3H-pyrazol-3-one;
cb5 - cucurbit[5]uril;
cb6 - cucurbit[6]uril;
cb7 - cucurbit[7]uril;
cb8 - cucurbit[8]uril;
cry - 2,2,2-cryptand, 4,7,13,16,21,24-hexaoxa-1,10-diazabicyclo[8.8.8]hexacosane;
dabco - 1,4-diazabicyclo[2.2.2]octane;
dcm - dichloromethane;
dea - diethylamine;
deda - diethylethylenediamine, N,N'-diethyl-1,2-ethanediamine;
diea - diisopropylethylamine, N-ethyl-N-isopropyl-2-propanamine;
dma - dimethylamine;
dmac - N,N-dimethylacetamide;
dmap - N,N-dimethyl-2-aminopyridine;
dmeda - N,N'-dimethylethylenediamine;
dmf - N,N-dimethylformamide;
dmh - N,N-dimethylhydroxylamine;
dmppz - 1,2-dimethylpiperazine;
dmso - dimethylsulfoxide;
dmu - N,N-dimethylurea;
dox - dioxane;
eda - ethylenediamine;
edpy - 4,4'-ethylenedipyridine;
eg - ethylene glycol;
eotp - (2-ethoxy-2-oxoethyl)(triphenyl)phosphonium;
etdpy - 1,2-bis(4-pyridyl)ethane;
EtOH - ethanol;
gua - guanidine;
H_2act - acetylenedicarboxylic acid;
H_2adc - 4,4'-azobenzenedicarboxylic acid;
H_2adp - adipic acid, butane-1,4-dicarboxylic acid;
H_2azl - azelaic acid, heptanes-1,7-dicarboxylic acid;
H_2bndc - (R,S)-1,1'-binaphthalene-2,2'-dicarboxylic acid;
H_2boda -1,2-phenylenedioxydiacetic acid, 2,2'-[1,2-phenylenebis(oxy)]diacetic acid;
H_2bpd - 4,4'-biphenyldicarboxylic acid;
H_2cbdc - 1,1-cyclobutanedicarboxylic acid;
H_2chdc - 1,3-cyclohexanedicarboxylic acid;
H_2cm - cinchomeronic acid, pyridine-3,4-dicarboxylic acid;
H_2cmpr - camphoric acid, 1,2,2-trimethylcyclopentane-1,3-dicarboxylic acid;
H_2dda - (R,S)-1,1'-biphenyl-6,6'-dinitro-2,2'-dicarboxylic acid;
H_2demln - diethylmalonic acid, pentane-3,3-dicarboxylic acid;
H_2dmmln - dimethylmalonic acid, propane-2,2-dicarboxylic acid;
H_2dpi - dipicolinic acid, pyridine-2,6-dicarboxylic acid;
H_2fmr - fumaric acid, trans-1,2-ethenedicarboxylic acid;
H_2glt - glutaric acid, propane-1,3-dicarboxylic acid;
H_2haa - hydroxiacetic acid, glycolic acid;
H_2icm - isocinchomeronic acid, pyridine-2,5-dicarboxylic acid;
H_2ida - diglycine, 2,2'-iminodiacetic acid;
H_2ipa - isophthalic acid, 1,3-benzenedicarboxylic acid;
H_2lti - lutidinic acid, pyridine-2,4-dicarboxylic acid;
H_2madc - adamantane-1,3-dicarboxylic acid;
H_2mddb - 3,3'-dithiodibenzoic acid;
H_2mln - malonic acid, methanedicarboxylic acid;

H_2mml - methylmalonic acid, ethylidenedicarboxylic acid;
H_2obtp - 2-bromoterephthalic acid, 2-bromo-1,4-benzenedicarboxylic acid;
H_2oda - diglicolic acid, 2,2'-oxydiacetic acid;
H_2odpydc - 2,2′-dipyridine-3,3′-dicarboxylic acid;
H_2onppc - 2,2'-dinitrobiphenyl-4,4'-dicarboxylic acid;
H_2ontp - 2-nitroterephthalic acid, 2-nitro-1,4-benzenedicarboxylic acid;
H_2ox - oxalic acid;
H_2pddb - 4,4'-dithiodibenzoic acid;
H_2pdmd - pyrazine-2,6-dicarboxylic acid;
H_2pdod - pyrazine-2,3-dicarboxylic acid;
H_2phndc - 1,10-Phenanthroline-2,9-dicarboxylic acid;
H_2phscc - phenylsuccinic acid, ethane-1-phenyl-1,2-dicarboxylic acid;
H_2pht - phthalic acid, 1,2-benzenedicarboxylic acid;
H_2pmdc - pyrazole-3,5-dicarboxylic acid;
H_2pml - pimelic acid, pentane-1,5-dicarboxylic acid;
H_2pndc - naphthalene-1,4-dicarboxylic acid;
H_2podb - 4,4'-oxydibenzoic acid;
H_2podc - pyrazole-4,5-dicarboxylic acid;
H_2ptpb - 1,1':4',1''-terphenyl-4,4''-dicarboxylic acid;
H_2pzdc - pyrazine-2,3-dicarboxylic acid;
H_2qui - quinolinic acid, pyridine-2,3-dicarboxylic acid;
H_2sbc - sebacic acid, octane-1,8-dicarboxylic acid;
H_2sbr - suberic acid, hexane-1,6-dicarboxylic acid;
H_2sq - squaric acid, 3,4-dihydroxy-3-cyclobutene-1,2-dione;
H_2suc - succinic acid, etane-1,2-dicarboxylic acid;
H_2ta - tartaric acid, 2,3-dihydroxybutanedioic acid;
H_2tpa - terephthalic acid, 1,4-benzenedicarboxylic acid;
H_3beica - 3,3',3''-((2,4,6-triethylbenzene-1,3,5-triyl)tris((1-oxoethane-2,1-diyl)imino)) tris(1,5,7-trimethyl-2,4-dioxo-3-azabicyclo[3.3.1]nonane-7-carboxylic acid;
H_3bta - benzene-1,3,5-triacetic acid;
H_3crm - citramalic acid, 2-hydroxy-2-methylbuthanedionic acid;
H_3hmm - hemimellitic acid, 1,2,3-benzenetricarboxylic acid;
H_3mpaa - methylphosphonoacetic acid, 2-phosphonopropanoic acid;
H_3nta - nitrilotriacetic acid;
H_3paa - phosphonoacetic acid;
H_3tma - trimellitic acid, 1,2, 4-benzenetricarboxylic acid;
H_3tms - trimesic acid, 1,3,5-benzenetricarboxylic acid;
H_3trc - tricarballylic acid, 1,2,3-propanetricarboxylic acid;
H_3ttpa - tris(2-carboxyethyl)isocyanuric acid;
H_4bota - bicyclo[2.2.2]oct-7-ene-2,3,5,6-tetracarboxylic acid;
H_4bpnt - benzophenone-3,3',4,4'-tetracarboxylic;
H_4bptc - 3,3',4,4'-biphenyltetracarboxylic acid;
H_4btca - 1,2,3,4-butanetetracarboxylic acid;
H_4btec - pyromellitic acid, 1,2,4,5-benzenetetracarboxylic acid;
H_4cbtc - 1,2,3,4-cyclobutanetetracarboxylic acid;
H_4cit - citric acid, 2-hydroxy-1,2,3-propanetricarboxylic acid;
H_4dcta - 1,2-diaminocyclohexane-N,N,N',N'-tetraacetic acid;
H_4dota - 1,7-diazonia-4,10-diazacyclododecane-N,N',N'',N'''-tetraacetic acid;
H_4pdtc - pyrazine-2,3,5,6-tetracarboxylic acid;
H_4teta - 1,4,8,11-tetraazacyclotetradecane-1,4,8,11-tetraacetic acid;
H_6mel - mellitic acid (1,2,3,4,5,6-benzenehexacarboxylic acid)
H_6hmel - 1,2,3,4,5,6-cyclohexanexexacarboxylic acid (hexahydromellitic acid)
Hac - acetic acid;
Hahba - 3-amino-5-hydroxybenzoic acid;
Hanca - 9-anthracenecarboxylic acid;
Hapa - pyromucic acid, 2-furoic acid, furan-2-carboxylic acid;
Harg - arginine, 2-amino-5-carbamimidamidopentanoic acid;
Hbeo - crotonic acid, 2-butenoic acid;

Hbox - benzoic acid;
Hbua - butyric acid;
Hcpym - pyrimidine-2-carboxylic acid;
Hdmae - 2-hydroxyethyldimethylamine;
Hdmb - 2,6- dimethoxybenzoic acid;
Heta - ethoxyacetic acid;
Hfa - formic acid;
Hgaba - γ-aminobutyric acid, 4-aminobutanoic acid;
Hgly - aminoacetic acid, glycine;
Hgpi - isonicotinic acid, γ-picolinic acid, pyridine-4-carboxylic acid;
Hgre - γ-resorcylic acid, 2,6-dihydroxybenzoic acid;
Hhmpa - acetonic acid, 2-hydroxy-2-methylpropanoic acid;
Hhpm - hydroxy-di-(2-pyridyl)methoxide;
Hisb - isobutyric acid, 2-methylpropanoic acid;
Hlac - lactic acid, 2-hydroxypropanoic acid;
Hmbba - 3-bromobenzoic acid;
Hmcod - pyridazine-3-carboxylic acid;
Hmcth - 5-chlorothiophene-2-carboxylic acid;
Hmeni - 5-ethylnicotinic acid, pyridine-5-ethyl-3-carboxylic acid;
Hmlm - malonamic acid, 3-amino-3-oxopropanoic acid;
Hmpaba - 3-methyl-4-aminobenzoic acid;
hmta - hexamethylenetetramine, 1,3,5,7-tetraazatricyclo[3.3.1.13,7]decane;
Hnic - nicotinic acid, pyridine-3-carboxylic acid;
Hoab - anthranilic acid, 2-aminobenzoic acid;
Hohb - salicylic acid, 2-hydroxybenzoic acid;
hpa - N-hydroxypropan-2-amine;
Hpaba - 4-aminobenzoic acid;
Hpamb - 4-(aminomethyl)benzoic acid;
Hpasa - 4-amino-salicylic acid;
Hpbba - 4-bromobenzoic acid;
Hpca - pyroglutamic acid, 2-pyrrolidone-5-carboxylic acid;
Hpcba - 4-chlorobenzoic acid;
Hpdab - 4-dimethylaminobenzoic acid;
Hpfb - pentafluorobenzoic acid;
Hpha - 2-phenylacetic acid;
Hphtob - 4,4''-dihydroxy-1,1':3',1''-terphenyl-2'-carboxylic acid;
Hpiba - 4-iodobenzoic acid;
Hpic - picolinic acid, pyridine-2-carboxylic acid;
Hpmb - 4-aminomethylbenzoic acid;
Hpmni - 6-methylnicotinic acid, pyridine-6-methyl-3-carboxylic acid;
Hpnba - 4-nitrobenzoic acid;
Hpoa - pyrazinoic acid, pyrazine-2-carboxylic acid;
Hppi - propionic acid;
Hptcp - 2-pyridin-4-yl-1,3-thiazole-4-carboxylic acid;
Hpyac - pyridine-2-acetic acid;
Hpypa - 3-pyridinepropanoic acid;
Hsbh - salicylidenebenzoylhydrazone;
Hscn - thiocyanic acid;
Htob - 2,6-biphenylbenzoic acid, [1,1':3',1'']terphenyl-2'-carboxylic acid;
hyd - hydrazine;
imd - imidazole;
lptz - lupetazine, N,N'-dimethyl-1,4-piperazine, N,N'-dimethyl-1,4-diazaciclohexane;
MeOH - methanol;
mz - 2-methylimidazole;
odpy - 2,2'-dipyridine;
pdpy - 4,4'-dipyridine;
phen - 1,10-phenanthroline;
ppz - piperazine, 1,4-diazaciclohexane;

py - pyridine;
pz - 2-phenylimidazole;
tea - triethylamine;
teda - N,N,N',N'-tetraethyl-1,2-ethanediamine;
teea - tetraethylammonium;
teeda - tetraethylethylenediamine;
tmeda - tetramethylethylenediamine, N,N,N',N'-trimethyl-1,2-ethanediamine;
urea - urea.

References

1. Chapelet-Arab, B.; Nowogrocki, G.; Abraham, F.; Grandjean, S., *Journal of Solid State Chemistry* **2005,** *178* (10), 3046-3054; Chapelet-Arab, B.; Nowogrocki, G.; Abraham, F.; Grandjean, S., *Journal of Solid State Chemistry* **2005,** *178* (10), 3055-3065.
2. Arab-Chapelet, B.; Grandjean, S.; Nowogrocki, G.; Abraham, F., *Journal of Alloys and Compounds* **2007,** *444*, 387-390.
3. Sylva, R. N.; Davidson, M. R., *Journal of the Chemical Society-Dalton Transactions* **1979,** (3), 465-471; Berto, S.; Crea, F.; Daniele, P. G.; Gianguzza, A.; Pettignano, A.; Sammartano, S., *Coordination Chemistry Reviews* **2012,** *256* (1-2), 63-81; Szabo, Z.; Toraishi, T.; Vallet, V.; Grenthe, I., *Coordination Chemistry Reviews* **2006,** *250* (7-8), 784-815.
4. Leciejewicz, J.; Alcock, N. W.; Kemp, T. J., *Coordination Chemistry* **1995,** *82*, 43-84; Fortier, S.; Hayton, T. W., *Coordination Chemistry Reviews* **2010,** *254* (3-4), 197-214; Wang, K. X.; Chen, J. S., *Accounts of Chemical Research* **2011,** *44* (7), 531-540.
5. Burns, P. C.; Ewing, R. C.; Hawthorne, F. C., *Canadian Mineralogist* **1997,** *35*, 1551-1570.
6. Qu, Z. R., *Chinese Journal of Inorganic Chemistry* **2007,** *23* (10), 1837-1839.
7. Alcock, N. W., *Journal of the Chemical Society-Dalton Transactions* **1973,** (16), 1610-1613; Chumaevskii, N. A.; Minaeva, N. A.; Mikhailov, Y. N.; Gorbunova, Y. E.; Beirakhov, A. G.; Shchelokov, R. N., *Zhurnal Neorganicheskoi Khimii* **1998,** *43* (5), 789-795.
8. Artem'eva, M. Y.; Serezhkin, V. N.; Smirnov, O. P.; Plakhtii, V. P., *Russian Journal of Inorganic Chemistry* **2006,** *51* (8), 1307-1310.
9. Jayadevan, N. C.; Mudher, K. D. S.; Chackraburtty, D. M., *Acta Crystallographica Section B-Structural Science* **1975,** *31* (SEP15), 2277-2280.
10. Alcock, N. W., *Journal of the Chemical Society-Dalton Transactions* **1973,** (16), 1616-1620.
11. Baeva, E. E.; Mikhailov, Y. N.; Gorbunova, Y. E.; Serezhkina, L. B.; Serezhkin, V. N., *Russian Journal of Inorganic Chemistry* **2003,** *48* (11), 1651-1657.
12. Alcock, N. W., *Journal of the Chemical Society-Dalton Transactions* **1973,** (16), 1614-1616.
13. Mikhailov, Y. N.; Gorbunova, Y. E.; Shishkina, O. V.; Serezhkina, L. B.; Serezhkin, V. N., *Russian Journal of Inorganic Chemistry* **1999,** *44* (9), 1370-1375.
14. Giesting, P. A.; Porter, N. J.; Burns, P. C., *Zeitschrift Fur Kristallographie* **2006,** *221* (4), 252-259.
15. Chapelet-Arab, B.; Nowogrocki, G.; Abraham, E.; Grandjean, S., *Radiochimica Acta* **2005,** *93* (5), 279-285.
16. Bressat, R.; Claudel, B.; Trambouze, Y., *Journal De Chimie Physique Et De Physico-Chimie Biologique* **1964,** *61* (6), 816-818.
17. Poojary, M. D.; Patil, K. C., *Proceedings of the Indian Academy of Sciences-Chemical Sciences* **1987,** *99* (5-6), 311-315.

18. Govindarajan, S.; Patil, K. C.; Poojary, M. D.; Manohar, H., *Inorganica Chimica Acta* **1986,** *120* (1), 103-107.
19. Artem'eva, M. Y.; Dolgushin, F. M.; Antipin, M. Y.; Serezhkina, L. B.; Serezhkin, V. N., *Russian Journal of Inorganic Chemistry* **2004,** *49* (3), 369-372.
20. Artem'eva, M. Y.; Mikhailov, Y. N.; Gorbunova, Y. E.; Serezhkina, L. B.; Serezhkin, V. N., *Russian Journal of Inorganic Chemistry* **2003,** *48* (9), 1337-1339.
21. Akhmerkina, Z. V.; Mikhailov, Y. N.; Gorbunova, Y. E.; Churakov, A. V.; Serezhkina, L. B.; Serezhkin, V. N., *Russian Journal of Inorganic Chemistry* **2005,** *50* (9), 1326-1331.
22. Serezhkina, L.; Marukhnov, A.; Peresypkina, E.; Virovets, A.; Medrish, I.; Pushkin, D., *Russian Journal of Inorganic Chemistry* **2008,** *53* (6), 837-841.
23. Medrish, I. V.; Peresypkina, E. V.; Virovets, A. V.; Serezhkina, L. B., *Russian Journal of Inorganic Chemistry* **2008,** *53* (7), 1040-1045.
24. Akhmerkina, Z. V.; Virovets, A. V.; Peresypkina, E. V.; Serezhkina, L. B., *Russian Journal of Inorganic Chemistry* **2006,** *51* (2), 229-234.
25. Shchelokov, R. N.; Mikhailov, Y. N.; Beirakhov, A. G.; Orlova, I. M.; Ashurov, Z. R., *Zhurnal Neorganicheskoi Khimii* **1986,** *31* (8), 2050-2054.
26. Frisch, M.; Cahill, C. L., *Journal of Solid State Chemistry* **2007,** *180* (9), 2597-2602.
27. Liu, D. S.; Shi, T. Q.; Liu, S. F.; Ying, S. M.; Li, X. F., *Acta Crystallographica Section E-Structure Reports Online* **2007,** *63*, M385-M387.
28. Serezhkina, L. B.; Vologzhanina, A. V.; Neklyudova, N. A.; Serezhkin, V. N., *Crystallography Reports* **2009,** *54* (1), 59-62.
29. Shilova, M. Y.; Vologzhanina, A. V.; Serezhkina, L. B.; Serezhkin, V. N., *Russian Journal of Coordination Chemistry* **2009,** *35* (2), 153-156.
30. Thuery, P., *Crystengcomm* **2008,** *10* (7), 808-810.
31. Serezhkina, L. B.; Vologzhanina, A. V.; Neklyudova, N. A.; Serezhkin, V. N.; Antipin, M. Y., *Russian Journal of Inorganic Chemistry* **2008,** *53* (8), 1193-1196.
32. Andrews, M. B.; Cahill, C. L., *Crystengcomm* **2011,** *13* (23), 7068-7078.
33. Thuery, P.; Masci, B., *Crystal Growth & Design* **2010,** *10* (2), 716-725.
34. Thuery, P., *Crystengcomm* **2010,** *12* (6), 1905-1911.
35. Serezhkina, L. B.; Peresypkina, E. V.; Virovets, A. V.; Neklyudova, N. A., *Russian Journal of Inorganic Chemistry* **2010,** *55* (7), 1020-1025.
36. Zachariasen, W. H.; Plettinger, H. A., *Acta Crystallographica* **1959,** *12* (7), 526-530.
37. Templeton, D. H.; Zalkin, A.; Ruben, H.; Templeton, L. K., *Acta Crystallographica Section C-Crystal Structure Communications* **1985,** *41* (OCT), 1439-1441; Navaza, A.; Charpin, P.; Vigner, D.; Heger, G., *Acta Crystallographica Section C-Crystal Structure Communications* **1991,** *47*, 1842-1845.
38. Lermontov, A. S.; Lermontova, E. K.; Wang, Y. Y., *Inorganica Chimica Acta* **2009,** *362* (10), 3751-3755.
39. Fankuchen, I., *The crystal structure of the uranyl acetates of sodium and of potassium*. Cornell University: 1933; p 108.
40. Ferrari, A.; Cavalca, L.; Tanni, M. E., *Ann. Chim. Ital.* **1959,** *48*.
41. Fankuchen, I., *Phys. Rev.* **1934,** *45* (8).

42. Serezhkina, L. B.; Vologzhanina, A. V.; Klepov, V. V.; Serezhkin, V. N., *Crystallography Reports* **2010,** *55* (5), 773-779.
43. Polyakova, I. N.; Seisenbaeva, G. A.; Santalova, N. A.; Dunaeva, K. M., *Koordinatsionnaya Khimiya* **1991,** *17* (3), 428-432.
44. Serezhkina, L. B.; Peresypkina, E. V.; Virovets, A. V.; Karasev, M. O., *Crystallography Reports* **2010,** *55* (1), 19-23.
45. Silva, M. R.; Beja, A. M.; Paixao, J. A.; da Veiga, L. A.; Martin-Gil, J., *Acta Crystallographica Section C-Crystal Structure Communications* **1999,** *55*, 2039-2041.
46. Anisimova, N.; Hoppe, R.; Serafin, M., *Zeitschrift Fur Anorganische Und Allgemeine Chemie* **1997,** *623* (1), 35-38.
47. Kim, J. Y.; Norquist, A. J.; O'Hare, D., *Chemistry of Materials* **2003,** *15* (10), 1970-1975.
48. Spitsyn, V. I.; Dunaeva, K. M.; Kolesnik, V. V.; Yuranov, I. A., *Zhurnal Neorganicheskoi Khimii* **1982,** *27* (4), 844-848.
49. Spitsyn, V. I.; Kolesnik, V. V.; Mistryukov, V. E.; Yuranov, I. A.; Mikhailov, Y. N.; Dunaeva, K. M., *Bulletin of the Academy of Sciences of the Ussr Division of Chemical Science* **1982,** *31* (4), 715-719.
50. Alcock, N. W.; Flanders, D. J.; Brown, D., *Inorganica Chimica Acta-F-Block Elements Articles and Letters* **1984,** *94* (6), 279-282.
51. Spencer, E. C.; Kalyanasundari, B.; Mariyatra, M. B.; Howard, J. A. K.; Panchanatheswaran, K., *Inorganica Chimica Acta* **2006,** *359* (1), 35-43.
52. Gulbaev, Y. I.; Azizov, T. A.; Khudoyarov, A. B.; Sharipov, K. T., *Uzbekskii Khimicheskii Zhurnal* **1997,** *28*, 5.
53. Bekaert, A.; Lemoine, P.; Brion, J. D.; Viossat, B., *Zeitschrift Fur Kristallographie-New Crystal Structures* **2006,** *221* (1), 45-46.
54. Grigoriev, M. S.; Antipin, M. Y.; Krot, N. N., *Acta Crystallographica Section E-Structure Reports Online* **2005,** *61*, M2078-M2079.
55. Mikhailov, Y. N.; Kanishcheva, A. S.; Gorbunova, Y. E.; Belomestnykh, V. I.; Sveshnikova, L. B., *Zhurnal Neorganicheskoi Khimii* **1997,** *42* (12), 1980-1985.
56. Charushnikova, I.; Krot, N.; Starikova, Z., *Radiochemistry* **2008,** *50* (2), 117-120.
57. Grigor'ev, M. S.; Antipin, M. Y.; Krot, N. N., *Radiochemistry* **2004,** *46* (3), 224-231.
58. Gutowski, K. E.; Cocalia, V. A.; Griffin, S. T.; Bridges, N. J.; Dixon, D. A.; Rogers, R. D., *Journal of the American Chemical Society* **2007,** *129* (3), 526-536.
59. Mentzen, B.; Giorgio, G., *Journal of Inorganic & Nuclear Chemistry* **1970,** *32* (5), 1509-&; Howatson, J.; Grev, D. M.; Morosin, B., *Journal of Inorganic & Nuclear Chemistry* **1975,** *37* (9), 1933-1935.
60. Cousson, A.; Proust, J.; Pages, M.; Robert, F.; Rizkalla, E. N., *Acta Crystallographica Section C-Crystal Structure Communications* **1990,** *46*, 2316-2318.
61. Charushnikova, I.; Grigor'ev, M.; Krot, N., *Radiochemistry* **2010,** *52* (2), 138-144.
62. Herrero, J. A.; Rojas, R. M.; Bermudez, J.; Gutierre.E, *Anales De Quimica* **1973,** *69* (4), 471-475.
63. Bismondo, A.; Casellato, U.; Graziani, R., *Inorganica Chimica Acta* **1994,** *223* (1-2), 151-153.

64. Benetollo, F.; Bombieri, G.; Herrero, P.; Rojas, R. M., *Journal of Alloys and Compounds* **1995,** *225* (1-2), 400-405.
65. Navaza, A.; Iroulart, M. G.; Nierlich, M.; Lance, M.; Vigner, J., *Acta Crystallographica Section C-Crystal Structure Communications* **1993,** *49*, 1767-1770.
66. Mougel, V.; Biswas, B.; Pecaut, J.; Mazzanti, M., *Chemical Communications* **2010,** *46* (45), 8648-8650.
67. Nierlich, M.; Iroulart, G.; Vigner, D.; Keller, N.; Lance, M., *Acta Crystallographica Section C-Crystal Structure Communications* **1990,** *46*, 2459-2460.
68. Cai, Y. G.; Zhang, W. H.; Sun, Q. J.; Zhang, W. P.; Zhao, J. S.; Miao, J. Y.; Ren, Z. L.; Liu, C. Y., *Journal of Coordination Chemistry* **2008,** *61* (20), 3350-3356.
69. Deifel, N. P.; Cahill, C. L., *Chemical Communications* **2011,** *47* (21), 6114-6116.
70. Thuery, P., *Crystal Growth & Design* **2012,** *12* (1), 499-507.
71. Bandoli, G.; Clemente, D. A., *Journal of Inorganic & Nuclear Chemistry* **1981,** *43* (11), 2843-2846.
72. Micera, G.; Erre, L. S.; Cariati, F.; Clemente, D. A.; Marzotto, A.; Valle, G., *Inorganica Chimica Acta-F-Block Elements Articles and Letters* **1985,** *109* (3), 173-177.
73. Das, S.; Madhavaiah, C.; Verma, S.; Bharadwaj, P. K., *Inorganica Chimica Acta* **2006,** *359* (2), 548-552.
74. Alcock, N. W.; Kemp, T. J.; Leciejewicz, J.; Pennington, M., *Acta Crystallographica Section C* **1989,** *45* (5), 719-721.
75. Alcock, N. W.; Kemp, T. J.; Roe, S. M.; Leciejewicz, J., *Inorganica Chimica Acta* **1996,** *248* (2), 241-246.
76. Cariati, F.; Erre, L.; Micera, G.; Clemente, D. A.; Cingi, M. B., *Inorganica Chimica Acta-Bioinorganic Chemistry* **1983,** *79* (1-6), 205-205.
77. Deacon, G. B.; Mackinnon, P. I.; Taylor, J. C., *Polyhedron* **1985,** *4* (1), 103-113.
78. Shchelokov, R. N.; Mikhailov, Y. N.; Orlova, I. M.; Sergeev, A. V.; Ashurov, Z. R.; Tashev, M. T.; Parpiev, N. A., *Koord.Khim.* **1985,** *11*, 1144.
79. Charushnikova, I. A.; Krot, N. N.; Starikova, Z. A., *Radiochemistry* **2004,** *46* (6), 556-559.
80. Go, Y. B.; Wang, X. Q.; Jacobson, A. J., *Inorganic Chemistry* **2007,** *46* (16), 6594-6600.
81. Kim, J. Y.; Norquist, A. J.; O'Hare, D., *Dalton Transactions* **2003,** (14), 2813-2814.
82. Borkowski, L. A.; Cahill, C. L., *Acta Crystallographica Section E-Structure Reports Online* **2004,** *60*, M198-M200.
83. Liao, Z. L.; Li, G. D.; Wei, X. A.; Yu, Y.; Chen, J. S., *European Journal of Inorganic Chemistry* **2010,** (24), 3780-3788.
84. Cousson, A.; Stout, B.; Nectoux, F.; Pages, M.; Gasperin, M., *Journal of the Less-Common Metals* **1986,** *125*, 111-115.
85. Jiang, Y. S.; Yu, Z. T.; Liao, Z. L.; Li, G. H.; Chen, J. S., *Polyhedron* **2006,** *25* (6), 1359-1366.

86. Volkringer, C.; Henry, N.; Grandjean, S.; Loiseau, T., *Journal of the American Chemical Society* **2012,** *134* (2), 1275-1283.
87. Qu, Z. R., *Chinese Journal of Inorganic Chemistry* **2007,** *23* (12), 2126-2127.
88. Qu, Z. R., *Chinese Journal of Inorganic Chemistry* **2007,** *23* (12), 2123-2125.
89. Rowland, C. E.; Belai, N.; Knope, K. E.; Cahill, C. L., *Crystal Growth & Design* **2010,** *10* (3), 1390-1398.
90. Albano, V. G.; Braga, D.; Concilio, C.; Roveri, N., *Cryst.Struct.Commun.* **1978,** *7*, 133.
91. Liao, Z. L.; Li, G. D.; Bi, M. H.; Chen, J. S., *Inorganic Chemistry* **2008,** *47* (11), 4844-4853.
92. Xia, Y.; Wang, K. X.; Chen, J. S., *Inorganic Chemistry Communications* **2010,** *13* (12), 1542-1547.
93. Wang, W.; Zhang, D. J.; Fan, Y.; Song, T. Y.; Zhang, P., *Acta Crystallographica Section E-Structure Reports Online* **2010,** *66*, M462-U1161.
94. Dalai, S.; Bera, M.; Rana, A.; Chowdhuri, D. S.; Zangrando, E., *Inorganica Chimica Acta* **2010,** *363* (13), 3407-3412.
95. Beer, S.; Berryman, O. B.; Ajami, D.; Rebek, J., *Chemical Science* **2010,** *1* (1), 43-47.
96. Ji, C. C.; Li, J.; Li, Y. Z.; Zheng, H. G., *Inorganic Chemistry Communications* **2010,** *13* (11), 1340-1342.
97. Thuery, P.; Masci, B., *CrystEngComm* **2012,** *14* (1).
98. Thuery, P., *Crystengcomm* **2009,** *11* (6), 1081-1088.
99. Cantos, P. M.; Frisch, M.; Cahill, C. L., *Inorganic Chemistry Communications* **2010,** *13* (9), 1036-1039.
100. Frisch, M.; Cahill, C. L., *Dalton Transactions* **2006,** (39), 4679-4690.
101. Cahill, C. L.; de Lill, D. T.; Frisch, M., *Crystengcomm* **2007,** *9* (1), 15-26.
102. Frisch, M.; Cahill, C. L., *Dalton Transactions* **2005,** (8), 1518-1523.
103. Jenniefer, S. J.; Muthiah, P. T., *Acta Crystallographica Section C-Crystal Structure Communications* **2011,** *67*, M69-M72.
104. Xie, Y. R.; Zhao, H.; Wang, X. S.; Qu, Z. R.; Xiong, R. G.; Xue, X. A.; Xue, Z. L.; You, X. Z., *European Journal of Inorganic Chemistry* **2003,** (20), 3712-3715.
105. Severance, R. C.; Vaughn, S. A.; Smith, M. D.; zur Loye, H. C., *Solid State Sciences* **2011,** *13* (6), 1344-1353.
106. Alcock, N. W.; Errington, W.; Kemp, T. J.; Leceiejewicz, J., *Acta Crystallographica Section C-Crystal Structure Communications* **1996,** *52*, 615-617.
107. Thuery, P., *Inorganic Chemistry Communications* **2009,** *12* (8), 800-803.
108. Jin, Y. B.; Hu, B.; Li, Y. X.; Wang, G. X., *Chinese Journal of Inorganic Chemistry* **2008,** *24* (1), 138-140.
109. Leciejewicz, J.; Starosta, W., *Acta Crystallographica Section E-Structure Reports Online* **2009,** *65*, M94-U980.
110. Cousson, A.; Nectoux, F.; Pages, M.; Rizkalla, E. N., *Radiochimica Acta* **1993,** *61* (3-4), 177-180.
111. Immirzi, A.; Bombieri, G.; Degetto, S.; Marangoni, G., *Acta Crystallographica Section B-Structural Science* **1975,** *31* (APR15), 1023-1028;

Jiang, Y. S.; Li, G. H.; Tian, Y.; Liao, Z. L.; Chen, J. S., *Inorganic Chemistry Communications* **2006,** *9* (6), 595-598.
112. Harrowfield, J. M.; Lugan, N.; Shahverdizadeh, G. H.; Soudi, A. A.; Thuery, P., *European Journal of Inorganic Chemistry* **2006,** (2), 389-396.
113. Mirzaei, M.; Eshtiagh-Hosseini, H.; Lippolis, V.; Aghabozorg, H.; Kordestani, D.; Shokrollahi, A.; Aghaei, R.; Blake, A. J., *Inorganica Chimica Acta* **2011,** *370* (1), 141-149.
114. Masci, B.; Thuery, P., *Polyhedron* **2005,** *24* (2), 229-237.
115. Cousson, A.; Proust, J.; Rizkalla, E. N., *Acta Crystallographica Section C-Crystal Structure Communications* **1991,** *47*, 2065-2069.
116. Masci, B.; Thuery, P., *Crystengcomm* **2008,** *10* (8), 1082-1087.
117. Masci, B.; Thuery, P., *Crystal Growth & Design* **2008,** *8* (5), 1689-1696.
118. Dean, N. E.; Hancock, R. D.; Cahill, C. L.; Frisch, M., *Inorganic Chemistry* **2008,** *47* (6), 2000-2010.
119. Borkowski, L. A.; Cahill, C. L., *Inorganic Chemistry* **2003,** *42* (22), 7041-7045.
120. Bombieri, G.; Benetollo, F.; Rojas, R. M.; Paz, M. L., *Eur. Cryst. Meeting* **1980,** *6*, 56; Bombieri, G.; Benetollo, F.; Rojas, R. M.; Depaz, M. L.; Delpra, A., *Inorganica Chimica Acta-Articles* **1982,** *61* (2), 149-154.
121. Grigor'ev, M.; Antipin, M.; Krot, N., *Radiochemistry* **2005,** *47* (2), 103-106.
122. Bombieri, G.; Benetollo, F.; Delpra, A.; Rojas, R., *Journal of Inorganic & Nuclear Chemistry* **1979,** *41* (2), 201-203.
123. Charushnikova, I. A.; Fedoseev, A. M.; Budantseva, N. A.; Polyakova, I. N.; Moisy, P., *Russian Journal of Coordination Chemistry* **2007,** *33* (1), 61-67.
124. Benetollo, F.; Bombieri, G.; Herrero, J. A.; Rojas, R. M., *Journal of Inorganic & Nuclear Chemistry* **1979,** *41* (2), 195-199.
125. Lu, S. M.; Ke, Y. X.; Li, J. M.; Zhou, S. X.; Wu, X. T.; Du, W. X., *Crystal Research and Technology* **2003,** *38* (11), 1004-1008.
126. Borkowski, L. A.; Cahill, C. L., *Crystal Growth & Design* **2006,** *6* (10), 2248-2259.
127. Zhang, Y. J.; Tilley, G. J.; Martin, L. R.; Collison, D.; Livens, F. R.; Helliwell, M.; Malik, K. M. A.; Hursthouse, M. B., *Journal of Nuclear Science and Technology* **2002,** *Supplement 3*, 457-460.
128. Kerr, A. T.; Cahill, C. L., *Crystal Growth & Design* **2011,** *11* (12), 5634-5641.
129. Thuery, P., *Crystal Growth & Design* **2008,** *8* (11), 4132-4143.
130. Zhang, Y. J.; Livens, F. R.; Collison, D.; Helliwell, M.; Heatley, F.; Powell, A. K.; Wocadlo, S.; Eccles, H., *Polyhedron* **2002,** *21* (1), 69-79.
131. Zhang, Y. J.; Collison, D.; Livens, F. R.; Helliwell, M.; Heatley, F.; Powell, A. K.; Wocadlo, S.; Eccles, H., *Polyhedron* **2002,** *21* (1), 81-96.
132. Thuery, P., *Crystal Growth & Design* **2011,** *11* (6), 2606-2620.
133. Mentzen, B. F.; Puaux, J. P.; Sautereau, H., *Acta Crystallographica Section B-Structural Science* **1978,** *34* (JUN), 1846-1849.
134. Thuery, P., *Inorganic Chemistry Communications* **2008,** *11* (6), 616-620.
135. Mentzen, B. F., *Acta Crystallographica Section B-Structural Science* **1977,** *33* (AUG15), 2546-2549.
136. Mentzen, B. F.; Puaux, J. P.; Loiseleur, H., *Acta Crystallographica Section B-Structural Science* **1977,** *33* (JUN15), 1848-1851.

137. Alcock, N. W.; Flanders, D. J.; Kemp, T. J.; Shand, M. A., *Journal of the Chemical Society-Dalton Transactions* **1985,** (3), 517-521.
138. Mentzen, B. F.; Sautereau, H., *Acta Crystallographica Section B-Structural Science* **1980,** *36* (SEP), 2051-2053.
139. Knope, K. E.; Cahill, C. L., *Inorganic Chemistry* **2008,** *47* (17), 7660-7672.
140. Knope, K. E.; Cahill, C. L., *Inorganic Chemistry Communications* **2010,** *13* (9), 1040-1042.
141. Bismondo, A.; Casellato, U.; Rizzo, L.; Graziani, R., *Inorganica Chimica Acta* **1992,** *191* (1), 69-73.
142. Spitsyn, V. I.; Kolesnik, V. V.; Mistriukov, V. E.; Mikhailov, I. N.; Dunaeva, K. M., *Doklady Akademii Nauk Sssr* **1983,** *273* (2), 355-359.
143. Burkov, V. I.; Mistryukov, V. E.; Mikhailov, Y. N.; Chuklanova, E. B., *Zhurnal Neorganicheskoi Khimii* **1997,** *42* (3), 391-395.
144. Ferrari, A.; Nardelli, M.; Tani, M. E., *Gazzetta Chimica Italiana* **1957,** *2*.
145. Yuranov, I. A.; Dunaeva, K. M., *Koordinatsionnaya Khimiya* **1989,** *15* (6), 845-847.
146. Yoshimura, T.; Kikunaga, H.; Shinohara, A., *Acta Crystallographica Section E-Structure Reports Online* **2009,** *65*, M355-U185.
147. Bismondo, A.; Casellato, U.; Forsellini, E.; Graziani, R., *Journal of Crystallographic and Spectroscopic Research* **1985,** *15* (3), 257-262.
148. Bismondo, A.; Casellato, U.; Sitran, S.; Graziani, R., *Inorganica Chimica Acta-F-Block Elements Articles and Letters* **1985,** *110* (3), 205-210.
149. Alcock, N. W.; Kemp, T. J.; Demeester, P., *Acta Crystallographica Section B-Structural Science* **1982,** *38* (JAN), 105-107.
150. Yokoyama, Y.; Inaba, A.; Hara, H.; Yamazaki, T.; Tamura, H.; Kushi, Y., *Chemistry Letters* **1990,** (4), 671-674.
151. Jiang, J.; Sarsfield, M. J.; Renshaw, J. C.; Livens, F. R.; Collison, D.; Charnock, J. M.; Helliwell, M.; Eccles, H., *Inorganic Chemistry* **2002,** *41* (10), 2799-2806.
152. Bombieri, G.; Croatto, U.; Graziani, R.; Forselli.E; Magon, L., *Acta Crystallographica Section B-Structural Science* **1974,** *30* (FEB15), 407-411.
153. Bombieri, G.; Forselli.E; Tomat, G.; Magon, L.; Graziani, R., *Acta Crystallographica Section B-Structural Science* **1974,** *30* (NOV15), 2659-2663.
154. Battiston, G. A.; Sbrignadello, G.; Bandoli, G.; Clemente, D. A.; Tomat, G., *Journal of the Chemical Society-Dalton Transactions* **1979,** (12), 1965-1971.
155. Thuery, P., *Polyhedron* **2007,** *26* (1), 101-106.
156. Thuery, P., *Crystengcomm* **2008,** *10* (1), 79-85.
157. Thuery, P., *Chemical Communications* **2006,** (8), 853-855.
158. Thuery, P.; Masci, B., *Crystal Growth & Design* **2008,** *8* (9), 3430-3436.
159. Thuery, P., *Inorganic Chemistry Communications* **2007,** *10* (4), 423-426.
160. Grigoriev, M. S.; Den Auwer, C.; Meyer, D.; Moisy, P., *Acta Crystallographica Section C-Crystal Structure Communications* **2006,** *62*, M163-M165.
161. Thuery, P., *Crystal Growth & Design* **2011,** *11* (1), 347-355.
162. Liang, L. L.; Cai, Y. G.; Weng, N. S.; Zhang, R. L.; Zhao, J. S.; Wang, J. F.; Wu, H. L., *Inorganic Chemistry Communications* **2009,** *12* (2), 86-88.
163. Thuery, P., *European Journal of Inorganic Chemistry* **2006,** (18), 3646-3651.

164. Thuery, P., *Crystal Growth & Design* **2009,** *9* (11), 4592-4594.
165. Thuery, P., *Crystengcomm* **2009,** *11* (2), 232-234.
166. Rusanova, J. A.; Rusanov, E. B.; Domasevitch, K. V., *Acta Crystallographica Section C-Crystal Structure Communications* **2010,** *66*, m207-m210.
167. Sather, A. C.; Berryman, O. B.; Rebek, J., *Journal of the American Chemical Society* **2010,** *132* (39), 13572-13574.
168. Andreev, G.; Budantseva, N.; Tananaev, I.; Myasoedov, B., *Inorganic Chemistry Communications* **2010,** *13* (5), 577-579.
169. Borkowski, L. A.; Cahill, C. L., *Acta Crystallographica Section E-Structure Reports Online* **2005,** *61*, M816-M817.
170. Borkowski, L. A.; Cahill, C. L., *Crystal Growth & Design* **2006,** *6* (10), 2241-2247.
171. Thuery, P., *Inorganic Chemistry* **2007,** *46* (6), 2307-2315.
172. Leroux, S. D.; Vantets, A.; Adrian, H. W. W., *Acta Crystallographica Section B-Structural Science* **1979,** *35* (DEC), 3056-3057.
173. Duvieubourg, L.; Nowogrocki, G.; Abraham, F.; Grandjean, S., *Journal of Solid State Chemistry* **2005,** *178* (11), 3437-3444.
174. Thuery, P., *Crystengcomm* **2009,** *11* (6), 1150-1156.
175. Thuery, P., *Acta Crystallographica Section C-Crystal Structure Communications* **2008,** *64*, M50-M52.
176. Alcock, N. W.; Kemp, T. J.; Leciejewicz, J., *Inorganica Chimica Acta* **1991,** *184* (2), 203-207.
177. Rowland, C. E.; Cahill, C. L., *Inorganic Chemistry* **2010,** *49* (14), 6716-6724.
178. Alcock, N. W.; Flanders, D. J.; Pennington, M.; Brown, D., *Acta Crystallographica Section C-Crystal Structure Communications* **1988,** *44*, 247-250.
179. Bharara, M. S.; Strawbridge, K.; Vilsek, J. Z.; Bray, T. H.; Gorden, A. E. V., *Inorganic Chemistry* **2007,** *46* (20), 8309-8315.
180. Nassimbeni, L. R.; Rodgers, A. L.; Haigh, J. M., *Inorganica Chimica Acta* **1976,** *20* (2), 149-153.
181. Villiers, C.; Thuery, P.; Ephritikhine, M., *Polyhedron* **2010,** *29* (6), 1593-1599.
182. Knope, K. E.; Cahill, C. L., *Inorganic Chemistry* **2009,** *48* (14), 6845-6851.
183. Thuery, P., *Crystal Growth & Design* **2011,** *11* (7), 3282-3294.
184. Charushnikova, I. A.; Krot, N. N.; Polyakova, I. N.; Makarenkov, V. I., *Radiochemistry* **2005,** *47* (3), 241-246.
185. Harrowfield, J. M.; Skelton, B. W.; White, A. H., *Comptes Rendus Chimie* **2005,** *8* (2), 169-180.
186. Turpeinen, U.; Hamalainen, R.; Mutikainen, I.; Orama, O., *Acta Crystallographica Section C-Crystal Structure Communications* **1996,** *52*, 1169-1171.
187. Serezhkina, L. B.; Vologzhanina, A. V.; Neklyudova, N. A.; Serezhkin, V. N., *Crystallography Reports* **2009,** *54* (3), 449-454.
188. Zheng, Y. Z.; Tong, M. L.; Chen, X. M., *European Journal of Inorganic Chemistry* **2005,** (20), 4109-4117.

189. Anisimova, N. Y.; Gorbunova, Y. E.; Mikhailov, Y. N.; Chumaevskii, N. A., *Russian Journal of Inorganic Chemistry* **2001,** *46* (4), 552-555.
190. Thuery, P., *Crystal Growth & Design* **2009,** *9* (2), 1208-1215.
191. Zhang, W. H.; Zhao, J. S., *Inorganic Chemistry Communications* **2006,** *9* (4), 397-399.
192. Zhang, W.; Zhao, J., *Journal of Molecular Structure* **2006,** *789* (1–3), 177-181.
193. Knope, K. E.; Cahill, C. L., *Inorganic Chemistry* **2007,** *46* (16), 6607-6612.
194. Charushnikova, I. A.; Krot, N. N.; Starikova, Z. A., *Radiochemistry* **2004,** *46* (5), 429-433.
195. Sarsfield, M. J.; Helliwell, M.; Raftery, J., *Inorganic Chemistry* **2004,** *43* (10), 3170-3179; Burns, C. J.; Clark, D. L.; Donohoe, R. J.; Duval, P. B.; Scott, B. L.; Tait, C. D., *Inorganic Chemistry* **2000,** *39* (24), 5464-5468; Cametti, M.; Nissinen, M.; Cort, A. D.; Mandolini, L.; Rissanen, K., *Journal of the American Chemical Society* **2005,** *127* (11), 3831-3837.
196. Kubatko, K. A.; Burns, P. C., *Inorganic Chemistry* **2006,** *45* (25), 10277-10281.
197. Lhoste, J.; Henry, N.; Roussel, P.; Loiseau, T.; Abraham, F., *Dalton Transactions* **2011,** *40* (11), 2422-2424.
198. Sullens, T. A.; Jensen, R. A.; Shvareva, T. Y.; Albrecht-Schmitt, T. E., *Journal of the American Chemical Society* **2004,** *126* (9), 2676-2677.
199. Severance, R. C.; Smith, M. D.; zur Loye, H. C., *Inorganic Chemistry* **2011,** *50* (17), 7931-7933.
200. Thuery, P., *Crystengcomm* **2008,** *10* (9), 1126-1128.
201. Thuery, P., *Crystengcomm* **2009,** *11* (11), 2319-2325.
202. Knope, K. E.; de Lill, D. T.; Rowland, C. E.; Cantos, P. M.; de Bettencourt-Dias, A.; Cahill, C. L., *Inorganic Chemistry* **2012,** *51* (1), 201-206.
203. Rojas, R. M.; Herrero, M. P.; Benetollo, F.; Bombieri, G., *Journal of the Less-Common Metals* **1990,** *162* (1), 105-116.
204. Thuery, P., *Crystal Growth & Design* **2010,** *10* (5), 2061-2063.

Chapter II
Uranyl Phthalates

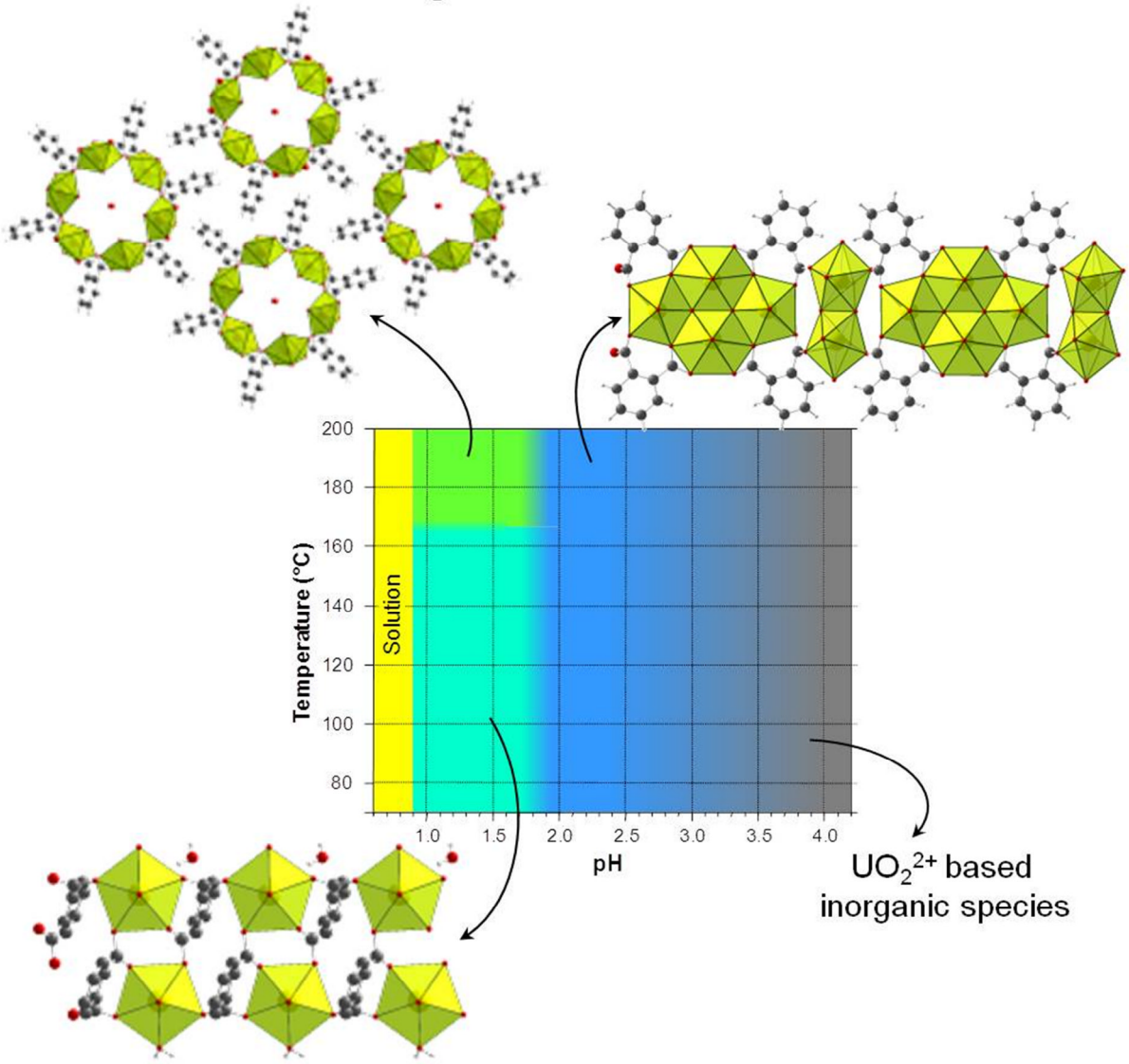

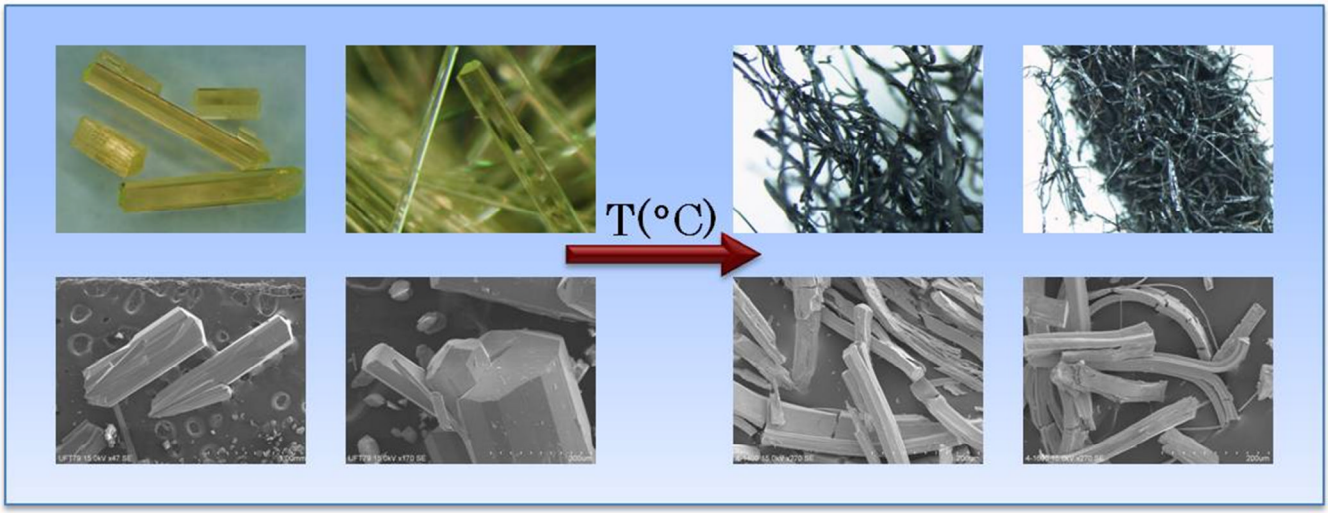

Chapter II Uranyl phthalates

II.1 . Introduction

The phthalic acid (noted H_2pht) has proven to be a prolific ligand. Varying the synthesis conditions in aqueous solvent, there have been obtained 4 compounds with this ditopic ligand from which two are isostructures, having different counter-cations. The structure of the uranyl-based compound $[UO_2(pht)(H_2O)]\cdot H_2O$ (noted hereafter **pht1**) has been previously encountered in literature[1] but only the structural characterization (from single-crystal XRD analysis) has been presented. The synthesis of a second complex $[UO_2(pht)(H_2O)]\cdot 0.32H_2O$ (**pht2**) has already reported in literature[2] but its structure has been determined for the neptunyl(VI) and plutonyl (VI) cation. The last two complexes $A[(UO_2)_3O(OH)(H_2O)(pht)_2]$[3] (A = K, noted **pht3**; NH_4, noted **pht4**) possess a unique structure having as SBUs alternating dimeric and tetrameric units interconnected via the carboxylate groups of the ligand. The type of tetranuclear brick present in compounds **pht3** and **pht4** has been previously reported also in some uranyl phthalates[4] $A_4[(UO_2)_4O_2(pht)_4]\cdot 3H_2O$ (where A = NH_4, K or Cs) but without being intercalated with the dimeric unit. The synthesis of these compounds implies the heating up to 70°C, during several hours, in an open reactor, of a diluted solution of uranyl nitrate containing the appropriate quantity of A_2pht salt. The crystallization takes place during 1-4 days statically at room temperature.

The synthesized compounds have been characterized by X-ray diffraction techniques, infrared and luminescence spectroscopy. Also the thermal behavior has been studied.

II.2 . Structure description

The structure of **pht1** complex has been already described in literature[1], and therefore no single crystal X-ray diffraction analysis has been conducted on this sample. The structural data of the other three uranyl phthalates (**pht2**, **pht3** and **pht4**) have been collected from single-crystal XRD analysis and the structure characteristics will be discussed in parallel with complex **pht1.** Details of crystal data are given in the Table II.2.1.

Table II.2.1 Crystal and refinement data for uranyl phthalate complexes.

Parameter*	pht1**	pht2	pht3	pht4
crystal system	triclinic	trigonal	triclinic	triclinic
space group	*P-1*	*R-3*	*P-1*	*P-1*
a/Å	6.757(1)	30.5385(7)	7.1113(3)	7.2962(3)
b/Å	8.150(1)	30.5385(7)	13.3625(5)	13.3376(4)
c/Å	10.632(2)	5.8489(2)	13.6784(5)	13.6850(4)
α/deg	95.24(2)	90	102.423(2)	102.294(2)
ß/deg	100.76(2)	90	104.864(2)	105.175(2)
γ/deg	103.75(1)	120	101.286(2)	101.557(2)
volume/Å^3	553.0(2)	4723.9(2)	1182.74(8)	1208.64(7)
Z, ρ_{calc}/g·cm^{-3}	2 2.823	12, 2.895	2, 3.441	2, 3.298
final R indices [$I > 2\sigma(I)$]	R1 = 0.0470 wR2 = 0.1133	R1 = 0.0221 wR2 = 0.0629	R1 = 0.0443 wR2 = 0.1227	R1 = 0.0256 wR2 = 0.0588
R indices (all data)	---	R1 = 0.0355 wR2 = 0.0674	R1 = 0.0610 wR2 = 0.1352	R1 = 0.0395 wR2 = 0.0731

*-a complete crystal and refinement data table for the phthalate system is given in the supplementary data chapter (figure VIII.1.1)
- **pht1 data was taken from literature[1]

Both **pht1** and **pht2** compounds possess in their structure one unique crystallographic site for the uranium atom, in both cases being situated in a 2i and respectively 18f general position. The SBUs of both structures are identical being type P monomeric units (pentagonal bipyramid). Also the similar uranium coordination sphere for both cases is formed by the two uranyl oxygen atoms and four oxygen atoms, each belonging to μ_2-bridging carboxylate group of the ligand and a fifth oxygen atom belonging to a coordinating water molecule.

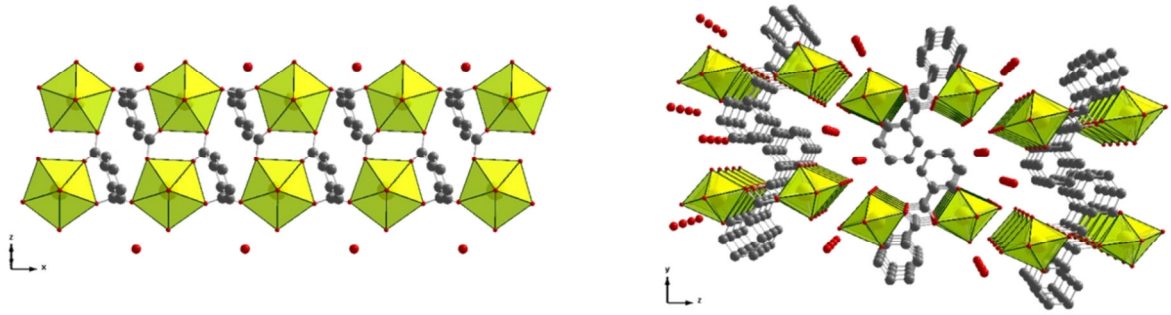

Figure II.2.1 Structure representation of complex **pht1** single chain along [010] (left) and view along [-100] direction (right).

For compound **pht1** (Figure II.2.1) the uranyl type U=O bonds have a length of 1.765(6) and 1.768(6) Å being close to the values obtained for compound **pht2** (Figure II.2.2) of 1.760(3) and 1.771(3) Å the latter phase possessing a less symmetrical SBU. Also there is a good concordance between the bond U–O lengths in the equatorial plane. The SBUs of both phases possess two short (average of 2.37 Å for **pht1** and of 2.36 Å for **pht2**) and two long (average of 2.42 Å for **pht1** and of 2.40 Å for **pht2**) bonds with the carboxylate type oxygen atoms and a even longer bond (of 2.425(7) Å for **pht1** and of 2.487(4) Å for **pht2**) with the oxygen atom belonging to the coordinating water molecule.

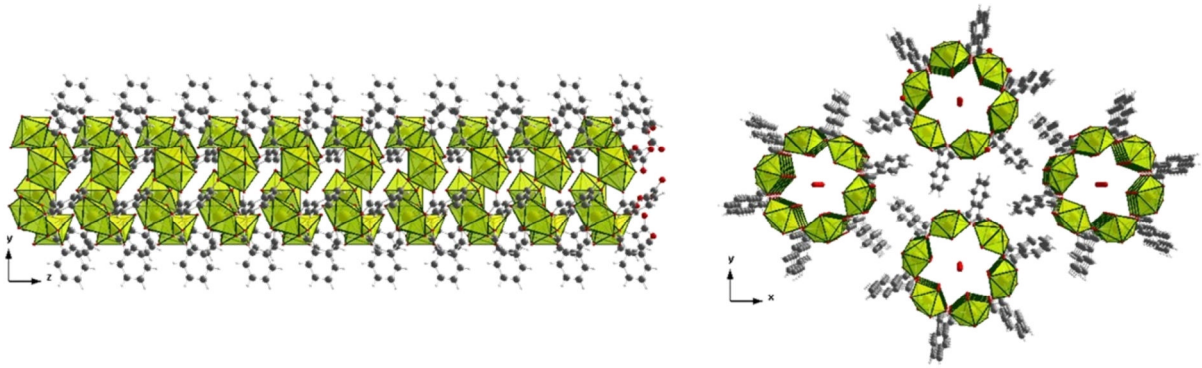

Figure II.2.2 Structure representation of complex **pht2** single nanotube, view along [100] direction (left) and complex view along [001] direction (right).

The major difference between the two complexes is the distinct mode of ligand coordination. Although in both cases four oxygen atoms belong to bridging carboxylate groups in the uranyl equatorial plane, the organic ligand adopts in complex **pht1**, a syn-anti & anti-anti μ_3-η_1:η_1:η_1:η_1 configuration, which differs from the case of complex **pht2** where the ligand adopts a syn-anti & syn-anti μ_4-η_1:η_1:η_1:η_1 configuration. Both structures show one-dimensional frameworks: for complex **pht1**, it consists of double chains of polyhedra interconnected by the ligand (Figure II.2.1.a)) and for complex **pht2**, it consists of parallel nanotubes

(Figure II.2.2.a)). Each nanotube is composed of piled interconnected six-member rings of uranyl polyhedra linked by the organic ligand. Beside the coordinating water molecules, each of the complexes contain also free water molecules, situated between the chains in complex **pht1** and inside the nanotubes in complex **pht2.**

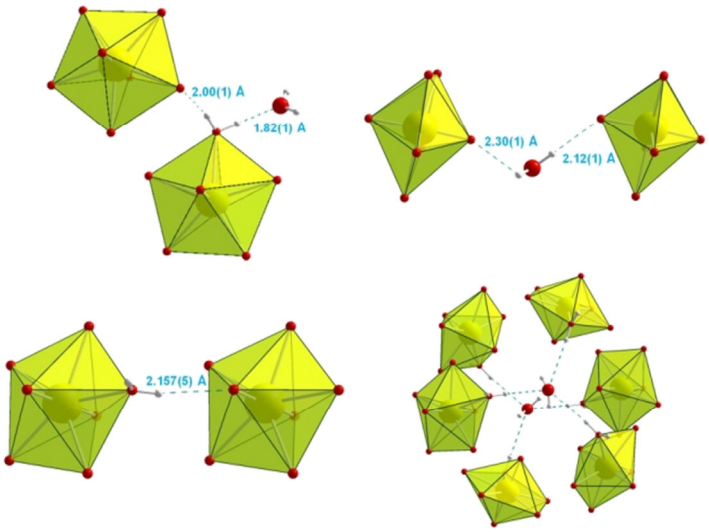

Figure II.2.3 Graphic representation of the hydrogen bond type interactions occurring in the structure of complex **pht1** (top) and complex **pht2** (bottom).

In both complexes the water molecules (free or coordinating) are involved in hydrogen bond type interactions (Figure II.2.3). In compound **pht1** hydrogen bond interactions appear between the hydrogen atoms of the coordinating water molecule and the oxygen atoms belonging to one free water molecule (H···O = 1.82(1) Å) and to a carboxylate group coordinating an adjacent uranium atom (H···O = 2.00(1) Å). This type of weak interactions appears between the hydrogen atoms of the free water molecule and the uranyl type oxygen atoms belonging to two adjacent uranyl polyhedra. In complex **pht2**, hydrogen bond interaction could take place, but because the hydrogen atom position has been automatically inserted in order to geometrically ride the parent atom and was not refined from the crystal data, the given H···O distances are guide lines for the actual values, being accurately measured but only for the chosen position of the hydrogen atoms. In this complex one of the H bonds takes place between one hydrogen atom belonging to the coordinating water molecule and one uranyl type oxygen atom belonging to the adjacent uranyl polyhedron. The other hydrogen bonds that could take place are between the coordinating water molecules, which for

each uranyl polyhedron is orientated toward the center of the nanotube, and the free water molecule situated in the center of the channel. Two H···O (2.56(17) and 2.70(23) Å) distances have been measured between the H atoms of the coordinating water molecule and the O atom of the free water molecule. But these measurements are not accurate, because of the high value of the U_{ij} anisotropic parameters and the mobility of the free water molecule along the nanotube, consistent with the *c* crystallographic axis. Basically the *z* atomic parameter for the oxygen atom of the free water molecule has been statistically chosen and refined, in reality having any possible value between zero and one.

It is interesting to notice that similar six-ring nanotube network possessing exactly the same type of SBU has been previously reported in one uranyl formate described by Thuéry[5]. No water molecule situated inside the nanotube has been reported for this compound.

Compounds **pht3** and **pht4** possess the same structure and will be discussed in parallel. Both structures have two distinct inorganic building blocks (Figure II.2.4) interconnected through the phthalate ligands.

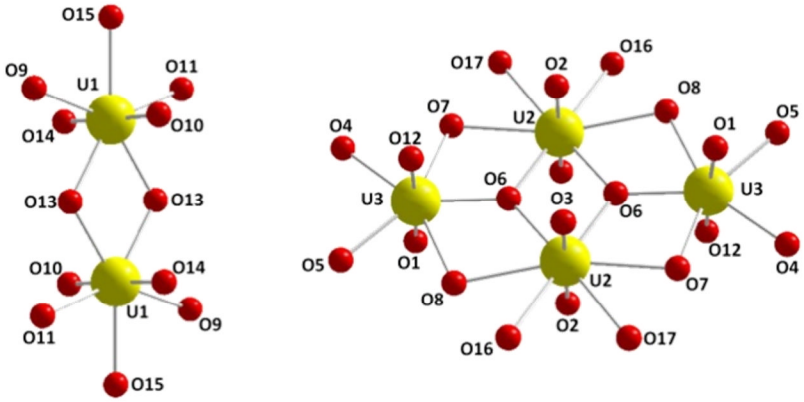

Figure II.2.4 Representation of the inorganic units of complexes **pht3** and **pht4**, dimeric unit (left) and tetrameric unit (right).

The first building unit, positioned on an inversion center (½ 0 0, *1d*) is a dinuclear species containing two 7-fold coordinated uranium atoms, both corresponding to the same crystallographic site (U1). This type of dimeric unit is quite common, appearing in more than twenty-four uranyl carboxylate complexes[6, 7] and it has been described in first chapter (figure I.2.14 α). Each uranium atom is linked with two short bonds by two uranyl type oxygen atoms (U=O = 1.773(9) - 1.778(10) Å and 1.764(4) - 1.767(4) Å for **pht3** and **pht4** respectively). The coordination sphere is completed by five other oxygen atoms.

Two of them (O13) ensure the edge shared between the two polyhedra and have been identified by bond valence calculations[8] to be μ_2-OH (calculated valence 1.2 v.u., expected value 1.2 v.u.) groups, other two (O9, O11) belong to the carboxylate groups of two different phthalate molecules, having a U—O distance range from 2.364(4) to 2.382(8) Å and the fifth oxygen atom in the equatorial plane (O15) has been attributed to a coordinating water molecule (U—O length of 2.439(8) Å and 2.438(4) Å for **pht3** and **pht4**, respectively). The second building unit, centered on an inversion center (½ ½ ½, *1h*), is tetranuclear and contains two independent uranium crystallographic sites. The tetrameric unit contains two uranium cations in 8-fold coordination (U2) and two in 7-fold coordination (U3) being previously encountered in the field of uranyl carboxylate complexes in structures containing the phthalic acid[4] and the acetic acid[9] as ligands (chapter I, figure I.2.17.a)). The coordination sphere of U2 is formed by two uranyl type oxygen atoms (U=O bond length ranging between 1.777(9) and 1.786(5) Å) in apical position (O2, O3) and other six oxygen atoms in the equatorial plane, from which four (O7, O8, O16, O17) belong to the carboxylate groups of the ligand, two (O7, O8) being shared with two different U3 atoms and the last two (O6 and O6#), completing the equatorial plane have been assigned as μ_3-oxo species (calculated valence of 2.08 v.u., expected value of 2.00), forming the edge shared between the two U2 hexagonal bipyramids. Each of the O6 oxo species is also shared with a U3 uranyl ion in order to form the tetranuclear SBU. The pentagonal bipyramid, belonging to the U3 uranium atom is also formed by two uranyl type oxygen atoms (U=O bond length ranging between 1.767(4) and 1.782(4) Å) O1 and O12 and in equatorial plane from the remaining five oxygen atoms, three are common to the adjacent U2 cation (O6-O8) and two (O4, O5) belong to the carboxylate groups of the ligand, groups ensuring the link between the two different SBUs. In the structure there are two different ligand molecules both adopting a μ_3-η_1:η_1:η_2:η_1 configuration, completing the bridge between the U2 and U3 polyhedra and at the same time ensuring the link between the two dimeric and tetrameric SBUs. This type of coordination generates infinite anionic chains (Figure II.2.5) of alternating dimeric and tetrameric inorganic units linked together by the phthalate ligand. The negative charge of the chain is

compensated by the countercation (K^+ for **pht3** and NH_4^+ for **pht4**). In both structures there are two crystallographic sites for the single charge cations, both between the chains, first (K1 or N1) situated nearby the dinuclear uranyl unit in a *1a* (0 0 0) special position and the second, situated between the tetrameric units in a *2i* general position has a 50% statistically occupancy. The cohesion between the chains is ensured by ionic interactions between the negatively charged chains and the single charged cations, by weak π-π interactions between the benzene rings and, in the case of complex **pht4**, by hydrogen bond interactions between the hydrogen atoms belonging to the ammonium group and the uranyl type oxygen atoms.

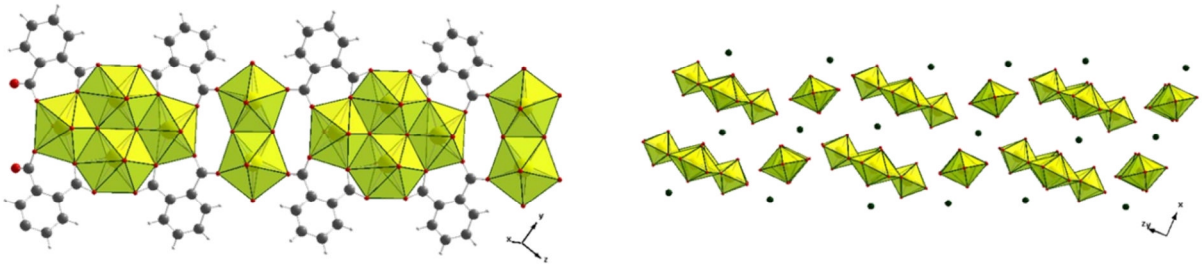

Figure II.2.5 Representation of complex **pht3** and **pht4** anionic single chain a) and countercation position relatively to the inorganic blocks, view along b axis (the ligand molecules have been removed for clarity) b).

II.3 . Synthesis

The compounds have been synthesized hydrothermally under autogenous pressure using 23 mL Teflon-lined Parr type autoclaves from a mixture of uranyl nitrate hexahydrate ($UO_2(NO_3)_2 \cdot 6H_2O$, Merck 99%), potassium hydroxide (KOH, Prolabo 85%), ammonia solution (Prolabo, 28%), phthalic acid (Acros Organics 99%) and deionized water. The starting reagents are commercially available and have been used without further purifications.

Compound **pht1** has been obtained by statically heating under hydrothermal conditions at 100°C a mixture of 0.502g (1 mmol) $UO_2(NO_3)_2 \cdot 6H_2O$, 0.083g (0.5 mmol) phthalic acid, 0.4 ml solution 2M ammonia and 4.6 mL (256 mmol) H_2O during 24h. The solution pH measured after synthesis was 2.1. The initial mixture pH could not be measured accurately due to the slow dissolution

of the organic ligand, constant modifying the reading. By the time the ligand is completely dissolved, an intermediate phase (yellow precipitate) began to appear, again modifying the pH reading. This phenomenon appears in all the syntheses being accentuated in the cases where the ligand has a very low solubility in water. After the hydrothermal reaction, all the ionic species are at equilibrium in solution and the final pH can be accurately measured. Similar results (pure phases) have been obtained using as pH corrector other organic or inorganic bases such as KOH, diaminopropane, hydrazine. The resulting yellow product has been filtered off, washed with water and dried at room temperature. The product has been analyzed by scanning electron microscopy and shows irregular needle like crystals with variable sizes of maximum 1 mm (Figure II.3.1).

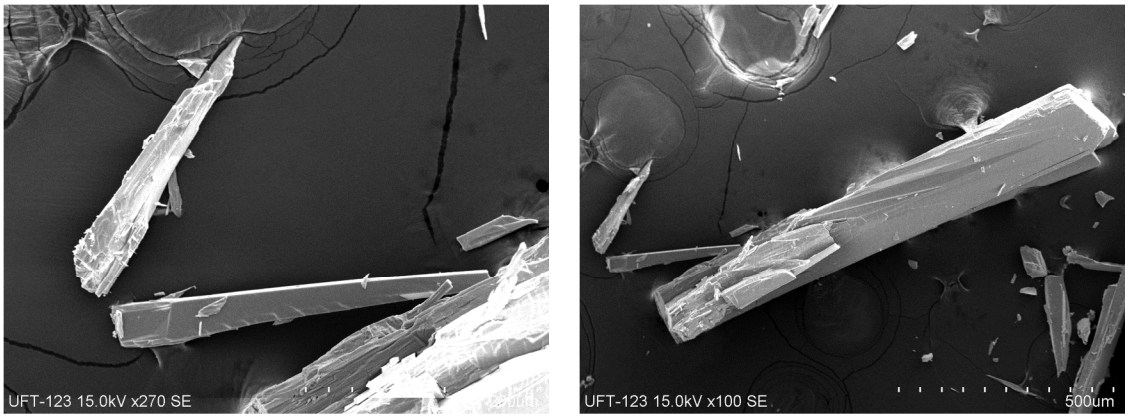

Figure II.3.1 SEM images of crystals belonging to complex **pht1**.

The synthesis method described in literature[1] implies the use of a lower temperature (80°C) and the use of a sealed glass vial. This indicates that phase **pht1** is obtained over a wide range of temperature (below 180°C), not requiring special reaction conditions such as high temperature or pressure.

For complex **pht2**, a mixture of 0.502 g (1 mmol) uranyl nitrate, 0.082 g (0.5 mmol) phthalic acid, 0.6 mL solution 1M KOH (0.6 mmol) and 4.4 mL (244 mmol) H_2O have been placed in a Parr type autoclave and heated statically during 24h at 200°C. The solution pH after reaction was 1.6. The obtained yellow product has been filtered off, washed with water and dried at room temperature. The obtained product has been analyzed by scanning electron microscopy and shows hexagonal shaped elongated crystals of millimeter size (Figure II.3.2).

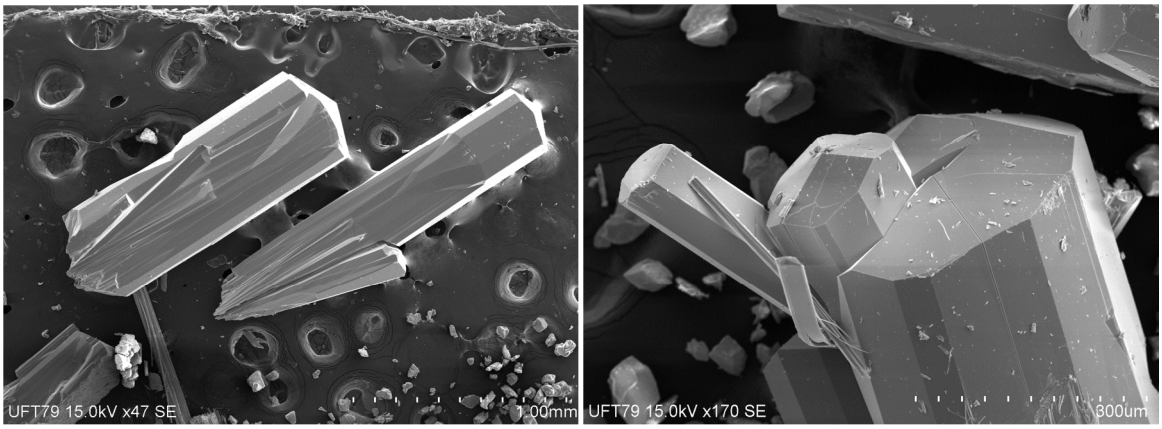

Figure II.3.2 SEM images of complex **pht2** crystals.

Due to the large size of the obtained crystals, photo images have been taken under the optic microscope, from which it can be observed a slightly change in crystal morphology when changing the nature and quantity of the pH moderator used in reaction. When using KOH the obtained crystals are very long and thin needle-like. When using ammonia solution in small quantity 0.2 mL sol 2M (0.4 mmol) the obtained crystals are also hexagonal based prisms but this time having a shorter height and a larger base (Figure II.3.3).

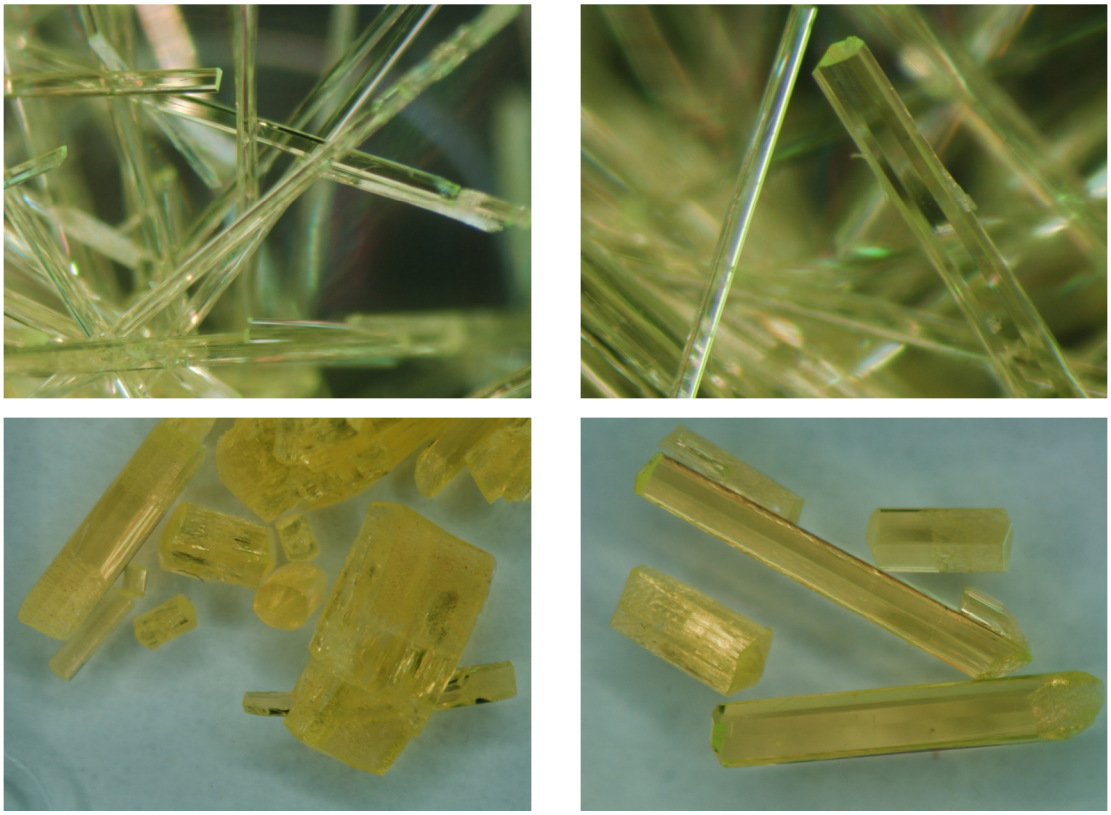

Figure II.3.3 Optic microscope photos of complex **pht2** crystals obtained using as pH corrector KOH (top) and ammonium (bottom).

Complex **pht3** has been synthesized by placing 0.502 g (1 mmol) uranium nitrate, 0.082 g (0.5 mmol) phthalic acid, 1.6 mL solution 1M (1.6 mmol) KOH and 3.4 mL (189 mmol) H_2O in a Parr bomb and statically heating the mixture during 24h at 200°C. The obtained yellow-orange product has been filtered off, washed with watered and dried at room temperature. The size of the obtained crystals is between 100 and 200 μm (Figure II.3.4).

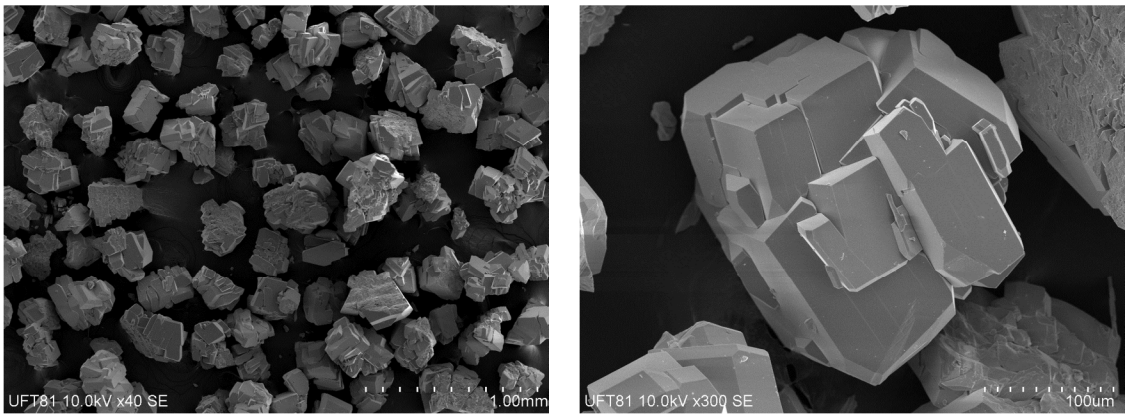

Figure II.3.4 SEM images of compound **pht3** crystals.

The last compound in this series, complex **pht4** has been synthesized by placing 0.502 g (1 mmol) uranium nitrate, 0.082 g (0.5 mmol) phthalic acid, 1.8 mL solution 2M (3.6 mmol) ammonia and 3.4 mL (189 mmol) H_2O in a Parr bomb and statically heating the mixture during 24h at 200°C. The obtained yellow-orange product has been filtered off, washed with watered and dried at room temperature. The size of the obtained crystals is between 80 and 300 μm (Figure II.3.5).

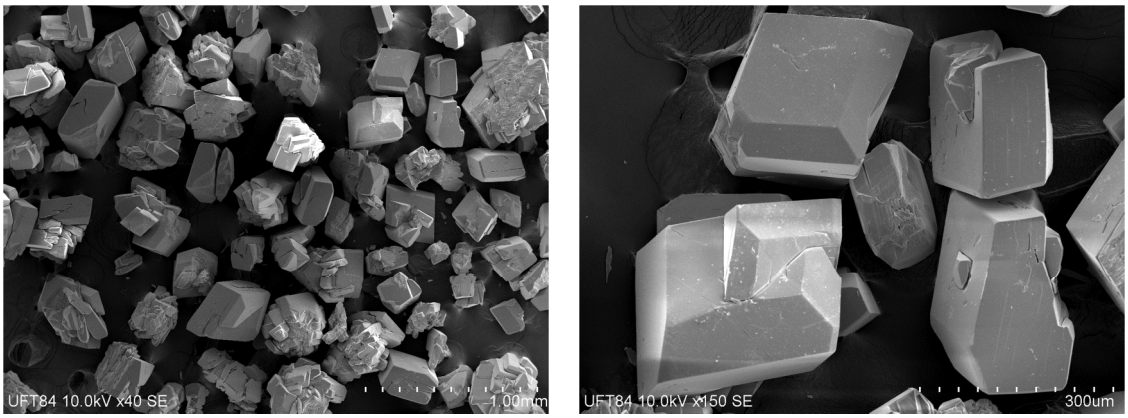

Figure II.3.5 SEM images of compound **pht4** crystals.

All four complexes have been obtained using in synthesis the same metal / ligand molar ratio of 2 and gradually modifying the reaction temperature and pH

(all the declared pH values are referring to the final pH values measured after the synthesis). The information about the uranyl - phthalate - H_2O - base system is the following: at low pH (0.9-1.6), independent of the nature of the pH corrector, the monomeric phases (complexes **pht1** and **pht2**) have been obtained. At this pH the ratio between the two monomeric phases is dictated by the applied temperature: complex **pht1** has been obtained pure using a synthesis temperature of 100°C (low-temperature phase) and complex **pht2** at a temperature of 200°C (high-temperature phase). Between 100 and 200°C, these two phases are formed, but **pht1** disappeared when increasing the temperature together with the formation of **pht2** (Figure II.3.6).

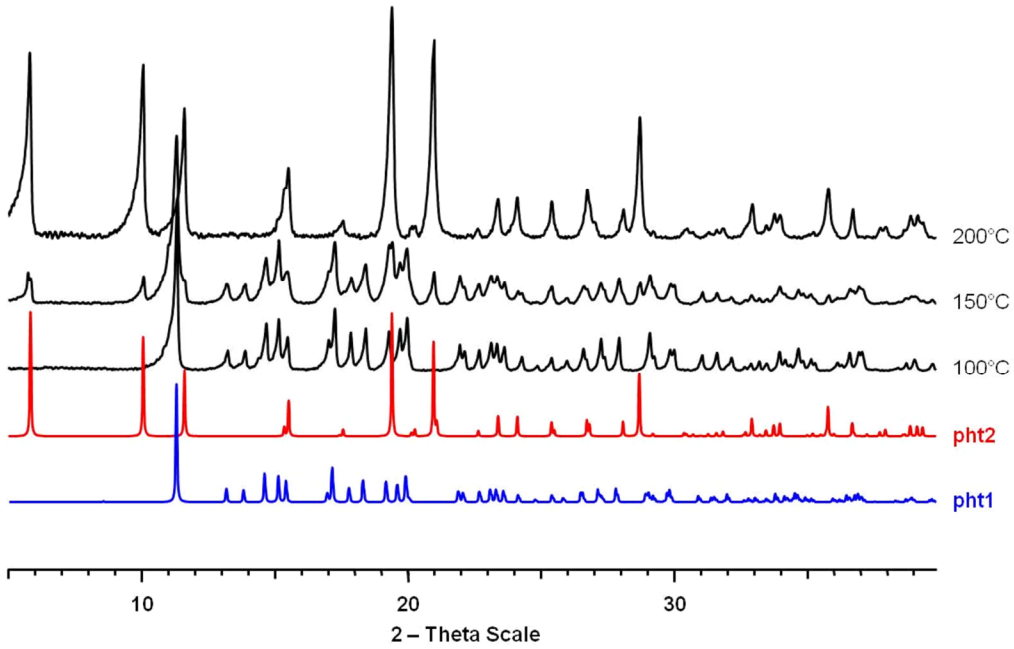

Figure II.3.6 Comparison between the crystal structure simulated PXRD patterns of complex **pht1** (blue), complex **pht2** (red) and experimental patterns of products synthesized at different temperatures (black).

At high pH (between 2 and 4), independent of the applied temperature (as long as it is in the hydrothermal domain) complexes **pht3** and **pht4** are synthesized as a function of the pH moderator's nature KOH or NH_4OH (Figure II.3.7-Figure II.3.8). Working at intermediate pH values, the obtained product is a mixture of monomer-based phase (complex **pht1** or **pht2**) with the dimer-tetramer-based phase (complex **pht3** or **pht4**).

Working at a pH superior to 3.5, the dimer-tetramer-based phase becomes impure, the impurity being formed by different uranyl oxo - hydroxide pure inorganic species (Figure II.3.7).

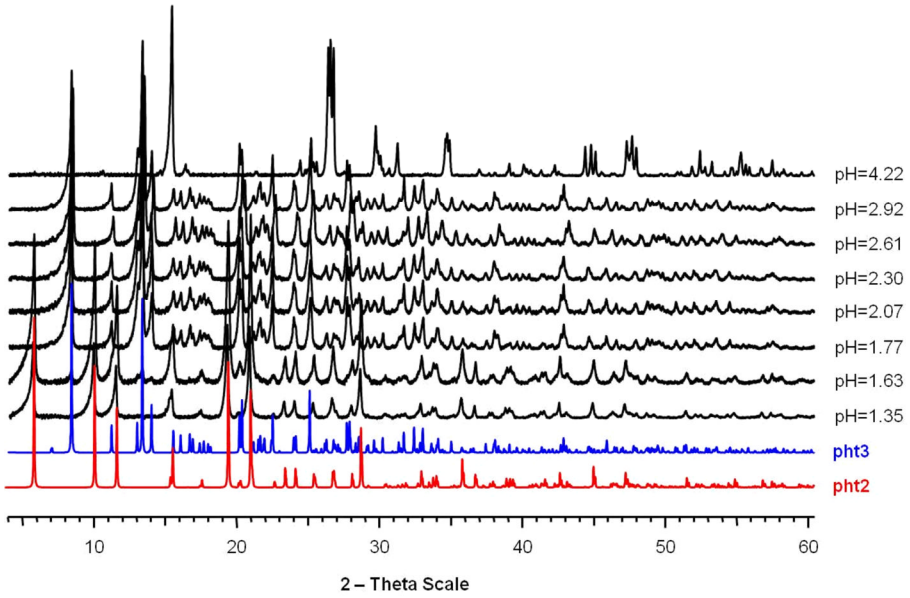

Figure II.3.7 PXRD patterns representation of the phase evolution as a pH function in the UO_2^{2+}-pht^{2-}-K^+-H_2O system. It shows the formation of **pht2** at low pH and then the formation of **pht3** a higher pH, from pH = 1.63.

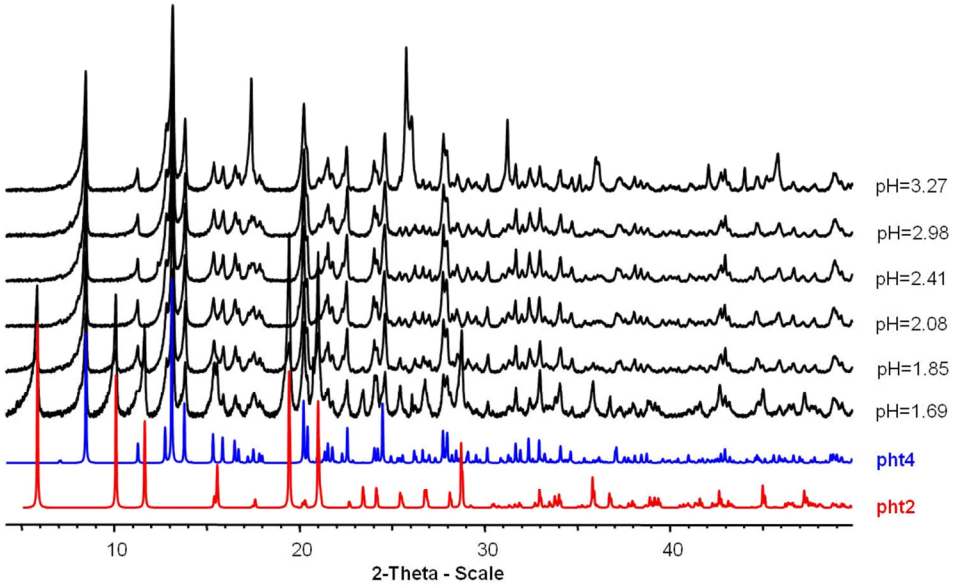

Figure II.3.8 PXRD patterns representation of the phase evolution as a pH function in the UO_2^{2+}-pht^{2-}-NH_4^+-H_2O system.

The hydrolysis process of uranyl cation in the particular uranyl-phthalate-base-water system (Figure II.3.9) is in good agreement with the study on the hydrolyzed species distribution as a function of pH presented in chapter I (Figure I.3.1) excepting the early apparition (pH = 2) of tetranuclear which in the mentioned study occurs at a pH value above 4. This difference can be easily explained by the two different working temperatures. The hydrolysis study has been conducted at room temperature and the phthalate ligand manages to stabilize the tetranuclear block under hydrothermal conditions at 200°C.

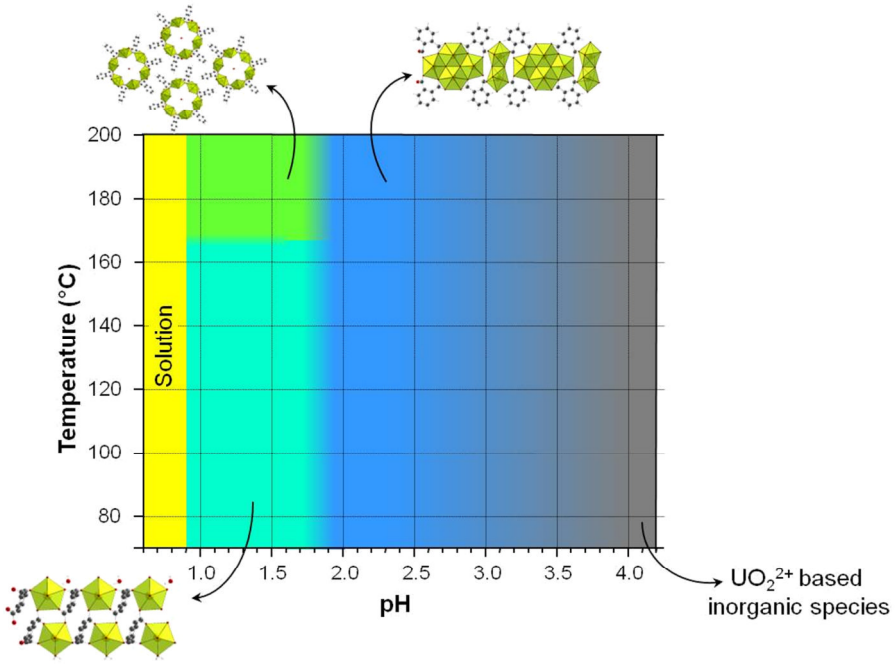

Figure II.3.9 Phase diagram (temperature and pH) for the uranyl phthalates system.

The purity of each of the phases has been established by comparing the simulated powder X-ray diffraction pattern from the crystal structure with the experimental PXRD pattern (see supplementary data chapter figures VIII.1.1 to VIII.1.4) and was confirmed by the SEM and thermogravimetric analysis.

II.4 . Thermal characterization

The thermogravimetric analyses and thermo-diffraction experiments have been conducted in parallel for each phase.

For **pht1** **$[(UO_2)(pht)(H_2O)]\cdot H_2O$**, the thermal degradation takes place in two steps. A first step (obs.: 7.6%) occurs around 95°C and corresponds to the departure of the water molecules, including also the coordinating water (7.7% calculated). This step is observed in the TDA curve (Figure II.4.1-left) as a small endothermic peak due to the water removal. At the same temperature its crystalline structure is changing (Figure II.4.1-right), resulting in an intermediate complex stable in the range of 100 to 400°C. This intermediate phase possesses a high crystallinity and most probably is the dehydrated form of complex **pht1**, with the corresponding chemical formula '$[UO_2(pht)]$', the uranyl ion being coordinated only by the carboxylate groups of the ligand. The resulting

polyhedron of the uranyl center would have a tetragonal bipyramidal geometry ($(UO_2)O_4$).

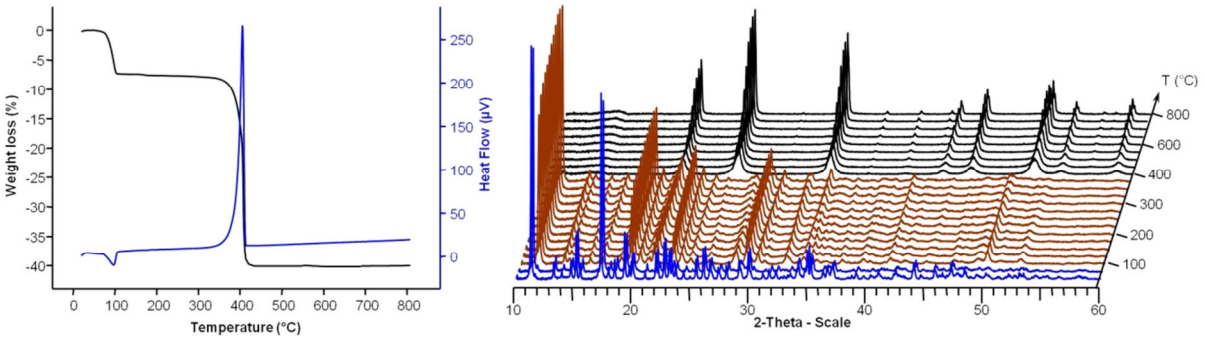

Figure II.4.1 Thermal behavior and stability of phase **pht1**. TGA/TDA curves (left), PXR thermo-diffraction patterns (right).

The crystalline structure of this intermediary phase could not be determined due to the poor quality PXRD pattern data and the instability of **pht1** crystals at heating, making impossible the collection of high temperature single crystal X-ray diffraction structural data. Starting from 350°C, the crystalline edifice of the intermediate phase starts to collapse. The organic part of the complex begins to burn, giving an intense exothermic peak in the TDA curve. The weight loss appearing in the TGA curve for this second step is 32.6% (32.6% calculated) and corresponds to the complete oxidation of the ligand and also the partial reduction of uranium from 6 to 5.33. The resulting product was identified as U_3O_8 (PDF No: 074-0562). Combining the two steps, there is an overall weight loss of 40.2% (40.3% calculated), corresponding to the entire degradation process. The degradation equation is presented below.

$$[(UO_2)(C_8H_4O_4)(H_2O)](H_2O) \xrightarrow[-2H_2O]{95°C} [(UO_2)(C_8H_4O_4)] \xrightarrow[-8CO_2\ -2H_2O]{350°C\ +7{,}3O_2} 1/3\,U_3O_8$$

For phase **pht2** $\mathbf{[(UO_2)(pht)(H_2O)]\cdot 0.33H_2O}$, the TGA curve shows different weight loss steps. A first event occurs around the temperature value of 100°C, without any visible changes in the TDA curve or in the PXRD patterns (Figure II.4.2). It consists in the loss of the free water molecules situated inside the nanotubes. The second step at 200°C is well defined from the TGA curve and giving a low intensity endothermic peak. This event gives also significant changes in the PXRD pattern since the compound passing through an amorphous

intermediate phase. During this transformation, the structure looses all the water molecules, including the uranyl coordinating ones. As consequence of this transformation, the initial crystalline edifice is completely and irreversibly destroyed. The first two steps are giving a total mass loss of 5.3% (obs.) corresponding to the loss of 1.33 water molecules per uranyl unit (calc: 5.2%). The occupancy of 0.33 free water molecules per uranyl unit has been established from the single crystal X-ray diffraction refinement and its in good agreement with the TGA experiment (obs: 0.28 free water molecules per uranyl unit).

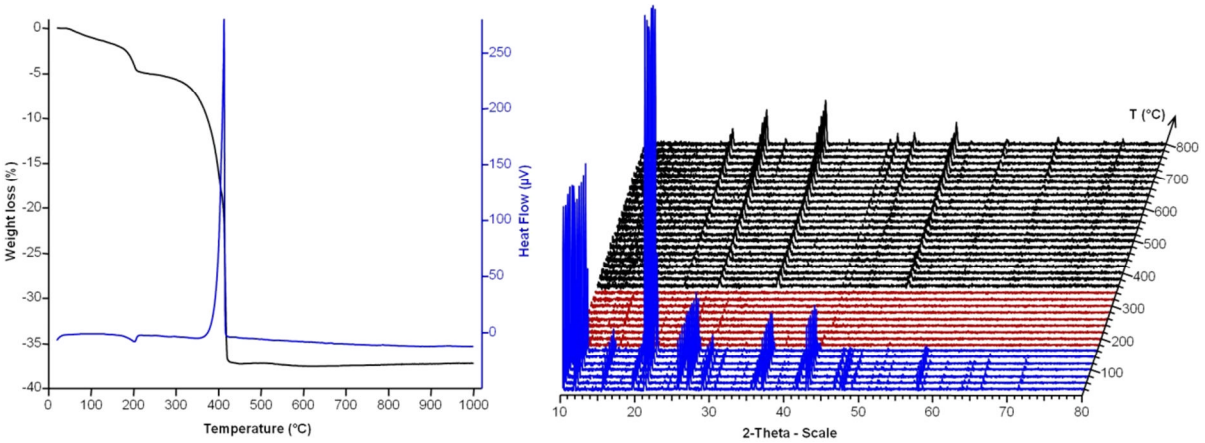

Figure II.4.2 Thermal behavior and stability of phase **pht2**. TGA/TDA curves (left), XRD thermo-diffraction (right).

The third step begins around 360°C and consists in the thermal decomposition of the organic ligand. This transformation gives an intense sharp exothermic peak in the TDA curve and it coincides in the thermodiffraction pattern with the slow crystallization of the final uranium oxide, which has been identified as α-U_3O_8 (PDF No: 002-0276). The overall mass loss corresponding to the transformation of the initial complex into the final uranium oxide is of 37.6%, in good agreement with the calculated one (38.7%) using the degradation equation below:

$$3[(UO_2)(C_8H_4O_4)(H_2O)]\cdot 0.33H_2O \xrightarrow[+10O_2\ -3.33H_2O\ -8CO_2]{400^{\circ}C} U_3O_8$$

The residuum (U_3O_8) obtained by the degradation of the **pht2** phase has been proven to maintain a morphology close to the one of the initial crystals (Figure II.4.3)

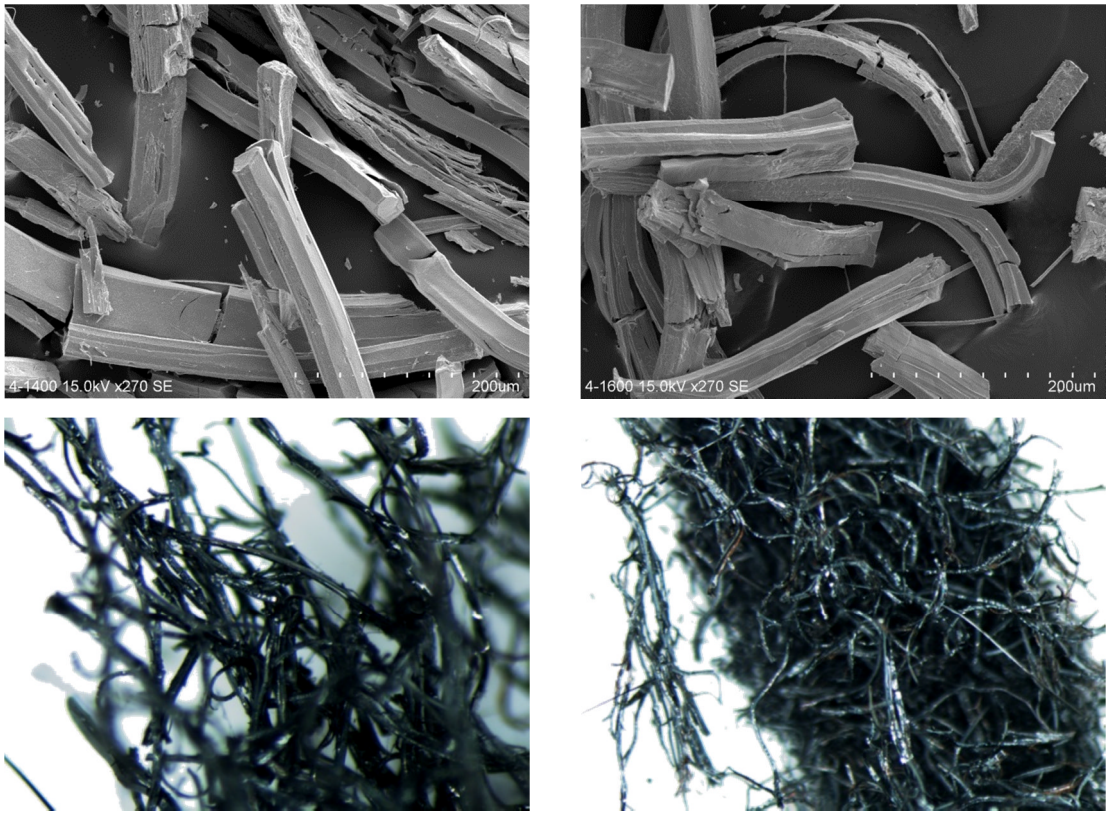

Figure II.4.3 SEM images (top) and optical microscope pictures (bottom) of the **pht2** degradation product.

In the case of **pht3** **$K[(UO_2)_3O(OH)(H_2O)(pht)_2]$** phase the thermal degradation takes place in three steps (Figure II.4.4). First event could correspond to the loss of the coordinating water molecules of the dimeric SBU (calc. 1.47%). It takes place between 60 and 200°C, being badly defined, and apparently it has no correspondence in the crystal structure since no transition appearing in the PXRD diagram in this temperature interval. The second step takes place between 220 and 260°C and has almost the same value of the weight loss as the first one, but this time better contoured. This step could be assigned to the loss of the hydroxo bridge, also belonging to the dimeric SBU. This loss also influences the crystal structure and a transition is recorded in the diffraction pattern at 220°C. The third event (the most well defined in the TGA curve) has been assigned to the total loss of the organic ligand. This fact is also confirmed by the intense exothermic peak in the heat flow diagram, appearing in the same range of temperature (360 - 400°C).

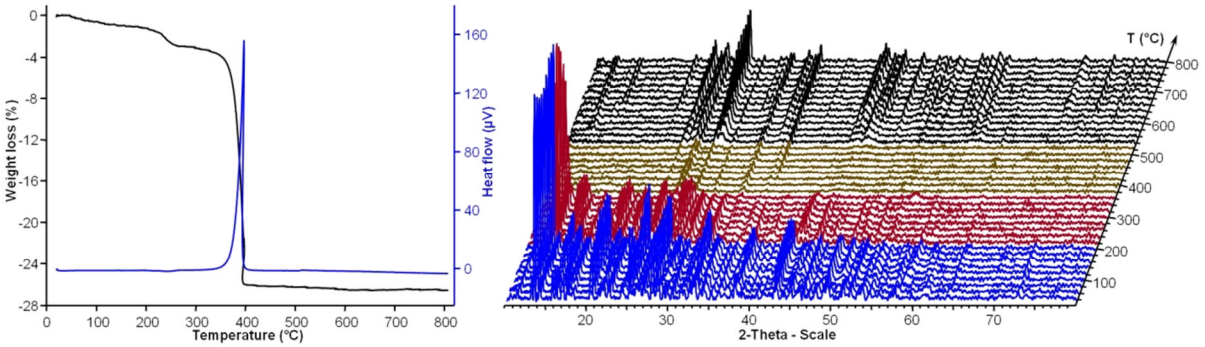

Figure II.4.4 Thermal behavior and stability of **pht3** phase. TGA/TDA curves (left), XRD thermo-diffraction (right).

During this step, the crystalline edifice is completely destroyed and the PXRD diagram corresponds to an amorphous compound in this temperature range. From 540°C, new sets of Bragg peaks are observed and these been identified as a mixture of two mixed oxides $K_2U_7O_{22}$ (PDF No. 029-1060) and $K_2U_4O_{13}$ (PDF No. 029-1059) having an approximate ratio between them of 2 (chapter VIII Figure VIII.1.5).

Combining the three degradation steps from the TGA curve there has been obtained an overall weight loss of 26.5%, corresponding to a calculated value of 26.3%, value obtained from a proposed degradation equation given below.

$$6K[(UO_2)_3(C_8H_4O_4)_2(OH)(H_2O)] \xrightarrow[+90O_2\ -33H_2O\ -96CO_2]{380°C} 2K_2U_7O_{22} + K_2U_4O_{13}$$

For the **pht4** $NH_4[(UO_2)_3O(OH)(H_2O)(pht)_2]$ complex, the structure is stable up to 200°C. Increasing the temperature, the phase begins to degrade, passing first through a crystalline intermediate stable up to 300°C (Figure II.4.5).

From 350°C upward the final uranium oxide U_3O_8 (PDF No. 089-4906) begins to crystallize. During the degradation of this phase there have not been observed any amorphous intermediates. From the TGA curve there can be identified three degradation steps, from which first two are not well defined and take place without major changes in the heat flow, the third one being attributed to the organic ligand degradation, exhibiting a major exothermic peak in the heat flow curve.

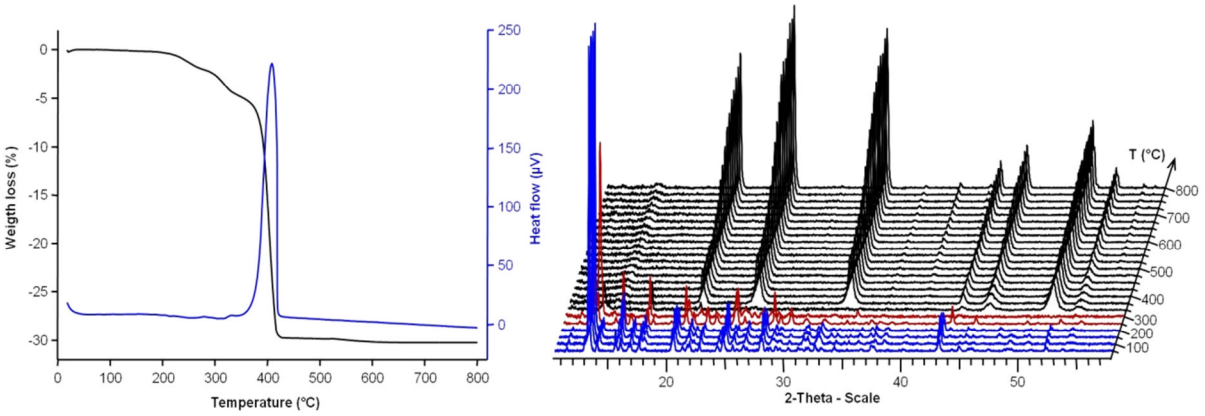

Figure II.4.5 Thermal behavior and stability of **pht4** phase. TGA/TDA curves (left), XRD thermo-diffraction (right).

Adding the three weight loss steps it has been obtained an overall value of 30.3%. This percentage is in good agreement with the calculated one (30.3%) using the thermal degradation equation displayed below.

$$NH_4[(UO_2)_3(C_8H_4O_4)_2O(OH)(H_2O)] \xrightarrow[-NH_3\ -16CO_2\ -4H_2O]{350°C\ +13.5O_2} U_3O_8$$

Starting from the idea of obtaining advanced nuclear fuels (especially uranium carbides) by thermal degradation of the obtained MOFs, the **pht2** has been the subject of multiple tries of degradation under different conditions in order to obtain the desired uranium carbide. The obtained data are resumed in Table II.4.1.

Table II.4.1 The various thermal degradation experiments conducted on pht2 phase

Heating time	Heating temperature	Atmosphere	Crucible material	Furnace inner tube material	Degradation Product
1h	1400°C	Air	Alumina	Alumina	U_3O_8
4h	1600°C	Air	Alumina	Alumina	U_3O_8
24h	1600°C	Ar	Alumina	Alumina	UO_2
24h	1600°C	95% Ar 5% H_2	Graphite	Alumina	UO_2
4h	850°C	H_2	Graphite	Quartz	UO_2

Unfortunately due to the high ratio of oxygen atoms in the initial phase and experimental issues (requirement of graphite furnace), the uranium carbide could not be obtained in all of the experiments. Varying different degradation parameters it has been observed that only the atmosphere inside the furnace has an influence on the final product. If an oxygen rich atmosphere is used, the uranium will be stabilized in a high oxidation state oxide (U_3O_8). If the atmosphere is inert (Ar), mild reducing (Ar + 5% H_2) or heavy reducing (pure H_2)

the uranium will be stabilized in a lower oxidation state oxide (UO_2). The temperature and the heating time had influences only on the crystallinity of the final product. The nature of the crucible or of the furnace inner tube had no notable influence on the nature of the final degradation products. Due to the negative result obtained on the **pht2** phase, no other degradation under reducing atmosphere experiments have been conducted with the other phases described in the thesis work.

II.5 . Spectroscopic characterization

Infrared spectroscopy

The infrared spectrum of **pht1** (Figure II.5.1) shows in the 2900 - 3800 cm^{-1} region three absorption peaks corresponding to the water molecule vibrations. All three have been attributed to the O—H stretching vibrations. First two belong to the free water molecules present in the structure, with two bands at 3588 and 3523 cm^{-1} being v_{asym}. The third broad peak centered at 3064 cm^{-1} covers stretching vibrations of water molecules involved in the hydrogen bond interactions (free water and coordinated water)[10].

Another region of interest is between 1600 and 1200 cm^{-1}, corresponding to the ligand specific vibrations. Those of carboxylate groups are the easiest to identify. The v_{asym}(COO) and v_{sym}(COO) vibrations give absorption peaks at 1509 and 1395 cm^{-1} respectively[11].

The third region is located in the IR spectrum below 1000 cm^{-1}, corresponding to the metal - oxygen bond vibrations, from which, the most important is the asymmetric v_3(U=O) bond vibration. This stretching vibration gives an intense peak situated at 927 cm^{-1} for this compound[12].

Counting on an empirical equation[13], the uranium oxygen distances can be calculated from the position where the specific peaks appear in the IR spectrum. The equation is given below.

$$\boldsymbol{d\,(U-O)(pm) = 9141[\nu_3(cm^{-1})]^{-2/3} + 80.4}$$

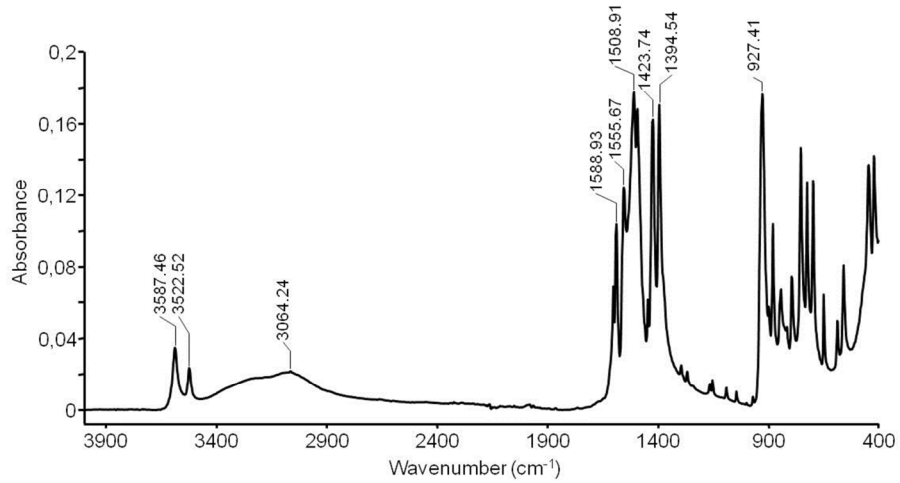

Figure II.5.1 Infrared spectrum of phase **pht1**.

Using this equation there have been found good correlations between the U—O distances given by the single crystal XRD technique and the one calculated from the IR spectrum, especially for the U═O bond, giving intense absorption peaks in the region of 900 cm^{-1}. The other U—O bonds from the equatorial plane give v_3 IR absorption peaks below this value, sometimes even below 400 cm^{-1}, region inaccessible for our IR spectrometer. For the U═O bond, the bond length calculated from the IR spectrum of 1.77 Å is in good concordance with the values from the single crystal X-Ray diffraction technique of 1.765(6) Å and 1.768(6) ÅÅ.

The **pht1** phase behavior upon heating has been followed by *in situ* infrared spectroscopy at different temperatures up to 210°C (Figure II.5.2). Three regions giving information about the thermal transformations have been examined. First region between 3640 and 3500 cm^{-1} reflects the presence of water molecules at room temperature (at 3588 and 3523 cm^{-1}). Starting with the temperature of 90°C in this region it can be observed the rapid disappearing (first order type transition) of the two peaks, corresponding to the departure of water molecules. The second domain at around 940 cm^{-1}, shows an important shift of the absorption peak belonging to the U═O bond vibration, from 928 cm^{-1} to 953 cm^{-1}. Applying the equation for bond length calculation it has been found a decreased value of the U═O bond length from 1.765 Å to 1.748 Å. This fact confirms major changes in the uranyl coordination environment, which can be reduced to a six-fold coordination sphere, as suggested by the chemical formula of the transient phase 'UO_2(pht)' from the TGA experiment. U=O distances are rather short for six-fold coordinated uranyl centers as we will observe in a series

of $UO_2(L)$ (L = ditopic carboxylate ligand) (see chapter V). The third region of interest is between 1650 and 1300 cm^{-1} (vibrations of C-O and C-C bonds). Upon increasing the temperature it can be observed a restructuring of the ligands molecules into a more symmetrical conformation. Three of the peaks appearing as doublets at room temperature, become shifted and converged to singlets at 210°C. The high temperature IR spectroscopy experiments have been conducted only for the phases that present major changes in the $T_{amb.}$-210°C temperature interval.

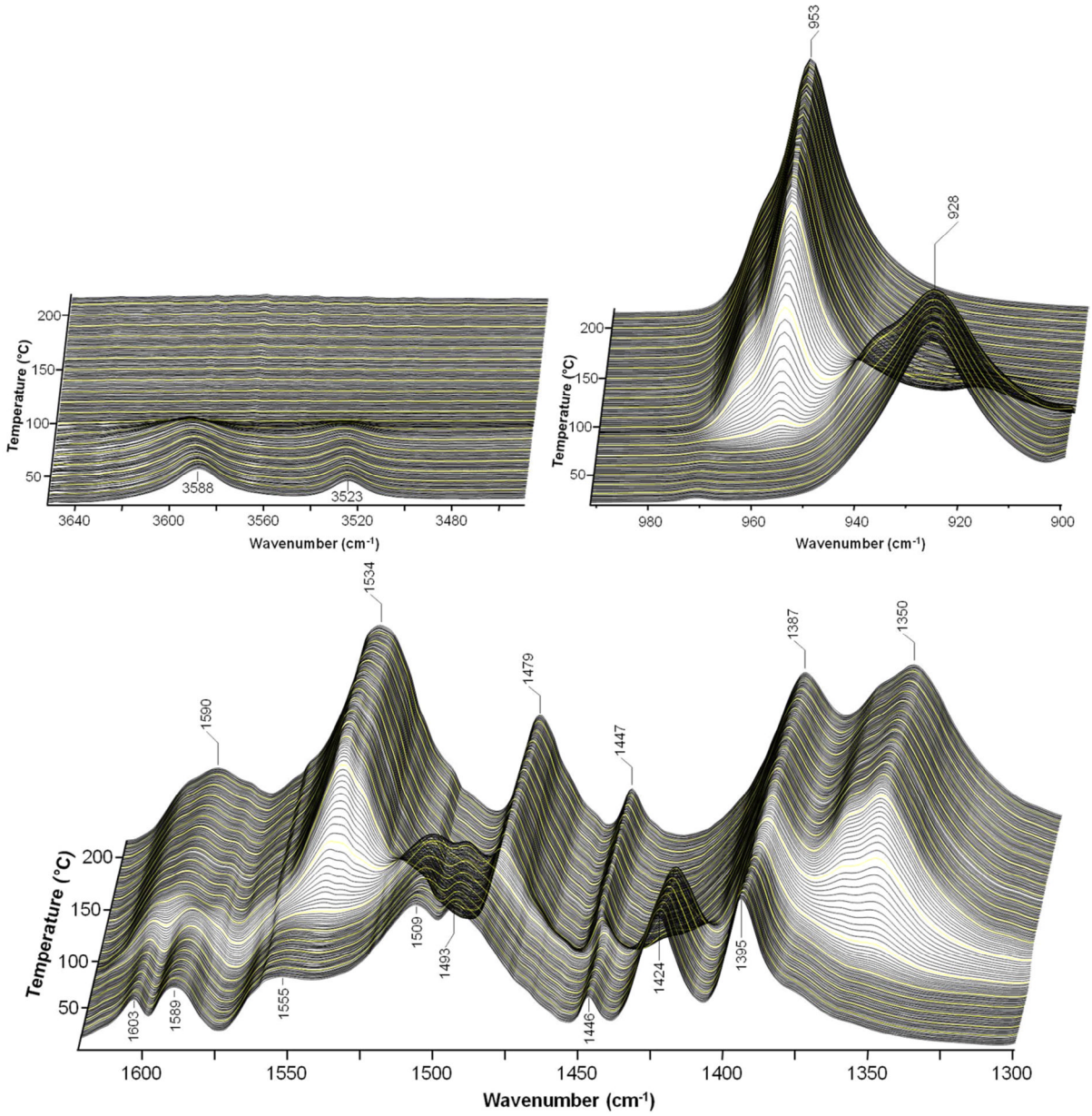

Figure II.5.2 Phase transformation of **pht1** observed by *in situ* infrared spectroscopy from room temperature to 210°C.

Infrared spectrum of **pht2** (Figure II.5.3) shows a broad absorption band centered at 3446 cm^{-1}, indicating the presence of water molecules and assigned to the ν(O—H) stretching vibration of water molecules. The peak appearing as a shoulder around 1596 cm^{-1} can be assigned to the δ(O—H) bending vibration of the same molecules.

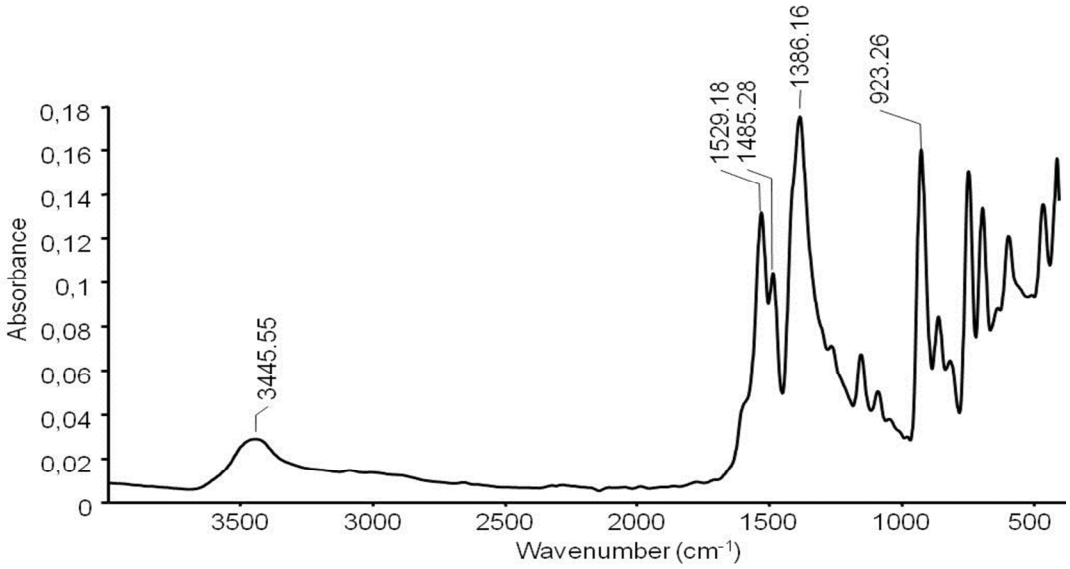

Figure II.5.3 Infrared spectrum of phase **pht2**.

The specific vibrations of the organic ligand give absorption maxima in the 1580 - 1000 cm^{-1} range. The ν_{asym}(COO) has been identified as a doublet at 1529 and 1485 cm^{-1} respectively, the ν_{sym}(COO) appearing at 1386 cm^{-1} as a much more intense single peak[11].

The uranyl related vibrations (ν_{asym}(U=O)) appear in the IR spectrum as absorption maxima at 923 cm^{-1}. All the other uranium - oxygen bond vibrations give absorption maxima below this value[12]. Based on this position, the U=O bond length has been calculated, obtaining a value of 1.768 Å, which is in good concordance with the average interatomic distances obtained by single crystal X-ray analysis technique (1.760(3) Å and 1.771(3) Å).

For the phase **pht3**, the IR spectrum (Figure II.5.4) shows a low intensity broad absorption band centered at 3245 cm^{-1} (ν_{sym}OH) which combined with the small peaks at 3644 cm^{-1}, 3566 cm^{-1} (ν_{asym}OH) and 1673 cm^{-1} (δHOH) indicating the presence of water molecules in the compound[10].

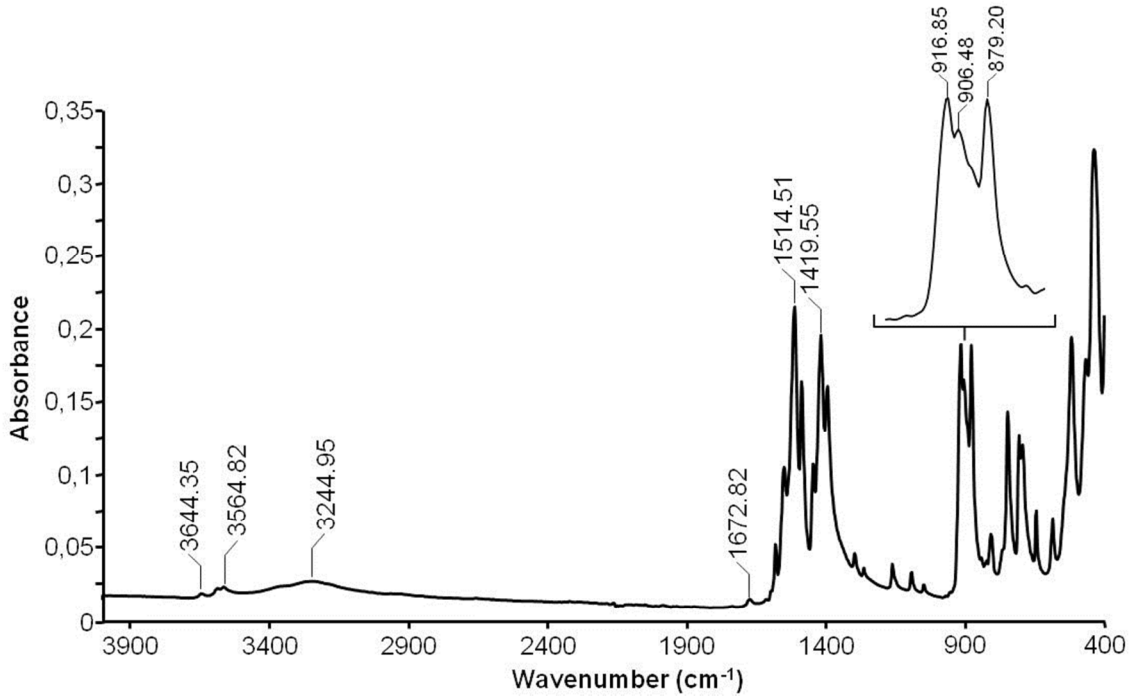

Figure II.5.4 Infrared spectrum of phase **pht3**.

In the region situated between 1640 and 1000 cm^{-1} are appearing the absorption maxima belonging to the organic ligand specific vibrations. From these, the most important are the ones of the carboxylate groups, giving peaks, for this complex as a doublet, at 1515 - 1488 cm^{-1} $\nu_{asym}(COO)$ and 1420 - 1396 cm^{-1} $\nu_{sym}(COO)$[11].

The peak attributed to the $\nu_3(U{=}O)$ bond vibration is broad and split, having two maxima and one shoulder. Applying the equation for bond length calculations, for the first maximum situated at 917 cm^{-1} it has been obtained a bond length value of 1.773 Å, value which is in good concordance with the values refined from the single crystal X-ray diffraction experiment of 1.773(9) Å and 1.778(10) Å for the uranium atoms constituting the dinuclear SBU. Calculating the bond length using the next two absorption peaks from 907 and 879 cm^{-1}, there have been obtained the values of 1.780 and 1.800 Å, which are attributed to the uranyl ions constituting the tetrameric SBU. The diffraction experiment gave the range of the U=O bond lengths between 1.774(9) Å and 1.783(9) Å. The value calculated from the last IR absorption peak is not included in this range, the corresponding maximum being shifted to lower wavenumbers. This shift can be explained by the influence exercised by the single charge cation, situated between the chains, on the uranyl type oxygen atoms from the SBUs, confining

their vibration. The distances between the potassium cation and the uranyl type oxygen atom are in a range 2.81(1) - 3.03(1) Å.

In the case of **pht4** phase, the infrared spectrum (Figure II.5.5) is quite similar to the one of **pht3**. The water presence in this compound is evidenced by three absorption peaks at 3571 cm^{-1} ($\nu_{asym}O{-}H$), 3232 cm^{-1} ($\nu_{sym}O{-}H$) and 1676 cm^{-1} ($\delta H{-}O{-}H$). Vibrations of the N–H bonds from ammonium groups can also be observed at 3232 cm^{-1} (broad band).

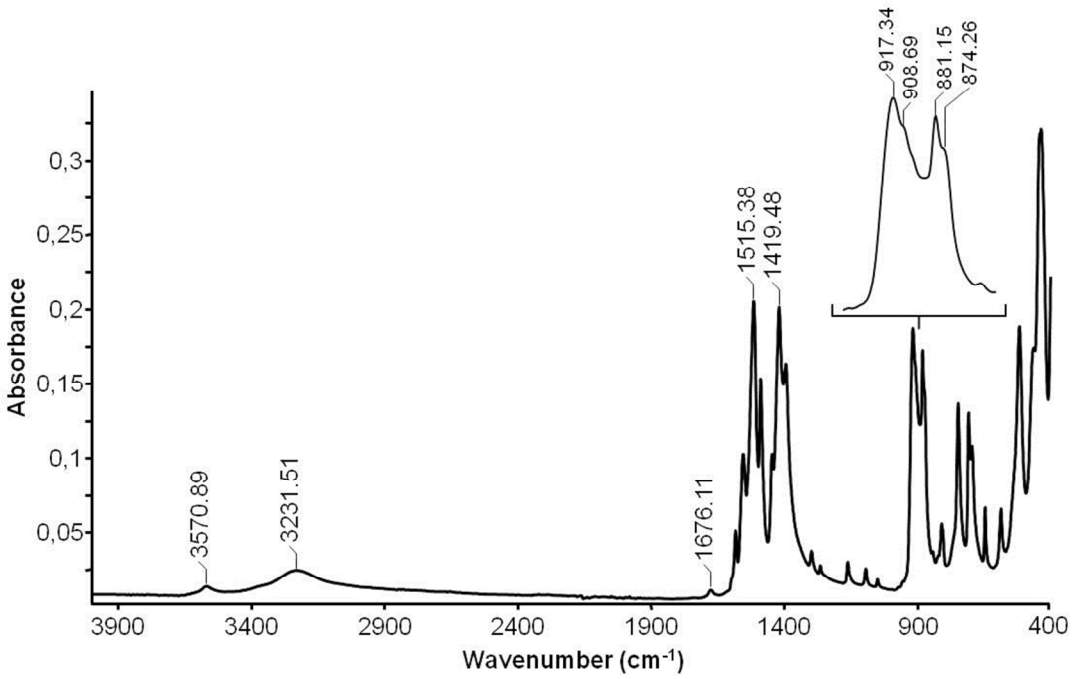

Figure II.5.5 Infrared spectrum of complex **pht4**.

The absorption peaks belonging to the phthalate vibrations are also in the 1640 - 1000 cm^{-1} region. The COO vibration bands are doubled and situated at the same wavenumbers as in the case of **pht3**.

The absorption peak corresponding to the U=O bond's vibration is also split and broad, having two maxima, each possessing one shoulder. The bond length calculated values from the position of these peaks are in the range 1.772 - 1.804 Å, all being larger than the values obtained from the single crystal X-ray diffraction experiment ranging from 1.764(4) Å to 1.786(5) Å. The reason could be the same interaction between the single charge cation and the uranyl type oxygen atoms, modifying their vibration and shifting the corresponding absorption peaks to lower wavenumbers. The distances between the nitrogen

atom of the ammonium group and the uranyl type oxygen atoms vary in the range of 2.92(1) to 3.17(1) Å.

Fluorescence Spectroscopy

The fluorescence experiments were conducted at room temperature, under excitation at 365 nm with the different powdered samples. The spectra were recorded between 440 nm and 640 nm, domain where the uranyl ion gives typical fluorescence emission in solid materials, as well as in solutions. As standard, it has been used the fluorescence emission spectrum of the uranyl dinitrate hexahydrate ($UO_2(NO_3)_2 \cdot 6H_2O$). This spectrum exhibits 6 peaks characteristics to the uranyl ion, 4 of them sharp and intense and 2 broad and of low intensity.

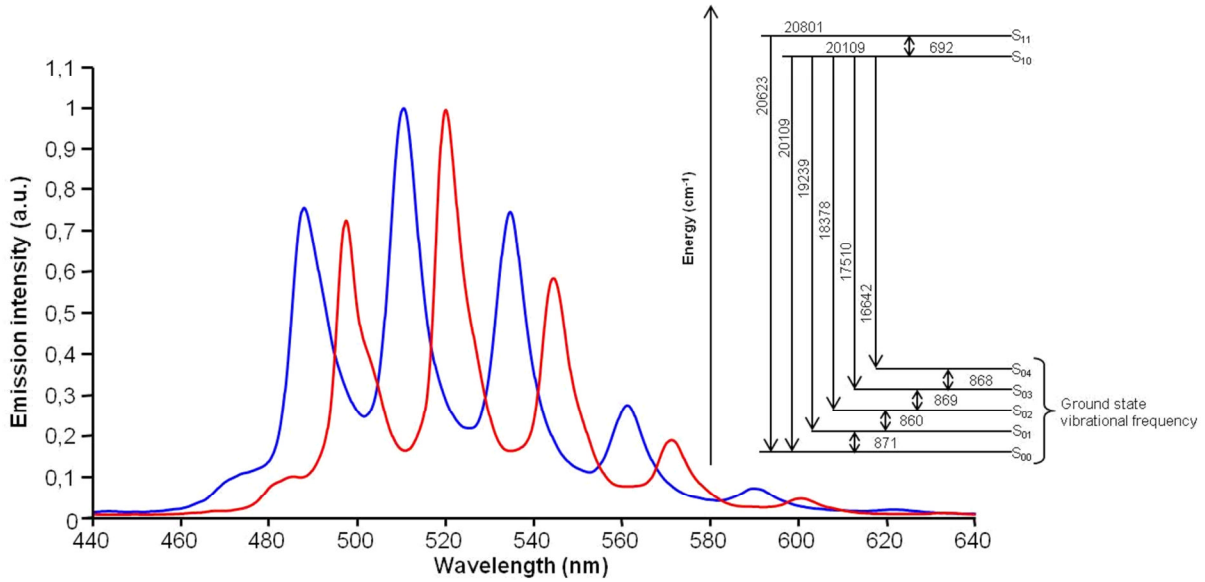

Figure II.5.6 Solid state emission spectra (left) of **pht1** (red), of uranyl nitrate hexahydrate (blue) and the electronic and vibronic transitions for **pht1** (right).

The emission spectrum of **pht1** phase (Figure II.5.6) has the same characteristic peaks but red-shifted with an approximate value of 12 nm. This red shift has been previously reported for this type of complexes[7, 14]. As expected the band spacing between the $S_{11}\rightarrow S_{00}$ and the $S_{10}\rightarrow S_{00}$ transitions is about 692 cm^{-1} and those between $S_{10}\rightarrow S_{0v}$ and $S_{10}\rightarrow S_{0(v+1)}$ transitions (v = 0-3) is around 867±7 cm^{-1}. The transitions $S_{04}\rightarrow S_{0v}$ (v = 0-3) are vibration transitions, including the $S_{0v}\rightarrow S_{0(v-1)}$ (v = 1-4) ones, which are directly related with the double uranyl bond specific symmetric vibrations observed in Raman spectroscopy.

The emission spectrum of the **pht2** phase (Figure II.5.7) has similar uranyl characteristic peaks, also with a red shift of 13 nm.

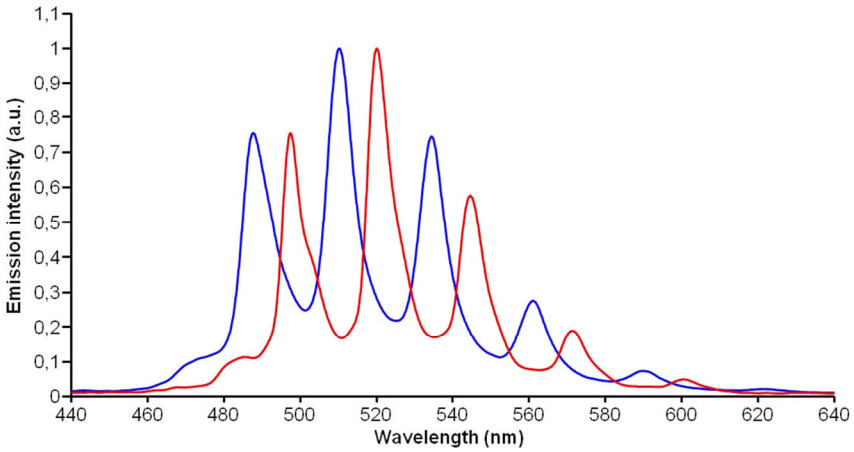

Figure II.5.7 Solid state emission spectra of **pht2** (red) and uranyl nitrate hexahydrate (blue).

The band spacing between the $S_{11}\rightarrow S_{00}$ and the $S_{10}\rightarrow S_{00}$ transitions is about 676 cm^{-1} and those between $S_{10}\rightarrow S_{0v}$ (v = 0-4) around 866±9 cm^{-1}. The obtained fluorescence data values for **pht2** are summarized and compared with the ones of **pht1** and uranium nitrate hexahydrate in Table II.5.1.

Table II.5.1 Fluorescence bands of uranyl dinitrate hexahydrate, phases pht1 and pht2.

Uranyl dinitrate hexahydrate			pht1			pht2		
λ (nm)	$\tilde{\nu}$ (cm^{-1})	$\Delta\tilde{\nu}$ (cm^{-1})	λ (nm)	$\tilde{\nu}$ (cm^{-1})	$\Delta\tilde{\nu}$ (cm^{-1})	λ (nm)	$\tilde{\nu}$ (cm^{-1})	$\Delta\tilde{\nu}$ (cm^{-1})
469,16	21315		480,75	20801		481,23	20780	
485,88	20581	733	497,29	20109	692	497,40	20105	676
507,98	19686	895	519,79	19239	871	519,89	19235	870
531,53	18814	872	544,12	18378	860	544,14	18378	857
557,36	17942	872	571,11	17510	869	571,32	17503	874
585,71	17073	868	600,90	16642	868	600,87	16642	861

For the case of **pht3** and **pht4** phases, the emission spectra (Figure II.5.8) suffer a drastic change from the typical one of the uranyl ion. Instead of the typical 6 peaks, the emission converged to a large broad band centered at 530 nm, split at top into 3 positions 522, 527 and 538 nm for the **pht3** and only in two, 527 and 538 nm, for the **pht4**. The emission bands of both of the compounds exhibit two shoulders around 560 and 590 nm. The position is consistent with the one of the last two peaks (557 and 586 nm) from the uranyl dinitrate hexahydrate emission spectrum. Other shoulders have been observed in the region 496 - 514 nm but with poor quality and their position could not be established accurately. This phenomenon of emission band convergence has been

previously encountered[15] and is explained by the nature of the oligomeric SBU, the number of electronic transitions being larger and not so well defined.

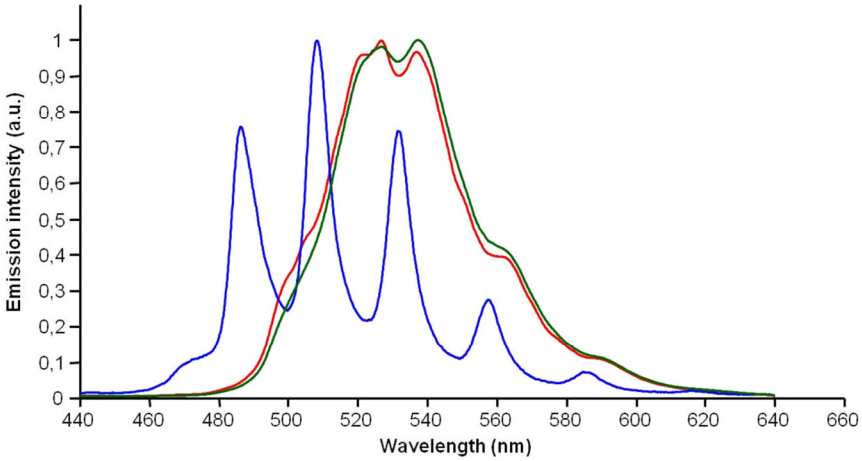

Figure II.5.8 Solid state emission spectra of **pht3** (red), **pht4** (green) and uranyl nitrate hexahydrate (blue).

Conclusion

In this chapter there have been described and characterized three new uranyl phthalate complexes **pht2** - **pht4** under hydrothermal conditions in the temperature range of 180-200°C. A previously described uranyl phthalate[1] **pht1** has also been obtained at lower temperature (100-120°C). As comparative elements there have been used two other uranyl phthalates, one neptunyl phthalate all described in literature[1, 2, 4]. Depending on the reaction pH, two structural types have been isolated. In a narrow pH domain (0.9-1.8): a trigonal 1D nanotubular structure (**pht2**) is observed with discrete pentagonal bipyramids UO_2X_5 (X = oxo group from carboxylate or water species) linked through the phthalate ligands. At higher pH values (up to 3.5), a second phase appears (**pht3** & **pht4**): it is built up from the connection of dinuclear $(UO_2)_2(\mu_2\text{-}OH)_2X_6$ and tetranuclear $(UO_2)4(\mu_3\text{-}O)_2X_{12}$ units to generate infinite chains. 7- and 8-fold coordinated uranium occurs in the tetramer, and only 7-fold coordinated uranium occurs in the dinuclear unit. These chains are intercalated by potassium or ammonium cations depending on the nature of the base used for the pH variation (KOH or NH_3). These observations indicate the polymerization process of the cationic uranyl species as a function of the hydrolysis rate related to the reaction

pH. Larger building blocks are observed at solid state when increasing pH, whereas isolated uranyl species are present under highly acidic conditions.

Bibliography

1. Charushnikova, I. A.; Krot, N. N.; Starikova, Z. A., *Radiochemistry* **2004,** *46* (6), 556-559.
2. Grigoriev, M. S.; Antipin, M. Y.; Krot, N. N.; Bessonov, A. A., *Radiochimica Acta* **2004,** *92* (7), 405-409.
3. Mihalcea, I.; Henry, N.; Loiseau, T., *Crystal Growth & Design* **2011,** *11* (5), 1940-1947.
4. Charushnikova, I. A.; Krot, N. N.; Polyakova, I. N.; Makarenkov, V. I., *Radiochemistry* **2005,** *47* (3), 241-246.
5. Thuery, P., *Inorganic Chemistry Communications* **2008,** *11* (6), 616-620.
6. Borkowski, L. A.; Cahill, C. L., *Acta Crystallographica Section E-Structure Reports Online* **2005,** *61*, M816-M817; Borkowski, L. A.; Cahill, C. L., *Inorganic Chemistry* **2003,** *42* (22), 7041-7045; Masci, B.; Thuery, P., *Polyhedron* **2005,** *24* (2), 229-237; Thuery, P., *Inorganic Chemistry* **2007,** *46* (6), 2307-2315; Leroux, S. D.; Vantets, A.; Adrian, H. W. W., *Acta Crystallographica Section B-Structural Science* **1979,** *35* (DEC), 3056-3057; Mikhailov, Y. N.; Kanishcheva, A. S.; Gorbunova, Y. E.; Belomestnykh, V. I.; Sveshnikova, L. B., *Zhurnal Neorganicheskoi Khimii* **1997,** *42* (12), 1980-1985; Andrews, M. B.; Cahill, C. L., *Crystengcomm* **2011,** *13* (23), 7068-7078; Duvieubourg, L.; Nowogrocki, G.; Abraham, F.; Grandjean, S., *Journal of Solid State Chemistry* **2005,** *178* (11), 3437-3444; Thuery, P., *Crystengcomm* **2009,** *11* (6), 1150-1156; Thuery, P., *Crystengcomm* **2008,** *10* (1), 79-85; Thuery, P., *Acta Crystallographica Section C-Crystal Structure Communications* **2008,** *64*, M50-M52; Jiang, J.; Sarsfield, M. J.; Renshaw, J. C.; Livens, F. R.; Collison, D.; Charnock, J. M.; Helliwell, M.; Eccles, H., *Inorganic Chemistry* **2002,** *41* (10), 2799-2806; Thuery, P., *Crystal Growth & Design* **2012,** *12* (1), 499-507.
7. Borkowski, L. A.; Cahill, C. L., *Crystal Growth & Design* **2006,** *6* (10), 2241-2247.
8. Burns, P. C.; Ewing, R. C.; Hawthorne, F. C., *Canadian Mineralogist* **1997,** *35*, 1551-1570.
9. Grigor'ev, M. S.; Antipin, M. Y.; Krot, N. N., *Radiochemistry* **2004,** *46* (3), 224-231.
10. Eriksson, A.; Lindgren, J., *Journal of Molecular Structure* **1978,** *48* (3), 417-430.
11. Loring, J. S.; Karlsson, M.; Fawcett, W. R.; Casey, W. H., *Spectrochimica Acta Part a-Molecular and Biomolecular Spectroscopy* **2001,** *57* (8), 1635-1642.
12. Kuppusamy, K.; Sivasankar, B. N.; Govindarajan, S., *Thermochimica Acta* **1996,** *274*, 139-148; Tellez, C.; Gomez, J.; Mondragon, M. A.; Castano, V. M.; Mena, G., *Vibrational Spectroscopy* **1995,** *9* (3), 279-285.
13. Bartlett, J. R.; Cooney, R. P., *Journal of Molecular Structure* **1989,** *193*, 295-300.

14. Borkowski, L. A.; Cahill, C. L., *Crystal Growth & Design* **2006,** *6* (10), 2248-2259.
15. Jiang, Y. S.; Yu, Z. T.; Liao, Z. L.; Li, G. H.; Chen, J. S., *Polyhedron* **2006,** *25* (6), 1359-1366; Clark, D. L.; Conradson, S. D.; Donohoe, R. J.; Keogh, D. W.; Morris, D. E.; Palmer, P. D.; Rogers, R. D.; Tait, C. D., *Inorganic Chemistry* **1999,** *38* (7), 1456-1466; Zheng, Y. Z.; Tong, M. L.; Chen, X. M., *European Journal of Inorganic Chemistry* **2005,** (20), 4109-4117; Almond, P. M.; Talley, C. E.; Bean, A. C.; Peper, S. M.; Albrecht-Schmitt, T. E., *Journal of Solid State Chemistry* **2000,** *154* (2), 635-641.

Chapter III
Uranyl Isophthalates

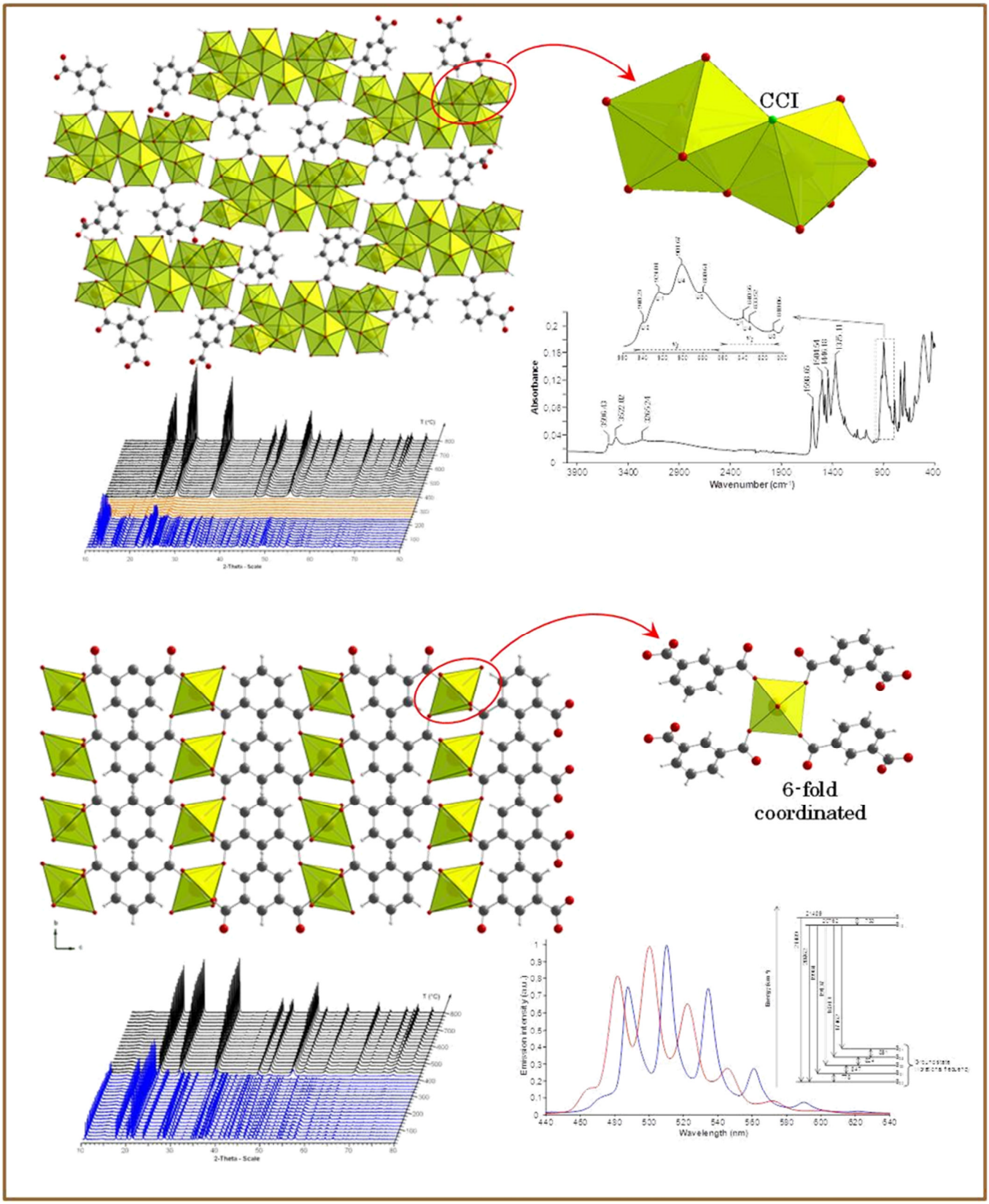

Chapter III Uranyl Isophthalates

III.1 . Introduction

Our investigations concerning the use of isophthalic acid (noted H_2ipa) as a ligand for uranyl ion complexation has shown that this crystal chemistry was much more complex and rich than that observed for the parent ditopic benzenedicarboxylate, with the 1,2-carboxylate function (see chapter II). Indeed, 10 compounds have been identified with distinct architectures. Beside the use of ammonium hydroxide or potassium hydroxide, we also examined the reactivity of two organic bases such as hydrazine or 1,3-diaminopropane. Two of the phases have been isolated in the presence of diprotonated 1,3-diaminopropane (H_2dap) as counter-cation. One of the two phases is closely related to that of an unique uranyl isophthalate[1] previously reported in literature by Prof. D. O'Hare, in the presence of *N,N*-dimethylformamide as main solvent. The influence of this diamine has been tested in order to estimate the structure-directing effect (or template effect) of this type of N-donor molecules with uranyl cations. Such a study was explored for instance by Prof. C Cahill[2] using linear dicarboxylic acids as ligands and bipyridyne derivatives as templates or Prof. F. Abraham[3] testing in an uranyl phosphate system, the structure-directing effect of different linear diamines. Hydrazine is commonly employed as reducing agent in nitric acid solution in order to maintain tetravalent oxidation state of uranium from after the dissolution the spent nuclear fuel and its use was tested in the chemical system involving isophthalic acid. All the obtained complexes $[(UO_2)(ipa)]$ (**iso1**)[4], $[(UO_2)(ipa)(H_2O)]\cdot 0.5H_2O$ (**iso2**), $[(UO_2)(Hipa)_2]$ (**iso3**), $(NH_4)[(UO_2)(ipa)(Hipa)]\cdot 3H_2O$ (**iso4**), $(H_2dap)[(UO_2)_3(ipa)_4(H_2O)_2]\cdot 4H_2O$ (**iso5**) (with dap standing for 1,3-diaminopropane), $(H_2dap)[(UO_2)_2(ipa)_3]\cdot 4H_2O$ (**iso6**), $[(UO_2)_4(ipa)_2(OH)_4(H_2O)_2]\cdot 2H_2O$ (**iso7**), $(NH_4)_2[(UO_2)_4(ipa)_2O_2(OH)_2(H_2O)_2]$ (**iso8**), $(NH_4)_2[(UO_2)_4(ipa)_2O_2(OH)_2(H_2O)_2]\cdot H_2O$ (**iso9**), and $[(UO_2)_4\text{-}(ipa)_2O(OH)_2(H_2O)_2]\cdot 2H_2O$ (**iso10**)[4] have been hydrothermally synthesized from a mixture of uranium nitrate

hexahydrate, phthalic acid, a pH moderator (NH_4OH, KOH, 1,3-diaminopropane or hydrazine) and as solvent deionized water.

The first synthesized complex (**iso1**) has a monomeric SBU containing six fold coordinated uranyl centers interlinked through the carboxylate groups of the ditopic ligand, in order to create the tridimensional edifice. The second complex (**iso2**) possesses a monomeric SBU with seven fold coordinated uranyl, interlinked into infinite unidimensional double chains. The next four complexes (**iso3** to **iso6**) are related, all possessing as monomeric SBU species of H type (hexagonal bipyramid) polyhedra (see chapter I Figure I.2.2). The difference between them is the ligand linkage configuration, the number of coordinating water molecules and the nature of different counter cations present in the crystal structure. One of the coordination polymer of this series is structurally related to that of the only uranyl isophthalate previously mentioned in literature[1] ($(Hdmf)_2[(UO_2)_3(ipa)_4(H_2O)_2]$). Another family of uranyl isophthalates is formed by the **iso7** to **iso9** complexes. All three complexes possess as SBU type (d) tetranuclear units (chapter I Figure I.2.17) linked by the isophthalate ligands in order to obtain infinite chains. The differences between them consist in the chains orientation, the position of the counter-cation (if present) and the nature of the μ_3 inter-polyhedra bridges. The last of the isophthalate coordination polymer (**iso10**) is the most unconventional one. It possesses an octameric SBU which was not previously mentioned in literature at all. The octanuclear brick is interconnected via the isophthalate ligand to other eight neighboring SBUs situated in different planes, in order to create the final high complexity tridimensional edifice. The octanuclear brick also presents an unusual cation-cation interaction which will be discussed at large further in this chapter. Details of crystal data are given in the III.1.1 - III.1.2 tables.

Table III.1.1 Condensed crystal and refinement data for iso6 to iso10 complexes.

Parameter*	iso1	iso2	iso3	iso4	iso5
crystal system	Monoclinic	Monoclinic	Triclinic	Monoclinic	Triclinic
space group	*C* 2/c	*C* c	*P* -1	*P* 2_1	*P* -1
a/Å	6.3566(2)	11.0614(4)	6.8234(4)	6.8634(1)	8.141(2)
b/Å	8.4626(2)	20.0758-7)	7.4026(5)	17.4997(3)	9.928(2)
c/Å	16.7062(4)	11.3468(5)	8.9551(9)	8.5229(1)	14.644(2)
α/deg	90	90	98.429(4)	90	97.922(9)

Parameter*	iso1	iso2	iso3	iso4	iso5
ß/deg	94.030(1)	119.160(2)	93.236(4)	108.639(1)	105.281(9)
γ/deg	90	90	114.433(3)	90	102.720(9)
volume/Å^3	896.46(4)	2200.4(2)	403.92(5)	969.97(2)	1089.5(3)
Z, ρ_{calc}/g·cm^{-3}	2, 3.217	4, 2.742	1, 2.468	2, 2.264	1, 2.479
final *R* indices [$I > 2\sigma(I)$]	R1 = 0.0182	R1 = 0.0636,	R1 = 0.0137	R1 = 0.0260	R1 = 0.0334
	wR2 = 0.0486	wR2 = 0.1976	wR2 = 0.0319	wR2 = 0.0614	wR2 = 0.0677
R indices (all data)	R1 = 0.0276	R1 = 0.0639,	R1 = 0.0137	R1 = 0.0339	R1 = 0.0524
	wR2 = 0.0534	wR2 = 0.1981	wR2 = 0.0319	wR2 = 0.0644	wR2 = 0.0796

* - a complete crystal and refinement data table is given in the supplementary data chapter (tables VIII.2.1- VIII.2.2).

Table III.1.2 Condensed crystal and refinement data for iso6 to iso9 complexes.

Parameter*	iso6	iso7	iso8	iso9	iso10
crystal system	Orthorhombic	Monoclinic	Monoclinic	Monoclinic	Triclinic
space group	$C\,222_1$	$P\,2/c$	$P\,2/c$	$P\,2_1/c$	$P\,\bar{1}$
a/Å	8.3339(3)	14.7096(3)	14.6171(8)	14.4967(7)	7.3934(3)
b/Å	18.0840(7)	7.0679(1)	6.9847(4)	12.0084(7)	13.3296(5)
c/Å	22.1394(9)	15.0958(3)	14.7297(9)	11.3516(7)	15.4432(5)
α/deg	90	90	90	90	111.865(2)
ß/deg	90	100.776(1)	99.306(3)	100.372(4)	90.637(2)
γ/deg	90	90	90	90	104.867(2)
volume/Å^3	3336.6(2)	1541.77(5)	1484.1(2)	1943.8(2)	1355.49(9)
Z, ρ_{calc}/g·cm^{-3}	4, 2.330	2, 3.301	2, 3.429	2, 2.645	2, 3.725
final *R* indices [$I > 2\sigma(I)$]	R1 = 0.0279	R1 = 0.0289	R1 = 0.0241	R1 = 0.0661	R1 = 0.0286
	wR2 = 0.0554	wR2 = 0.0666	wR2 = 0.0516	wR2 = 0.1908	wR2 = 0.0671
R indices (all data)	R1 = 0.0368	R1 = 0.0428	R1 = 0.0354	R1 = 0.0813	R1 = 0.0485
	wR2 = 0.0711	wR2 = 0.0889	wR2 = 0.0691	wR2 = 0.1999	wR2 = 0.0835

* - a complete crystal and refinement data table is given in the supplementary data chapter (tables VIII.2.2- VIII.2.3).

III.2 . Structure description

The structure of **iso1** [(UO_2)(ipa)] possesses one unique crystallographic site for the uranium atoms, situated on a *4a* (0,0,0) special position. The environment of the uranium atom is formed by six oxygen atoms, two of them in axial position, O1 and its symmetry equivalent (O1#), with an expected 180° angle around the uranium atom and a typical shorter U=O distance of 1.759(2) Å. The other 4 oxygen atoms O2, O3 and their symmetry equivalents, belonging to the carboxylate groups of the ligand molecules, are situated in the equatorial plane at a distance of 2.331(2) Å and 2.290(2) Å respectively from the uranium atom, forming the square base of the bipyramid (Figure III.2.1).

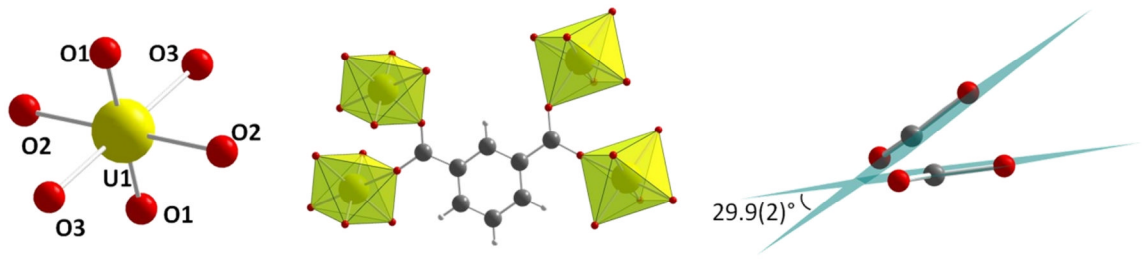

Figure III.2.1 Representation of uranium environment (left), the ligand's coordination configuration (middle) and the angle formed by the two carboxylate groups of the ligand (right) for **iso1** phase.

The UO_6 building units are discrete species surrounded and interlinked by the organic ligand in order to form a tridimensional structure (Figure III.2.2). The carboxylate groups of the isophthalate adopt a bidentate syn-anti coordination configuration making the ligand a tetradentate one of μ_4-η_1:η_1:η_1:η_1 type. Each of the carboxylate group bridges two UO_6 square bipyramids, creating two different types of infinite chains, with different propagation directions. The angle between the two directions is 60.35(4)°. This orientation is favored by the distance between the two carboxylate groups of the ligand (position 1-3 on the benzene ring) and also by the torsion angle between them of ~30° (usually a carboxylate group belonging to an aromatic cycle is coplanar with the ring).

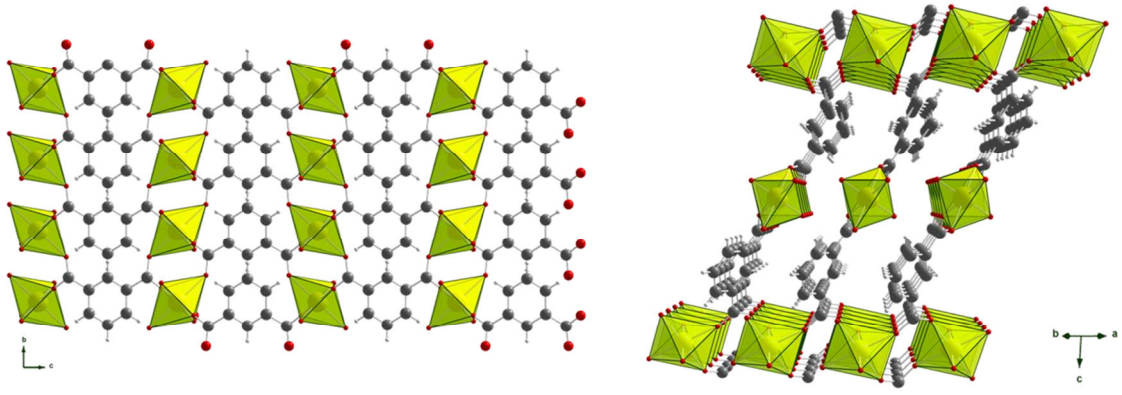

Figure III.2.2 Structure representation for the 3D edifice of **iso1**, view along the [100] crystallographic direction (left) and perspective view along [110] direction (right).

Although **iso1** is one of the densest compounds (ρ_{calc} = 3.217 g/cm^3) its structure presents infinite flat narrow channels, along the [110] direction. These channels are too narrow (shortest C···C and terminal O1···O1 distances of 3.487(2) and 3.074 Å respectively) to host any inclusion compound or free water molecules.

It may be noticed that the occurrence of six-fold coordination for uranyl cations is quite uncommon with carboxylate ligands. Indeed, very few examples of such an uranyl environment are known in literature and was previously reported in several UOFs (see chapter I)

The **iso2** complex ($[(UO_2)(ipa)(H_2O)]\cdot 0.5H_2O$) presents two different crystallographic sites for the uranium atoms (U1 and U2), both being situated on *4a* general positions. Both monomeric SBUs of this structure (Figure III.2.3) are discrete pentagonal bipyramids formed by two uranyl type oxygen atoms, in the apical position and other five oxygen atoms in the equatorial plane. From the latter five, one belongs to a coordinating water molecule, the remaining four being carboxyl type belonging to the ligand's molecules. For the U1 atom the coordinating uranyl type oxygen atoms are O3 and O6, situated at distances of 1.75(1) and 1.76(1) Å respectively and forming an O=U=O angle of 174(1)°. The carboxyl type oxygen atoms from the equatorial plane are O1, O2, O7 and O8, each having a U–O bond length of 2.47(1), 2.29(1), 2.47(1) and 2.31(1) Å respectively. The coordination sphere surrounding the U1 atom is completed by the O9 water molecule situated at a relatively short distance of 2.39(1) Å from the central metal atom. The bond valence calculation gives a value of 0.52 v.u. for the O9 atom, in good agreement with the assignment of aquo species[5]. The U2 polyhedron is formed by O4 and O5 apical uranyl type oxygen atoms, presenting U=O distances of 1.73(1) and 1.76(1) Å respectively and an O=U=O angle of 179(1)°, four equatorial carboxyl oxygen atoms O10 and O12 to O14, each presenting U–O distances ranging from 2.31(1) to 2.48(1) Å and one coordinating water molecule (O11) situated at 2.42(1) Å (valence value of 0.49 v.u.) from the uranium atom.

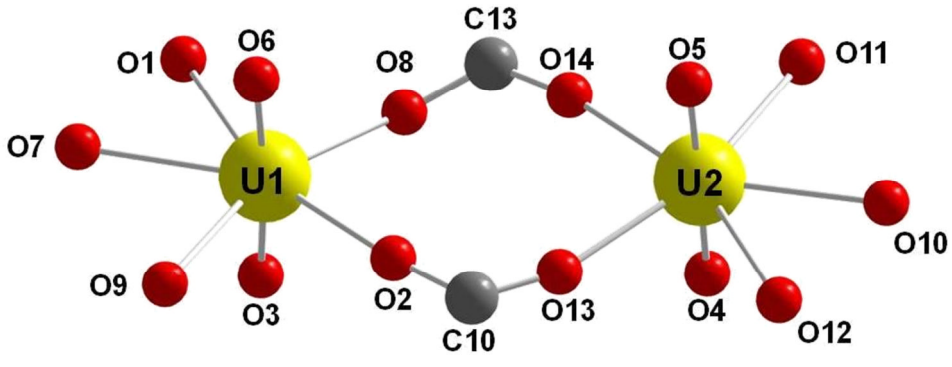

Figure III.2.3 Uranium coordination environment for **iso2** complex.

The two SBUs are interconnected through the ligand molecules to form infinite double chains (ribbons) propagating along [100] direction. The ligand molecules occupy two different crystallographic sites A and B (Figure III.2.4). The ligand molecule of the A site chelates with one carboxylate arm the U1 atom and bridges with the second arm two other U1 and U2 polyhedra in a bidentate manner. The type B ligand molecule presents a symmetrical opposite coordination configuration, chelating the U2 atom with one carboxylate arm and with the second one bridging two other U1 and U2 polyhedra.

The polymeric ribbons are forming along the [100] direction two alternating layers stacked along the [001] direction. Each of the two layers presents a different orientation of the ribbons, with a plane angle of 12.65(1)° from the [010] direction and of 25.31(1)° from an adjacent chain of an adjacent layer.

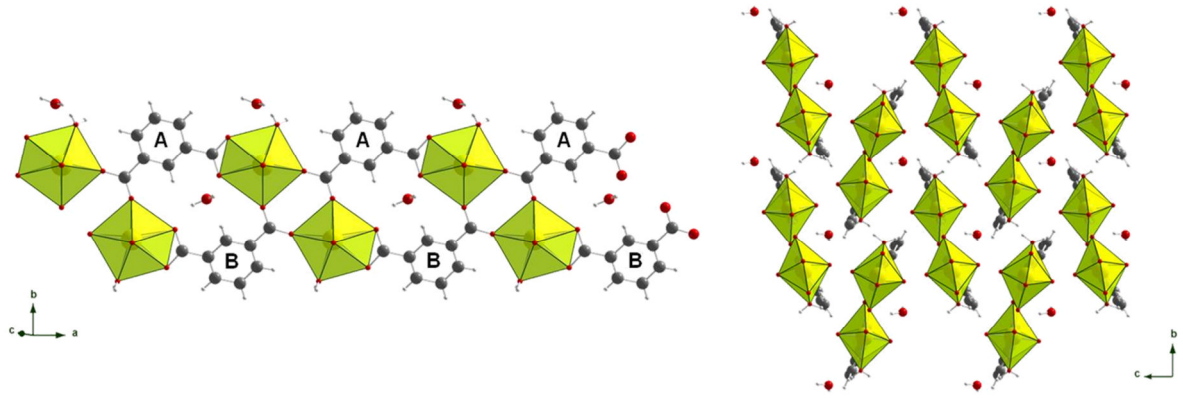

Figure III.2.4 Structure representation of **iso2** complex. View toward the (001) plane (left) and along [100] axis (right).

The structure of **iso2** contains one free water molecule (Ow1) per each two SBUs, intercalated between the polymeric chains (Figure III.2.5). This molecule has in the immediate proximity two U1 polyhedra belonging to two different chains. From one of the SBU the aquo O9 oxygen atom belonging to the coordinating water molecule is situated at 2.60(2) Å from the Ow1 oxygen atom, permitting a hydrogen bond interaction.

Also in close proximity to Ow1 (2.88(1) Å), there is the O1 carboxyl type oxygen atom belonging to the second U1 polyhedron permitting a second hydrogen bond interaction.

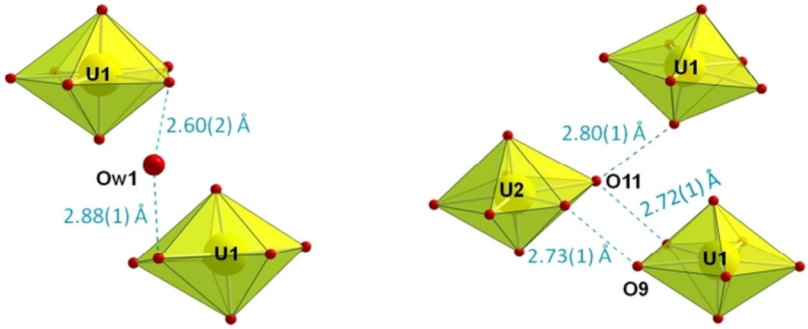

Figure III.2.5 The environment surrounding the coordinating and free water molecules present in the structure of **iso2.**

The O9 aquo atom, beside the interaction with Ow1, can interact through the second hydrogen atom with a proximal carboxyl type oxygen atom (O10) belonging to an adjacent U2-centered polyhedron. A similar interaction takes place between one hydrogen atom belonging to the O11 coordinating water molecule of U2-centered SBU and the carboxyl type oxygen atom (O7) belonging to the U1 polyhedron. Through the second hydrogen atom, the O11 water molecule interacts with the uranyl type oxygen atom (O3) belonging to a second U1-centered polyhedron (O11····O3 = 2.80(1) Å).

The structure of the **iso3** ([$(UO_2)(Hipa)_2$]) coordination polymer contains a single unique crystallographic site, situated on the *1h* (½,½,½) special position. The coordination sphere of the uranium atom is formed by eight oxygen atoms (Figure III.2.6). Two of them, O4 and its symmetry equivalent, are forming the uranyl bond and are located at a distance of 1.756(2) Å from the metal atom, with an expected O═U═O angle of 180°. The other remaining six oxygen atoms, O1, O2, O3 and their symmetry equivalents are situated in the equatorial plane at a distance of 2.454(2) Å, 2.502(2) Å and 2.514(2) Å respectively, forming the hexagonal base of the bipyramid (Figure III.2.6).

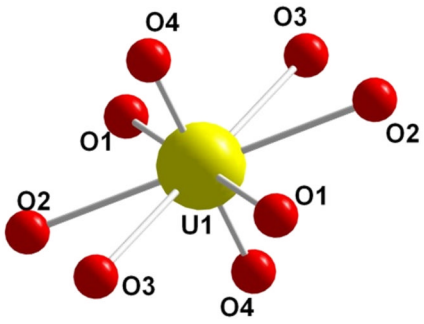

Figure III.2.6 The uranium coordination environment for **iso3** (hexagonal bipyramid with O4=U1=O4 axial uranyl bonds).

The discrete mononuclear building units are interconnected by the organic ligand into infinite chains, propagating along the [001] direction (Figure III.2.7). The carboxylate groups of the ligand coordinate the uranyl ion in a distinct manner: one adopting chelating mode with one uranium atom, the second monodentate bridging a second SBU, giving the final ligand coordination configuration of μ_2-η_1:η_1:η_1. The coordinating groups of the ligand being nearly coplanar with the benzene ring and the monodentate coordinating group being protonated determine the low dimensionality of the structure. The lack of hydrogen bonds interactions between the chains are giving the conclusion that the cohesion between the chains, supporting the crystalline edifice is ensured by π-π stacking interactions between the aromatic rings. The distance between the centers of two adjacent aromatic rings is of 3.8731(4) Å.

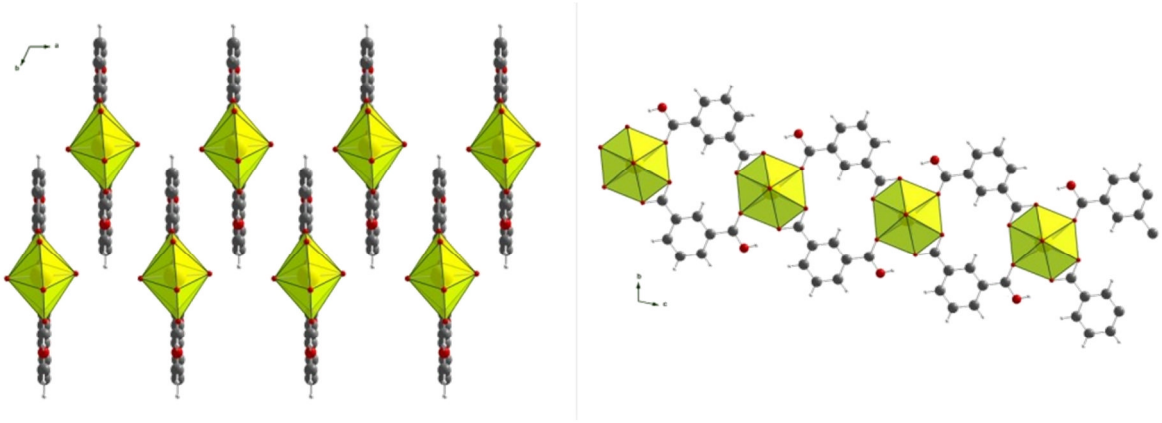

Figure III.2.7 Polymer chain intercalation, view along the [001] axis (left) and chain orientation, view along [100] axis for **iso3** complex.

The structure of complex **iso4** ($(NH_4)[(UO_2)(ipa)(Hipa)]\cdot 3H_2O$) exhibits a unique crystallographic site for the uranium atom, situated on a *2a* general crystallographic position. The SBU is a discrete polyhedron with hexagonal bipyramidal geometry similar to the one of **iso3** complex. The environment surrounding the uranium atom is formed by eight oxygen atoms (Figure III.2.8). Two of them, O5 and O6, form the uranyl bond being situated at the distance of 1.768(3) and 1.776(3) Å respectively and make an angle around the central metal atom of nearly 180° (179.1(4)°). The remaining six oxygen atoms O1-O4, O7 and O8 form in the equatorial plane the hexagonal base of the bipyramid, being all situated at a distance from the central uranium atom ranging from 2.433(8) to 2.495(3) Å.

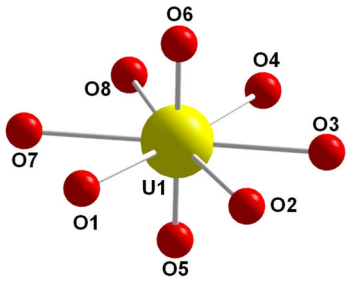

Figure III.2.8 The uranium coordination environment for **iso4** (hexagonal bipyramid with O5=U1=O6 axial uranyl bonds).

The monomeric inorganic units are, as in the previous case (**iso3**), interconnected by the isophthalate ligand to form infinite polymeric chains, running along *b* axis. The structure of **iso4** (Figure III.2.9), contains two independent sites for the organic ligand. The first ligand molecule has one carboxylate group (O1, O7) chelating a uranyl-centered polyhedron, the second group (O9, O10) being protonated and non-coordinating. The C—O9 and C═O10 bond lengths are 1.32(1) and 1.23(1) Å assessing the existence of a hydrogen atom bonded to O9 atom (carboxylic acid function). The coordination configuration for this molecule is μ_2-η_1:η_1. The second ligand molecule chelates with both carboxylate groups (O2, O3 and O4, O8) and binds two hexagonal bipyramids ensuring the chain propagation. The latter ligand molecule presents a μ_4-η_1:η_1:η_2:η_2 coordination configuration.

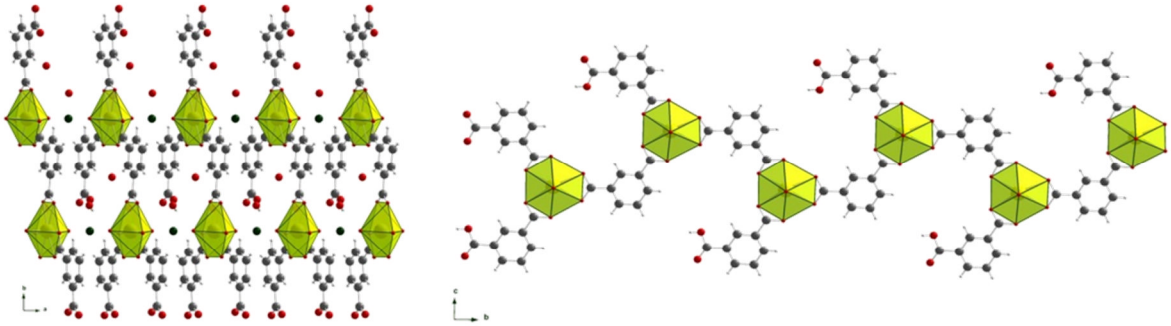

Figure III.2.9 structure **iso4** representation, view along the [001] axis (left) and along [100] axis (right).

The structure of **iso4** exhibits free molecular H_2O and cationic NH_4^+ species. The ammonium ion occurs in a molar ratio of 1:1 with the uranyl ion and its presence is required to compensate the negative charge adopted by the [(UO_2)(ipa)(Hipa)] infinite ribbons. The water molecules have three unique crystallographic positions in the structure and together with the ammonium ion create multiple hydrogen bond type interactions (Figure III.2.10). The

ammonium ion is situated in the proximity (less than 3 Å) of four oxygen atoms. Two of them (O5 and O6) are uranyl type and are situated at distances of 2.45(1) and 1.839(4) Å respectively from the nitrogen atom. The other two (O9 and O10) are carboxyl type oxygen atoms, belong to the non-coordinating carboxylate group and are having a N···O distance of 2.72(1) and 2.50(1) Å respectively. From the three free water molecules (Ow1 - Ow3) present in structure, first one (Ow1) is situated at close enough distance to form hydrogen bonds to four adjacent oxygen atoms. Two of them, O1 and O4, are coordinating carboxylate type. The third O10 belongs to the protonated non coordinating carboxylate group and the fourth is the Ow3 atom belonging to an adjacent water molecule. The distances between these atoms and Ow1 are in a range of 2.77(1) to 2.91(1) Å.

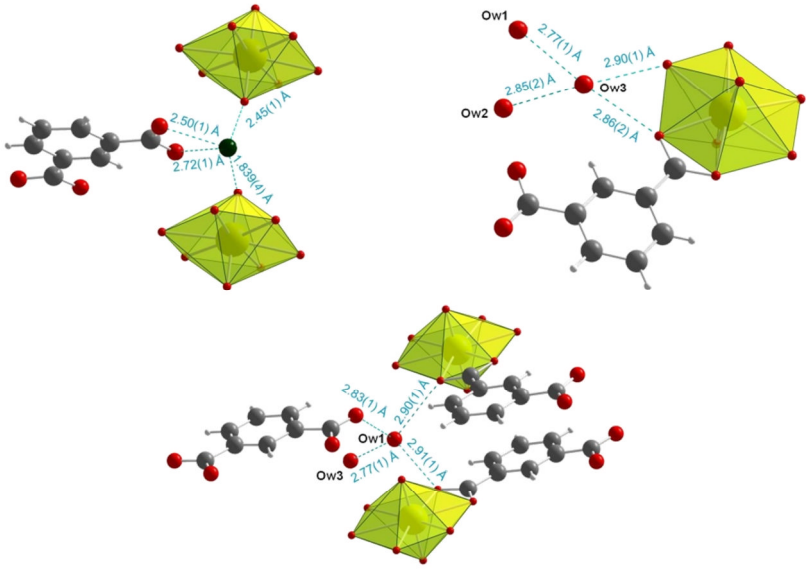

Figure III.2.10 View of the extended hydrogen bond network of **iso4** complex.

The second water molecule Ow2 has in immediate vicinity only the Ow3 molecule (Ow2···Ow3 = 2.85(2) Å). The third water molecule Ow3, beside the two interactions with Ow1 and Ow2, can create two others with O7 and O8 coordinating carboxylate type oxygen atoms, with distances of 2.86(2) and 2.90(1) Å. The cohesion between the polymeric chains is ensured by the ionic interactions of the ammonium cation, the extended network of hydrogen bonds and also by π-π stacking interactions between the aromatic rings. The distance between the centers of two adjacent aromatic rings belonging to two distinct polymeric chains, stacking along the [100] direction, is of 3.68(1) Å.

The compound **iso5** ($(H_2dap)[(UO_2)_3(ipa)_4(H_2O)_2]\cdot 4H_2O$) exhibits two distinct crystallographic sites for the uranium atom. First atom U1 is situated on a *1d* (½ 0 0) special position, the second U2 on a *2i* general position. Both metal centers are described as monomeric SBUs with hexagonal bipyramidal geometry, involving eight oxygen atoms (Figure III.2.11). For U1, the oxygen atoms forming the uranyl ion O5 and its symmetry generated equivalent O5# are symmetrically situated from the U atom at a distance of 1.776(8) Å and form a O═U═O angle of 180°. The U2-centered polyhedron is less symmetrical, the oxygen atoms forming the uranyl bond, O10 and O12, being situated at a distance of 1.753(7) and 1.750(7) Å respectively from the central uranium atom and forming a 178.4(3)° angle around it.

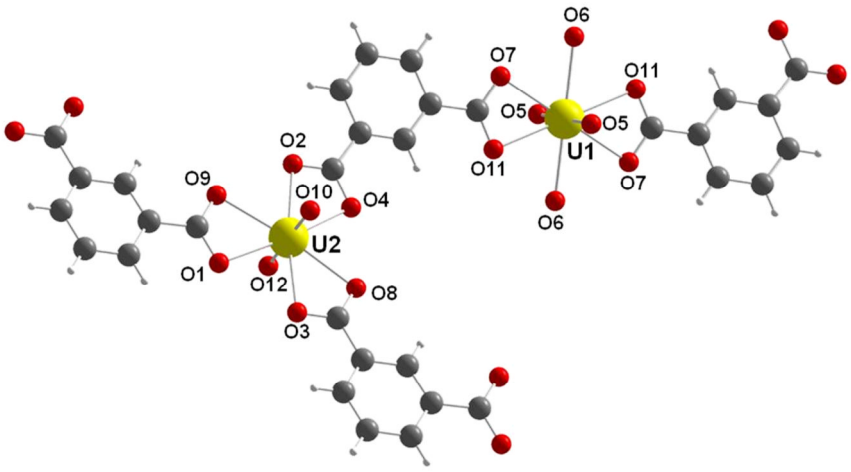

Figure III.2.11 Coordination environment (hexagonal bipyramid) surrounding the metal atoms for **iso5** complex.

The equatorial coordination plane is completed in the case of U1 by two oxygen atoms (O6 and O6#) having a U—O distance of 2.455(7) Å, belonging to two terminal coordinating water molecules and other four (O7, O11 and their symmetric equivalents) belonging to the carboxylate groups of two different ligand molecules having a U—O distance of 2.463(7) and 2.510(6) Å, respectively. The bond valence calculation gives a value of 0.46 v.u. on the oxygen atom belonging to the coordinating water molecule, value confirming the aqua nature of the O6 oxygen atom[5]. For the U2 atom, the equatorial coordination plane is completed by six carboxylate type oxygen atoms (O1-O4, O8 and O9) belonging to three different ligand molecules and all having a U—O distance ranging from 2.444(7) to 2.491(6) Å, corresponding to chelating bonding mode.

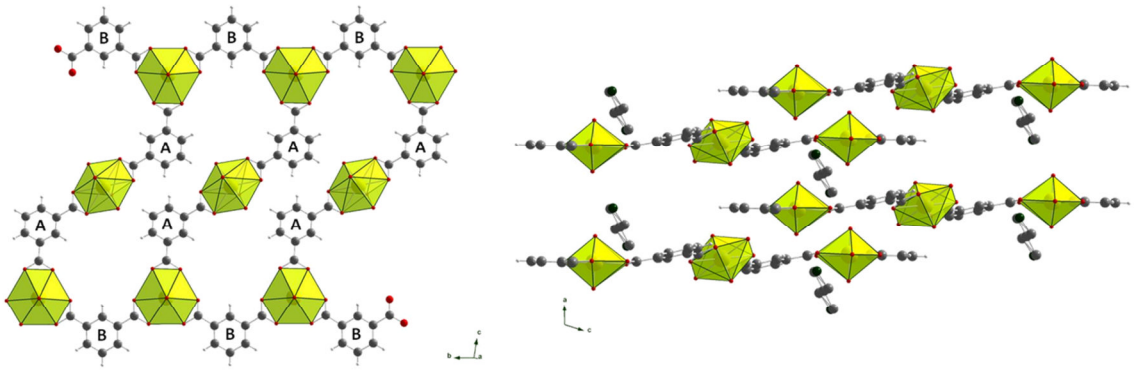

Figure III.2.12 View of the two types of ligand molecules, A and B, (left) and the intercalation of the H_2dap between the polymer ribbons (right) for **iso5** complex.

The structure of **iso5** complex also exhibits two non equivalent crystallographic positions for the ligands molecule. Both organic linkers are chelating through the carboxylate groups a different uranyl ion, interlinking the two polyhedra. First ligand molecule noted **A** (Figure III.2.12) interlinks one U1 center with a U2 one inside the chain. The second (**B**) binds together two U2 polyhedra forming the final ladder type unidimensional infinite structure developing along [010] direction.

Between the intercalated polymeric ribbons there are two water molecules (Ow1 and Ow2) and di-protonated 1,3-diaminopropane molecules. The latter ones compensate the negative charge of the $[(UO_2)_3(ipa)_4(H_2O)_2]^{2-}$ ribbon. Both 1,3-diaminopropane and water molecules are situated close enough to adjacent oxygen atoms for exhibiting weak hydrogen bond type interactions (Figure III.2.13).

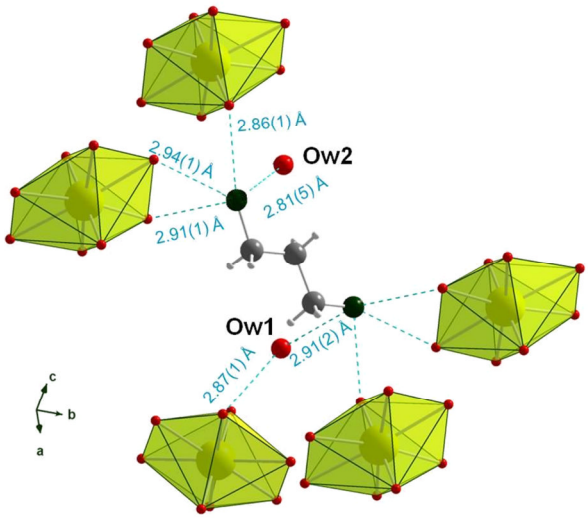

Figure III.2.13 View of the hydrogen bonds scheme appearing in the **iso5** complex.

Both nitrogen atoms belonging to the 1,3-diaminopropane molecules are in vicinity of one uranyl type oxygen atom (O12), at a distance of 2.86(1) Å and of two carboxyl type oxygen atoms, O2 and O9, with distances of 2.94(1) and 2.91(1) Å, respectively. One nitrogen atom is also close (2.91(2) Å) to the Ow1 free water molecule, the second having as neighbor the Ow2 free water molecule at a distance of 2.81(5) Å. The crystalline structure is mainly stabilized by the H-bond interactions with the intercalated species (di-protonated diamine and water).The distance between the planes of two adjacent benzene rings (4.56(2) Å) is large enough to diminish the π-π stacking interactions.

A closely related chain-like structure was described by O'Hare[1] in another uranyl isophthalate $(Hdmf)_2[(UO_2)_3(ipa)_4(H_2O)_2]$ with intercalated protonated *N,N*-dimethylformamide (Hdmf) molecules. The latter was used as a co-solvent during the hydrothermal reaction. The coordination environment of uranium is identical for both compounds with chelating bridging fashion for the carboxylates groups. The only difference is the tilt angle between the flat ribbons: in **iso5**, they are strictly perpendicular to the stacking axis, whereas in $(Hdmf)_2[(UO_2)_3(ipa)_4(H_2O)_2]$[1], the ribbons are slightly tilted (±12.92°) from the stacking direction (Figure III.2.14).

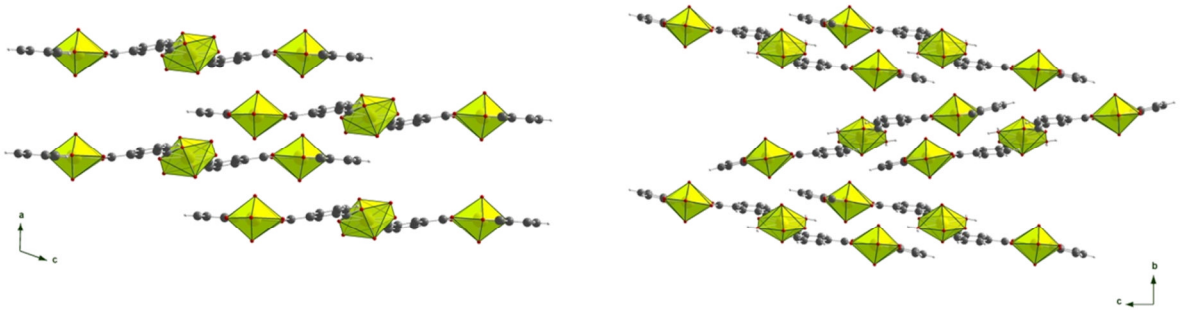

Figure III.2.14 Structure representation of **iso5** (left) and $(Hdmf)_2[(UO_2)_3(ipa)_4(H_2O)_2]$[1] (right). View along the ribbon's propagation direction for both of the compounds. The inclusion compounds have been omitted for clarity.

It is noticeable that the amine molecules in the uranyl-isophthalate system seem to play the role of structure-directing agent and favor the formation of chain-like networks with the same environment for uranium.

The phase **iso6** $((H_2dap)[(UO_2)_2(ipa)_3]\cdot 4H_2O)$ also consists of monomeric hexagonal bipyramidal units for the uranyl group (Figure III.2.15). Its structure exhibits one unique crystallographic site for the uranium atom, situated on an *8c*

general position. Similar to the previous cases (**iso3** to **iso5**) the uranium atom is coordinated by eight oxygen atoms. Two of them form the uranyl ion (O1 and O2) and are situated at a distance of 1.779(4) and 1.759(4) Å respectively from the uranium atom, having a O=U=O angle of 178.5(2)°. The remaining six form the equatorial plane and belong to three carboxylate groups coming from three different ligand molecules.

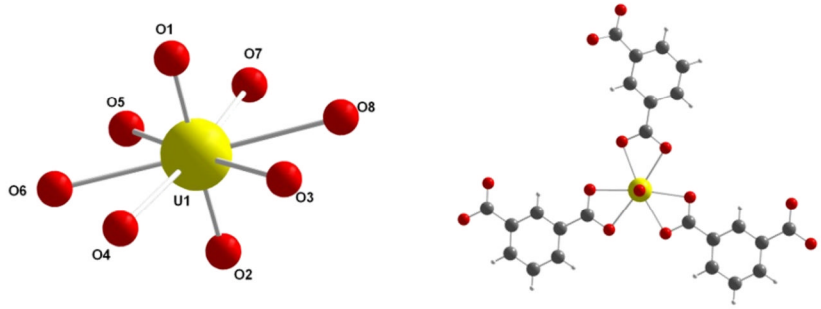

Figure III.2.15 The hexagonal bipyramidal environment of the uranium atom in the **iso6** complex.

There is also a unique crystallographic site for the organic ligand. Each of the carboxylate groups are chelating two neighboring uranyl centers in two different planes, interlinking them in order to obtain the final infinite double layered structure (Figure III.2.16).

The structure of **iso6** also exhibits, like in the case of **iso5**, trapped water and di-protonated diaminopropane molecules. The amine groups are protonated to compensate the negative charges of the $[(UO_2)_2(ipa)_3]^{2-}$ layers. The water molecules (Ow1 and Ow2) are situated between the double layer, unlike the 1,3-diaminopropane molecules that are positioned between the layers and acting as pillars between the uranyl-isophthalate sheets.

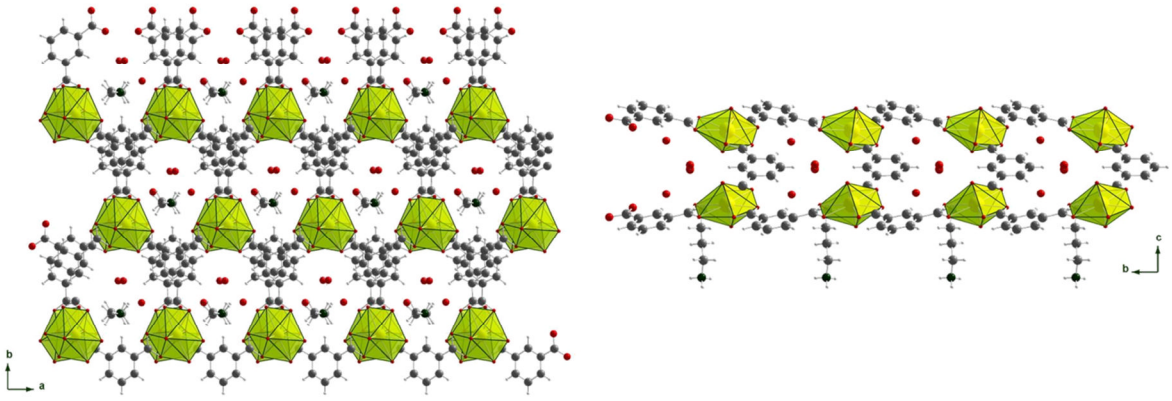

Figure III.2.16 Representation of **iso6** complex, view along the [001] direction (left) and the [100] direction (right

The 1,3-diaminopropane creates at both ends of its molecule, through the nitrogen atoms, hydrogen bond interactions (Figure III.2.17). Two of them are with two carboxyl oxygen atoms coordinating two different adjacent uranyl-centered polyhedra (O4 and O7, having N···O distances of 2.91(1) and 2.94(1) Å respectively), the third being with the Ow1 oxygen atom of a free water molecule (N···Ow1 distance of 2.89(1) Å). The Ow1 water molecule also links through hydrogen bonds another carboxyl oxygen atom (O5), being situated at a distance of 2.86(1) Å. The Ow2 water molecule link only one uranyl oxygen atom (O1) (Ow2···O1 = 2.97(1) Å).

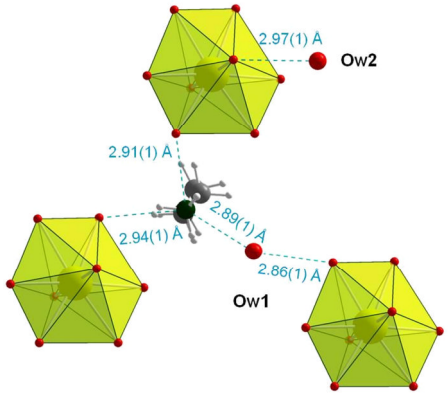

Figure III.2.17 The hydrogen bond interactions appearing in the **iso6**'s structure.

The cohesion between the uranyl phthalate layers is ensured by the diamine molecules through hydrogen bond interactions.

The **iso7** ($[(UO_2)_4(ipa)_2(OH)_4(H_2O)_2]\cdot 4H_2O$) complex is the first member of the series containing tetranuclear uranyl-centered motif with the isophthalate linker. Its structure exhibits two distinct crystallographic sites for the uranium atom, both situated on a *4g* general position and having seven-fold coordination (pentagonal bipyramid) (Figure III.2.18). For the U1 atom, the uranyl type oxygen atoms (O3 and O5) are situated at the U=O distance of 1.752(6) and 1.768(6) Å respectively and form a O=U=O angle of 177.3(2)°. Nearly perpendicular to this axis, in the equatorial plane, the coordination sphere is completed by three hydroxo groups (O1, O2 and O2#), with the U–O distance ranging from 2.406(5) to 2.459(5) Å, one coordinating water molecule (O4), situated at 2.435(6) Å from the uranium atom and one carboxyl type oxygen atom (O6) belonging to the ligand, which forms a U–O bond of 2.339(6) Å. The nature of the coordinating water molecule and the hydroxo bridges has been established

by bond valence calculation[5]. The resulted valence values are: 1.06 v.u. for the O1 (μ_2-OH) group, 1.39 v.u. for the O2 (μ_3-OH) group and 0.48 v.u. for the O4 atom belonging to the coordination water molecule. A complete bond valence calculation table for **iso7** is given in the supplementary data chapter Table VII.2.30. The coordination environment surrounding the U2 atom also contains two apical uranyl type oxygen atoms (O9 and O11) situated at 1.775(6) and 1.757(7) Å respectively, forming an O=U=O angle of 177.2(3)°. The equatorial plane in this case is composed by three carboxyl oxygen atoms (O7, O8 and O10), with U—O distances ranging from 2.309(6) to 2.452(7) Å and two hydroxo bridges (O1 and O2) situated at 2.356(6) and 2.452(5) Å distance from the U2 metal central atom.

The two uranium atoms are symmetrically doubled by the *2e* (0 y ¼) twofold rotation axis, resulting in a tetrameric unit, centered on this symmetry element. All the uranium atoms are seven fold coordinated, defining a resulting SBU being of type i), based on the classification established in first chapter (Figure I.3.17). This type of tetranuclear SBU is quite common in the class of uranyl carboxylates being encountered in literature[6] in more than 16 compounds (see chapter I table I.3.12).

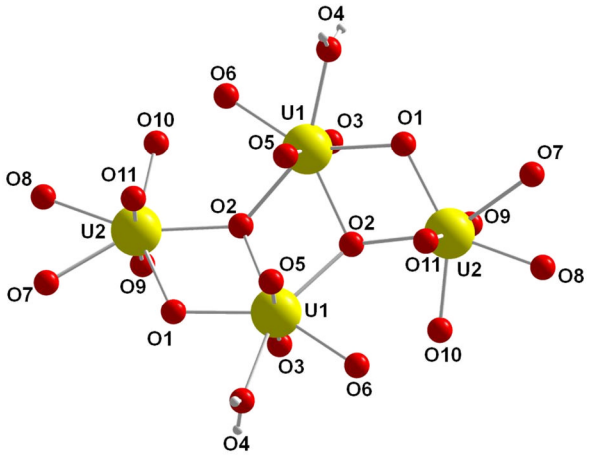

Figure III.2.18 The seven fold coordination environment of uranyl centers involved in the tetranuclear block of **iso7** complex.

The unique independent organic ligand chelates with one carboxylate group the U2 atom of one SBU, and adopts a bidentate bridging mode between two uranium atoms (U1 and U2) of a second neighboring SBU; this corresponding to the μ_3-η_1:η_1:η_1:η_1 coordination configuration. Each of the SBUs is bridged with

the next one through two ligand molecules in order to form infinite neutral ribbons $[(UO_2)_4(ipa)_2(OH)_4(H_2O)_2]$ propagating along the [100] direction and having the SBU orientated in the (101) plane (Figure III.2.19).

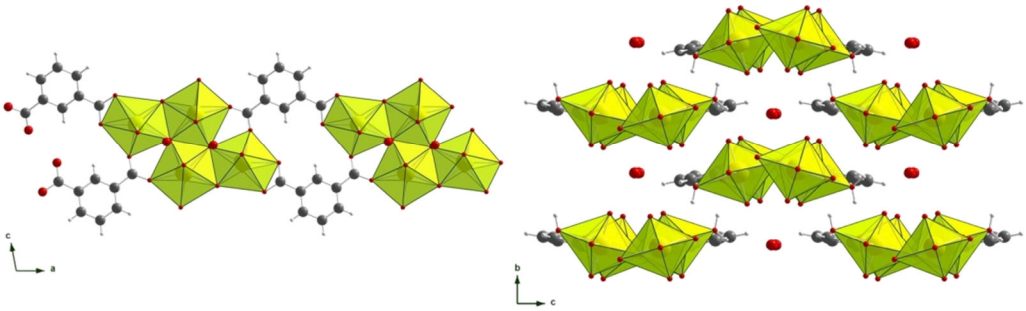

Figure III.2.19 View of **iso7** structure along [010] (left) and [100] (right) directions.

Viewing the structure through the (011) plane, there can be observed that the intercalated ribbons are orientated perpendicular to the stacking direction [010], nearly parallel to each other and contain in between free water molecules (one molecule per each uranyl unit). The cohesion between the ribbons, maintaining the stability of the crystalline edifice is mainly ensured by the hydrogen bonds sub-network. But also the occurrence of π-π stacking interactions cannot be ignored since the distance between the centers of two adjacent parallel benzene rings is of 3.68(1) Å along the chains stacking direction [010].

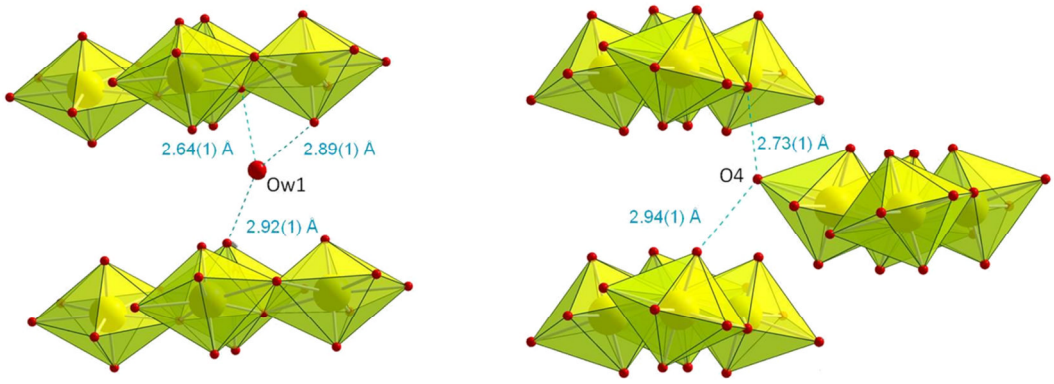

Figure III.2.20 Representation of the weak interactions occurring in the structure of **iso7** complex.

The hydrogen bonds are manifesting between the Ow1 non-coordinating water molecule and three oxygen atoms, O2-hydroxo and O9-uranyl (Ow···O distance of 2.64(1) and 2.89(1) Å respectively), belonging to one SBU and O5-uranyl (Ow···O distance of 2.92(1) Å) belonging to a second tetranuclear unit (Figure III.2.20). The coordinating water molecule (O4) is situated in close range (interatomic

distances of 2.73(1) and 2.94(1) Å) from two oxygen atoms (O1-hydroxo and O9-uranyl respectively) belonging to two adjacent SBUs, in order to interact through hydrogen bonds.

At the first sight, the structure of the **iso8** ($(NH_4)_2[(UO_2)_4(ipa)_2O_2(OH)_2(H_2O)_2]$) complex seems to be identical to that of **iso7**. Both structures are crystallizing in the same space group, have nearly the same cell parameters, with similar SBUs geometry and connection of the organic ligand generating infinite ribbons stacked in the same manner. First noticeable difference between the two structures consists in the position of the, initially unidentified (ammonium ion or water molecule), inclusion entity. This difference is well evidenced in the Figure III.2.19 and III.2.22 figures, where viewing toward the (011) plane the inserted atoms are positioned nearly one behind the other. This forms a single line parallel to the [100] axis for **iso7** whereas for **iso8** they are distinct positions in the (011) plane, creating two lines of atoms parallel with the [100] axis.

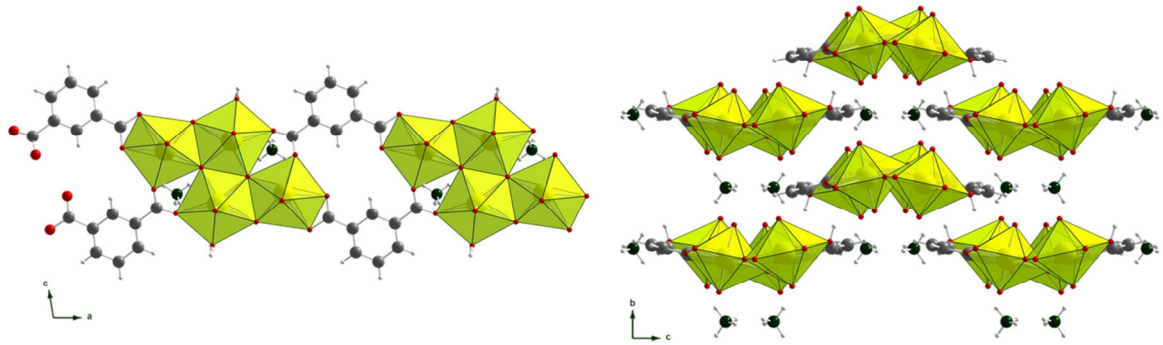

Figure III.2.21 View of **iso8** structure along [010] (left) and [100] (right) directions.

The most significant difference between the two structures is given by the bond valence calculations. The obtained values indicate the nature of the bridges anions within the SBU. The bond valence calculations have given the values of 0.45 v.u. for the O9 coordinating water molecule, 1.10 v.u. for the μ_2-O2 bridge, identifying it as a hydroxo group and 1.98 v.u. for the μ_3-O3 bridge, identifying it as an oxo group (it was μ_3-OH in **iso7**). As a consequence, the formula of the polymeric ribbons is $[(UO_2)_4(ipa)_2O_2(OH)_2(H_2O)_2]^{2-}$ which turns out to be negatively charged, implying an external positive compensation from a counter-cation. The fact that in the synthesis of this product the ammonium hydroxide has been used as a pH corrector, conducts toward the conclusion that the inclusion atoms are not water molecule, like in the case of **iso7**, but ammonium

cations. A comparative analysis of the interatomic distances, in SBUs belonging to the two structures, is given inTable III.2.1

Table III.2.1 Comparison between the bond lengths and bond valences of the oxygen atoms constituting the SBUs of iso7 and iso8 complexes

Interatomic bond		Interatomic distance (Å)		Bond valence /oxygen atom valence (v.u.)		Oxygen atom type	
iso7	iso8	iso7	iso8	iso7	iso8	iso7	iso8
U(1)-O(5)	U(2)-O(4)	1.752(6)	1.790(4)	1.78 / 1.78	1.65 / 1.65	uranyl	uranyl
U(1)-O(3)	U(2)-O(6)	1.768(6)	1.803(4)	1.73 / 1.73	1.61 / 1.61	uranyl	uranyl
U(1)-O(6)	U(2)-O(1)	2.339(6)	2.448(4)	0.57 / 1.88	0.47 / 1.74	carboxyl	carboxyl
U(1)-O(1)	U(2)-O(2)	2.406(5)	2.423(4)	0.50 / 1.06	0.49 / 1.10	hydroxyl	hydroxyl
U(1)-O(4)	U(2)-O(9)	2.435(6)	2.460(4)	0.48 / 0.48	0.45 / 0.45	water	water
U(1)-O(2)#1	U(2)-O(3)	2.445(5)	2.258(4)	0.47 / 1.39	0.67 / 1.98	hydroxyl	oxo
U(1)-O(2)	U(2)-O(3)#1	2.459(5)	2.304(4)	0.46 / 1.39	0.61 / 1.98	hydroxyl	oxo
U(2)-O(11)	U(1)-O(11)	1.757(7)	1.791(4)	1.76 / 1.76	1.65 / 1.65	uranyl	uranyl
U(2)-O(9)	U(1)-O(8)	1.775(6)	1.802(4)	1.70 / 1.70	1.62 / 1.62	uranyl	uranyl
U(2)-O(10)	U(1)-O(7)	2.309(6)	2.365(4)	0.61 / 1.89	0.55 / 1.79	carboxyl	carboxyl
U(2)-O(1)	U(1)-O(2)	2.356(6)	2.310(4)	0.56 / 1.06	0.61 / 1.10	hydroxyl	hydroxyl
U(2)-O(8)	U(1)-O(10)	2.387(6)	2.433(4)	0.52 / 1.78	0.48 / 1.75	carboxyl	carboxyl
U(2)-O(2)	U(1)-O(3)	2.452(5)	2.241(4)	0.46 / 1.39	0.69 / 1.98	hydroxyl	oxo
U(2)-O(7)	U(1)-O(5)	2.452(7)	2.542(5)	0.46 / 1.70	0.39 / 1.62	carboxyl	carboxyl

In comparison with the case of **iso7** (for O2), the μ_3 bridge (O3) has significantly shorter bonds with any of the linked uranium atoms in the case of **iso8**. This fact increases the valence value of the oxygen atom, determining the loss of the proton. Relative to the SBUs of the two structures, no other noticeable differences could be observed since the remaining coordination environment (Figure III.2.22) (beside O3 bridge) are similar to the one of **iso7**.

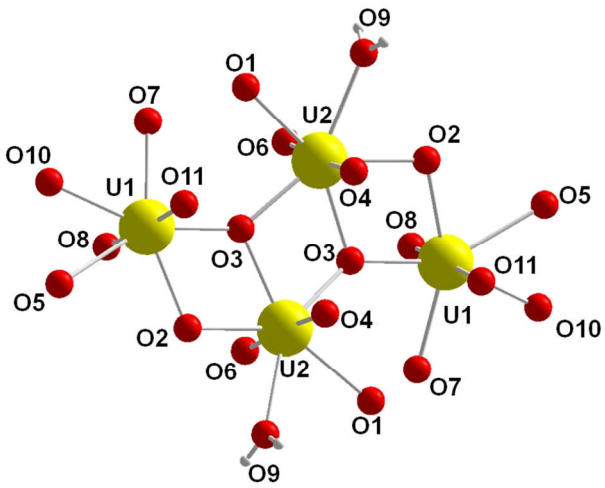

Figure III.2.22 The seven fold coordination environment of uranyl centers involved in the tetranuclear block in **iso8** complex.

The cohesion between the polymeric chains is maintained by hydrogen bonds between the O9 coordinating water molecule and two neighboring oxygen atoms (O7-carboxyl and O8-uranyl) belonging to two distinct adjacent SBUs. Weak π-π stacking interactions could take place, the distance between the centers of two neighboring aromatic rings being of 3.731(4) Å along the [010] stacking direction of the polymeric chains. The previously encountered (**iso7**) hydrogen bonds between the free water molecules and the adjacent SBUs are, in the case of **iso8**, replaced by interactions between the ammonium cation and the negatively charged ribbons surrounding it. The nitrogen atom of the countercation is situated in the vicinity of five oxygen atoms, members of three distinct SBUs: two (O6-uranyl and O7-carboxyl), members of the SBU "above", having N···O distances of 2.99(1) and 2.97(1) Å respectively, one (O5-carboxyl), belonging to the SBU "beside", situated at the distance of 2.91(1) Å and the last two (O4-uranyl and O11 uranyl) belonging to the SBU "beneath" the ammonium cation (Figure III.2.23) having the N···O distances of 2.86(1) and 2.95(1) Å, respectively.

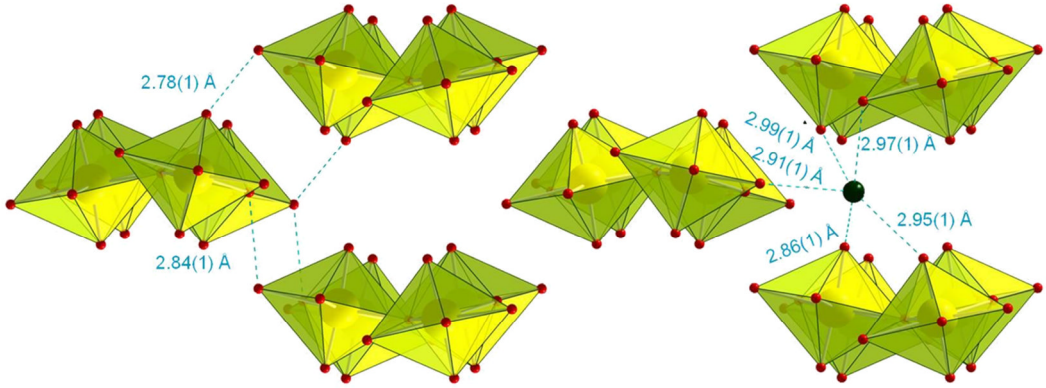

Figure III.2.23 Possible ionic and hydrogen bond interactions in **iso8** complex.

The structure of **iso9** ($(NH_4)_2[(UO_2)_4(ipa)_2O_2(OH)_2(H_2O)_2]\cdot H_2O$) complex exhibits a similar SBU with the one of **iso8**. It presents two crystallographic sites for the uranium atom, both situated in general positions and both doubled by a *2b* (½ 0 0) inversion center, the tetranuclear unit being centered on this symmetry element. The coordination sphere around the uranium atoms (Figure III.2.24) is also similar to the one of **iso8**, with apical U=O distances ranging from 1.70(4) to 1.78(3) Å and equatorial U–O distances ranging between 2.21(4) and 2.56(3) Å.

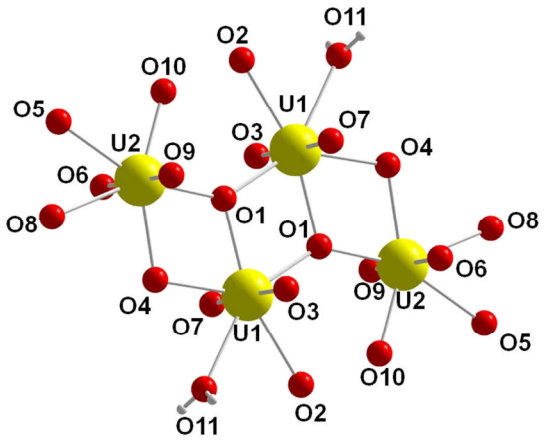

Figure III.2.24 Representation of the inorganic tetranuclear building unit showing the seven-fold coordination around the uranium atoms in the **iso9** complex.

The bond valence calculation gave the values of 2.05 and 1.15 v.u. for the μ_3-O1 and μ_2-O4 bridges, identifying them as oxo and respectively hydroxo species, similar to the case of **iso8**. A comparative analysis of interatomic distances and calculated valence values for the SBUs of **iso8** and **iso9** is given in Table III.2.2.

Table III.2.2 Comparison between the bond lengths and bond valences of the oxygen atoms constituting the SBUs of iso8 and iso9 complexes.

Interatomic bond		Interatomic distance (Å)		Bond valence /oxygen atom valence (v.u.)		Oxygen atom type
iso8	iso9	iso8	iso9	iso8	iso9	
U(2)-O(4)	U(1)-O(7)	1.790(4)	1.71(3)	1.65 / 1.65	1.93 /1.93	uranyl
U(2)-O(6)	U(1)-O(3)	1.803(4)	1.78(3)	1.61 / 1.61	1.69 / 1.69	uranyl
U(2)-O(1)	U(1)-O(2)	2.448(4)	2.44(2)	0.47 / 1.74	0.47 / 1.83	carboxyl
U(2)-O(2)	U(1)-O(4)	2.423(4)	2.37(3)	0.49 / 1.10	0.54 / 1.15	hydroxyl
U(2)-O(9)	U(1)-O(11)	2.460(4)	2.56(3)	0.45 / 0.45	0.38 / 0.38	water
U(2)-O(3)	U(1)-O(1)	2.258(4)	2.26(2)	0.67 / 1.98	0.67 / 2.05	oxo
U(2)-O(3)#1	U(1)-O(1)#1	2.304(4)	2.28(2)	0.61 / 1.98	0.64 / 2.05	oxo
U(1)-O(11)	U(2)-O(9)	1.791(4)	1.70(4)	1.65 / 1.65	1.97 / 1.97	uranyl
U(1)-O(8)	U(2)-O(6)	1.802(4)	1.71(3)	1.62 / 1.62	1.69 / 1.69	uranyl
U(1)-O(7)	U(2)-O(10)	2.365(4)	2.21(4)	0.55 / 1.79	0.74 / 2.00	carboxyl
U(1)-O(2)	U(2)-O(4)	2.310(4)	2.31(3)	0.61 / 1.10	0.61 / 1.15	hydroxyl
U(1)-O(10)	U(2)-O(5)	2.433(4)	2.48(2)	0.48 / 1.75	0.44 / 1.75	carboxyl
U(1)-O(3)	U(2)-O(1)	2.241(4)	2.21(2)	0.69 / 1.98	0.74 / 2.05	oxo
U(1)-O(5)	U(2)-O(8)	2.542(5)	2.49(2)	0.39 / 1.62	0.43 / 1.82	carboxyl

In this complex, the bridging mode of the organic ligand is identical to that found in **iso7** and **iso8** with one chelating mode for one carboxylate arm and one bidentate bridging mode for the other one. It results in the generation of infinite anionic chain $[(UO_2)_4(ipa)_2O_2(OH)_2(H_2O)_2]^{2-}$ running along the [100] direction.

The major difference from the **iso8** compound is the chains orientation in the (011) plane. For **iso8** all the chains are parallel and orientated along [001] direction. Contrarily, in the case of **iso9** each of the chains are perpendicular to all four adjacent chains and all make a ±45° angle with each of the [010] and [001] directions (Figure III.2.25).

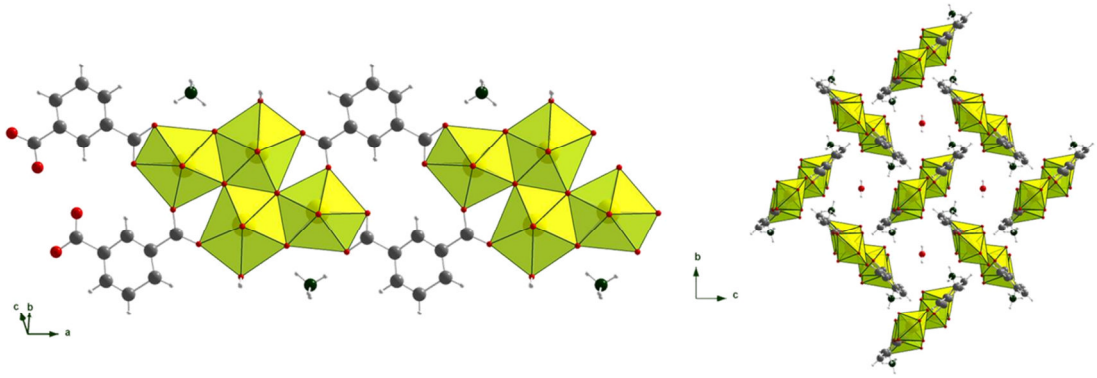

Figure III.2.25 View of **iso9** complex: single chain representation (left) and chain orientation in the (011) plane (right).

The perpendicular positioning of the chains creates infinite open channels orientated parallel to the chains along [100]. Free water molecules (Ow1) are encapsulated at the center of each channel, with distances of more than 3 Å from any neighboring oxygen atoms, indicative of rather weak hydrogen bond interactions.

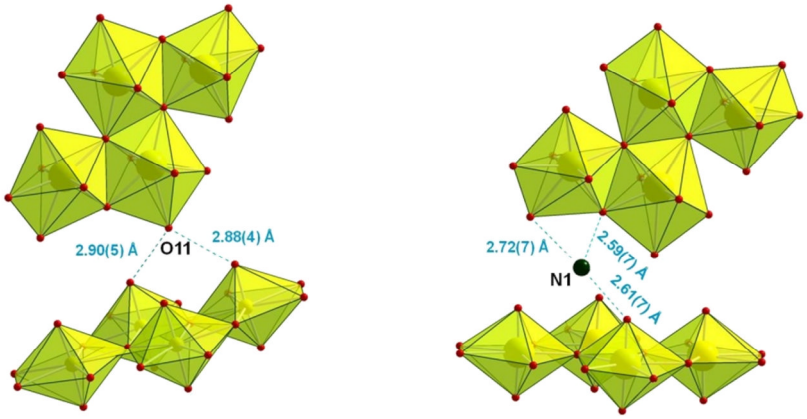

Figure III.2.26 View of the weak ionic and hydrogen bond interactions in **iso9** complex.

Some strong hydrogen bond interactions take place between the coordinating water molecule (O11) and the uranyl oxygen atoms (O3 and O6) belonging to an adjacent SBU (Figure III.2.26), with the interatomic distances of

2.90(5) and 2.88(4) Å, respectively. Other ionic interactions are occurring between the ammonium cation (N1) and the two adjacent SBUs. The closest oxygen atoms to the ammonium ion are O4 (μ_2-OH) and O8 (carboxyl), belonging to one SBU, with distances of 2.57(7) and 2.72(7) Å respectively and O7 (uranyl), belonging to a second SBU situated at a distance of 2.61(7) Å.

It is interesting to notice that the coordination complexes **iso8** and **iso9** constitute two polymorphic assemblies (Figure III.2.27) from a given motif with identical chemical formula and exhibiting two distinct structural arrangements. Apparently the driven force favoring the formation of one given structure is the nature of the pH moderator, **iso8** being identified in chemical systems using ammonium or KOH and **iso9** in systems using 1,3-diaminopropane as pH correctors (Figure III.3.1).

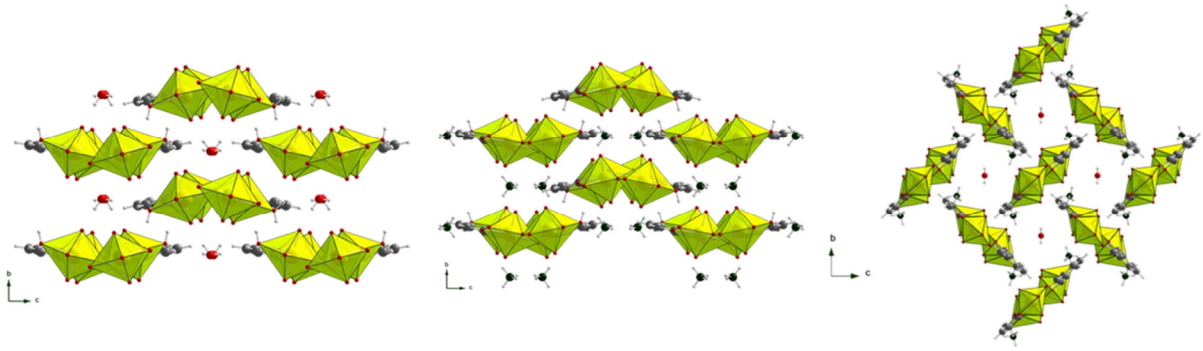

Figure III.2.27 Views of the different modes of assemblies of uranyl-centered tetramer-based ribbons $[(UO_2)_4(ipa)_2X_6]$ (X= O, OH, H_2O) in **iso7** (left), **iso8** (center) and **iso9** (right).

The uranyl phthalates **iso10** $[(UO_2)_4(ipa)_2O(OH)_2(H_2O)_2]\cdot 2H_2O$ is the most interesting and unusual one for its novelty. It exhibits a building unit containing eight uranyl centers, which are seven-fold coordinated and interconnected through μ_3-OH and μ_3-O bridges (Figure III.2.28). The octanuclear SBU is the largest discrete block of interconnected uranyl polyhedra so far reported in literature[7]. The previous largest unit reported in carboxylates-based compounds (excepting peroxo type clusters) was a hexanuclear SBU[8] (see chapter I figure I.3.19). The structure of **iso10** has four crystallographic sites for the uranium atoms, each situated in a *2i* (x y z) general position. All four uranium atoms positions are being symmetrically doubled by a *1b* (0 0 ½) inversion center, on which the SBU is situated, resulting in an octanuclear motif (Figure III.2.28).

The coordination sphere of U1 atom is formed by two uranyl type oxygen atoms (O8 and O18) in apical position (U═O distances of 1.773(3) and 1.775(3) Å respectively) forming a 178.9(2)° angle around the uranium atom and by other five oxygen atoms in the equatorial plane. Two of them (O11, O20) are carboxyl types belonging to the ligand (U─O bond lengths of 2.360(3) and 2.398(3) Å respectively); the remaining three oxygen atoms (O1, O2 and O2#) are μ_3-OH groups (U─O bond lengths of 2.406(3), 2.416(3) and 2.586(3) Å, respectively). For U2 atom the coordination environment, beside the two uranyl type oxygen atoms (O15 and O16) situated at 1.765(3) and 1763(3) Å from the uranium atom and creating a O═U═O angle of 177.5(2)°, is formed in the equatorial plane by other five oxygen atoms. Two of them (O7 and O17) are carboxyl type (U─O bond lengths of 2.448(3) and 2.296(3) Å respectively). The third (O1) is a μ_3-OH group (U─O distance of 2.556(3) Å). The fourth (O3) is a μ_3-O group (UO distance of 2.249(3) Å) and the fifth (O19) belongs to the coordinating water molecule forming a U─O bond of 2.491(3) Å. For the coordination sphere of U3 atom one of the two (O10 and O14) uranyl type oxygen atoms (U═O distances of 1.823(3) and 1.770(3) Å respectively and U═O═U angle of 176.8(2)°), the O10 is shared with U4 atom forming a U3═O10─U4 angle of 109.1(1)°. The U3═O10 bond (1.823(3) Å) is slightly longer than the typical uranyl bond (1.763(3)-1.823(3) Å) due to the implication of the O10 into a second bonding into the equatorial plane of U4 polyhedron. The pentagonal base of the polyhedra is completed by other five oxygen atoms from which one (O13) is carboxyl type (U─O distances of 2.311(3) Å), the second (O21) belongs to a coordinating water molecule (U─O distances of 2.432(3) Å), the next two (O1 and O2) are μ_3-OH groups (U─O bond lengths of 2.456(3) and 2.426(3) Å, respectively), the fifth (O_3) being a μ_3-O group, situated at 2.217(3) Å distance from the uranium atom. The last uranium atom U4, completing half of the compound's SBU is also composed of 7 oxygen atoms from which 2 (O9 and O12) positioned in apical position (U═O distances of 1.777(3) and 1.780(3) Å respectively) are forming the uranyl ion (O═U═O angle of 176.3(1)°), the remaining five oxygen atoms are: one (O10) uranyl type belonging to U3 coordination sphere (U4─O10 bond length of 2.548(3) Å), one μ_3-O group (O3) having a U─O bond length of 2.267(3) Å and three carboxylate type (O4-O6)

belonging to the organic linker (U—O distances of 2.346(3), 2.385(3) and 2.352(3) Å respectively), forming the equatorial coordination plane.

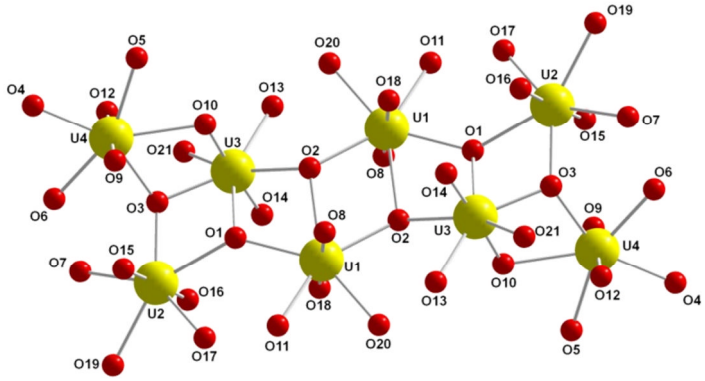

Figure III.2.28 The octanuclear building unit showing the 7-fold coordination around uranium atoms in the **iso10** complex.

The bonding between the uranium polyhedra is ensured by two μ_3-O and four μ_3-OH bridges as follows: U1 polyhedron shares two edges, O2-O2 and O1-O2, with U1 polyhedron and respectively with U3 and two corners, O1 and O2, with U2 and U3 respectively; U2 polyhedron also shares the O1-O3 edge with U3 and one corner ,O3, with U4; U3 polyhedron shares the O3-O10 CCI edge with U4, the latter one having no other interaction with different polyhedra beside the already mentioned ones.

The assignments of the oxo, hydroxo and aquo species have been done based on bond valence calculation[5], the expected values being 0.4 for water molecule, 1.2 for hydroxyl groups and 2 for O^{2-} groups. These assignments are summarized in Table III.2.3.

Table III.2.3 Assignments of the oxygen atoms from the octanuclear SBU in **iso10** complex.

Atom	Atom bond	Bond length	bond valence [v.u.]	atom valence [v.u.] / assignment
O1	U(1)-O(1)	2.406	0.50	1.33 / hydroxo
	U(2)-O(1)	2.566	0.37	
	U(3)-O(1)	2.456	0.46	
O2	U(1)-O(2)	2.586	0.36	1.34 / hydroxo
	U(1)-O(2)#1	2.416	0.49	
	U(3)-O(2)	2.426	0.49	
O3	U(2)-O(3)	2.249	0.68	2.07 / oxo
	U(3)-O(3)	2.217	0.73	
	U(4)-O(3)	2.267	0,66	
O10	U(3)-O(10)	1.823	1.55	1.94 / oxo-uranyl (CCI)
	U(4)-O(10)	2.550	0.38	
O21	U(3)-O(21)	2.432	0.48	0.48 / aquo

An interesting feature about this SBU is the cation-cation interaction (CCI) between the U3 and U4 uranium atoms through the O10 oxygen atom. As it was previously described (chapter I Figure I.3.22) a CCI is mainly the atypical bonding of a uranyl type oxygen atom (usually chemically inert) with a second metal atom. All the reported uranyl homometallic CCIs take place as a corner sharing bonding, **iso10** being so far the only compound in which this atypical bonding appears as edge sharing (Figure III.2.29). The two involved uranium atoms also share, beside the uranyl type oxygen atom (O10), a μ_3-oxo bridging group (O3).

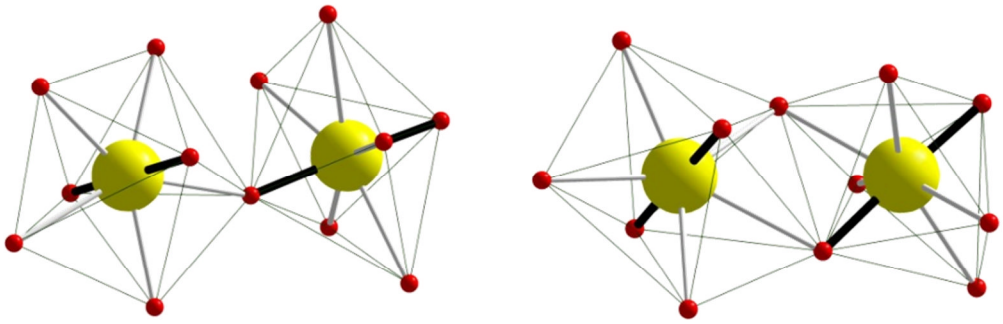

Figure III.2.29 Model of a corner-sharing CCI (left) and of an edge-sharing CCI (right). With black bold have been marked the U=O uranyl type bonds.

Although the inorganic motif of **iso10** phase has a high complexity, it possesses only two independent crystallographic isophthalate molecules (Figure III.2.30-left). First ligand molecule (A) bridges through one carboxylate arm the U1 and U2 polyhedra, belonging both to the same SBU and through the second arm two uranium polyhedra (U4 and U4#) but this time each belonging to 2 different SBUs. The coordination configuration for the first ligand molecule is μ_4-η_1:η_1:η_1:η_1 binding together three octanuclear SBUs. The second ligand molecule (B) bridges through one carboxylate group the U1 and U2 polyhedra of one SBU, while through the second one it bridges the U3 and U4 polyhedra belonging to a neighbor SBU. The coordination configuration is also μ_4-η_1:η_1:η_1:η_1, but the ligand binds together only two SBUs. Globally each SBU is interlinked by the ligand molecules with other eight adjacent ones in order to form the final 3D edifice. The resulting structure exhibits along [010] direction open channels in which free water molecules are present, which together with the coordinating

water molecule create an extended network of weak hydrogen bond type interactions (Figure III.2.31).

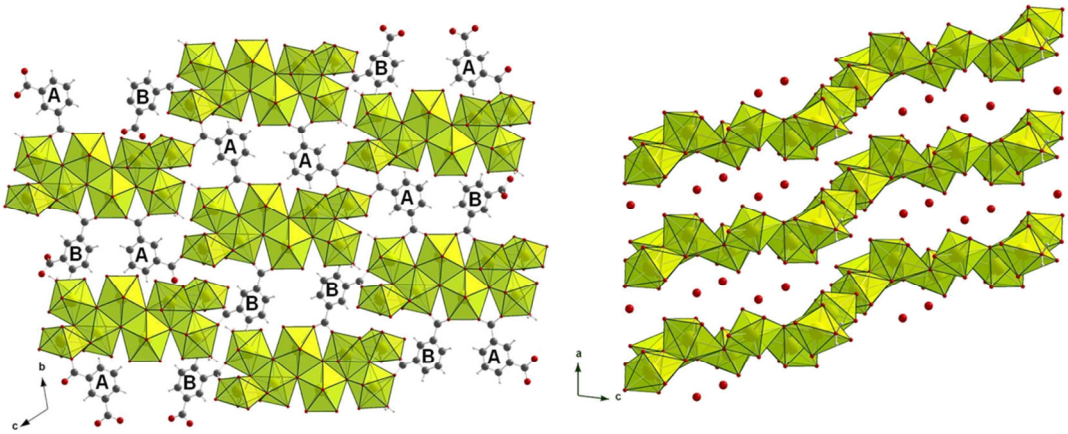

Figure III.2.30 Representation of **iso10**: the two different bonding configuration of the ligand (the free water molecules and different ligand molecules have been omitted for clarity), view along [100] axis (left) and the position of the free water molecules intercalated between the inorganic SBUs (the ligand's molecules have been omitted for clarity) (right).

The first free water molecule (Ow1) is situated at a close enough distance (below 3 Å) to four different oxygen atoms for interacting through hydrogen bonds. The closest one (2.72(1) Å) is a μ_3-hydroxo group (O1) belonging to a first SBU. The remaining three are: one uranyl type (O9) belonging to the same SBU (Ow1···O9 = 2.96(1) Å), another uranyl type oxygen atom (O14) belonging to a second SBU (Ow1···O14 = 3.00(1) Å) and the second free water molecule (Ow1···Ow2 = 3.00(1) Å). Beside the link with Ow1, the Ow2 water molecule can interact with a μ_3-hydroxo group (O2) belonging to the first SBU (Ow2···O2 = 2.68(1) Å) and with a uranyl type oxygen atom (O8), belonging to the second SBU(Ow2···O8 = 2.94(1) Å). The first bonded water molecule (O19) belonging to the U2 coordination sphere interacts with the carboxyl type oxygen atom (O7) also from a U2 coordination sphere but from an adjacent SBU. The O19 bonded water molecule belonging to the second SBU binds in the same manner the O7 oxygen atom from the first, resulting for each two SBUs in the structure a double hydrogen bond interaction, at a distance of 2.90(1) Å, between the U2 polyhedra of each. The second bonded water molecule (O21) belonging to U3 polyhedron is at suitable distance to interact with two oxygen atoms belonging to two different adjacent SBUs, first being a carboxyl type (O5) (O21···O5 = 2.67(1) Å), the second a uranyl type one (O12) (O21···O12 = 2.85(1) Å).

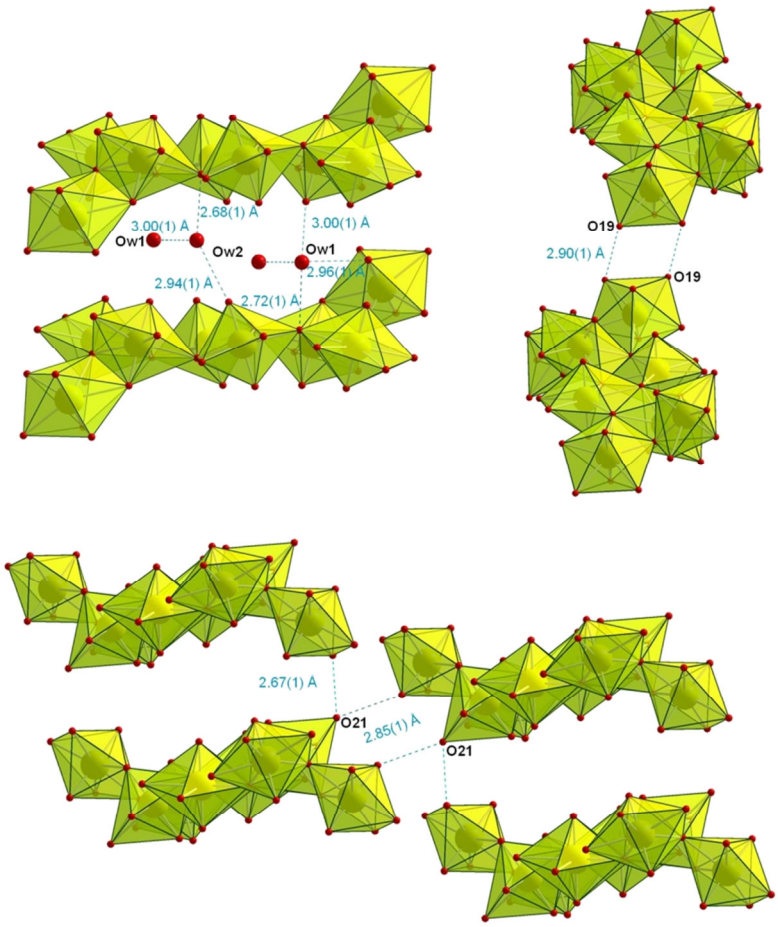

Figure III.2.31 The hydrogen bond interactions appearing in the structure of **iso10.**

III.3 . Synthesis

The **ison** (n = 1-10) compounds have been hydrothermally synthesized under autogenous pressure using 23 mL Teflon-lined Parr type autoclaves. The starting reagents have been: uranyl nitrate hexahydrate ($UO_2(NO_3)_2 \cdot 6H_2O$, Merck 99%), isophthalic acid (Aldrich 99%), KOH (Prolabo 85%), ammonia solution (Prolabo 28%), 1,3-diaminopropane (Acros Organics 99%), hydrazine solution (Acros Organics 51%). All are commercially available and have been used without further purifications.

Using the isophthalic acid as a ditopic ligand, three chemical systems have been studied with constant reaction time and temperature (arbitrarily for 24 hours at 200°C). The variation of the reaction pH has been investigated in order to analyze the effect of the hydrolysis of uranyl species in the presence of the isophthalate ligand. Four different base molecules have been tested, and these

define four systems corresponding to the addition of ammonium hydroxide (system 1), potassium hydroxide (system 2), hydrazine (system 3) and 1,3-diaminopropane (system 4). In the case of hydrazine system the variation of the metal / ligand ratio also gave significant changes in the final products, generating three subsystems (3.1 - 3.3). A summary of the different phases, which have been identified in our study, is presented in the Figure III.3.1 showing the phase diagram as a function of reaction pH. The pH value corresponds to that of the supernatant liquid measured after the hydrothermal reaction, before recovering the powdered product. The different coordination complexes have been generally crystallized in acidic conditions, but for pH greater than ≈1. At higher pH, dense uranium oxides could be obtained under the forms of $UO_{2+\delta}$ (fluorite)[9], U_3O_8[10] or mixed valence U^{IV}/U^{VI} oxide $[U_2(UO_2)_4O_6(OH)_4(H_2O)_4]\cdot 5H_2O$ (ianthinite)[11].

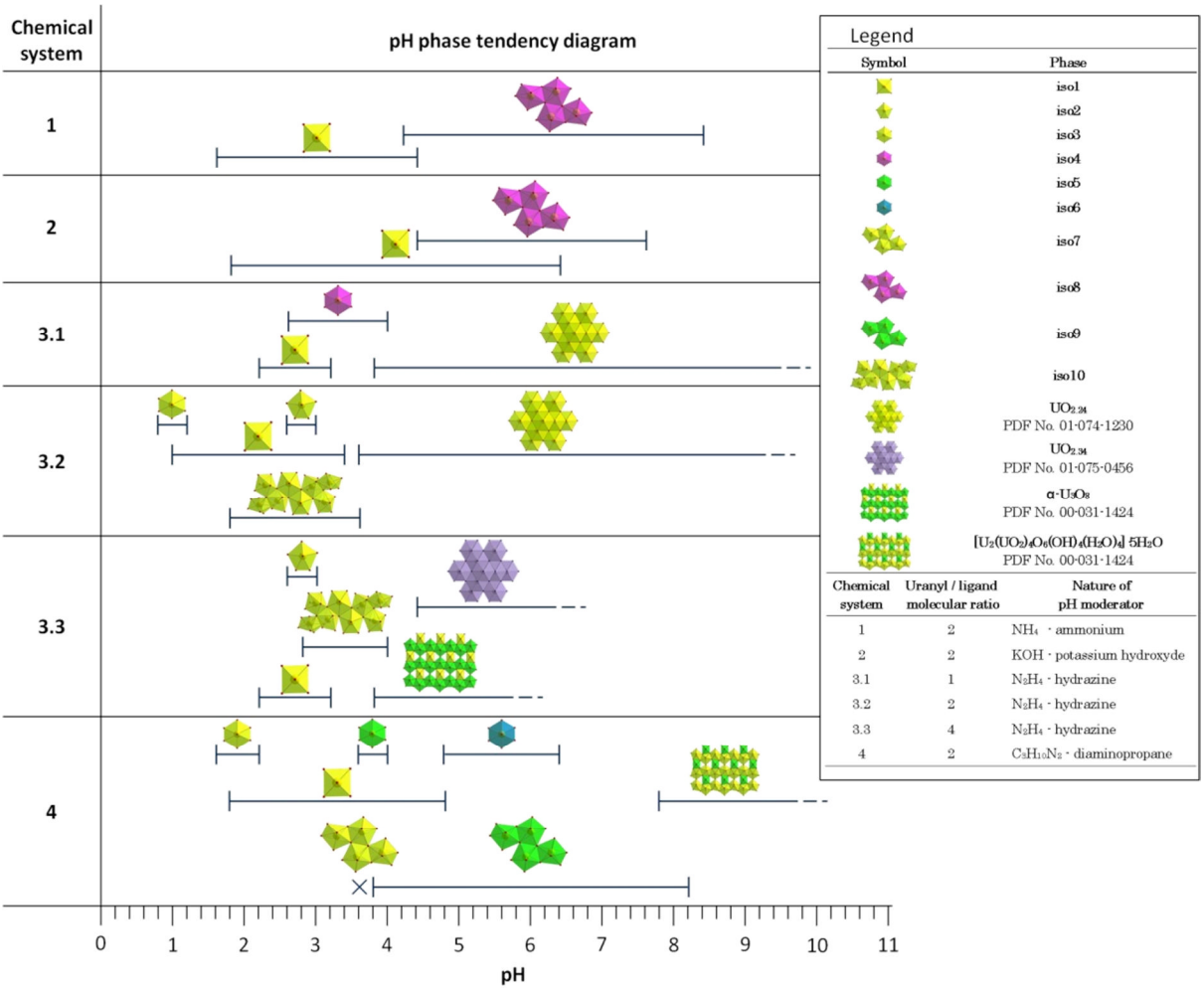

Figure III.3.1 Phase tendency diagram as a function of pH for different chemical systems belonging to the uranyl isophthalates compounds (after hydrothermal heating at 200°C for 24 h).

The **iso1** phase [(UO_2)(ipa)] (, isolated square bipyramid) appeared in all the studied systems, usually at low pH, traces of this compound appearing even at pH = 5. Pure phases of **iso1** have been obtained on a narrow domain of pH, generally between 2 and 3, the exact domain varying from one system to another. As typical synthesis route it has been arbitrarily chosen the system using 1,3-diaminopropane as base (system 4) since largest sizes of crystals have been generated in this particular case. The preparation possessing the highest purity and crystallinity of **iso1** phase has been obtained by statically heating under hydrothermal conditions at 200°C a mixture of 0.502 g (1 mmol) uranyl nitrate hexahydrate, 0.083 g (0.5 mmol) isophthalic acid, 0.2 mL solution 2M (0.4 mmol) 1,3-diaminopropane and 4.2 ml (233 mmol) water during 24h. The solution pH after synthesis was 1.7.

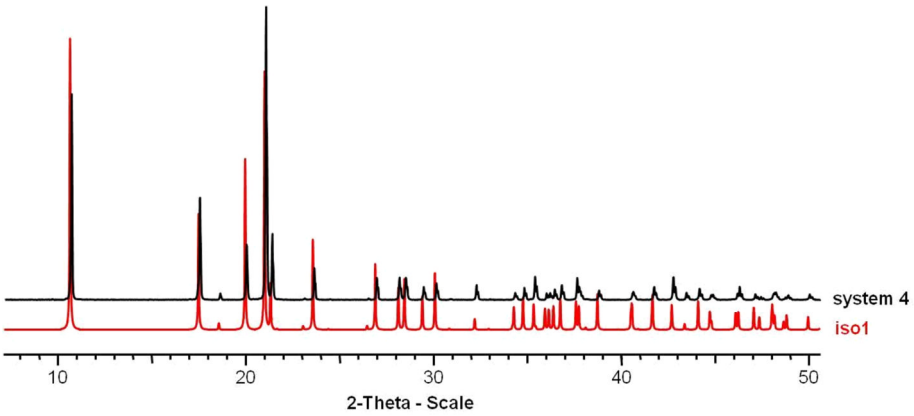

Figure III.3.2 Comparison between the calculated and experimental PXRD patterns of **iso1** phase, indicating its purity in one of the chemical system 4 preparations.

The resulting yellow solid product has been filtered off, washed with water and dried at room temperature. The product has been analyzed by scanning electron microscopy and shows irregular shaped crystals with sizes of 400 - 600 µm (Figure III.3.3).

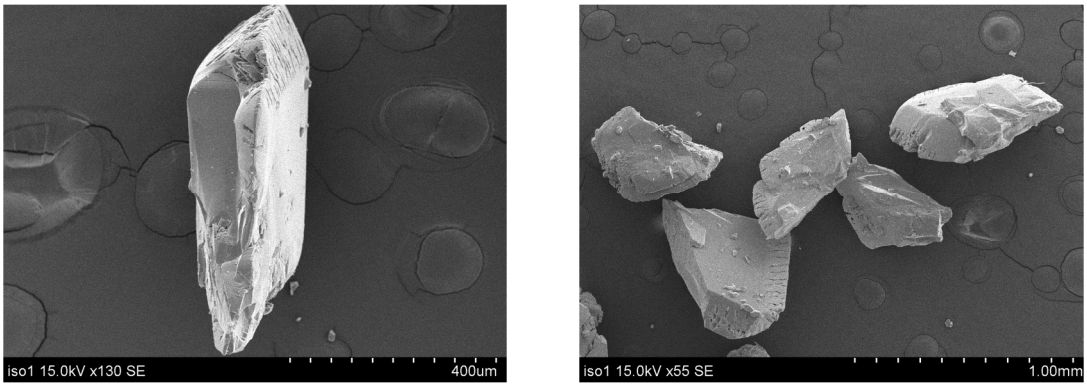

Figure III.3.3 SEM photographs of **iso1** complex.

Compound **iso2** $[(UO_2)(ipa)(H_2O)]\cdot 0.5H_2O$ (, isolated pentagonal bipyramid) has been identified in two of the subsystems implying hydrazine as a base. In both cases small amounts of **iso2** crystals have been identified as impurities for the same narrow domain of pH (2.8 - 3.2). The main phase is **iso1,** which also crystallized in the presence of small quantities of unidentified phases (Figure III.3.4).

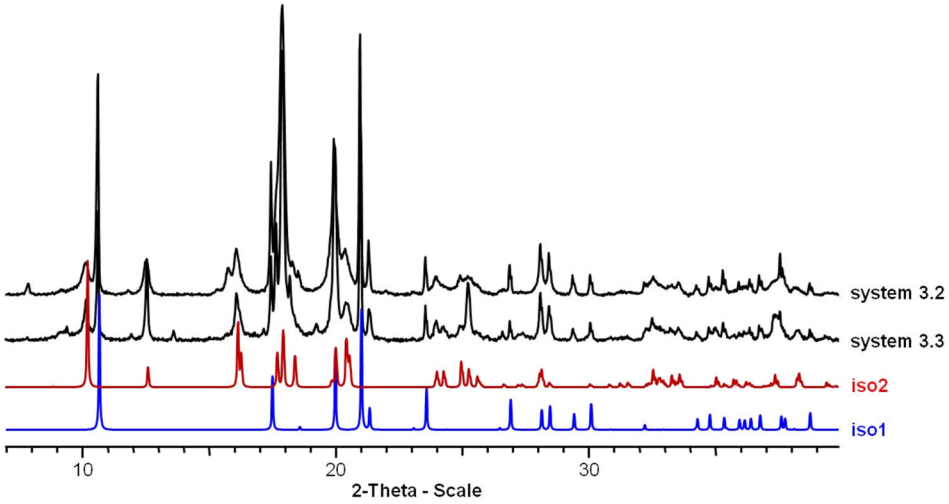

Figure III.3.4 Comparison between the calculated (**iso1** and **iso2**) and experimental (systems 3.2 and 3.3) PXRD patterns (cooper radiation) concerning **iso2** phase.

In first case (system 3.2), the preparation has been obtained by statically heating at 200°C during 24 h a mixture of 0.502g (1 mmol) uranyl nitrate hexahydrate, 0.083 g (0.5 mmol) isophthalic acid, 0.3 mL solution 2M (0.6 mmol) hydrazine and 4.7 ml (261 mmol) water. The final solution pH was 3.0.

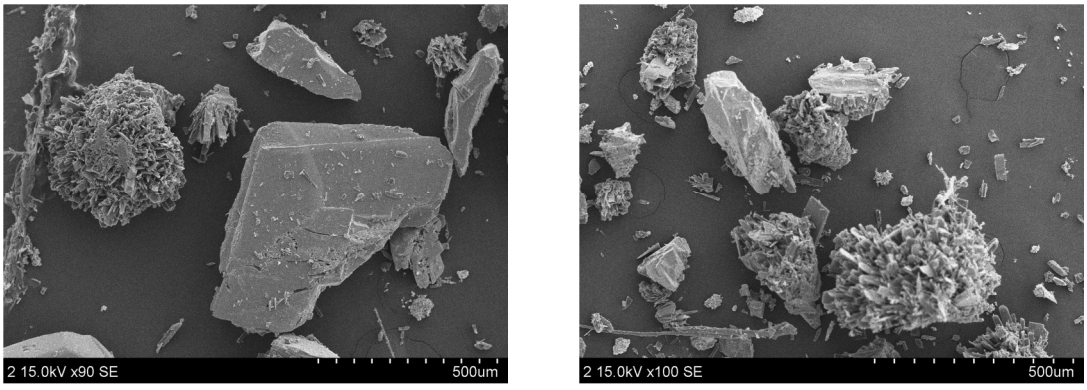

Figure III.3.5 SEM images of the system 3.3 product.

For the second case (system 3.3), under same conditions there have been used 0.502 g (1 mmol) uranyl nitrate hexahydrate, 0.042 g (0.25 mmol) isophthalic acid, 0.2 mL solution 2M (0.4 mmol) hydrazine and 4.8 ml (267 mmol) water. The final solution pH was 2.8.

The product obtained in the 3.3 chemical system has been also by SEM (Figure III.3.5), revealing a mixture between typical **iso1** crystals (large irregular shaped blocks) and small crystals of **iso2** phase.

The phase **iso3** [$(UO_2)(Hipa)_2$] (, isolated hexagonal bipyramid) also appeared in two different chemical systems (3.2 and 4) involving different organic amines, at about the same range of pH (0.8 - 2.2) in both cases. In the chemical system implying hydrazine as base (system 3.2) the preparation containing the largest amount of **iso3** phase has been obtained by statically heating a mixture of 0.502 g (1 mmol) uranyl nitrate hexahydrate, 0.083 g (0.5 mmol) isophthalic acid, 0.2 mL solution 2M (0.4 mmol) hydrazine and 4.8 mL (267 mmol) water. After the synthesis the supernatant solution pH was 1.0. In the system 4 (1,3-diaminopropane), the largest amount of **iso3** phase has been obtained using 0.502 g (1 mmol) uranyl nitrate hexahydrate, 0.083 g (0.5 mmol) isophthalic acid, 0.3 mL solution 2M (0.6 mmol) 1,3-diaminopropane and 4.7 mL (261 mmol) water. After the synthesis the solution pH was 1.9. In both cases **iso3** phase appeared together with large amounts of **iso1** and traces of unidentified impurity (Figure III.3.6).

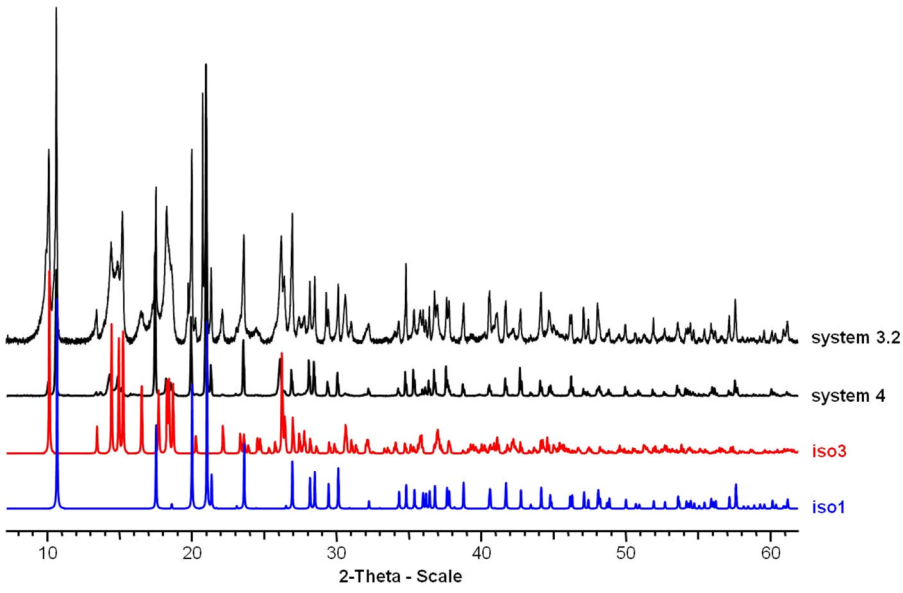

Figure III.3.6 Comparison between the calculated (**iso1** and **iso3**) and experimental (systems 3.2 and 4) PXRD patterns (cooper radiation) of systems producing **iso3** phase.

SEM investigation on the product of the 3.2 system revealed a mixture of **iso1** typical crystals (large irregular shaped blocks) and prism shaped crystals of **iso3** phase (Figure III.3.7).

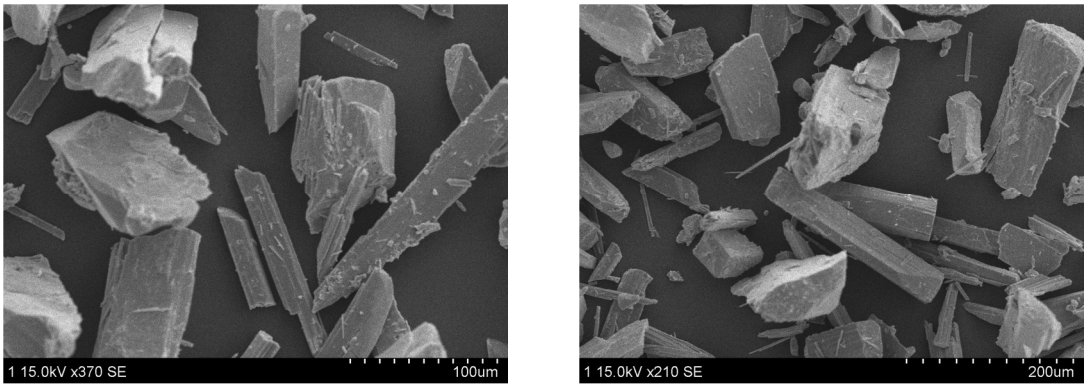

Figure III.3.7 SEM images of the system 3.2 product.

Crystals of **iso4** $(NH_4)[(UO_2)(ipa)(Hipa)]\cdot 3H_2O$ (, isolated hexagonal bipyramid) complex have been isolated from one chemical subsystem containing hydrazine as base, system 3.1. This phase appeared only in the conditions of this system, in the 2.4 - 4.0 pH range. The largest amount of phase has been obtained in a preparation by statically heating a mixture of 0.502 g (1 mmol) uranyl nitrate, 0.166 g (1 mmol) isophthalic acid, 1.0 mL solution 2M (2.0 mmol) hydrazine and 4.0 mL (222 mmol) water. The solution pH after synthesis was 2.4. In these conditions, **iso4** phase appeared as minor phase in mixture with **iso1** together with an unknown phase. (Figure III.3.8). Moreover, the crystal structure of **iso4** has shown the occurrence of ammonium groups as counter-cation, which would come from the *in-situ* chemical decomposition of hydrazine molecules under hydrothermal condition.

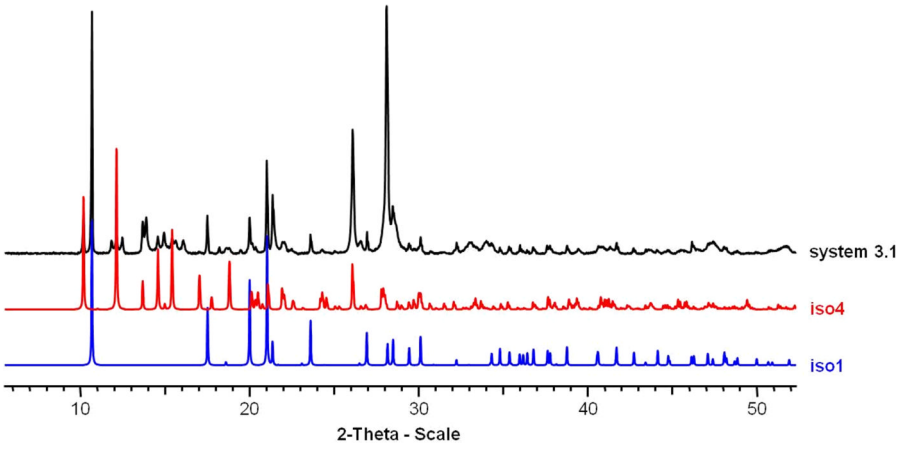

Figure III.3.8 Identification of **iso4** phase in a preparation belonging to the 3.1 chemical system.

The preparation containing the **iso4** phase has been investigated by SEM and revealed a mixture of small (~50 μm) prism shaped **iso4** crystals and large

undefined shape crystal blocks of **iso1**, both surrounded by unidentified powder (Figure III.3.9).

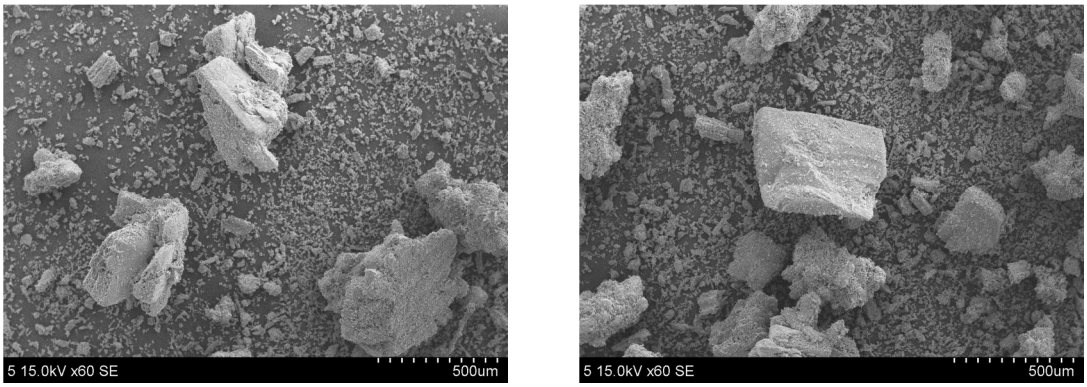

Figure III.3.9 SEM photographs of the preparation containing the **iso4** phase.

The **iso5** phase $(H_2dap)[(UO_2)_3(ipa)_4(H_2O)_2]\cdot 4H_2O$ (, isolated hexagonal bipyramid) has been obtained in a system 4 preparation by statically heating a mixture of 0.502 g (1 mmol) uranyl nitrate, 0.083 g (0.5 mmol) isophthalic acid 0.6 mL solution 2M (1.2 mmol) 1,3-diaminopropane and 4.4 mL (244 mmol) water. The solution pH after synthesis was 3.8. In these conditions **iso5** phase is obtained in large quantities, as major phase, but having as impurities the **iso1** and other unidentified phases (Figure III.3.10). The pH domain in which this phase is forming is very narrow, from 3.6 to 4.0.

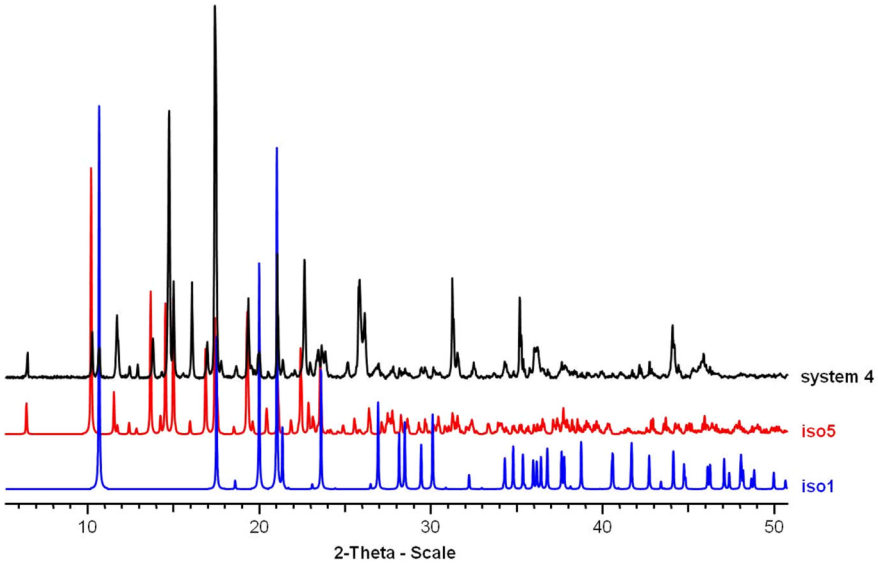

Figure III.3.10 Identification of **iso5** phase from chemical system 4.

Iso6 phase $(H_2dap)[(UO_2)_2(ipa)_3]\cdot 4H_2O$ (, isolated hexagonal bipyramid) is the second uranyl isophthalate containing diprotonated 1,3-diaminopropane cations, from chemical system 4. This phase appeared on a relatively broad

domain of pH, from 4.8 to 6.4, this region being unexpectedly for the isolation of monomeric species (see figure speciation diagram chapter I). The largest quantity of **iso6** has been obtained by statically heating under hydrothermal conditions a mixture of 0.502 g (1 mmol) uranyl nitrate, 0.083 g (0.5 mmol) isophthalic acid 0.8 mL solution 2M (1.6 mmol) diaminopropane and 4.2 mL (233 mmol) water. The final pH of the supernatant solution was 4.8. Under these conditions the product is a multiphase mixture of **iso6**, **iso1** and other unidentified impurities (Figure III.3.11).

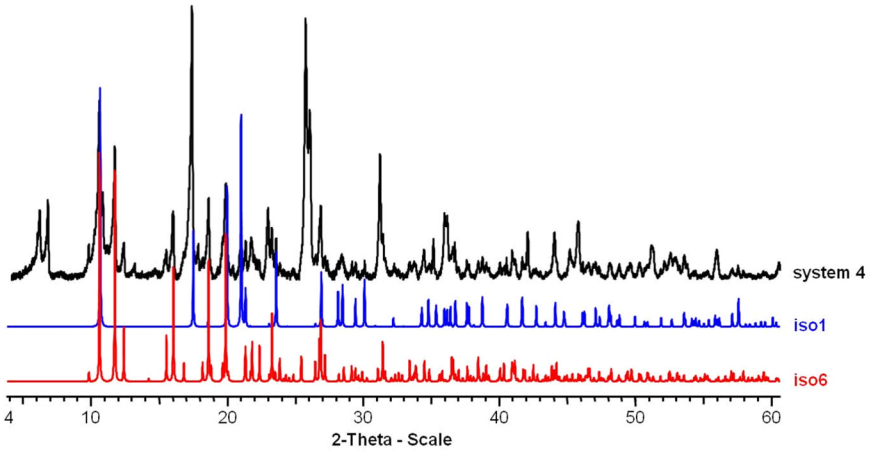

Figure III.3.11 Identification of **iso6** phase in one of the preparations of chemical system 4, from PXRD pattern comparison against calculated patterns.

The system 4 preparation containing the **iso6** phase was also investigated by SEM, the pictures revealing thin **iso6** needle shaped crystals of 100 µm in length together with block-like **iso1** crystals and some unidentified powder (Figure III.3.12).

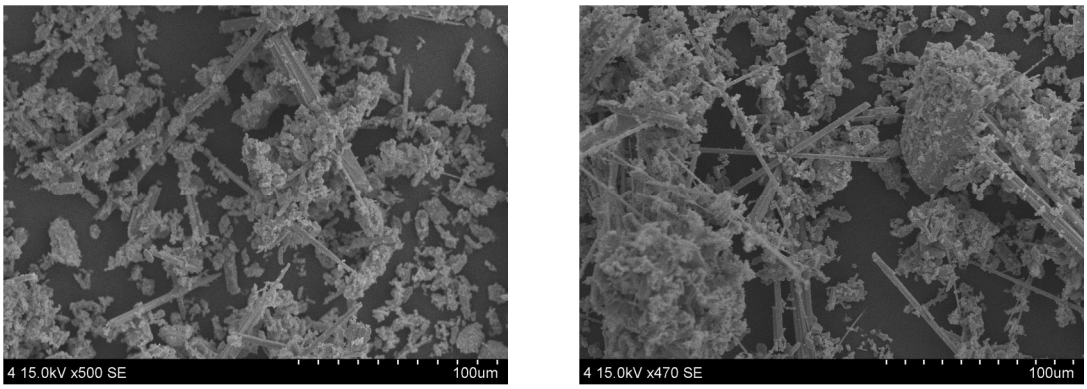

Figure III.3.12 SEM pictures of one system 4 preparation containing the **iso6** phase

A single crystal of **iso7** $[(UO_2)_4(ipa)_2(OH)_4(H_2O)_2]\cdot 2H_2O$ (, tetramer of pentagonal bipyramids) phase has been isolated and its structure has been determined by refining the single crystal X-ray diffraction data. The crystal has

been picked up from a preparation of chemical system 4 obtained by statically heating under hydrothermal conditions a mixture of 0.502 g (1 mmol) uranyl nitrate, 0.083 g (0.5 mmol) isophthalic acid 0.4 mL solution 2M (0.8 mmol) diaminopropane and 4.6 mL (256 mmol) water. The final solution pH was 3.6. The PXRD pattern of this preparation does not indicate any traces of **iso7** phase, showing an almost pure **iso1** phase, the small quantity of impurities remaining unidentified (Figure III.3.13).

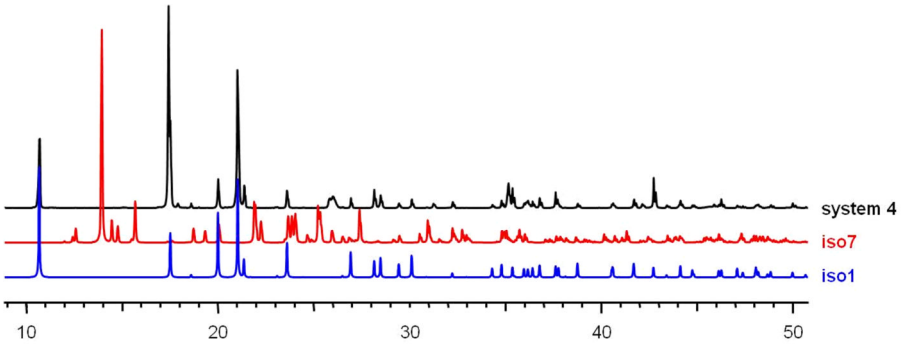

Figure III.3.13 Comparison between calculated (**iso1** and **iso7**) and experimental (system 4) PXRD patterns showing the absence of **iso7** phase from the preparations where the crystal was isolated.

In all uranyl isophthalate preparations the **iso7** phase is absent. This fact raises the question if **iso7** PXRD pattern was not confused with that of **iso8**. Both phases crystallize in the same space group and have close values of the cell parameters. The answer is no, since noticeable differences between the PXRD patterns of the two phases are observed (Figure III.3.14). The conclusion is that the **iso7** phase does not appear, in large enough quantities (> 5%) to give measurable X-ray diffraction signal, in any of the preparations (Figure III.3.14).

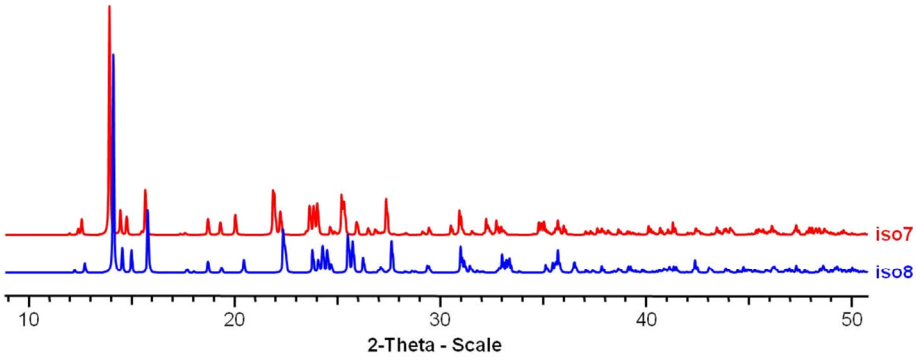

Figure III.3.14 Comparison between the calculated PXRD patterns of **iso7** and **iso8** phases.

Iso8 $(NH_4)_2[(UO_2)_4(ipa)_2O_2(OH)_2(H_2O)_2]$ (, tetramer of pentagonal bipyramids) phase is specific to the chemical system 1, containing ammonium

counter-cations in solution. It appeared in different preparations on a large domain of pH (4.2 - 8.4). The largest quantity of **iso8** phase have been obtained together with small quantities of unidentified impurities by statically heating under hydrothermal conditions a mixture of 0.502 g (1 mmol) uranyl nitrate, 0.083 g (0.5 mmol) isophthalic acid 1.4 mL solution 2M (0.8 mmol) ammonium hydroxide and 3.6 mL (200 mmol) water. The final solution pH was 4.3.

Similar PXRD patterns to the ones of **iso8** have been acquired from preparations belonging to the chemical system 2, in which the potassium hydroxide has been used as a base. The domain of pH in which the phase appeared is close to that of chemical system 1, between 4.4 and 7.6. The largest amount of phase has been obtained under the same conditions as in the previous system, using 2.0 mL solution 1M (2.0 mmol) KOH, 3 mL (167 mmol) water and the same quantities of metal source and ligand. The solution pH after synthesis was 3.1 and the phase was obtained together with **iso1** and other small quantities of unidentified phases (Figure III.3.15). These results conducted to the conclusion that an isotype of **iso8** phase containing potassium instead of ammonium as counter-cation was forming under these conditions. The proposed chemical formula would be $K_2[(UO_2)_4(ipa)_2O_2(OH)_2(H_2O)_2]$ by analogy the ammonium-based uranyl isophthalate **iso8**. This case was similar to that reported for the uranyl phthalates **pht3** and **pht4**[12] (chapter II). From this chemical system, no crystal structure was obtained by single X-ray diffraction structure determination due to the lack of suitable crystals.

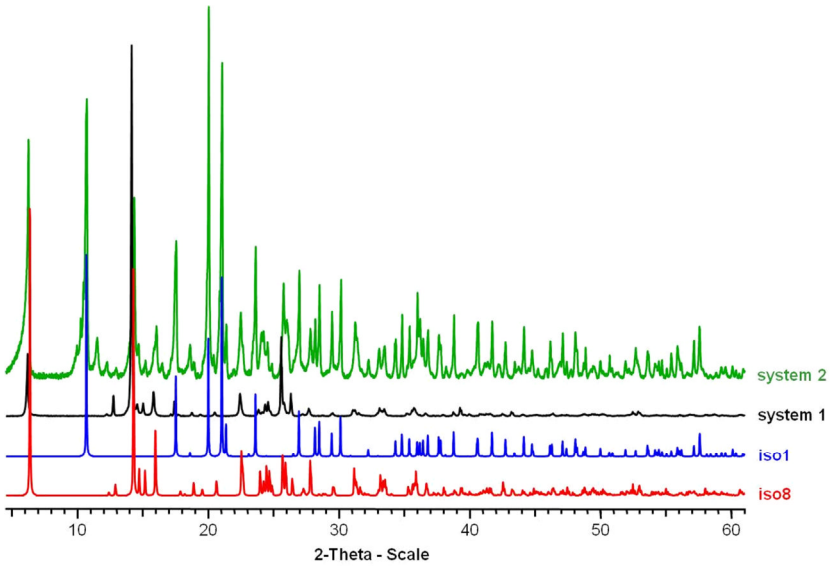

Figure III.3.15 Identification of **iso8** phase in two distinct chemical systems

One system 1 preparation, containing the **iso8** phase has been investigated by SEM (Figure III.3.16) and revealed a mixture of **iso8** needle-like crystals and **iso1** block-like ones, surrounded by an unidentified powder.

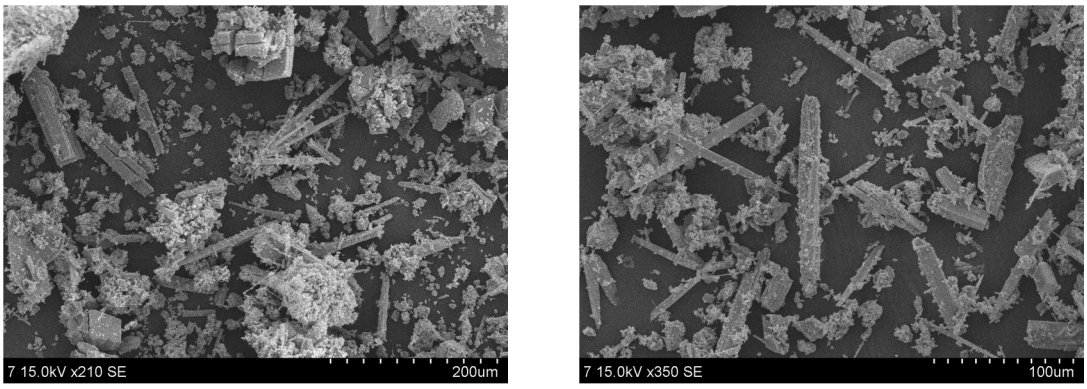

Figure III.3.16 SEM picture of one system 1 preparation containing the **iso9** phase.

Although the structure of **iso9** $(NH_4)_2[(UO_2)_4(ipa)_2O_2(OH)_2(H_2O)_2]\cdot H_2O$ (,tetramer of pentagonal bipyramids) incorporates ammonium cations, this phase appeared only in chemical system 4, system involving 1,3-diaminopropane as pH moderator. This phenomenon suggested the in-situ decomposition of the diamine under the hydrothermal conditions and the release of ammonium cationic species.

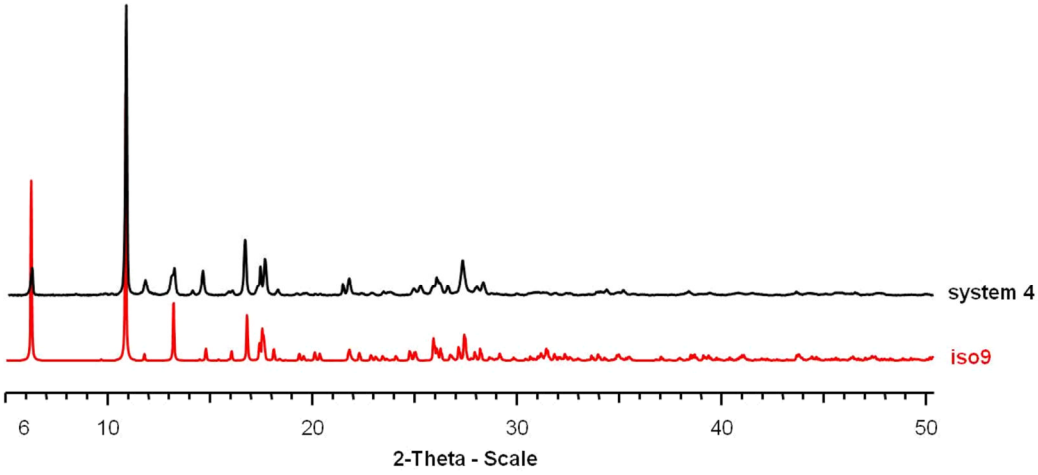

Figure III.3.17 Identification by PXRD pattern comparison of **iso9** in one of the chemical system 4 preparations.

The **iso9** phase crystallized on a broad domain of pH, from 3.8 to 8.2. The best yield for this phase has been obtained by statically heating under hydrothermal conditions a mixture of 0.502 g (1 mmol) uranyl nitrate, 0.083 g (0.5 mmol) isophthalic acid 1.0 mL solution 2M (2.0 mmol) 1,3-diaminopropane and 4.0 mL (222 mmol) water. The final solution pH was 7.9. In the latter

mentioned conditions the compound was obtained as major phase; the PXRD pattern also indicated the presence of small amount of unidentified impurities (Figure III.3.17).

The system 4 preparation containing **iso9** as major phase was also investigated by SEM. The photographs (Figure III.3.18) revealed large (~500 µm length) prismatic crystals of **iso9** phase surrounded by relatively large quantity of unidentified powder.

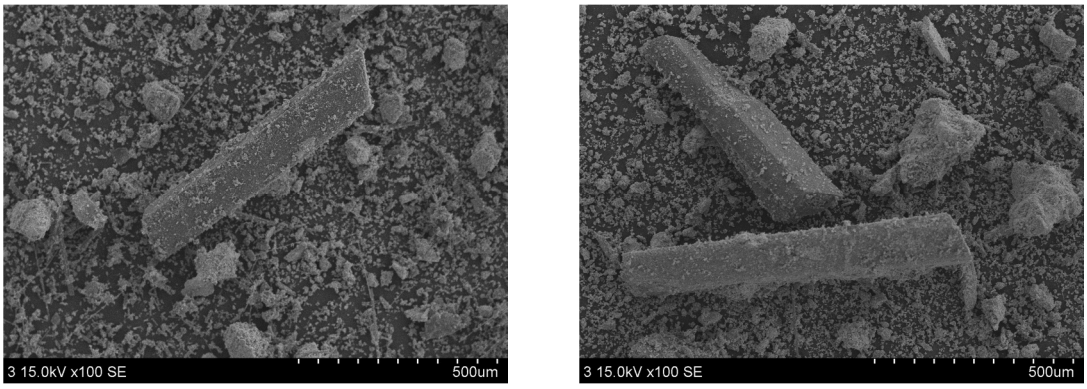

Figure III.3.18 SEM pictures of one system 4 preparation containing the **iso9** phase.

The **iso10** $[(UO_2)_4(ipa)_2O(OH)_2(H_2O)_2]\cdot 2H_2O$ (, octamer of pentagonal bipyramids) phase was obtained only in the presence of hydrazine, for which the metal / ligand ratio is higher of equal to 2 (chemical subsystems 3.2 and 3.3). In these systems the phase is formed on a relatively broad domain of pH, from 1.8 to 4.0 (Figure III.3.19). As pure phase, the compound has been produced by statically heating under hydrothermal conditions a mixture of 0.502 g (1 mmol) uranyl nitrate, 0.042 g (0.25 mmol) isophthalic acid 0.6 mL solution 2M (2.0 mmol) hydrazine and 4.4 mL (244 mmol) water. The final solution pH was 3.0.

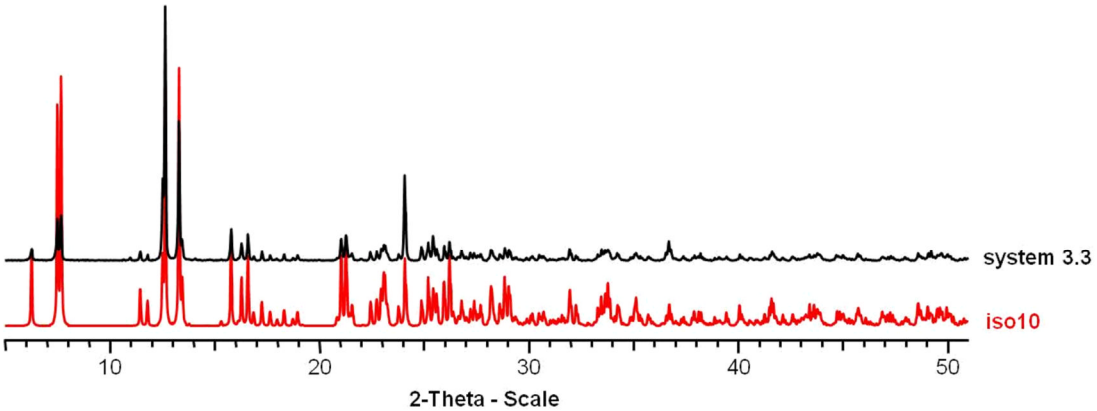

Figure III.3.19 Comparison between the calculated and experimental PXRD patterns of **iso10** indicating the phase purity in one of the chemical system 3.3 preparations.

The obtained crystalline product has been analyzed by scanning electron microscopy and shows irregular shaped crystals with sizes of 300 - 400 µm (Figure III.3.20).

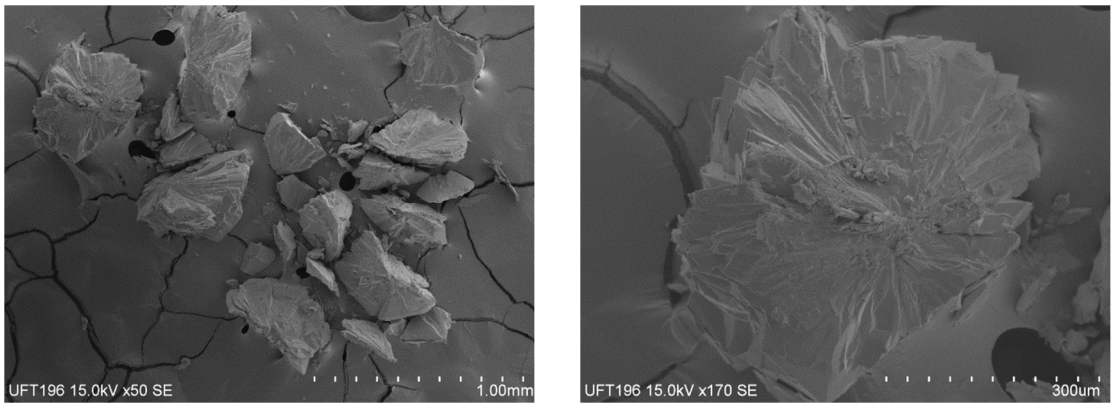

Figure III.3.20 SEM pictures of **iso10** crystals.

Due to the fact that only **iso1** and **iso10** coordination complexes have been obtained pure, they were the only two available for further analyses.

III.4 . Thermal characterization

The TGA curve of phase **iso1 [UO_2(ipa)]** (Figure III.4.1) exhibits a unique weight loss step near 420°C of approximately 35.3% (35.3% calculated) corresponding to the total degradation of the phase into α-U_3O_8 oxide (PDF No. 031-1424) respecting the degradation equation:

$$3[UO_2(C_8H_4O_4)] \xrightarrow[+4O_2\ -2H_2O\ -8CO_2]{420°C} U_3O_8$$

Around the same temperature the TD curve presents an intense exothermic peak corresponding to the oxidation of the organic ligand.

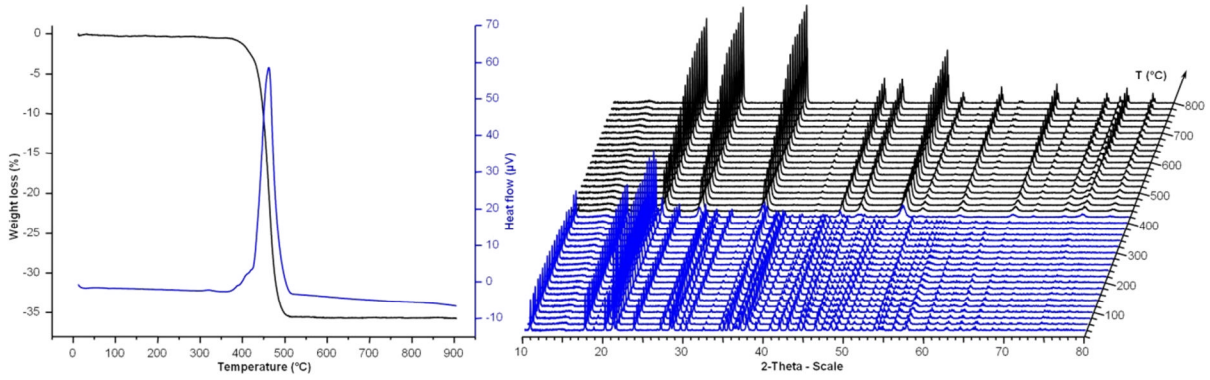

Figure III.4.1 Thermal behavior of phase **iso1**. TGA/TDA curves (left), thermodiffraction patterns (right).

The stability of **iso1** phase up to 400°C is confirmed also by thermodiffraction experiment, the crystalline structure remaining nearly unchanged (except slight cell parameters dilatation) up to this temperature. The transformation at 420°C into the final oxide takes place suddenly without passing through an amorphous intermediary phase.

The thermal degradation of **iso10** complex takes place in multiple steps evidenced in the TG curve by successive weight loss steps, by exothermic or endothermic peaks in TD curve and by changes in the diffraction patterns in the thermodiffraction diagram (Figure III.4.2). The first step appears in the TG curve as a smooth slope beginning around 120°C and ending around 320°C. It corresponds to a weight loss of 6.2% and has been assigned to a long process of water removal (5.3 H_2O molecules per $(UO_2)_4$ unit based on the weight of the residue). The weight loss value suggests that **iso10** contains a larger number of free water molecules than the one given by the solved structure. The chemical formula is $[(UO_2)_4(ipa)_2O(OH)_2(H_2O)_2]\cdot 3.3H_2O$. Due to the compactness of the structure, the free water molecules are not removed from pores at the specific temperature (below 100°C) but persist up to 200 - 270°C. For this reason in this first degradation step it was taken into account the whole water content regardless of type (free or bonded). This process is evidenced also in the TD curve by a low intensity broad endothermic peak centered at approximately 270°C. In the thermodiffraction diagram this process is seen as a change from the diffraction pattern of the initial complex into a pattern of an amorphous phase, this change occurring at 240°C. The second step has a weight loss of 18.7% and corresponds to the decomposition of the organic ligand. The calculated weight loss for this process is of 21.1%. The disagreement between the experimental and the calculated weight loss values indicates that the ligand molecules does not pass entirely into gaseous products, some of the carboxylate type oxygen atoms remaining in the uranium coordination sphere, possibly as carbonate species. In the TD curve this step is evidenced by two intense exothermic peaks, indicating that the oxidation of the ligand's organic molecule is a two-step process. In the thermodiffraction patterns this step corresponds to the passage from the amorphous phase to a poor crystalline one corresponding to a form of U_3O_8. The

last two steps at 520 and 630°C together summing a weight loss of 1.83% correspond to the atoms reorganization in the oxide structure, the reduction of uranium valence from 6 in the initial complex to 5.33 in the final oxide identified as U_3O_8 (PDF No. 01-089-4906) and the decomposition of the carbonate species. These two steps take place without thermal effect, the TD curve presenting no inflections in the region, and also without major changes in the thermodiffraction patterns beside the appearance of some low intensity peaks (starting with 600°C) corresponding to the final form of the uranium oxide and the crystallinity growth of the oxide phase with the temperature.

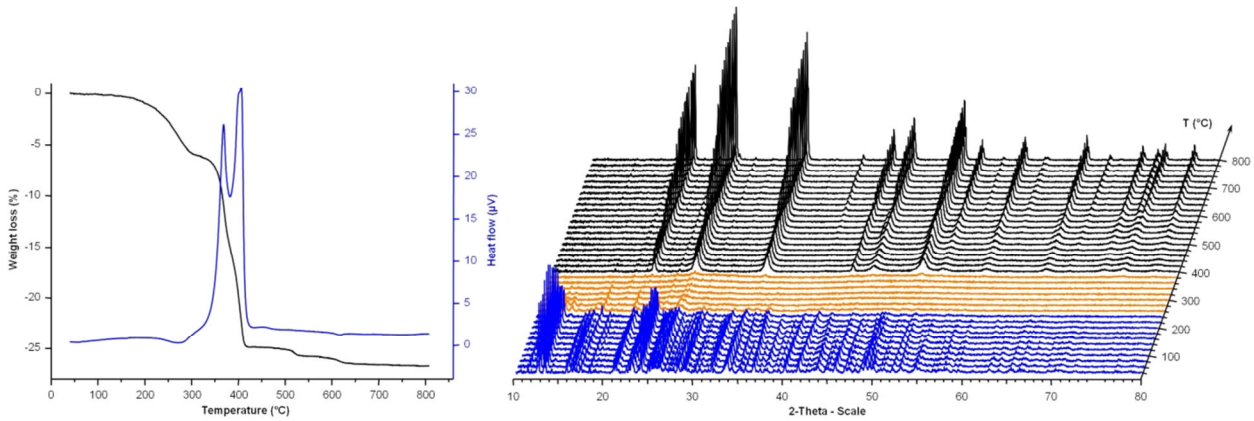

Figure III.4.2 Thermal behavior and thermal stability of phase **iso10**. TGA/TDA curves (left), thermodiffraction patterns (right).

All four degradation steps are summing a total weight loss of 26.69%, value which is in agreement with the calculated one 27.76% based on the degradation equation below:

$$3[(UO_2)_4(C_8H_4O_4)_2O(OH)_2(H_2O)_2]\cdot 3.32H_2O \xrightarrow[-48\,CO_2\ -30.96\,H_2O]{650°C\ +43\,O_2} 4U_3O_8$$

III.5 . Spectroscopic characterization

Infrared spectroscopy

The IR spectrum of **iso1** complex (Figure III.5.1) shows no absorption maxima above 1700 cm^{-1} indicating the absence of any kind of water molecule in the crystalline structure.

The ligand specific vibration appears in spectrum as absorption peaks in the region 1700 - 960 cm^{-1}, with the vibrations of the carboxylate groups giving maxima at 1501.4 cm^{-1} $\nu_{asym}(COO)$ and 1390.7 cm^{-1} $\nu_{sym}(COO)$. The other ligand related vibrations give low intensity absorption peaks and could not be accurately attributed.

The vibration corresponding to the uranium-oxygen bonds give peaks below 1000 cm^{-1}. The most intense band is at 936.6 cm^{-1} and has been attributed to the ν_3 asymmetrical vibration of the uranyl double bond O═U═O. The empirical equation[13]

$$\boldsymbol{d\,(U-O)(pm) = 9141[\nu_3(cm^{-1})]^{-2/3} + 80.4}$$

can be applied for calculating the U═O bond length based on the position of the corresponding IR absorption peak. It has been found a distance of 1.759 Å, which is in perfect agreement with the one refined from the structure determination by single crystal X-ray diffraction experiment of 1.759(2) Å.

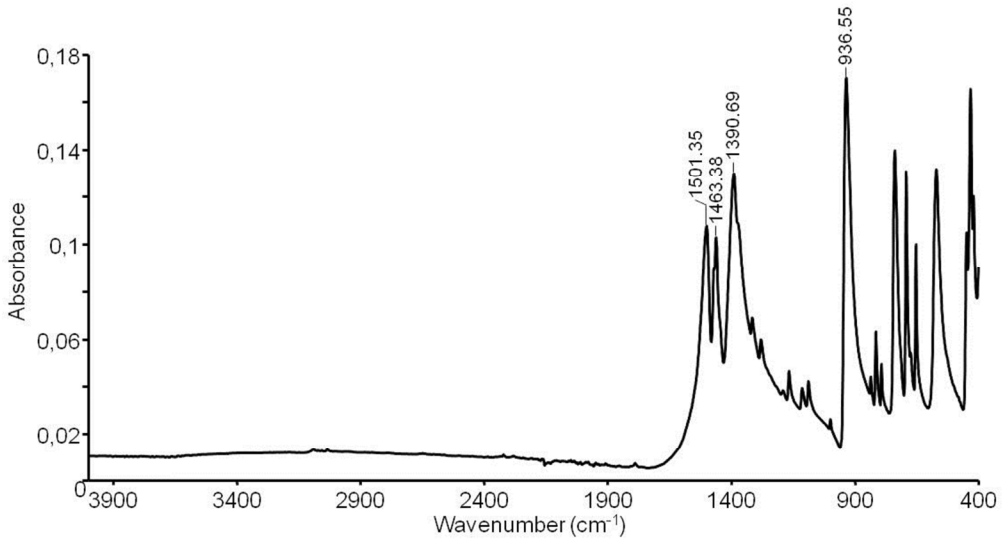

Figure III.5.1 Infrared spectrum of **iso1** complex

The infrared spectrum of **iso10** (Figure III.5.2) shows in the 2900 - 3700 cm^{-1} region three absorption peaks corresponding to the water molecule vibrations. All three have been attributed to the O─H stretching vibrations. First two belong to the free water molecules present in the structure, with two bands at 3596 and 3522 cm^{-1} being ν_{asym}. The third, a broad band, is centered at 3265 cm^{-1} covering the stretching vibrations of water molecules involved in the hydrogen bond interactions (free water and coordinated water). Also indicating

the presence of water molecules in complex is the intense peak at 1599 cm^{-1} which has been attributed to the δ vibrations[14].

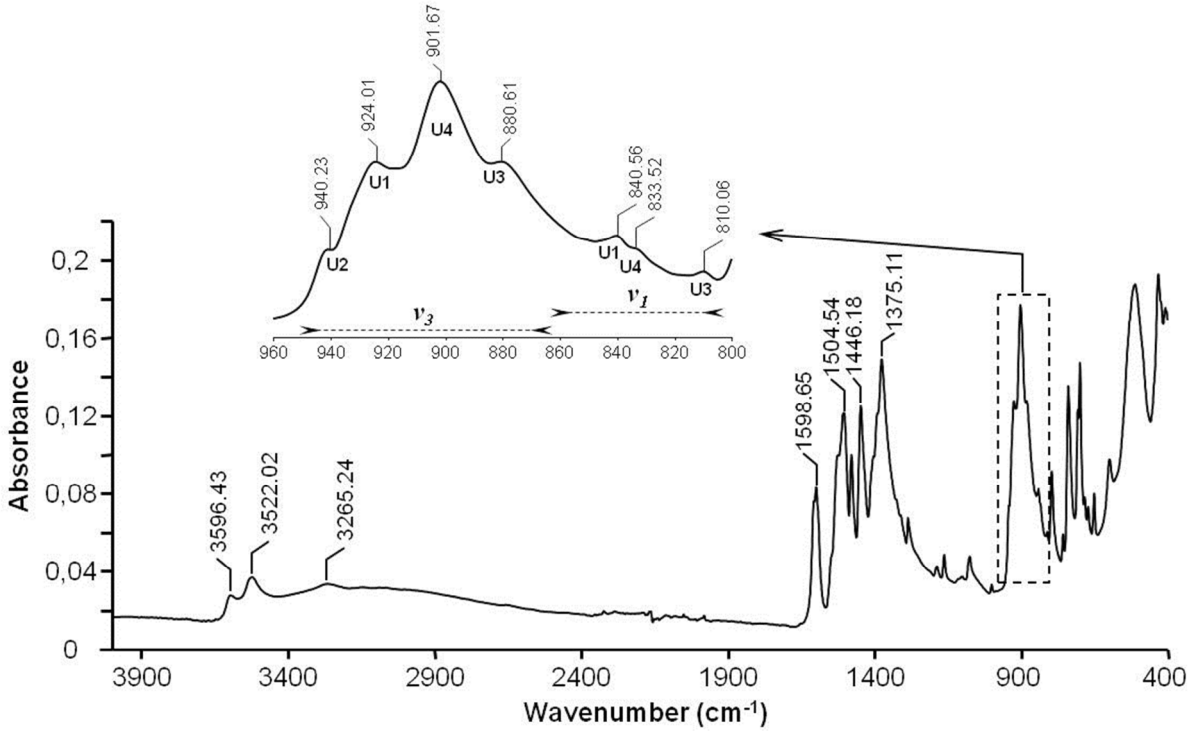

Figure III.5.2 Infrared spectrum of **iso10** complex.

The second important region of the IR spectrum is in the range 1570 - 1250 cm^{-1}. The absorption peaks appearing in this region belong to the vibrations of the ligand molecule. From these, the ones at 1505 and 1446 cm^{-1} have been assigned to the stretching vibrations of the carboxylate groups, $\nu_{asym}(COO)$ and $\nu_{sym}(COO)$ respectively and the one at 1375 cm^{-1} covers the C-C and ring vibrations of the organic molecule.

In the region below 970 cm^{-1} are concentrated the peaks corresponding to the U—O bond vibrations, from which, the most important and easy to assign is the one of U═O bond, appearing in our case at 902 cm^{-1} and having 6 shoulders, each of them being assigned to the different ν_3 and ν_1 (normally absent in IR) vibrations of the different uranyl bonds in the structure.

These vibrations are also visible in the Raman spectrum (collaboration with Pr. N. Dacheux & Dr N. Clavier, ISCM, Marcoule)(Figure III.5.3), the assignments been summarized in Table III.5.1.

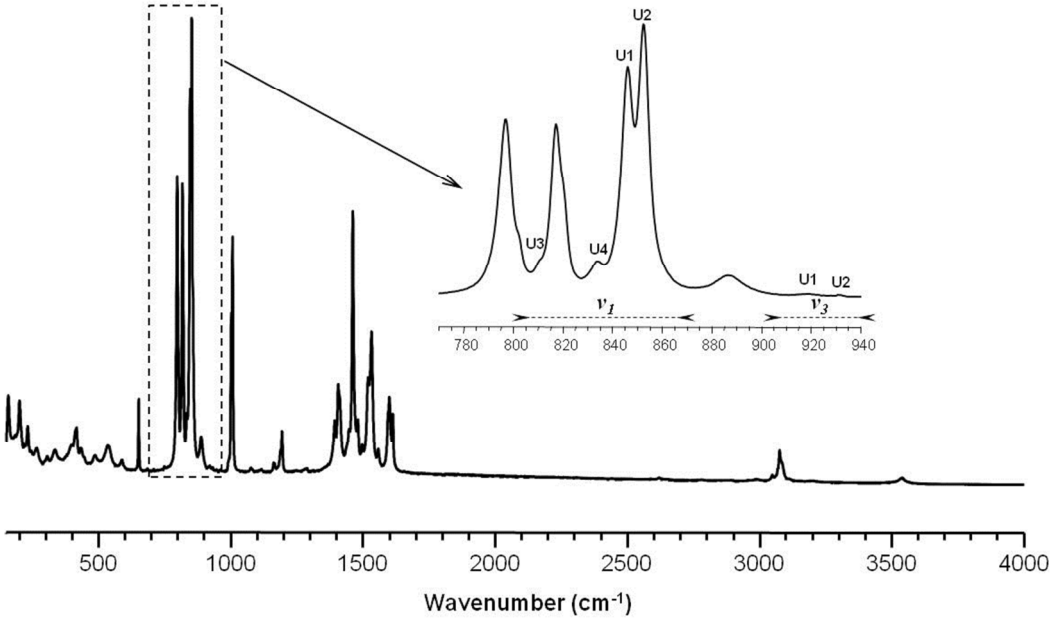

Figure III.5.3 The Raman diffusion spectrum of **iso10** complex

The interatomic distances have been calculated using the two empirical equations[13] below:

$$d\,(U-O)(pm) = 9141[\nu_3(cm^{-1})]^{-2/3} + 80.4$$
$$d\,(U-O)(pm) = 10650[\nu_1(cm^{-1})]^{-2/3} + 57.5$$

Table III.5.1 Correlation between the U=O distances obtained by refinement of the X-ray single crystal diffraction data and by empirical calculus based on the peak positions in the IR spectrum.

Bond	X-ray		IR				Raman			
			ν_3		ν_1		ν_3		ν_1	
	BL* (Å)	$\overline{BL}$ (Å)	σ** (cm^{-1})	BL (Å)	σ (cm^{-1})	BL (Å)	σ (cm^{-1})	BL (Å)	σ (cm^{-1})	BL (Å)
U1=O8	1.773(3)	1.774	924	1.768	841	1.770	919	1.771	846	1.766
U1=O18	1.775(3)									
U2=O15	1.765(3)	1.764	940	1.757	-	-	932	1.762	852	1.760
U2=O16	1.763(3)									
U3=O14	1.770(3)	1.797	881	1.799	810	1.801	-	-	810	1.801
U3=O10	1.823(3)									
U4=O9	1.777(3)	1.779	902	1.783	834	1.777	-	-	834	1.777
U4=O12	1.780(3)									

*BL - bond length
** σ - peak position

The calculated distances are in good agreement with the ones obtained from structure determination by single crystal X-ray diffraction experiment. The strong asymmetry of the O14=U3=O10 uranyl motif (1.770(3) and 1.823(3) Å for the U3=O14 and respectively for U3=O10 bonds) determined by the U3=O10–U4 CCI was difficult to confirm by IR and Raman spectroscopy. The Raman

vibration located at 797 cm^{-1} (v_1) corresponding to a bond length of 1.814 Å could correspond to the elongated U3═O10 (1.823(3) Å from X-ray) but also could correspond to a ligand vibration mode. Moreover the corresponding v_3 vibration was not observed in the IR spectrum in the 861 cm^{-1} region. Consequently the vibrations of the asymmetric U3 uranyl motif were assigned to the bands located at 810 cm^{-1} (v_1) in Raman spectrum and at 881 cm^{-1} (v_3) in the IR spectrum. The associated bond length determined from IR and Raman of 1.799 and 1.801 Å are in good agreement with the average uranyl bond length (for U3 motif) of 1.797 Å determined from X-ray.

Fluorescence spectroscopy

As in the previously discussed cases (**pht1**, **pht2**), the fluorescence experiments have also been conducted at room temperature, under excitation at 365 nm for the isophthalate phases **iso1** and **iso10**. The emission spectra were recorded in the same 440-640 nm wavelength range and compared with that of uranyl nitrate hexahydrate.

The emission spectrum of **iso1** (Figure III.5.4) presents the same uranyl characteristic peaks as the uranyl nitrate but is blue-shifted with a value of 8 nm. The value of the shift increases linearly with the wavelength from 3.81 nm for the first peak to 13.05 nm for the last one.

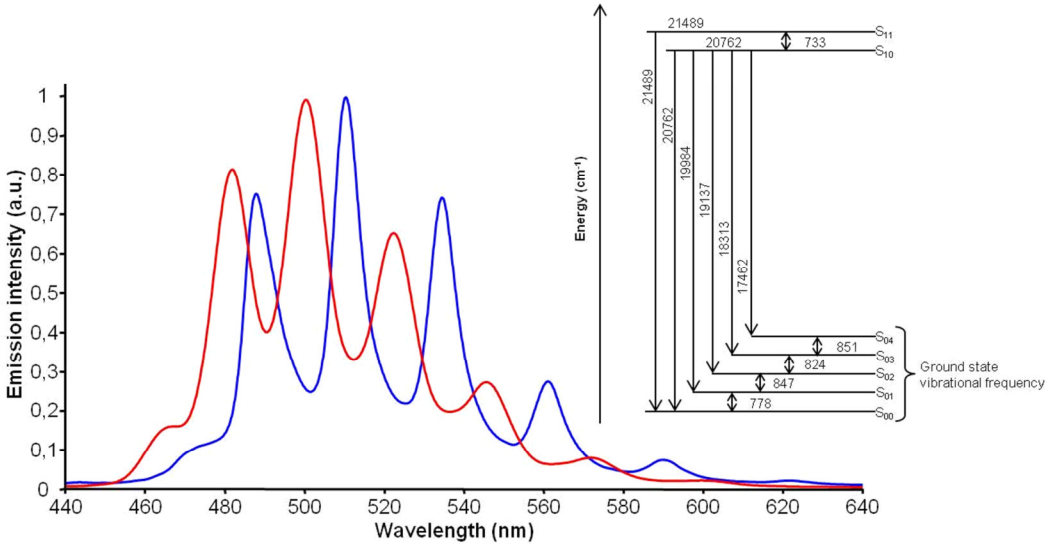

Figure III.5.4 Solid state emission spectra (left) of **iso1** (red), of uranyl nitrate hexahydrate (blue) and the electronic and vibronic transitions for **iso1** (right).

The blue-shift could be explained by the type of the uranyl polyhedron. It is a square bipyramid in **iso1** by comparison with the hexagonal bipyramid one of uranyl nitrate or of the previously studied phases (**pht1** and **pht2**).

Table III.5.2 Fluorescence bands of uranyl dinitrate hexahydrate and iso1 complex.

Uranyl dinitrate hexahydrate			iso1		
λ (nm)	$\tilde{\nu}$ (cm^{-1})	$\Delta\tilde{\nu}$ (cm^{-1})	λ (nm)	$\tilde{\nu}$ (cm^{-1})	$\Delta\tilde{\nu}$ (cm^{-1})
469,16	21315		465.35	21489	
485,88	20581	733	481.66	20762	733
507,98	19686	895	500.39	19984	778
531,53	18814	872	522.56	19137	847
557,36	17942	872	546.05	18313	824
585,71	17073	868	572.66	17462	851

As expected the band spacing between the $S_{11}\rightarrow S_{00}$ and the $S_{10}\rightarrow S_{00}$ transitions is about 733 cm^{-1} and those between $S_{10}\rightarrow S_{0v}$ and $S_{10}\rightarrow S_{0(v+1)}$ (v = 0-3) have a value ranging from 778 to 851 cm^{-1}. The transitions $S_{04}\rightarrow S_{0v}$ (v = 0-3) are vibration transitions, including the $S_{0v}\rightarrow S_{0(v-1)}$ (v = 1-4) ones, which are directly related with the double uranyl bond specific symmetric vibrations observed by Raman spectroscopy. The fluorescence data values for **iso1** complex are summarized and compared with those of uranyl nitrate hexahydrate in Table III.5.2.

The fluorescence solid state emission spectrum of **iso10** (Figure III.5.5), as in the cases of **pht3**, **pht4** phases (chapter II figure II.3.13), exhibits broad bands, having poor resolution, which would be due to the nature of the oligomeric SBU. The most intense band is centered at 520 nm, which is split at top on 3 positions at 495, 512 and 531 nm. These positions are consistent with those of the most intense 3 peaks in the emission spectrum of the uranyl nitrate. The broad band presents two shoulders on each side, at 487 and 552 nm. Their positions are consistent with those of the first and fourth peak respectively in the uranyl nitrate spectrum. The position of the fifth peak could not be accurately identified in the **iso10** spectrum.

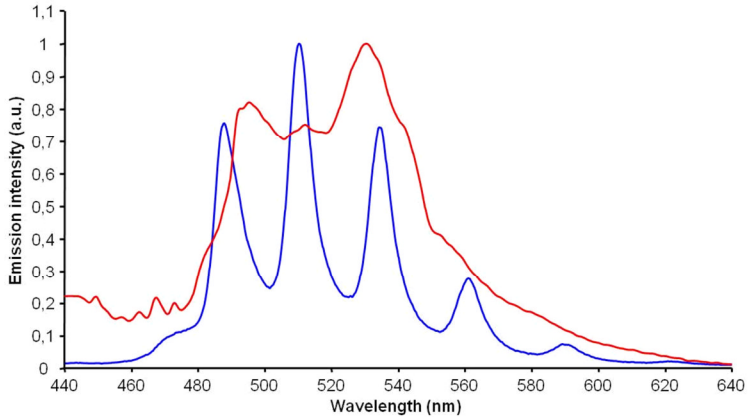

Figure III.5.5 Solid state emission spectra (left) of **iso9** (red) and uranyl nitrate hexahydrate (blue).

Conclusion

In this chapter there have been described and structurally characterized 10 new uranyl isophthalate complexes obtained in aqueous medium under mild hydrothermal conditions. As comparative elements it has been used one other uranyl isophthalate previously described in literature[1] and the uranium nitrate hexahydrate for the fluorescence spectroscopy experiments. The crystal chemistry of this system is quite rich since different building motifs for uranyl cations have been observed. At low pH, isolated monomeric uranyl species with different coordination environments have been identified and are present with the typical seven- and eight-fold coordinated states, as well as the six-fold one, which is less common in carboxylate chemistry. At higher pH, tetrameric building blocks are stabilized in one-dimensional networks. However, the most striking feature is the occurrence of a previously unknown octanuclear building brick (in **iso10**), for which a configuration of cation-cation interaction (U=O-U bond) has been observed.

Bibliography

1. Kim, J. Y.; Norquist, A. J.; O'Hare, D., *Dalton Transactions* **2003,** (14), 2813-2814.
2. Kerr, A. T.; Cahill, C. L., *Crystal Growth & Design* **2011,** *11* (12), 5634-5641.
3. Jouffret, L.; Rivenet, M.; Abraham, F., *Inorganic Chemistry* **2011,** *50* (10), 4619-4626.
4. Mihalcea, I.; Henry, N.; Bousquet, T.; Volkringer, C.; Loiseau, T., *Crystal Growth & Design* **2012,** *12* (9), 4641-4648.
5. Burns, P. C.; Ewing, R. C.; Hawthorne, F. C., *Canadian Mineralogist* **1997,** *35*, 1551-1570.
6. Liao, Z. L.; Li, G. D.; Wei, X. A.; Yu, Y.; Chen, J. S., *European Journal of Inorganic Chemistry* **2010,** (24), 3780-3788; Thuery, P., *Crystal Growth & Design* **2011,** *11* (6), 2606-2620; Harrowfield, J. M.; Skelton, B. W.; White, A. H., *Comptes Rendus Chimie* **2005,** *8* (2), 169-180; Borkowski, L. A.; Cahill, C. L., *Crystal Growth & Design* **2006,** *6* (10), 2248-2259; Turpeinen, U.; Hamalainen, R.; Mutikainen, I.; Orama, O., *Acta Crystallographica Section C-Crystal Structure Communications* **1996,** *52*, 1169-1171; Thuery, P., *Crystal Growth & Design* **2012,** *12* (1), 499-507; Serezhkina, L. B.; Vologzhanina, A. V.; Neklyudova, N. A.; Serezhkin, V. N., *Crystallography Reports* **2009,** *54* (3), 449-454; Villiers, C.; Thuery, P.; Ephritikhine, M., *Polyhedron* **2010,** *29* (6), 1593-1599.
7. Mihalcea, I.; Henry, N.; Clavier, N.; Dacheux, N.; Loiseau, T., *Inorganic Chemistry* **2011,** *50* (13), 6243-6249.
8. Zheng, Y. Z.; Tong, M. L.; Chen, X. M., *European Journal of Inorganic Chemistry* **2005,** (20), 4109-4117.
9. Bevan, D. J. M.; Grey, I. E.; Willis, B. T. M., *Journal of Solid State Chemistry* **1986,** *61* (1), 1-7; Gronvold, F.; Haraldsen, H., *Nature* **1948,** *162* (4106), 69-70.
10. Baenziger, N. C., The crystal structures of some thorium and uranium compounds. Iowa State College Journal of Science: 1952; Vol. 27, p 126.
11. Burns, P. C.; Finch, R. J.; Hawthorne, F. C.; Miller, M. L.; Ewing, R. C., *Journal of Nuclear Materials* **1997,** *249* (2–3), 199-206.
12. Mihalcea, I.; Henry, N.; Loiseau, T., *Crystal Growth & Design* **2011,** *11* (5), 1940-1947.
13. Bartlett, J. R.; Cooney, R. P., *Journal of Molecular Structure* **1989,** *193*, 295-300.
14. Eriksson, A.; Lindgren, J., *Journal of Molecular Structure* **1978,** *48* (3), 417-430.

Chapter IV
Uranyl Pyromellitates

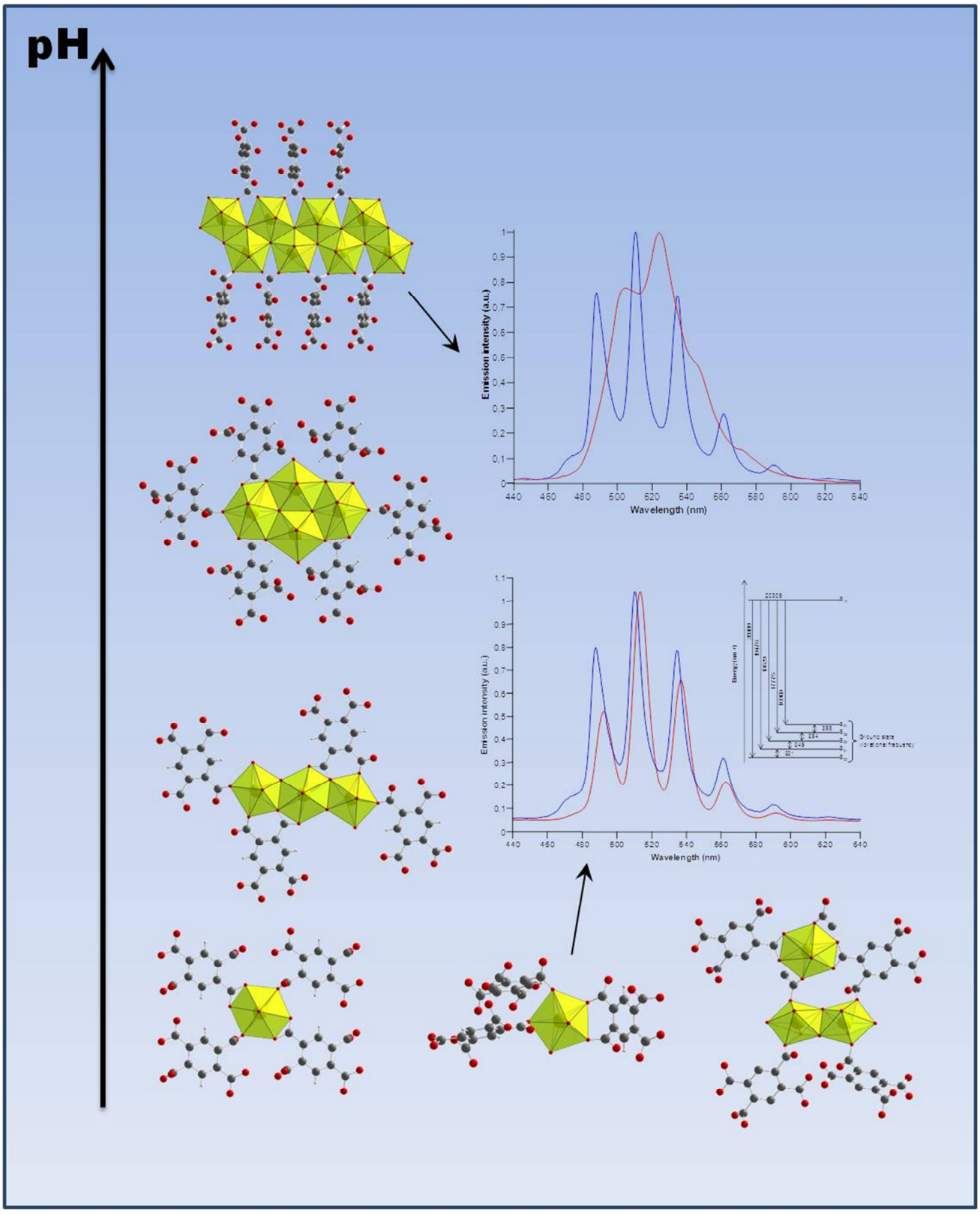

Chapter IV Uranyl Pyromellitates

IV.1 . Introduction

The pyromellitic acid (noted H_4btec) is a tetradentate ligand with four carboxylate groups and has been used in the preparation of different metal-organic complexes. The most common compounds involve 3d transition metals such as iron[1], cobalt[2], nickel[3] zinc[4]… and also with p block elements (aluminum[5], gallium[6] or indium[7]), or lanthanides[8]. Concerning the actinides, the pyromellitate ligand has been reported in three uranyl complexes from which one[9] has been obtained pure also in our work. This complex $[UO_2(H_2btec)(H_2O)_2]\cdot 2H_2O$ will be noted hereafter as **A** phase and will be used as comparison element in the solid state fluorescence spectroscopy experiments.

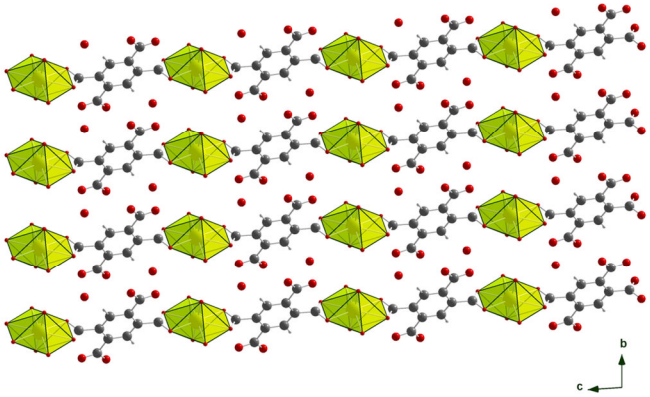

Figure IV.1.1 Structure representation of phase **A** $[UO_2(H_2btec)(H_2O)_2\cdot 2H_2O$. View along the [100] axis.

Its structure (Figure IV.1.1) contains infinite chains of hexagonal bipyramidal polyhedra as motifs, interlinked by the organic ligand. The polyhedra are also coordinated by two water molecules and two of the carboxylate groups of the ligand are protonated and not coordinating the metal. The structure also contains a free water molecule positioned between the chains. From the other two uranyl pyromellitates mentioned in literature, one employs 1,10-phenanthroline as a secondary ligand[10] and the other is a mixed uranyl/silver complex[11]. The literature also mentions the synthesis and structure of one neptunyl pyromellitate[12].

Following the same strategy with the pyromellitate ligand that was used in the previous cases (phthalate and isophthalate), we proceeded from a mixture of the H_4btec molecule, uranyl nitrate hexahydrate as metal source, different inorganic and organic bases as pH moderator and deionized water as under hydrothermal conditions. In our investigations, 7 new complexes have been identified. The first compound $[(UO_2)_2(btec)(H_2O)_2]\cdot H_2O$[13] (**pyr1**) presents a tridimensional compact structure with a monomeric seven fold coordinated uranyl linked to each other through the organic molecule and one encapsulated free water molecule (per uranyl unit). The second and third complexes $(NH_4)_2[(UO_2)(btec)]\cdot 4H_2O$[13] (**pyr2**) and $(Hdma)_2[(UO_2)(btec)]$ (**pyr3**) (where dma = dimethylamine) possess the same bidimensional sheets containing isolated eight fold coordinated uranyl centers linked through the btec molecules, which have for two opposite carboxylate groups a nonbonded, deprotonated oxygen atom interacting with the intercalated ammonium or dimethylammonium cations. In the latter case the dimethylammonium countercation is obtained *in situ* by the degradation of the dimethylformamide molecules introduced as pH moderator. The fourth phase $(NH_4)[(UO_2)_2(OH)(H_2O)(btec)]\cdot 2H_2O$ (**pyr4**), presents a tridimensional structure built up from a dimeric unit of two seven fold coordinated uranyl units sharing a hydroxo edge and a monomeric eight fold coordinated unit, both interlinked by the organic ligand. Water molecules are encapsulated within narrow channels of the structure. The fifth complex $[(UO_2)_3(btec)(OH)_2(H_2O)_2]$ (**pyr5**) is also a lamellar one, but this time containing a unique type of linear trimeric SBU, perfectly compensating the four negative charges of the ligand, no other countercation being required. The SBU is formed by two pentagonal bipyramids on each side, sharing one edge with the central hexagonal bipyramid. The sixth complex $(Hdma)_2[(UO_2)_2O(btec)]$ (**pyr6**) exhibits a 2D structure, in which the btec molecules, like in the case of **pyr2** and **pyr3**, present two carboxylate groups, each with a nonbonded, deprotonated oxygen atom, interacting with the countercation. The SBU is formed of four bipyramids, all edge sharing interconnected, two seven fold coordinated uranyl units in the center and two eight fold coordinated on each side. The last phase $(NH_4)_4[(UO_2)_{12}O_4(OH)_8(btec)_3]\cdot 22H_2O$[13] (**pyr7**) presents in its structure large

rhombus-shaped open channel (8.2 × 8.6 Å) delimited by infinite ribbons of seven fold coordinated uranyl polyhedra sharing edges and the ligand's molecules. Within the channels, charge compensating, ammonium countercations and trapped water molecules, are present.

The **pyr1**, **pyr2** and **pyr7** phases have been obtained pure and fully characterized (also complex **A** has been obtained pure). For the cases of **pyr3** - **pyr6**, only a small number of crystals have been isolated from preparations and picked up for the structure determination. Details of crystal data are given in IV.1.1 - IV.1.2 tables.

Table IV.1.1 Structure refinement and crystal data for pyr1 - pyr3 uranyl pyromellitates.

Parameter*	pyr1	pyr2	pyr3
crystal system	Orthorhombic	Monoclinic	Monoclinic
space group	*P bcn*	*C* 2/*c*	*P* 2$_1$/*n*
a/Å	12.8489(2)	55.631(2)	7.2181(6)
b/Å	12.7051(2)	7.1082(3)	13.686(1)
c/Å	9.97360(10)	13.1074(5)	9.2779(7)
α/deg	90	90	90
β/deg	90	95.831(1)	92.580(2)
γ/deg	90	90	90
volume/Å^3	1628.16(4)	5156.4(4)	915.6(1)
Z, ρ_{calc}/g·cm^{-3}	4, 3.485	4, 2.365	2, 2.2204
final *R* indices [$I > 2\sigma(I)$]	R1 = 0.0164 wR2 = 0.0428	R1 = 0.0277 wR2 = 0.0309	R1 = 0.0484 wR2 = 0.0418
R indices (all data)	R1 = 0.0237 wR2 = 0.0471	R1 = 0.0396 wR2 = 0.0324	R1 = 0.1268 wR2 = 0.0496

* - a complete crystal and refinement data table is given in the supplementary data chapter (table VIII.3.1)

Table IV.1.2 Structure refinement and crystal data for pyr4 – pyr7 uranyl pyromellitates.

Parameter*	pyr4	pyr5	pyr6	pyr7
crystal system	Monoclinic	Triclinic	Monoclinic	Orthorhombic
space group	*P* 2$_1$/n	*P* -1	*P* 2$_1$/*c*	*P nnm*
a/Å	9.1844(2)	5.5266(3)	13.5550(5)	13.198(2)
b/Å	21.6150(5)	7.6559(3)	14.6014(4)	14.852(2)
c/Å	11.5401(2)	11.3208(4)	11.7868(4)	23.407(4)
α/deg	90	100.846(2)	90	90
β/deg	112.701(1)	100.440(2)	110.728(2)	90
γ/deg	90	96.940(2)	90	90
volume/Å^3	2113.5(1)	456.66(3)	2181.9(1)	4588.1(12)
Z, ρ_{calc}/g·cm^{-3}	4, 2.729	1, 4.088	4, 2.784	4, 3.183
final *R* indices [$I > 2\sigma(I)$]	R1 = 0.0336 wR2 = 0.0947	R1 = 0.0188 wR2 = 0.0683	R1 = 0.0346 wR2 = 0.0727	R1 = 0.0444 wR2 = 0.0733
R indices (all data)	R1 = 0.0459 wR2 = 0.1138	R1 = 0.0244 wR2 = 0.0844	R1 = 0.0600 wR2 = 0.0972	R1 = 0.0634 wR2 = 0.0747

* - a complete crystal and refinement data table is given in the supplementary data chapter (table VIII.3.2)

IV.2 . Structures description

The structure of **pyr1** $[(UO_2)_2(btec)(H_2O)_2]\cdot H_2O$ possesses one unique crystallographic site for the uranium atom, situated on a 8d general position. The coordination sphere surrounding the metal has a pentagonal bipyramidal geometry formed by two uranyl type oxygen atoms (O1 and O2) in apical positions (U=O distances of 1.764(3) and 1.758(3) Å respectively) forming an O=U=O angle of 177.7(1)° and other five oxygen atoms in the equatorial plane (Figure IV.2.1). Four of the oxygen atoms (O3-O6) forming the equatorial plane belong to carboxylate groups of the ligand (U—O distances ranging from 2.343(2) to 2.438(2) Å). The fifth oxygen atom (O7) completing the pentagonal base belongs to a coordinating water molecule, situated at the distance of 2.415(3) Å from the uranium atom (bond valence of 0.5; expected 0.4 for aquo species).

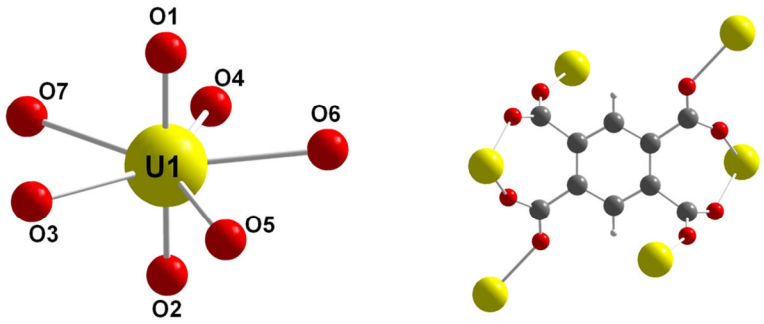

Figure IV.2.1 Coordination sphere of the uranium atom (left) and the ligand coordination configuration of the organic ligand (right) for **pyr1** complex.

The $UO_6(H_2O)$ building units are discrete species surrounded and interlinked by the organic ligand in order to form a tridimensional edifice (Figure IV.2.2). Each carboxylate group of the ligand coordinates uranium atoms adopting a syn-anti and anti-anti respectively bidentate coordination configuration, making the ligand a hexadentate one of μ_6-η_1:η_1:η_1:η_1:η_1:η_1 type. Two carboxyl oxygen atoms belonging to two neighboring (1,2 and 4,5 positions) carboxylate groups chelate one uranium center, the remaining two oxygen atoms bridging other two uranium atoms. The torsion angles of the carboxylate groups from the plane of the benzene ring of 30.2(2)° and 62.7(2)° together with the syn-anti and anti-anti coordination configuration are supporting the tridimensional development of the structure.

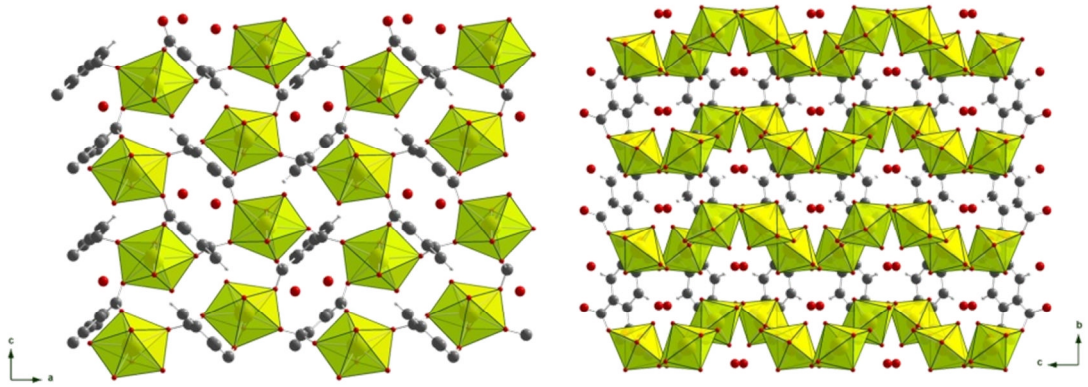

Figure IV.2.2 Representation of the tridimensional structure of **pyr1**. View along [010] axis (left) and along [100] axis (right).

Although the structure is relatively compact, it also contains disordered free water molecules. The presence of free and coordinating water molecules in such structures implies the apparition of hydrogen bonds (Figure IV.2.3). The O7 coordinating water molecule links through hydrogen bonds the Ow1 free water molecule, at the distance of 2.527(4) Å and the O4 carboxyl oxygen atom (belonging to an adjacent monomer) at the distance of 2.752(4) Å. The Ow1 free water molecule, beside the interaction with O7 also binds the O6 carboxyl oxygen atom at 2.948(4) Å.

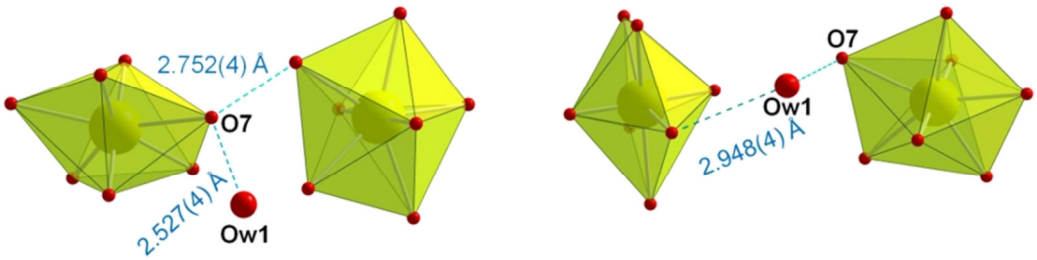

Figure IV.2.3 The hydrogen bond interactions scheme in the structure of **pyr1** compound.

The **pyr2** complex $(NH_4)_2[(UO_2)(btec)]\cdot 4H_2O$ presents two unique crystallographic sites for the uranium atom (Figure IV.2.4). One uranium atom (U1) is situated on an *8f* general position, the second on a *4e* (½ y ¼) special position. Both metal centers form distinct monomeric units with hexagonal bipyramidal geometries. Around U1, the apical positions are occupied by the O2 and O4 uranyl oxygen atoms (U=O distances of 1.781(3) and 1.775(3) Å respectively forming an O=U=O angle of 179.8(2)°). The equatorial plane is entirely formed by carboxyl type oxygen atoms (O1, O5, O6, O8, O10 and O11) belonging to four different ligand molecules. The U–O distances are in the range 2.399(3)-2.545(3) Å. The U2-centered polyhedron possesses symmetrical uranyl

bonds, with the lengths of 1.776(3) Å and forming a 178.9(2)° angle around the uranium atom. The coordination equatorial plane around U2 is also formed entirely by carboxyl oxygen atoms (O7, O9, O12 and their symmetry equivalents) belonging to four different ligand molecules, with U—O distances in the range of 2.423(3)-2.537(3) Å. Both polyhedra are chelated by two carboxylate arms of the ligand and monodentate coordinated by other two. The main difference between them is that in the case of U1 the chelating groups are situated in opposite positions (*trans*- position) around the uranium atom and in the case of U2 the two chelating groups are positioned one beside the other (*cis*- position).

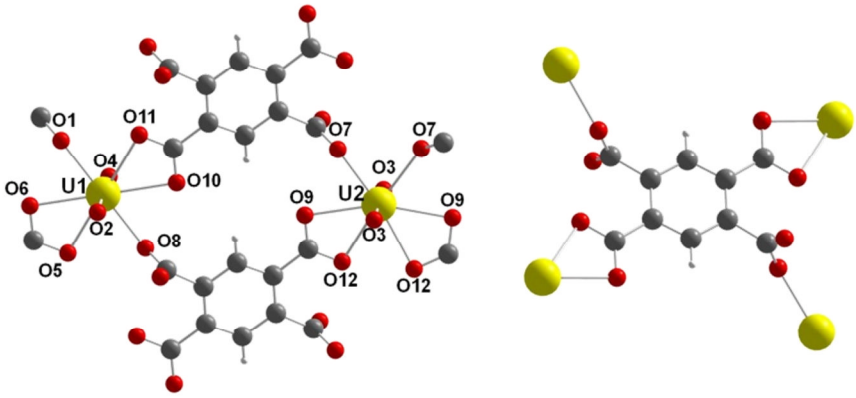

Figure IV.2.4 The coordination environment surrounding the metal centers (left) and the coordination configuration of the ligand molecule (right) for the **pyr2** compound.

The structure of **pyr2** also exhibits two distinct unique positions for the organic ligand. For both cases the coordination configuration is identical. The ligand, with two opposite arms (positions 1 and 4 on the ring) chelates two different metal centers while the remaining two (positions 2 and 5) monodentate coordinates another two distinct metal centers. The monodentate coordinating carboxylate arms are using only one oxygen atom to bind the uranium center, the second being free. The relatively short C—O distances (1.234(4) to 1.246(4) Å) for the noncoordinating oxygen atoms indicate that those are nonprotonated. Each organic ligand molecule binds four different uranium atoms and each uranium center is coordinated by four distinct ligand molecules. The result is a mixed organic-inorganic layer in which the inorganic bricks are strictly alternating with the organic molecules (Figure IV.2.5).

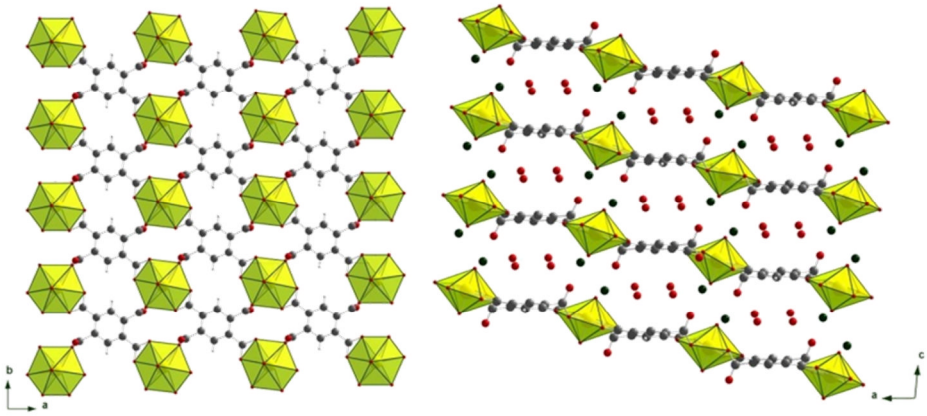

Figure IV.2.5 Structure representation of **pyr2**. View along [001] axis (left) and [010] axis (right).

The deprotonated, non coordinating carboxyl oxygen atoms are giving a -2 charge to the $[UO_2(btec)]$ layer, which needs to be compensated by the ammonium cations situated between the layers. Four water molecules, together with the ammonium cations are situated between the sheets and creating a network of hydrogen bonds interactions. (Figure IV.2.6).

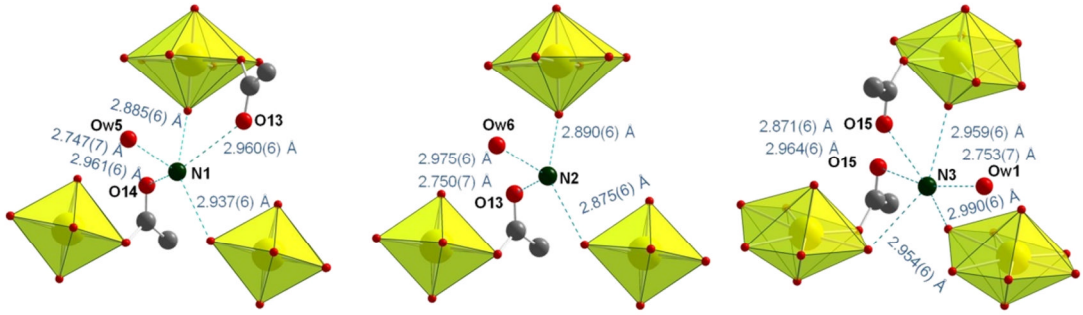

Figure IV.2.6 Weak interactions appearing between the ammonium cations and neighboring oxygen atoms in the structure of **pyr2** compound.

The N1 ammonium cation is situated in the vicinity of five oxygen atoms. Two of them are noncoordinating carboxyl type (O13 and O14, N···O = 2.96(1) Å), one is coordinating carboxyl type (O1, N···O = 2.94(1) Å), the fourth is a uranyl oxygen atom (O4, N···O = 2.89(1) Å) and the fifth belongs to a noncoordinating water molecule (Ow5, N···O = 2.75(1) Å. The N2 cation has four neighboring oxygen atoms: the previously mentioned O13 (N···O = 2.75(1) Å), one coordinating carboxyl type (O8, N···O = 2.88(1) Å), one uranyl type (O2, N···O = 2.89(1) Å) and one oxygen atom belonging to the Ow6 free water molecule (N···O = 2.98(1) Å). Another weak interaction appears, as in the case of N1, with the O14 oxygen atom, the N···O distance being 3.05(1) Å. The N3 cation presents four weak interactions with neighboring oxygen atoms. Two of them occur with non

coordinating carboxyl type oxygen atoms (O15 and its equivalent O15#, N···O = 2.96(1) and 2.87(1) Å) and other two are with coordinating carboxyl oxygen atoms (O7 and O12, N···O = 2.95(1) and 2.99(1) Å respectively).

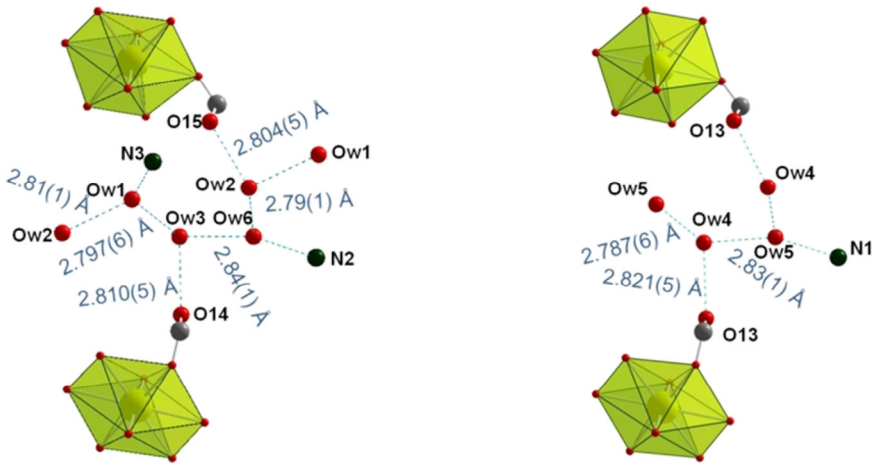

Figure IV.2.7 View of the hydrogen bonds manifesting in the structure of **pyr2** complex.

The large number of free water molecules (Ow1 to Ow6) present between the polymeric layers gives rise to an extended network of hydrogen bond interactions manifesting at O···O distances ranging from 2.79(1) to 2.84(1) Å (Figure IV.2.7). The cohesion between the layers is ensured exclusively by hydrogen bond interactions, the distance between two adjacent aromatic rings being too large (7.29(1) Å) for the existence of π-π stacking interactions.

The structure of **pyr3** $(Hdma)_2[(UO_2)(btec)]$ exhibits a single unique crystallographic site situated on *2a* (0 0 0) special position. The central uranium atom is eight-fold coordinated and adopts the hexagonal bipyramidal geometry (Figure IV.2.8-left). The axial positions are occupied by two uranyl oxygen atoms (O1u and its symmetry equivalent) at the distance of 1.716(4) Å, forming an O=U=O angle of 180°. The other six positions in the equatorial plane are occupied exclusively by carboxyl oxygen atoms, two carboxylate groups chelating (*trans*-position) and other two monodentate coordinating the uranium atom (similar to the case of U1-centered polyhedron of the **pyr2** phase). The ligand molecule (one single crystallographic site) presents the same coordination configuration as in the case of **pyr2** structure: two opposite carboxylate arms (positions 1 and 4) chelate two distinct uranium atoms, the remaining two (positions 2 and 5) monodentate coordinating other two uranium centers (Figure

IV.2.8-right). The free carboxyl oxygen atoms are deprotonated interacting with the dimethylammonium cation. The equatorial U—O bond lengths are in the range of 2.445(4)-2.528(4) Å.

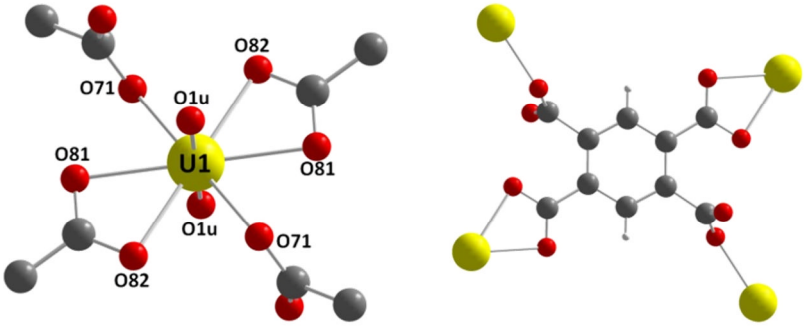

Figure IV.2.8 Representation of the coordination sphere around the uranium atom (left) and the ligand's coordination configuration (right) for **pyr3** phase.

The coordination manner of the organic ligand gives rise to infinite layers of alternating organic and inorganic motifs developing in the [110] plane and stacking along [110] direction (Figure IV.2.9). Intercalated between the polymeric layers, the structure exhibits dimethylammonium cations interacting with the noncoordinating carboxyl functions.

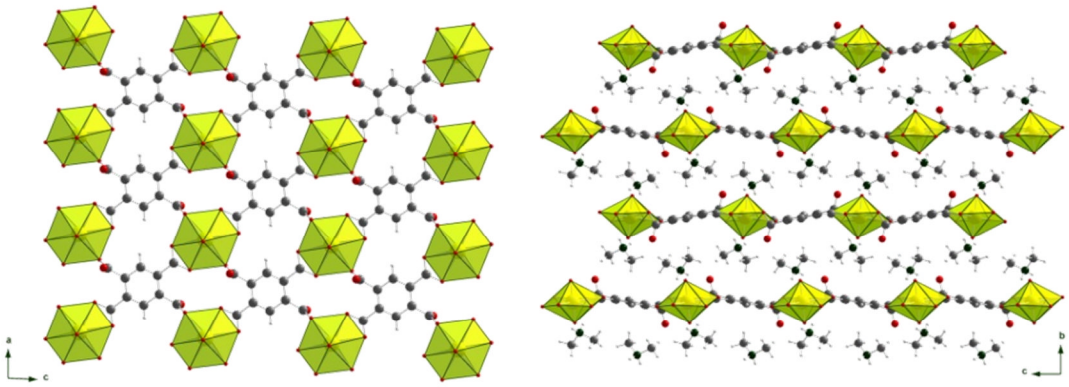

Figure IV.2.9 Structure representation of the **pyr3** phase. View along [010] ([(UO_2)btec] single layer representation) (left) and along [100] direction (right).

Each dimethylammonium cation interacts through hydrogen bonds with one coordinating (O71) and one free (O72) carboxyl oxygen atoms at distances of 1.992(4) and 1.948(5) Å respectively (Figure IV.2.10). The cohesion between the polymeric layers in ensured by Van der Waals weak interactions, no stacking interactions occurring due to the large distance (8.94(1) Å) between two adjacent benzene rings.

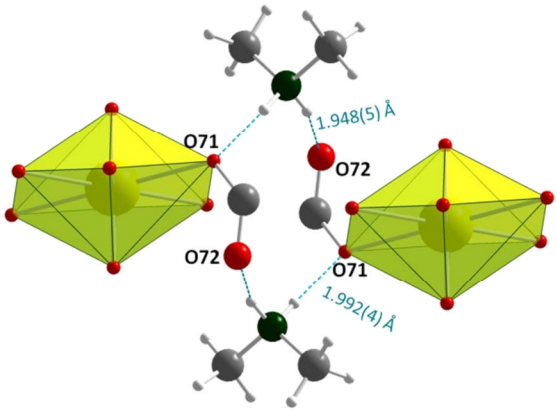

Figure IV.2.10 Representation of the hydrogen bonds occurring in the structure of **pyr3** complex.

The structure of **pyr4** $(NH_4)[(UO_2)_2(OH)(H_2O)(btec)]\cdot 2H_2O$ exhibits two distinct crystallographic sites for the uranium atom, situated on *4e* general positions. Each uranium atom adopts a different coordination environment (Figure IV.2.11). U1 atom is eight-fold coordinated and adopts a hexagonal bipyramidal geometry, with two uranyl oxygen atoms (O4 and O5) in apical position and other six oxygen atoms in the equatorial plane (O2, O3, O6, O9, O11 and O13). The uranyl oxygen atoms form typical short bonds with the central metal atom of 1.76(1) and 1.77(1) Å respectively and a nearly 180° (179.4(4)°) angle around it. The equatorial coordination plane is formed exclusively by carboxyl oxygen atoms belonging to ligand molecules, the U—O bond lengths being in the range 2.43(1)-2.51(1) Å. The U2 uranium atom is seven-fold coordinated and adopts the pentagonal bipyramid geometry, also possessing two uranyl oxygen atoms (O10 and O12) in apical position and only five oxygen atoms in the equatorial plane. The uranyl oxygen atoms are situated at U═O distances of 1.77(1) and 1.78(1) Å respectively and form a O═U═O angle of 179.0(4)°. Two of the atoms in the equatorial plane are carboxyl type belonging to the ligand (O7 and O8, U—O = 2.38(1) and 2.33(1) Å respectively), other two (O14 and its symmetry equivalent, U—O = 2.34(1) and 2.35(1) Å respectively) are hydroxo species. The terminal position is occupied by a coordinating water molecule (O1, U—O = 2.51(1) Å). The nature of the hydroxo and aquo species has been determined by bond valence calculations, obtaining values of 1.14 v.u. (expected 1.2) for the hydroxo and 0.42 v.u. (expected 0.4) for the aquo ones[14].

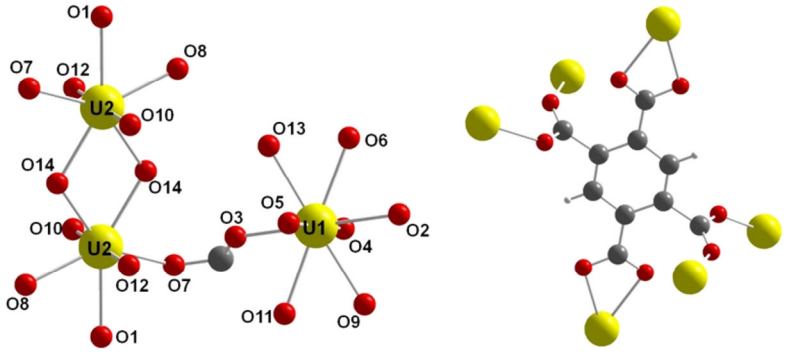

Figure IV.2.11 Representation of the coordination environment surrounding the uranium atoms (left) and the ligand's coordination configuration (right) for the **pyr4** compound.

The structure of **pyr4** presents two types of building motifs. The polyhedron formed around the U1 atom is distinct monomeric species. The polyhedron formed around the U2 atom is situated in the proximity of the *2c* (0 ½ 0) inversion center. This symmetry operation doubles the position of each atom in the U2 bipyramid and creates a dinuclear SBU, for which the two polyhedra are linked through the μ_2-O14–μ_2-O14 hydroxo edge. The coexistence in the same structure of a monomeric and a dimeric bricks is a rare combination since only a few cases[15, 16] have been reported in literature.

Only one unique crystallographic site exists for the organic ligand. All of its carboxylate arms are coordinating uranium atoms. Two opposite groups (positions 1,4 on the benzene ring) chelate each a distinct uranium atom belonging to the monomeric unit (U1), each of the remaining two arms (positions 2,5) bidentate bridging in a *syn-anti* manner two uranium atoms U1 and U2. The distinct nature of the two building blocks and the coordination configuration of the organic linker are the main factors determining the complexity and the tridimensional expansion of the **pyr4** structure.

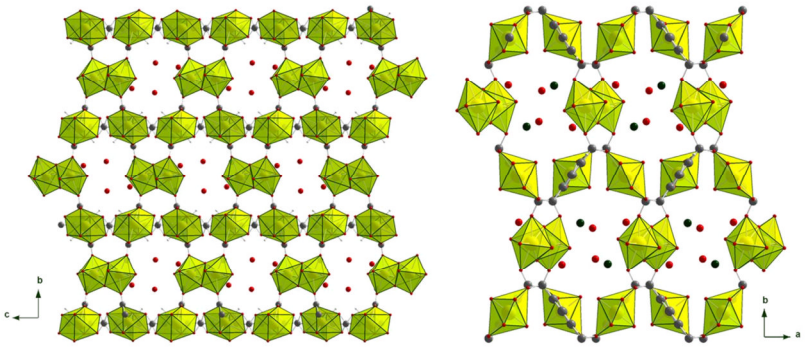

Figure IV.2.12 Structure representation of the **pyr4** complex. View along the [100] (left) and [001] (right) axes.

Along [100] and [001] directions, the structure of **pyr4** (Figure IV.2.12) presents narrow channels in which ammonium cations and free water molecules are present. The ammonium cations are required for compensating the negative charge of the hydroxo species present in the dimeric SBU and together with the free water molecules are creating a network of weak interactions increasing the stability of the structure (Figure IV.2.13).

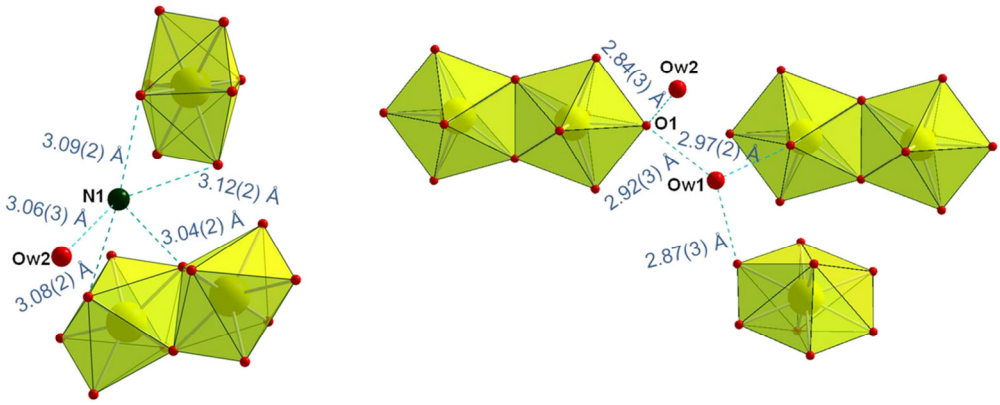

Figure IV.2.13 Representation of the weak hydrogen bond interactions manifesting in the structure of **pyr4.**

The ammonium cation (N1) binds through weak interactions the O5-uranyl and O2-carboxyl oxygen atoms, belonging to the monomer, the O10-uranyl and O14-hydroxyl atoms belonging to the dimeric SBU and the Ow2 atom belonging to a noncoordinating water molecule. The bonds range is 3.04(2)-3.12(2) Å. The O1 coordinating water molecule, belonging to the dimeric SBU, binds the Ow1 and Ow2 water molecules at the distance of 2.84(3) and 2.92(3) Å, respectively. The Ow1, beside the interaction with O1, also binds the O12-uranyl (dinuclear SBU) and O11-carboxyl (monomer) oxygen atoms at distances of 2.97(2) and 2.87(3) Å, respectively. The structure's tridimensional cohesion is mainly ensured by ligand binding together the SBUs but also favored by the hydrogen bonds. The fact that the benzene rings are not positioned parallel one to the other and the distance between two adjacent rings is 5.83(1) Å excludes the possibility of π-π stacking interactions.

The structure of **pyr5** $[(UO_2)_3(btec)(OH)_2(H_2O)_2]$ presents two distinct crystallographic sites for the uranium atom. U1 atom is situated on a *1d* (½ 0 0) inversion center, the second one (U2) is on a *2i* general position.

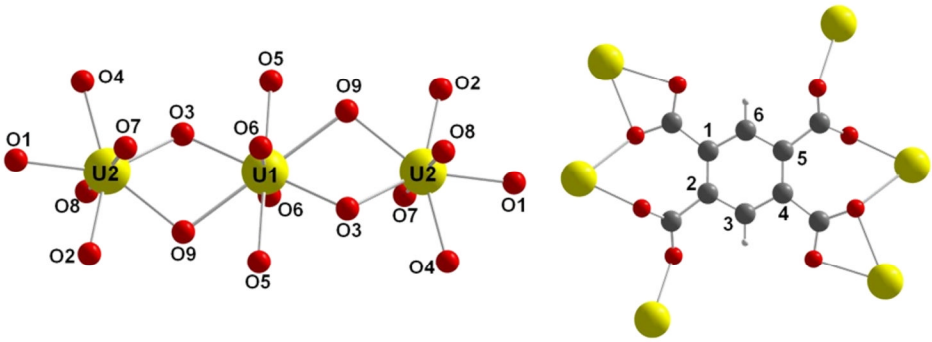

Figure IV.2.14 Representation of the coordination environment surrounding the uranium atoms (left) and the ligand's coordination configuration (right) for the **pyr5** complex.

The U1 atom is eight-fold coordinated and adopts the hexagonal bipyramidal geometry, possessing two uranyl oxygen atoms in axial positions (O6 and its symmetry equivalent), forming two typical U=O short bonds of 1.800(4) Å (O=U=O angle of 180.0(3)°) and other six oxygen atoms (O3, O5, O9 and their symmetry equivalents) in the equatorial plane. The oxygen atoms in the equatorial coordination plane are carboxyl (O5 and O9) and hydroxyl (O3) species and coordinate the uranium atom at distances ranging from 2.321(3) to 2.589(3) Å. The hydroxo nature of the O3 oxygen atom has been determined by bond valence calculation[14, 17], the obtained valence value being 1.19 v.u. (expected value for hydroxo specie of 1.2 v.u.). The U2 atom is seven-fold coordinated, forming a polyhedron with pentagonal bipyramidal geometry. The apical positions, situated at 1.759(4) and 1.779(4) Å from the uranium atom, are occupied by two uranyl oxygen atoms (O8 and O7 respectively) and form an O=U=O angle of 177.1(2)°. The five equatorial positions are occupied by three carboxyl oxygen atoms (O1, O2 and O9), one hydroxyl oxygen atoms (O3) and in terminal position by one oxygen atom belonging to a coordinating water molecule. The equatorial U–O distances are ranging from 2.305(4) to 2.470(4) Å. The U2-centered polyhedron shares the O3-O9 edge with the U1 polyhedron. The U1 bipyramid symmetrically shares a second O3-O9 edge with a second U2 polyhedron, the result being a trinuclear SBU, centered around the U1 atom, on the *1d* inversion center (Figure IV.2.14). This type of trimeric unit is new in literature, only combinations of three seven-fold coordinated uranium centers being previously reported [16, 18, 19] (see chapter I).

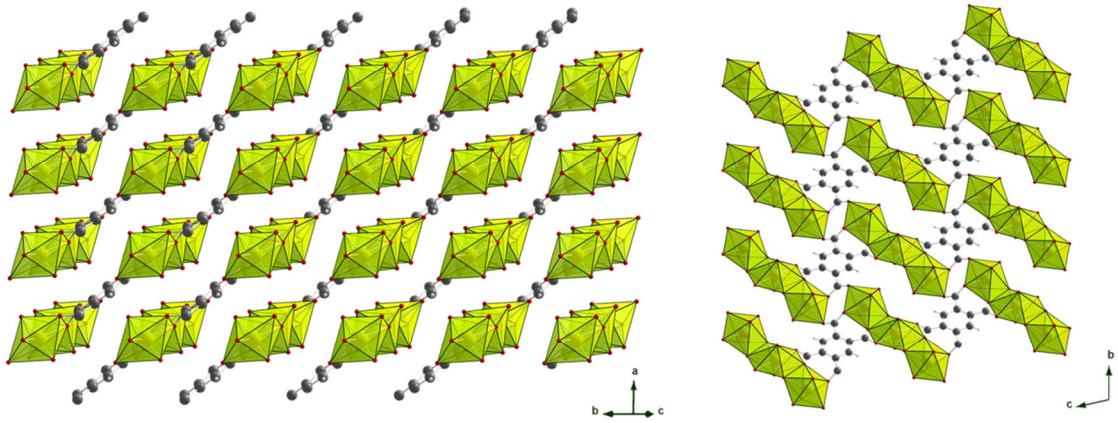

Figure IV.2.15 Structure representation of complex **pyr5**. View along [011] (left) and [100] (right) directions.

For the organic ligand there is a single unique crystallographic site. One ligand molecule coordinates through the four carboxylate arms six uranium atoms belonging to four distinct SBUs. Two of the carboxylate groups (positions 1,4 on the ring) are each bidentate bridging in a *syn-anti* fashion two U2 polyhedra belonging to two distinct SBUs, each of the remaining two arms (positions 2,5) are chelating the U1 atom and bridging one of the two U2 atoms of the same SBU. The result is a neutral layer of alternating inorganic SBUs and organic ligand molecules developing in the (110) plane (Figure IV.2.15). The cohesion between the layers is ensured only by the hydrogen bonds formed by the coordinating water molecule and the hydroxyl groups with the adjacent oxygen atoms (Figure IV.2.16).

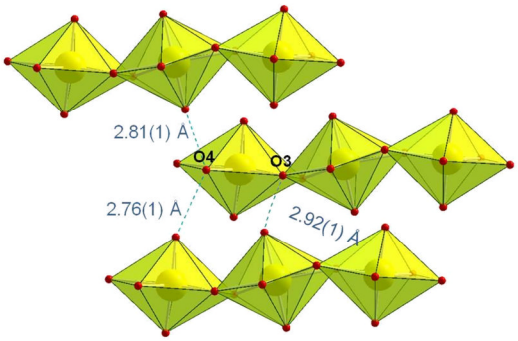

Figure IV.2.16 Representation of the hydrogen bonds in the structure of **pyr5.**

The O4 coordinating water molecule binds through hydrogen bonds two uranyl oxygen atoms O6 (U1-centered polyhedron) and O7 (U2-centered polyhedron) belonging to two different layers, at the distance of 2.81(1) and 2.76(1) Å, respectively. The O3 hydroxo group binds at a distance of 2.92(1) Å the

O6 uranyl oxygen atom belonging to the SBU where one of the U2-centered polyhedra has been bound by the O4 water molecule.

The structure of **pyr6** complex $(Hdma)_2[(UO_2)_2O(btec)]$ presents two distinct crystallographic sites for the uranium atoms, both situated on *4e* general positions but in the proximity of an *2d* (½ 0 ½) inversion center. The U1 atom is seven-fold coordinated adopting the expected pentagonal bipyramidal geometry, with two uranyl oxygen atoms (O5 and O6) in apical positions (U=O bond lengths of 1.78(1) and 1.77(1) Å respectively, forming an O=U=O angle of 176.2(4)°) and other five oxygen atoms forming the pentagonal base of the bipyramid. From the latter five, three (O8, O10 and O11) are carboxyl oxygen atoms belonging to the carboxylate arms of the organic ligand. The remaining two (O9 and its symmetry equivalent O9#) are oxo groups. The nature of these groups has been established by bond valence calculation[14, 17], the obtained value being 2.07 v.u. (expected value of 2 for oxo species). The U—O bond lengths for the equatorial plane are ranging between 2.26(1) and 2.45(1) Å. The second uranium atom (U2) is eight-fold coordinated with a hexagonal bipyramidal geometry presenting in axial positions two uranyl oxygen atoms (O3 and O4 with U=O bond lengths of 1.77(1) and 1.75(1) respectively, forming an O=U=O angle of 177.0(3)°) and in the equatorial plane six oxygen atoms. Five of the coordinating oxygen atoms (O1, O2, O7, O10 and O11) in the equatorial coordination plane are carboxyl type belonging to the ligand, the sixth being the already mentioned (O9) oxo group. The two polyhedra are symmetrically doubled by the adjacent inversion center, resulting in a tetranuclear SBU formed by two central pentagonal bipyramids and two hexagonal bipyramids on each side (Figure IV.2.17). All four polyhedra are interconnected by edge sharing as follows: each U1 polyhedron shares one edge (O9 - O9#) with the second U1 polyhedron (U1#) and two edges (O9 - O11 and O9# - O10) with the two adjacent U2 polyhedra (U2 and U2#); each U2 polyhedron shares two edges (O9 - O11 and O9 - O10) with the two neighboring U1 polyhedra (U1 and U1#). In the structure of **pyr6** there is a single crystallographic site for the organic ligand, each ligand molecule adopting the same coordination configuration. The carboxylate arms situated at 1 and 2 positions on the benzene ring are both coordinating the same SBU, first (position

1) chelating one U2 atom and at the same time bridging a neighboring U1 atom and the second monodentate coordinating the previously mentioned U1 atom. The carboxylate group situated at position 4 has the same coordination configuration as the group in position 1, simultaneously chelating and bridging U2 and respectively the U1 atoms belonging to an adjacent SBU. The last carboxylate group situated at position 5 monodentate coordinates the U2 atom belonging to a third SBU. The carboxylate monodentate coordinating arms (positions 2,5) present a noncoordinating oxygen atom, which has been proven to be nonprotonated, indicated by the short C–O bonds of 1.22(1) Å. The ligand molecule behaves as a pentadentate linker with μ_5-η_2:η_1:η_1:η_0:η_1:η_2:η_1:η_0 coordination configuration.

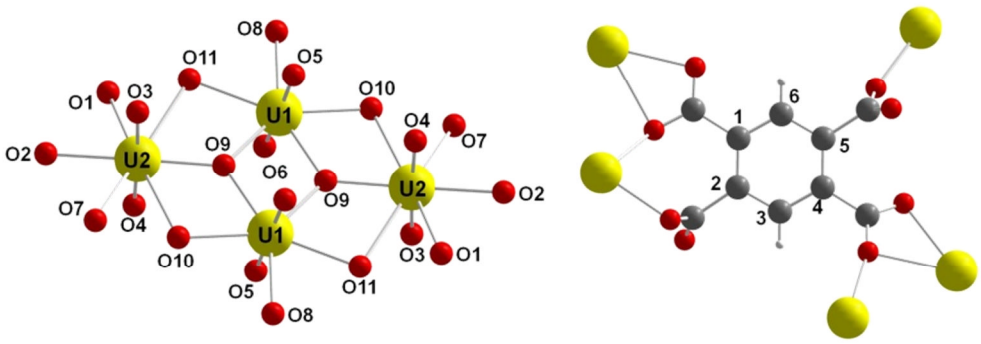

Figure IV.2.17 Coordination sphere surrounding the uranium atoms (left) and the ligand molecule coordination configuration (right) for **pyr6** complex.

Each ligand molecules interlinks three SBUs and each SBU is coordinated by six ligand molecules resulting in a single layered negatively charged bidimensional edifice ($[(UO_2)_2O(btec)]^{2-}$) developing in the (010) plane (Figure IV.2.18).

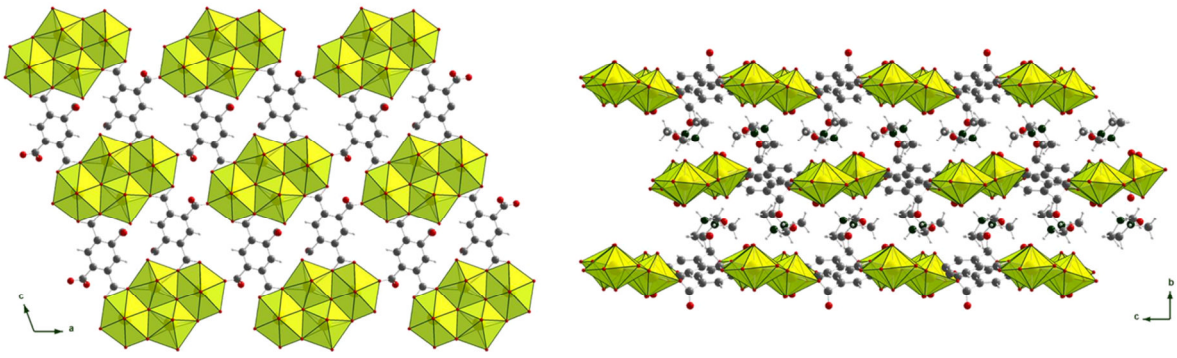

Figure IV.2.18 Structure representation for **pyr6** complex. View along [010] (left) and [100] (right) axes.

Two distinct crystallographic sites for the dimethylammonium cation are located between the polymeric layers. The protonated organic species are required for compensating the negative charges of the layers. A noncoordinating water molecule is also found intercalated between the sheets (Figure IV.2.19).

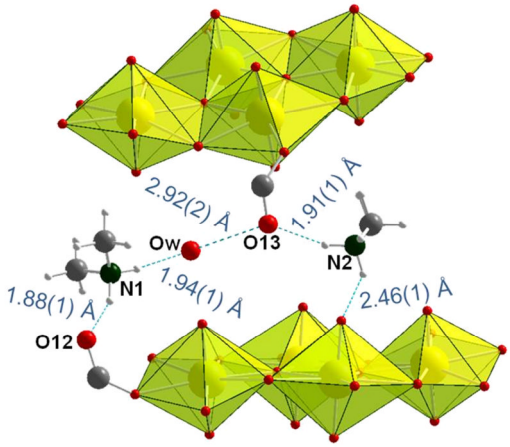

Figure IV.2.19 Representation of the weak hydrogen bond interactions appearing in the structure of **pyr6**.

The N1 nitrogen atom, with the two riding hydrogen atoms, interacts through hydrogen bonds with the O12 noncoordinating carboxyl oxygen atom belonging to the ligand and with the Ow (water) oxygen atom. The lengths of these hydrogen bonds are 1.88(1) and 1.94(1) Å, respectively. The second cation (N2) binds the O13 noncoordinating carboxyl oxygen atom and the O5 uranyl oxygen atom, both belonging to two different layers. The corresponding hydrogen bond lengths are 1.91(1) and 2.46(1) Å. The Ow free water molecule is situated at suitable distance (2.92(2) Å) from the O13 oxygen atom for the hydrogen bonds. The interlayer cohesion is maintained only by the weak hydrogen bond interactions without any π-π stacking interactions (C···C distances of 9.95(3) Å).

The structure of **pyr7** $(NH_4)_4[(UO_2)_{12}O_4(OH)_8(btec)_3]\cdot 22H_2O$ complex contains three crystallographic independent sites for the uranium atoms located on *8h* general positions. All three uranium atoms are seven-fold coordinated, adopting the pentagonal bipyramidal geometry (Figure IV.2.20). The typical short apical U═O bonds have the length in the range 1.748(6)-1.778(6) Å. The U─O bond lengths in the equatorial plane are ranging between 2.390(6) and 2.414(6) Å for the carboxyl oxygen atoms, 2.415(6) and 2.516(6) Å for the hydroxo groups and between 2.251(6) and 2.279(6) Å for the oxo groups.

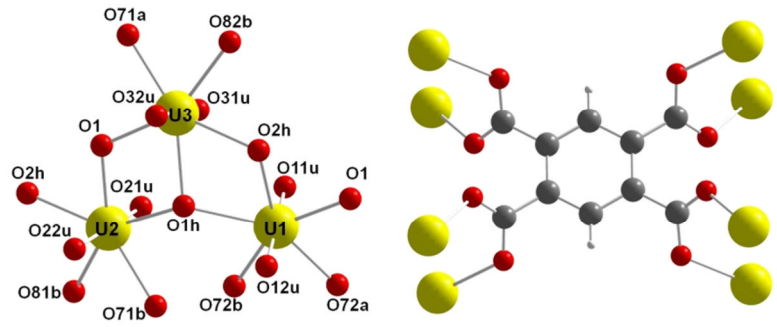

Figure IV.2.20 Coordination environment of the uranium atoms (left) and the ligand's coordination configuration (right) for the **pyr7** complex.

The nature of the oxo and hydroxo groups present in the structure has been established by bond valence calculation[14, 17]. The obtained values are 1.97 v.u. for the oxo group (expected value of 2) and 1.37, 1.40 v.u. for the two hydroxo groups (expected value of 1.2).

The uranium-centered polyhedra are interconnected via edge sharing through oxo-hydroxo bridges in such a manner to form infinite inorganic ribbons, running along the [100] axis (Figure IV.2.21). The infinite ribbons are interconnected transversally by the four carboxylate arms of the pyromellitate ligand generating the final tridimensional framework. The latter exhibits one-dimensional channels running parallel with the infinite ribbons along the *a* axis. The shape of the channels is rhombic prism with the window size of ~ 8.2 × 8.6 Å, considering the ionic radius for the oxygen atoms of 1.35 Å. Each channel is delimited on the edges by four inorganic ribbons and the corners correspond to the ligand molecules (Figure IV.2.22).

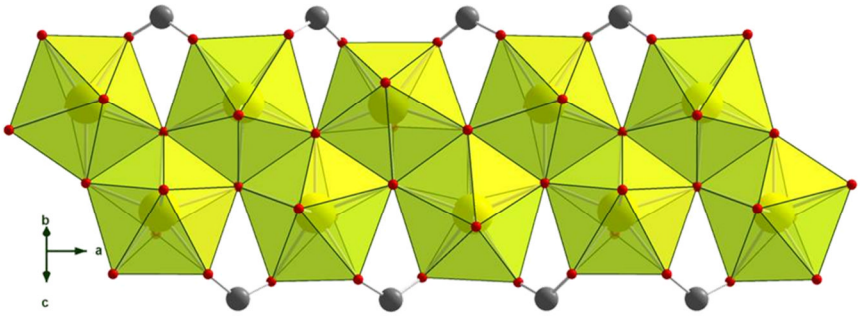

Figure IV.2.21 View (along the [021] axis) of a single infinite ribbon of interconnected uranium polyhedra in **pyr7** complex.

The pyromellitate molecule behaves as octadentate ligand (μ_8-η_1:η_1:η_1:η_1:η_1:η_1:η_1:η_1), connecting eight uranyl cations, with each carboxylate arm bridging in a *syn-anti* bidentate bridging mode. The benzene ring plane is perpendicular to the chain axis, each carboxylate group bridges two uranyl

centers of an inorganic ribbon, consequently, each ligand molecule is bind to four distinct chains.

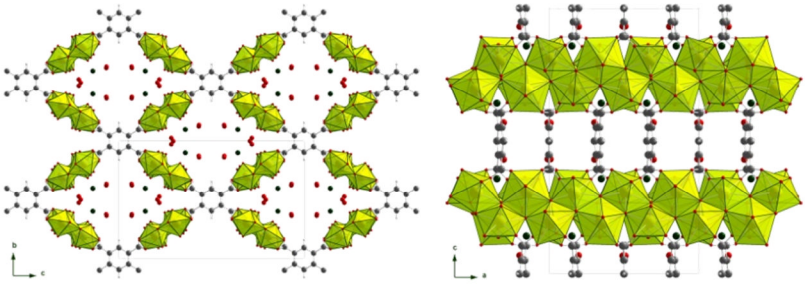

Figure IV.2.22 Structure representation of **pyr7** complex. View along [100] (left) and [010] (right) axes.

The channels are filled with ammonium cations, required to compensate the negative charges of the $[(UO_2)_{12}O_4(OH)_8(btec)_3]^{4-}$ framework, and noncoordinating water molecules, interacting with the framework through hydrogen bonds (Figure IV.2.23).

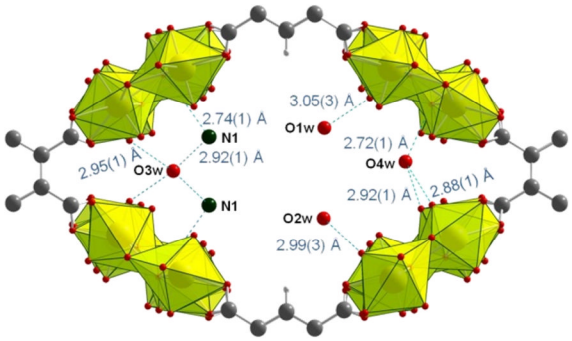

Figure IV.2.23 Hydrogen bonds and ionic interactions manifesting in the structure of **pyr7** phase.

Each ammonium cation (N1) is situated in the proximity of one hydroxo group belonging to the inorganic ribbon (O2h; N···O = 2.74(1) Å) and one free water molecule (O3w; N···O = 2.91(1) Å). The O3w free water molecule is located at equal distances (symmetric hydrogen bonds) from two uranyl oxygen atoms (O12u and its equivalent; O···O = 2.95(1) Å) belonging to two neighboring ribbons. The O1w and O2w crystallization water molecules are in the proximity of one uranyl oxygen atom (O21u and O32u respectively, with O···O distances of 3.05(1) and 2.99(1) Å respectively), each belonging to a different ribbon. The O4w free water molecule is situated adjacent to three oxygen atoms: two of them are uranyl types (O22u and O31u, with O···O distances of 2.88(1) and 2.92(1) Å respectively), like the case of O3w molecule, and the third (O1h; O···O = 2.72(1)

Å) belongs to a hydroxo bridge of the inorganic ribbon. Although the structure presents an extended network of hydrogen bonds, the tridimensional cohesion is ensured by the framework itself (the ligand coordination configuration and the oxo/hydroxo bridges) and only reinforced by the weak interactions manifesting inside the channels. This structural arrangement is particularly remarkable because most of the uranyl carboxylates consist of molecular packing of discrete or low-dimensional inorganic building blocks. Indeed, the number of 3D networks is rather small, and they were reported in some examples, exhibiting exclusively quite narrow pore systems[19, 20]. However, a very recent contribution also shows such closely related open-framework solid with uranyl cations and incorporating tripodal carboxylate ligand[21].

IV.3 . Synthesis

The **pyr1** to **pyr7** complexes have been synthesized hydrothermally under autogenous pressure using 23 mL Teflon-lined Parr type autoclaves. The starting reagents have been: uranyl nitrate hexahydrate ($UO_2(NO_3)_2 \cdot 6H_2O$, Merck 99%), neodymium nitrate hexahydrate ($Nd(NO_3)_3 \cdot 6H_2O$, Aldrich 99.9%), pyromellitic acid (1,2,4,5-$C_6H_2(COOH)_4$, Aldrich 96%), potassium hydroxide (KOH, Prolabo 85%), ammonia solution (NH_3, Prolabo 28%), hydrazine solution (N_2H_4, Acros Organics 51%), N,N-dimethylformamide ($(CH_3)_2NCHO$, Sigma Aldrich 99%), ammonium carbonate ($(NH_4)_2CO_3$, Aldrich 99%), and lithium carbonate (Li_2CO_3, Aldrich 99%). All are commercially available and have been used without further purifications.

Using the pyromellitic acid as ligand, six chemical systems have been studied. In each of them, the optimal reaction time and temperature were maintained constant (at 200°C during 24 h), and were varied the nature and the quantity of pH moderator. It is shown in Figure IV.3.1 that six bases were used, one for each system. In the chemical system 2 (ammonium carbonate), it has been observed that a new uranyl pyromellitate phase (**pyr4**) is obtained during the investigations of the mixed system uranyl-neodymium we studied in the chapter VI. This fact has generated the two subsystems, 2.1 and 2.2.

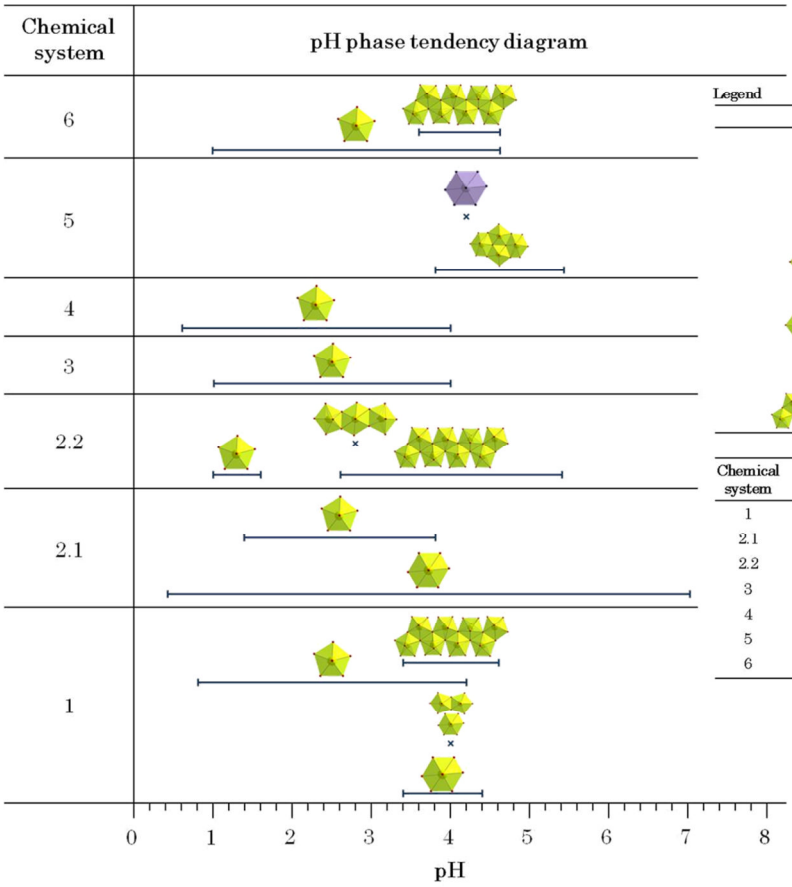

Legend

Symbol	Phase
	pyr1
	pyr2
	pyr3
	pyr4
	pyr5
	pyr6
	pyr7

Chemical system	U / Nd / Ligand molar ratio	Nature of pH moderator
1	1 : 0 : 0.5	NH_4OH - ammonium hydroxide
2.1	1 : 0 : 0.5	$(NH_4)_2CO_3$ - ammonium carbonate
2.2	0.5 : 0.5 : 0.5	$(NH_4)_2CO_3$ - ammonium carbonate
3	1 : 0 : 0.5	KOH - potassium hydroxide
4	1 : 0 : 0.5	N_2H_4 - hydrazine
5	1 : 0 : 0.5	C_3H_7NO - N,N-dimethylformamide
6	1 : 0 : 0.5	Li_2CO_3 - Lithium hydroxide

Figure IV.3.1 pH phase tendency diagram for the uranyl pyromellitate chemical systems.

The **pyr1** phase $[(UO_2)_2(btec)(H_2O)_2]\cdot H_2O$ ( ) appears in all six studied chemical systems, starting from a very low pH of 0.6, traces of this complex being identified up to pH of 4.6 depending on the system. As a general method for obtaining the pure **pyr1** phase it has been chosen a synthesis from chemical system 1: a mixture of 0.502 g (1 mmol) $UO_2(NO_3)_2\cdot 6H_2O$, 0.127 g (0.5 mmol) pyromellitic acid, 0.2 mL solution 2M (0.4 mmol) NH_4OH and 4.8 mL H_2O (267 mmol) was placed in a Parr type autoclave. The solution pH at the end of synthesis was 0.8.

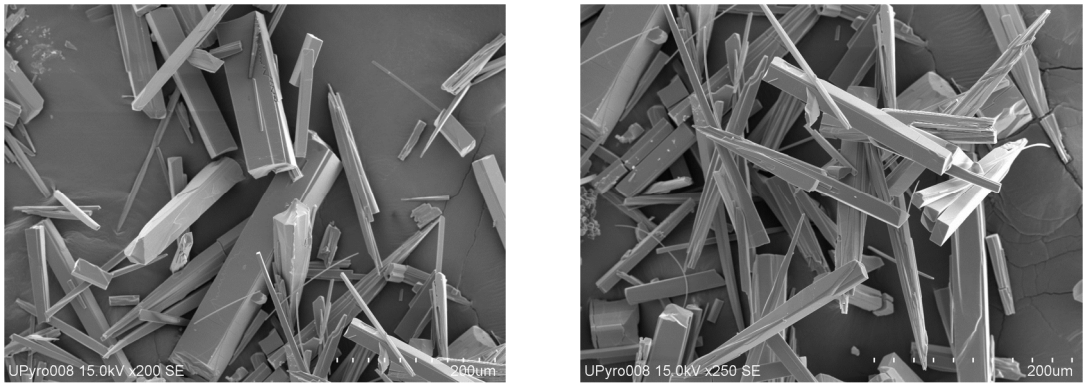

Figure IV.3.2 SEM pictures of **pyr1** complex.

The resulting yellow product has been filtered off, washed with water and then dried at room temperature. The **pyr1** product has been analyzed by scanning electron microscopy and shows typical needle-like crystals of 100 - 200 µm in size (Figure IV.3.2).

The **pyr2** phase $(NH_4)_2[(UO_2)(btec)]\cdot 4H_2O$ ( ) has been obtained in two of the studied cases. In chemical system 1, employing the ammonium hydroxide as base, the phase appears on a relatively restrained pH domain, from 3.4 to 4.4. In the chemical system 2.1 employing the ammonium carbonate as base, the pH range in which the phase appears is broad, beginning at 0.4, traces of the phase still being observed at pH 7. The general synthesis method for obtaining the **pyr2** phase pure belongs to the 2.1 chemical system and consists in the statically heating of a mixture of 0.502 g (1 mmol) $UO_2(NO_3)_2\cdot 6H_2O$, 0.127 g (0.5 mmol) pyromellitic acid, 0.058 g (0.6 mmol) $(NH_4)_2CO_3$ and 5 mL (278 mmol) H_2O. The pH after synthesis was 0.9. The obtained yellow product has been filtered off, washed with water and dried at room temperature. The SEM (Scanning Electron Microscopy) analyzes reveal small crystallites with a specific plate shape of 1 to 10 µm in size (Figure IV.3.3).

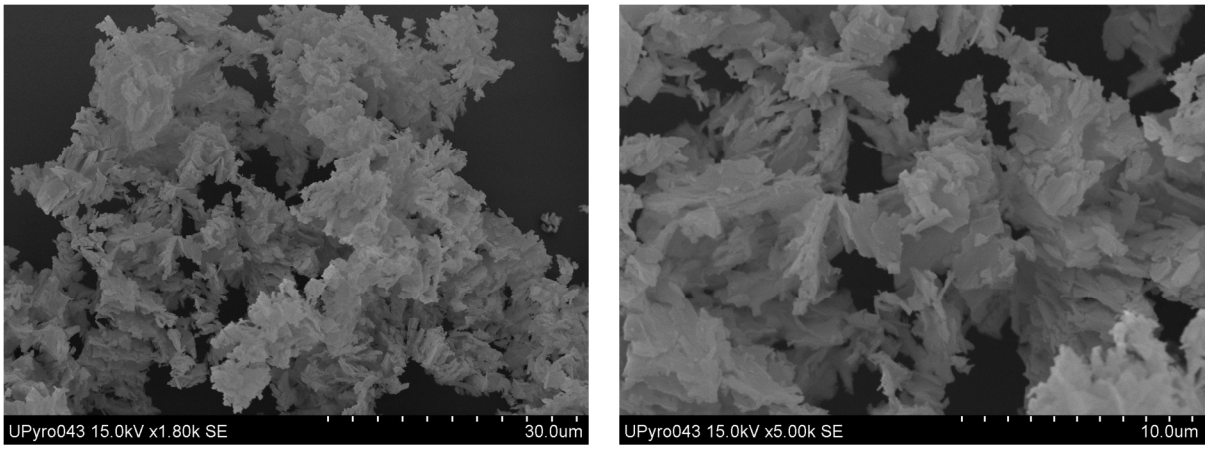

Figure IV.3.3 SEM pictures of **pyr2** phase.

The **pyr3** $(Hdma)_2[(UO_2)(btec)]$ ( ) and **pyr6** $(Hdma)_2[(UO_2)_2O(btec)]$ ( ) phases have been both obtained in the same preparation under the same reaction conditions by heating under hydrothermal conditions, a mixture of 0.502 g (1 mmol) $UO_2(NO_3)_2\cdot 6H_2O$, 0.127 g (0.5 mmol) pyromellitic acid, 1 mL (~13 mmol) N,N-dimethylformamide and 4 mL (222 mmol) H_2O. The pH after synthesis was 4.8. Both of the phases contain dimethylammonium cations resulted from the *in-*

situ degradation of the N,N-dimethylformamide molecules employed as pH moderator, consequently they can only be obtained in chemical system 5. Crystals of **pyr3** complex were isolated only from one preparation (pH = 4.8) although the PXRD pattern of this preparation shows no traces of the phase. The **pyr6** phase appears in small quantities on a relatively broad domain of pH, from 3.8 to 5.4 and always together with various quantities of unidentified impurities (Figure IV.3.4).

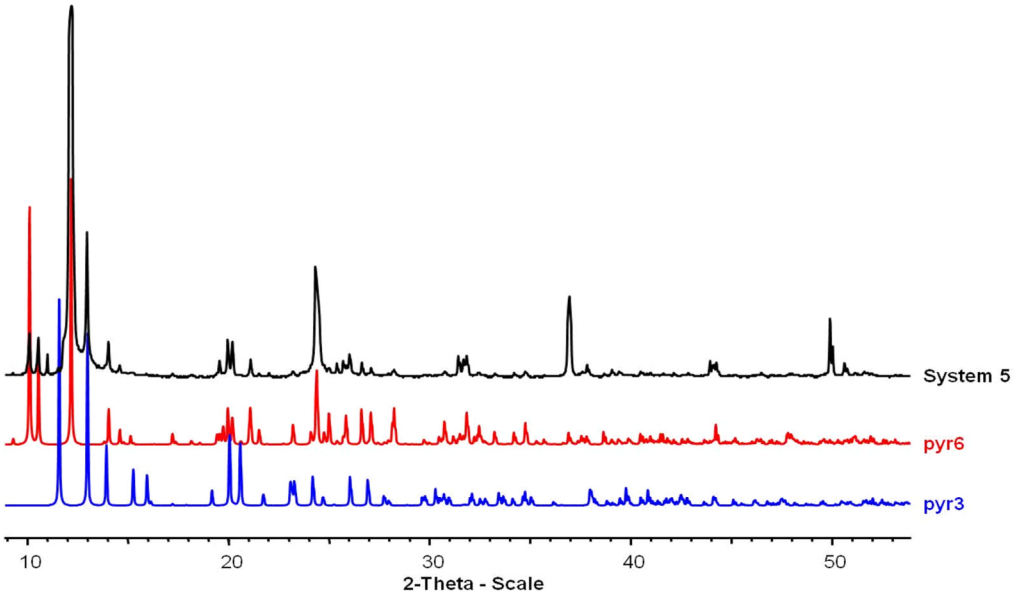

Figure IV.3.4 Comparison between the experimental PXRD pattern of a preparation belonging to chemical system 5 and the simulated patterns of the **pyr3** and **pyr6** phases.

The **pyr4** phase $(NH_4)[(UO_2)_2(OH)(H_2O)(btec)]\cdot 2H_2O$ ( ) has only been observed in one preparation of the chemical system 1. The synthesis consists in the statically heating at 200°C during 24 h, under hydrothermal conditions, of a mixture containing 0.502 g (1 mmol) $UO_2(NO_3)_2\cdot 6H_2O$, 0.127 g (0.5 mmol) pyromellitic acid, 1.2 mL solution 2M (2.4 mmol) NH_4OH and 3.8 mL (211 mmol) H_2O. The solution pH after synthesis was 4.0. The yellow product obtained has been filtered off, washed with water and dried at room temperature. From this preparation one crystal has been characterized by single crystal X-ray diffraction technique, determining the **pyr4** structure. The PXRD pattern (Figure IV.3.5) of this preparation shows only a mixture of **pyr1**, **pyr2** and **pyr7** phases, not presenting any traces of **pyr4**. The conclusion is that **pyr4** phase appears in this system as an impurity, in very small quantities.

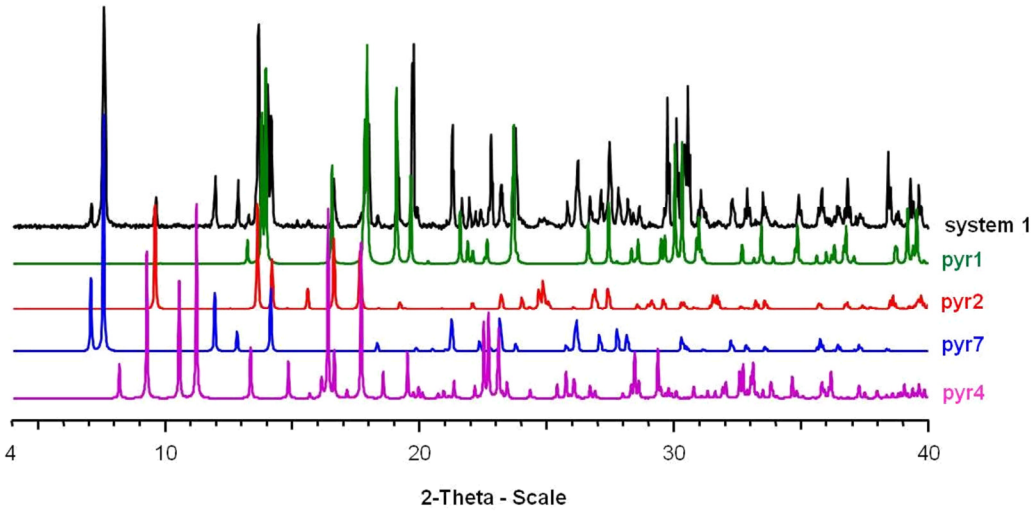

Figure IV.3.5 Comparison between the experimental PXRD pattern of the preparation where crystals of **pyr3** phase were found (black) and the simulated patterns of **pyr1** (green), **pyr2** (red), **pyr6** (blue) and **pyr3** (purple) phases.

The **pyr5** phase $[(UO_2)_3(btec)(OH)_2(H_2O)_2]$ () has been obtained in the chemical subsystem 2.2, employing the ammonium carbonate as a base and the neodymium nitrate hexahydrate as a source of secondary cation. Mixed uranyl-lanthanide cations have been use for the synthesis of mixed U/Ln carboxylates, phases that will be presented in chapter VI. In one of the system 2.2 preparation a few crystals of the **pyr5** phase have been separated and the structure has been determined. The preparation has been obtained by statically heating under hydrothermal conditions at 200°C during 24 h a mixture of 0.251 g (0.5 mmol) $UO_2(NO_3)_2{\cdot}6H_2O$, 0.219 g (0.5 mmol) $Nd(NO_3)_3{\cdot}6H_2O$, 0.117 g (1.2 mmol) $(NH_4)_2CO_3$ and 5 mL (278 mmol). The pH after synthesis was 2.8.

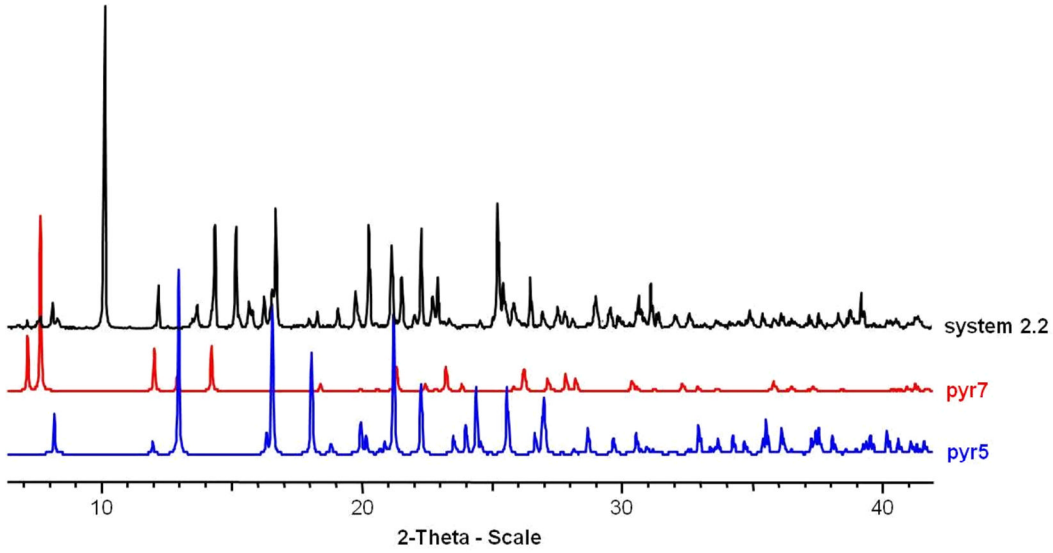

Figure IV.3.6 Comparison between the experimental PXRD pattern of the preparation where crystals of **pyr5** phase appear and the simulated patterns of the **pyr7** (red) and **pyr5** (blue) phases.

The resulting yellow product has been filtered off, washed with water and dried at room temperature. Beside the crystals of **pyr5**, no other crystals were suited for structure determination by single crystal X-ray diffraction technique. The PXRD experimental diagram of this preparation does not match the **pyr5** simulated one, the only phase identified by this method is **pyr7**, phase appearing in very small quantities (Figure IV.3.6).

The **pyr7** phase $(NH_4)_4[(UO_2)_{12}O_4(OH)_8(btec)_3]\cdot 22H_2O$ ( ) has been obtained in three different chemical systems 1, 2.2 and 6 at relatively high values of pH, ranging from 2.6 to 5.4. As a major phase, with very small quantity of impurities this complex has been obtained by slightly modifying reaction conditions of system 1. A better yield was obtained when the synthesis took place at 110°C during 24 h instead of 200°. The product has been thus obtained in these conditions from a mixture of 1.005 g (2 mmol) $UO_2(NO_3)_2\cdot 6H_2O$, 0.064 g (0.25 mmol) pyromellitic acid, 1.0 mL solution 2M (2.0 mmol) NH_4OH and 4 mL (222 mmol) H_2O. The solution pH after synthesis was 2.7. For improving the purity of the phase a microwave-assisted procedure was attempted using a MarsX oven (microwave accelerated reaction system). A mixture of 1.005 g (2 mmol) $UO_2(NO_3)_2\cdot 6H_2O$, 0.064 g (0.25 mmol) pyromellitic acid, 1.3 mL solution 2M (2.6 mmol) NH_4OH and 8.7 mL (483 mmol) H_2O was placed in a 100 mL Teflon autoclave and heated statically at 110°C during 2 h. After filtration, the product was dried at room temperature.

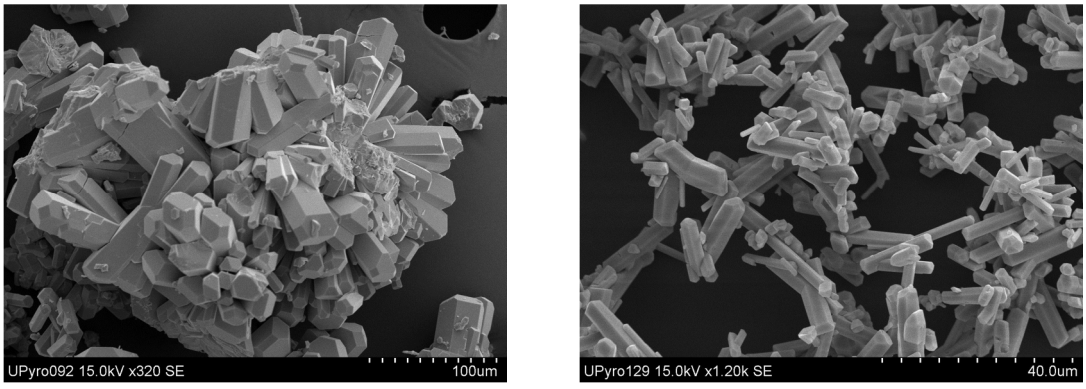

Figure IV.3.7 SEM pictures of **pyr7** phase obtained by conventional hydrothermal (left) and by microwave-assisted (right) methods

SEM examination of both preparations, obtained by conventional and microwave-assisted methods, indicated crystal morphologies with a block shape of 20 - 80 μm in size for the first case and with a pseudohexagonal needlelike

shape of 5 - 30 μm in size for the second case (Figure IV.3.7). A difference in crystal size and shape for the products obtained by the two techniques has been previously reported for the preparation of MOF-type materials and was attributed to the fast nucleation kinetics occurring under microwave irradiation[22].

Due to the fact that only **pyr1**, **pyr2** and **pyr7** coordination complexes have been obtained pure, the three of them were the only available for further analyses.

IV.4 . Spectroscopic characterization.

Infrared spectroscopy

Infrared spectrum of $[(UO_2)_2(btec)(H_2O)_2]\cdot(H_2O)_2$ (**pyr1**) shows a very broad band of absorption in the 3650-3200 cm^{-1} range, indicating the presence of hydrogen bonds between the coordinating water and the free water molecules. For the water molecules, the asymmetric stretching [ν_{asym}(O—H)] has been assigned at 3577 cm^{-1}, the ν_{sym}(O—H) occurs in the range of 3500-3000 cm^{-1} as a low intensity broad band and the peak at 1626 cm^{-1} has been assigned to the δ(H—O—H) bending[23].

The ν_{asym}(COO) and ν_{sym}(COO) stretching vibrations of the uranyl coordinating groups belonging to the ligand were observed in the 1567-1430 cm^{-1} domain. The intense peak appearing at 1386 cm^{-1} has been assigned to the C=C ring vibration. The absence of any absorption near the value of 1694 cm^{-1} confirms the absence of non coordinating carboxylate groups, consequently, the absence of the free acid in the sample[24].

The uranyl related vibrations give IR absorbance in the 1000-200 cm^{-1} domain. In our case only the $\nu_{asym.}$(U=O) and could be assigned at 925 cm^{-1}. The peaks appearing at a wavenumbers value below 550 cm^{-1} could belong to the $\nu_{st.}$(U-O) vibration but could not be precisely assigned[25]. The absorption peak that appears at 925 cm^{-1} has been assigned to the ν_3 asymmetrical stretching

vibration of the uranyl bond. The position of this peak, using the empirical equation previously described[26], gives an approximate U═O bond length of 1.767 Å, value which is in good agreement with the bond lengths obtained from the single crystal X-ray diffraction data of 1.764(3) and 1.758(3) Å.

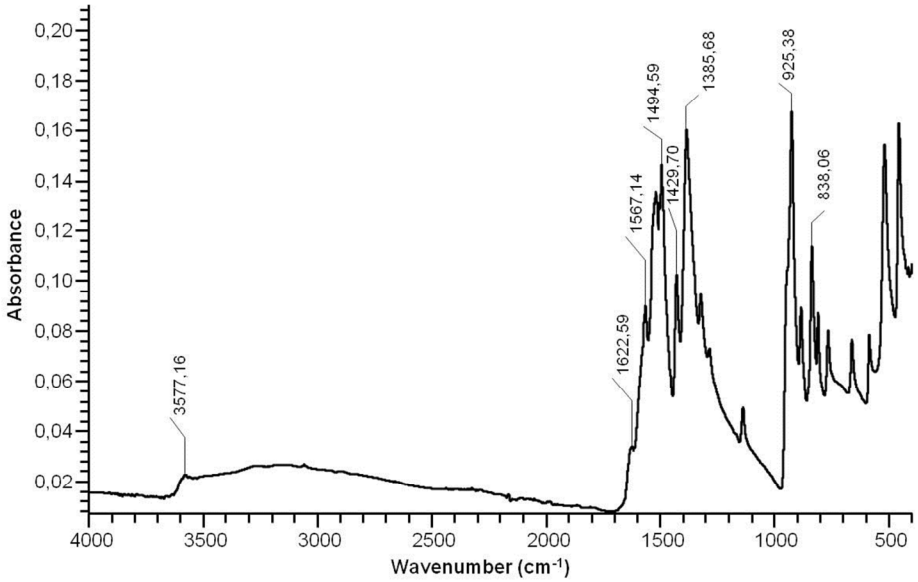

Figure IV.4.1 IR absorption spectrum of **pyr1** complex.

In the case of $(NH_4)_2[UO_2(btec)]\cdot(H_2O)_4$ (**pyr2**) the IR spectrum (Figure IV.4.2) is more explicit in the 3600-2600 cm-1 region. There could be assigned to the H_2O ν_{asym}(O-H) absorption band centered at 3550 cm^{-1}, the H_2O ν_{sym}(O-H) absorption band centered at 3198 cm^{-1} and the NH_4 ν(N─H) band centered at 2761 cm^{-1}.

In the structure, two of the carboxylate groups contain a non coordinating oxygen atom, this particularity giving the broad peak centered at 1683 cm^{-1}, peak assigned to the ν(C=O) vibration. The peaks corresponding to the ν_{asym}(COO) and ν_{sym}(COO) vibrations have been found in the 1545-1430 cm^{-1} domain and the intense peak from 1360 cm^{-1} has been attributed to the ν(C=C) ring vibration.

The uranyl ν_{asym}(U=O) has been found at 924 cm^{-1}. The uranyl ν_{sym}(U=O) and ν(U-O) could not be precisely assigned but they are found in the region below 880 cm^{-1}. The position of the peak (924 cm^{-1}) corresponding to the ν_3 vibration of the uranyl bond gives by empirical calculus the U═O bond length of 1.768 Å, value which is in agreement with the bond lengths obtained from the crystallographic data refinement of 1.781(3) and 1.775(3) Å.

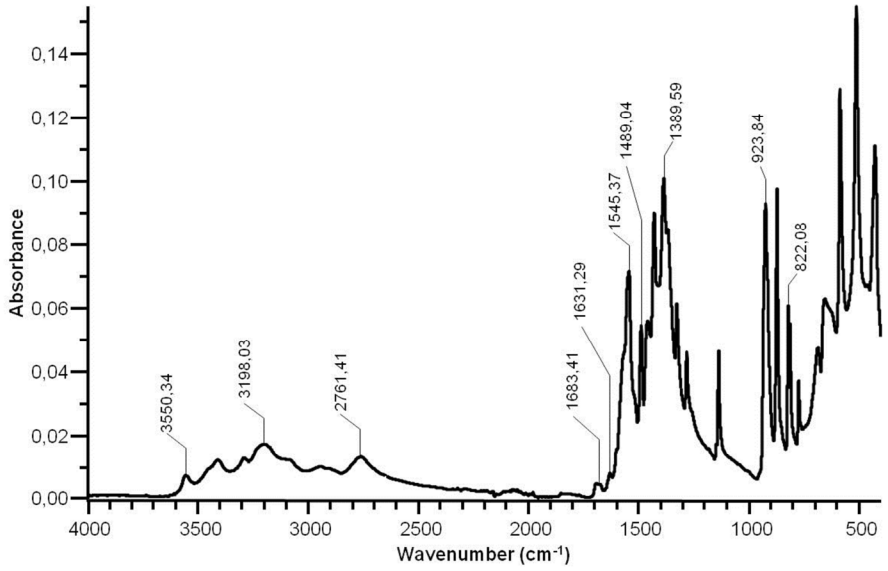

Figure IV.4.2 IR absorption spectrum of **pyr2** complex.

For the $(NH_4)_4[(UO_2)_{12}O_4(OH)_8(btec)_3]\cdot 22H_2O$ (**pyr7**) compound the IR spectrum (Figure IV.4.3), like in the previous case, presents a very broad, low intensity absorption band centered at 3250 cm^{-1}. This band has been assigned to the ν_{asym}(O-H) and ν_{sym}(O-H) of water molecules, to the hydrogen bonds vibration and also to the ν(N-H) vibrations from the NH_4^+ groups. The δ(H-O-H) vibration of the water molecules has been found at 1633 cm^{-1}.

The ligand related vibrations have been assigned as follows: the asymmetric and symmetric COO stretching vibrations have been found in the 1564-1437 cm^{-1} area and the aromatic C=C stretch vibration appears at 1393 cm^{-1}. The absence of any absorption peak near the 1694 cm^{-1} value, confirms the absence of the free acid in sample.

The peak at 918 cm^{-1} and its shoulder at 942 cm^{-1} have been assigned to the ν_{asym}(U=O). Other peaks appearing below 880 cm^{-1} are belonging to the ν_{asym}(U=O) and the ν(U–O) vibrations but could not be precisely assigned. Applying the empirical calculations[26] for obtaining the U=O bond length from the position of the IR absorption peaks belonging to the ν_3 uranyl vibration, the resulting values were 1.770 and 1.755 Å respectively. These values are in agreement with those obtained from the crystallographic data refinement, which vary between 1.748(6) and 1.778(6) Å

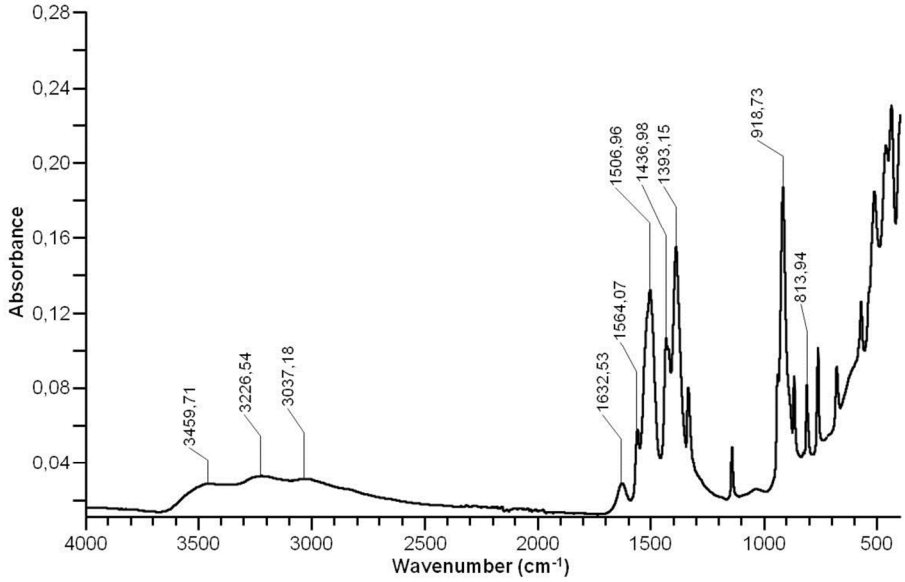

Figure IV.4.3 IR absorption spectrum of **pyr7** complex.

Fluorescence spectroscopy

For the pyromellitate phases obtained pure, **pyr1**, **pyr2**, **pyr7** and **A**, the solid state fluorescence emission spectra have been recorded at room temperature under excitation at 365 nm. The emission spectra of each compound have been recorded in the 440-640 nm range and have been compared with that of uranyl nitrate hexahydrate.

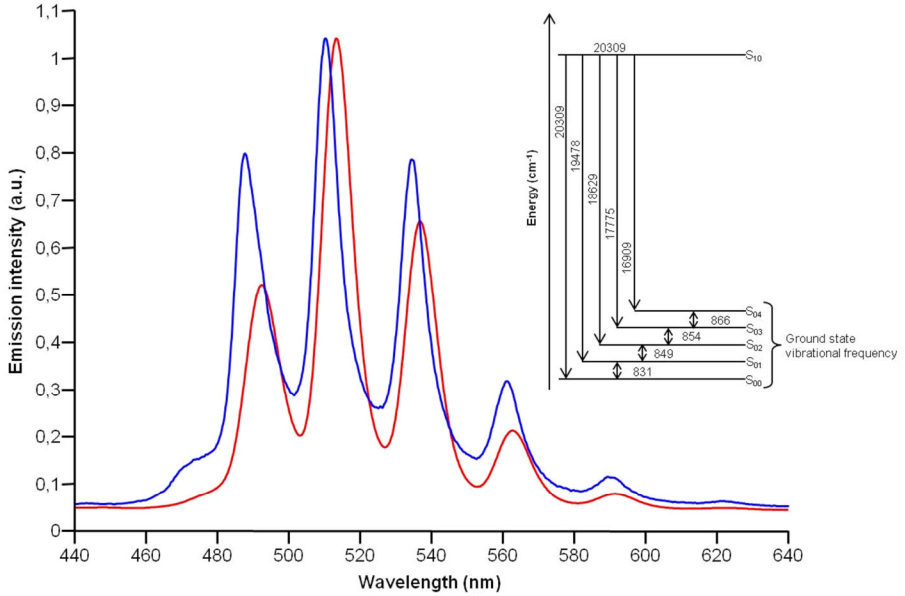

Figure IV.4.4 Solid state emission spectra (left) of **pyr1** (red), of uranyl nitrate hexahydrate (blue) and the electronic and vibronic transitions (right) for **pyr1** complex.

The fluorescence emission spectrum of **pyr1** phase (Figure IV.4.4) maintains the same uranyl characteristic peaks as the uranyl nitrate, with a very small red shift of ~5.6 nm (average) and excepting the $S_{11}\rightarrow S_{00}$ transition, which for this compound was not observed. The spacing between two consecutive bands $S_{10}\rightarrow S_{0v}$ and $S_{10}\rightarrow S_{0(v+1)}$ (v = 0-3) electronic transitions takes values ranging from 831 to 866 cm^{-1} and corresponds to the vibronic transitions $S_{0v}\rightarrow S_{0(v-1)}$ (v = 1-4) observed in Raman diffusion spectroscopy.

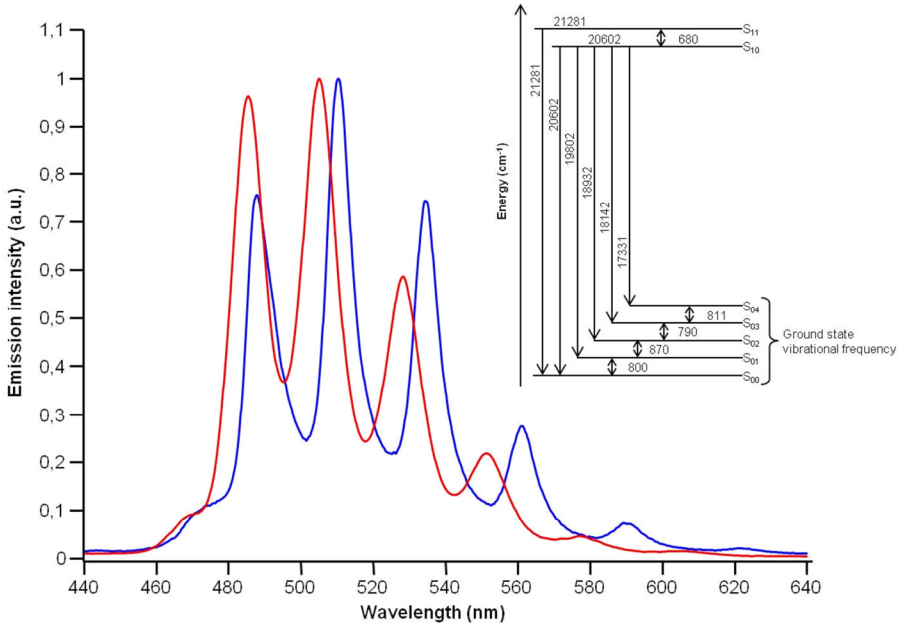

Figure IV.4.5 Solid state emission spectra (left) of **pyr2** (red), of uranyl nitrate hexahydrate (blue) and the electronic and vibronic transitions (right) for **pyr2** complex.

For the **pyr2** phase the solid state fluorescence emission spectrum (Figure IV.4.5) shows all six electronic transitions specific to the uranyl ion. Compared with the spectrum of uranyl nitrate hexahydrate, the one of **pyr2** presents a blue shift of maximum 8.7 nm on the last peak. The spacing between two consecutive bands $S_{10}\rightarrow S_{0v}$ and $S_{10}\rightarrow S_{0(v+1)}$ (v = 0-3) electronic transitions takes values ranging from 790 to 870 cm^{-1} and corresponds to the vibronic transitions $S_{0v}\rightarrow S_{0(v-1)}$ (v = 1-4) observed in Raman diffusion spectroscopy. The spacing between the $S_{11}\rightarrow S_{00}$ and $S_{10}\rightarrow S_{00}$ electronic transitions has, as expected, a lower value of 687 nm.

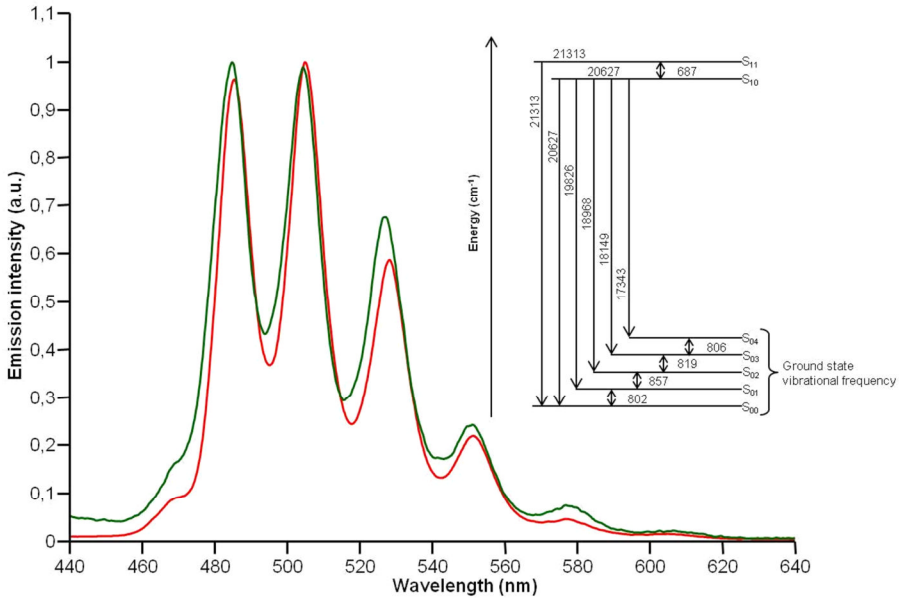

Figure IV.4.6 Solid state emission spectra (left) of **pyr2** (red), of phase **A** (blue) and the electronic and vibronic transitions (right) for phase **A**.

The emission spectrum of the **A** phase (Figure IV.4.6) is almost identical to the one of **pyr2**, with small variations in the intensity of the peaks and a very small blue shift (0.6 nm) of the **A** phase spectrum from the one of the **pyr2**. The resemblance between the two spectra was expected, the uranyl-centered monomeric unit of both phases being similar. More fluorescence data values have been summarized in Table IV.4.1.

Table IV.4.1 Fluorescence bands for uranyl nitrate, pyr1, pyr2 and A phases.

Uranyl dinitrate hexahydrate			pyr1			pyr2			phase A		
λ (nm)	$\tilde{\nu}$ (cm^{-1})	$\Delta\tilde{\nu}$ (cm^{-1})	λ (nm)	$\tilde{\nu}$ (cm^{-1})	$\Delta\tilde{\nu}$ (cm^{-1})	λ (nm)	$\tilde{\nu}$ (cm^{-1})	$\Delta\tilde{\nu}$ (cm^{-1})	λ (nm)	$\tilde{\nu}$ (cm^{-1})	$\Delta\tilde{\nu}$ (cm^{-1})
469,16	21315		-	-		469,9	21281		469,2	21313	
485,88	20581	733	492,4	20309	-	485,4	20602	680	484,8	20627	686
507,98	19686	895	513,4	19478	831	505.0	19802	800	504,4	19826	802
531,53	18814	872	536,8	18629	849	528,2	18932	870	527,2	18968	857
557,36	17942	872	562,6	17775	854	551,2	18142	790	551.0	18149	819
585,71	17073	868	591,4	16909	866	577.0	17331	811	576,6	17343	806

The fluorescence solid-state emission spectrum of **pyr7** (Figure IV.4.7) exhibits broad bands, having poor resolution due to the polymeric nature of the SBU. It presents two main peaks at 504.4 and 523.8 nm, which could correspond to the second and the third peak in the uranyl nitrate spectrum and two shoulders at 544.6 and 571 nm possibly corresponding to the forth and the fifth peak in the latter mentioned spectrum.

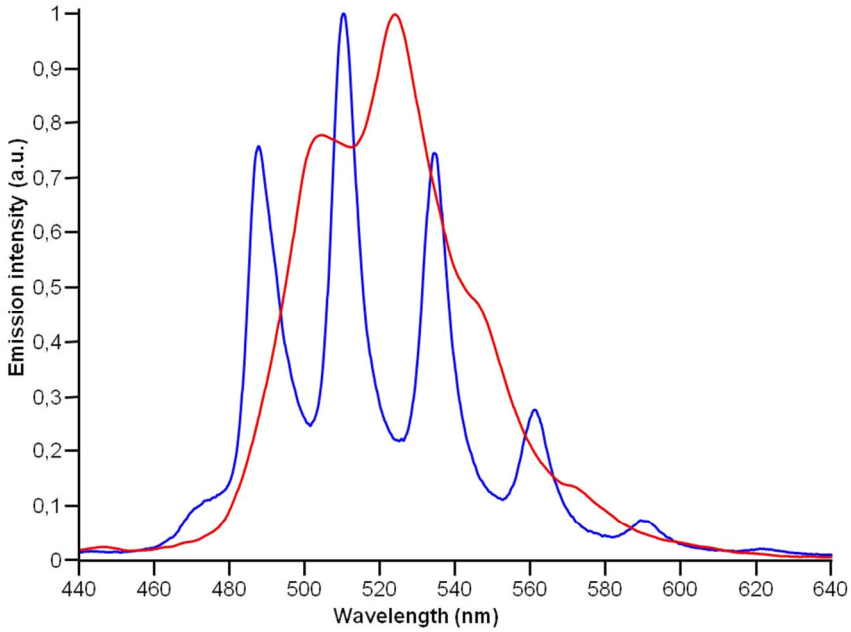

Figure IV.4.7 Solid state emission spectra for uranyl nitrate hexahydrate (blue), and for **pyr7** complex (red).

It is interesting to note the band shift could be correlated to the different structural assemblies of uranyl for a given polycarboxylate ligand, here pyromellitate. We observed that the shift seems to depend on the coordination state of the uranyl centers. The most intense peaks are located at 513.4 and 524.0 nm (red-shifted) for pentagonal bipyramidal environments (for **pyr1** and **pyr7**, respectively) and 505.0 and 504.4 nm (blue-shifted) for hexagonal bipyramidal environments (for **pyr2** and **A**, respectively). Compared to the spectrum of the uranyl dinitrate hexahydrate (maximum at 508.0 nm), the difference between those containing 8-fold coordinated uranyl centers (**pyr2** and **A**) is quite small ($\Delta\lambda$ = 3 - 3.6 nm), whereas it is higher for those containing 7-fold coordinated uranyl centers ($\Delta\lambda$ = 5.4 and 16.0 nm for **pyr1** and **pyr7**, respectively). The coordination sphere around uranyl center in the uranyl dinitrate is defined by a hexagonal bipyramid[27] and relatively slight differences in the band positions are observed with those of compounds **pyr2** and **A**. These variations of positions could be due to the effect of the rigid benzene-containing tetracarboxylate ligand, which may shift the emission intensity of the whole spectrum. Such analyses of red-shifted or blue-shifted fluorescence spectra have been previously reported in a series of uranyl phases associated with aliphatic carboxylates[28] for instance, but no clear assignment depending on the uranyl coordination state had been made because of the different natures of ligands attached to the actinide cation.

IV.5 . Thermal characterization

The TGA/TDA experiments were conducted under air from ambient temperature up to 800°C with a heating rate of 1°C/min. The thermodiffraction experiments were conducted under the same conditions as the TGA/TDA but with a heating rate of 5°C/min. X-ray powder diffraction patterns were recorded at each 20°C.

The thermal degradation of **pyr1** $[(UO_2)_2(btec)(H_2O)_2]\cdot H_2O$ complex exhibits five distinct events for the thermogravimetric curve (Figure IV.5.1). The first step takes place between 30 and 85°C and has been attributed to the loss of the crystallization water molecules. On this domain of temperature the TG curve records a weight loss of 1.9%, percentage found to be in agreement to the calculated value of 2.1% corresponding to the free water molecules (one water molecule per formula unit). This step is also evidenced in the TD curve by a low intensity broad endothermic peak. Apparently the loss of crystallization water does not influence the crystallinity of the compound, since no change takes place for the PXRD patterns in this temperature range (Figure IV.5.1).

The second degradation step takes place between 175 and 225°C and has been assigned to the loss of the coordination water. In the TG curve this step is evidenced by a weight loss of 4.3%, corresponding to the calculated value of 4.3% for the loss of coordinating water molecules (two molecules per formula unit). In the TD curve this step appears as a broad endothermic peak, more intense than the previous one. In the thermodiffraction powder patterns, a change of positions of Bragg peaks occurs at about 160°C, indicating the formation of a crystalline intermediate, stable up to 300°C. From the TG data, the formula for this intermediate phase should be '$(UO_2)_2(btec)$', corresponding to an anhydrous form of **pyr1**. In this case, the coordination state of uranyl cation would become six (square bipyramid). Attempts have been made for indexation of the Bragg peaks of the intermediate phase, but no satisfactory cell parameters have been obtained.

The third degradation step takes place between 340 and 445°C and appears in the TG curve as a massive weight loss of 25.9%. It has been assigned

to the oxidation of the ligand molecules. The calculated percentage for the total burning of the organic ligand is 29.7%. The 3.8% difference between the experimental and calculated values suggests that the organic molecules are not fully oxidized (to CO_2 and H_2O), some small parts remaining attached to the metal centers possibly as carbonate species. This step is evidenced in the TD curve as an intense exothermic peak. The thermodiffraction patterns diagram shows the transition from the crystalline intermediate '$(UO_2)_2$(btec)', toward the formation of α-U_3O_8 (PDF No. 00-031-1424) transient oxide form.

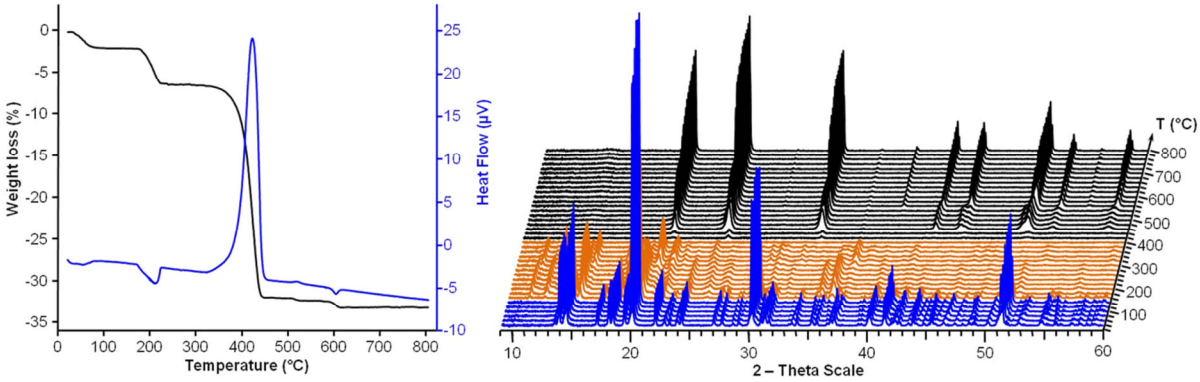

Figure IV.5.1 Thermal stability and thermal behavior of **pyr1** phase. TGA/TDA curves (left) and thermodiffraction patterns (right).

Between 510 and 615°C, the last two steps have been assigned to a structural reorganization of the oxide phase and the loss of the remaining functions belonging to the ligand. In the TG curve they are represented by a summed weight loss of 1.2%, the last step also giving a very weak endothermic peak in the TD curve. After cooling down, this phase passes into a second oxide form: U_3O_8 (PDF No. 01-072-1078). The total weight loss is 33.3% value, which is in agreement with the calculated one (34.9%), based on the degradation equation below:

$$3\left[(UO_2)_2{-}H_2O_2(C_{10}H_2O_8)\right]\cdot H_2O \xrightarrow[-9H_2O]{230^\circ C} 3[(UO_2)_2(C_{10}H_2O_8)] \xrightarrow[-30CO_2]{620^\circ C\ +20.5O_2} \xrightarrow{-H_2O} 2U_3O_8$$

For this compound, an *in situ* high temperature IR experiment has been conducted between room temperature and 210°C (Figure IV.5.2).

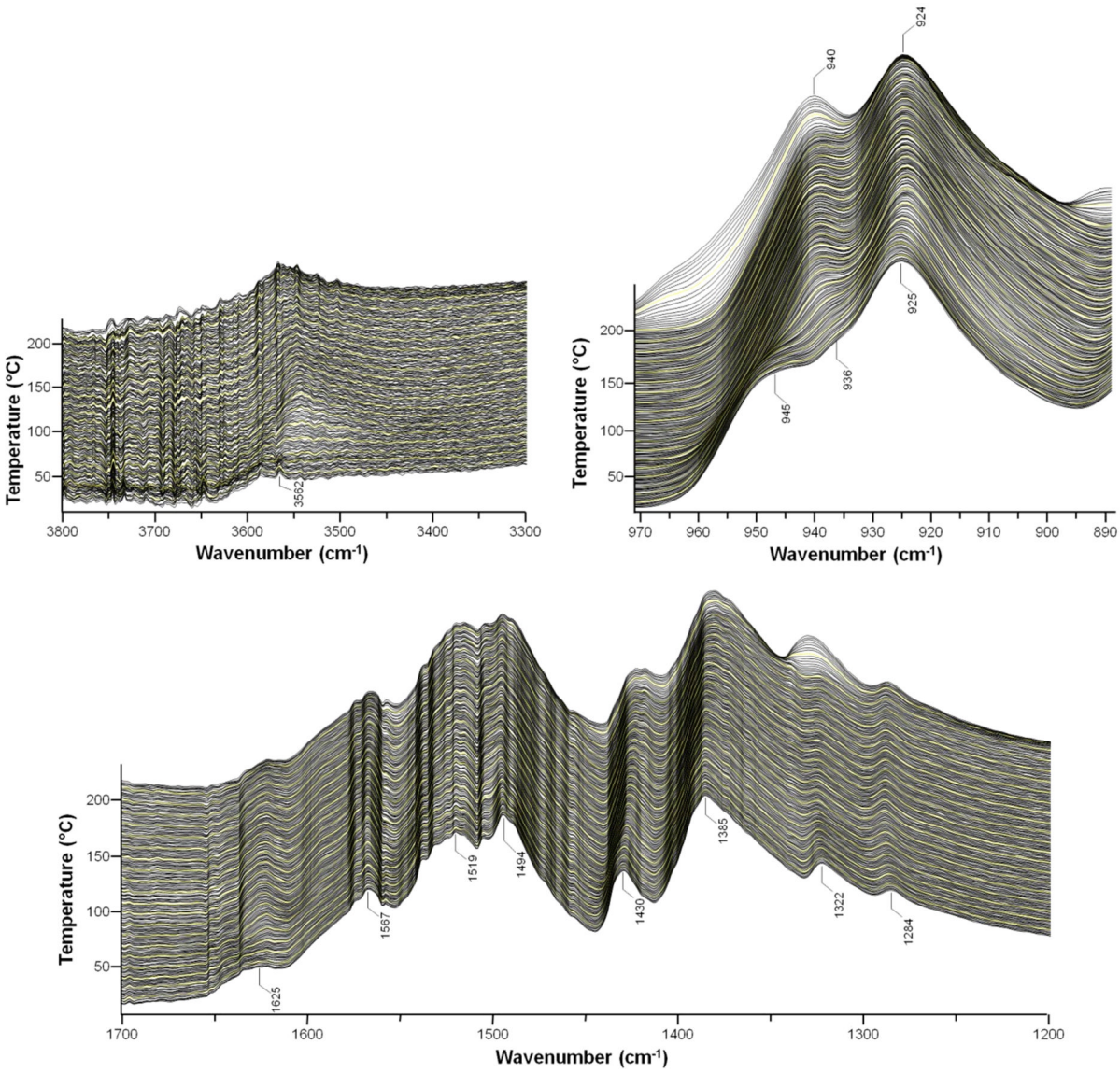

Figure IV.5.2 Temperature in situ IR spectra evolution for **pyr1** phase

Concerning the *in situ* IR experiment only the transformation corresponding to the departure of the crystallization water molecules could be observed. The main changes appear in the 970-890 cm^{-1} region (region specific to the uranyl bond vibration), where the shoulder at 945 cm^{-1} disappears at about 80°C, being replaced by the one at 940 cm^{-1}. The shift of the uranyl bond vibration at such low temperature could be explained by the influence of the non-coordinating water molecules on the uranyl oxygen atoms through the hydrogen bonds network. Once the water molecules are removed, their influence disappears modifying the U═O bond vibrations and implicitly the position of the corresponding peaks in the IR spectrum. In the organic ligand region (1700-1200 cm^{-1}), no changes have been recorded up to 200°C, the pyromellitate

molecules maintaining the same coordination configuration during the experiment. This indicates that the coordination state of the uranyl center would decrease to six [$(UO)_2O_4$] since no change implying the creation of new U-O bonds of the pyromellitate linker is observed. In the region 3800-3300 cm^{-1}, corresponding to the O—H vibration of the water molecules, it can be observed that the coordinating water molecules are stable up to 200°C. At the end of the experiment, around 210°C, small changes begin to appear, the broad band centered at 3550 cm^{-1} beginning to decrease in intensity.

The thermogravimetric curve of **pyr2** $(NH_4)_2[(UO_2)(btec)]\cdot 4H_2O$ complex takes place in four steps. The first step has been assigned to the removal of free water molecules. The transformation begins at about 60°C and is finished at around 110°C. The weight loss measured on this step is of 11.9%, corresponding to the removal of four water molecules per formula unit (calculated value of 11.5%). This step is represented in the heat flow curve by a relatively intense endothermic peak centered at 95°C. In the thermodiffraction powder patterns (Figure IV.5.3), this step is correlated with two transformations. The first one occurs at 60°C with the formation of a transient dehydrated form of the phase. This form is stable up to 80°C, temperature at which it already passes into an amorphous phase. The latter persists up to 360°C, when the uranium oxide begins to crystallize. On this amorphous domain, no transformation could be observed by this technique. The second step on the thermogravimetric curve, measuring a weight loss of 9.0%, has been assigned to the removal of the two ammonium cations per formula unit. This process begins at 190°C and ends at about 330°C. The calculated weight loss for this step is only of 5.7%, the difference, up to 9% being attributed to an early, partial decomposition of the organic ligand. In the TD curve, this process is evidenced by a broad, low intensity, endothermic peak.

The third step, occurring between 340 and 440°C, has the highest weight loss of approximately 32.2% and corresponds to the burning of the organic part of the complex. The calculated weight loss for the total removal of the ligand molecules is 39.8%. The disagreement between the calculated and experimental weight loss values of this step has been attributed to two phenomena: the early

decomposition of the ligand in the second event and the partial degradation of the ligand in the third step, which would conduct to the formation of possible carbonate species. This step has been evidenced in the heat flow curve as an intense exothermic peak centered at 400°C and also in the thermodiffraction patterns diagram, where at 380°C the crystalline pattern of the final uranium oxide begins to appear.

The fourth step occurring between 500 and 650°C and measuring a weight loss of ~2% has been assigned to the total elimination of the organic part and to different processes of reorganization of the final oxide phase. These processes are taking place without a thermal effect and without observable changes in the PXRD patterns.

All four steps are summing a total weight loss of 55.1%, which is in good agreement with the calculated value of 55.3%, considering the U_3O_8 as final product. The final residue has been identified to be U_3O_8 (PDF No. 01-076-1850). The chemical equation for the degradation process is:

$$3(NH_4)_2[(UO_2)(C_{10}H_2O_8)] \cdot 4H_2O \xrightarrow[+22O_2\ -18H_2O\ -30CO_2\ -6NH_3]{\sim 600^\circ C} U_3O_8$$

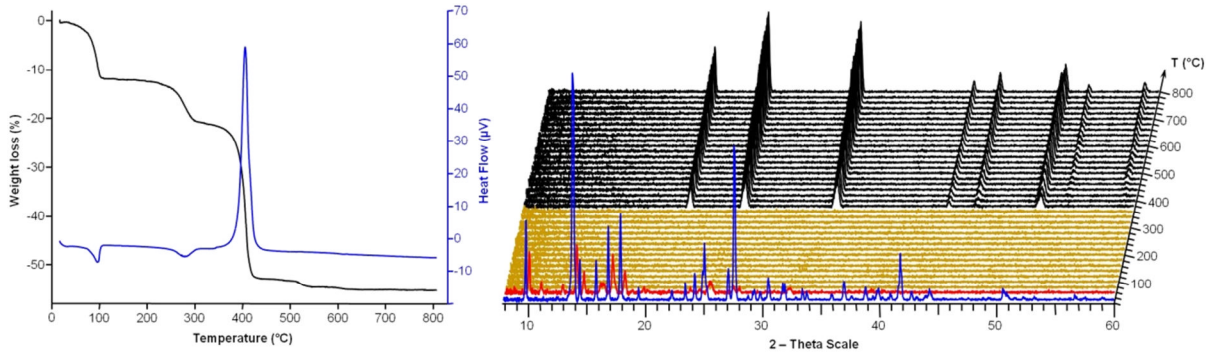

Figure IV.5.3 Thermal stability and thermal behavior of **pyr2** phase. TGA/TDA curves (left) and thermodiffraction patterns (right).

The *in situ* temperature IR experiment carried out **on pyr2** phase (Figure IV.5.4) shows that the changes with the temperature are consistent with the first step of degradation observed in the TG curve due to the loss of crystallization water. The dehydration phenomenon is observed in the 3600 - 3000 cm^{-1} region, where the two broad bands corresponding to the water O—H

vibrations are decreasing in intensity with the temperature and are completely extinguished at about 100°C.

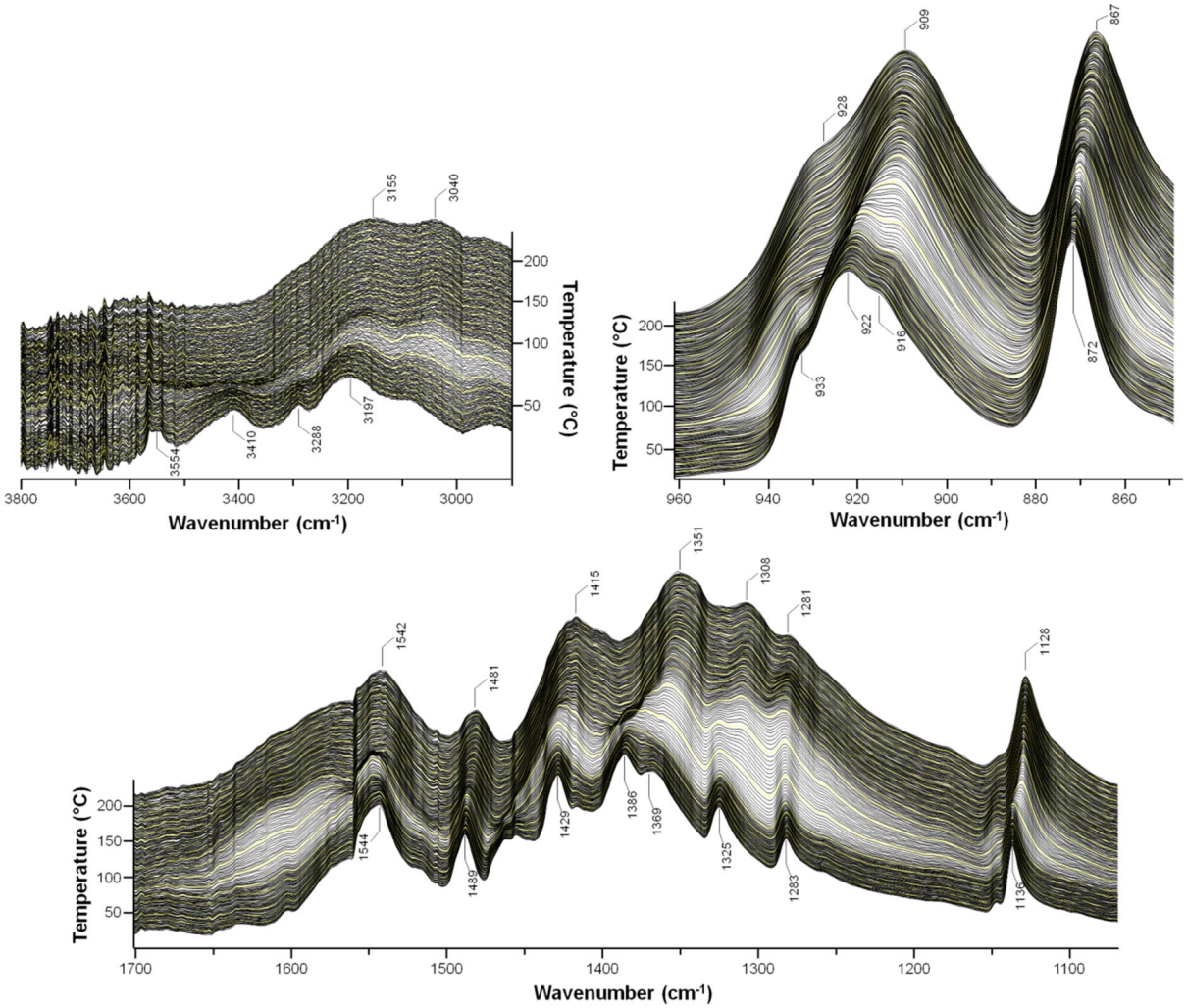

Figure IV.5.4 Temperature in situ IR spectra evolution for **pyr2** phase.

The water loss influences the uranyl bonds and also the ligand's conformation. The band corresponding to the uranyl bond vibration, containing at room temperature one main peak at 922 cm^{-1} and two shoulders on each side at 933 and 916 cm^{-1}, appears at 200°C as a main peak centered at 909 cm^{-1} and one shoulder at 926 cm^{-1}. Also in the 1700-1100 cm^{-1} region, where the vibrations corresponding to the organic linker give absorption, some shifts have been observed suggesting a change in the bond lengths and implicitly in the ligand's conformation in the structure. This change is compatible with the destruction of the crystalline edifice and the apparition of the amorphous phase observed in the thermodiffraction patterns diagram.

The **pyr7** phase $(NH_4)_4[(UO_2)_{12}O_4(OH)_8(btec)_3]\cdot 22H_2O$ presents a thermogravimetric curve showing three events (Figure IV.5.5). The first step occurring between 30 and 160°C has been assigned to the loss of the crystallization water molecules. Based on the quantity of residue (72.4%) remained after total degradation and identifying the residue as a U_3O_8 oxide phase, the water content removed in the first degradation step has been approximated at 22 molecules per formula unit (experimental weight loss of 9.0%, estimated 8.5). This dehydration process is also identified in the heat flow curve as a low intensity endothermic peak, centered at 130°C. In the thermodiffraction patterns diagram this process is observed late, at around 240°C and is indicated by a structural transition into an amorphous phase (absence of diffracted intensities). The second and the third decomposition steps have been assigned to the removal of the charge compensating ammonium cations and to the burning of the organic ligand respectively. The border between the second and the third decompositions steps is not well defined for the TG curve. The range of temperature where the two steps are taking place is 220-480°C, measuring a summed experimental weight loss of 18.6% (calculated: 17.6%), which corresponds to the total loss of ammonium cations and organic molecules from the compound. In the TD curve, the removal of ammonium cations is giving a very weak endothermic peak, almost indistinguishable, while the burning of the ligand molecules is giving an expected very intense exothermic peak. In the thermodiffraction diagram, a change occurs at 400°C showing the slow crystallization of the final oxide phase. The final oxide has been identified as U_3O_8 (PDF No 01-077-0144) at 800°C, stabilizing at room temperature into the α-U_3O_8 (PDF No 00-002-0276) form. The thermal degradation equation for the whole process is:

$$(NH_4)_4[(UO_2)_{12}O_4(OH)_8(C_{10}H_2O_8)_3]\cdot 23H_2O \xrightarrow[+O_2,\ -CO_2,\ -H_2O,\ -NH_3]{\sim 500^\circ C} 4U_3O_8$$

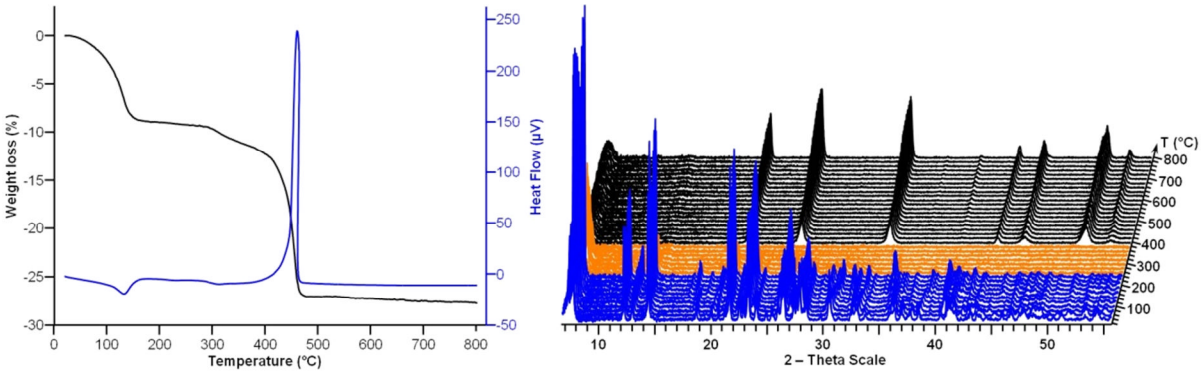

Figure IV.5.5 Thermal stability and thermal behavior of **pyr7** phase. TGA/TDA curves (left) and thermodiffraction patterns (right).

The *in situ* temperature IR spectroscopy experiment conducted on **pyr7** has shown only the transition corresponding to the first step of thermal degradation that consists in the removal of the crystallization water molecules.

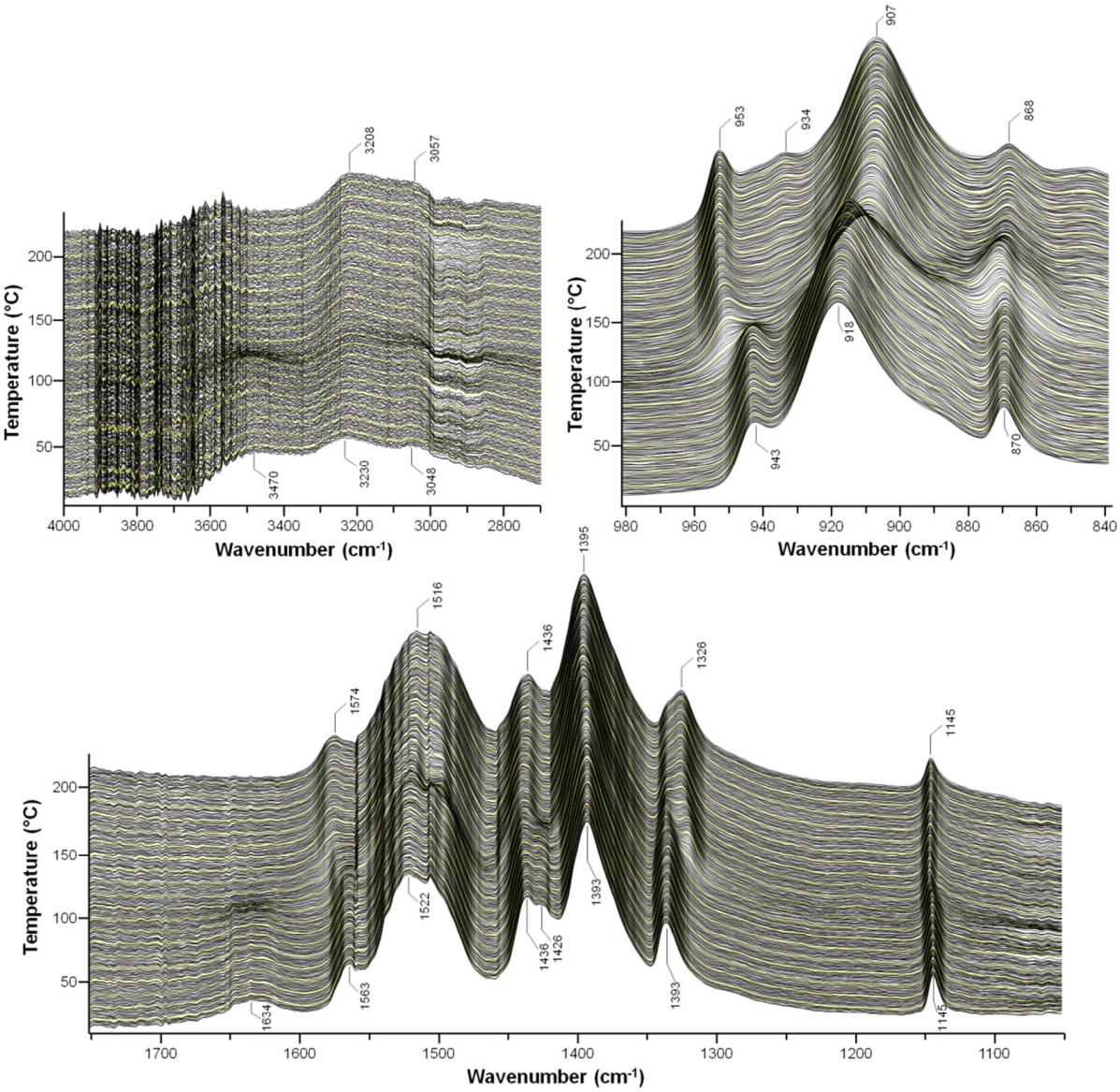

Figure IV.5.6 High temperature in situ IR spectra diagram for **pyr7** phase.

In the IR spectra this transition is observed at around 110°C and consists in the disappearing of the absorption bands corresponding to the stretching and the bending vibrations of the O—H bond of water molecules. These bands, at room temperature, have been identified at 3740 and 1634 cm^{-1} respectively. The removal of the water molecules from complex also has an influence on the bond vibrations of the organic ligand and also on the uranyl bond vibrations. Minor shifts of the IR absorption peaks in the region 1600 - 1300 are suggesting a small change in the ligand's molecule conformation but maintaining the same coordination type.

Conclusion

In this chapter there have been described and characterized 7 uranyl pyromellitate complexes, which are formed in aqueous medium after hydrothermal treatment. It revealed the wide diversity of connecting modes of this particular tetracarboxylate linker, offering the possibility of coordination via monodendate, bidendate, or chelating bridging types from four to eight uranyl centers. A previous work describing the room-temperature crystallization of the uranyl pyromellitate UO_2(btec)·$2H_2O$5ref (phase **A**) also reported the formation of a one-dimensional assembly composed of 8-fold coordinated uranyl cations linked through two carboxylate arms of the organic ligand (chelating mode). This example provided another illustration of the manner of connection of this tetracarboxylate. Depending on the reaction pH, on observe the occurrence of different inorganic building motifs [monomer (**pyr1**, **pyr2**, **pyr3** and **pyr4**), dimer (**pyr4**), trimer (**pyr5**), tetramer (**pyr6**) or infinite ribbon (**pyr7**)], which contributed to the richness of the crystal chemistry for the uranyl-organic assemblies. In fact, a new trinuclear unit with 8-fold coordinated uranium trans-connected to 7-fold coordinated uranium has been observed in compound **pyr5**. Moreover, the formation of a porous open-framework, containing large one-dimensional channel system for compound **pyr7** with such a tetratopic ligand is quite unexpected because we think that the relatively high number of carboxylate groups together with its possible rotations around the benzene plane might allow metal linkages

in many directions, which would induce the formation of rather complicated and compact three-dimensional networks as we observed in compounds **pyr1** and **pyr4**. In other structures, the connection via the oxo groups of the equatorial plane of the bipyramidal polyhedra is favoured the formation of lower-dimension networks such as compounds **pyr2**, **pyr3**, **pyr5**, **pyr6**, and $UO_2(H_2O)_2(H_2btec)\cdot 2H_2O$ (**A**) as well. Although it was suggested that the formation of a 3D framework could be favoured by using flexible aliphatic linkers[28, 29], we observed in compound **pyr7** the existence of a porous network via association of a rigid ligand (btec) together with straight infinite double chains of uranyl-centered polyhedra. It results in a unique architecture for hexavalent uranium based on one-dimensional channel systems with a potential free diameter of 8.2 Å × 8.6 Å. Fluorescence spectra of compounds **pyr1**, **pyr2**, **pyr7**, and $UO_2(H_2O)_2(btec)\cdot 2H_2O$[9] (**A**) indicate red-shifted emission bands for structures containing seven-fold coordinated uranyl centers and blue-shifted emission bands for structures containing eight-fold coordinated uranyl centers, compared to that of uranyl dinitrate hexahydrate.

Bibliography

1. Li, Y.; Zhang, Z. X.; Hong, P. Z.; Wua, Z. X.; Li, K. C., *Inorganic Chemistry Communications* **2008,** *11* (7), 761-764; Kumagai, H.; Chapman, K. W.; Kepert, C. J.; Kurmoo, M., *Polyhedron* **2003,** *22* (14-17), 1921-1927; Sanselme, M.; Greneche, J. M.; Riou-Cavellec, M.; Ferey, G., *Chemical Communications* **2002,** (18), 2172-2173; Zhang, L. J.; Xu, J. Q.; Shi, Z.; Xu, W.; Wang, T. G., *Dalton Transactions* **2003,** (6), 1148-1152.
2. Song, P.; Liu, B.; Li, Y. Q.; Yang, J. Z.; Wang, Z. M.; Li, X. G., *Crystengcomm* **2012,** *14* (6), 2296-2301; Huang, Q.; Diao, L. H.; Zhang, C.; Lei, F. H., *Inorganic Chemistry Communications* **2011,** *14* (12), 1889-1893; Jin, J.; Li, D.; Li, L.; Han, X.; Cong, S. M.; Chi, Y. X.; Niu, S. Y., *Inorganica Chimica Acta* **2011,** *379* (1), 44-55.
3. Sun, L. P.; Niu, S. Y.; Jin, J.; Yang, G. D.; Ye, L., *European Journal of Inorganic Chemistry* **2006,** (24), 5130-5137.
4. Shao, K. Z.; Zhao, Y. H.; Lan, Y. Q.; Wang, X. L.; Su, Z. M.; Wang, R. S., *Crystengcomm* **2011,** *13* (3), 889-896; Zhao, L. M.; Li, H. H.; Wu, Y.; Zhang, S. Y.; Zhang, Z. J.; Shi, W.; Cheng, P.; Liao, D. Z.; Yan, S. P., *European Journal of Inorganic Chemistry* **2010,** (13), 1983-1990.
5. Volkringer, C.; Loiseau, T.; Haouas, M.; Taulelle, F.; Popov, D.; Burghammer, M.; Riekel, C.; Zlotea, C.; Cuevas, F.; Latroche, M.; Phanon, D.; Knofelv, C.; Llewellyn, P. L.; Ferey, G., *Chemistry of Materials* **2009,** *21* (24), 5783-5791; Volkringer, C.; Loiseau, T.; Guillou, N.; Ferey, G.; Haouas, M.; Taulelle, F.; Elkaim, E.; Stock, N., *Inorganic Chemistry* **2010,** *49* (21), 9852-9862.
6. Hajjar, R.; Volkringer, C.; Loiseau, T.; Guillou, N.; Marrot, J.; Ferey, G.; Margiolaki, I.; Fink, G.; Morais, C.; Taulelle, F., *Chemistry of Materials* **2011,** *23* (1), 39-47.
7. Mazaj, M.; Volkringer, C.; Loiseau, T.; Kaucic, V.; Ferey, G., *Solid State Sciences* **2011,** *13* (8), 1488-1493; Han, Z. B.; Li, B. Y.; Ji, J. W.; Du, Y. E.; An, H. Y.; Zeng, M. H., *Dalton Transactions* **2011,** *40* (36), 9154-9158.
8. Guo, L.; Wu, G.; Li, H. H., *Journal of Chemical Crystallography* **2012,** *42* (3), 192-198; Hou, K. L.; Bai, F. Y.; Xing, Y. H.; Wang, J. L.; Shi, Z., *Crystengcomm* **2011,** *13* (11), 3884-3894; Zhang, H. B.; Tian, C. B.; Wu, S. T.; Lin, J. D.; Li, Z. H.; Du, S. W., *Journal of Molecular Structure* **2011,** *985* (2-3), 355-360.
9. Cousson, A.; Stout, B.; Nectoux, F.; Pages, M.; Gasperin, M., *Journal of the Less-Common Metals* **1986,** *125*, 111-115.
10. Jiang, Y. S.; Yu, Z. T.; Liao, Z. L.; Li, G. H.; Chen, J. S., *Polyhedron* **2006,** *25* (6), 1359-1366.
11. Yu, Z.-T.; Liao, Z.-L.; Jiang, Y.-S.; Li, G.-H.; Chen, J.-S., *Chemistry – A European Journal* **2005,** *11* (9), 2642-2650.
12. Nectoux, F.; Abazli, H.; Jove, J.; Cousson, A.; Pages, M.; Gasperin, M.; Choppin, G., *Journal of the Less-Common Metals* **1984,** *97* (FEB), 1-10.
13. Mihalcea, I.; Henry, N.; Volkringer, C.; Loiseau, T., *Crystal Growth & Design* **2012,** *12* (1), 526-535.

14. Burns, P. C.; Ewing, R. C.; Hawthorne, F. C., *Canadian Mineralogist* **1997,** *35*, 1551-1570.
15. Thuery, P., *Crystengcomm* **2008,** *10* (1), 79-85; Knope, K. E.; Cahill, C. L., *Inorganic Chemistry* **2009,** *48* (14), 6845-6851; Zhang, Y. J.; Collison, D.; Livens, F. R.; Helliwell, M.; Heatley, F.; Powell, A. K.; Wocadlo, S.; Eccles, H., *Polyhedron* **2002,** *21* (1), 81-96; Zhang, Y. J.; Livens, F. R.; Collison, D.; Helliwell, M.; Heatley, F.; Powell, A. K.; Wocadlo, S.; Eccles, H., *Polyhedron* **2002,** *21* (1), 69-79; Thuery, P.; Masci, B., *Crystal Growth & Design* **2010,** *10* (2), 716-725.
16. Knope, K. E.; Cahill, C. L., *Inorganic Chemistry* **2008,** *47* (17), 7660-7672.
17. Brese, N. E.; Okeeffe, M., *Acta Crystallographica Section B-Structural Science* **1991,** *47*, 192-197.
18. Thuery, P., *Crystal Growth & Design* **2011,** *11* (7), 3282-3294.
19. Thuery, P., *Crystal Growth & Design* **2011,** *11* (6), 2606-2620.
20. Borkowski, L. A.; Cahill, C. L., *Inorganic Chemistry* **2003,** *42* (22), 7041-7045; Rowland, C. E.; Cahill, C. L., *Inorganic Chemistry* **2010,** *49* (19), 8668-8673; Liao, Z. L.; Li, G. D.; Wei, X. A.; Yu, Y.; Chen, J. S., *European Journal of Inorganic Chemistry* **2010,** (24), 3780-3788; Thuery, P.; Masci, B., *Crystal Growth & Design* **2008,** *8* (9), 3430-3436; Mihalcea, I.; Henry, N.; Clavier, N.; Dacheux, N.; Loiseau, T., *Inorganic Chemistry* **2011,** *50* (13), 6243-6249; Thuery, P., *Chemical Communications* **2006,** (8), 853-855; Masci, B.; Thuery, P., *Crystengcomm* **2008,** *10* (8), 1082-1087.
21. Wu, H.-Y.; Wang, R.-X.; Yang, W.; Chen, J.; Sun, Z.-M.; Li, J.; Zhang, H., *Inorganic Chemistry* **2012,** *51* (5), 3103-3107.
22. Ni, Z.; Masel, R. I., *Journal of the American Chemical Society* **2006,** *128* (38), 12394-12395; Haque, E.; Khan, N. A.; Park, J. H.; Jhung, S. H., *Chemistry-a European Journal* **2010,** *16* (3), 1046-1052; Klinowski, J.; Paz, F. A. A.; Silva, P.; Rocha, J., *Dalton Transactions* **2011,** *40* (2), 321-330.
23. Eriksson, A.; Lindgren, J., *Journal of Molecular Structure* **1978,** *48* (3), 417-430.
24. Diniz, R.; De Abreu, H. A.; De Almeida, W. B.; Fernandes, N. G.; Sansiviero, M. T. C., *Spectrochimica Acta Part a-Molecular and Biomolecular Spectroscopy* **2005,** *61* (8), 1747-1757.
25. Kuppusamy, K.; Sivasankar, B. N.; Govindarajan, S., *Thermochimica Acta* **1996,** *274*, 139-148; Tellez, C.; Gomez, J.; Mondragon, M. A.; Castano, V. M.; Mena, G., *Vibrational Spectroscopy* **1995,** *9* (3), 279-285.
26. Bartlett, J. R.; Cooney, R. P., *Journal of Molecular Structure* **1989,** *193*, 295-300.
27. Taylor, J. C.; Mueller, M. H., *Acta Crystallographica* **1965,** *19*, 536-&.
28. Borkowski, L. A.; Cahill, C. L., *Crystal Growth & Design* **2006,** *6* (10), 2241-2247; Borkowski, L. A.; Cahill, C. L., *Crystal Growth & Design* **2006,** *6* (10), 2248-2259.
29. Kerr, A. T.; Cahill, C. L., *Crystal Growth & Design* **2011,** *11* (12), 5634-5641.

Chapter V
Six-fold coordinated uranyl cations

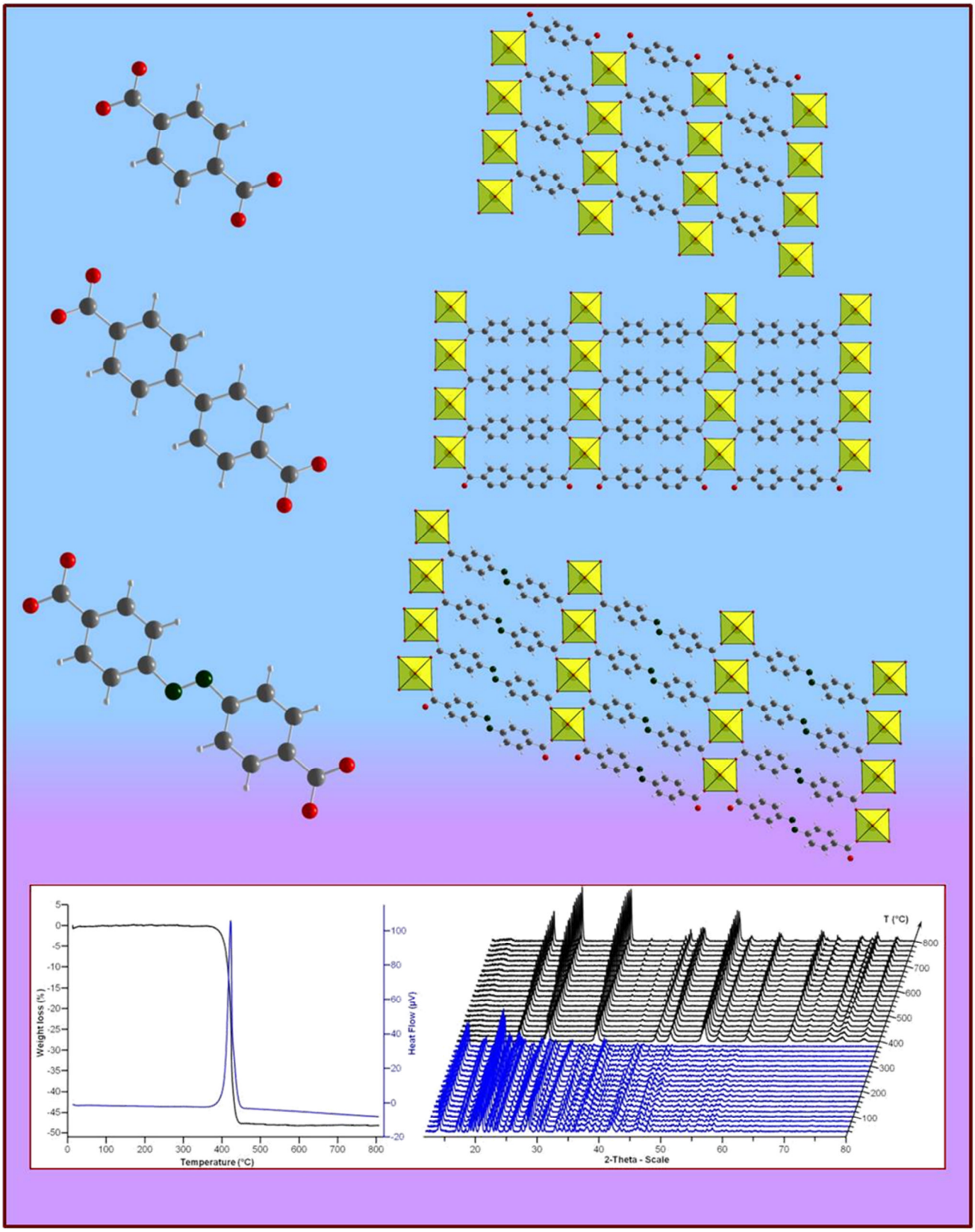

Chapter V Six-fold coordinated uranyl cations

V.1 . Introduction

Using different aromatic dicarboxylic acid molecules in complexation of uranyl cations it has been observed that those having the carboxylate groups disposed in opposite positions (*para*) have a preference to form specific complexes containing layered extended assemblies and possessing as SBU monomeric six-fold coordinated uranyl species. In this chapter there are described three of this type of complexes $[UO_2(tpa)]$ **ter1**, $[UO_2(bpd)]$ **bpd1**, $[UO_2(adc)]$ **adc1**[1], containing terephthalate, 4,4'-biphenyldicarboxylate and respectively 4,4'-azobenzene-dicarboxylate rigid organic molecules (Figure V.1.1).

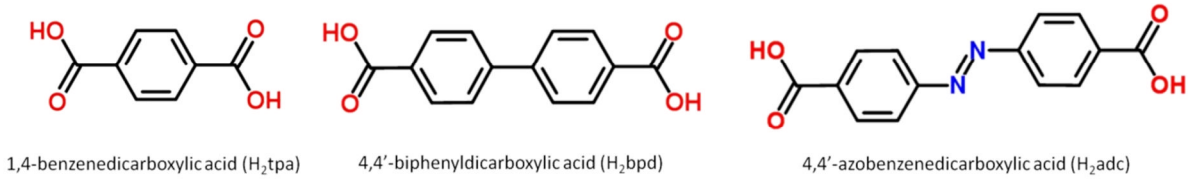

Figure V.1.1 Representation of the three ditopic organic ligand molecules used in the synthesis of the specific six-fold coordinated uranyl complexes.

The first complex **ter1** has been synthesized using the terephthalic acid as organic linker. This ligand has been previously used for the construction of many highly porous metal organic framework type compounds, such as MOF-5[2] or MIL-101[3], and also has been previously reported in an uranyl-organic framework.[4] Also terephthalate derivatives such as 2-bromo- or 2-nitroterephthalic acid have been used in combination with the uranyl ion in the construction of coordination polymers[4, 5]. The other two complexes **bpd1** and **adc1** have been synthesized using derivatives of the terephthalic acid, both maintaining the two specific properties: the molecule rigidity and the opposite positions of the two carboxylate groups. Crystal data of the three complexes are given in

Table V.1.1.

Table V.1.1 Crystal and refinement data for the six-fold coordinated uranyl carboxylate complexes.

Parameter*	ter1	bpd1	adc1
crystal system	triclinic	monoclinic	triclinic
space group	*P*-1	*C*2/*m*	*P*-1
a/Å	5.1144(2)	9.0105(2)	5.137(1)

Parameter*	ter1	bpd1	adc1
b/Å	5.5731(2)	14.4741(3)	5.611(1)
c/Å	8.4717(3)	5.3067(1)	12.944(2)
α/deg	90.004(2)	90	95.95(1)
ß/deg	94.397(2)	103.364(1)	90.63(1)
γ/deg	107.984(2)	90	107.04(1)
volume/Å^3	228.92(2)	673.35(2)	354.4(1)
Z, ρ_{calc}/g·cm^{-3}	1, 3.149	2, 2.517	1, 2.522
final *R* indices [$I > 2\sigma(I)$]	R1 = 0.0147 wR2 = 0.0276	R1 = 0.0219 wR2 = 0.0461	R1 = 0.0188 wR2 = 0.0450
R indices (all data)	R1 = 0.0148 wR2 = 0.0277	R1 = 0.0231 wR2 = 0.0466	R1 = 0.0188 wR2 = 0.0450

* - a complete crystal and refinement data table is given in the supplementary data chapter (table VIII.4.1)

V.2 . Structures description

The structure of **ter1** ([UO_2(tpa)]) complex possesses one unique crystallographic site for the uranium atom, situated on a *1a* (0,0,0) special position. The coordination sphere around the uranium atom (Figure V.2.1) is formed by six oxygen atoms. Two of them (O2 and its symmetry equivalent) are situated in axial position and have a typical shorter U=O bond of 1.765(1) Å with an expected O=U=O angle of 180.0°. The other four oxygen atoms (O1, O3 and their symmetry equivalents) are situated in the equatorial plane at distances of 2.326(1) and 2.289(1) Å respectively from the uranium atom and form the square base of the bipyramid. All four oxygen atoms in the equatorial plane are carboxyl type belonging to the ligand's molecules. Both carboxylate arms of the ligand are each bidentate bridge between two distinct uranyl polyhedra, giving a final μ_4-η_1:η_1:η_1:η_1 coordination configuration.

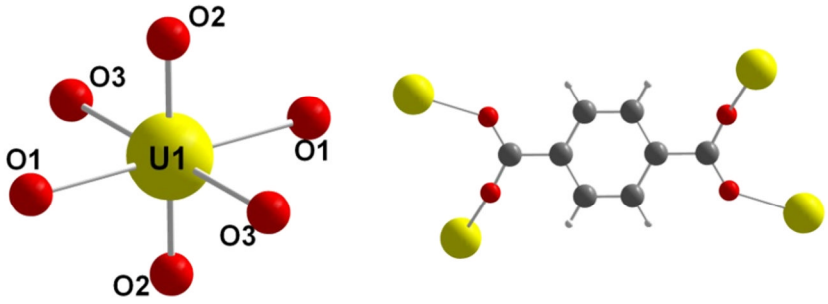

Figure V.2.1 Representation of the coordination sphere around the uranium atom (left) and of the ligand's coordination configuration (right) for the **ter1** complex.

Each ligand molecule binds together four inorganic blocks almost in the same plane, resulting in neutral infinite polymeric layers. Each layer contains

alternating organic (ligand molecules) and inorganic (uranyl polyhedra) rows orientated parallel with the (100) direction (Figure V.2.2).

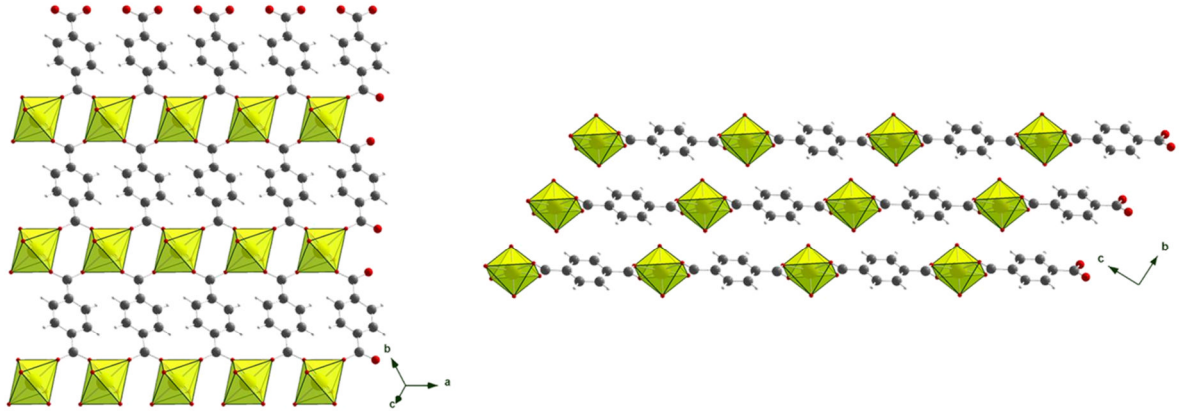

Figure V.2.2 Structure representation of **ter1** complex. View along the (111) (left) and the (100) (right) directions.

The structure of **bpd1** ([UO_2(bpd)]) also presents an unique crystallographic site for the uranium atom, situated on a *2b* (0 ½ 0) special position. The polyhedron formed around the uranium atom is similar to the one of **ter1** complex, with two uranyl oxygen atoms (O2 and its symmetry equivalent) in apical position with a U=O bond of 1.749(4) Å and an expected O=U=O angle of 180° and other four carboxyl oxygen atoms (O1 and its other three symmetry equivalents) in the equatorial plane with a U–O bond length of 2.287(3) Å (Figure V.2.3).

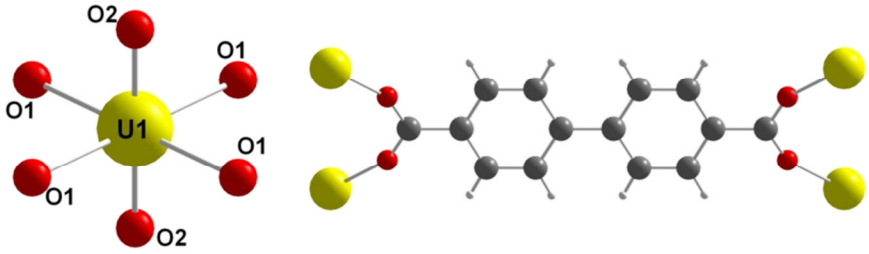

Figure V.2.3 Representation of the coordination sphere around the uranium atom (left) and of the ligand's coordination configuration (right) for the **bpd1** complex.

Each carboxylate arms of the ligand bridges with a bidentate mode two distinct uranyl polyhedra, conferring, like in the **ter1** case a μ_4-η_1:η_1:η_1;η_1 coordination configuration for the organic linker. This type of bonding generates neutral infinite polymeric bidimensional layers stacking along the (100) direction (Figure V.2.4). Each layer presents alternating inorganic and organic rows orientated parallel to the (001) direction.

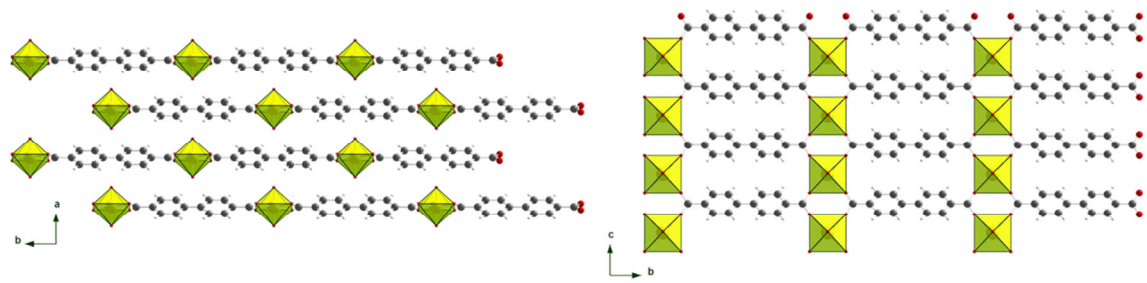

Figure V.2.4 Structure representation of **bpd1** complex. View along the (001) (left) and the (100) (right) directions.

The structure of **adc1**[UO_2(adc)] complex contains its unique crystallographic site of the uranium atom on a *1h* (½ ½ ½) special position. The polyhedron around the uranium atom (Figure V.2.5) is formed by two uranyl oxygen atoms (O1 and its symmetry equivalent) with a U═O bond of 1.752(3) Å and a O═U═O angle of 180.0° and, as expected, four carboxyl type oxygen atoms (O2, O3 and their symmetry equivalents) forming the square base of the bipyramid. The U─O bond lengths are of 2.330(3) and 2.282(3) Å for O2 and O3, respectively.

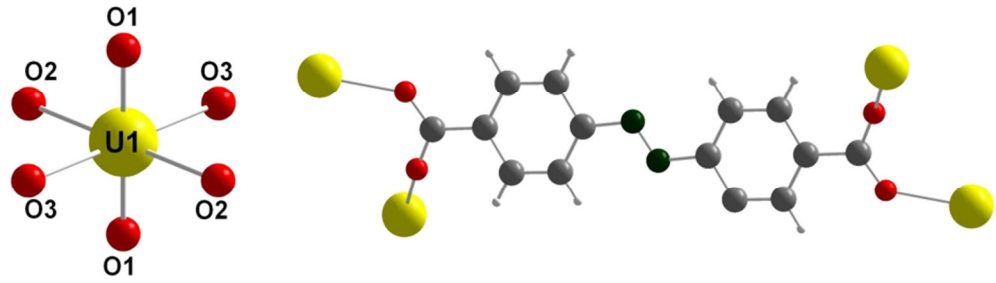

Figure V.2.5 Representation of the coordination sphere around the uranium atom (left) and of the ligand's coordination configuration (right) for the **adc1** complex.

The ligand molecules adopt the μ_4-η_1:η_1:η_1;η_1 coordination configuration, forming the expected bidimensional polymeric layers, in which the ligand's molecules and the uranyl polyhedra are disposed in alternating parallel rows orientated, in this case, along the (100) direction (Figure V.2.6).

From the structural point of view the three complexes possess many common features, such as the six fold coordinated uranyl polyhedra, the μ_4-η_1:η_1:η_1;η_1 coordination configuration respected by the organic ligand, the bidimensional expansion of the structure, creating neutral layers with parallel organic-inorganic pavement.

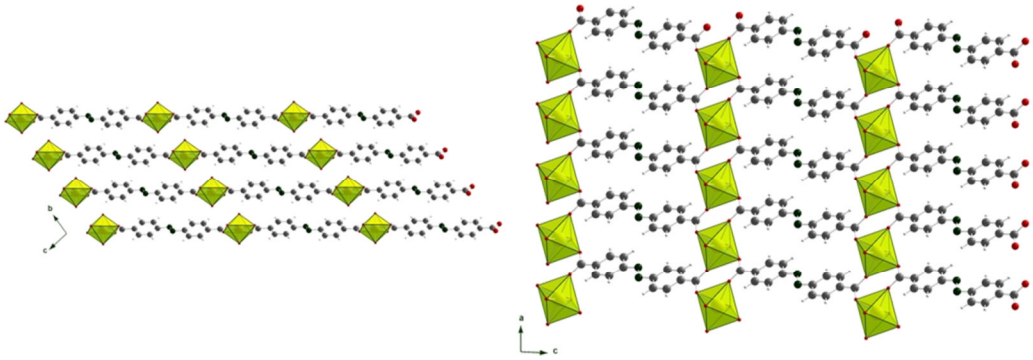

Figure V.2.6 Structure representation of **adc1** complex. View along the (100) (left) and the (010) (right) directions.

Six-fold coordinated uranyl cations are rarely reported in UOF-type coordination complexes involving carboxylate ligands since pentagonal or hexagonal bipyramidal environments are the most commonly encountered cases. Nevertheless, this state of coordination is well-defined in the crystal chemistry of purely inorganic oxide-based solids bearing hexavalent uranium and reported several times in dense phases. It is interesting to notice that such a surrounding was previously reported in very few complexes. A first illustration is found in the uranyl benzoate $UO_2(box)_2$ described by Cousson et al. in 1990[6] and exhibits a chain-like assembly. A second example is reported in a uranyl dicarboxylate involving the 3,3'-dithiobisbenzoate group ($UO_2(mddb)_4$)[7], with a 1D network. In this phase, the ligand is closely related to the 4,4'-azobenzenedicarboxylate used for the formation of **adc1**, with the double nitrogen bonding N=N replaced by the sulfur bonding S=S. The positions of the carboxylate arms (4,4'- and 3,3'-) also differ and induce a V-shape conformation for the dithio-based ligand. The latter generates a unidimensional structure instead of a bidimensional one for **adc1**. It was also described in the uranyl isophthalate series studied in this work (see chapter III, phase **iso1**). In other complexes, this type of square bipyramidal moiety is encountered in heterometallic assemblies with copper ($UO_2Cu(pmdc)_2(H_2O)_2$)[8] involving the 3,5-pyrazoledicarboxylate (pmdc) linker (2D network) or lanthanide ($[(UO_2)_2Ln(OH)(H_2O)_3(mel)]\cdot 2.5H_2O$[9]; Ln = Ce or Nd) with the mellitate (mel) linker (3D network). The last example is related to uranyl cations interacting with a 2,2-dinitro derived 4,4'-biphenyldicarboxylate (onppc) ligand in the complex $[(UO_2)_2U(OH)_4(H_2O)(onppc)_3]\cdot 5H_2O$[10]. The positions of nitro groups attached to each benzene ring of the onppc molecule induce a torsion of the

organic ligands, which resulted in the formation of a three-dimensional framework instead of the layered network exhibited by the **bpd1** phase (involving the nonfunctionalized 4,4'-biphenyldicarboxylate).

In these different coordination complexes, it is noteworthy to observe that the 6-fold coordinated uranyl cations are occurring as monomeric building unit only. The second feature is the implication of aromatic ditopic carboxylate molecules as linker between the uranyl centers (except for the phase based on the hexadentate mellitate[9] molecule). To our knowledge, this type of coordination was not found in complexes with aliphatic carboxylates. Nevertheless, 6-fold coordinated uranyl species were found in a larger oligomer containing six metallic centers, surrounded by other types of O-donor ligands such as the p-benzylcalix[7]arene (H_7L) in $[(UO_2)_6(L)_2(O)_2(Hdabco)_6]\cdot 3CH_3CN\cdot CHCl_3\cdot 5CH_3OH\cdot 3H_2O$[11].

V.3 . Synthesis

The **ter1**, **bpd1** and **adc1** complexes have been synthesized hydrothermally under autogenous pressure using 23 mL Teflon-lined Parr type autoclaves. The starting reagents have been: uranyl nitrate hexahydrate ($UO_2(NO_3)_2\cdot 6H_2O$, Merk 98%), terephthalic acid (1,4-benzene dicarboxylic acid noted H_2tpa, Aldrich 98%), 4,4'-biphenyl dicarboxylic acid (noted H_2bpd, Aldrich 97%), 4,4'-azobenzene-dicarboxylic acid (noted H_2adc), ammonium hydroxide solution (NH_4OH, Prolabo 28%) and deionized water. All reagents are commercially available (except H_2adc) and have been used without further purification. The 4,4'-azobenzenedicarboxylic acid was prepared by Dr T. Bousquet (UCCS) following a synthetic procedure previously described in literature[12].

The **ter1** [$UO_2(tpa)$] complex has been obtained pure by statically heating at 200°C under hydrothermal conditions during 24 h a mixture of 0.503 g (1 mmol) $UO_2(NO_3)_2\cdot 6H_2O$, 0.083 g (0.5 mmol) terephthalic acid, 0.8 mL solution 2M (1.6 mmol) NH_4OH and 4.2 mL (233 mmol) deionized water. The solution pH after the reaction was 2.6. The resulting yellow product has been filtered off, washed with water and then dried at room temperature.

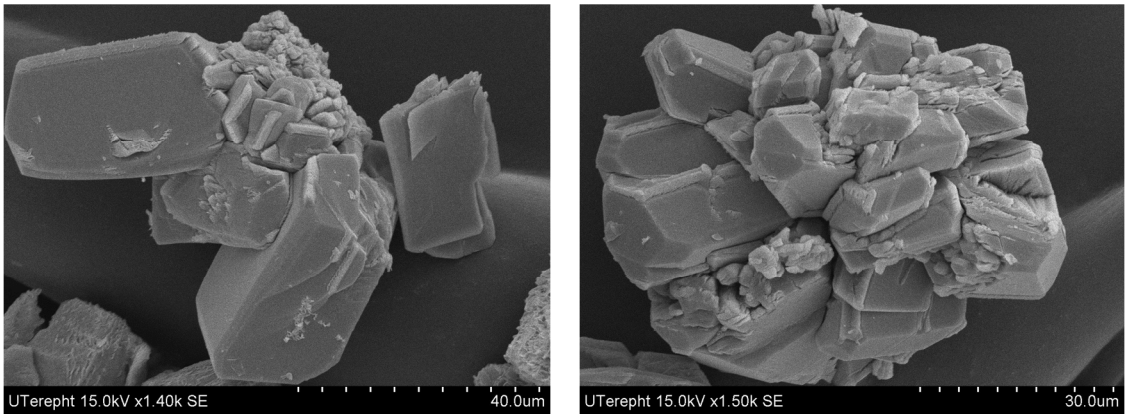

Figure V.3.1 SEM photographs of the **ter1** phase.

SEM pictures taken of this product showed conglomerates of parallelepiped shaped crystallites of 10 to 20 μm in size (Figure V.3.1). This phase has been obtained over the 2.0 to 3.4 range of pH by varying the NH_4OH concentration.

The **bpd1** [UO_2(bpd)] complex has been obtained pure by statically heating at 200°C under hydrothermal conditions during 24 h a mixture of 0.503 g (1 mmol) $UO_2(NO_3)_2 \cdot 6H_2O$, 0.121 g (0.5 mmol) 4,4'-biphenyl dicarboxylic acid, 0.6 mL solution 2M (1.2 mmol) NH_4OH and 4.4 mL (244 mmol) deionized water. The solution pH after the reaction was 2.6. The resulting yellow product has been filtered off, washed with water and then dried at room temperature. SEM pictures of this preparation showed undefined shaped crystals of 50 to 200 μm in size (Figure V.3.2). This phase has been obtained over the 2.6 to 3.1 range of pH by varying the base concentration in reaction.

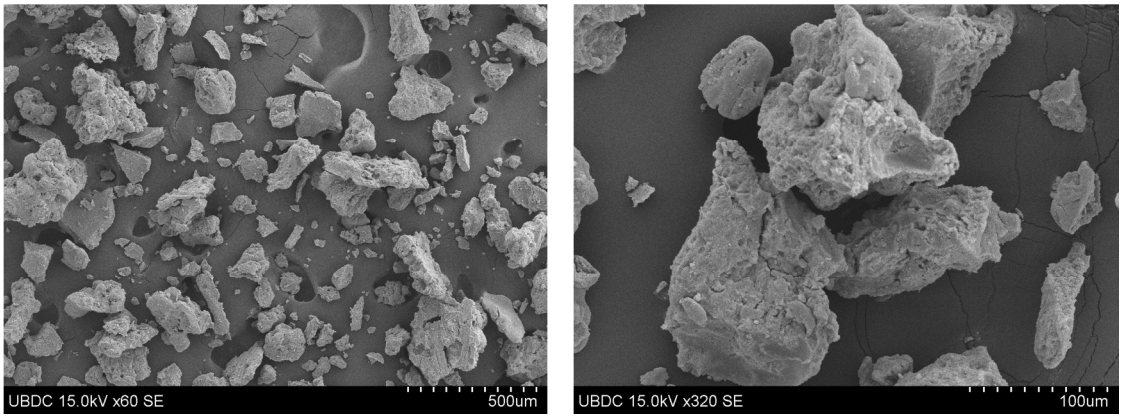

Figure V.3.2 SEM photographs of **bpd1** phase.

The **adc1** [UO2(adc)] complex has been obtained pure by statically heating at 200°C under hydrothermal conditions during 24 h a mixture of 0.503 g (1 mmol) $UO_2(NO_3)_2 \cdot 6H_2O$, 0.139 g (0.5 mmol) 4,4'-azobenzenedicarboxylic acid, 0.6 mL solution 2M (1.2 mmol) NH_4OH and 4.4 mL (244 mmol) deionized water. The solution pH after the reaction was 2.3. The resulting yellow product has been filtered off, washed with water and then dried at room temperature. SEM pictures of this preparation showed typical needlelike crystals of 5 to 10 μm in size (Figure V.3.3). This phase has been obtained over the 2.3 to 3.2 range of pH by varying the base concentration in reaction.

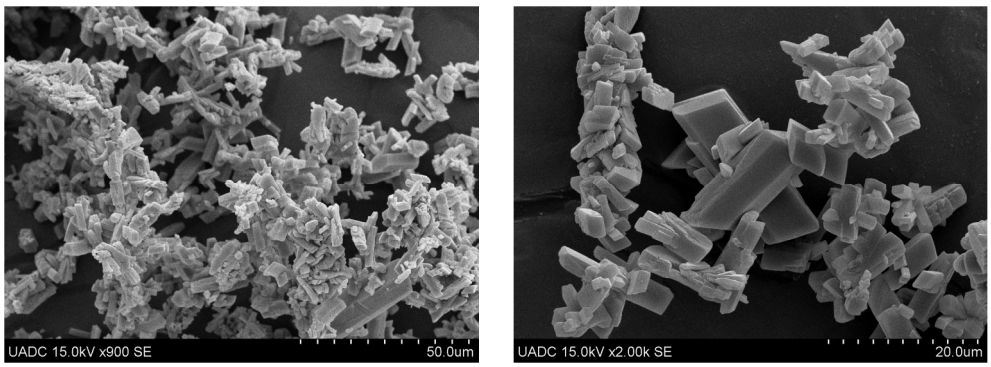

Figure V.3.3 SEM photographs of **adc1** phase.

V.4 . Thermal characterization

The thermogravimetric analyzes were conducted under air with a heating rate of 1°C/min. The thermodiffraction experiments were also conducted under air, with a heating rate of 5°C/min, one PXRD pattern being recorded at each 20°C. All three six fold coordinated uranyl carboxylates present a one step thermal degradation process that corresponds to the burning of the organic linker.

For **ter1** [UO_2(tpa)] the burning process is evidenced in the TG curve (Figure V.4.1-left) as a weight loss of 36.3%, which is in good agreement with the calculated one of 35.4% using the equation below:

$$3[UO_2(C_8H_4O_4)] \xrightarrow[-6H_2O\ -24CO_2]{380°C\ +22O_2} U_3O_8.$$

This process is observed in the TG curve between 360°C and 510°C and the TD curve shows an exothermic peak centered at 430°C. The thermodiffraction patterns diagram (Figure V.4.1-right) indicates a direct structural transition

from the PXRD pattern of the initial phase to the pattern of the final oxide at 380°C. The residue after the thermal decomposition of the **ter1** phase has been identified as α'-U_3O_8 (PDF No: 031-1425) at 800°C, this oxide passing into a form α-U_3O_8 (PDF No: 031-1424) by cooling down to room temperature.

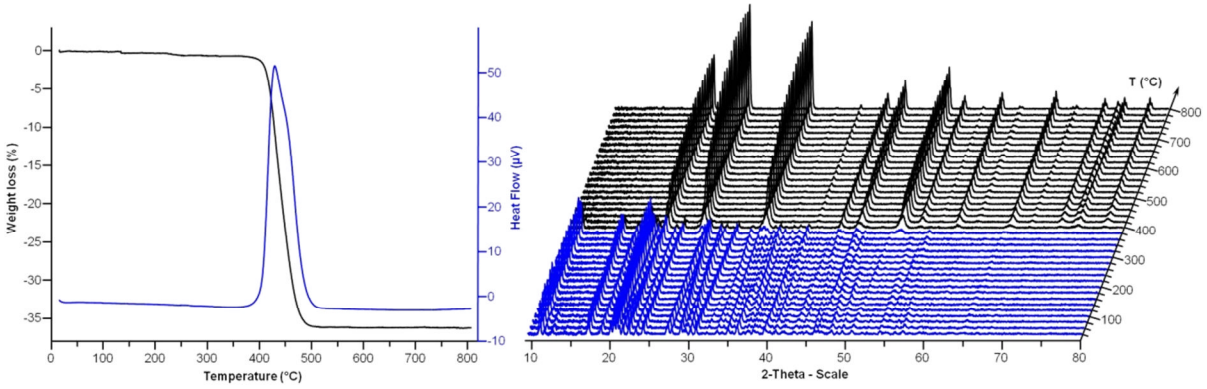

Figure V.4.1 Thermal behavior and thermal stability of phase **ter1**. TG/TD curves (left), X-ray thermodiffraction patterns (right).

For the **bpd1** [UO_2(bpd)] phase the thermal degradation process begins at 365°C and ends at 450°C. This process is represented in the TG curve (Figure V.4.2-left) as a weight loss of 44.9%, in good agreement with the calculated one of 45.0% using the equation:

$$3[UO_2(C_{14}H_8O_4)] \xrightarrow[-42CO_2\ -12H_2O]{360°C\ +43O_2} U_3O_8.$$

The degradation process is also evidenced in the heat flow curve by an exothermic peak centered at 430°C. The thermodiffraction patterns diagram (Figure V.4.2-right) indicates a direct transition from the PXRD pattern of the initial phase to the pattern of the final oxide. The residue has been identified as U_3O_8 (PDF No. 074-0562) at 800°C.

The thermal degradation process of the **adc1** [UO_2(adc)] phase begins at 360°C and ends at 450°C. This process records in the TG curve a weight loss of 48.3%, which is in good agreement with the calculated one of 47.9% based on the equation below:

$$3[UO_2(C_{14}H_8O_4N_2)] \xrightarrow[-42CO_2\ -12H_2O\ -3N_2]{360°C\ +43O_2} U_3O_8$$

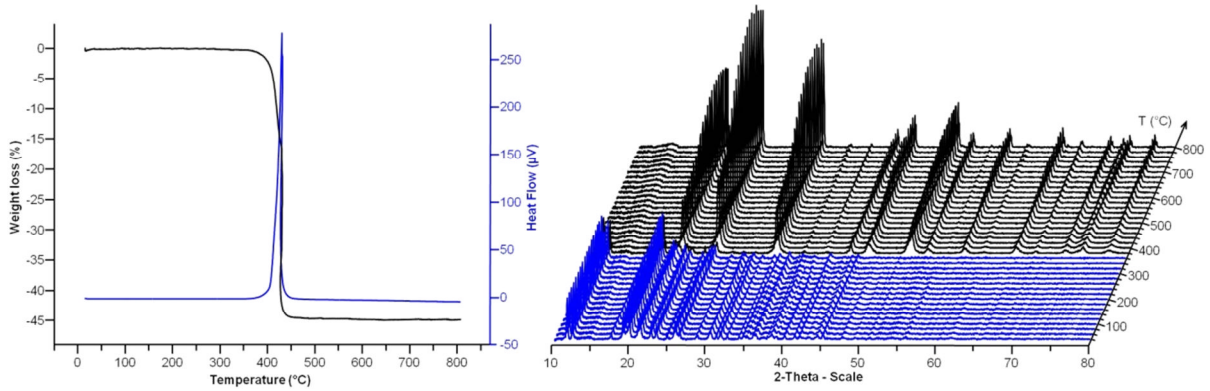

Figure V.4.2 Thermal behavior and thermal stability of phase **bpd1**. TG/TD curves (left), X-ray thermodiffraction patterns (right).

This process is well observed also in the TD curve as an exothermic peak centered at 420°C together with a structural transition from the PXRD pattern of the initial phase to the pattern of the final oxide in the thermodiffraction patterns. The residue after degradation has been identified as U_3O_8 (PDF No: 074-0562) at 800°C.

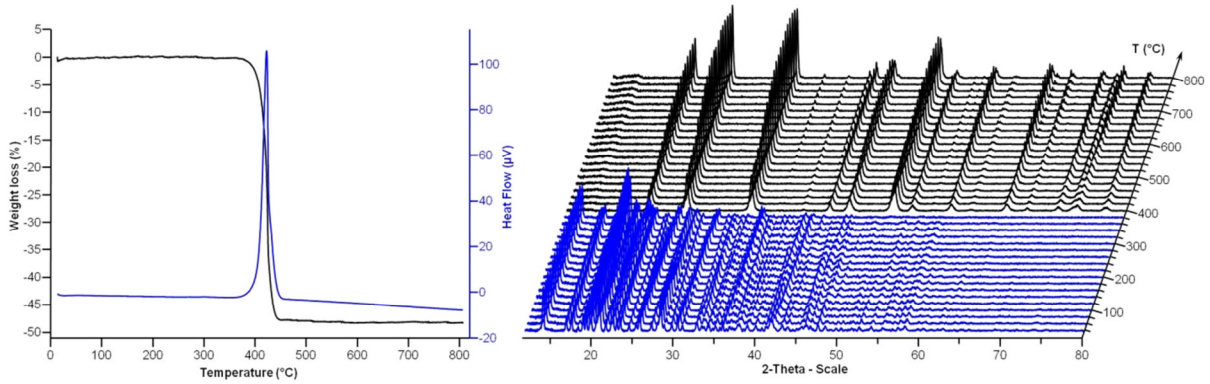

Figure V.4.3 Thermal behavior and thermal stability of phase **adc1**. TG/TD curves (left), X-ray thermodiffraction patterns (right).

The *in situ* evolution of the XRD powder patterns as a function of temperature was identical for the three compounds (also similar to **iso1**). The Bragg peaks of the different phases were visible up to 360 °C for **bpd1**, 380 °C for **ter1** and **adc1**, indicating their relative good thermal stability. Above these temperatures, the structural collapse was observed being immediately followed by the crystallization of the U_3O_8 uranium oxide. This structural transformation differed from those of other uranyl polycarboxylates, which have been previously characterized by XRD thermodiffraction. For instance, the uranyl phthalates[13] (**pht1** - **pht4**), pyromellitates[14] (**pyr1**, **pyr2** and **pyr7**) or mellitates[9] were decomposed at lower temperatures or sometimes transformed into a transient

phase, followed by the occurrence of amorphous phase, which then crystallized in uranium oxide U_3O_8 at temperature close to 400 °C. For the present study, it seems that the uranyl-organic networks based on 6-fold coordinated uranyl centers were quite thermally stable compared to the others, for which one of their structural features was the existence of 7- or 8-fold coordinated uranyl centers. This would be due to the nature of additional coordinating ligands around the uranyl (hydroxo or aquo groups), which may undergo dehydroxylation or dehydration transformations upon heating, which results in the formation of intermediate or structural decomposition before 400 °C. For the present phases, the temperature of decomposition of the organic part matched well with that of the crystallization of U_3O_8.

V.5 . Spectroscopic characterization

Infrared spectroscopy

The IR spectra of the three phases **ter1**, **bpd1** and **adc1** (Figure V.5.1) show no absorption maxima in the region above 1700 cm^{-1} confirming the absence of water molecules in the structure.

The ligand related vibrations give IR absorption peaks in the region 1600-1000 cm^{-1}, where the most intense are those corresponding to the carboxylate groups $\nu_{asym}(COO)$ at 1504, 1480, 1491 cm^{-1} and the $\nu_{sym}(COO)$ at 1377, 1404 and 1403 cm^{-1} for the **ter1**, **bdc1** and **adc1** complexes, respectively. The other ligand related vibrations give low intensity absorption peaks and could not be accurately attributed.

The vibration corresponding to the uranium-oxygen bonds give peaks below 1000 cm^{-1}, from which the most intense are located at 904, 936 and 934 cm^{-1} for the compounds **ter1**, **bpd1** and **adc1**, respectively. These maxima have been assigned to the ν_3 asymmetrical vibration of the U=O uranyl bond.

The position of the IR absorption maximum corresponding to the ν_3 uranyl vibration gives information about the length of the uranyl bond. Using the empirical equation $d\,(U-O)(pm) = 9141[\nu_3(cm^{-1})]^{-2/3} + 80.4$ [15], there have been found uranyl bond lengths of 1.782, 1.759 and 1.761 Å for **ter1**, **bdc1** and **adc1**,

respectively. The calculated values are in agreement with the values obtained from the structure determination by single crystal X-ray diffraction technique of 1.765(1), 1.749(2) and 1.752(1) Å, respectively.

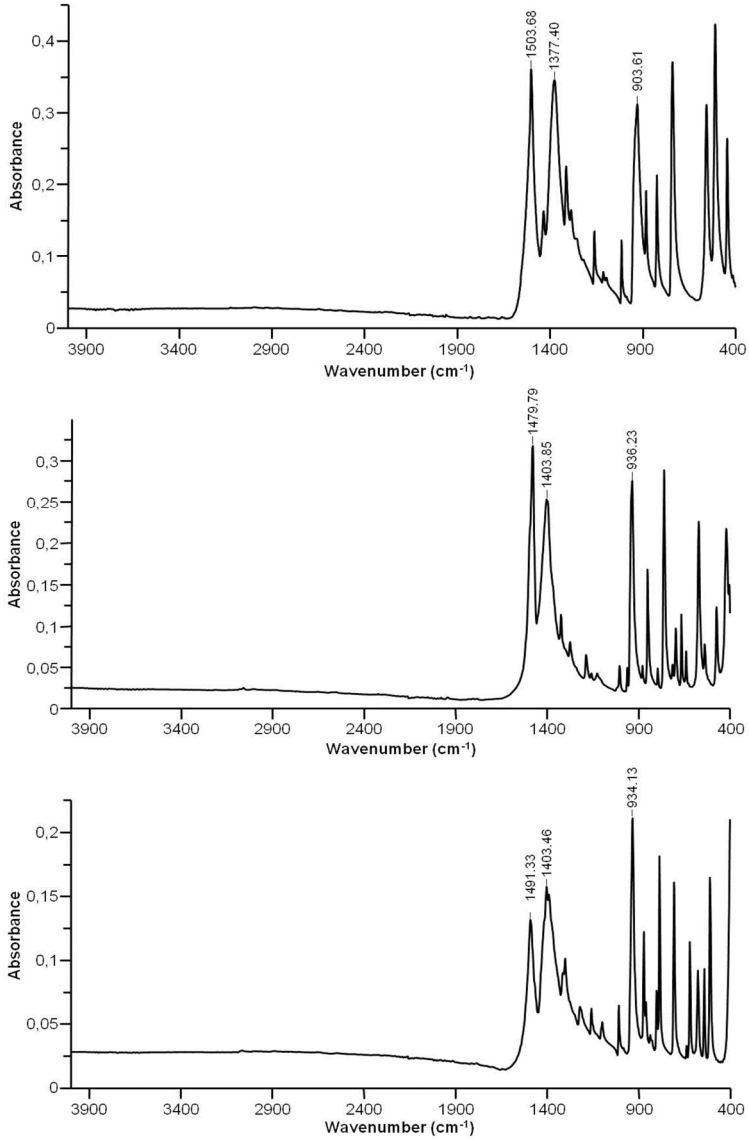

Figure V.5.1 IR spectra of the **ter1** phase (top), **bpd1** phase (middle), and **adc1** phase (bottom).

Fluorescence spectroscopy

The solid state fluorescence spectroscopic analyzes were conducted at room temperature. Each spectrum was measured in the 440-640 nm range under excitation at the wavelength of 365 nm.

The solid state emission spectrum of **ter1** (Figure V.5.2) presents the same electronic transitions (specific to the uranyl ion) as the reference compound (uranyl nitrate hexahydrate) but with a red shift of 12.2 nm (average).

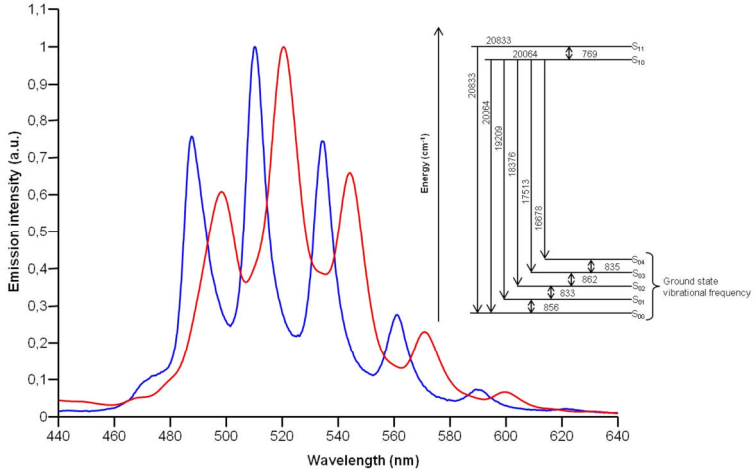

Figure V.5.2 Solid state emission spectra (left) of **ter1** (red), of uranyl nitrate hexahydrate (blue) and the electronic and vibronic transitions of **ter1** (right).

As expected the band spacing between the $S_{11}\rightarrow S_{00}$ and the $S_{10}\rightarrow S_{00}$ transitions is about 769 cm^{-1} and those between $S_{10}\rightarrow S_{0v}$ and $S_{10}\rightarrow S_{0(v+1)}$ (v = 0-3) have a value ranging from 833 to 862 cm^{-1}. The transitions $S_{04}\rightarrow S_{0v}$ (v = 0-3) are vibration transitions, including the $S_{0v}\rightarrow S_{0(v-1)}$ (v = 1-4) ones, which are directly related with the double uranyl bond specific symmetric vibrations observed in Raman spectroscopy. The fluorescence data values for **ter1** complex are summarized and compared with the ones of uranyl nitrate hexahydrate in Table V.5.1.

Table V.5.1 Fluorescence bands of uranyl dinitrate hexahydrate and ter1 complex.

Uranyl dinitrate hexahydrate			ter1		
λ (nm)	$\tilde{\nu}$ (cm^{-1})	$\Delta\tilde{\nu}$ (cm^{-1})	λ (nm)	$\tilde{\nu}$ (cm^{-1})	$\Delta\tilde{\nu}$ (cm^{-1})
469,16	21315		480.0	20833	
485,88	20581	733	498.4	20064	769
507,98	19686	895	520.6	19209	856
531,53	18814	872	544.2	18376	833
557,36	17942	872	571.0	17513	862
585,71	17073	868	599.6	16678	835

The solid state fluorescence emission spectrum (Figure V.5.3) of the **bpd1** phase presents six broad bands, giving maxima at 444.0, 467.4, 491.8, 525.4, 549.4 and 576.2 nm. Due to the poor resolution, the position of these peaks could not be assigned to the typical uranyl fluorescence electronic transitions. Although the organic ligand by its own (H_2bpd) does not give fluorescence emission in the 440-640 nm area, it seems to influence the uranyl fluorescence spectrum, resulting the atypical fluorescence spectrum of the **bpd1** complex.

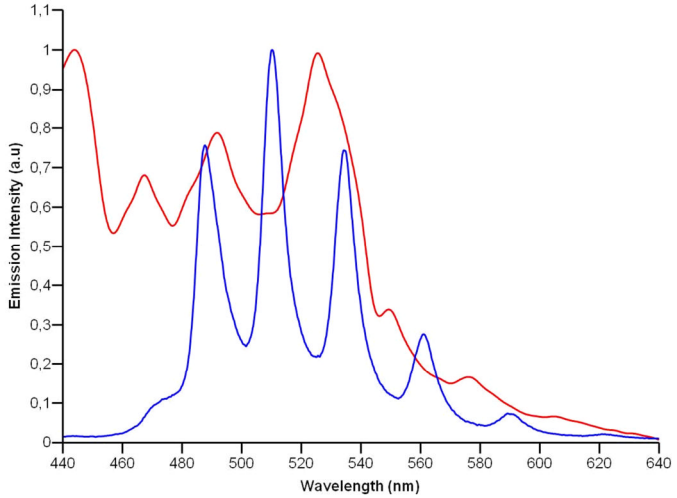

Figure V.5.3 Solid state emission spectra of **bdc1** (red) and of uranyl nitrate hexahydrate (blue).

Also in the case of the **adc1** complex it can be observed the influence of the organic ligand over the fluorescence spectrum of the complex. In this case the typical uranyl fluorescence spectrum is completely hidden by the ligand spectrum. As it can be observed in the figure, the emission spectrum of the complex nearly coincides with the one of the ligand.

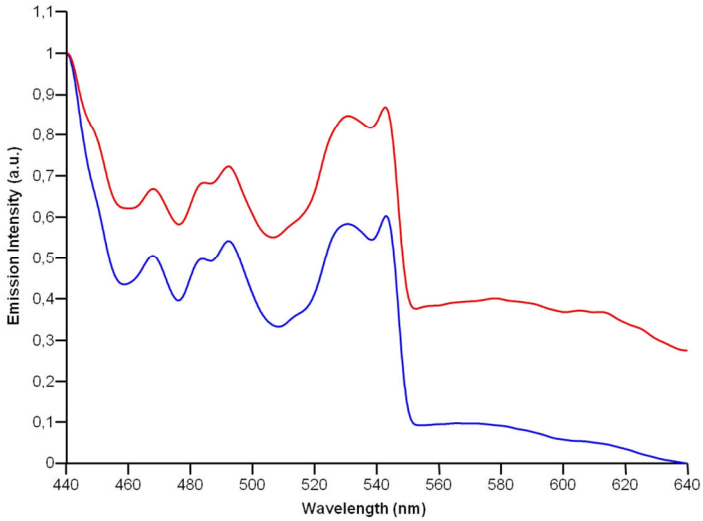

Figure V.5.4 Solid state emission spectra of **adc1** (red) and H_2adc (blue).

Conclusions

In this chapter there have been described and characterized quite unique cases of MOF type uranyl carboxylates, exhibiting six-fold coordination environments and each containing as ligand a specific ditopic aromatic carboxylate. All three ligands (1,4-benzene dicarboxylic acid, 4,4'-biphenyl

dicarboxylic acid and 4,4'-azobenzene dicarboxylic acid) have as specific property the para position of the two coordinating groups, which seems to favor this six-fold coordination around the uranium metal.

The thermal stability and heating behavior has been determined by TGA and thermo-diffraction analyses and indicated for all three samples a single step decomposition process in the 360 - 420°C range.

References

1. Mihalcea, I.; Henry, N.; Bousquet, T.; Volkringer, C.; Loiseau, T., *Crystal Growth & Design* **2012,** *12* (9), 4641-4648.
2. Li, H.; Eddaoudi, M.; O'Keeffe, M.; Yaghi, O. M., *Nature* **1999,** *402* (6759), 276-279.
3. Ferey, G.; Mellot-Draznieks, C.; Serre, C.; Millange, F.; Dutour, J.; Surble, S.; Margiolaki, I., *Science* **2005,** *309* (5743), 2040-2042.
4. Go, Y. B.; Wang, X. Q.; Jacobson, A. J., *Inorganic Chemistry* **2007,** *46* (16), 6594-6600.
5. Severance, R. C.; Smith, M. D.; zur Loye, H. C., *Inorganic Chemistry* **2011,** *50* (17), 7931-7933.
6. Cousson, A.; Proust, J.; Pages, M.; Robert, F.; Rizkalla, E. N., *Acta Crystallographica Section C-Crystal Structure Communications* **1990,** *46*, 2316-2318.
7. Rowland, C. E.; Belai, N.; Knope, K. E.; Cahill, C. L., *Crystal Growth & Design* **2010,** *10* (3), 1390-1398.
8. Frisch, M.; Cahill, C. L., *Dalton Transactions* **2005,** (8), 1518-1523.
9. Volkringer, C.; Henry, N.; Grandjean, S.; Loiseau, T., *Journal of the American Chemical Society* **2012,** *134* (2), 1275-1283.
10. Qu, Z. R., *Chinese Journal of Inorganic Chemistry* **2007,** *23* (10), 1837-1839.
11. Thuery, P.; Nierlich, M.; Souley, B.; Asfari, Z.; Vicens, J., *Journal of the Chemical Society, Dalton Transactions* **1999,** (15), 2589-2594.
12. Liu, D. B.; Xie, Y. Y.; Shao, H. W.; Jiang, X. Y., *Angewandte Chemie-International Edition* **2009,** *48* (24), 4406-4408.
13. Mihalcea, I.; Henry, N.; Loiseau, T., *Crystal Growth & Design* **2011,** *11* (5), 1940-1947.
14. Mihalcea, I.; Henry, N.; Volkringer, C.; Loiseau, T., *Crystal Growth & Design* **2012,** *12* (1), 526-535.
15. Bartlett, J. R.; Cooney, R. P., *Journal of Molecular Structure* **1989,** *193*, 295-300.

Chapter IV
Mixed U^{VI}-Ln^{III} aromatic carboxylates

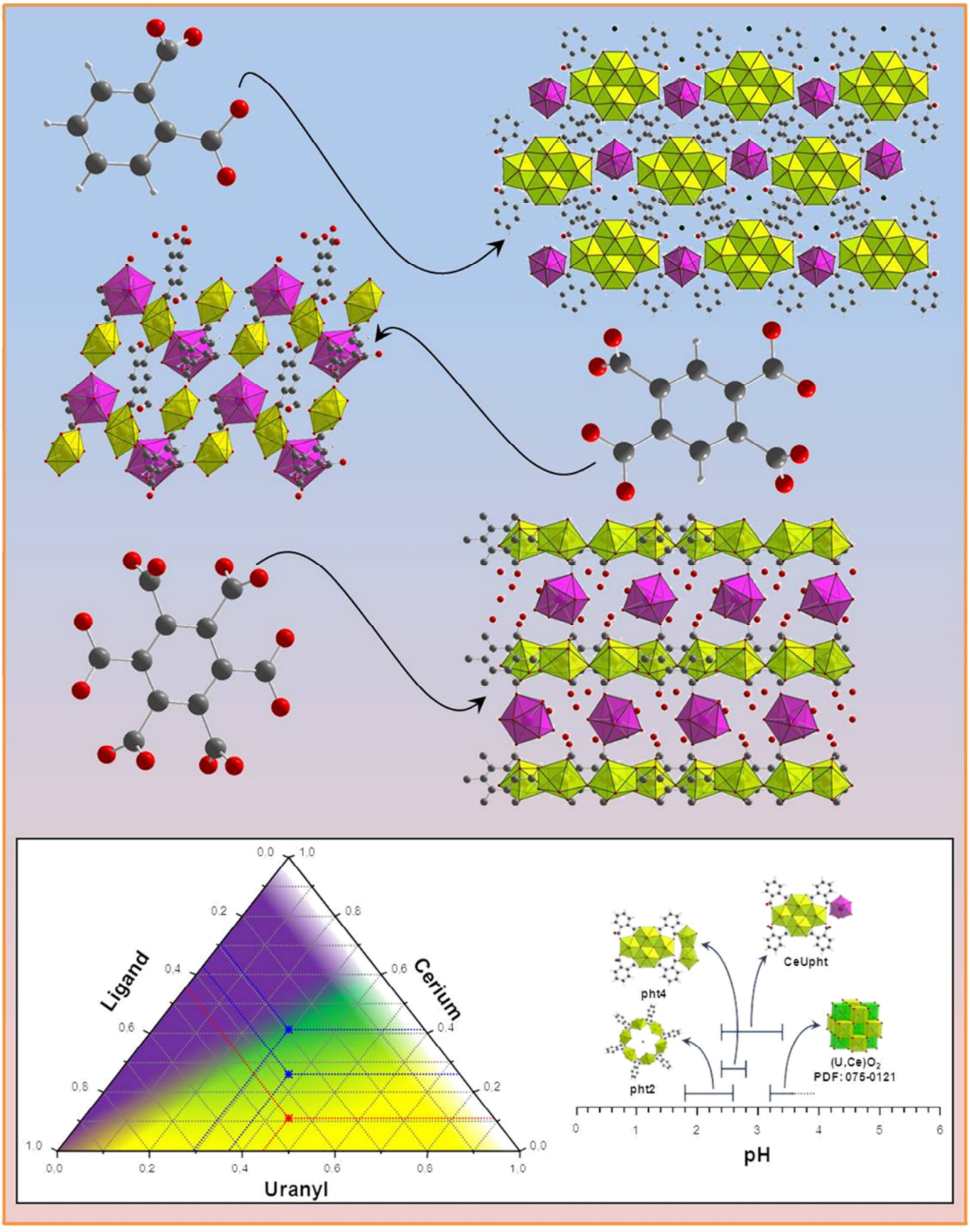

Chapter VI Mixed U^{VI}-Ln^{III} aromatic carboxylates

VI.1 . Introduction

The second major objective of this thesis work was to synthesize and structurally characterize mixed cation U^{VI}-Ln^{III} coordination polymers in order to analyze the formation of mixed heterometallic oxide upon thermal degradation. Several ligands of aromatic multidentate carboxylate type have been used for this purpose. As discussed in the introduction (chapter I, page 40), literature surprisingly described very few examples of such mixed *4f-5f* complexes. One of the major remark, reported by Thuéry[1] is the difficulty to synthesize homogenously pure *4f-5f* compounds since phase segregation often occurs with the formation of at least biphasic mixtures of products involving pure uranyl- or lanthanide-based complexes. One of the first illustrations of the successful synthesis of such mixed phase has been shown in our group by Volkringer et al.[2], who prepared Ce^{3+}-UO_2^{2+} and Nd^{3+}-UO_2^{2+} complexes by means of the hexadentate mellitate linker. The latter molecule (1,2,3,4,5,6-benzenehexacarboxylate) as well as oxalate was also assumed to be found in highly nitric solution when dissolving uranium carbide[3]. Therefore, this example incited us to continue this study by examining the reactivity of the different polycarboxylates we used in this thesis work. We thus tested the ligands phthalate (pht) and pyromellitate (btec) and also found another series of phase with the mellitate (mel)[4]. Other attempts have been done with the other ditopic molecules (isophthalate, terephthalate, etc…), but no mixed U-Ln phase has been obtained. These compounds have been hydrothermally synthesized starting from mixtures of uranyl nitrate, lanthanide (Nd or Ce) nitrate, ligand, ammonia solution and water as solvent. Here the choice of cerium or neodymium has been driven by the possibility to simulate the reactivity of heavy actinides such as plutonium or americium for instance. One noticed that the crystallization domain of such compounds is quite narrow and the technique of microwave heating has been used for some cases, in order to play

with crystal growth parameters (nucleation-growth process) for the isolation of pure *4f-5f* phases. The structures refined from the single crystal X-ray diffraction data revealed that the phthalate complexes $NH_4[(UO_2)_4O_2Ln(H_2O)_7(pht)_4]\cdot xH_2O$ (Ln = Ce (**CeUpht**), Nd (**NdUpht**); x = 1 for **CeUpht** and 0 for **NdUpht**) are based on the connection of tetranuclear $[(UO_2)_4O_2]$ uranyl building units with discrete lanthanide monomeric units $[Ln(H_2O)_7]$ via the organic ligand, generating infinite chains intercalated by free ammonium cations. The pyromellitate phases $[(UO_2)_3Ln_2(H_2O)_{12}(btec)_3]\cdot 5H_2O$ (Ln = Ce (**CeUpyr**), Nd (**NdUpyr**)) contain layers of pentagonal and hexagonal monomeric uranyl-centered bipyramids interconnected by the carboxylate arms of the organic ligand. Intercalated between the layers are situated lanthanide monomeric species $[Ln(H_2O)_7]$ which ensure the three-dimensionality of the structure, being coordinated by two ligand carboxylate arms of two adjacent layers. The structures of the mellitate series $[(UO_2)_2(OH)Ln(H_2O)_7(mel)]\cdot 5H_2O$ are built up from dimeric uranyl-centered units interconnected by the ligand carboxylate groups in order to create infinite layers which are further connected to each other through discrete monomeric lanthanide $[Ln(H_2O)_6]$ species. Details of the crystal data for the six phases are given in the Table VI.1.1 - Table VI.1.2 tables.

Table VI.1.1 Refinement and crystal data for the CeUpht, NdUpht and CeUpyr phases.

Parameter*	CeUpht	NdUpht	CeUpyr
crystal system	monoclinic	monoclinic	triclinic
space group	*P*2/*n*	*P*2/*n*	*P*-1
a/Å	15.9635(2)	15.9634(6)	10.9229(2)
b/Å	19.9741(3)	19.9848(8)	11.5371(3)
c/Å	7.2160(1)	7.1993(3)	13.4516(3)
α/deg	90	90	69.5020(5)
ß/deg	95.3854(7)	95.430(2)	80.0490(6)
γ/deg	90	90	62.2530(5)
volume/Å^3	2289.63(5)	2286.5(2)	1405.14(6)
Z, ρ_{calc}/g·cm^{-3}	2, 2.974	2, 2.960	1, 2.496
final *R* indices [$I > 2\sigma(I)$]	R1 = 0.0594 wR2 = 0.0793	R1 = 0.0561 wR2 = 0.0562	R1 = 0.0332 wR2 = 0.0500
R indices (all data)	R1 = 0.0694 wR2 = 0.0799	R1 = 0.1507 wR2 = 0.0789	R1 = 0.0380 wR2 = 0.0505

* - a complete crystal and refinement data table is given in the supplementary data chapter (table VIII.5.1)

Table VI.1.2 Refinement and crystal data for the NdUpyr, CeUmel and NdUmel phases.

Parameter*	NdUpyr	CeUmel	NdUmel
crystal system	triclinic	orthorhombic	orthorhombic
space group	*P*-1	$Pna2_1$	$Pna2_1$
a/Å	10.8981(13)	15.8523(8)	15.8367(8)
b/Å	11.5452(14)	8.3188(5)	8.3203(6)
c/Å	13.4086(16)	21.5884(12)	21.5047(3)
α/deg	69.399(3)	90	90
ß/deg	79.959(3)	90	90
γ/deg	62.242(2)	90	90
volume/Å^3	1397.4(3)	2846.9(3)	2833.6(3)
Z, ρ_{calc}/g·cm^{-3}	1, 2.520	4, 2.856	4, 2.879
final *R* indices [$I > 2\sigma(I)$]	R1 = 0.0304 wR2 = 0.0418	R1 = 0.0365 wR2 = 0.0375	R1 = 0.0313 wR2 = 0.0351
R indices (all data)	R1 = 0.0456 wR2 = 0.0430	R1 = 0.0612 wR2 = 0.0400	R1 = 0.0443 wR2 = 0.0375

* - a complete crystal and refinement data table is given in the supplementary data chapter (table VIII.5.2)

VI.2 . Structure description

The phases of the phthalate system $NH_4[(UO_2)_4O_2Ln(H_2O)_7(pht)_4]\cdot xH_2O$ (Ln = Ce and Nd; x = 1 and 0 for **CeUpht** and **NdUpht**) present similar structures, excepting one free water molecule appearing only in the **CeUpht** phase. Both phthalate phases contain three distinct crystallographic sites for the uranium atoms and one for the lanthanide atom. First two uranium atoms (U1 and U2) and the lanthanide atom are situated on *2f* (¾ y ¼) special position, the third uranium atom being situated on a *4g* general position. The U1 and U2 atoms are forming hexagonal bipyramidal polyhedra whereas the U3 atom forms a pentagonal bipyramidal shaped coordination sphere. For the three uranium cations typically short uranyl bonds are observed with lengths in the range of 1.719(9)-1.779(2) Å for **CeUpht** and 1.760(6)-1.764(6) Å for **NdUpht**. In both phases the U—O equatorial bonds are ranging from 2.241(6) to 2.636(9) Å for the eight-fold coordinated uranium atoms (U1 and U2) and from 2.192(6) to 2.414(9) Å for the seven-fold coordinated uranium atoms (U3). The U1 and U2 polyhedra are edge sharing connected (through the O1····O1 edge), each of the two also sharing two other edges (O1····O81b) with two distinct U3 polyhedra. The O1 atom, possessing a μ_3 coordination configuration has been found by bond valence calculations[5] to be an oxo bridge (values of 2.10 and 2.09 v.u. for **CeUpht** and

NdUpht respectively, expected value of 2.00 v.u. for oxo species). All other oxygen atoms in the equatorial plane of the uranium polyhedra are carboxylate type belonging to the ligand. From the latter ones, the O81a and O81b oxygen atom presents a second type of μ_3-connection mode, simultaneously coordinating two uranium centers (U2, U3 and U1, U3 respectively) and binding one carbon atom from carboxylate group. The edge sharing connection occurring between the uranium polyhedra gives rise to a discrete tetrameric SBU (Figure VI.2.1-left) previously encountered in other two uranyl phthalate phases (**pht3** and **pht4**, chapter II). The lanthanide's coordination sphere is formed by two carboxylate oxygen atoms (O11b and its symmetry equivalent) situated at distances of 2.53(1) Å from the central metal ion (for both phases) and other seven oxygen atoms belonging to coordinating water molecules, possessing Ln—O bond lengths ranging from 2.48(3) to 2.66(3) Å for **CeUpht** and from 2.47(2) to 2.57(2) Å for **NdUpht** phase (Figure VI.2.1-center). The uranyl-lanthanide phthalate structures possess two distinct positions for the organic ligand molecules (Figure VI.2.1-right). First molecule chelates the U1 atom with one carboxylate arm and simultaneously also bridges the U3 center. With the second carboxylate arm it bridges in bidentate manner, the U3 atom and the lanthanide center. The total coordination configuration for this ligand molecule is μ_5-η_1:η_1:η_2:η_2:η_3.

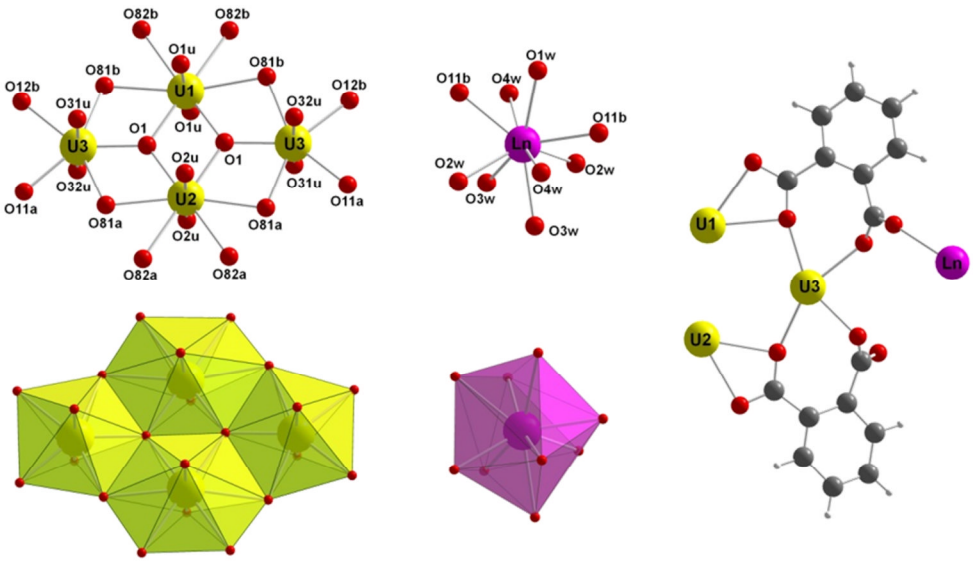

Figure VI.2.1 Coordination environment surrounding the uranium atoms (left), surrounding the lanthanide atom (center) and the coordination configuration of the ligand (right) for the mixed uranyl-lanthanide phthalate phases.

The second ligand molecule, chelates the U2 with one carboxylate arm and bridges the U3 atoms and coordinates the U3 center with the other monodentate group. The total coordination configuration for this molecule is μ_4-η_1:η_1:η_2:η_2.
The ligand molecules are binding alternating uranyl and lanthanide building units into polymeric chains. These chains are almost similar to the ones present in the **pht3** and **pht4** phases. The difference between them is the replacement of the dimeric uranyl unit from the uranyl pure phthalates with a lanthanide monomeric unit (Figure VI.2.2). The lanthanide polyhedron occupies only one side of the chain, leaving two carboxylate oxygen atoms free. The negative charges of the noncoordinating carboxylate oxygen atoms and the oxo groups present in the tetrameric units are compensated by ammonium countercations intercalated between the chains.

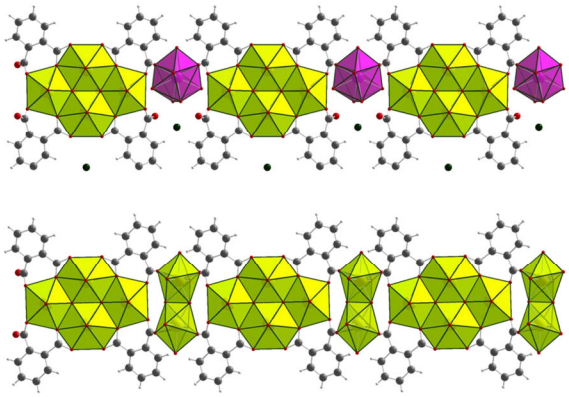

Figure VI.2.2 Comparison between the polymeric chains of the **LnUpht** (Ln = Ce and Nd) phases (top) and of the **pht3** and **pht4** phases (bottom).

The infinite polymeric chains are running along the [100] direction and in the (011) plane are orientated parallel with the [010] direction (Figure VI.2.3). The stacking direction of the chains is [001].

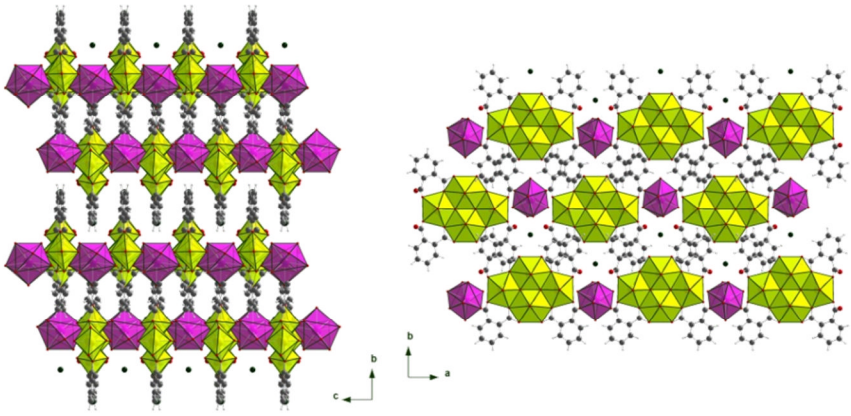

Figure VI.2.3 View of the **LnUpht** (Ln = Ce and Nd) structures along the [100] (left) and [001] (right) directions.

Due to the fact that seven of the nine positions in the coordination sphere of the lanthanide atom are occupied by water molecules, complex networks of hydrogen bonds are present in the structure fixing the lanthanide polyhedra into position (Figure VI.2.4).

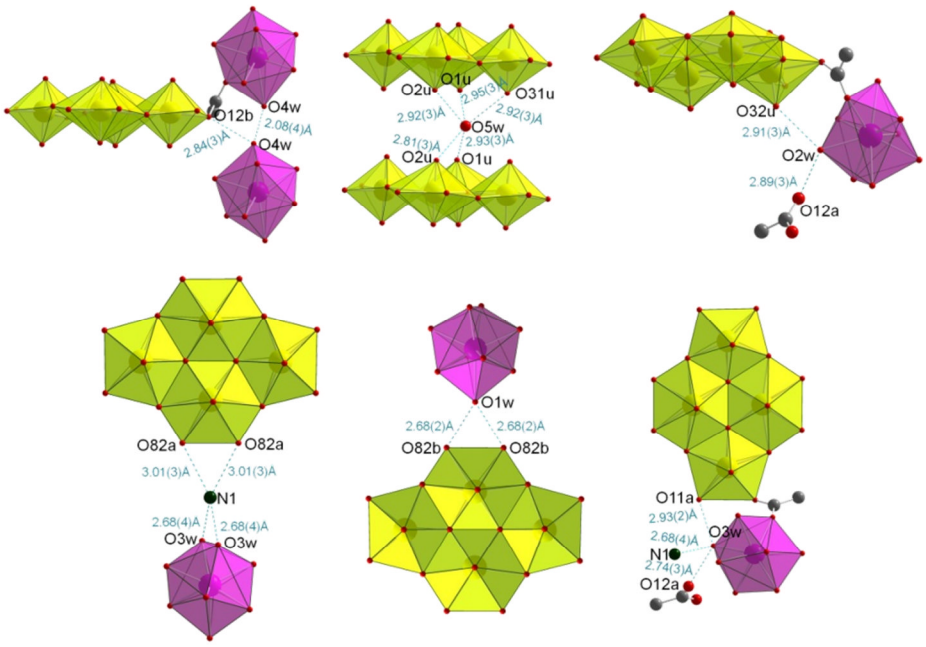

Figure VI.2.4 Representation of the hydrogen bond interactions occurring in the **LnUpht** (Ln = Ce and Nd) structures.

The Ow1 water molecule binds two O82b coordinating carboxylate oxygen atoms; the Ow2 interacts with O32u uranyl and O12a free carboxylate oxygen atoms; the Ow3 interacts with the N1 ammonium cation, with the O12a free carboxylate and O11a coordinating carboxylate oxygen atoms. The Ow4 water molecule interacts with the O12b coordinating carboxylate oxygen atom and another Ow4 coordinating water molecule belonging to an adjacent lanthanide polyhedron. These interactions manifest at a O····O distance ranging from 2.08(4) to 2.93(2) Å. The structure of the **CeUpht** phase also contains the Ow5 free water molecule situated between two uranyl tetranuclear SBUs. This water molecule interacts with the adjacent uranyl oxygen atoms through five possible hydrogen bonds, the O····O distances ranging from 2.81(3) to 2.95(3) Å.

The contribution to the tridimensional stability of the structure is divided between the hydrogen bond interactions and the π-π stacking interactions, manifesting between the benzene rings along the stacking axis. The distance

between the centers of two adjacent benzene rings, belonging to two different chains is of 3.71(2) Å.

The phases of the pyromellitate system $[(UO_2)_3Ln_2(H_2O)_{12}(btec)_3]\cdot 5H_2O$ (where Ln = Ce for **CeUpyr** phase and Nd for **NdUpyr**) both exhibit similar structure, excepting slight disorders on the oxygen atoms belonging to water molecules and for the **CeUpyr** phase a cationic disorder on the cerium atom. An interesting fact was that no disorder was found on the coordination sphere surrounding this cation. The structures of both phases present two distinct crystallographic sites for the uranium atom and one for the lanthanide atom. The U1 atom is situated on a *1g* (0 ½ ½) special position; the second uranium atom (U2) and the lanthanide atom are situated on *2i* general positions. All the metal atoms in the structures are forming distinct mononuclear SBUs (Figure VI.2.5). The U1 atom is eight-fold coordinated forming a U^{VI} typical hexagonal bipyramidal shaped polyhedron. The apical positions are occupied symmetrically by the O11u uranyl oxygen atom and its equivalent, forming a U═O uranyl bond of 1.764(5) and 1.752(5) Å for **CeUpyr** and **NdUpyr** respectively and a 180° angle around the uranium atom for both phases. The equatorial plane of the bipyramid, formed entirely by carboxyl oxygen atoms is distorted. The plane of the O71b and O72b oxygen atoms is tilted from the plane of the O81 atoms with 21.67(9) and respectively with 21.63(7)° for the two phases. The U─O equatorial bonds involving oxygen atoms of bridging carboxylate arms (O81) are shorter (2.404(3) Å for **CeUpyr** and 2.396(4) Å for **NdUpyr**) than the ones involving oxygen atoms (O71b, O72b) of chelating groups (2.496(4)-2.573(4) Å for **CeUpyr** and 2.485(4)-2.598(4) Å for **NdUpyr**). The U2 atom is seven-fold coordinated forming the typical pentagonal bipyramidal polyhedron. It possesses two asymmetrical short uranyl bonds in axial position of 1.757(4)-1.780(4) Å (for **CeUpyr**) and 1.767(4)-1.770(4) Å (for **NdUpyr**), with the O21u and O22u uranyl oxygen atoms and other five longer bonds in the equatorial plane with carboxyl type oxygen atoms. As observed in the U1 case, also for the U2 atom the equatorial U─O bonds involving oxygen atoms of bridging carboxylate arms (O82b, O92 and O101) are shorter (2.339(5)-2.376(3) Å and respectively 2.338(5) - 2.367(3) Å) than the ones involving oxygen atoms (O71 and O72) belonging to

chelating carboxylate arms (2.455(5), 2.434(4) Å and 2.450(4), 2.422(3) respectively for the **CeUpyr** and **NdUpyr** phases). The lanthanide atom is nine-fold coordinated and forms an irregular polyhedron. Six of the coordinating oxygen atoms (O1w to O6w) are belonging to water molecules. The remaining three (O82, O91 and O102) oxo groups are carboxyl oxygen atoms belonging to bridging carboxylate arms of the ligand. The Ln—O bonds involving the carboxyl oxygen atoms are slightly shorter (ranging from 2.468(5) to 2.541(6) Å for **CeUpyr** and from 2.432(4) to 2.523(5) Å for **NdUpyr**) than the ones involving aquo oxygen atoms (2.504(4)-2.630(7) Å and 2.465(5)-2.576(6) Å, respectively).

The structures of the two mixed U^{VI}/Ln^{III} pyromellitates exhibit two distinct crystallographic positions for the organic linker (Figure VI.2.6). First ligand molecule binds only uranium centers, creating an infinite layer of interconnected uranyl polyhedra. With two opposite carboxylate arms (positions 1 and 4 on the ring) it chelates two U1 atoms, with the remaining two (positions 2 and 5 on the ring) monodentate binding two U2 atoms. The coordination configuration of this first ligand molecule is μ_6-η_1:η_1:η_2:η_1:η_1:η_2.

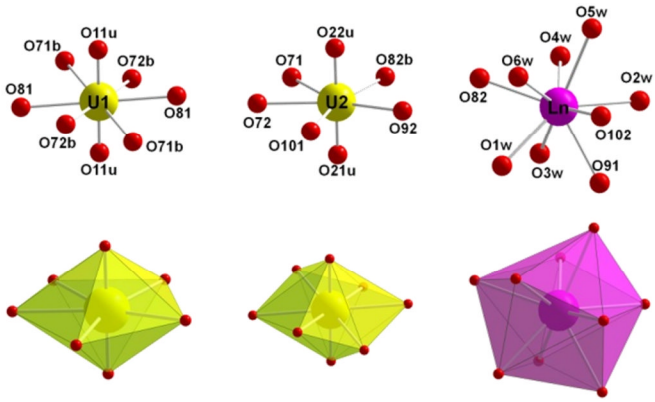

Figure VI.2.5 Coordination environment surrounding the metallic centers in **LnUpyr** structures (Ln = Ce, Nd).

The second ligand molecule is responsible with the connection between the layers and also binds the lanthanide center. First carboxylate arm (position 1) bridges the U1 and the lanthanide metal centers; the second one (position 2) chelates the U2 atom; the remaining two (positions 4 and 5) are having the same coordination mode, bridging one U2 and one Ln atoms. Both of the latter two arms are coordinating the same lanthanide atom but distinct U2 centers. The total coordination configuration of the second ligand molecule is μ_8-η_1:η_2:η_2:η_2:η_2:η_3:η_3:η_2.

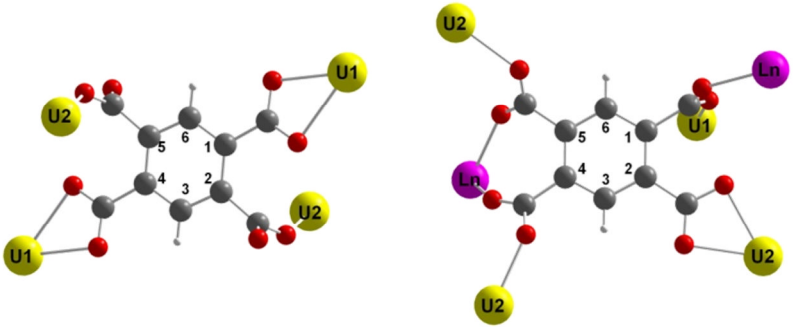

Figure VI.2.6 Coordination configuration of the pyromellitate ligand in the two **LnUpyr** phases (Ln = Ce, Nd).

The layers formed by the first ligand molecule interconnecting uranium polyhedra are developing along the (110) plane and contain intercalated lanthanide polyhedra bonded by the second ligand molecule (Figure VI.2.7).

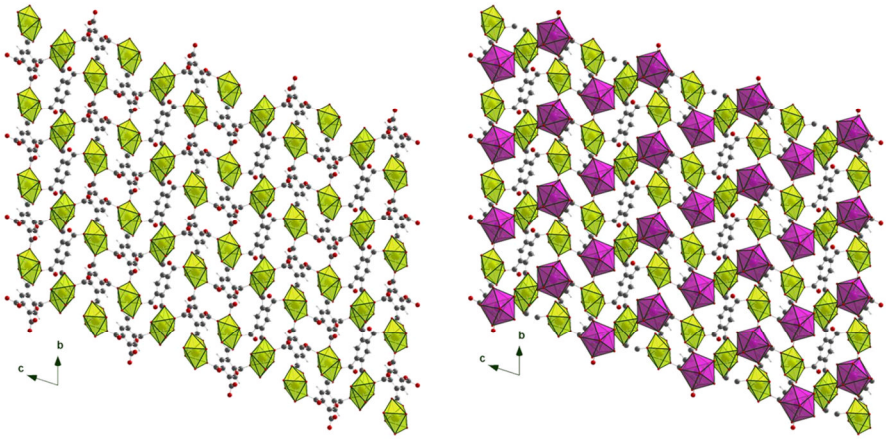

Figure VI.2.7 Structure of **LnUpyr** phases (Ln = Ce, Nd). View along the [100] axis. Representation omitting lanthanide centers (left) and containing the lanthanide centers (right).

Also intercalated in the structure, there are three distinct crystallographic positions for free water molecules (Figure VI.2.8).

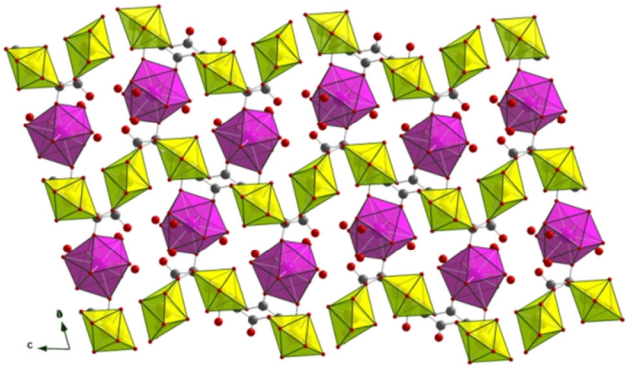

Figure VI.2.8 Structure representation of the **LnUpyr** phases (Ln = Ce, Nd). View along the [-110] direction showing the alternating layers of uranyl and lanthanide polyhedra and the intercalated free water molecules.

Due to the large number of coordinating and free water molecules in the structures of the **LnUpyr** phases it results an extended network of hydrogen

bonds (Figure VI.2.9). The most frequently encountered hydrogen bonds are the ones between the lanthanide coordinating water molecules and the free uranyl coordinating carboxyl type oxygen atoms. The O····O distances for these interactions range from 2.71(1) to 2.98(1) Å for **CeUpyr** and from 2.71(1) to 3.00(1) Å for **NdUpyr** phases. Also frequently encountered in these two phases are the interactions between the free water molecules and also between the coordinating and free water molecules. These interactions occur at O····O distances ranging from 2.60(4) to 2.98(1) Å for **CeUpyr** and from 2.72(1) to 2.96(1) Å for the **NdUpyr** phases.

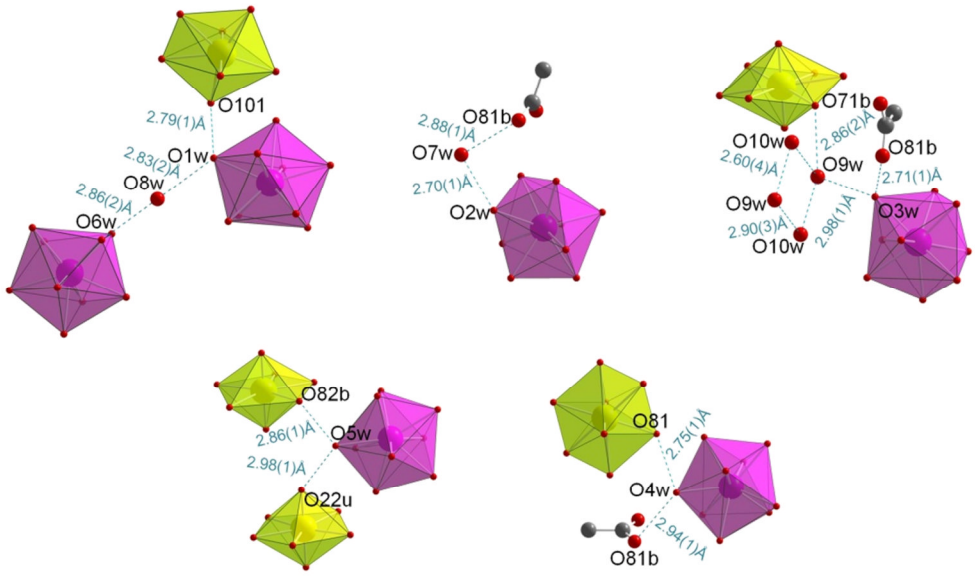

Figure VI.2.9 Hydrogen bond interactions occurring in the structures of the **CeUpyr** phase. Similar interactions occur in the structure of **NdUpyr** with slightly modified bond length values.

The tridimensional stability of the structure is mainly ensured by the coordination configuration of the ligand molecules and reinforced by the large number of hydrogen bonds. No π-π stacking interactions could take place due to the orientation of the benzene rings (71.2(2)° between the planes of two adjacent ligand molecules) and also due to the large distances between them (5.98(1) Å between the centers of two closest benzene rings).

The third series of mixed uranyl-lanthanide carboxylates contain as organic ligand the mellitic acid (H_6mel). Both phases of the series possess the same structure $[(UO_2)_2(OH)Ln(H_2O)_7(mel)]\cdot 5H_2O$, where Ln = Ce for **CeUmel** or Nd for **NdUmel**. The **LnUmel** phases contain two distinct crystallographic sites for the uranium atoms and one for the lanthanide atom, all three situated on *4a*

general positions (Figure VI.2.10). Both uranium atoms are seven-fold coordinated and adopt the pentagonal bipyramidal geometry. The typically shorter uranyl bonds are ranging from 1.764(6) to 1.782(7) Å for the **CeUmel** phase and from 1.766(5) to 1.789(6) Å for the **NdUmel** one. The O=U=O angle for both of the uranium atoms of both of the phases varies between 177.9(3) and 179.4(3)°. The equatorial plane for each uranyl polyhedron is composed of four carboxyl type oxygen atoms belonging to the organic ligand and a fifth oxygen atom, which is common for both polyhedra. This fifth atom (O1h) connects the two pentagonal bipyramids forming a dinuclear SBU. The μ_2-OH nature of the O1h atom has been established by bond valence calculation[5, 6]. The obtained values were 1.23 and 1.25 v.u. for the **CeUmel** and respectively for the **NdUmel** phases (expected valence value for hydroxo species: 1.00 v.u.). For both complexes, the equatorial U–OH bonds are shorter (2.293(5) to 2.309(5) Å) than the ones involving carboxyl oxygen atoms (2.354(6) to 2.499(5) Å).

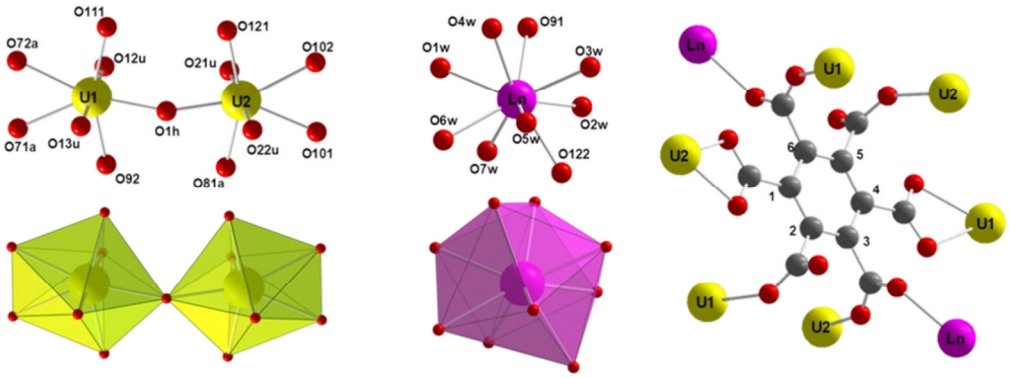

Figure VI.2.10 Coordination environment of uranyl polyhedra (left), of lanthanide polyhedron (center) and the coordination configuration of the organic ligand (right) for the **LnUmel** phases.

For the organic linker, the structure possesses only one unique crystallographic site. Pairs of opposite carboxylate arms of the ligand are adopting the same coordination mode: first and fourth of the arms (positions 1 and 4 on the ring) are both adopting the symmetric chelating mode but each on a different uranium atom (group 1 chelates the U2 atom and group 4 the U1 atom); the second and the fifth arms (positions 2 and 5 on the ring) are monodentate coordinating a single uranium atom, the second oxygen atom remaining free (group 2 coordinates the U1 atom and group 5 the U2); the last two groups (position 3 and 6 on the ring) are each bridging the lanthanide atom with a

distinct uranium atom (group 3 bridges the U2 center while group 6 bridges the U1 one). The total coordination configuration of the mellitate ligand in these two phases is μ_{10}-η_1:η_1:η_2:η_1:η_3:η_2:η_2:η_1:η_2:η_3.

Ignoring the bond with the lanthanide center, the organic ligand creates infinite sheets of interconnected uranyl SBUs developing in the (110) plane and stacking on the [001] direction (Figure VI.2.11). The lanthanide centers are bound in between the layers ensuring the tridimensional cohesion of the structure. Also three distinct crystallographic sites assigned to free water molecules are located between the layers .

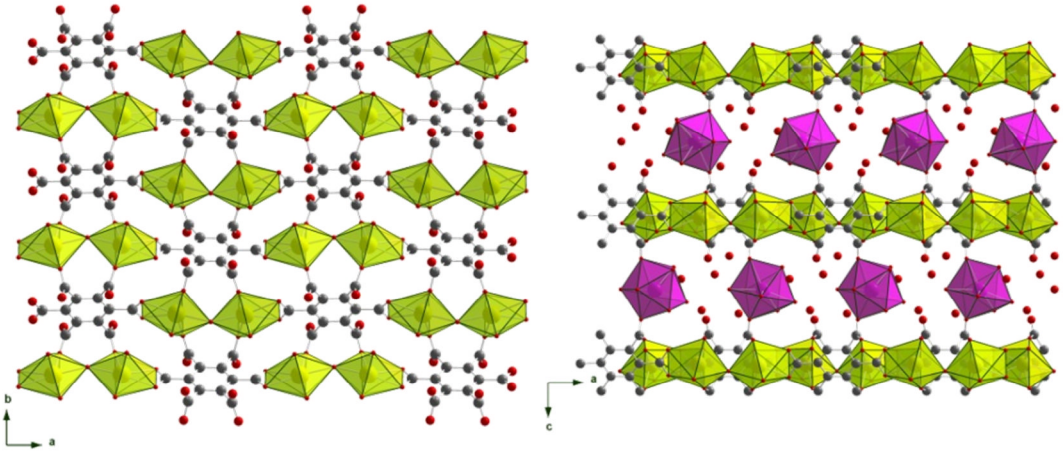

Figure VI.2.11 Structure representation of **LnUmel** phase. View along the [001] direction of a single uranyl-ligand layer (left) and along the [010] direction the alternating uranyl and lanthanide layers.

These free water molecules, together with the coordinating water molecules surrounding the lanthanide cation are "weaving" a complex network of hydrogen bonds contributing to the stability of the complex.

The most important hydrogen bond interactions are the ones occurring between the coordinating water molecules and the carboxyl oxygen atoms, with O····O distances ranging from 2.72(1) to 2.92(1) Å for both **LnUmel** structures (Figure VI.2.12). There are also hydrogen bonds occurring between the free water molecules and the adjacent uranyl, carboxyl and aquo type oxygen atoms. The O····O distances at which these interactions take place are ranging between 2.60(2) and 2.98(1) Å.

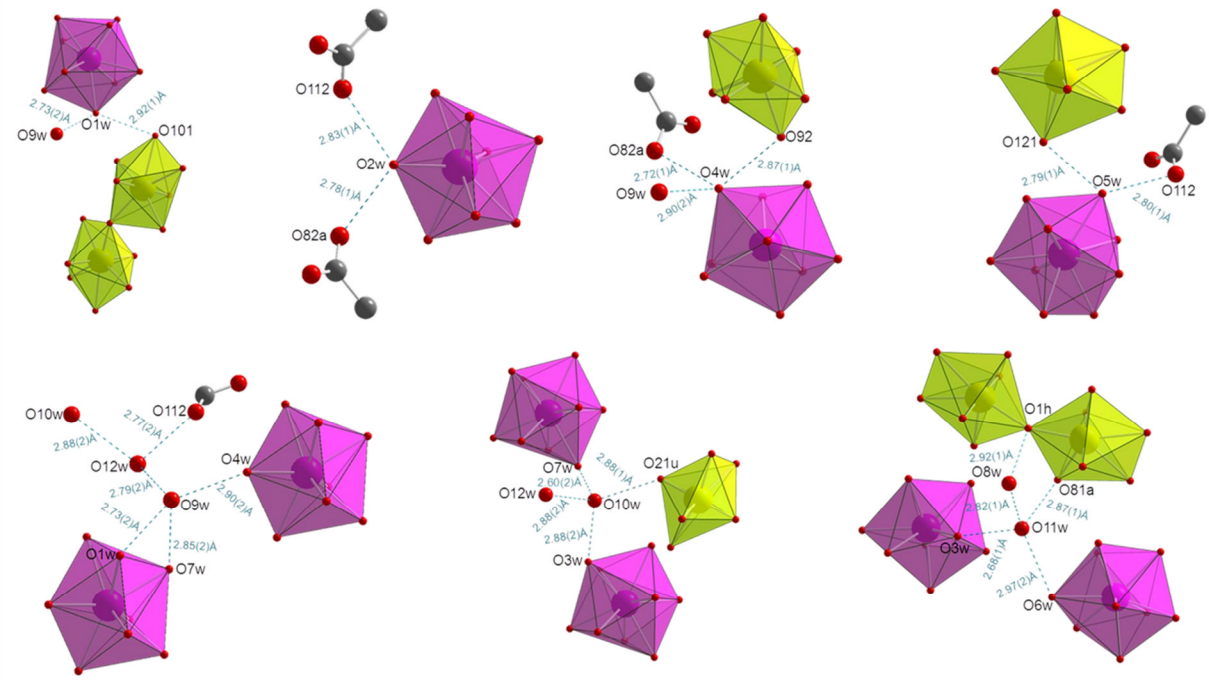

Figure VI.2.12 Representation of the hydrogen bonds occurring in the structure of **CeUmel**. Similar interactions occur also in the structure of **NdUmel** at slightly different O····O distances.

The stability of the tridimensional edifice is mainly ensured by the coordination configuration of the organic ligand by bridging the two uranyl and lanthanide types of layers. Also contributing to the stability of the structure is the complex network of hydrogen bonds. For the two **LnUmel** structures, no π-π stacking interaction could occur due to the large distance between the uranyl layers, which also contain the organic benzene rings of the ligand. The distance between two consecutive uranyl-ligand layers is of 10.79(1) Å.

VI.3 . Synthesis

The **LnUpht**, **LnUpyr** and **LnUmel** phases (where Ln = Ce and Nd) have been synthesized hydrothermally under autogenous pressure using 23 mL Teflon-lined stainless steel autoclaves. The starting reagents have been: uranyl nitrate hexahydrate ($UO_2(NO_3)_2 \cdot 6H_2O$, Merck 99%), cerium nitrate hexahydrate ($Ce(NO_3)_3 \cdot 6H_2O$, Aldrich 99%), neodymium nitrate hexahydrate ($Nd(NO_3)_3 \cdot 6H_2O$, Aldrich 99%), phthalic acid (o-$C_6H_4(COOH)_2$, 1,2-benzenedicarboxylic acid or H_2pht, Acros Organics, 99%), pyromellitic acid ($C_6H_2(COOH)_4$, 1,2,4,5-benzenetetracarboxylic acid or H_4btec, Aldrich 96%), mellitic acid ($C_6(COOH)_6$,

benzenehexacarboxylic acid or H_6mel, Aldrich, 99%), ammonia solution (Prolabo 28%), sodium hydroxide (NaOH, Aldrich 98%) and deionized water. These reagents are commercially available and have been used without further purification.

For the synthesis of **CeUpht** phase $NH_4[(UO_2)_4O_2Ce(H_2O)_7(pht)_4]\cdot H_2O$, the first reaction conditions that have been optimized and after maintained constant were the reaction time and temperature of 24 h at 150°C. A higher temperature favors the formation of the cerium and/or the (Ce,U) mixed oxide depending of the initial cationic ratio used. The next parameter that was optimized was the ratio between precursors (Ce, U and ligand). Pure and major phases (very low quantities of impurities) of the **CeUpht** compound have been synthesized maintaining the U/Ce ratio between 0.75 and 1.33 and the total metal/ligand ratio above 1.5. Varying the cationic ratio outside the given domain or decreasing the metal/ligand ratio will favor the phase segregation. As expected, enriched-cerium phase was observed when increasing the Ce/U ratio and enriched-uranyl phase was observed when decreasing the Ce/U ratio. As it can be observed in the ratio phase tendency diagram (Figure VI.3.1-left) there is a relatively large difference between the U/Ln ratio applied in synthesis and the ratio given by the phase stoichiometry. Lower quantities of uranyl source and ligand and higher quantities of cerium source are required, which must be in excess for its reaction with uranyl. The use of a lower metal/ligand ratio is also motivated by the presence of the excess cerium-enriched phases.

The last reaction parameter that has been optimized in this system has been the solution pH. The pH phase diagram depends on the previously discussed conditions. If these conditions are maintained in optimal ranges the pH influence on the nature of the final products is the one given in the pH phase diagram (Figure VI.3.1-right). A low pH (beneath 2.8) favors the formation of pure uranyl phases (**pht2** and **pht4**). A high pH (above 3.2) favors the redox reaction between U^{VI} and Ce^{III}, resulting in the crystallization $(Ce,U)^{IV}O_2$ mixed oxide of fluorite type. The narrow domain of pH where the **CeUpht** phase has been obtained pure is in between the 2.8-3.2 limits.

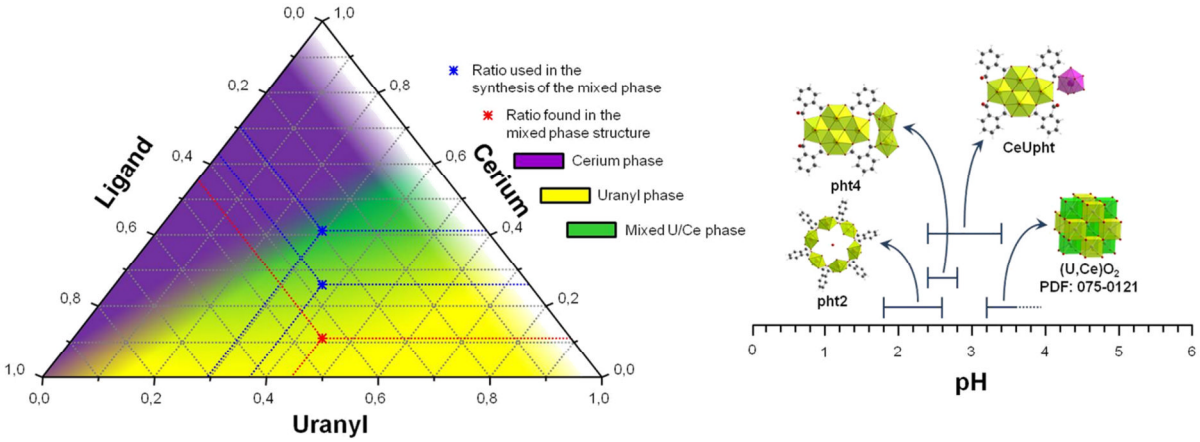

Figure VI.3.1 Phase tendency diagrams as a function of the reagents used ratio (left) and of the reaction pH (right) for the **CeUpht** phase.

The phase has been obtained as major phase by statically heating under hydrothermal conditions at 150°C during 24 h a mixture of 0.502 g (1 mmol) $UO_2(NO_3)_2 \cdot 6H_2O$, 0.614 g (1.4 mmol) $Ce(NO_3)_3 \cdot 6H_2O$, 0.166 g (1 mmol) 1,2-$C_6H_4(COOH)_2$, 1.8 ml solution 2M (3.6 mmol) NH_3 and 3.2 mL (178 mmol) H_2O. The final solution pH was 2.9. The resulting product was then filtered off, washed with water and dried at room temperature. The PXRD pattern of this product showed small traces of impurities. As pure phase, the **CeUpht** phase has been obtained using a microwave accelerating reaction system (MARS CEM oven) from a mixture of 0.502 g (1 mmol) $UO_2(NO_3)_2 \cdot 6H_2O$, 0.614 g (1.4 mmol) $Ce(NO_3)_3 \cdot 6H_2O$, 0.166 g (1 mmol) 1,2-$C_6H_4(COOH)_2$, 1.6 ml solution 2M (3.2 mmol) NH_3 and 8.6 mL (478 mmol) H_2O, heated hydrothermally for 2 h at 150°C. The final solution ph was 2.6. The obtained product has been filtered off, washed with water and dried at room temperature. SEM examination of the two products shows that the one obtained by electric traditional heating presents crystalline conglomerates of 100-500 µm in size whereas the one obtained by microwave heating presents isolated crystals of 30 - 100 µm in size (Figure VI.3.2).

The good result obtained by microwave assisted synthesis suggests that the mixed phase is the kinetic one and its formation is actually favored by a shorter reaction time.

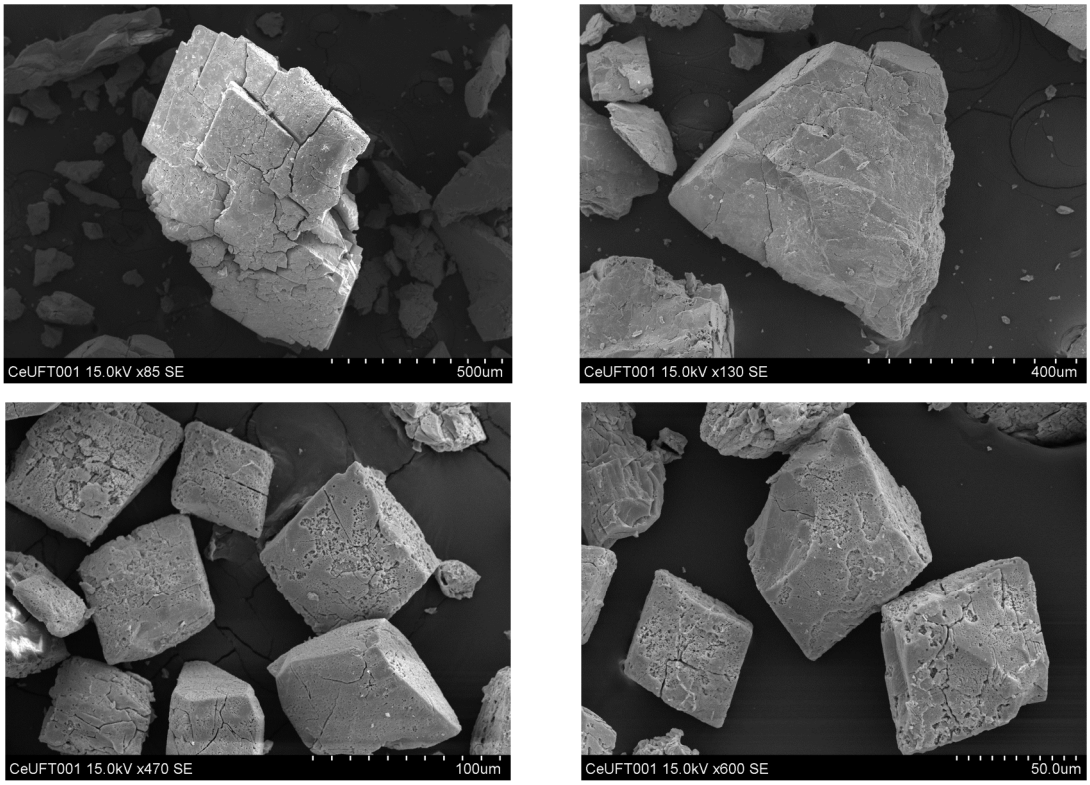

Figure VI.3.2 SEM images of the **CeUpht** phase obtained by traditional electric heating (top) and by microwave heating (bottom).

For the **NdUpht** phase $NH_4[(UO_2)_4O_2Nd(H_2O)_7(pht)_4]$, the optimum reaction time and temperature have been fixed to 24 h and 200°C. In these conditions, the optimal U/Nd ratio has been found to be ranging from 0.75 to 1 while the optimal metal/ligand ratio should be maintained above 1.5.

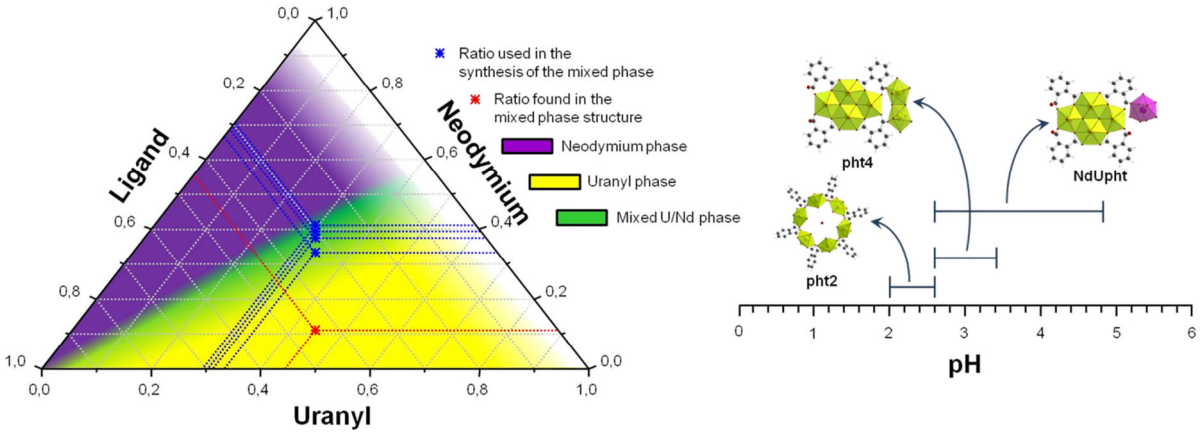

Figure VI.3.3 Phase tendency diagrams as a function of the reagents used ratio (left) and of the reaction pH (right) for the **NdUpht** phase.

As in the **CeUpht** case, the uranyl/lanthanide/ligand ratio required in synthesis is different from the stoichiometry of the final product, the system requiring an excess of neodymium ions to remain in solution and to crystallize

the **NdUpht** phase (Figure VI.3.3). In the given conditions, the solution pH permitting the formation of the mixed phase varies between 2.6 and 4.8. Preparations obtained at pH above 5 gave unidentified powders with no crystals suitable for the single crystal X-ray structure determination.

Major phase has been obtained by hydrothermally heating at 200°C during 24 h a mixture of 0.254 g (0.5 mmol) $UO_2(NO_3)_2 \cdot 6H_2O$, 0.310 g (0.7 mmol) $Nd(NO_3)_3 \cdot 6H_2O$, 0.083 g (0.5 mmol) 1,2-$C_6H_4(COOH)_2$, 0.8 ml solution 2M (1.6 mmol) NH_3 and 8.2 mL (456 mmol) H_2O. The final solution pH was 3.5. The resulting product was filtered off, washed with water and dried at room temperature. The PXRD pattern of this product showed beside the **NdUpht** phase the presence in low quantities (traces) of unidentified impurities. This complex has been obtained pure (from XRD analyses) by microwave heating under hydrothermal conditions, during 2 h at 150°C a mixture of 0.502 g (1 mmol) $UO_2(NO_3)_2 \cdot 6H_2O$, 0.620 g (1.4 mmol) $Nd(NO_3)_3 \cdot 6H_2O$, 0.166 g (1 mmol) 1,2-$C_6H_4(COOH)_2$, 1.6 ml solution 2M (3.2 mmol) NH_3 and 8.4 mL (467 mmol) H_2O. The final solution pH was 3.5.

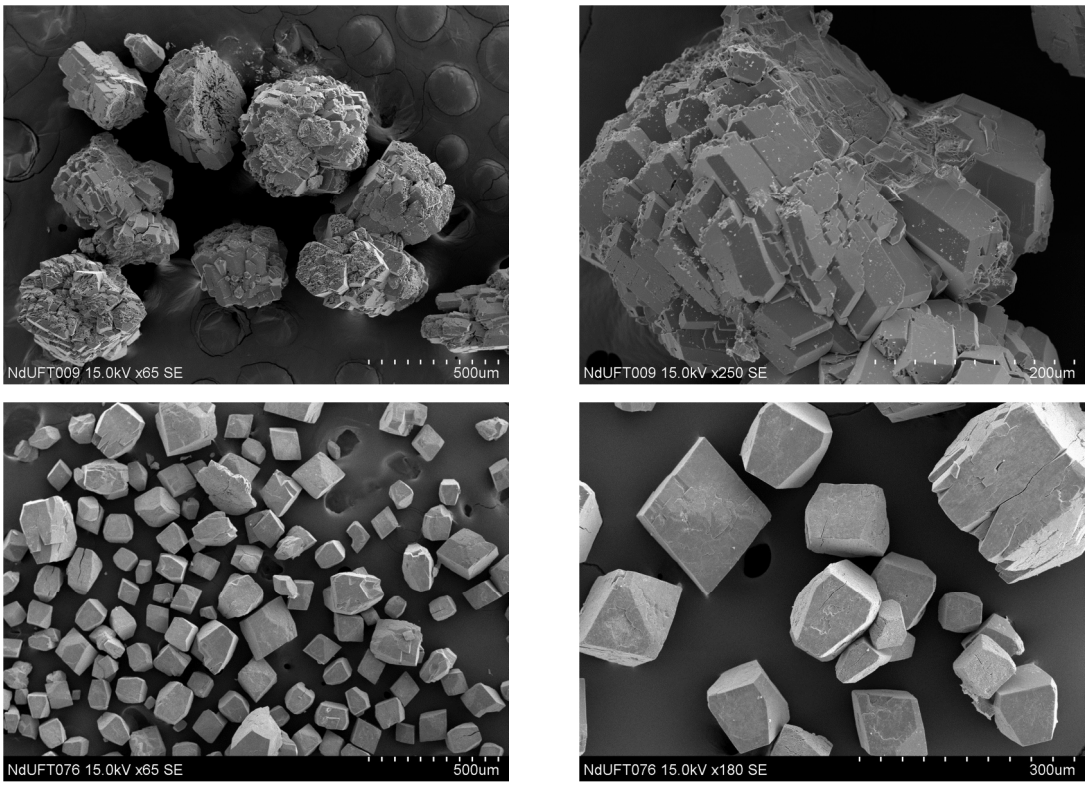

Figure VI.3.4 SEM images of the **NdUpht** phase obtained by traditional electric heating (top) and by microwave heating (bottom).

SEM examination of the two products revealed that for the one obtained by conventional electric heating the crystals are gathered into large conglomerates of 150-400 µm in size, while for the one obtained by microwave heating the crystals are discrete, well defined and multifaceted with sizes in the range of 50-250 µm (Figure VI.3.4).

The **CeUpyr** phase $[(UO_2)_3Ce_2(H_2O)_{12}(btec)_3]\cdot 5H_2O$ has been obtained by hydrothermally heating during 24 h at 150°C a mixture of 0.502 g (1 mmol) $UO_2(NO_3)_2\cdot 6H_2O$, 0.351 g (0.8 mmol) $Ce(NO_3)_3\cdot 6H_2O$, 0.132 g (0.5 mmol) 1,2,4,5-$C_6H_2(COOH)_4$, 1.2 ml solution 2M (2.4 mmol) NH_3 and 3.8 mL (211 mmol) H_2O. The solution pH after synthesis was 2.7. The obtained product was filtered off, washed with water and dried at room temperature. A synthesis temperature superior to 150°C favors the formation of $(U,Ce)O_2$ type oxide phases (fluorite type) and decreases the yield for the mixed U-Ce pyromellitate phase. As it can be observed in the reagents ratio based tendency diagram (Figure VI.3.5-left), the reagents ratio used for obtaining the pure **CeUpyr** mixed phase differs from the stoichiometric ratio of the phase. The main difference is in the ligands ratio, which has been reduced for avoiding phase segregation.

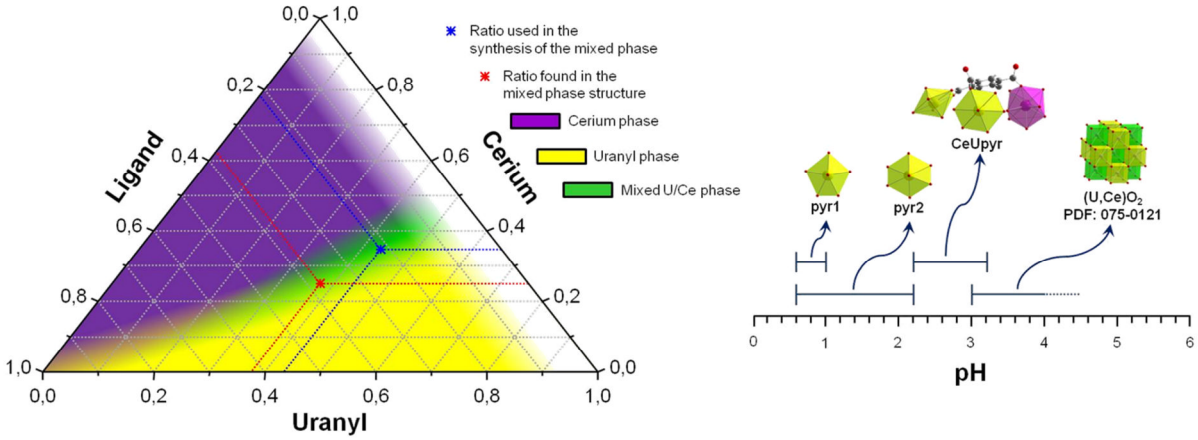

Figure VI.3.5 Phase tendency diagrams as a function of the reagents used ratio (left) and of the reaction pH (right) for the **CeUpyr** phase.

In the optimum conditions of reaction time, temperature and reagents ratio, the pH influence over the nature of the final products is the one illustrated in the pH phase diagram (Figure VI.3.5-right). At low pH (below 2.2), the cerium cations are remaining soluble, only pure uranium pyromellitates crystallizing. A high pH (above 3.0) favors the formation of MO_2 fluorite type oxide phases (where M = Ce or Ce,U). The optimum pH range for obtaining the mixed **CeUpyr** phase

is between 2.2 and 3.0. The SEM examination of the product revealed thin elongated plate crystallites with variable sizes (Figure VI.3.6).

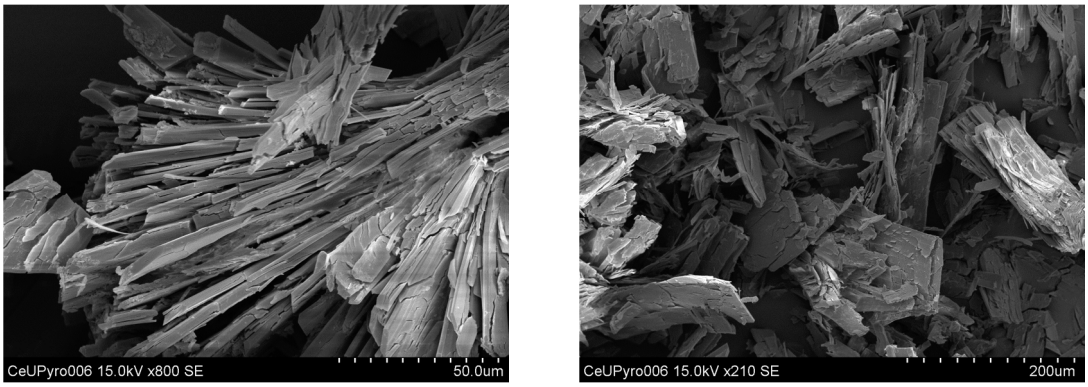

Figure VI.3.6 SEM images of the **CeUpyr** phase.

The **NdUpyr** phase $[(UO_2)_3Nd_2(H_2O)_{12}(btec)_3]\cdot 5H_2O$ has been obtained over a wide range of U/Nd ratios (0.6 to 1.1) but maintaining the total metal/ligand ratio above 2 (Figure VI.3.7-left). An increased ratio of the ligand favors the phase segregation resulting in mixtures of neodymium and uranyl pyromellitates. The used reagents ratio in the synthesis contains a larger amount of neodymium by comparison with the ratio given by the crystal structure of the phase, quantities of this cation being required to remain in solution. The optimum reaction time and temperature have been found to be 6 h and 150°C. The preferred decreased reaction time proves that the mixed phase is the kinetic one since a longer reaction time favored the formation of pure uranyl pyromellitates.

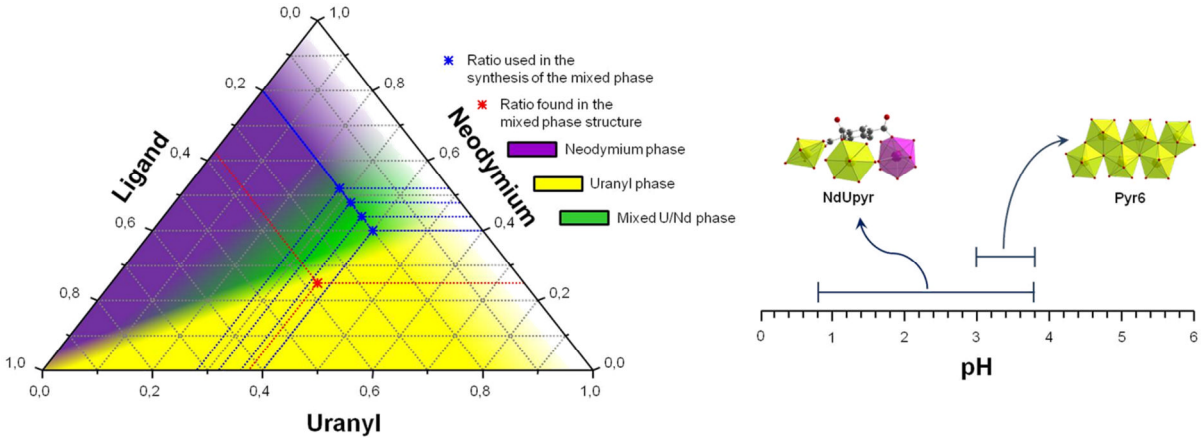

Figure VI.3.7 Phase tendency diagrams as a function of the reagents used ratio (left) and of the reaction pH (right) for the **NdUpyr** phase.

Under optimum reaction conditions, the **NdUpyr** mixed phase has been obtained over a wide range of pH, between 0.8 and 3.8 but starting from the pH value of 3.0 it has been obtained in mixture with the **pyr6** uranyl phase (Figure

VI.3.7-right). At pH values above 3.8 unidentified phases have been obtained, not possessing suitable crystal for structure determination.

Pure **NdUpyr** phase has been obtained by statically heating under hydrothermal conditions at 150° during 6 h a mixture of 0.502 g (1 mmol) $UO_2(NO_3)_2 \cdot 6H_2O$, 0.442 g (1.0 mmol) $Nd(NO_3)_3 \cdot 6H_2O$, 0.132 g (0.5 mmol) 1,2,4,5-$C_6H_2(COOH)_4$, 1.2 ml solution 2M (2.4 mmol) NH_3 and 3.8 mL (211 mmol) H_2O. The resulting product was then filtered off, washed with water and dried at room temperature. SEM examination of this product showed thin plate crystals with various sizes (Figure VI.3.8).

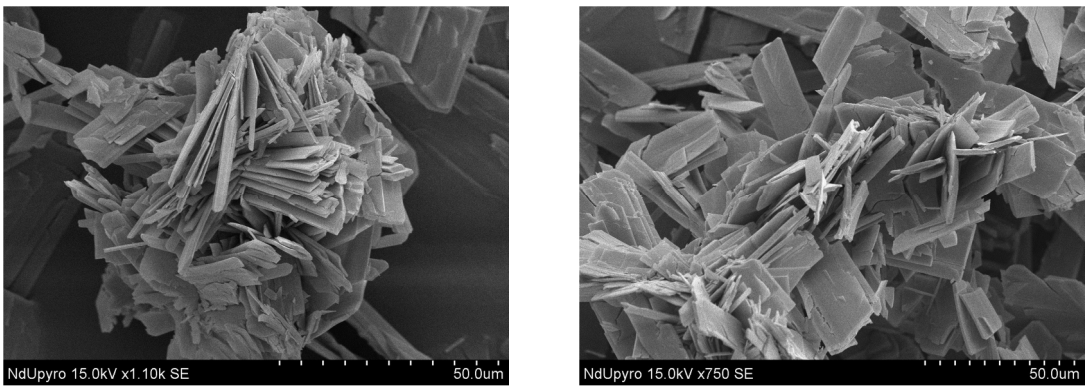

Figure VI.3.8 SEM pictures of the **NdUpyr** phase.

For the **CeUmel** phase ($[(UO_2)_2(OH)Ce(H_2O)_7(mel)] \cdot 5H_2O$) the optimum reaction time and temperature have been found to be 4 h and 150°C. The relatively short reaction time demonstrates fast formation kinetics for the mixed complex, while the low temperature suggests the reduced stability of the complex. The ratio of the used precursors in the synthesis of the pure **CeUmel** complex contains more lanthanide and less uranyl cations than the ratio given by the crystal structure (Figure VI.3.9-left). Pure mixed phase has been obtained maintaining the U/Ce ratio in the range of 4-4.7 and the total metal/ligand ratio above 2.3. Using these optimal conditions, at low pH, beneath 1.6, a mixture of two already mentioned in literature[2] phases has been obtained: one **Cemel** $[Ce_2(H_2O)_6(mel)]$ containing only Ce cations and the other **Umel** $[(UO_2)_3(H_2O)_6(mel)]_2 \cdot 11.5H_2O$ containing only uranyl cations. Reaching the pH of 2.8 and above, the MO_2 oxide phase begins to appear and increase in yield with the pH. The optimum pH for the synthesis of this phase is in the range 1.8-2.4 (Figure VI.3.9-right).

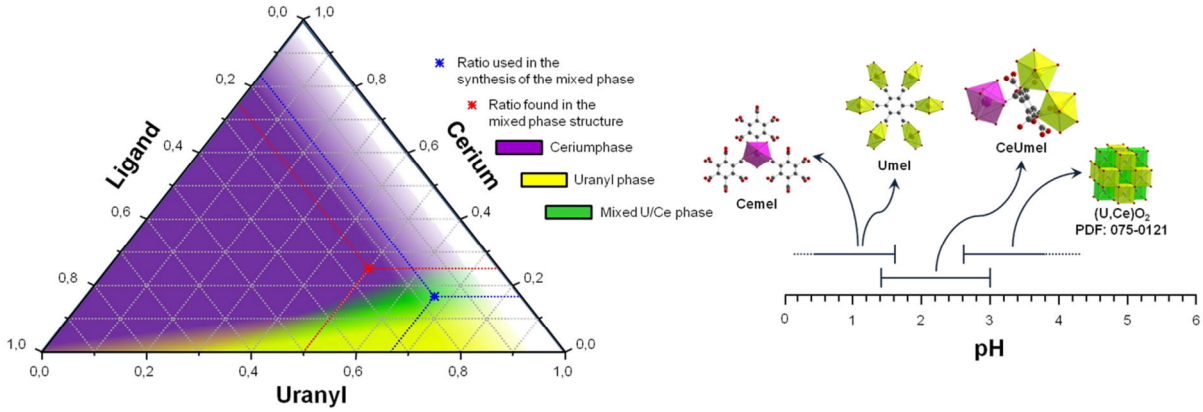

Figure VI.3.9 Phase tendency diagrams as a function of the reagents used ratio (left) and of the reaction pH (right) for the **CeUmel** phase.

Pure **CeUmel** phase has been obtained by statically heating under hydrothermal conditions at 150°C during 4 h a mixture of 0.502 g (1 mmol) $UO_2(NO_3)_2 \cdot 6H_2O$, 0.100 g (0.23 mmol) $Ce(NO_3)_3 \cdot 6H_2O$, 0.085 g (0.25 mmol) $C_6(COOH)_6$, 0.3 ml solution 4M (1.2 mmol) NaOH and 5 mL (278 mmol) H_2O. The solution pH after synthesis was 1.8.

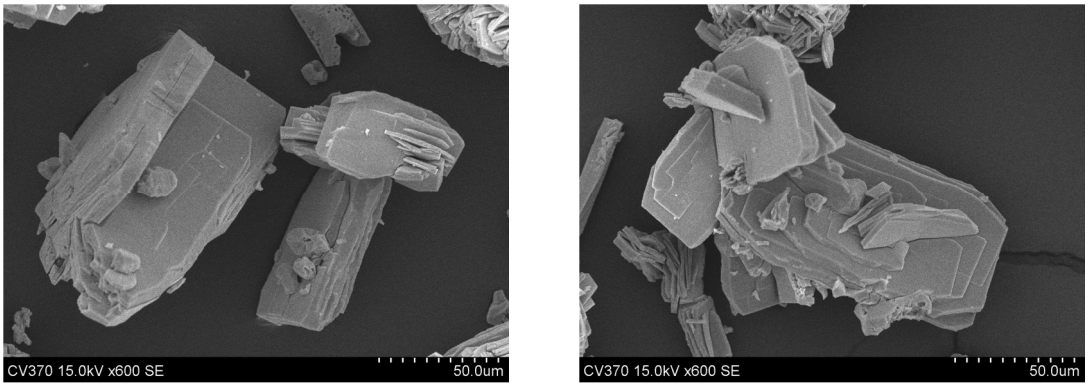

Figure VI.3.10 SEM pictures of the **CeUmel** phase.

The resulting product was then filtered off, washed with water and dried at room temperature. SEM examination of the obtained product revealed conglomerates of 50-100 µm in size containing stacked plate like shaped crystals (Figure VI.3.10).

The **NdUmel** phase ($[(UO_2)_2(OH)Nd(H_2O)_7(mel)] \cdot 5H_2O$) has been obtained at the same temperature as the Ce containing one (150°C) but during a longer reaction time (24 h) suggesting a slower reaction kinetics. The precursors ratio used in the synthesis is close to that given by the crystal structure. Pure **NdUmel** phase has been obtained using a U/Nd ratio in the 1.8-2.6 range and maintaining the metal/ligand ratio above 2.3 (Figure VI.3.11-left). In these conditions, at low pH (below 1) two previously mentioned phases are appearing: the pure

neodymium phase **Ndmel** (similar to **Cemel**) and the pure uranyl phase **Umel**[2]. At an intermediate pH, between 1 and 1.8 the mixed **NdUmel** phase is obtained and furthermore increasing the pH, unidentified phases begin to appear (Figure VI.3.11).

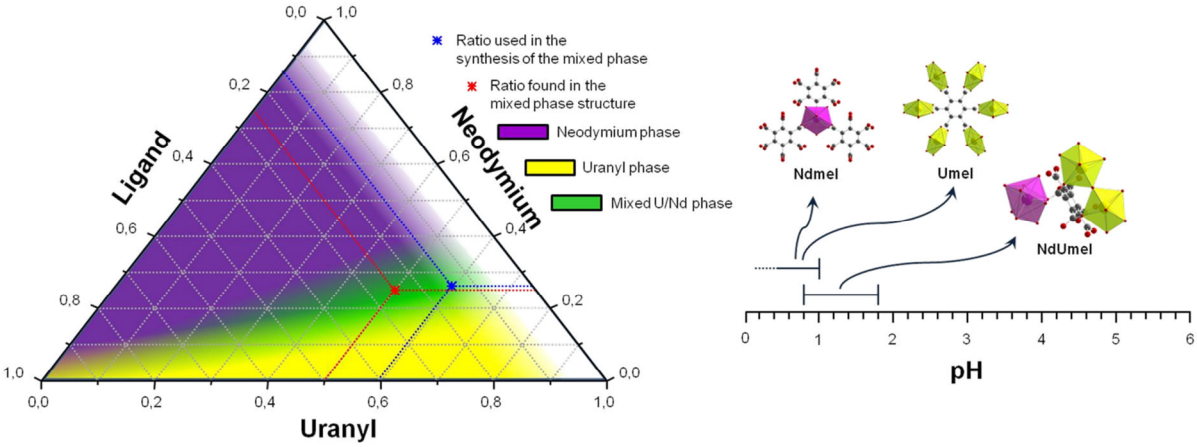

Figure VI.3.11 Phase tendency diagrams as a function of the reagents used ratio (left) and of the reaction pH (right) for the **NdUmel** phase.

Pure phase of **NdUmel** has been synthesized by statically heating under hydrothermal conditions at 150°C during 24 h a mixture of 0.502 g (1 mmol) $UO_2(NO_3)_2 \cdot 6H_2O$, 0.200 g (0.46 mmol) $Nd(NO_3)_3 \cdot 6H_2O$, 0.085 g (0.25 mmol) $C_6(COOH)_6$, 0.1 ml solution 4M (0.4 mmol) NaOH and 5 mL (278 mmol) H_2O. The solution final pH was 0.9. The obtained product has been filtered off, washed with water and dried at room temperature. SEM investigation on this product revealed large blocks of conglomerate crystals, having 0.2 to 1 mm in size (Figure VI.3.12).

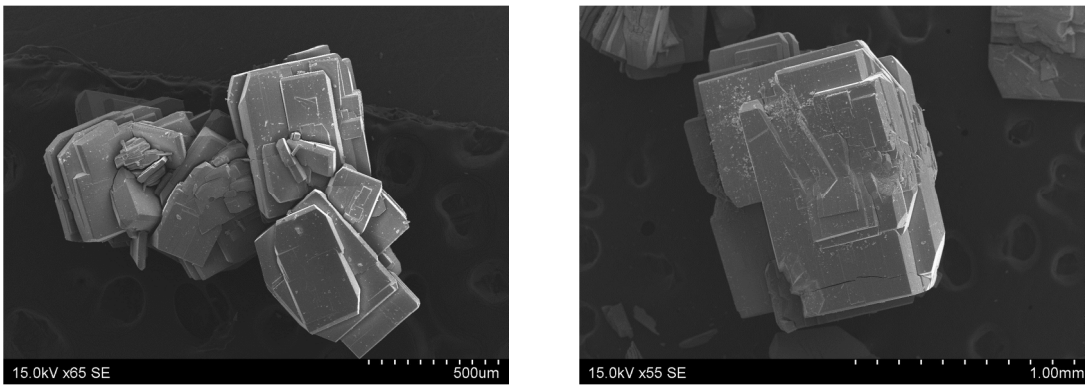

Figure VI.3.12 SEM pictures of the **NdUmel** phase.

VI.4 . Thermal characterization

The thermal stability and heating behavior of the different mixed uranyl-lanthanide phases have been studied by thermogravimetric analysis and *in situ* high temperature powder X-ray diffraction up to 800°C (upper limit of our diffractometer apparatus) followed by *ex situ* PXRD on the calcined products at 1400-1500°C.

The thermogravimetric curve of **CeUpht** phase (Figure VI.4.1-left) shows a number of five loss events. First three weight loss steps occurring at 35°C (1.7%), 140°C (1.7%) and 205°C (3.2%) have been assigned to the successive departure of the free and coordinating water molecules. They cumulate a total weight loss of 6.6%, which is in agreement with the calculated one of 7.0% corresponding to the loss of the eight water molecules. The fourth step, occurring at 310°C and presenting a weight loss of only 1% has been assigned to the loss of the ammonium cation. The weight loss corresponds with the calculated one of 0.9% for the loss of one ammonium cation per formula unit. The fifth step, corresponding to the burning of the organic ligand at 420°C, measures a weight loss of 28.5%, (calc.: 31.7%). The remaining residue weights 63.9% and corresponds to the stoichiometric mixture of 4/3 U_3O_8 and CeO_2 (calc.: 65.9%). The heat flow curve presents four endothermic peaks corresponding to the loss of the water molecules and the ammonium cation, the fourth having a very low intensity and one intense exothermic peak that corresponds to the degradation of the organic ligand.

The thermodiffraction diagram (Figure VI.4.1-right) indicates that the **CeUpht** phase is quite unstable upon heating, since the PXRD patterns of the complex are visible up to 60°C only. It is transformed into an intermediate form above 60°C, which is stable up to 180°C where it passes into an almost amorphous phase, only one peak appearing at 2θ value of 7°. This phase is stable up to 340°C where it passes into a total amorphous phase. Starting from 500°C the final oxide form begins to crystallize and has been identified (from PXRD) as α'-U_3O_8 at 800°C as well as after cooling down to room temperature. The presence of CeO_2 cannot be observed by PXRD in this case.

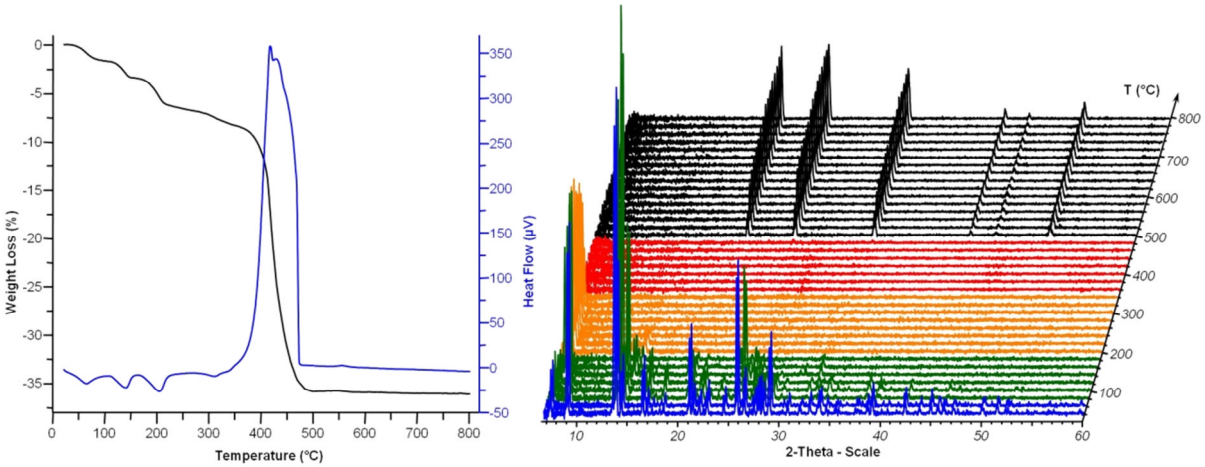

Figure VI.4.1 Thermogravimetric analysis (left) and thermodiffraction diagram (right) for the **CeUpht** phase.

The presence of cerium in the final residue has been evidenced by calcinating the sample at 1400°C in air. The obtained residue has been identified by PXRD as being $Ce_{0.5}U_{0.5}O_2$ fluorite type mixed oxide (PDF No. 01-075-0127).

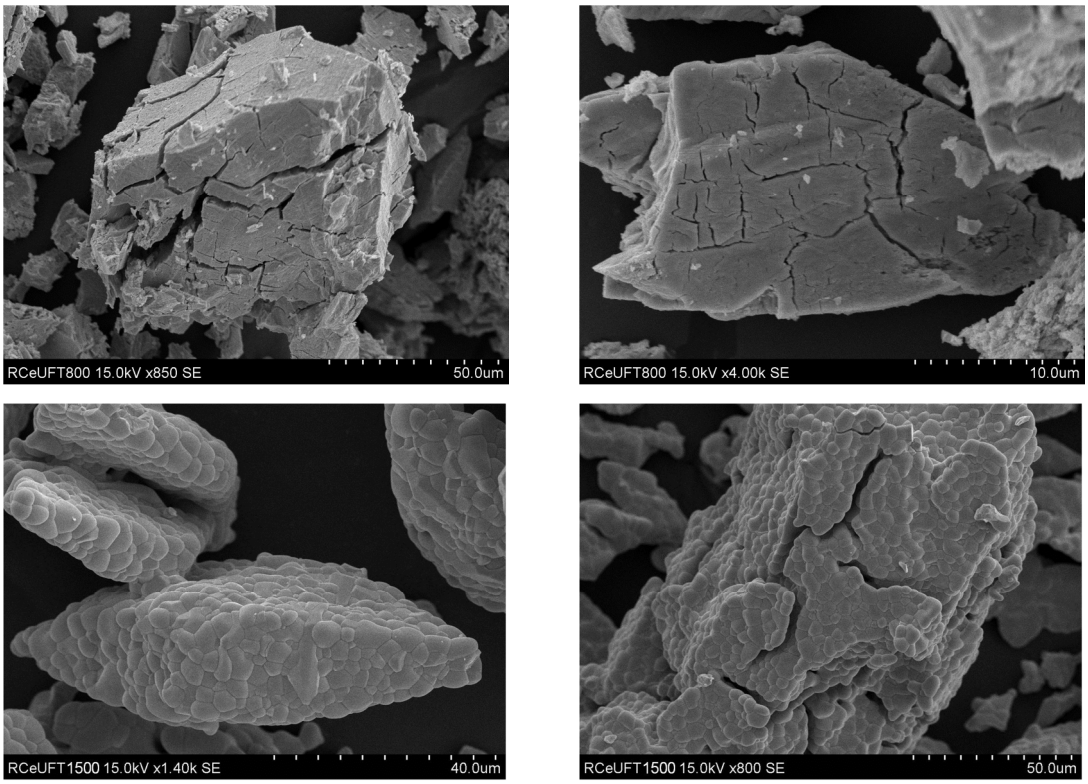

Figure VI.4.2 SEM images of the **CeUpht** residue calcined at 800°C (top) and 1500°C (bottom).

In the absence of cerium, a pure uranyl carboxylate by burning in air atmosphere always gives as residue the U_3O_8 oxide form and not the reduced UO_2 form. For confirmation, on both residues (obtained at 800°C and at 1500°C) ICP-AES (Inductively Coupled Plasma Atomic Emission Spectrometry)

investigation has been conducted and gave the composition $Ce_{0.77}U_{0.23}O_2$. The results confirmed the U/Ce ratio of 4/1 given by the crystal structure.

Also, the two residues, calcined at 800 and 1500°C have been investigated by SEM and revealed crystals with same morphology as the parent compound. For the residue calcined at 1500°C, crystallites of 4 to 10 µm in size and typical flat domains of $(U,Ce)O_2$ fluorite phase are visible (Figure VI.4.2).

The thermogravimetric curve of **NdUpht** (Figure VI.4.3-left) presents multiple weight loss steps, from which the first three events have been assigned to the successive departures of water molecules from the structure. These three steps occur at 35, 105 and 180°C and correspond to a total weight loss of 7.0%. The calculated weight loss for the departure of the seven water molecules of the structure is 6.1%. The difference from the experimental value could be explained by the adsorbed attached water molecules, which are removed in the first degradation step at 36°C. The step corresponding to the possible loss of the ammonium cation is a long process, occurring between 210 and 300°C (obs.: 1.2%; calc.: 0.9%). The organic ligand starts to decompose at 320°C, with a weight loss of 27.2%. The calculated weight loss value for the decomposition of the four ligand molecules is of 31.9%. The disagreement between the calculated and experimental weight loss values for this step could be explained by the partial decomposition of the ligand with the transient formation of carbonate species. These species are stable up to 575°C when the last decomposition process occurs, measuring a weight loss of 1.7%. The remaining residue weight is 63.0% and close to the calculated value of 62.8% for a stoichiometric ratio of 4/3 U_3O_8 and 1/2 Nd_2O_3. The PXRD of the TGA residue showed only the presence of the crystalline U_3O_8 oxide (PDF No. 01-074-2102). The heat flow curve exhibits three low intensity endothermic peaks corresponding to the water release processes and one intense exothermic peak corresponding to the decomposition of the organic ligand. The likely processes of ammonium cations removal and degradation of the carbonate species take place without thermal effect.

The thermodiffraction diagram (Figure VI.4.3-right) shows that the **NdUpht** phase is stable up to 80°C where it is transformed into a crystalline intermediate form. This form at 140°C passes into an almost amorphous phase

presenting one single diffraction peak at 7° (2θ). This phase persists up to 340°C where it passes into a total amorphous phase. Starting with 500°C, the final oxide form begins to crystallize, the diffraction peaks increasing in intensity with the temperature. The residue has been identified by PXRD to be α-U_3O_8 (PDF No. 00-031-1424).

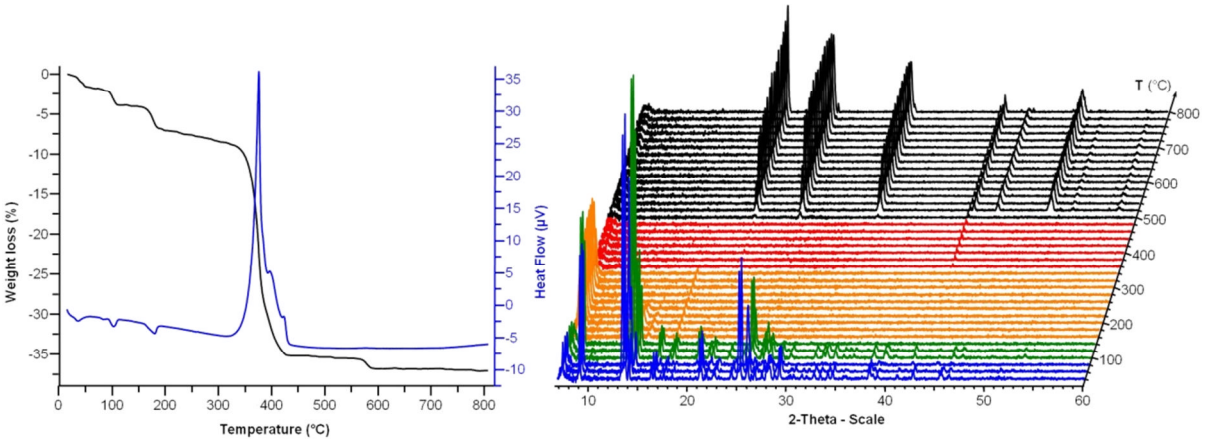

Figure VI.4.3 Thermogravimetric analysis (left) and thermodiffraction diagram (right) for the NdUpht phase.

Increasing the degradation temperature up to 1400°C, the residue has been identified as $Nd_{2.81}U_{1.19}O_{7.3}$ (PDF No. 01-075-0089) fluorite type mixed oxide. ICP-AES analyzes conducted on both of the residues obtained at 800 and 1400°C have confirmed the 4/1 cationic ratio between uranium and neodymium, with a composition of $U_{0.79}Nd_{0.21}O_{2-\delta}$. SEM investigation of the residue calcined at 1400°C revealed crystals with close morphologies to those of the initial phase and presenting crystallites with sizes up to 10 µm with typical flat grains of $(U,Nd)O_{2-\delta}$ fluorite phase (Figure VI.4.4).

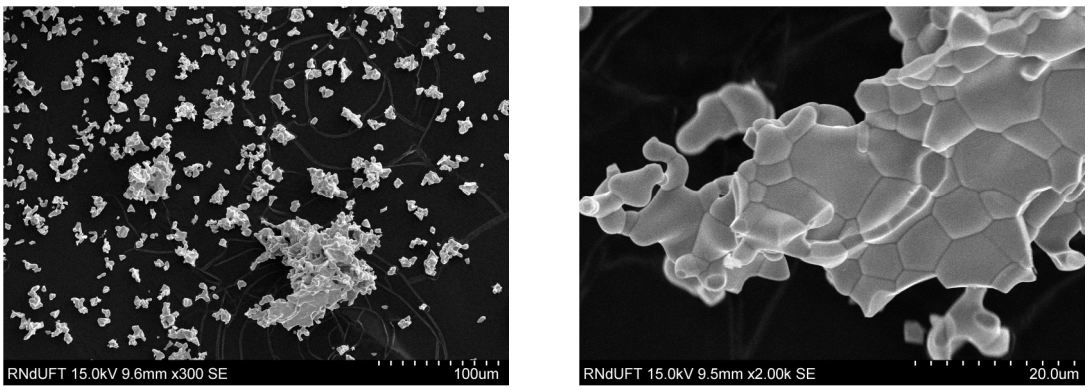

Figure VI.4.4 SEM images of the **NdUpht** phase after calcination at 1400°C.

The **CeUpyr** phase presents on the TG curve (Figure VI.4.5-left) three major degradation steps. The first two steps occurring at 95 and 250°C,

corresponds to a total weight loss of 15.8% (calculated value: 14.3% for the loss of all water molecules). The third and last degradation step occurs at 400°C and measures a weight loss of 29.0%, which corresponds to the calculated value of 30.5% for the loss of three ligand molecules. The remaining residue is 55.2%, and agrees well with the calculated one of 55.3% for the stoichiometric ratio of U_3O_8/ $2CeO_2$. The heat flow curve exhibits two endothermic peaks corresponding to the two water release processes and one intense exothermic peak corresponding to the decomposition of the organic ligand. The TG residue has been identified by PXRD to be a mixture of U_3O_8 (PDF No. 01-074-2102) and CeO_2 (PDF No. 00-043-1002).

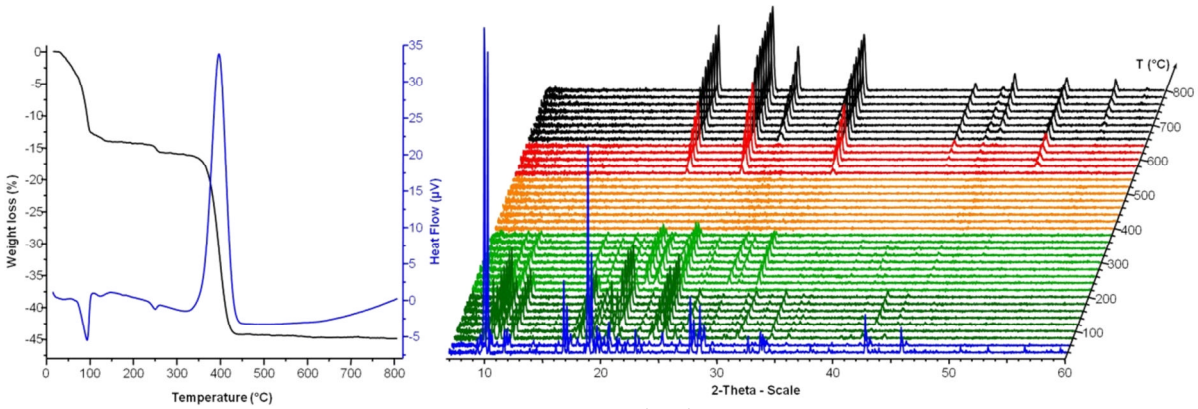

Figure VI.4.5 Thermogravimetric analysis (left) and thermodiffraction diagram (right) for the **CeUpyr** phase.

The thermodiffraction diagram (Figure VI.4.5-right) shows that the initial CeUpyr phase is stable only up to 60°C, and then transformed into a first well crystalline dehydrated form. This intermediate phase is stable up to 200°C, where is transformed into a less crystalline phase. From 400°C a completely amorphous phase appears and persists up to 560°C, where a first oxide form U3O8 (PDF No. 01-089-4906) begins to crystallize. The second oxide begins to crystallize at 640°C and has been identified as CeO2 (PDF No. 00-043-1002).

The mixed uranium-cerium oxide has been obtained by calcination the **CeUpyr** phase at 1400°C, the PXRD pattern of the resulted phase matching the simulated one of the $Ce_{0.66}U_{0.34}O_2$ (PDF No. 01-075-0124) mixed oxide. The U/Ce ratio in both calcination residues obtained at 800 and 1400°C has proven to be identical by ICP-AES analyzes, to the one in the parent complex (measured composition $U_{0.57}Ce_{0.43}O_2$). SEM examination of the calcined sample showed

crystals of 20 to 60 µm in size containing crystalline grains with sizes up to 10 µm (Figure VI.4.6), with flat growth domains of fluorite type.

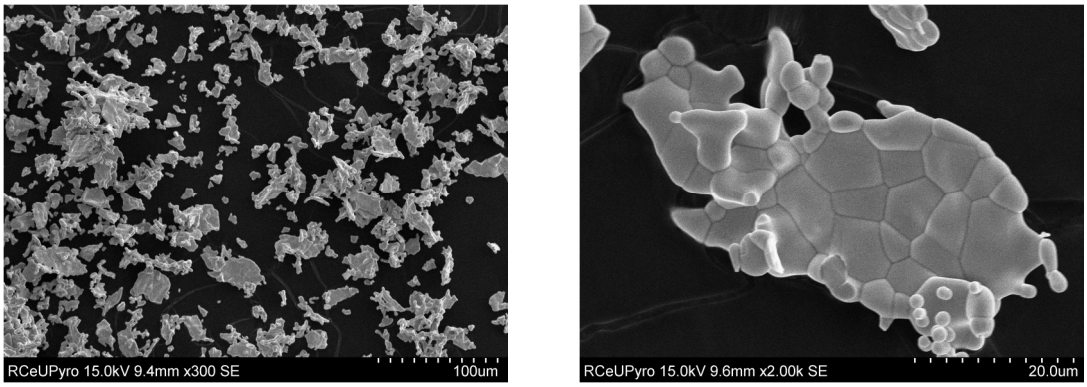

Figure VI.4.6 SEM images of the **CeUpyr** phase after calcination at 1400°C.

The thermogravimetric curve of **NdUpyr** phase (Figure VI.4.7-left) exhibits four degradation steps. The first two events, occurring at 85 and 260°C (obs.: 16%), have been assigned to the loss of the water molecules of the structure. The calculated weight loss for these two steps is 14.2%. The difference of 1.8% between the experimental and calculated values can be explained by a certain amount of adsorbed water molecules. The third step, occurring at 410°C and measuring a weight loss of 29.5% corresponds to the decomposition of the organic ligand. The calculated weight loss value for the degradation of the three ligand molecules is 31.1%. The difference between the calculated and experimental weight loss of this process could be explained by the formation of carbonate species during the degradation of the ligand. These species, in this case, are stable up to 580°C when the fourth degradation step occurs. The carbonate elimination measures a weight loss of 1.1%. At 800°C, the resulting residue, is 53.4%, and agrees well with the calculated one of 54.7% for the stoichiometric ratio 1:1 of U_3O_8 and Nd_2O_3. As expected, the heat flow presents two endothermic peaks corresponding to the water removal processes and one intense exothermic peak corresponding to the ligand decomposition. The last process of carbonate species removal takes place without a major thermal effect.

The thermodiffraction diagram (Figure VI.4.7-right) shows that the **NdUpyr** phase is unstable, passing into a dehydrated at 60°C but still crystalline intermediate. This intermediate form is stable up to 220°C where is transformed into a second phase with lesser crystallinity. The latter one is stable up to 380°C

where it passes into a total amorphous phase. Starting from 560°C the first oxide phase begins to crystallize. This phase has been identified as a mixture between the U_3O_8 (PDF No. 01-076-1851) uranium oxide and the $Nd_{2.4}U_{1.6}O_{7.87}$ (PDF No. 00-031-1424) fluorite type mixed oxide. At 780°C the uranium oxide is transformed into the α-U_3O_8 form (PDF No. 00-031-1424).

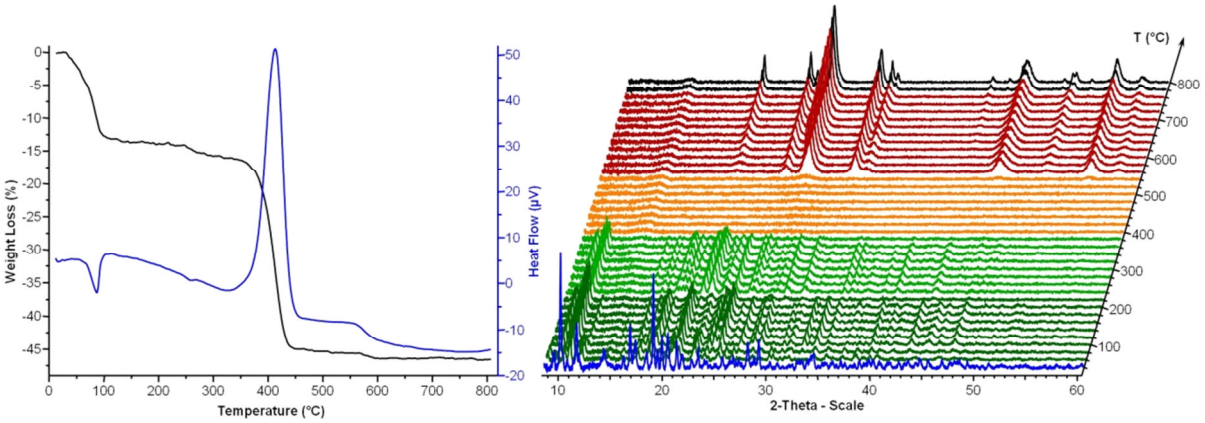

Figure VI.4.7 Thermogravimetric analysis (left) and thermodiffraction diagram (right) for the **NdUpyr** phase.

The **NdUpyr** sample calcined at 1400°C gives the pure fluorite type mixed oxide, the PXRD pattern of this phase matching the simulated one for the $Nd_3UO_{7.17}$ (PDF No. 01-075-0090). The Nd/U ratio of the initial complex has been found also in both of the calcination residues at 800 and 1400°C (measured composition $U_{0.55}Nd_{0.45}O_{2-\delta}$).

SEM examination (Figure VI.4.8) of the calcination residue revealed crystals of different sizes with close morphology to the one of the initial phase, presenting crystallites grown up to 10 µm in size with flat domains of fluorite type oxide.

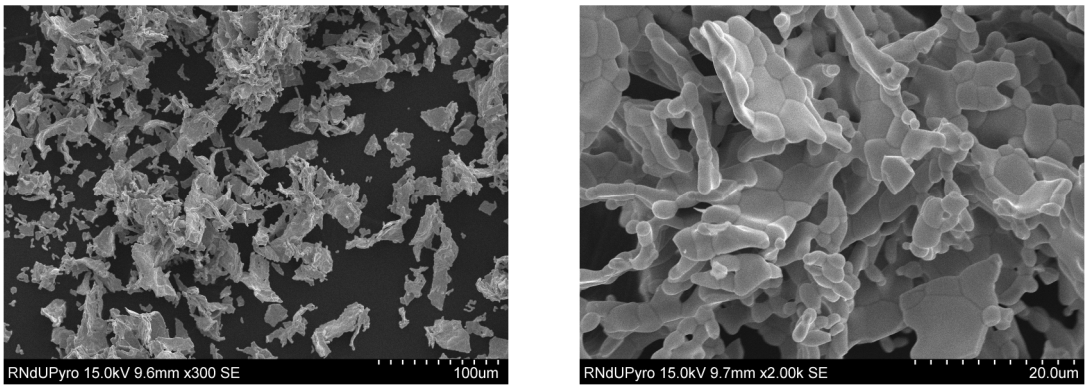

Figure VI.4.8 SEM images of the **NdUpyr** phase after calcination at 1400°C.

The thermogravimetric curve of the **CeUmel** phase (Figure VI.4.9-left) presents two major weight loss steps. The first event has been assigned to a continuous process of water removal with a weight loss of 16.8%. This value is in good agreement with the calculated one of 17.3% corresponding to the removal water molecules. The heat flow curve for this step presents four low intensity endothermic peaks, suggesting that the dehydration of the complex is a multistep process. The second degradation step measures a weight loss of 24.0% and corresponds to the total decomposition of the organic ligand. The calculated weight loss for this process is 23.9% and corresponds to the loss of one ligand molecule. The heat flow curve indicates by the presence of three exothermic peaks that the ligand's decomposition is a three step process. Two of them are minor processes, occur at 330°C and 540°C and represent an early partial ligand decomposition and respectively the removal of carbonate species. The main decomposition process takes place at 390°C when almost all the mass of the ligand molecules is lost, some carbonate species remaining attached to the metal centers. At 800°C the remaining residue is 40.8%, which is in good agreement with the calculated value of 41.3% corresponding to the stoichiometric ratio of 2/3 to 1 between the U_3O_8 and CeO_2 oxides.

The thermodiffraction diagram (Figure VI.4.9-right) shows that the **CeUmel** complex is stable up to 60°C. From 60 to 200°C the sample, loosing water molecules passes through numerous crystalline intermediate phases. From 200 to 500°C the sample is completely amorphous, at 520°C the final oxide phase beginning to crystallize. At 800°C the residue has been identified as a mixture of U_3O_8 (PDF No. 01-074-0562) and CeO_2 (PDF No. 00-002-1306).

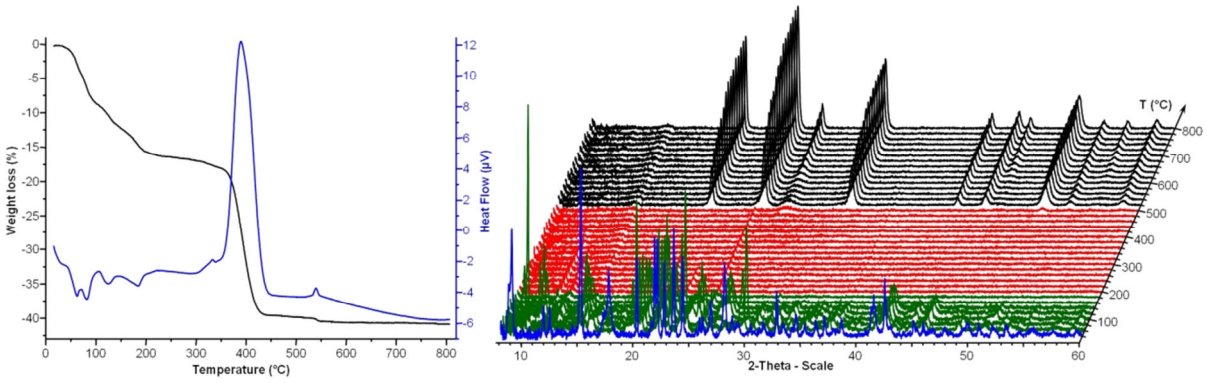

Figure VI.4.9 Thermogravimetric analysis (left) and thermodiffraction diagram (right) for the **CeUmel** phase.

The fluorite type Ce/U mixed oxide has been obtained by calcination the **CeUmel** phase at 1400°C. The resulting product has been identified by PXRD pattern matching as $Ce_{0.66}U_{0.34}O_2$ (PDF No. 01-075-0124) mixed oxide. Both products, calcined at 800 and 1400°C gave, by the ICP-AES analyses, appropriate U/Ce ratio with the one of the **CeUmel** crystal structure (measured composition $U_{0.67}Ce_{0.33}O_2$). SEM investigation of the product calcined at 1400°C revealed crystals with sizes in the range 10 - 80 µm presenting crystallites grown up to 18 µm in size (Figure VI.4.10) with the expected grains of fluorite type oxide.

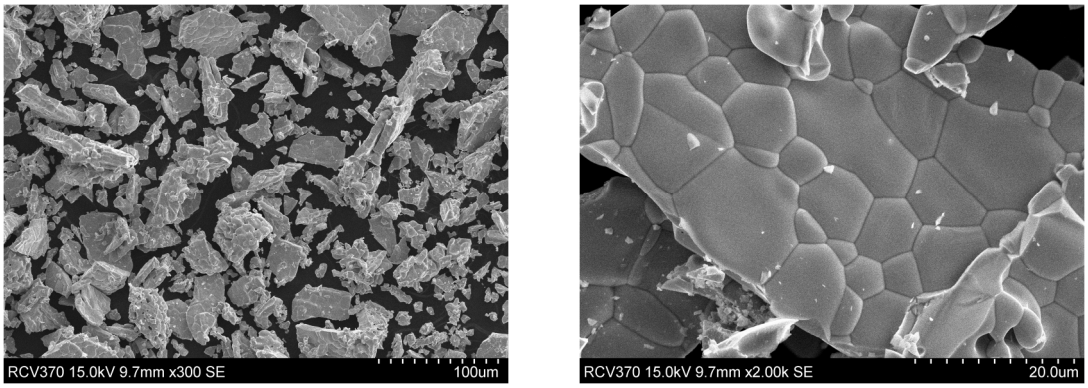

Figure VI.4.10 SEM images of the **CeUmel** phase after calcination at 1400°C.

The thermogravimetric analysis of **NdUmel** phase (Figure VI.4.11-left) shows two major degradation steps. The first step is a continuous of water removal from structure which finishes at around 230°C. It is a weight loss of 15.7% (calc.: 17.2%) corresponding the removal of water molecules. The difference between these two values indicates that the complex would be already partially dehydrated before the analysis.

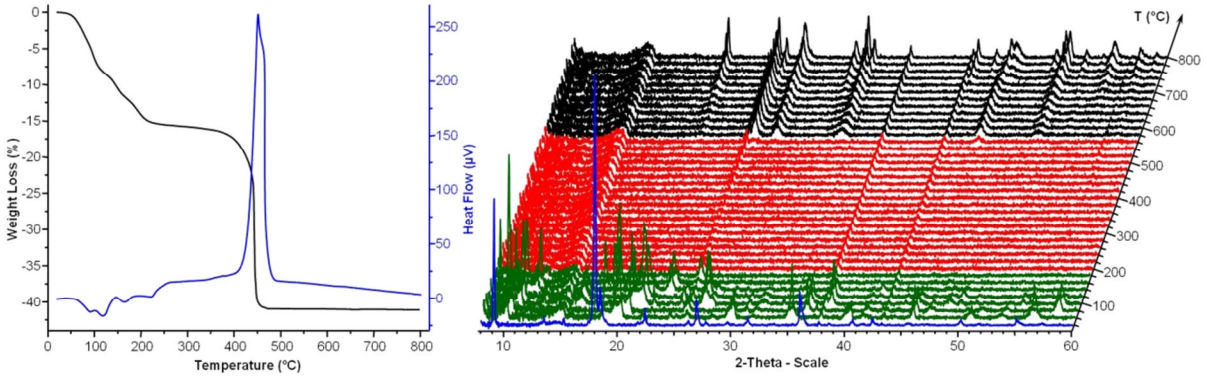

Figure VI.4.11 Thermogravimetric analysis (left) and thermodiffraction diagram (right) for the **NdUmel** phase.

The second degradation step occurs at 450°C and corresponds to the degradation of the organic ligand. It measures a weight loss of 25.3%, which is in

good agreement with the calculated value for the removal of one ligand molecule. The residue obtained after degradation is 41% corresponding to the calculated value of 41.8% for a stoichiometric ratio of $2/3U_3O_8$: $1/2Nd_2O_3$

The thermodiffraction diagram (Figure VI.4.11-right) shows that the **NdUmel** complex is stable up to 60°C. From 60 to 200°C the sample, loosing water molecules passes through numerous crystalline intermediate phases. From 200 to 560°C the sample is completely amorphous, and at 580°C the final oxide phase begins to crystallize. At 800°C the residue has been identified as a mixture of U_3O_8 (PDF No. 01-089-4906) and Nd_2O_3 (PDF No. 03-065-3184).

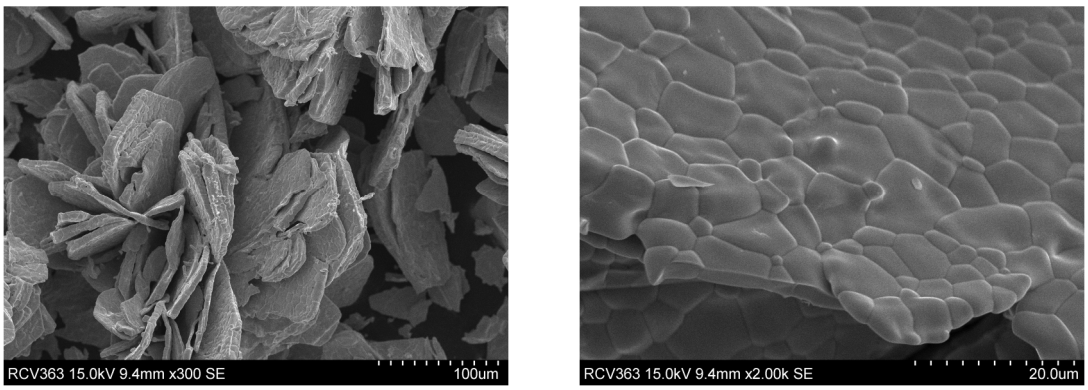

Figure VI.4.12 SEM images of the **NdUmel** phase after calcination at 1400°C.

The fluorite type Nd/U mixed oxide has been obtained by calcination of the NdUmel phase at 1400°C. The resulting product has been identified by PXRD pattern matching as Nd3UO7.17 (PDF No. 01-075-0090) mixed oxide. Both products, calcined at 800 and 1400°C gave in the ICP-AES analyses the same U/Nd ratio as the one of the NdUmel crystal structure. SEM investigation of the product calcined at 1400°C revealed crystals with similar morphology as the crystals of the parent complex presenting crystallites grown up to 15 μm in size (Figure VI.4.12).

VI.5 . Spectral characterization

Infrared Spectroscopy

Infrared spectra of **CeUpht** and **NdUpht** phases (Figure VI.5.1) show a very broad absorption band in the 3650-3000 cm^{-1} range, indicating the presence of hydrogen bond type interactions between the coordinating water molecules, free water molecules and ammonium groups. In this region there have been identified two broad absorption maxima; first around 3405 cm^{-1} being assigned to the ν_{asym}(H-O-H) vibration and the second at 3200 cm^{-1} belonging to the ν_{sym}(H-O-H). Also the low intensity peak present at 1630 cm^{-1} could belong to the δ(H-O-H) vibration.

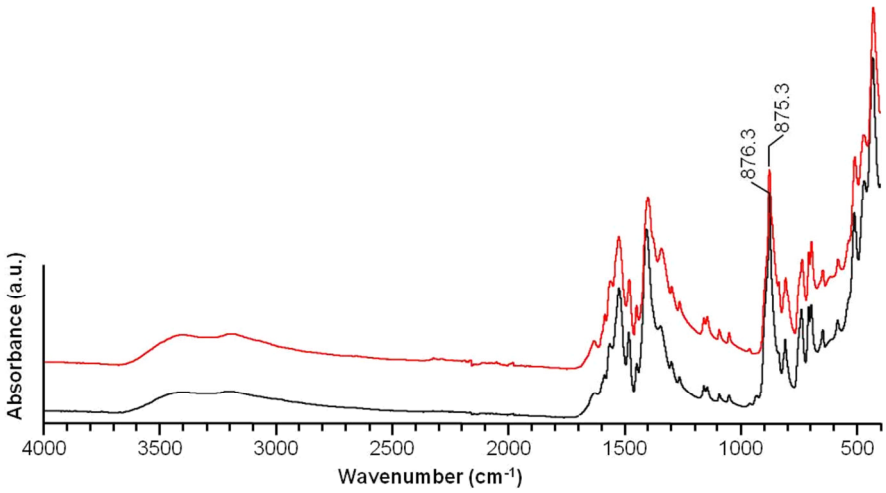

Figure VI.5.1 Infrared spectra of the **CeUpht** (red) and **NdUpht** (black) compounds.

In the same region, the ν(C=O) vibration belonging to a non coordinating carboxylate group of the ligand, can be overlapped with the δ(H-O-H) vibration. The COO stretching vibrations of the uranyl coordinating carboxylate groups have been observed in the region 1560-1340 cm-1; the vasym(COO) has been attributed to the peak from 1523 cm-1 and the vsym(COO) has been found as a doublet having maxima at 1399 and 1377 cm-1. The low intensity peaks present in the region 1600-1000 cm-1 have been assigned to the ν(CC) and δ(CH) benzene ring vibrations.

The uranyl related vibrations give IR absorbance in the region below

940 cm-1. The intense peak having maxima around 876 cm-1 has been assigned to the vasym(U=O).

The infrared spectra of **CeUpyr** and **NdUpyr** phases (Figure VI.5.2) present a very broad, low intensity band in the range 3680-2800 cm^{-1} having two maxima, first around 3526 cm^{-1} being assigned to the ν_{asym}(H-O-H) and the second at 3366 cm^{-1} corresponding to the symmetrical stretching vibration ν_{sym}(H-O-H). The δ type vibration of the water molecules should be observed around 1620 cm^{-1} but apparently it is overlapped with the ν(C=O) vibration of free carboxylate functions having IR absorption maximum at 1614 cm^{-1}. Other ligand related vibrations have been identified in the region 1100-1700 cm^{-1}. The ν_{asym}(COO) vibration is centered at 1524 cm^{-1} and has two maxima at 1542 and 1496 cm^{-1}. The ν_{sym}(COO) vibration is centered at 1360 cm^{-1} and also has two peaks at 1360 and 1325 cm^{-1}.

The uranyl related vibration and all other metal-oxygen vibrations are appearing in the IR spectrum below 960 cm^{-1}. In this region it has been found the ν_{asym}(U=O) vibration, giving absorption in the region of 913 cm^{-1}.

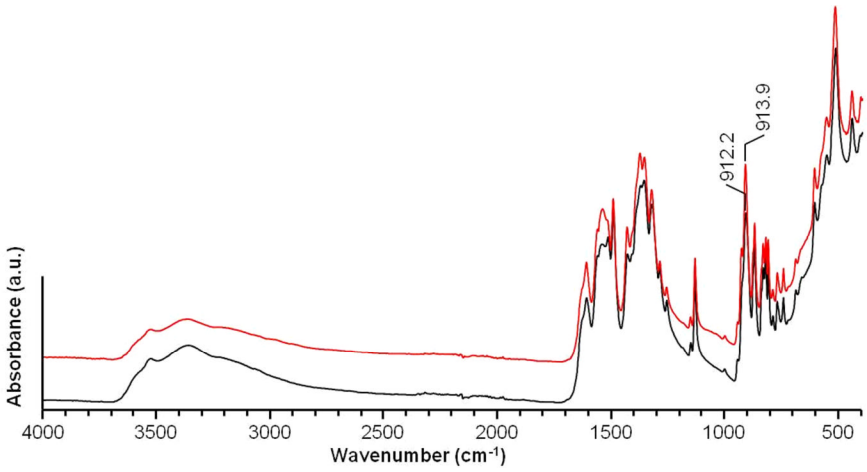

Figure VI.5.2 Infrared spectra of the **CeUpyr** (red) and **NdUpyr** (black) compounds.

The infrared spectra of **CeUmel** and **NdUmel** present a very broad, low intensity band in the range 3700-2800 cm^{-1} having several maxima, first around 3500 cm^{-1} assigned to the ν_{asym}(H—O—H) and the second at 3200 cm^{-1} corresponding to the symmetrical stretching vibration ν_{sym}(H—O—H). The vibration bands around 1600 cm^{-1} (ν_{asym} C=O) and 1300 cm^{-1} (ν_{sym} C=O) are assigned to carboxylate functions linked to uranyl and lanthanide cations. Other

vibration modes of the ligand are also localized in the range 1538-1470 cm^{-1} (ν C—C).

The asymmetric vibration of the double uranyl bond is located at 913.9 cm^{-1} and 911 cm^{-1} for **CeUmel** and **NdUmel** phase, respectively.

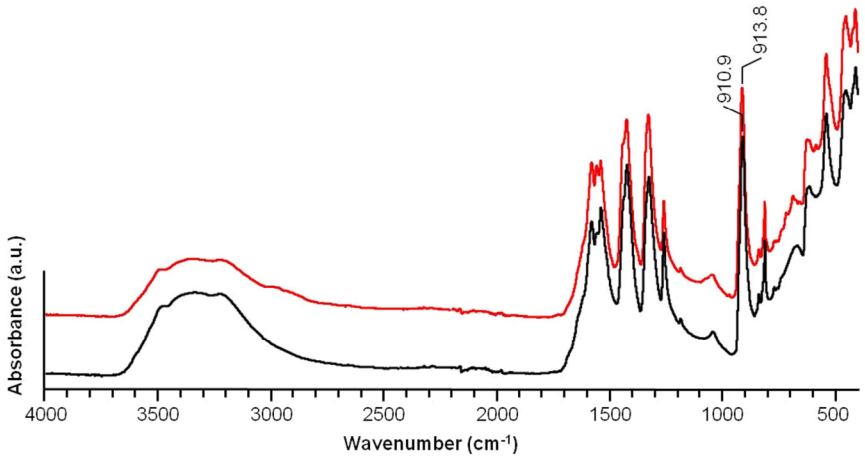

Figure VI.5.3 Infrared spectra of the **CeUmel** (red) and **NdUmel** (black) compounds.

Applying the empirical equation[7] that relate the U=O bond length with the position of the corresponding IR absorption peak, good bond length correlations have been obtained by comparison with the values obtained from single crystal X-ray diffraction analyses. The results have been summed in Table VI.5.1.

Table VI.5.1 Correlation between the U=O bond length values obtained by X-ray data refinement and by IR spectroscopy.

Compound	X-ray		IR	
	Bond	Bond length (Å)	Peak position (cm^{-1})	Bond length (Å)
CeUpht	U1-O1u	1.73(1)	899	1.79
	U2-O2u	1.72(1)	889	1.79
	U3-O31u	1.779(2)	876	1.80
	U3-O32u	1.77(1)	862	1.81
NdUpht	U1-O1u	1.76(1)	899	1.79
	U2-O2u	1.76(1)	889	1.79
	U3-O31u	1.76(1)	875	1.80
	U3-O32u	1.79(1)	863	1.81
CeUpyr	U1-O11u	1.764(5)	949	1.75
	U2-O21u	1.757(4)	933	1.76
	U2-O22u	1.780(4)	914	1.78
NdUpyr	U1-O11u	1.751(5)	949	1.75
	U2-O21u	1.770(4)	931	1.76
	U2-O22u	1.767(4)	912	1.78
CeUmel	U1-O12u	1.782(7)	929	1.76
	U1-O13u	1.781(6)	913	1.77
	U2-O21u	1.764(6)	911	1.78
	U2-O22u	1.764(6)		
NdUmel	U1-O12u	1.777(6)	928	1.76
	U1-O13u	1.766(5)	915	1.77
	U2-O21u	1.789(6)	910	1.78
	U2-O22u	1.769(5)		

Fluorescence Spectroscopy

The fluorescence experiments have been conducted at room temperature under excitation at 365 nm. The emission spectra have been recorded in the 440-640 nm wavelength domain. The emission spectrum of uranyl nitrate hexahydrate has been used as comparative element.

Because of the tetrameric uranyl unit present in the structures of the **LnUpht** phases, their emission spectra (Figure VI.5.4) resembles with the ones of the **pht3** and **pht4** uranyl phthalate compounds (Chapter II Figure II.3.13). The fluorescence emission spectrum of **CeUpht** presents an intense broad band centered on 530 nm having the top split on two positions with maxima at 524 and 536 nm. The fluorescence spectrum of **NdUpht** phase exhibits also a broad band centered at 530 nm with the top split into two maxima, positioned in this case at 526 and 536 nm.

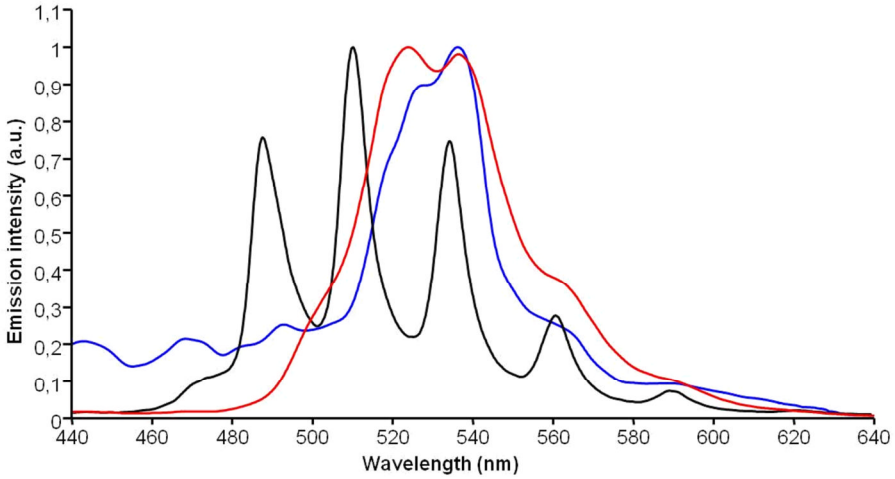

Figure VI.5.4 Solid state fluorescence emission spectra for the **CeUpht** (red), **NdUpht** (blue) and uranyl nitrate hexahydrate (black).

The deconvoluted fluorescence spectra of the **LnUpht** phases (Figure VI.5.5) reveal the fluorescence bands masked by the poor resolution. The deconvoluted spectrum of the **CeUpht** presents six fluorescence bands (resembling to the typical uranyl fluorescence spectrum) with maxima at 483, 501, 521, 538, 562 and 589 nm. The deconvolution of the **NdUpht** fluorescence spectrum has revealed a complex set of peaks, from which the most intense ones have maxima at 518, 526 and 538 nm.

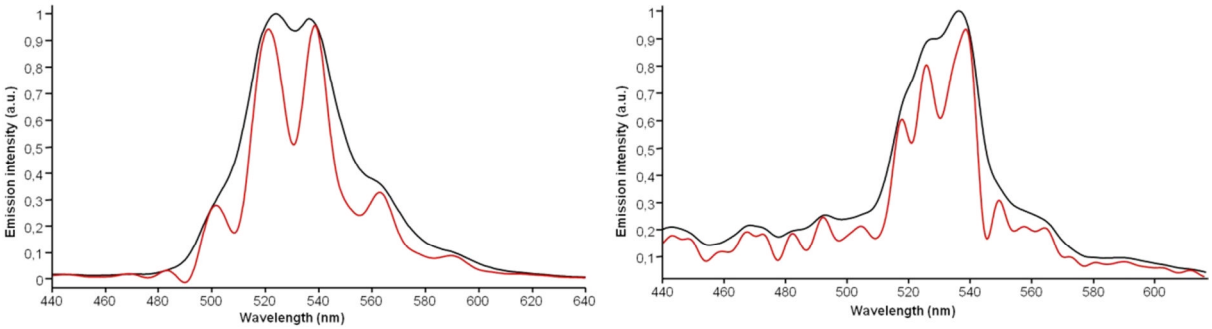

Figure VI.5.5 Comparison between the experimental (black) and deconvoluted (red) fluorescence spectra of **CeUpht** (left) and **NdUpht** (right).

The fluorescence spectra (Figure VI.5.6) of the **LnUpyr** phases are exhibiting multiple fluorescence bands, which due to the poor resolution have been impossible to be attributed either to the uranyl or the lanthanide electronic transitions. Although neodymium does not present fluorescence bands in the 440-640 nm range (when excited at 365 nm), the spectrum of **NdUpyr** exhibits supplementary peaks to the ones uranyl specific, proving an influence, in this structure, of the neodymium cation on the overall electronic transitions of the phase. Supplementary fluorescence bands to the uranyl ones are to be expected and do appear in the case of **CeUpyr**, cerium possessing its own fluorescence spectrum in the examined domain.

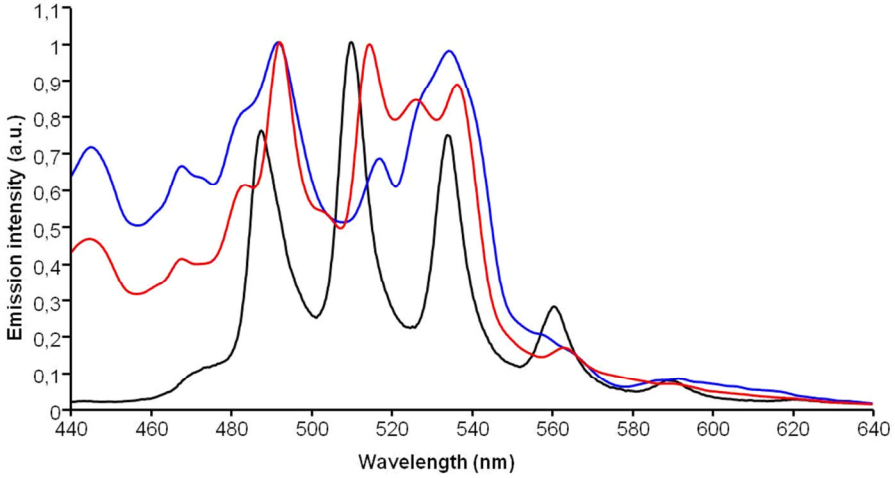

Figure VI.5.6 Solid state fluorescence emission spectra for the **CeUpyr** (red), **NdUpyr** (blue) and uranyl nitrate hexahydrate (black).

The **NdUmel** phase presents a fluorescence spectrum (Figure VI.5.7-blue) resembling with the typical uranyl one, exhibiting maxima at 467, 493, 510, 534 and 558 nm. It also presents an extra low intensity band at 446 nm, caused most probably by the neodymium influence on the structure's electronic transitions. In

the **CeUmel** phase, cerium manifests a major influence over the uranyl electronic transitions, making difficult to identify the uranyl specific fluorescence bands.

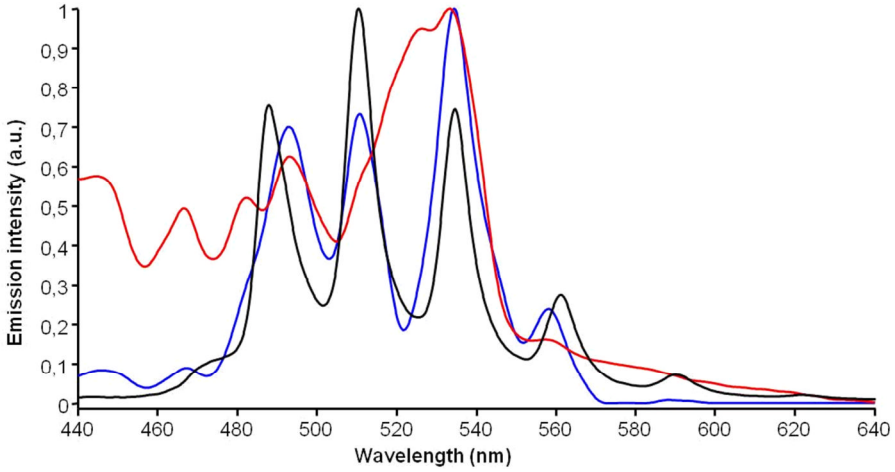

Figure VI.5.7 Solid state fluorescence emission spectra for the **CeUmel** (red), **NdUmel** (blue) and uranyl nitrate hexahydrate (black).

The **CeUmel** emission spectrum (Figure VI.5.7-red) presents low intensity bands at 444, 467, 482, 493 and 557 nm and an intense broad band centered at 526 nm having the top split into two positions at 526 and 533 nm. The deconvolution of this broad band reveals four peaks having maxima at 511, 519, 525 and 534 nm.

Conclusion

The six new mixed U^{VI}-Ln^{III} (Ln = Ce, Nd) coordination polymers presented in this chapter, containing as organic ligand the phthalic, pyromellitic or mellitic acids have been synthesized hydrothermally using either the conventional electric heating or the microwave assisted heating.

One of the structural features of these different mixed uranyl-lanthanide coordination polymers lies on the existence of uranyl networks (isolated building unit, or mixed uranyl-organic layer) linked to each other through discrete lanthanide polyhedra centers. In each case, the connection between the 4f-5f elements is ensured by two or three bidentate carboxylate arms from the organic molecules. The lanthanide cations are therefore surrounded by seven or six water molecules, which do not further participate to the condensation scheme of the

final network. A similar observation was reported in the previous example of mixed uranyl-lanthanide assembly $[(UO_2)Ln(H_2O)_7(Hhmel)]\cdot H_2O$ (Ln = Pr, Eu, Tb, Er)[1] with the aliphatic equivalent of the mellitate ligand. The occurrence of monomeric lanthanide species with high hydration state (6 or 7 H_2O) seems to be a characteristic in this class of heterometallic coordination complexes. The second aspect concerns the U/Ln ratio, which also depends on the nature of the organic ligand and the uranyl oligomer size. It is 4U/1Ln based on tetrameric blocks in **CeUpht** and **NdUpht**; 1.5U/1Ln based on discrete hexagonal and pentagonal bipyramids in **CeUpyr** and NdUpyr; 2U/1Ln based in dimeric blocks in **CeUmel** and **NdUmel** and 1U/1Ln based in discrete hexagonal bipyramid[1]. Uranyl cations are known to condense upon hydrolysis to generate different oligomeric species, with the formation of di-, tri-, or tetranuclear centers[8].

From the crystal chemistry point of view, these different motifs are observed in the final coordination assemblies, but higher condensed polynuclear blocks, containing six[9, 10] or eight[11] uranyl centers or ribbon-like motifs are also encountered[10, 12] and could result from the condensation of low nuclearity uranyl oligomers. However, considering the reaction pH range (0.9-3.5), it was reported that lanthanide cations could also undergo hydrolysis reaction since formation of precipitate appears above pH 6 in aqueous solution[13]. In fact, lanthanide cations of the present study, are surrounded by solvation water species, and their coordination sphere are completed only by two or three carboxyl oxo ligands, which would correspond to the first steps of water exchange reactions with the multidentate carboxylic acids. In the presence of uranyl cations, further condensation processes (to form higher nuclearity building unit) seem to be stopped for lanthanide cations in these cases, although highly condensed building unit occurs in pure lanthanide carboxylates.

Another type of heterometallic U-Ln assembly was also reported with the organic linker mellitate, $(UO_2)_2Ln(OH)(H_2O)(mel)_2$ (Ln = Ce, Nd) in our group[2]. These compounds were hydrothermally synthesized at 200 °C and their structures consist of direct bonding via oxo (cation-cation interaction) and hydroxo bridging ligands between uranyl and lanthanide centers. In this particular case, it seems that the reaction temperature has a drastic role for the

crystallization of the different phases: lower temperature (150 °C) favored the formation of uranyl networks intercalated by isolated lanthanide cations, through carboxylate (**CeUmel**, **NdUmel**) whereas higher temperature (200 °C) gave rise to the formation of more condensed networks with the occurrence of direct U-O-Ln bonding[2].

For each of the six obtained samples two calcination experiments were conducted. First reaching a maximum temperature of 800°C gave in all the cases a mixture of U_3O_8 and CeO_2 or Nd_2O_3 (depending on the sample). The second experiment conducted at 1500°C for the LnUpht and at 1400°C for the other four phases gave for all of the phases a $(Ln,U)O_2$ fluorite type mixed oxide. ICP-AES analyzes were conducted for each phases on both residues obtained at 800°C and 1400-1500°C, revealing a close cationic ratio to the one given by the initial compounds stoichiometry.

References

1. Thuery, P., *Crystal Growth & Design* **2010,** *10* (5), 2061-2063.
2. Volkringer, C.; Henry, N.; Grandjean, S.; Loiseau, T., *Journal of the American Chemical Society* **2012,** *134* (2), 1275-1283.
3. Ferris, L. M.; Bradley, M. J., *Journal of the American Chemical Society* **1965,** *87* (8), 1710-1714.
4. Mihalcea, I.; Volkringer, C.; Henry, N.; Loiseau, T., *Inorganic Chemistry* **2012,** *51* (18), 9610-9618.
5. Burns, P. C.; Ewing, R. C.; Hawthorne, F. C., *Canadian Mineralogist* **1997,** *35*, 1551-1570.
6. Brese, N. E.; Okeeffe, M., *Acta Crystallographica Section B-Structural Science* **1991,** *47*, 192-197.
7. Bartlett, J. R.; Cooney, R. P., *Journal of Molecular Structure* **1989,** *193*, 295-300.
8. Sylva, R. N.; Davidson, M. R., *Journal of the Chemical Society-Dalton Transactions* **1979,** (3), 465-471; Berto, S.; Crea, F.; Daniele, P. G.; Gianguzza, A.; Pettignano, A.; Sammartano, S., *Coordination Chemistry Reviews* **2012,** *256* (1-2), 63-81; Szabo, Z.; Toraishi, T.; Vallet, V.; Grenthe, I., *Coordination Chemistry Reviews* **2006,** *250* (7-8), 784-815.
9. Thuery, P.; Nierlich, M.; Souley, B.; Asfari, Z.; Vicens, J., *Journal of the Chemical Society, Dalton Transactions* **1999,** (15), 2589-2594.
10. Zheng, Y. Z.; Tong, M. L.; Chen, X. M., *European Journal of Inorganic Chemistry* **2005,** (20), 4109-4117.

11. Mihalcea, I.; Henry, N.; Clavier, N.; Dacheux, N.; Loiseau, T., *Inorganic Chemistry* **2011,** *50* (13), 6243-6249.
12. Kerr, A. T.; Cahill, C. L., *Crystal Growth & Design* **2011,** *11* (12), 5634-5641; Severance, R. C.; Vaughn, S. A.; Smith, M. D.; zur Loye, H. C., *Solid State Sciences* **2011,** *13* (6), 1344-1353; Duvieubourg, L.; Nowogrocki, G.; Abraham, F.; Grandjean, S., *Journal of Solid State Chemistry* **2005,** *178* (11), 3437-3444; Anisimova, N. Y.; Gorbunova, Y. E.; Mikhailov, Y. N.; Chumaevskii, N. A., *Russian Journal of Inorganic Chemistry* **2001,** *46* (4), 552-555; Thuery, P., *Crystal Growth & Design* **2009,** *9* (2), 1208-1215; Kim, J. Y.; Norquist, A. J.; O'Hare, D., *Chemistry of Materials* **2003,** *15* (10), 1970-1975; Borkowski, L. A.; Cahill, C. L., *Crystal Growth & Design* **2006,** *6* (10), 2241-2247; Zhang, W. H.; Zhao, J. S., *Inorganic Chemistry Communications* **2006,** *9* (4), 397-399; Thuery, P., *Crystal Growth & Design* **2011,** *11* (7), 3282-3294; Jiang, Y. S.; Yu, Z. T.; Liao, Z. L.; Li, G. H.; Chen, J. S., *Polyhedron* **2006,** *25* (6), 1359-1366; Zhang, W.; Zhao, J., *Journal of Molecular Structure* **2006,** *789* (1–3), 177-181; Thuery, P., *Inorganic Chemistry Communications* **2008,** *11* (6), 616-620; Dalai, S.; Bera, M.; Rana, A.; Chowdhuri, D. S.; Zangrando, E., *Inorganica Chimica Acta* **2010,** *363* (13), 3407-3412; Knope, K. E.; Cahill, C. L., *Inorganic Chemistry* **2007,** *46* (16), 6607-6612; Frisch, M.; Cahill, C. L., *Dalton Transactions* **2006,** (39), 4679-4690; Charushnikova, I. A.; Krot, N. N.; Starikova, Z. A., *Radiochemistry* **2004,** *46* (5), 429-433.
13. Baes, C. F.; Mesmer, R. E., *The hydrolysis of Cations*. Krieger Publishing Compagny: Malabar, Florida, 1986.

Conclusions and perspectives

This thesis work describes the synthesis and structural characterization of 25 new uranyl carboxylates (so-called uranyl-organic framework or UOF), obtained with 7 distinct aromatic poly-carboxylate ligands. Such high number of phases together with the synthesis conditions does offer important information on the influence of different parameters over the nature of the final product. One significant parameter appears to be the synthesis pH, implicitly the quantity of pH moderator added into reaction, which is related to the hydrolysis rate toward the inorganic uranyl moiety. It is known that at room temperature a uranyl solution could contain various ratios of oligomeric species depending on the solution pH. At low pH only monomeric species exist. Increasing the pH these species are condensing into larger oligomeric units (dimers to polymeric chains) through hydroxo bridges. The concentration evolution in solution, at room temperature, of some oligomeric units is presented in chapter I figure I.3.1. Our work has shown this trend since a similar evolution takes place also in the hydrothermal systems. At relatively low pH only structures containing isolated monomeric uranyl species were obtained (**pht2**, **iso1** - **iso6**, **pyr1**, **pyr2** etc.), unlike the much larger tetrameric (**pht3**, **iso7** - **iso9**, **pyr6**) or even octameric (**iso10**) SBUs obtained at a higher pH. For the phases where the uranyl-ligand backbone is negatively charged, this charge is compensated by countercations provided by the pH moderator. In these cases, the nature of the countercation also influences the structure of the final complex for example the cases of **iso5** and $(Hdmf)_2[(UO_2)_3(ipa)_4(H_2O)_2]$ or **pyr2** and **pyr3**. This influence is manifesting only when the difference in size between two countercations is large enough, for example no structural changes occur when a metal countercation (Na^+, K^+) is replaced with a small organic countercation (NH_4^+), the cases of **pht3** and **pht4**.

A very important role in the complexity of the UOF final structure is played by the organic ligand, which by its geometry, rigidity/flexibility and the number of coordination groups governs the dimensionality and architecture of the final structure. In our work, using only rigid aromatic molecules, the number and the position on the benzene ring of the carboxyl arms were the determinant

factors for the final structure geometry. It has been observed that ligands containing carboxylate arms situated in close proximity one from the other (phthalate, isophthalate, pyromellitate, mellitate) favors the formation of high complexity, high dimensionality structures, while ligands presenting carboxylate arms in *para* position one from the other (terephthalate, 4,4'-biphenyl dicarboxylate, 4,4'-azobenzene dicarboxylate) are favoring bidimensional structures with a strict alternating organic/inorganic pavement and a rare six fold coordinated uranium atom as SBU (see chapter V). It is also interesting to notice that an unique case of open-framework structure (**pyr7**) has been isolated by using pyromellitate ligand and this led to the generation of large one-dimensional tunnel framework, which quite unknown and unexpected for uranyl cation, due to the preferential condensation along the planar oxo group, favoring the formation of low-dimensional networks. The other point is the occurrence of the inorganic octanuclear motif in **iso10**, which exhibits one rare situation of cation-cation interaction (U=O-U bonding) through edge-sharing polyhedra, in hybrid organic-inorganic compounds. This bonding configuration is sometimes encountered in some purely inorganic solids but less often observed in UOF-type phases.

The synthesis temperature manifested significant importance only in a few cases such as the **pht1** (obtained at 100°C) and **pht2** (obtained at 200°C) phases or the cases of complex **A** (80-100°C) and **pyr2** (200°C). This influence has been observed only for the cases of low pH phases. For the phases obtained at high pH a decrease of the reaction temperature only diminished the yield and the purity of the product. An interesting case is the mixed uranyl-lanthanide complexes, where a lower temperature (~150°C) favors the formation of the mixed phase with isolated uranyl and lanthanide species whereas higher temperature generate direct bonding between the 4f and 5f metals in the case of mellitate, for instance.

For other synthesis parameters such as reaction time, precursor's ratio, the dilution of the chemical system or the reactor volume, no general tendency could be established, their influence varying from one system to another.

From the thermal degradation point of view it has been noticed that for simple products (no coordination water molecules, no free water molecules and no countercations) such as the six-fold coordinated uranyl complexes (see chapter V and **iso1** phase of chapter III) the thermal degradation is a single step process, the decomposition of the organic ligand being rapidly followed by the crystallization if the oxide phase, while for the complex structures such as **iso10** or **pyr7** the thermal degradation is a multistep process due to the presence of hydroxo, or aquo groups. The initial phase passes through multiple intermediate crystalline and amorphous states before the final oxide crystallizes. Concerning the nature of the thermal degradation residue, our study has shown that starting from uranyl carboxylate type coordination polymers by thermal degradation only uranyl oxide phases can be obtained. No matter the degradation conditions, there were no uranyl carbide phases identified in the residue. Also it has been shown that the nature of the degradation atmosphere influences the type of uranium oxide obtained after burning. Under oxygen rich atmospheres such as air, from the degradation pure uranyl carboxylates only U_3O_8 phases have been obtained. Under inert (N_2), mild reducing (Ar + 5% H_2) or heavy reducing (H_2) atmospheres the thermal degradation products were UO_2 fluorite type uranium oxides. For the case of mixed uranyl - lanthanide carboxylates the thermal degradation at low temperature (800°C) gave a mixture of U_3O_8 and CeO_2 when the lanthanide was Ce and a mixture of U_3O_8 and Nd_2O_3 when the lanthanide was Nd. The calcination of these carboxylates at a higher temperature (1400 - 1500°C) gave pure $(U,Ce)O_2$ and respectively $(U,Nd)O_2$ fluorite type mixed oxides. Apparently the presence of the lanthanide atoms are favoring the formation of the fluorite type oxide although the calcination took place under air.

For all the phases that have been obtained pure, the solid state fluorescence emission spectrum was recorded. It has been observed that the structures possessing monomeric SBUs (**pht1**, **pht2**, **iso1**) present the typical uranyl spectrum, resembling to the one of the uranyl nitrate hexahydrate, while structures possessing large SBUs (**pht2**, **pht3**, **iso10**, **pyr7**) present an intense emission band of low resolution, making impossible interpretation of the electronic transitions. For the **bpd1** and **adc1** compounds it has been observed an

influence of the organic ligand over the uranyl fluorescence spectrum, for the latter case, the fluorescence spectrum of the ligand completely quenching the fluorescence emission of the uranyl ion.

As perspectives, the investigations should be continued on these chemical systems, since unidentified phases have been produced as mixtures with others, and efforts should be made in order to access to their atomic assemblies. This is mainly due to the fact that several polymeric species co-exist when increasing the hydrolysis rate and is reflected by the formation of mixtures of compounds. Therefore, knowing the different phases described in this thesis work, careful influence of the different conditions synthesis should be studied in order to complete the difference phase diagrams. For instance, the influence on temperature or reactants concentrations should be examined in more details. Another aspect, which was not developed in this work, is the understanding of the chemical mechanisms for the formation of such UOF solids. Indeed, the use *in situ* techniques would be a good help for attempting to highlight the reaction mechanisms occurring during the hydrothermal treatment. These measurements could be done for our system, but one may also think about another probe such as Raman spectroscopy with the typical O=U=O vibration at 800 cm^{-1}. There now exists Raman probe system, which can be inserted directly in the hydrothermal cell and allow for the following of the Raman spectra during the crystal growth of the final UOF. The latter technique would be appropriate for the system using phthalate ligands since all the crystalline phases have been identified and their formation could be thus followed easily.

A review of the new synthesized phases

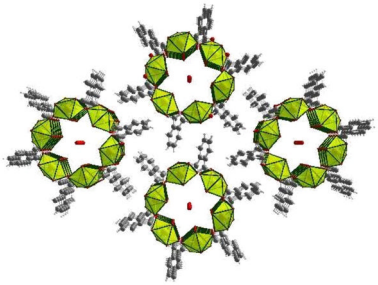

pht2 $[UO_2(pht)(H_2O)]\cdot 0.32H_2O$

monomeric seven-fold coordinated uranyl; 2D dimensionality; presents free and coordinating water molecules.

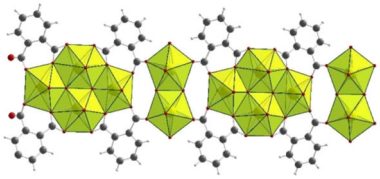

pht3-pht4 $A[(UO_2)_3O(OH)(H_2O)(pht)_2]$

tetrameric SBU seven- and eight-fold coordinated uranyl-centered polyhedra and dimeric SBU of seven-fold coordinated bipyramids; 2D structure; presents coordinating water molecules and potassium or ammonium (A) counter-cations.

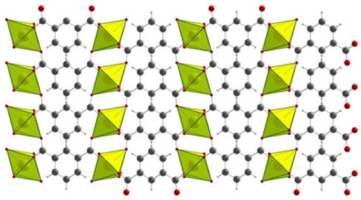

iso1 $[(UO_2)(ipa)]$

monomer, six-fold coordinated uranyl-centered polyhedra; bidimensional structure.

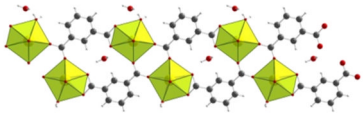

iso2 $[(UO_2)(ipa)(H_2O)]\cdot 0.5H_2O$

monomer, seven-fold coordinated uranyl-centered polyhedra; 1D structure; contains free and coordinating water molecules.

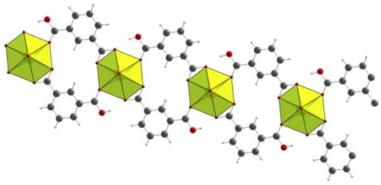

iso3 $[(UO_2)(Hipa)_2]$

monomer, eight-fold coordinated uranyl centered polyhedra, unidimensional structure; contains one protonated carboxyl oxygen atom per ligand molecule.

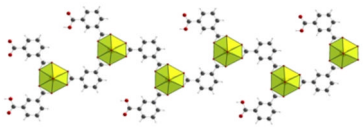

iso4 $(NH_4)[(UO_2)(ipa)(Hipa)]\cdot 3H_2O$

monomer; hexagonal bipyramidal geometry polyhedra; 1D structure; contains free water molecules, ammonium countercations and one protonated carboxylic group per each two ligand molecules.

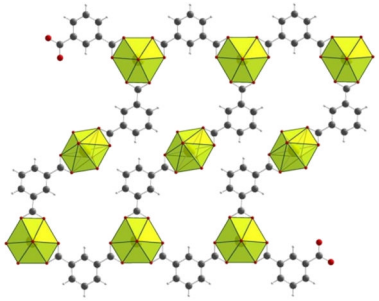

iso5 $(H_2dap)[(UO_2)_3(ipa)_4(H_2O)_2]\cdot 4H_2O$
monomer; hexagonal bipyramidal shaped polyhedra; 1D structure; contains propane-1,3-diammonium countercations, free and coordinating water molecules.

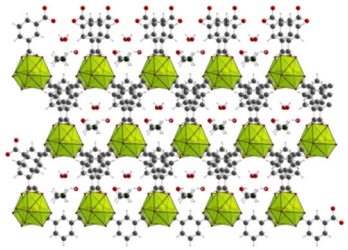

iso6 $(H_2dap)[(UO_2)_2(ipa)_3]\cdot 4H_2O$
monomer; hexagonal bipyramidal shaped polyhedra; 2D structure; contains propane-1,3-diammonium countercations and free water molecules.

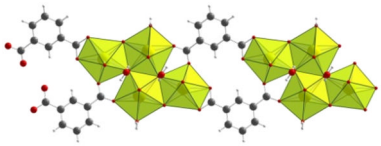

iso7 $[(UO_2)_4(ipa)_2(OH)_4(H_2O)_2]\cdot 2H_2O$
tetrameric SBU; pentagonal bipyramidal shaped polyhedra; 1D structure; contains free and coordinating water molecules

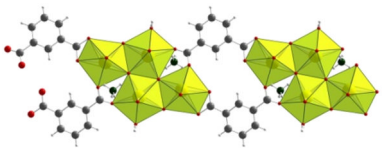

iso8 $(NH_4)_2[(UO_2)_4(ipa)_2O_2(OH)_2(H_2O)_2]$
tetrameric SBU; pentagonal bipyramidal shaped polyhedra; 1D structure; contains coordinating water molecules and ammonium countercations.

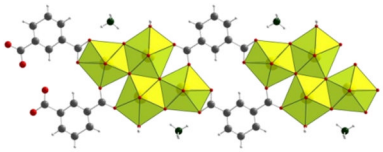

iso9 $(NH_4)_2[(UO_2)_4(ipa)_2O_2(OH)_2(H_2O)_2]\cdot H_2O$
tetrameric SBU; pentagonal bipyramidal shaped polyhedra; 1D structure; contains coordinating water molecules and ammonium countercations.

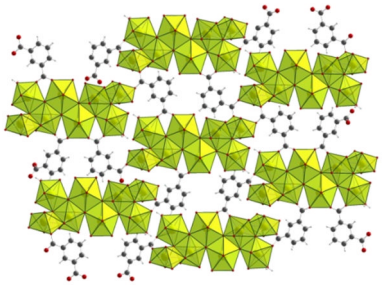

iso10 $[(UO_2)_4(ipa)_2O(OH)_2(H_2O)_2]\cdot 2H_2O$
octameric SBU; pentagonal bipyramidal shaped polyhedra; tridimensional stricture; contains free and coordinating water molecules. Also presents an unique case of edge sharing cation-cation interaction (CCI).

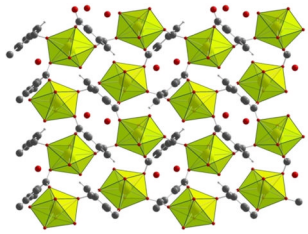

pyr1 $[(UO_2)_2(btec)(H_2O)_2]\cdot H_2O$
monomer; pentagonal bipyramidal shaped polyhedra, tridimensional structure; contains free and coordinating water molecules.

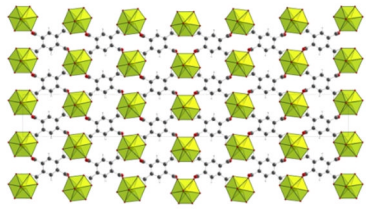

pyr2 $(NH_4)_2[(UO_2)(btec)]\cdot 4H_2O$

monomer; hexagonal bipyramidal shaped polyhedra, bidimensional structure; contains ammonium countercations and free water molecules. Also the organic ligand presents two deprotonated non-coordinating carboxyl oxygen atoms per ligand molecule.

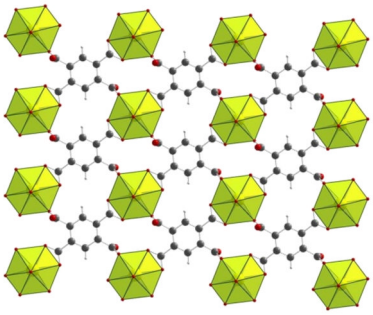

pyr3 $(Hdma)_2[(UO_2)(btec)]$

monomer; hexagonal bipyramidal shaped polyhedra, bidimensional structure; contains dimethylammonium countercations. Also the organic ligand presents two deprotonated non-coordinating carboxyl oxygen atoms per ligand molecule.

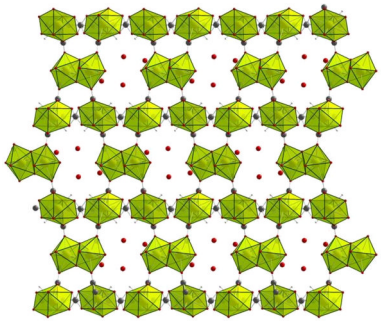

pyr4 $(NH_4)[(UO_2)_2(OH)(H_2O)(btec)]\cdot 2H_2O$

dimeric SBU containing pentagonal bipyramidal shaped polyhedra and monomeric SBU containing hexagonal bipyramidal shaped polyhedra; 3D structure; contains ammonium countercations, free and coordinating water molecules.

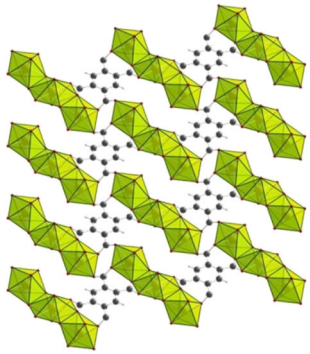

pyr5 $[(UO_2)_3(btec)(OH)_2(H_2O)_2]$

trimeric SBU containing pentagonal and hexagonal bipyramidal shaped polyhedra; bidimensional structure; contains coordinating water molecules.

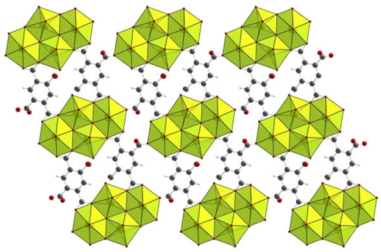

pyr6 $(Hdma)_2[(UO_2)_2O(btec)]$

tetrameric SBU containing pentagonal and hexagonal bipyramidal shaped polyhedra; bidimensional structure; contains dimethylammonium countercations. Also the organic ligand presents two deprotonated non-coordinating carboxyl oxygen atoms per ligand molecule.

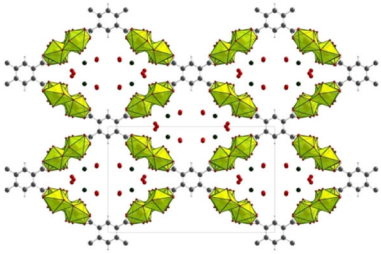

pyr7 $(NH_4)_4[(UO_2)_{12}O_4(OH)_8(btec)_3]\cdot 22H_2O$
polymeric chain-like SBU containing pentagonal bipyramidal shaped polyhedra; 3D structure; contains ammonium countercations and free water molecules.

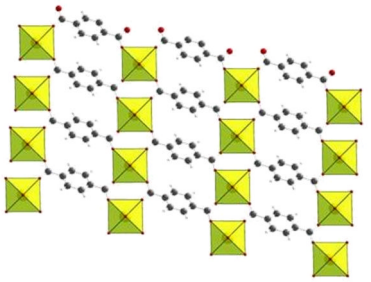

ter1 $[UO_2(tpa)]$
monomer containing tetragonal bipyramidal shaped polyhedra; bidimensional structure.

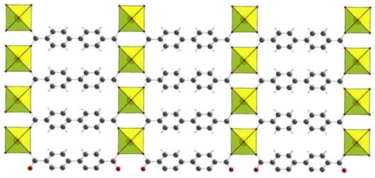

bpd1 $[UO_2(bpd)]$
monomer containing tetragonal bipyramidal shaped polyhedra; bidimensional structure.

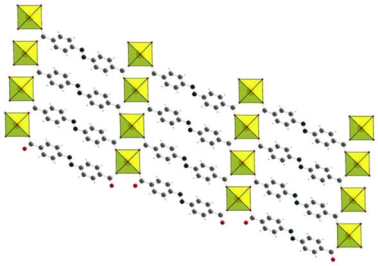

adc1 $[UO_2(adc)]$
monomer containing tetragonal bipyramidal shaped polyhedra; bidimensional structure.

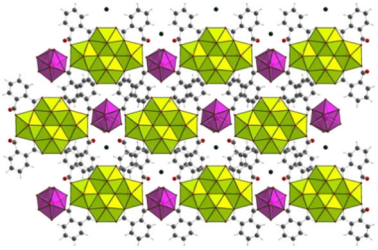

LnUpht $NH_4[(UO_2)_4O_2Ln(H_2O)_7(pht)_4]\cdot xH_2O$
tetrameric uranyl SBU containing pentagonal and hexagonal bipyramidal shaped polyhedra and monomeric lanthanide unit containing nine-fold coordinated, lanthanide centered polyhedra; bidimensional structure; contains ammonium countercations, free and coordinating water molecules.

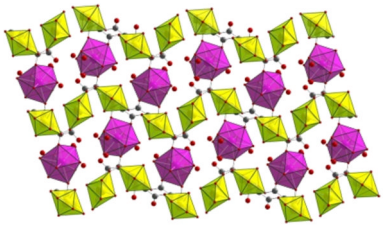

LnUpyr $[(UO_2)_3Ln_2(H_2O)_{12}(btec)_3]\cdot 5H_2O$
monomeric uranyl containing pentagonal and hexagonal bipyramidal shaped polyhedra and monomeric lanthanide unit containing nine-fold coordinated, lanthanide centered polyhedra; 3D structure; contains free and coordinating water molecules.

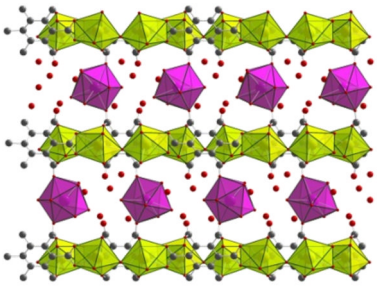

LnUmel $[(UO_2)_2(OH)Ln(H_2O)_7(mel)]\cdot 5H_2O$
dimeric uranyl SBU containing pentagonal bipyramidal shaped polyhedra and monomeric lanthanide unit containing nine-fold coordinated, lanthanide centered polyhedra; 3D structure; contains free and coordinating water molecules.

Abstract:

This thesis work concerns the synthesis, crystal structural study and thermal behavior of coordination polymers type uranyl and mixed uranyl-lanthanide aromatic carboxylates. Using a series of 7 aromatic carboxylate ligands, more than 25 new uranyl (so-called Uranyl-Organic Framework or UOF) and mixed uranyl-lanthanide coordination polymers have been synthesized and described in this manuscript. Some of the ligands have proven to be very prolific such as the isophthalic acid, which is present in 10 coordination polymers and with others (such as terephthalic acid) only one complex could be isolated. Some of the obtained phases contain typical monomeric or tetrameric SBUs and others possess unique features such as octanuclear SBU with an edge sharing CCI (U=O-U), linear trinuclear SBU or polymeric SBU delimiting large tunnel systems. The synthesis of all these phases conducted to a better understanding of the hydrothermal reactions and the influence of different parameters over the final reaction product. For each of the phases obtained pure the thermal behavior and thermal stability have been studied. These experiments offer a better understanding of the relation between the structure of the initial complex, the thermal degradation conditions and the nature of final oxide. Also for these phases the fluorescence emission spectra were recorded, offering information about the influence of different ligands or different type of SBUs over the typical uranyl spectrum.

Keywords:

Metal-organic frameworks, coordination polymers, hydrothermal synthesis, uranyl, mixed coordination polymers, thermal degradation.

Résumé:

Ce travail de thèse décrit la synthèse, l'étude cristallochimique et le comportement thermique de polymères de coordination à base de cations uranyle, ou mixtes uranyle-lanthanide complexés par des ligands carboxylates aromatiques (acide phthalique et dérivés). L'emploi de 7 molécules polycarboxylates a conduit à la formation de plus de 25 nouveaux composés type *Uranyl-Organic Framework* (UOF) ou hybrides uranyle-organique, ou encore mixtes uranyle-lanthanide-organique. Certains de ces ligands on montré une grande diversité d'arrangements atomiques, avec par exemple, l'isophthalate qui conduit à la formation de 10 complexes de coordination, alors que d'autres (par exemple terephthalate) ont permis d'isoler un seul type d'assemblage. Certaines de ces phases contiennent classiquement des briques de construction inorganiques monomériques ou tétramériques alors que d'autres mettent en évidence des blocs trimériques linéaires ou octamériques originals, ou encore des systèmes de chaînes inorganiques générant des structures à tunnels inédits. Une configuration rare d'interaction cation-cation (CCI ou U=O-U) a été également identifiée dans l'isophthalate à base d'unité octamérique. La synthèse de toutes ces phases a permis une meilleure compréhension des réactions hydrothermales et de l'influence de différents paramètres influant la formation du produit final. Pour les phases obtenues sous formes pures, les comportements thermiques et leur stabilité ont été étudiés. Ces expériences ont permis d'établir des relations entre le précurseur initial, la dégradation thermique et les conditions de formation de l'oxyde final. Les spectres de fluorescence ont été collectés et indiquent des informations sur l'influence de la nature du ligand organique ou du type du motif de construction inorganique.

Mots-clé:

Assemblage métal-organique, polymères de coordination, synthèse hydrothermale, uranyle, mixte uranyle-lanthanide, dégradation thermique

UNIVERSITÉ LILLE 1 - SCIENCES ET TECHNOLOGIES

ÉCOLE DOCTORALE SCIENCES DE LA MATIÉRE DU RAYONNEMENT ET DE L'ENVIRONNEMENT

THÈSE

pour obtenir le grade de

DOCTEUR DE L'UNIVERSITE LILLE 1 SCIENCES ET TECHNOLOGIES

Spécialité: Molécules et Matière Condensée

Soutenance publique prévue le 21 décembre 2012 par

Ionut MIHALCEA

Crystal Chemistry of Coordination Polymers Based on Uranyl and Mixed Uranyl / Lanthanide Carboxylates

ANNEXES

Contents

TABLE OF CONTENTS

Annex A

Materials and Methods

Annex A. Materials and methods

Synthesis

The MOF type uranyl carboxylates have been synthesized by using the hydrothermal route. This method is characterized by conditions of high pressure (autogenous created 10 - 30 bar) and temperature (180 - 220°C). Within this method, two different heating techniques were used: the traditional electric heating and the microwave assisted heating.

For the traditional electric heating syntheses, the employed ovens were Heraeus® Thermo Scientific (Figure 0.1-right) with an interior volume of 200 L (0.2 m^3) and reaching a maximum temperature of 250°C.

Figure 0.1 Pictures of Parr type autoclave (left) and Heraeus® oven (right) employed in the hydrothermal syntheses of the uranyl coordination polymers.

The reactors for this type of synthesis are Teflon-lined stainless steel Parr autoclaves with the volume of 23 mL (Figure 0.1-left). Due to the high pressures generated during heating it is recommended that the content of the reactor to occupy less than 50% of the total inside volume.

The oven used for the microwave assisted syntheses was a CEM Mars 5® Microwave Accelerated Reaction System (Figure 0.2-left) equipped with an optic fiber infrared temperature sensor and a load-cell pressure sensor (Figure 0.2-right). The reactors were CEM XP-1500® autoclaves (Figure 0.2) confectioned of

TFM® fluoropolymer, designed to resist at pressures of 1500 psi (~102.1Atm; $10.3 \cdot 10^6$ Pa) and temperatures of 300°C.

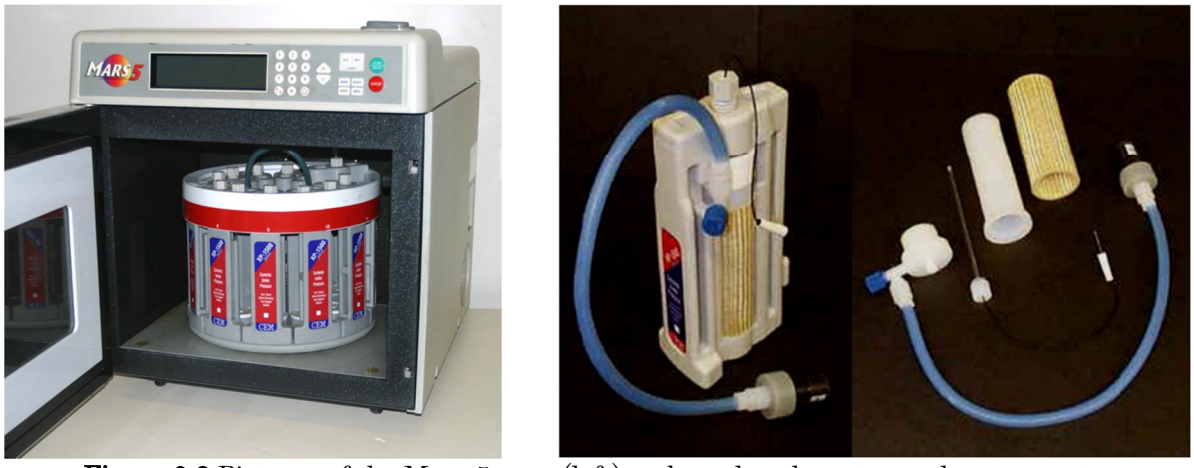

Figure 0.2 Pictures of the Mars 5 oven (left) and employed reactor and components.

The pH of the supernatant solution after each synthesis was measured with an Orion 420A pH meter equipped with a Schott Silamid® N65 glass KCl electrode (Figure 0.3).

Figure 0.3 Picture of the Orion 420A (left) and of the Schott Silamid® N65 electrode (right)

For the mixed U-Ln carboxylate phases (chapter VI) the U/Ln ratio in the calcined residues was determined by ICP-AES (Inductively Coupled Plasma Atomic Emission Spectrometry), also referred to as inductively coupled plasma optical emission spectrometry (ICP-OES), is an analytical technique used for the detection of trace metals. It is a type of emission spectroscopy that uses the inductively coupled plasma to produce excited atoms and ions that emit electromagnetic radiation at characteristic wavelengths. The intensity of this emission is indicative of the concentration of the element within the sample. The ICP-AES is composed of two parts: the ICP and the optical spectrometer. The ICP

torch consists of three concentric quartz glass tubes. The output coil of the radio frequency generator surrounds part of this quartz torch. Argon gas is typically used to create the plasma. When the torch is turned on, an intense electromagnetic field is created within the coil by the high power radio frequency signal flowing in the coil. The argon gas flowing through the torch is ignited with a Tesla unit that creates a brief discharge arc through the argon flow to initiate the ionization process. Once the plasma is ignited, the Tesla unit is turned off. The argon gas is ionized in the intense electromagnetic field and flows in a particular rotationally symmetrical pattern towards the magnetic field. Stable, high temperature plasma of about 7000 K is then generated as the result of the inelastic collisions created between the neutral argon atoms and the charged particles. A peristaltic pump delivers an aqueous or organic sample into a nebulizer where it is changed into mist and introduced directly inside the plasma flame. The sample immediately collides with the electrons and charged ions in the plasma and is itself broken down into charged ions. The various molecules break up into their respective atoms which then lose electrons and recombine repeatedly in the plasma, giving off radiation at the characteristic wavelengths of the elements involved. One or two transfer lenses are then used to focus the emitted light on a diffraction grating where it is separated into its component wavelengths in the optical spectrometer. Within the optical chamber the light intensity is measured with a photomultiplier tube or the separated colors fall upon an array of semiconductor photodetectors such as charge coupled devices (CCDs). In units using these detector arrays, the intensities of all wavelengths (within the system's range) can be measured simultaneously, allowing the instrument to analyze for every element to which the unit is sensitive all at once. Thus, samples can be analyzed very quickly. The intensity of each line is then compared to previously measured intensities of known concentrations of the elements, and their concentrations are then computed by interpolation along the calibration lines[1].

In our experiments a Varian® Vista-MPX CCD Simultaneous ICP-OES spectrometer (Figure 0.4) was used equipped with a CCD array detector with the ability to capture the entire wavelength spectrum in one reading without

scanning and a compact 40 MHz radio frequency generator ensuring superior plasma performance.

Figure 0.4 Picture of a Varian® Vista-MPX CCD Simultaneous ICP-OES spectrometer

Crystal Morphology characterization

Microscopic pictures of the samples were taken using a Nikon® SMZ800 optic microscope (Figure 0.1-d) with a zoom range of 1X to 6.3X, equipped with a high definition Digital Sight DS-Fi1 digital camera (Figure 0.1-c) with a 5 megapixel CCD (charge-coupled device) sensor, a resolution of 2560 × 1920 pixels and a frame rate of 12 frames per second. The microscope is also equipped with a Schott® KL 1500 LCD 150-watt halogen cold light source illuminator (Figure 0.1-a). The light is transported from source to the microscope through a flexible optic fiber light guide (Figure VII.2.1-b) possessing a terminal annular ringlight equipped with a polarization filter.

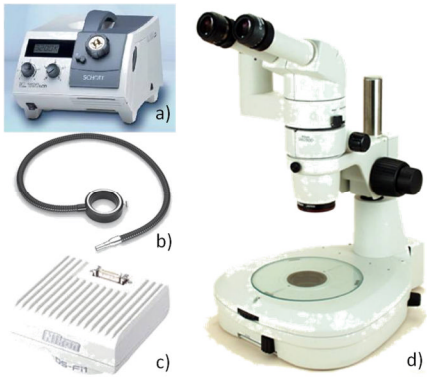

Figure 0.1 Pictures of the optic microscope d) and accessories a), b) and c).

Photographs of the samples with higher resolution and magnification were taken by scanning electron microscopy (SEM). The scanning electron microscope

generates a high-energy focused beam of electrons to produce a variety of signals at the surface of solid samples. The signals that derive from electron-sample interactions reveal information about the sample including external morphology, chemical composition, and crystalline structure and orientation of materials making up the sample. In most applications, data are collected over a selected area of the sample's surface, and a bidimensional image is generated that displays spatial variations in these properties. In a scanning electron microscope, the accelerated electrons carry significant amounts of kinetic energy, this energy being dissipated as a variety of signals produced by electron-sample interactions when the incident electrons are decelerated in the solid sample. These signals include secondary electrons (that produce SEM images), backscattered electrons, diffracted backscattered electrons, X photons, visible light, and heat. Secondary electrons valuable for showing morphology and topography and backscattered electrons valuable for illustrating contrasts in the composition of multiphase samples are commonly used for imaging samples. SEM analysis is considered to be non-destructive, the electron interactions not leading to volume loss of the sample. The SEM is routinely used to generate high-resolution images of objects shapes and to show spatial variations in chemical compositions[2].

For our experiments, the utilized microscope was the Hitachi® S-3400N model, equipped with an Everhardt Thornley secondary electrons detector and a high sensitivity semiconductor 4+1-segment backscattered electrons detector (Figure 0.2).

Figure 0.2 Picture of the Hitachi® S-3400N scanning electron microscope

X-ray characterization

Single crystal X-ray structure determination

The single crystal X-ray diffraction technique is the most used characterization technique for structure determination of crystalline materials. Generally it consists in the "bombardment" of a crystal sample with a monochromatic X-ray beam and the analysis of the secondary beams scattered by the atoms of the crystallographic planes, offering structural information of the analyzed sample. The existential condition for a diffracted beam is described by the Bragg's law:

$$2d_{hkl}sin\theta = n\lambda$$

where θ is the X-ray incidence angle, λ is the wavelength of the incident X-ray beam, d is the lattice planes spacing and n is the order of the diffracted beam. The interaction of the incident X-ray beam with each individual crystallographic plane generates different directions and different amplitudes for the diffracted beams. This generation of different amplitudes leads to the structure factor F(hkl):

$$F(hkl) = \sum_{n=1}^{N} f_n e^{2\pi i(hx_n + ky_n + lz_n)}$$

where the structure factor is dependent of the atomic scattering (f_n) and the atomic position (xyz). The intensity of the diffracted beams can be found from:

$$I(hkl) = F(hkl)F(hkl)^*$$

where $F(hkl)^*$ represents the complex conjugate of F(hkl). With some approximations (Lorentz polarization, absorption correction, data reduction …) these equation link the observed diffracted intensities to the internal structure of the unit cell.

For all the described phases a single crystal (of each) was selected under a polarizing optical microscope and glued on a glass fiber for a single-crystal X-ray diffraction experiment. X-ray intensity data were collected on a Bruker® X8-APEX2 CCD area-detector diffractometer (Figure 0.1) using Mo-Kα radiation (λ = 0.71073 Å) equipped with an optic fiber collimator. Several sets of narrow data

frames (20 s per frame) were collected with ω and φ scans. Data reduction was accomplished using SAINT V7.53a[3]. The substantial redundancy in data collection allowed a semi-empirical absorption correction method to be applied (SADABS V2.10)[4], on the basis of multiple measurements of equivalent reflections. The structures were solved by either direct or Patterson methods, developed by successive difference Fourier syntheses, and refined by full-matrix least-squares on all F^2 data using
SHELX[5] program. Hydrogen atoms of the benzene rings were included in calculated positions and allowed to ride on their parent atoms.

Figure 0.1 Picture of the Bruker® X8-APEX2 diffractometer.

For each successfully determined structure, the nature of oxo, hydroxo or aquo species was determined by bond valence calculation. This method is based on the work of Brese and Okeeffe from 1991[6] which consider that for an atom *i* bonded with a number *n* of *j* atoms, the valence of atom i is equal to the sum of its bond valences:

$$V_i = \sum_{j=1}^{n} v_{ij}$$

where v_{ij} is the bond valence of the i-j pair. For each bond, the bond valence is calculated with formula:

$$v_{ij} = exp\left(\frac{R_{ij} - d_{ij}}{b}\right)$$

where d_{ij} is the i-j interatomic distance, R_{ij} is a constant specific to each *ij* pair and *b* is a constant that generally takes the value 0.37 Å. In 1997 Burns has demonstrated that for the case of uranyl ion, the R_{UO} constant has the value 2.051 Å and the *b* constant has the value 0.519 Å[7].

Powder X-ray diffraction

Powder X-Ray diffraction (PXRD) is a rapid analytical technique, mainly used for phase identification but can also provide information about unit cell dimensions and about crystallite dimensions of the sample. The interaction of the incident rays with the sample produces constructive interference (diffracted beams) only when the Bragg's law is satisfied ($2d\ sin\theta = n\lambda$). By scanning a sample through a range of 2θ angles, all the corresponding possible diffracted rays are detected, processed and counted (ideal case of a totally random orientation of the sample crystallites). Conversion of the diffraction peaks from the 2θ scale to *d*-spacing scale permits the identification of the phase, each phase possessing a unique set of *d*-spacing.

All the PXRD experiments were conducted on a Bruker AXS® D8 Advance diffractometer (Figure 0.2) with DAVINCI design equipped with a fast Lynxeye high-resolution energy-dispersive 1D detector and a sample auto-changer with the capacity of 45 (samples optional modules up to 90 samples).

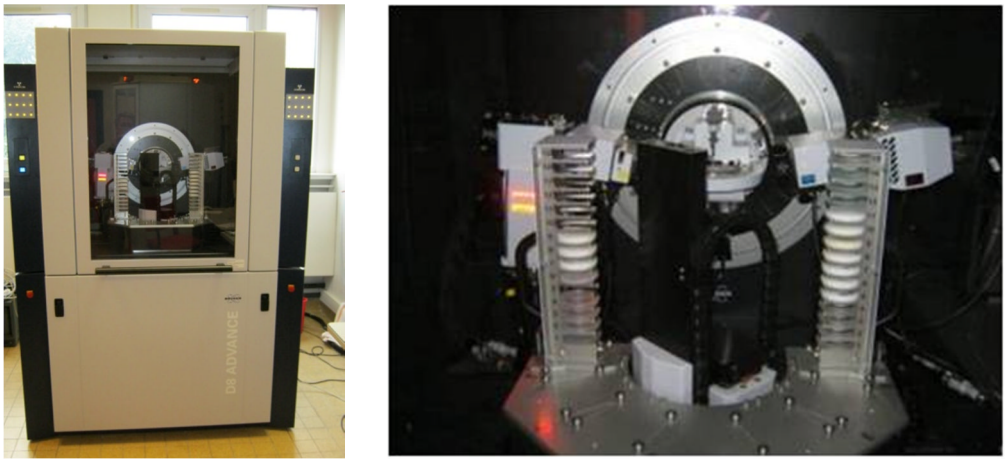

Figure 0.2 Pictures of the Bruker® D8 Advance powder diffractometer.

Thermal characterization

Thermogravimetric analysis

The thermogravimetric analysis (TGA) measures the changes in weight of a sample in relation to a temperature program in a controlled atmosphere.. Knowing the mass of the original mixture and the total mass of impurities liberating upon heating, the stoichiometric ratio can be used to calculate the percent mass of the substance in a sample. TGA is commonly employed in research and testing to determine characteristics of materials such as polymers, to determine degradation temperatures, absorbed moisture content of materials, the level of inorganic and organic components in materials, decomposition points of explosives, and solvent residues. It is also often used to estimate the corrosion kinetics in high temperature oxidation.

Differential thermal analysis (DTA) is a thermoanalytic technique in which the material under study and an inert reference are made to undergo identical thermal cycles, while recording any temperature difference between sample and reference. Changes in the sample, either exothermic or endothermic, can be detected relative to the inert reference. Thus, a DTA curve provides data on the transformations that have occurred, such as glass transitions, crystallization, melting and sublimation. The area under a DTA peak is the enthalpy change and is not affected by the heat capacity of the sample.

Simultaneous TGA-DTA measures both heat flow and weight changes in a material as a function of temperature or time in a controlled atmosphere. Simultaneous measurement of these two material properties not only improves productivity but also simplifies interpretation of the results. The complementary information obtained allows differentiation between endothermic and exothermic events with no associated weight loss (e.g. melting and crystallization) and those that involve a weight loss (e.g. degradation)[8].

In our case, for the obtained pure samples, the TGA/DTA analyses provided information about the thermal stability of the compounds and the different degradation steps. The experiments were carried out on a TGA 92

SETARAM® thermoanalyzer under air atmosphere with a heating rate of 1°C/min from room temperature up to 800°C.

Figure 0.1 Pictures of the TGA 92 SETARAM® thermoanalyzer.

Thermodiffraction analysis

The *in situ* high-temperature powder x-ray diffraction technique studies the changes of the crystalline parameters of a sample during temperature variations. This technique is very versatile permitting variations in a large number of parameters such as the atmosphere, temperature domain and heating rate, 2θ domain, acquisition time for each pattern and the frequency of pattern acquisition.

For our experiments a Bruker® X8 Advance powder diffractometer equipped with an Anton Paar XRK900 reactive room was used to follow the thermal degradation processes of the synthesized phases. The experiments took place under air, with a heating rate of 5°C/min. At each 20°C one PXRD pattern was recorded.

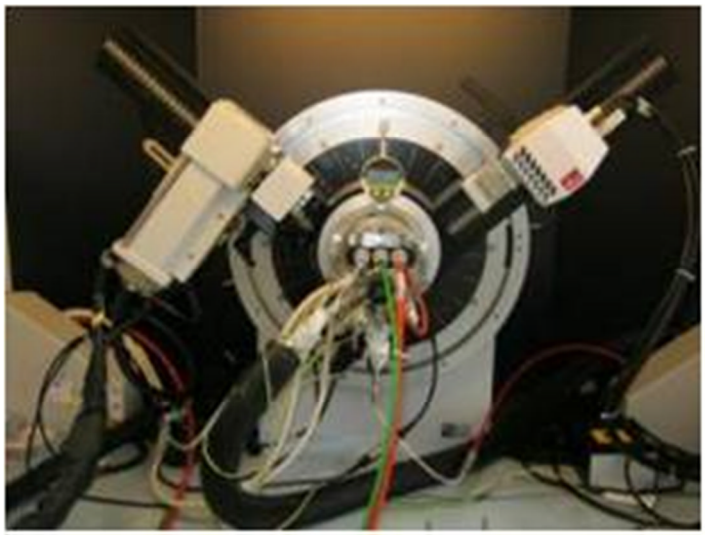

Figure 0.2 Picture of the Bruker® X8 Advance - XRK900 diffractometer.

Spectral analysis

Infrared Spectroscopy

Infrared (IR) spectroscopy is one of the most common spectroscopic techniques used by organic and inorganic chemistry. It represents the absorption measurement of different IR frequencies by a sample positioned in the path of an IR beam. The main goal of IR spectroscopic analysis is to determine the chemical functional groups in the sample. Different functional groups absorb characteristic frequencies of IR radiation. Using various sampling accessories, IR spectrometers can accept a wide range of sample types such as gases, liquids, and solids. IR absorption information is generally presented in the form of a spectrum with wavelength or wavenumber as the x-axis and absorption intensity or percent transmittance as the y-axis. The infrared domain of the electromagnetic spectrum is usually divided into three regions; the near-, mid- and far- infrared, named for their relation to the visible spectrum. The higher-energy near-IR, approximately 14000 - 4000 cm^{-1} can excite overtone or harmonic vibrations. The mid-infrared, approximately 4000-400 cm^{-1} (2.5 - 25 µm) may be used to study the fundamental vibrations and associated rotational-vibrational structure. The far-infrared, approximately 400 - 10 cm^{-1} (25 - 1000 µm), lying adjacent to the

microwave region, has low energy and may be used for rotational spectroscopy. Infrared spectroscopy exploits the fact that molecules absorb specific frequencies that are characteristic of their structure. The frequency of the absorbed radiation matches the transition energy of the bond or group that vibrates. The vibrational energies are determined by the shape of the molecular potential energy surfaces, the masses of the atoms, and the associated vibronic coupling[9].

For this work the IR spectra of the synthesized samples were recorded on a Perkin Elmer® Spectrum2 spectrometer equipped with a diamond ATR accessory. The *in situ* high temperature spectra were recorded with the same spectrometer but equipped with a Pike® GaldiATR module capable of heating the sample up to 210°C. All the IR spectra were recorded in the 4000 - 400 cm^{-1} domain with a resolution of 4 cm^{-1}. For the high temperature spectra the heating rate was of 10°C/min, during this period 195 spectra being recorded.

Figure 0.1 Pictures of the Perkin Elmer® Spectrum2 (left) and the Pike GaldiATR accessory (right).

Fluorescence spectroscopy

Fluorescence spectroscopy is a type of electromagnetic spectroscopy which analyzes fluorescence from a sample. It uses a beam of light, usually ultraviolet light, that excites the electrons in molecules of certain compounds and causes them to emit light, typically (not necessarily) visible light. Fluorescence spectroscopy is primarily concerned with electronic and vibrational states. Generally, the species being examined possess a ground electronic state, and an excited electronic state of higher energy. Within each of these electronic states

are various vibrational states. In fluorescence spectroscopy, the species is first excited, by absorbing a photon, from its ground electronic state to one of the various vibrational states in the excited electronic state. Collisions with other molecules cause the excited molecule to lose vibrational energy until it reaches the lowest vibrational state of the excited electronic state. The molecule then drops down to one of the various vibrational levels of the ground electronic state again, emitting a photon in the process. As molecules may drop down into any of several vibrational levels in the ground state, the emitted photons will have different energies, and thus frequencies. Therefore, by analyzing the different frequencies of light emitted in fluorescent spectroscopy, along with their relative intensities, the structure of the different vibrational levels can be determined. In a typical experiment, the different wavelengths of fluorescent light emitted by a sample are measured using a monochromator, holding the excitation light at a constant wavelength. This is called an emission spectrum. An excitation spectrum is the opposite, whereby the emission light is held at a constant wavelength, and the excitation light is scanned through many different wavelengths. Devices that measure fluorescence are called fluorimeters.

In our experiments, the SAFAS® Xenius XC spectrofluorimeter was used to record the fluorescence spectra of the uranyl based complexes. All the solid state fluorescence spectra were recorded at room temperature, under excitation at 365 nm, the scanned area being between 440 and 640 nm[10].

Figure 0.2 Picture of a SAFAS® Xenius XC spectrofluorimeter.

References

1. Stefánsson, A.; Gunnarsson, I.; Giroud, N., *Analytica Chimica Acta* **2007,** *582* (1), 69-74; Mermet, J. M., *Journal of Analytical Atomic Spectrometry* **2005,** *20* (1), 11-16; Aceto, M.; Abollino, O.; Bruzzoniti, M. C.; Mentasti, E.; Sarzanini, C.; Malandrino, M., *Food Additives and Contaminants* **2002,** *19* (2), 126-133; Benramdane, L.; Bressolle, F.; Vallon, J. J., *Journal of Chromatographic Science* **1999,** *37* (9), 330-344; Ma, R.; McLeod, C. W.; Tomlinson, K.; Poole, R. K., *ELECTROPHORESIS* **2004,** *25* (15), 2469-2477.
2. Goldstein, J.; Newbury, D. E.; Joy, D. C.; Lyman, C. E.; Echlin, P.; Lifshin, E.; Sawyer, L.; Michael, J. R., *Scanning Electron Microscopy and X-ray Microanalysis*. Springer: 2003; Egerton, R. F., Physical Principles of Electron Microscopy: An Introduction to TEM, SEM, and AEM. Springer: 2005.
3. SAINT Plus, version 7.53a, Bruker Analytical X-Ray Systems: Madison. WI, 2008.
4. Sheldrick, G. M., SADABS, Bruker-Siemens Area Detector Absorption and Other Corrections, version 2008/1, 2008.
5. Sheldrick, G. M., *Acta Crystallographica Section A* **2008,** *64*, 112-122.
6. Brese, N. E.; Okeeffe, M., *Acta Crystallographica Section B-Structural Science* **1991,** *47*, 192-197.
7. Burns, P. C.; Ewing, R. C.; Hawthorne, F. C., *Canadian Mineralogist* **1997,** *35*, 1551-1570.
8. Mansfield, E.; Kar, A.; Quinn, T. P.; Hooker, S. A., *Analytical Chemistry* **2010,** *82* (24), 9977-9982; Bud, R.; Warner, D. J., *Instruments of Science: An Historical Encyclopedia*. Garland Publishing Inc: 1998.
9. Atkins, P., Elements of physical chemistry. Oxford University Press: Oxford New York, 2009; Harwood, L., Experimental organic chemistry : principles and practice. Blackwell Scientific Publications: Oxford England Boston, 1990; Kazuo, N., Infrared and Raman Spectra of Inorganic and Coordination Compounds. Part A: Theory and Applications in Inorganic Chemistry. John Wiley & Sons, Inc.: Hoboken, New Jersey, 2009.
10. Valeur, B., *Molecular Fluorescence: Principles and Applications*. Wiley-VCH Verlag GmbH: 2001; Rabinowitch, E.; Belford, L. R., *Spectroscopy and Photochemistry of Uranyl Compounds*. Pergamon Press: 1964.

Annex B

Supplementary Materials

Annex B. Supplementary materials

Phthalate system

Table 0.1 Crystal data and structure refinement for uranyl phthalate complexes.

	pht2	pht3	pht4
formula	$C_{12}H_9O_{11}U_{1.50}$	$C_{16}H_8KO_{17}U_3$	$C_{16}H_8NO_{17}U_3$
formula weight	686.24	1225.41	1200.32
temperature/K	293(2)	293(2)	293(2)
crystal type	yellow needle	yellow parallelepiped	yellow parallelepiped
crystal size/mm	0.65 × 0.08 × 0.08	0.18 × 0.08 × 0.03	0.17 × 0.16 × 0.05
crystal system	trigonal	triclinic	triclinic
space group	*R*-3	*P*-1	*P*-1
a/Å	30.5385(7)	7.1113(3)	7.2962(3)
b/Å	30.5385(7)	13.3625(5)	13.3376(4)
c/Å	5.8489(2)	13.6784(5)	13.6850(4)
α/deg	90	102.423(2)	102.294(2)
ß/deg	90	104.864(2)	105.175(2)
γ/deg	120	101.286(2)	101.557(2)
volume/Å^3	4723.9(2)	1182.74(8)	1208.64(7)
Z, ρ_{calc}/g·cm^{-3}	12, 2.895	2, 3.441	2, 3.298
μ/mm^{-1}	15.483	20.747	20.132
Θ range/deg	2.31–35.93	1.60–31.37	1.61–32.60
limiting indices	$-49 \le h \le 48$ $-48 \le k \le 49$ $-7 \le l \le 9$	$-10 \le h \le 10$ $-19 \le k \le 19$ $-19 \le l \le 19$	$-11 \le h \le 11$ $-20 \le k \le 20$ $-20 \le l \le 20$
collected reflections	97670	38015	66799
unique reflections	4662 [R(int) = 0.0424]	7705 [R(int) = 0.0495]	8737 [R(int) = 0.0459]
parameters	155	336	341
goodness-of-fit on F^2	1.310	1.146	1.135
final R indices [$I > 2\sigma(I)$]	R1 = 0.0221 wR2 = 0.0629	R1 = 0.0443 wR2 = 0.1227	R1 = 0.0256 wR2 = 0.0588
R indices (all data)	R1 = 0.0355 wR2 = 0.0674	R1 = 0.0610 wR2 = 0.1352	R1 = 0.0395 wR2 = 0.0731
largest diff peak and hole/e·Å^{-3}	1.610 and −1.826	6.872 and −1.758	2.265 and −1.226

Table 0.2 Atomic coordinates (x10^4) and equivalent isotropic displacement parameters (A^{2}x10^3) for complex pht2.

Atom	x	y	z	U(eq)
U(1)	6198(1)	1613(1)	9713(1)	18(1)
O(1)	6347(1)	2160(1)	8086(5)	24(1)
O(2)	6051(1)	1069(1)	11315(6)	32(1)
O(3)	6622(1)	1364(1)	6985(5)	25(1)
O(4)	5443(1)	1569(1)	10997(5)	23(1)
O(5)	7041(1)	1987(1)	10998(5)	23(1)
O(6)	5565(1)	1089(1)	6996(5)	26(1)
O(7)	6342(2)	2148(2)	13152(8)	50(1)
C(1)	4967(1)	1299(1)	10923(6)	16(1)
C(2)	5287(1)	1182(1)	5755(6)	17(1)
C(3)	4883(1)	756(1)	4409(6)	18(1)
C(4)	4707(1)	820(1)	12272(6)	19(1)
C(5)	4300(2)	406(2)	11226(8)	27(1)
C(6)	4648(2)	277(2)	5424(8)	27(1)

Atom	x	y	z	U(eq)
C(7)	7706(2)	909(2)	2300(10)	36(1)
C(8)	7471(2)	738(2)	4415(10)	39(1)
OW1	6668(2)	3334(2)	6704(10)	165(15)
OW2	6668(2)	3334(2)	13963(10)	320(30)

Table 0.3 Bond lengths for complex pht2.

Bond	Bond lengths [Å]	Bond	Bond lengths [Å]
U(1)-O(2)	1.760(3)	C(2)-C(3)	1.493(5)
U(1)-O(1)	1.771(3)	C(3)-C(6)	1.400(5)
U(1)-O(5)	2.356(3)	C(3)-C(4)#3	1.412(5)
U(1)-O(4)	2.364(3)	C(4)-C(5)	1.396(5)
U(1)-O(6)	2.393(3)	C(4)-C(3)#4	1.412(5)
U(1)-O(3)	2.408(3)	C(5)-C(8)#2	1.387(7)
U(1)-O(7)	2.487(4)	C(6)-C(7)#5	1.386(7)
O(3)-C(1)#1	1.262(4)	C(7)-C(6)#6	1.386(7)
O(4)-C(1)	1.264(4)	C(7)-C(8)	1.394(8)
O(5)-C(2)#1	1.269(4)	C(8)-C(5)#1	1.387(7)
O(6)-C(2)	1.254(4)	OW1-OW2#3	1.6032
C(1)-O(3)#2	1.261(4)	OW2-OW2#7	0.736(12)
C(1)-C(4)	1.492(5)	OW2-OW1#4	1.6032
C(2)-O(5)#2	1.269(4)		

Table 0.4 Bond Angles for complex pht2.

Bond	Angle [°]	Bond	Angle [°]
O(2)-U(1)-O(1)	179.66(17)	C(1)#1-O(3)-U(1)	129.6(2)
O(2)-U(1)-O(5)	89.35(13)	C(1)-O(4)-U(1)	142.9(3)
O(1)-U(1)-O(5)	90.61(12)	C(2)#1-O(5)-U(1)	143.6(3)
O(2)-U(1)-O(4)	89.78(14)	C(2)-O(6)-U(1)	130.2(3)
O(1)-U(1)-O(4)	90.47(12)	O(3)#2-C(1)-O(4)	122.5(3)
O(5)-U(1)-O(4)	136.38(10)	O(3)#2-C(1)-C(4)	117.7(3)
O(2)-U(1)-O(6)	89.01(14)	O(4)-C(1)-C(4)	119.8(3)
O(1)-U(1)-O(6)	90.85(12)	O(6)-C(2)-O(5)#2	123.1(4)
O(5)-U(1)-O(6)	148.96(11)	O(6)-C(2)-C(3)	117.8(3)
O(4)-U(1)-O(6)	74.61(11)	O(5)#2-C(2)-C(3)	119.1(3)
O(2)-U(1)-O(3)	88.70(14)	C(6)-C(3)-C(4)#3	119.3(4)
O(1)-U(1)-O(3)	90.97(12)	C(6)-C(3)-C(2)	117.1(3)
O(5)-U(1)-O(3)	74.61(11)	C(4)#3-C(3)-C(2)	123.5(3)
O(4)-U(1)-O(3)	148.96(11)	C(5)-C(4)-C(3)#4	119.4(4)
O(6)-U(1)-O(3)	74.37(11)	C(5)-C(4)-C(1)	116.9(3)
O(2)-U(1)-O(7)	93.83(19)	C(3)#4-C(4)-C(1)	123.4(3)
O(1)-U(1)-O(7)	86.47(18)	C(8)#2-C(5)-C(4)	120.7(4)
O(5)-U(1)-O(7)	68.39(13)	C(7)#5-C(6)-C(3)	120.6(4)
O(4)-U(1)-O(7)	68.16(13)	C(6)#6-C(7)-C(8)	120.0(4)
O(6)-U(1)-O(7)	142.64(13)	C(5)#1-C(8)-C(7)	120.0(4)
O(3)-U(1)-O(7)	142.86(13)	OW2#7-OW2-OW1#4	179.5(15)

Table 0.5 Bond valence calculation for complex pht2.

Atom	Atom bond(s)	Bond length [Å]	Bond valence [vu]	Atom valence [vu]
U1	U(1)-O(2)	1,76	1,75	6,02
	U(1)-O(1)	1,771	1,72	
	U(1)-O(5)	2,356	0,56	
	U(1)-O(4)	2,364	0,55	
	U(1)-O(6)	2,393	0,52	
	U(1)-O(3)	2,408	0,50	
	U(1)-O(7)	2,487	0,43	
O1	U(1)-O(1)	1,771	1,72	1,72
O2	U(1)-O(2)	1,76	1,75	1,75
O3	U(1)-O(3)	2,408	0,50	1,92
	O(3)-C(1)#1	1,262	1,41	

Atom	Atom bond(s)	Bond length [Å]	Bond valence [vu]	Atom valence [vu]
O4	U(1)-O(4)	2,364	0,55	1,95
	O(4)-C(1)	1,264	1,41	
O5	U(1)-O(5)	2,356	0,56	1,94
	O(5)-C(2)#1	1,269	1,39	
O6	U(1)-O(6)	2,393	0,52	1,96
	O(6)-C(2)	1,254	1,44	
O7	U(1)-O(7)	2,487	0,43	0,43

Table 0.6 Atomic coordinates (x10⁴) and equivalent isotropic displacement parameters (A²x10³) for complex pht3.

Atom	x	y	z	U(eq)
U(1)	5205(1)	9124(1)	952(1)	23(1)
U(2)	4957(1)	5916(1)	4153(1)	20(1)
U(3)	3127(1)	2829(1)	2747(1)	20(1)
K(1)	10000	10000	0	42(1)
K(2)	10654(8)	5720(4)	5732(4)	34(1)
O(1)	5582(14)	2781(7)	2703(7)	36(2)
O(2)	2426(13)	5919(7)	4078(7)	36(2)
O(3)	7485(14)	5962(7)	4163(7)	38(2)
O(4)	2114(13)	2520(6)	884(6)	29(2)
O(5)	2258(13)	940(6)	2317(6)	29(2)
O(6)	4345(15)	4201(6)	4176(6)	35(2)
O(7)	3713(16)	4488(6)	2287(6)	38(2)
O(8)	3865(14)	2252(6)	4349(6)	31(2)
O(9)	4558(15)	10018(7)	2474(6)	36(2)
O(10)	7833(14)	9734(8)	1502(8)	43(2)
O(11)	5957(17)	7551(7)	142(7)	42(2)
O(12)	619(15)	2824(8)	2725(8)	42(2)
O(13)	5418(18)	9301(7)	-659(7)	45(3)
O(14)	2575(16)	8488(9)	418(8)	49(2)
O(15)	5540(20)	8017(7)	2157(7)	55(3)
O(16)	4144(14)	2155(6)	5928(6)	32(2)
O(17)	4040(15)	6113(6)	2280(6)	34(2)
C(1)	3559(17)	5156(7)	1765(8)	23(2)
C(2)	3179(18)	340(7)	2730(8)	26(2)
C(3)	2953(16)	2867(7)	267(7)	23(2)
C(4)	3637(16)	1690(8)	4971(8)	23(2)
C(5)	2806(16)	4830(8)	596(8)	25(2)
C(6)	2523(16)	3839(8)	-65(8)	24(2)
C(7)	2798(14)	503(8)	4579(8)	22(2)
C(8)	2527(17)	-84(8)	3571(9)	25(2)
C(9)	2252(19)	-30(10)	5287(10)	34(3)
C(10)	2373(17)	5658(9)	138(9)	27(2)
C(11)	1710(20)	5472(10)	-948(9)	35(3)
C(12)	1450(20)	4487(11)	-1591(9)	40(3)
C(13)	1570(20)	-1099(10)	5025(11)	37(3)
C(14)	1892(19)	3676(9)	-1159(8)	31(2)
C(15)	1771(19)	-1189(9)	3280(11)	37(3)
C(16)	1270(20)	-1687(9)	4005(12)	40(3)

Table 0.7 Bond lengths for complex pht3.

Bond	Bond lengths [Å]	Bond	Bond lengths [Å]
U(1)-O(10)	1.773(9)	K(2)-O(2)#3	2.885(10)
U(1)-O(14)	1.778(10)	K(2)-O(2)#9	2.892(10)
U(1)-O(13)	2.306(8)	K(2)-O(1)#4	2.979(11)
U(1)-O(13)#1	2.329(8)	K(2)-O(12)#3	2.994(11)
U(1)-O(9)	2.368(8)	K(2)-U(2)#4	4.137(5)
U(1)-O(11)	2.382(8)	K(2)-U(2)#9	4.173(5)
U(1)-O(15)	2.439(8)	K(2)-U(2)#3	4.217(5)
U(1)-U(1)#1	3.8534(7)	K(2)-U(3)#4	4.223(5)

Bond	Bond lengths [Å]	Bond	Bond lengths [Å]
U(1)-K(1)	4.0084(4)	O(1)-K(2)#4	2.979(11)
U(1)-K(1)#2	4.0795(4)	O(2)-K(2)#3	2.885(10)
U(2)-O(2)	1.777(9)	O(2)-K(2)#2	2.892(10)
U(2)-O(3)	1.783(9)	O(3)-K(2)#4	2.834(10)
U(2)-O(6)	2.256(7)	O(4)-C(3)	1.266(12)
U(2)-O(6)#3	2.258(7)	O(4)-K(1)#5	3.224(7)
U(2)-O(17)	2.561(7)	O(5)-C(2)	1.267(13)
U(2)-O(16)#3	2.565(7)	O(5)-K(1)#5	3.014(8)
U(2)-O(7)	2.650(8)	O(6)-U(2)#3	2.258(7)
U(2)-O(8)#3	2.656(7)	O(7)-C(1)	1.262(11)
U(2)-C(4)#3	3.025(10)	O(8)-C(4)	1.270(11)
U(2)-C(1)	3.034(10)	O(8)-U(2)#3	2.656(7)
U(2)-U(2)#3	3.7135(6)	O(9)-C(2)#10	1.243(14)
U(2)-U(3)	3.9505(5)	O(11)-C(3)#8	1.218(14)
U(3)-O(12)	1.774(9)	O(12)-K(2)#3	2.994(11)
U(3)-O(1)	1.775(9)	O(13)-U(1)#1	2.329(8)
U(3)-O(6)	2.214(7)	O(14)-K(1)#2	3.028(11)
U(3)-O(5)	2.379(7)	O(16)-C(4)	1.245(13)
U(3)-O(4)	2.382(7)	O(16)-U(2)#3	2.565(7)
U(3)-O(7)	2.420(7)	O(17)-C(1)	1.252(12)
U(3)-O(8)	2.442(7)	C(1)-C(5)	1.484(14)
U(3)-U(2)#3	3.9659(5)	C(2)-O(9)#11	1.243(14)
U(3)-K(2)#4	4.223(5)	C(2)-C(8)	1.519(14)
U(3)-K(2)#3	4.300(5)	C(3)-O(11)#8	1.218(14)
U(3)-K(1)#5	4.4348(4)	C(3)-C(6)	1.524(14)
K(1)-O(10)	2.906(10)	C(4)-C(7)	1.503(14)
K(1)-O(10)#6	2.906(10)	C(4)-U(2)#3	3.025(10)
K(1)-O(5)#7	3.014(8)	C(5)-C(6)	1.379(14)
K(1)-O(5)#8	3.014(8)	C(5)-C(10)	1.430(14)
K(1)-O(14)#1	3.028(11)	C(6)-C(14)	1.402(14)
K(1)-O(14)#9	3.028(11)	C(7)-C(8)	1.377(15)
K(1)-O(13)	3.040(12)	C(7)-C(9)	1.407(13)
K(1)-O(13)#6	3.040(12)	C(8)-C(15)	1.398(14)
K(1)-O(4)#7	3.224(8)	C(9)-C(13)	1.350(17)
K(1)-O(4)#8	3.224(8)	C(10)-C(11)	1.388(16)
K(1)-U(1)#6	4.0084(4)	C(11)-C(12)	1.363(19)
K(2)-K(2)#4	2.294(11)	C(12)-C(14)	1.393(17)
K(2)-O(3)	2.809(11)	C(13)-C(16)	1.38(2)
K(2)-O(3)#4	2.834(10)	C(15)-C(16)	1.387(17)

Table 0.8 Bond valence calculation for complex pht3.

Atom	Atom bond(s)	Bond length [Å]	Bond valence [vu]	Atom valence [vu]
U1	U(1)-O(10)	1,773	1,71	6,14
	U(1)-O(14)	1,778	1,69	
	U(1)-O(13)	2,306	0,61	
	U(1)-O(13)#1	2,329	0,59	
	U(1)-O(9)	2,368	0,54	
	U(1)-O(11)	2,382	0,53	
	U(1)-O(15)	2,439	0,47	
U2	U(2)-O(2)	1,777	1,70	6,09
	U(2)-O(3)	1,783	1,68	
	U(2)-O(6)	2,256	0,67	
	U(2)-O(6)#3	2,258	0,67	
	U(2)-O(17)	2,561	0,37	
	U(2)-O(16)#3	2,565	0,37	
	U(2)-O(7)	2,650	0,32	
	U(2)-O(8)#3	2,656	0,31	
U3	U(3)-O(12)	1,774	1,71	6,16
	U(3)-O(1)	1,775	1,70	
	U(3)-O(6)	2,214	0,73	
	U(3)-O(5)	2,379	0,53	
	U(3)-O(4)	2,382	0,53	

Atom	Atom bond(s)	Bond length [Å]	Bond valence [vu]	Atom valence [vu]
	U(3)-O(7)	2,420	0,49	
	U(3)-O(8)	2,442	0,47	
O1	U(3)-O(1)	1,775	1,70	1,70
O2	U(2)-O(2)	1,777	1,70	1,70
O3	U(2)-O(3)	1,783	1,68	1,68
O4	U(3)-O(4)	2,382	0,53	1,80
	O(4)-C(3)	1,266	1,27	
O5	U(3)-O(5)	2,379	0,53	1,80
	O(5)-C(2)	1,267	1,27	
O6	U(2)-O(6)	2,256	0,67	2,08
	U(2)-O(6)#3	2,258	0,67	
	U(3)-O(6)	2,214	0,73	
O7	U(2)-O(7)	2,650	0,32	2,09
	U(3)-O(7)	2,420	0,49	
	O(7)-C(1)	1,262	1,28	
O8	U(2)-O(8)#3	2,656	0,31	2,04
	U(3)-O(8)	2,442	0,47	
	O(8)-C(4)	1,270	1,26	
O9	U(1)-O(9)	2,368	0,54	1,87
	O(9)-C(2)#10	1,243	1,33	
O10	U(1)-O(10)	1,773	1,71	1,71
O11	U(1)-O(11)	2,382	0,53	1,92
	O(11)-C(3)#8	1,218	1,39	
O12	U(3)-O(12)	1,774	1,71	1,71
O13	U(1)-O(13)	2,306	0,61	1,20
	U(1)-O(13)#1	2,329	0,59	
O14	U(1)-O(14)	1,778	1,69	1,69
O15	U(1)-O(15)	2,439	0,47	0,47
O16	U(2)-O(16)#3	2,565	0,37	1,69
	O(16)-C(4)	1,245	1,32	
O17	U(2)-O(17)	2,561	0,37	1,68
	O(17)-C(1)	1,252	1,30	

Table 0.9 Bond Angles for complex pht3.

Bond	Angle [°]	Bond	Angle [°]	Bond	Angle [°]
O(10)-U(1)-O(14)	178.6(5)	O(1)-U(3)-O(8)	88.0(4)	K(2)#4-K(2)-O(1)#4	145.3(4)
O(10)-U(1)-O(13)	88.8(4)	O(6)-U(3)-O(8)	68.6(3)	O(3)-K(2)-O(1)#4	133.7(3)
O(14)-U(1)-O(13)	92.2(5)	O(5)-U(3)-O(8)	69.7(2)	O(3)#4-K(2)-O(1)#4	88.9(3)
O(10)-U(1)-O(13)#1	91.5(4)	O(4)-U(3)-O(8)	153.1(3)	O(2)#3-K(2)-O(1)#4	132.1(3)
O(14)-U(1)-O(13)#1	89.8(5)	O(7)-U(3)-O(8)	137.1(3)	O(2)#9-K(2)-O(1)#4	89.0(3)
O(13)-U(1)-O(13)#1	67.5(3)	O(12)-U(3)-U(2)	90.4(3)	K(2)#4-K(2)-O(12)#3	141.4(4)
O(10)-U(1)-O(9)	92.1(4)	O(1)-U(3)-U(2)	92.1(3)	O(3)-K(2)-O(12)#3	86.4(3)
O(14)-U(1)-O(9)	87.8(4)	O(6)-U(3)-U(2)	28.17(19)	O(3)#4-K(2)-O(12)#3	134.0(3)
O(13)-U(1)-O(9)	141.4(3)	O(5)-U(3)-U(2)	166.42(18)	O(2)#3-K(2)-O(12)#3	84.4(3)
O(13)#1-U(1)-O(9)	73.9(3)	O(4)-U(3)-U(2)	109.99(18)	O(2)#9-K(2)-O(12)#3	135.9(3)
O(10)-U(1)-O(11)	88.6(4)	O(7)-U(3)-U(2)	40.95(18)	O(1)#4-K(2)-O(12)#3	73.3(3)
O(14)-U(1)-O(11)	90.7(5)	O(8)-U(3)-U(2)	96.71(17)	K(2)#4-K(2)-U(2)#4	74.5(3)
O(13)-U(1)-O(11)	74.5(3)	O(12)-U(3)-U(2)#3	90.1(3)	O(3)-K(2)-U(2)#4	136.7(3)
O(13)#1-U(1)-O(11)	142.0(3)	O(1)-U(3)-U(2)#3	92.7(3)	O(3)#4-K(2)-U(2)#4	20.47(19)
O(9)-U(1)-O(11)	144.1(3)	O(6)-U(3)-U(2)#3	27.79(19)	O(2)#3-K(2)-U(2)#4	97.4(2)
O(10)-U(1)-O(15)	88.7(5)	O(5)-U(3)-U(2)#3	110.49(18)	O(2)#9-K(2)-U(2)#4	70.2(2)
O(14)-U(1)-O(15)	89.9(5)	O(4)-U(3)-U(2)#3	165.93(18)	O(1)#4-K(2)-U(2)#4	74.2(2)
O(13)-U(1)-O(15)	145.4(3)	O(7)-U(3)-U(2)#3	96.82(18)	O(12)#3-K(2)-U(2)#4	136.9(3)
O(13)#1-U(1)-O(15)	147.1(3)	O(8)-U(3)-U(2)#3	40.90(17)	K(2)#4-K(2)-U(2)	73.4(3)
O(9)-U(1)-O(15)	73.2(3)	U(2)-U(3)-U(2)#3	55.950(10)	O(3)-K(2)-U(2)	19.57(19)
O(11)-U(1)-O(15)	70.9(3)	O(12)-U(3)-K(2)#4	146.9(4)	O(3)#4-K(2)-U(2)	134.6(3)
O(10)-U(1)-U(1)#1	90.2(3)	O(1)-U(3)-K(2)#4	36.1(3)	O(2)#3-K(2)-U(2)	69.8(2)
O(14)-U(1)-U(1)#1	91.2(3)	O(6)-U(3)-K(2)#4	56.0(3)	O(2)#9-K(2)-U(2)	96.7(2)
O(13)-U(1)-U(1)#1	33.9(2)	O(5)-U(3)-K(2)#4	113.8(2)	O(1)#4-K(2)-U(2)	136.4(2)
O(13)#1-U(1)-U(1)#1	33.6(2)	O(4)-U(3)-K(2)#4	114.3(2)	O(12)#3-K(2)-U(2)	72.8(2)
O(9)-U(1)-U(1)#1	107.50(19)	O(7)-U(3)-K(2)#4	75.7(2)	U(2)#4-K(2)-U(2)	147.91(14)
O(11)-U(1)-U(1)#1	108.4(2)	O(8)-U(3)-K(2)#4	75.9(2)	K(2)#4-K(2)-U(2)#9	75.2(3)
O(15)-U(1)-U(1)#1	178.7(3)	U(2)-U(3)-K(2)#4	60.70(7)	O(3)-K(2)-U(2)#9	97.6(2)

Bond	Angle [°]	Bond	Angle [°]	Bond	Angle [°]
O(10)-U(1)-K(1)	40.7(3)	U(2)#3-U(3)-K(2)#4	61.18(7)	O(3)#4-K(2)-U(2)#9	70.2(2)
O(14)-U(1)-K(1)	140.0(3)	O(12)-U(3)-K(2)#3	33.8(4)	O(2)#3-K(2)-U(2)#9	137.4(2)
O(13)-U(1)-K(1)	48.9(3)	O(1)-U(3)-K(2)#3	149.2(3)	O(2)#9-K(2)-U(2)#9	20.42(18)
O(13)#1-U(1)-K(1)	83.5(3)	O(6)-U(3)-K(2)#3	57.1(3)	O(1)#4-K(2)-U(2)#9	74.3(2)
O(9)-U(1)-K(1)	127.2(2)	O(5)-U(3)-K(2)#3	114.6(2)	O(12)#3-K(2)-U(2)#9	138.2(3)
O(11)-U(1)-K(1)	72.2(2)	O(4)-U(3)-K(2)#3	114.4(2)	U(2)#4-K(2)-U(2)#9	53.08(7)
O(15)-U(1)-K(1)	116.2(3)	O(7)-U(3)-K(2)#3	81.8(3)	U(2)-K(2)-U(2)#9	117.14(13)
U(1)#1-U(1)-K(1)	62.482(10)	O(8)-U(3)-K(2)#3	80.6(2)	K(2)#4-K(2)-U(2)#3	73.1(3)
O(10)-U(1)-K(1)#2	138.4(3)	U(2)-U(3)-K(2)#3	61.30(7)	O(3)-K(2)-U(2)#3	69.7(2)
O(14)-U(1)-K(1)#2	42.9(4)	U(2)#3-U(3)-K(2)#3	60.29(7)	O(3)#4-K(2)-U(2)#3	96.2(2)
O(13)-U(1)-K(1)#2	82.1(3)	K(2)#4-U(3)-K(2)#3	113.09(12)	O(2)#3-K(2)-U(2)#3	19.42(18)
O(13)#1-U(1)-K(1)#2	47.5(3)	O(12)-U(3)-K(1)#5	82.6(3)	O(2)#9-K(2)-U(2)#3	135.2(2)
O(9)-U(1)-K(1)#2	72.0(2)	O(1)-U(3)-K(1)#5	94.4(3)	O(1)#4-K(2)-U(2)#3	135.7(2)
O(11)-U(1)-K(1)#2	126.8(3)	O(6)-U(3)-K(1)#5	172.9(3)	O(12)#3-K(2)-U(2)#3	71.8(2)
O(15)-U(1)-K(1)#2	120.7(3)	O(5)-U(3)-K(1)#5	39.67(18)	U(2)#4-K(2)-U(2)#3	116.70(12)
U(1)#1-U(1)-K(1)#2	60.621(10)	O(4)-U(3)-K(1)#5	44.97(18)	U(2)-K(2)-U(2)#3	52.62(7)
K(1)-U(1)-K(1)#2	123.103(9)	O(7)-U(3)-K(1)#5	113.89(18)	U(2)#9-K(2)-U(2)#3	148.27(14)
O(2)-U(2)-O(3)	176.1(4)	O(8)-U(3)-K(1)#5	108.95(17)	K(2)#4-K(2)-U(3)#4	124.8(3)
O(2)-U(2)-O(6)	91.2(4)	U(2)-U(3)-K(1)#5	153.694(10)	O(3)-K(2)-U(3)#4	138.2(2)
O(3)-U(2)-O(6)	91.7(4)	U(2)#3-U(3)-K(1)#5	148.701(10)	O(3)#4-K(2)-U(3)#4	73.9(2)
O(2)-U(2)-O(6)#3	91.7(4)	K(2)#4-U(3)-K(1)#5	130.47(7)	O(2)#3-K(2)-U(3)#4	137.1(2)
O(3)-U(2)-O(6)#3	91.7(4)	K(2)#3-U(3)-K(1)#5	116.34(7)	O(2)#9-K(2)-U(3)#4	73.9(2)
O(6)-U(2)-O(6)#3	69.3(3)	O(10)-K(1)-O(10)#6	180.0(4)	O(1)#4-K(2)-U(3)#4	20.56(18)
O(2)-U(2)-O(17)	85.7(4)	O(10)-K(1)-O(5)#7	61.6(3)	O(12)#3-K(2)-U(3)#4	93.8(2)
O(3)-U(2)-O(17)	90.7(4)	O(10)#6-K(1)-O(5)#7	118.4(3)	U(2)#4-K(2)-U(3)#4	56.39(7)
O(6)-U(2)-O(17)	112.6(3)	O(10)-K(1)-O(5)#8	118.4(3)	U(2)-K(2)-U(3)#4	149.87(14)
O(6)#3-U(2)-O(17)	176.9(3)	O(10)#6-K(1)-O(5)#8	61.6(3)	U(2)#9-K(2)-U(3)#4	56.37(7)
O(2)-U(2)-O(16)#3	92.5(3)	O(5)#7-K(1)-O(5)#8	180.000(1)	U(2)#3-K(2)-U(3)#4	149.14(14)
O(3)-U(2)-O(16)#3	84.6(4)	O(10)-K(1)-O(14)#1	82.1(3)	U(3)-O(1)-K(2)#4	123.3(4)
O(6)-U(2)-O(16)#3	175.9(3)	O(10)#6-K(1)-O(14)#1	97.9(3)	U(2)-O(2)-K(2)#3	127.9(4)
O(6)#3-U(2)-O(16)#3	112.4(3)	O(5)#7-K(1)-O(14)#1	102.0(3)	U(2)-O(2)-K(2)#2	125.0(4)
O(17)-U(2)-O(16)#3	66.0(2)	O(5)#8-K(1)-O(14)#1	78.0(3)	K(2)#3-O(2)-K(2)#2	46.8(2)
O(2)-U(2)-O(7)	90.8(4)	O(10)-K(1)-O(14)#9	97.9(3)	U(2)-O(3)-K(2)	128.6(4)
O(3)-U(2)-O(7)	88.1(4)	O(10)#6-K(1)-O(14)#9	82.1(3)	U(2)-O(3)-K(2)#4	125.7(4)
O(6)-U(2)-O(7)	64.3(2)	O(5)#7-K(1)-O(14)#9	78.0(3)	K(2)-O(3)-K(2)#4	48.0(2)
O(6)#3-U(2)-O(7)	133.5(2)	O(5)#8-K(1)-O(14)#9	102.0(3)	C(3)-O(4)-U(3)	133.0(7)
O(17)-U(2)-O(7)	48.5(2)	O(14)#1-K(1)-O(14)#9	180.000(2)	C(3)-O(4)-K(1)#5	112.2(6)
O(16)#3-U(2)-O(7)	113.9(2)	O(10)-K(1)-O(13)	57.9(2)	U(3)-O(4)-K(1)#5	103.6(2)
O(2)-U(2)-O(8)#3	87.9(4)	O(10)#6-K(1)-O(13)	122.1(2)	C(2)-O(5)-U(3)	129.3(7)
O(3)-U(2)-O(8)#3	92.0(4)	O(5)#7-K(1)-O(13)	117.8(2)	C(2)-O(5)-K(1)#5	114.1(6)
O(6)-U(2)-O(8)#3	133.3(2)	O(5)#8-K(1)-O(13)	62.2(2)	U(3)-O(5)-K(1)#5	110.1(3)
O(6)#3-U(2)-O(8)#3	64.1(2)	O(14)#1-K(1)-O(13)	57.7(3)	U(3)-O(6)-U(2)	124.2(3)
O(17)-U(2)-O(8)#3	113.9(2)	O(14)#9-K(1)-O(13)	122.3(3)	U(3)-O(6)-U(2)#3	125.0(3)
O(16)#3-U(2)-O(8)#3	48.7(2)	O(10)-K(1)-O(13)#6	122.1(2)	U(2)-O(6)-U(2)#3	110.7(3)
O(7)-U(2)-O(8)#3	162.4(2)	O(10)#6-K(1)-O(13)#6	57.9(2)	C(1)-O(7)-U(3)	160.5(7)
O(2)-U(2)-C(4)#3	91.4(3)	O(5)#7-K(1)-O(13)#6	62.2(2)	C(1)-O(7)-U(2)	95.1(6)
O(3)-U(2)-C(4)#3	86.9(4)	O(5)#8-K(1)-O(13)#6	117.8(2)	U(3)-O(7)-U(2)	102.3(3)
O(6)-U(2)-C(4)#3	157.6(3)	O(14)#1-K(1)-O(13)#6	122.3(3)	C(4)-O(8)-U(3)	158.4(7)
O(6)#3-U(2)-C(4)#3	88.5(3)	O(14)#9-K(1)-O(13)#6	57.7(3)	C(4)-O(8)-U(2)#3	94.1(6)
O(17)-U(2)-C(4)#3	89.8(3)	O(13)-K(1)-O(13)#6	180.0	U(3)-O(8)-U(2)#3	102.1(2)
O(16)#3-U(2)-C(4)#3	24.0(2)	O(10)-K(1)-O(4)#7	99.9(2)	C(2)#10-O(9)-U(1)	139.7(8)
O(7)-U(2)-C(4)#3	137.9(2)	O(10)#6-K(1)-O(4)#7	80.1(2)	U(1)-O(10)-K(1)	115.8(5)
O(8)#3-U(2)-C(4)#3	24.7(2)	O(5)#7-K(1)-O(4)#7	61.03(19)	C(3)#8-O(11)-U(1)	149.4(8)
O(2)-U(2)-C(1)	87.8(4)	O(5)#8-K(1)-O(4)#7	118.97(19)	U(3)-O(12)-K(2)#3	126.9(5)
O(3)-U(2)-C(1)	89.7(4)	O(14)#1-K(1)-O(4)#7	61.6(3)	U(1)-O(13)-U(1)#1	112.5(3)
O(6)-U(2)-C(1)	88.6(2)	O(14)#9-K(1)-O(4)#7	118.4(3)	U(1)-O(13)-K(1)	96.2(4)
O(6)#3-U(2)-C(1)	157.9(3)	O(13)-K(1)-O(4)#7	117.0(2)	U(1)#1-O(13)-K(1)	98.0(4)
O(17)-U(2)-C(1)	24.0(2)	O(13)#6-K(1)-O(4)#7	63.0(2)	U(1)-O(14)-K(1)#2	113.6(5)
O(16)#3-U(2)-C(1)	89.8(2)	O(10)-K(1)-O(4)#8	80.1(2)	C(4)-O(16)-U(2)#3	99.2(6)
O(7)-U(2)-C(1)	24.5(2)	O(10)#6-K(1)-O(4)#8	99.9(2)	C(1)-O(17)-U(2)	99.7(6)
O(8)#3-U(2)-C(1)	137.9(2)	O(5)#7-K(1)-O(4)#8	118.97(19)	O(17)-C(1)-O(7)	116.8(9)
C(4)#3-U(2)-C(1)	113.7(3)	O(5)#8-K(1)-O(4)#8	61.03(19)	O(17)-C(1)-C(5)	121.1(8)
O(2)-U(2)-U(2)#3	91.8(3)	O(14)#1-K(1)-O(4)#8	118.4(3)	O(7)-C(1)-C(5)	122.1(9)

Bond	Angle [°]	Bond	Angle [°]	Bond	Angle [°]
O(3)-U(2)-U(2)#3	92.1(3)	O(14)#9-K(1)-O(4)#8	61.6(3)	O(17)-C(1)-U(2)	56.3(5)
O(6)-U(2)-U(2)#3	34.65(18)	O(13)-K(1)-O(4)#8	63.0(2)	O(7)-C(1)-U(2)	60.5(5)
O(6)#3-U(2)-U(2)#3	34.62(18)	O(13)#6-K(1)-O(4)#8	117.0(2)	C(5)-C(1)-U(2)	176.7(7)
O(17)-U(2)-U(2)#3	147.15(17)	O(4)#7-K(1)-O(4)#8	180.000(1)	O(9)#11-C(2)-O(5)	125.1(10)
O(16)#3-U(2)-U(2)#3	146.83(17)	O(10)-K(1)-U(1)	23.5(2)	O(9)#11-C(2)-C(8)	115.5(9)
O(7)-U(2)-U(2)#3	98.91(16)	O(10)#6-K(1)-U(1)	156.5(2)	O(5)-C(2)-C(8)	119.3(10)
O(8)#3-U(2)-U(2)#3	98.70(15)	O(5)#7-K(1)-U(1)	84.94(16)	O(11)#8-C(3)-O(4)	124.7(10)
C(4)#3-U(2)-U(2)#3	123.06(19)	O(5)#8-K(1)-U(1)	95.06(16)	O(11)#8-C(3)-C(6)	115.2(9)
C(1)-U(2)-U(2)#3	123.26(17)	O(14)#1-K(1)-U(1)	73.40(19)	O(4)-C(3)-C(6)	119.9(9)
O(2)-U(2)-U(3)	89.5(3)	O(14)#9-K(1)-U(1)	106.60(19)	O(16)-C(4)-O(8)	117.7(9)
O(3)-U(2)-U(3)	91.8(3)	O(13)-K(1)-U(1)	34.89(15)	O(16)-C(4)-C(7)	120.5(8)
O(6)-U(2)-U(3)	27.60(18)	O(13)#6-K(1)-U(1)	145.11(15)	O(8)-C(4)-C(7)	121.8(9)
O(6)#3-U(2)-U(3)	96.85(19)	O(4)#7-K(1)-U(1)	112.68(15)	O(16)-C(4)-U(2)#3	56.8(5)
O(17)-U(2)-U(3)	84.97(17)	O(4)#8-K(1)-U(1)	67.32(15)	O(8)-C(4)-U(2)#3	61.1(5)
O(16)#3-U(2)-U(3)	150.64(16)	O(10)-K(1)-U(1)#6	156.5(2)	C(7)-C(4)-U(2)#3	175.1(7)
O(7)-U(2)-U(3)	36.76(16)	O(10)#6-K(1)-U(1)#6	23.5(2)	C(6)-C(5)-C(10)	118.5(9)
O(8)#3-U(2)-U(3)	160.68(15)	O(5)#7-K(1)-U(1)#6	95.06(16)	C(6)-C(5)-C(1)	126.8(9)
C(4)#3-U(2)-U(3)	174.58(18)	O(5)#8-K(1)-U(1)#6	84.94(16)	C(10)-C(5)-C(1)	114.6(9)
C(1)-U(2)-U(3)	61.03(17)	O(14)#1-K(1)-U(1)#6	106.60(19)	C(5)-C(6)-C(14)	119.7(9)
U(2)#3-U(2)-U(3)	62.235(11)	O(14)#9-K(1)-U(1)#6	73.40(19)	C(5)-C(6)-C(3)	126.4(9)
O(12)-U(3)-O(1)	176.9(5)	O(13)-K(1)-U(1)#6	145.11(15)	C(14)-C(6)-C(3)	113.8(9)
O(12)-U(3)-O(6)	90.9(4)	O(13)#6-K(1)-U(1)#6	34.89(15)	C(8)-C(7)-C(9)	118.6(10)
O(1)-U(3)-O(6)	92.2(4)	O(4)#7-K(1)-U(1)#6	67.32(15)	C(8)-C(7)-C(4)	123.7(8)
O(12)-U(3)-O(5)	90.5(4)	O(4)#8-K(1)-U(1)#6	112.68(15)	C(9)-C(7)-C(4)	117.7(10)
O(1)-U(3)-O(5)	87.5(3)	U(1)-K(1)-U(1)#6	180.000(11)	C(7)-C(8)-C(15)	119.8(10)
O(6)-U(3)-O(5)	138.3(3)	K(2)#4-K(2)-O(3)	66.6(3)	C(7)-C(8)-C(2)	125.9(9)
O(12)-U(3)-O(4)	89.4(4)	K(2)#4-K(2)-O(3)#4	65.4(3)	C(15)-C(8)-C(2)	113.9(10)
O(1)-U(3)-O(4)	88.1(4)	O(3)-K(2)-O(3)#4	132.0(2)	C(13)-C(9)-C(7)	122.1(12)
O(6)-U(3)-O(4)	138.2(3)	K(2)#4-K(2)-O(2)#3	66.8(3)	C(11)-C(10)-C(5)	120.7(10)
O(5)-U(3)-O(4)	83.6(3)	O(3)-K(2)-O(2)#3	84.6(3)	C(12)-C(11)-C(10)	120.1(10)
O(12)-U(3)-O(7)	93.2(4)	O(3)#4-K(2)-O(2)#3	76.9(3)	C(11)-C(12)-C(14)	120.1(10)
O(1)-U(3)-O(7)	87.6(4)	K(2)#4-K(2)-O(2)#9	66.4(3)	C(9)-C(13)-C(16)	119.1(11)
O(6)-U(3)-O(7)	69.0(3)	O(3)-K(2)-O(2)#9	77.2(3)	C(12)-C(14)-C(6)	120.9(10)
O(5)-U(3)-O(7)	152.4(3)	O(3)#4-K(2)-O(2)#9	84.0(3)	C(16)-C(15)-C(8)	119.9(12)
O(4)-U(3)-O(7)	69.2(3)	O(2)#3-K(2)-O(2)#9	133.2(2)	C(15)-C(16)-C(13)	120.4(11)
O(12)-U(3)-O(8)	93.5(4)				

Table 0.10 Atomic coordinates (x10⁴) and equivalent isotropic displacement parameters (A²x10³) for complex pht4.

Atom	x	y	z	U(eq)
U(1)	5210(1)	9120(1)	956(1)	22(1)
U(2)	4949(1)	5920(1)	4150(1)	24(1)
U(3)	3131(1)	2817(1)	2745(1)	22(1)
N(1)	10000	10000	0	40(2)
N(2)	10683(12)	5765(7)	5783(7)	30(2)
O(1)	5523(6)	2761(3)	2691(3)	36(1)
O(2)	2484(7)	5934(3)	4071(3)	40(1)
O(3)	7415(7)	5978(3)	4147(3)	42(1)
O(4)	2123(6)	2516(3)	887(3)	28(1)
O(5)	2279(6)	921(3)	2326(3)	27(1)
O(6)	4351(8)	4200(3)	4177(3)	45(1)
O(7)	3709(7)	4480(3)	2286(3)	43(1)
O(8)	3865(7)	2240(3)	4347(3)	35(1)
O(9)	4466(7)	9977(3)	2454(3)	38(1)
O(10)	7741(6)	9785(4)	1563(4)	44(1)
O(11)	6044(7)	7588(3)	178(3)	42(1)
O(12)	696(7)	2810(4)	2722(4)	43(1)
O(13)	5478(7)	9323(3)	-646(3)	39(1)
O(14)	2681(6)	8431(4)	375(4)	44(1)
O(15)	5585(8)	8016(3)	2166(3)	49(1)
O(16)	4163(7)	2152(3)	5933(3)	34(1)
O(17)	4047(7)	6111(3)	2277(3)	37(1)

Atom	x	y	z	U(eq)
C(1)	3526(8)	5154(4)	1765(3)	24(1)
C(2)	3154(8)	310(4)	2734(3)	24(1)
C(3)	2909(8)	2860(3)	253(3)	24(1)
C(4)	3640(7)	1678(3)	4971(3)	22(1)
C(5)	2771(7)	4838(4)	584(3)	22(1)
C(6)	2524(7)	3830(4)	-75(3)	21(1)
C(7)	2807(7)	501(3)	4589(4)	21(1)
C(8)	2557(8)	-114(3)	3575(4)	23(1)
C(9)	2300(8)	-21(4)	5302(4)	30(1)
C(10)	2358(8)	5650(4)	138(4)	26(1)
C(11)	1718(9)	5484(5)	-942(4)	34(1)
C(12)	1472(9)	4490(5)	-1590(4)	35(1)
C(13)	1540(9)	-1122(4)	5020(5)	36(1)
C(14)	1900(8)	3671(4)	-1162(4)	29(1)
C(15)	1817(9)	-1215(4)	3310(5)	34(1)
C(16)	1292(9)	-1708(4)	4021(5)	39(1)

Table 0.11 Bond lengths for complex pht4.

Bond	Bond lengths [Å]	Bond	Bond lengths [Å]
U(1)-O(10)	1.764(4)	O(6)-U(2)#2	2.260(4)
U(1)-O(14)	1.767(4)	O(7)-C(1)	1.267(5)
U(1)-O(13)	2.319(4)	O(8)-C(4)	1.270(5)
U(1)-O(13)#1	2.330(3)	O(8)-U(2)#2	2.660(3)
U(1)-O(11)	2.364(4)	O(9)-C(2)#3	1.246(6)
U(1)-O(9)	2.374(3)	O(11)-C(3)#4	1.248(6)
U(1)-O(15)	2.438(4)	O(13)-U(1)#1	2.330(3)
U(1)-U(1)#1	3.8662(3)	O(16)-C(4)	1.251(5)
U(2)-O(2)	1.778(4)	O(16)-U(2)#2	2.558(3)
U(2)-O(3)	1.786(5)	O(17)-C(1)	1.245(5)
U(2)-O(6)	2.257(4)	C(1)-C(5)	1.498(6)
U(2)-O(6)#2	2.260(4)	C(2)-O(9)#5	1.246(6)
U(2)-O(17)	2.555(3)	C(2)-C(8)	1.509(7)
U(2)-O(16)#2	2.558(3)	C(3)-O(11)#4	1.248(6)
U(2)-O(7)	2.650(4)	C(3)-C(6)	1.509(6)
U(2)-O(8)#2	2.660(3)	C(4)-C(7)	1.486(6)
U(2)-C(1)	3.025(4)	C(4)-U(2)#2	3.027(4)
U(2)-C(4)#2	3.027(4)	C(5)-C(10)	1.398(6)
U(2)-U(2)#2	3.7228(3)	C(5)-C(6)	1.399(6)
U(2)-U(3)	3.9569(3)	C(6)-C(14)	1.392(6)
U(3)-O(12)	1.767(4)	C(7)-C(9)	1.396(6)
U(3)-O(1)	1.782(4)	C(7)-C(8)	1.398(6)
U(3)-O(6)	2.220(4)	C(8)-C(15)	1.390(7)
U(3)-O(4)	2.373(3)	C(9)-C(13)	1.390(7)
U(3)-O(5)	2.382(3)	C(10)-C(11)	1.381(7)
U(3)-O(7)	2.417(4)	C(11)-C(12)	1.377(8)
U(3)-O(8)	2.442(3)	C(12)-C(14)	1.395(7)
U(3)-U(2)#2	3.9691(3)	C(13)-C(16)	1.368(9)
O(4)-C(3)	1.272(6)	C(15)-C(16)	1.375(8)
O(5)-C(2)	1.265(6)		

Table 0.12 Bond valence calculation for complex pht4.

Atom	Atom bond(s)	Bond length [Å]	Bond valence [vu]	Atom valence [vu]
U1	U(1)-O(10)	1,764	1,74	6,21
	U(1)-O(14)	1,767	1,73	
	U(1)-O(13)	2,319	0,60	
	U(1)-O(13)#1	2,330	0,58	
	U(1)-O(11)	2,364	0,55	
	U(1)-O(9)	2,374	0,54	
	U(1)-O(15)	2,438	0,47	

Atom	Atom bond(s)	Bond length [Å]	Bond valence [vu]	Atom valence [vu]
U2	U(2)-O(2)	1,778	1,69	6,08
	U(2)-O(3)	1,786	1,67	
	U(2)-O(6)	2,257	0,67	
	U(2)-O(6)#2	2,260	0,67	
	U(2)-O(17)	2,555	0,38	
	U(2)-O(16)#2	2,558	0,38	
	U(2)-O(7)	2,650	0,32	
	U(2)-O(8)#2	2,660	0,31	
U3	U(3)-O(12)	1,767	1,73	6,16
	U(3)-O(1)	1,782	1,68	
	U(3)-O(6)	2,220	0,72	
	U(3)-O(4)	2,373	0,54	
	U(3)-O(5)	2,382	0,53	
	U(3)-O(7)	2,417	0,49	
	U(3)-O(8)	2,442	0,47	
O1	U(3)-O(1)	1,782	1,68	1,68
O2	U(2)-O(2)	1,778	1,69	1,69
O3	U(2)-O(3)	1,786	1,67	1,67
O4	U(3)-O(4)	2,373	0,54	1,79
	O(4)-C(3)	1,272	1,26	
O5	U(3)-O(5)	2,382	0,53	1,80
	O(5)-C(2)	1,265	1,27	
O6	U(3)-O(6)	2,220	0,72	2,06
	U(2)-O(6)	2,257	0,67	
	U(2)-O(6)#2	2,260	0,67	
O7	U(3)-O(7)	2,417	0,49	2,08
	U(2)-O(7)	2,650	0,32	
	O(7)-C(1)	1,267	1,27	
O8	U(2)-O(8)#2	2,660	0,31	2,04
	U(3)-O(8)	2,442	0,47	
	O(8)-C(4)	1,270	1,26	
O9	U(1)-O(9)	2,374	0,54	1,86
	O(9)-C(2)#3	1,246	1,32	
O10	U(1)-O(10)	1,764	1,74	1,74
O11	U(1)-O(11)	2,364	0,55	1,86
	O(11)-C(3)#4	1,248	1,31	
O12	U(3)-O(12)	1,767	1,73	1,73
O13	U(1)-O(13)#1	2,330	0,58	1,18
	U(1)-O(13)	2,319	0,60	
O14	U(1)-O(14)	1,767	1,73	1,73
O15	U(1)-O(15)	2,438	0,47	0,47
O16	U(2)-O(16)#2	2,558	0,38	1,68
	O(16)-C(4)	1,251	1,31	
O17	U(2)-O(17)	2,555	0,38	1,70
	O(17)-C(1)	1,245	1,32	

Table 0.13 Bond Angles for complex pht4.

Bond	Angle [°]	Bond	Angle [°]	Bond	Angle [°]
O(10)-U(1)-O(14)	178.3(2)	O(7)-U(2)-C(1)	24.68(11)	O(1)-U(3)-U(2)#2	93.10(13)
O(10)-U(1)-O(13)	89.6(2)	O(8)#2-U(2)-C(1)	138.02(11)	O(6)-U(3)-U(2)#2	27.89(9)
O(14)-U(1)-O(13)	91.82(19)	O(2)-U(2)-C(4)#2	91.12(16)	O(4)-U(3)-U(2)#2	165.64(8)
O(10)-U(1)-O(13)#1	91.21(19)	O(3)-U(2)-C(4)#2	86.37(17)	O(5)-U(3)-U(2)#2	110.10(8)
O(14)-U(1)-O(13)#1	90.1(2)	O(6)-U(2)-C(4)#2	157.43(12)	O(7)-U(3)-U(2)#2	96.74(8)
O(13)-U(1)-O(13)#1	67.48(14)	O(6)#2-U(2)-C(4)#2	88.55(12)	O(8)-U(3)-U(2)#2	40.94(8)
O(10)-U(1)-O(11)	89.76(19)	O(17)-U(2)-C(4)#2	89.96(11)	U(2)-U(3)-U(2)#2	56.029(5)
O(14)-U(1)-O(11)	89.78(19)	O(16)#2-U(2)-C(4)#2	24.05(11)	C(3)-O(4)-U(3)	134.2(3)
O(13)-U(1)-O(11)	74.55(13)	O(7)-U(2)-C(4)#2	138.14(11)	C(2)-O(5)-U(3)	130.4(3)
O(13)#1-U(1)-O(11)	142.01(13)	O(8)#2-U(2)-C(4)#2	24.75(11)	U(3)-O(6)-U(2)	124.20(16)
O(10)-U(1)-O(9)	91.00(19)	C(1)-U(2)-C(4)#2	113.82(12)	U(3)-O(6)-U(2)#2	124.76(16)
O(14)-U(1)-O(9)	88.44(19)	O(2)-U(2)-U(2)#2	92.44(13)	U(2)-O(6)-U(2)#2	111.01(15)
O(13)-U(1)-O(9)	141.47(13)	O(3)-U(2)-U(2)#2	92.74(14)	C(1)-O(7)-U(3)	160.2(3)
O(13)#1-U(1)-O(9)	73.98(13)	O(6)-U(2)-U(2)#2	34.52(9)	C(1)-O(7)-U(2)	94.5(3)

Bond	Angle [°]	Bond	Angle [°]	Bond	Angle [°]
O(11)-U(1)-O(9)	143.98(13)	O(6)#2-U(2)-U(2)#2	34.48(9)	U(3)-O(7)-U(2)	102.60(13)
O(10)-U(1)-O(15)	87.9(2)	O(17)-U(2)-U(2)#2	147.03(8)	C(4)-O(8)-U(3)	158.3(3)
O(14)-U(1)-O(15)	90.4(2)	O(16)#2-U(2)-U(2)#2	146.85(8)	C(4)-O(8)-U(2)#2	94.0(3)
O(13)-U(1)-O(15)	145.22(13)	O(7)-U(2)-U(2)#2	98.66(8)	U(3)-O(8)-U(2)#2	102.08(12)
O(13)#1-U(1)-O(15)	147.23(13)	O(8)#2-U(2)-U(2)#2	98.67(7)	C(2)#3-O(9)-U(1)	143.0(4)
O(11)-U(1)-O(15)	70.76(13)	C(1)-U(2)-U(2)#2	123.17(8)	C(3)#4-O(11)-U(1)	152.4(4)
O(9)-U(1)-O(15)	73.28(14)	C(4)#2-U(2)-U(2)#2	123.00(8)	U(1)-O(13)-U(1)#1	112.52(14)
O(10)-U(1)-U(1)#1	90.49(15)	O(2)-U(2)-U(3)	90.01(13)	C(4)-O(16)-U(2)#2	99.5(3)
O(14)-U(1)-U(1)#1	91.18(15)	O(3)-U(2)-U(3)	92.08(14)	C(1)-O(17)-U(2)	99.7(3)
O(13)-U(1)-U(1)#1	33.83(9)	O(6)-U(2)-U(3)	27.65(9)	O(17)-C(1)-O(7)	117.1(4)
O(13)#1-U(1)-U(1)#1	33.65(9)	O(6)#2-U(2)-U(3)	96.62(9)	O(17)-C(1)-C(5)	120.3(4)
O(11)-U(1)-U(1)#1	108.37(9)	O(17)-U(2)-U(3)	84.92(8)	O(7)-C(1)-C(5)	122.6(4)
O(9)-U(1)-U(1)#1	107.63(9)	O(16)#2-U(2)-U(3)	150.68(8)	O(17)-C(1)-U(2)	56.4(2)
O(15)-U(1)-U(1)#1	178.18(13)	O(7)-U(2)-U(3)	36.60(8)	O(7)-C(1)-U(2)	60.8(2)
O(2)-U(2)-O(3)	174.81(18)	O(8)#2-U(2)-U(3)	160.57(7)	C(5)-C(1)-U(2)	176.2(3)
O(2)-U(2)-O(6)	91.92(19)	C(1)-U(2)-U(3)	61.02(8)	O(9)#5-C(2)-O(5)	124.1(4)
O(3)-U(2)-O(6)	92.1(2)	C(4)#2-U(2)-U(3)	174.66(8)	O(9)#5-C(2)-C(8)	115.4(4)
O(2)-U(2)-O(6)#2	92.10(19)	U(2)#2-U(2)-U(3)	62.150(5)	O(5)-C(2)-C(8)	120.4(4)
O(3)-U(2)-O(6)#2	92.38(19)	O(12)-U(3)-O(1)	176.4(2)	O(11)#4-C(3)-O(4)	123.7(4)
O(6)-U(2)-O(6)#2	68.99(15)	O(12)-U(3)-O(6)	91.0(2)	O(11)#4-C(3)-C(6)	115.2(4)
O(2)-U(2)-O(17)	85.59(17)	O(1)-U(3)-O(6)	92.60(19)	O(4)-C(3)-C(6)	120.9(4)
O(3)-U(2)-O(17)	89.85(17)	O(12)-U(3)-O(4)	89.33(17)	O(16)-C(4)-O(8)	117.5(4)
O(6)-U(2)-O(17)	112.56(12)	O(1)-U(3)-O(4)	87.79(16)	O(16)-C(4)-C(7)	120.5(4)
O(6)#2-U(2)-O(17)	177.23(15)	O(6)-U(3)-O(4)	137.77(13)	O(8)-C(4)-C(7)	122.1(4)
O(2)-U(2)-O(16)#2	91.96(16)	O(12)-U(3)-O(5)	90.58(18)	O(16)-C(4)-U(2)#2	56.5(2)
O(3)-U(2)-O(16)#2	83.90(17)	O(1)-U(3)-O(5)	86.99(16)	O(8)-C(4)-U(2)#2	61.2(2)
O(6)-U(2)-O(16)#2	175.78(16)	O(6)-U(3)-O(5)	137.96(12)	C(7)-C(4)-U(2)#2	174.7(3)
O(6)#2-U(2)-O(16)#2	112.53(12)	O(4)-U(3)-O(5)	84.25(12)	C(10)-C(5)-C(6)	119.4(4)
O(17)-U(2)-O(16)#2	66.09(11)	O(12)-U(3)-O(7)	93.16(19)	C(10)-C(5)-C(1)	115.3(4)
O(2)-U(2)-O(7)	91.01(18)	O(1)-U(3)-O(7)	87.81(18)	C(6)-C(5)-C(1)	125.2(4)
O(3)-U(2)-O(7)	87.84(18)	O(6)-U(3)-O(7)	68.87(12)	C(14)-C(6)-C(5)	118.7(4)
O(6)-U(2)-O(7)	64.15(12)	O(4)-U(3)-O(7)	68.96(12)	C(14)-C(6)-C(3)	114.0(4)
O(6)#2-U(2)-O(7)	133.12(12)	O(5)-U(3)-O(7)	152.88(12)	C(5)-C(6)-C(3)	127.3(4)
O(17)-U(2)-O(7)	48.58(11)	O(12)-U(3)-O(8)	93.48(18)	C(9)-C(7)-C(8)	118.3(4)
O(16)#2-U(2)-O(7)	114.10(11)	O(1)-U(3)-O(8)	88.14(17)	C(9)-C(7)-C(4)	117.6(4)
O(2)-U(2)-O(8)#2	87.67(17)	O(6)-U(3)-O(8)	68.70(12)	C(8)-C(7)-C(4)	124.1(4)
O(3)-U(2)-O(8)#2	91.92(17)	O(4)-U(3)-O(8)	153.39(12)	C(15)-C(8)-C(7)	119.4(4)
O(6)-U(2)-O(8)#2	133.15(12)	O(5)-U(3)-O(8)	69.28(11)	C(15)-C(8)-C(2)	115.3(4)
O(6)#2-U(2)-O(8)#2	64.21(11)	O(7)-U(3)-O(8)	137.11(12)	C(7)-C(8)-C(2)	125.2(4)
O(17)-U(2)-O(8)#2	114.10(11)	O(12)-U(3)-U(2)	90.37(15)	C(13)-C(9)-C(7)	121.6(5)
O(16)#2-U(2)-O(8)#2	48.73(10)	O(1)-U(3)-U(2)	92.62(13)	C(11)-C(10)-C(5)	121.6(5)
O(7)-U(2)-O(8)#2	162.67(11)	O(6)-U(3)-U(2)	28.15(9)	C(12)-C(11)-C(10)	118.9(5)
O(2)-U(2)-C(1)	87.25(17)	O(4)-U(3)-U(2)	109.62(8)	C(11)-C(12)-C(14)	120.5(5)
O(3)-U(2)-C(1)	89.60(17)	O(5)-U(3)-U(2)	166.11(8)	C(16)-C(13)-C(9)	119.1(5)
O(6)-U(2)-C(1)	88.66(12)	O(7)-U(3)-U(2)	40.81(8)	C(6)-C(14)-C(12)	120.9(5)
O(6)#2-U(2)-C(1)	157.62(12)	O(8)-U(3)-U(2)	96.83(8)	C(16)-C(15)-C(8)	121.2(5)
O(17)-U(2)-C(1)	23.93(11)	O(12)-U(3)-U(2)#2	90.22(15)	C(13)-C(16)-C(15)	120.4(5)
O(16)#2-U(2)-C(1)	89.85(11)				

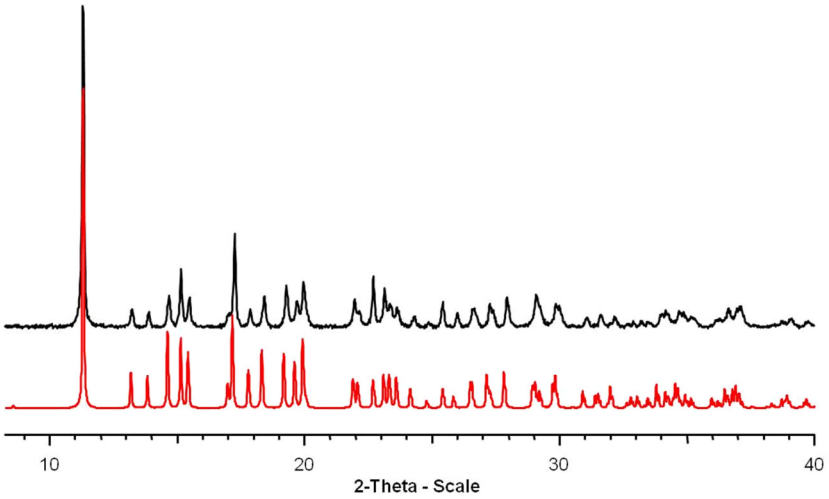

Figure 0.1 Comparison between the calculated (red) and experimental (black) PXRD patterns for the **pht1** phase.

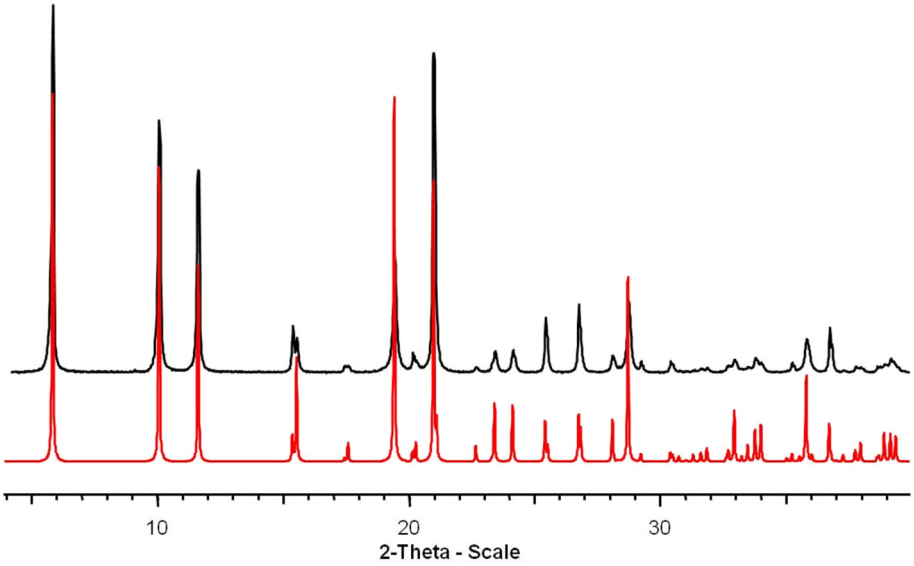

Figure 0.2 Comparison between the calculated (red) and experimental (black) PXRD patterns for the **pht2** phase.

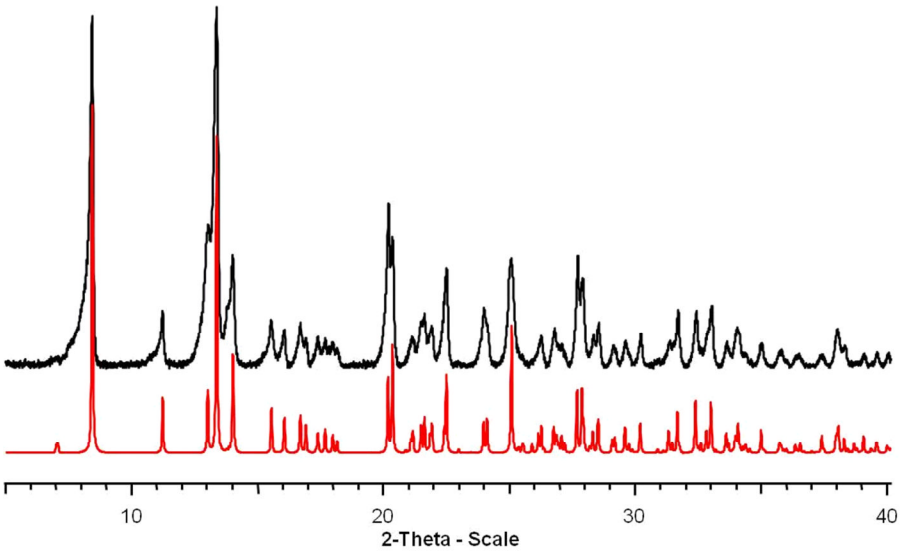

Figure 0.3 Comparison between the calculated (red) and experimental (black) PXRD patterns for the **pht3** phase.

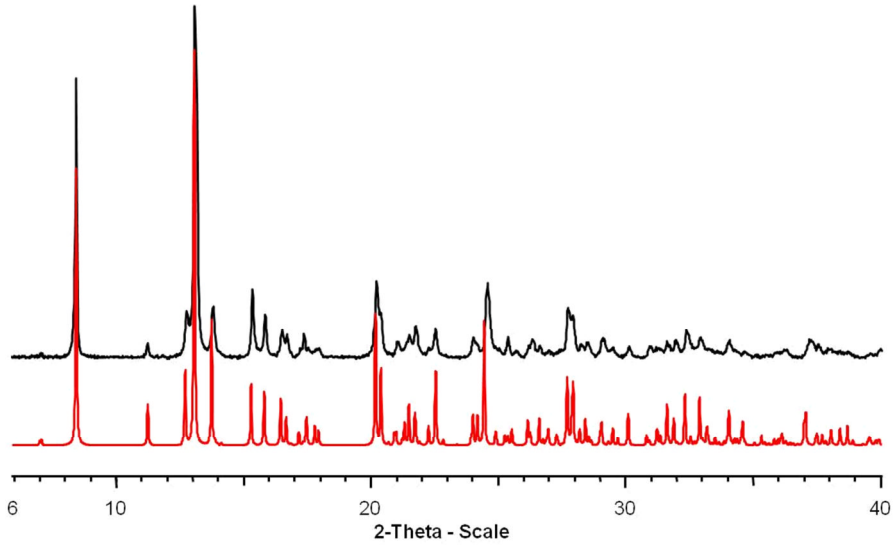

Figure 0.4 Comparison between the calculated (red) and experimental (black) PXRD patterns for the **pht4** phase.

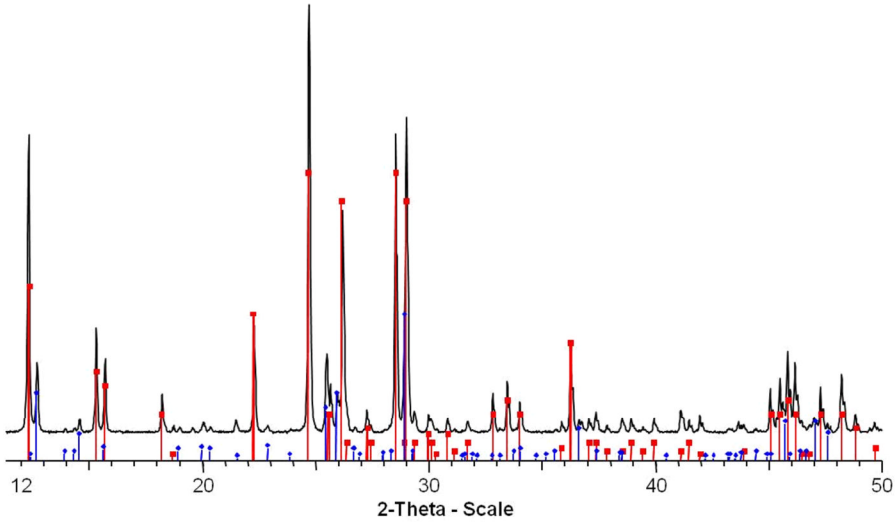

Figure 0.5 Identification of the thermo-degradation residue of **pht3** phase: $K_2U_7O_{22}$ - red (preset to 66% intensity) and $K_2U_4O_{13}$ - blue (preset to 33%).

Isophthalate system

Table 0.1 Crystal data and structure refinement for uranyl phthalate complexes iso1 to iso4.

	iso1	iso2	iso3	iso4
formula	$C_{16}H_8O_{12}U_2$	$C_{16}H_{10}O_{15}U_2$	$C_{16}H_{10}O_{10}U$	$C_{16}H_9NO_{13}U$
formula weight	868.28	918.30	600.27	661.27
temperature/K	293(2)	293(2)	293(2)	293(2)
crystal type	yellow block	yellow needle	yellow plate	yellow block
crystal size/mm	0.23 x 0.19 x 0.18	0.24 x 0.08 x 0.04	0.21 x 0.15 x 0.06	0.24 x 0.14 x 0.10
crystal system	Monoclinic	Monoclinic	Triclinic	Monoclinic
space group	C 1 2/c 1	C 1 c 1	P -1	P 1 21 1
a/Å	6.3566(2)	11.0612(4)	6.8234(4)	6.8634(1)
b/Å	8.4626(2)	20.0762-7)	7.4026(5)	17.4997(3)
c/Å	16.7062(4)	11.3466(5)	8.9551(9)	8.5229(1)
α/deg	90	90	98.429(4)	90
ß/deg	94.030(1)	119.165(2)	93.236(4)	108.639(1)
γ/deg	90	90	114.433(3)	90
volume/Å^3	896.46(4)	2200.3(2)	403.92(5)	969.97(2)
Z, ρ_{calc}/g·cm^{-3}	2, 3.217	4, 2.766	1, 2.468	2, 2.264
μ/mm^{-1}	18.111	14.776	10.105	8.440
Θ range/deg	2.44 - 36.38	2.03 - 37.37	2.32 - 29.56	2.52 to 29.32
limiting indices	-10<=h<=10 -13<=k<=12 -27<=l<=27	-18<=h<=18, -33<=k<=30, -18<=l<=18	-9<=h<=9 -10<=k<=10 -12<=l<=12	-9<=h<=9 -24<=k<=24 -11<=l<=11
collected reflections	18917	53577	22549	51748
unique reflections	2112 [R(int) = 0.0376]	10010 [R(int) = 0.0278]	2272 [R(int) = 0.0353]	5301 [R(int) = 0.0546]
parameters	71	299	125	261
goodness-of-fit on F^2	1.190	1.054	1.066	1.022
final R indices [$I > 2\sigma(I)$]	R1 = 0.0182 wR2 = 0.0486	R1 = 0.0382, wR2 = 0.1018	R1 = 0.0137 wR2 = 0.0319	R1 = 0.0260 wR2 = 0.0614
R indices (all data)	R1 = 0.0276 wR2 = 0.0534	R1 = 0.0440, wR2 = 0.1040	R1 = 0.0137 wR2 = 0.0319	R1 = 0.0339 wR2 = 0.0644
largest diff peak and hole/e·Å^{-3}	0.580 and -2.415	2.965 and -2.978	1.544 and -0.588	0.736 and -1.367

Table 0.2 Crystal data and structure refinement for uranyl phthalate complexes iso5 to iso8.

	iso5	iso6	iso7	iso8
formula	$C_{35}H_{16}N_2O_{28}$ U_3	$C_{27}H_{22}N_2O_{20}U_2$	$C_{16}H_8N_2O_{22}U_4$	$C_{16}H_8N_2O_{22}U_4$
formula weight	1626.59	1170.53	1532.36	1532.36
temperature/K	293(2)	293(2)	293(2)	293(2)
crystal type	yellow needle	yellow needle	yellow blck	yellow needle
crystal size/mm	0.22 x 0.05 x 0.04	0.24 x 0.07 x 0.04	0.23 x 0.11 x 0.07	0.18 x 0.03 x 0.03
crystal system	Triclinic	Orthorhombic	Monoclinic	Monoclinic
space group	*P*-1	*C* 2 2 2_1	*P* 1 2/*c* 1	*P* 1 2/*c* 1
a/Å	8.141(2)	8.3339(3)	14.7096(3)	14.6171(8)
b/Å	9.928(2)	18.0840(7)	7.0679(1)	6.9847(4)
c/Å	14.644(2)	22.1394(9)	15.0958(3)	14.7297(9)
α/deg	97.922(9)	90	90	90
ß/deg	105.281(9)	90	100.776(1)	99.306(3)
γ/deg	102.720(9)	90	90	90
volume/Å^3	1089.5(3)	3336.6(2)	1541.77(5)	1484.1(2)
Z, ρ_{calc}/g·cm^{-3}	1, 2.479	4, 2.330	2, 3.301	2, 3.429
μ/mm^{-1}	11.222	9.784	21.033	21.851
Θ range/deg	1.47 to 23.80	1.84 to 33.80	1.41 to 29.00	1.41 - 31.50
limiting indices	-9<=h<=9 -11<=k<=11 -16<=l<=16	-12<=h<=11 -28<=k<=27 -34<=l<=32	-20<=h<=18 -9<=k<=9 -20<=l<=20	-21<=h<=21 -10<=k<=10 -21<=l<=21
collected reflections	39418	41271	41864	57659
unique reflections	3332 [R(int) = 0.1369]	6645 [R(int) = 0.0412]	4118 [R(int) = 0.0652]	4946 [R(int) = 0.0533]

	iso5	iso6	iso7	iso8
parameters	309	232	200	195
goodness-of-fit on F^2	1.054	1.363	1.395	1.417
final R indices [$I > 2\sigma(I)$]	R1 = 0.0334 wR2 = 0.0677	R1 = 0.0279 wR2 = 0.0554	R1 = 0.0289 wR2 = 0.0666	R1 = 0.0241 wR2 = 0.0516
R indices (all data)	R1 = 0.0524 wR2 = 0.0796	R1 = 0.0368 wR2 = 0.0711	R1 = 0.0428 wR2 = 0.0889	R1 = 0.0354 wR2 = 0.0691
largest diff peak and hole/e·Å^{-3}	0.884 and -0.996	0.836 and -1.220	2.683 and -1.263	3.483 and -1.454

Table 0.3 Crystal data and structure refinement for uranyl phthalate complexes iso9 and iso10.

	iso9	iso10
formula	$C_{16}H_8N_2O_{23}U_4$	$C_{16}H_8O_{23}U_4$
formula weight	1548.36	1520.34
temperature/K	293(2)	293(2)
crystal type	yellow parallelepiped	yellow parallelepiped
crystal size/mm	0.19 x 0.08 x 0.07	0.25 x 0.20 x 0.11
crystal system	Monoclinic	Triclinic
space group	P 1 21/c 1	P -1
a/Å	14.4967(7)	7.3934(3)
b/Å	12.0084(7)	13.3296(5)
c/Å	11.3516(7)	15.4432(5)
α/deg	90	111.865(2)
ß/deg	100.372(4)	90.637(2)
γ/deg	90	104.867(2)
volume/Å^3	1943.8(2)	1355.49(9)
Z, ρ_{calc}/g·cm^{-3}	2, 2.645	2, 3.725
μ/mm^{-1}	16.686	23.923
Θ range/deg	2.22 - 21.49	1.43 to 40.68
limiting indices	-14<=h<=14 -12<=k<=12 -11<=l<=10	-13<=h<=13 -24<=k<=24 -28<=l<=28
collected reflections	14551	95298
unique reflections	2225 [R(int) = 0.0660]	17449 [R(int) = 0.0566]
parameters	195	388
goodness-of-fit on F^2	1.142	1.072
final R indices [$I > 2\sigma(I)$]	R1 = 0.0661 wR2 = 0.1908	R1 = 0.0286 wR2 = 0.0671
R indices (all data)	R1 = 0.0813 wR2 = 0.1999	R1 = 0.0485 wR2 = 0.0835
largest diff peak and hole/e·Å^{-3}	1.706 and -1.655	2.480 and -2.940

Table 0.4 Atomic coordinates (x10^4) and equivalent isotropic displacement parameters (A^{2}x10^3) for iso1.

Atom	x	y	z	U(eq)
U(1)	0	0	0	12(1)
O(1)	1580(3)	1329(2)	586(1)	24(1)
O(2)	665(3)	-1860(2)	1016(1)	19(1)
O(3)	2087(3)	-4060(2)	578(1)	23(1)
C(1)	1145(3)	-3293(3)	1096(1)	14(1)
C(2)	0	-3309(5)	2500	14(1)
C(3)	576(4)	-4141(3)	1827(1)	14(1)
C(4)	5000	-1614(5)	2500	21(1)
C(5)	599(4)	-5788(3)	1834(2)	20(1)

Table 0.5 Bond lengths for complex iso1.

Bond	Bond lengths [Å]	Bond	Bond lengths [Å]
U(1)-O(1)	1.7589(2)	O(3)-U(1)#4	2.290(2)
U(1)-O(1)#1	1.7589(2)	C(1)-C(3)	1.483(3)
U(1)-O(3)#2	2.290(2)	C(2)-C(3)	1.396(3)

Bond	Bond lengths [Å]	Bond	Bond lengths [Å]
U(1)-O(3)#3	2.290(2)	C(2)-C(3)#5	1.396(3)
U(1)-O(2)#1	2.331(2)	C(3)-C(5)	1.395(5)
U(1)-O(2)	2.331(2)	C(4)-C(5)#6	1.390(3)
O(2)-C(1)	1.256(3)	C(4)-C(5)#7	1.390(3)
O(3)-C(1)	1.265(3)	C(5)-C(4)#8	1.390(3)

Table 0.6 Bond Angles for complex iso1.

Bond	Angle [°]	Bond	Angle [°]
O(1)-U(1)-O(1)#1	180.0(1)	O(3)#3-U(1)-O(2)	87.82(6)
O(1)-U(1)-O(3)#2	89.44(8)	O(2)#1-U(1)-O(2)	180.00(8)
O(1)#1-U(1)-O(3)#2	90.56(8)	C(1)-O(2)-U(1)	139.5(1)
O(1)-U(1)-O(3)#3	90.56(8)	C(1)-O(3)-U(1)#4	154.4(2)
O(1)#1-U(1)-O(3)#3	89.44(8)	O(2)-C(1)-O(3)	123.1(2)
O(3)#2-U(1)-O(3)#3	180.00(8)	O(2)-C(1)-C(3)	118.9(2)
O(1)-U(1)-O(2)#1	92.31(8)	O(3)-C(1)-C(3)	118.0(2)
O(1)#1-U(1)-O(2)#1	87.69(8)	C(3)-C(2)-C(3)#5	119.4(3)
O(3)#2-U(1)-O(2)#1	87.82(6)	C(2)-C(3)-C(5)	120.1(2)
O(3)#3-U(1)-O(2)#1	92.18(6)	C(2)-C(3)-C(1)	120.8(2)
O(1)-U(1)-O(2)	87.69(8)	C(5)-C(3)-C(1)	119.1(2)
O(1)#1-U(1)-O(2)	92.31(8)	C(5)#6-C(4)-C(5)#7	119.6(4)
O(3)#2-U(1)-O(2)	92.18(6)	C(4)#8-C(5)-C(3)	120.4(2)

Table 0.7 Bond valence calculation for complex iso1.

Atom	Atom bond	Bond length	Bond valence [vu]	Atom valence [vu]
U1	U(1)-O(1)	1,759	1,76	5,94
	U(1)-O(1)#1	1,759	1,76	
	U(1)-O(3)#2	2,290	0,63	
	U(1)-O(3)#3	2,290	0,63	
	U(1)-O(2)#1	2,331	0,58	
	U(1)-O(2)	2,331	0,58	
O1	U(1)-O(1)	1,759	1,76	1,76
O2	U(1)-O(2)	2,331	0,58	1,88
	O(2)-C(1)	1,256	1,29	
O3	U(1)-O(3)#2	2,290	0,63	1,90
	O(3)-C(1)	1,265	1,27	

Table 0.8 Atomic coordinates ($x10^4$) and equivalent isotropic displacement parameters (A^2x10^3) for complex iso2.

Atom	x	y	z	U(eq)
U(1)	3322(1)	2113(1)	3676(1)	26(1)
U(2)	1339(1)	5103(1)	2762(1)	27(1)
O(1)	1157(8)	1832(3)	3691(11)	44(2)
O(2)	5310(8)	1957(4)	3564(11)	48(2)
O(3)	4207(12)	2039(5)	5440(11)	49(2)
O(4)	2237(11)	4952(5)	4480(10)	47(2)
O(5)	413(12)	5275(5)	1018(13)	58(3)
O(6)	2390(10)	2266(9)	1924(11)	85(5)
O(7)	1684(7)	2884(3)	3869(9)	41(2)
O(8)	3301(11)	960(3)	3647(15)	64(3)
O(9)	4147(8)	3232(3)	3917(9)	42(2)
O(10)	2922(7)	4348(3)	2440(9)	38(2)
O(11)	431(9)	3978(4)	2348(9)	45(2)
O(12)	3519(9)	5392(3)	2809(11)	45(2)
O(13)	6607(11)	1219(4)	3329(14)	75(4)
O(14)	-688(10)	5266(5)	2844(14)	60(3)
C(1)	-2530(8)	2302(4)	3827(10)	30(2)
C(2)	2143(10)	-42(5)	2563(12)	36(2)
C(3)	-66(9)	-350(4)	2329(11)	32(2)
C(4)	3750(8)	4799(4)	2561(11)	32(2)

Atom	x	y	z	U(eq)
C(5)	-340(8)	2594(4)	4007(11)	33(2)
C(6)	887(10)	2425(4)	3830(11)	34(2)
C(7)	1075(10)	81(4)	2842(14)	35(2)
C(8)	-1359(11)	2123(4)	3689(13)	34(2)
C(9)	-2615(10)	2922(5)	4302(11)	35(2)
C(10)	6373(9)	1791(4)	3507(13)	37(2)
C(11)	-408(10)	3222(5)	4512(12)	38(2)
C(12)	-1555(11)	3372(5)	4664(14)	45(3)
C(13)	-1668(10)	5428(4)	3036(14)	43(3)
C(14)	-85(10)	-898(6)	1618(14)	46(3)
C(15)	2094(11)	-598(6)	1813(14)	49(3)
C(16)	1028(12)	-1030(8)	1363(16)	58(4)
OW1	4226(14)	3706(6)	6087(12)	80(4)

Table 0.9 Bond lengths for complex iso2.

Bond	Bond lengths [Å]	Bond	Bond lengths [Å]
U(1)-O(3)	1.75(1)	O(13)-U(2)#2	2.31(1)
U(1)-O(6)	1.76(1)	O(14)-C(13)	1.25(1)
U(1)-O(2)	2.29(1)	C(1)-C(9)	1.38(1)
U(1)-O(8)	2.31(1)	C(1)-C(8)	1.43(1)
U(1)-O(9)	2.39(1)	C(1)-C(10)#3	1.49(1)
U(1)-O(1)	2.47(1)	C(2)-C(7)	1.39(1)
U(1)-O(7)	2.47(1)	C(2)-C(15)	1.39(2)
U(1)-C(6)	2.85(1)	C(2)-C(13)#2	1.49(1)
U(2)-O(4)	1.73(1)	C(3)-C(14)	1.36(1)
U(2)-O(5)	1.76(1)	C(3)-C(7)	1.40(1)
U(2)-O(13)#1	2.31(1)	C(3)-C(4)#4	1.49(1)
U(2)-O(14)	2.31(1)	C(4)-C(3)#5	1.49(1)
U(2)-O(11)	2.42(1)	C(5)-C(8)	1.38(1)
U(2)-O(12)	2.46(1)	C(5)-C(11)	1.40(1)
U(2)-O(10)	2.48(1)	C(5)-C(6)	1.50(1)
U(2)-C(4)	2.85(1)	C(9)-C(12)	1.38(1)
O(1)-C(6)	1.26(1)	C(10)-C(1)#6	1.49(1)
O(2)-C(10)	1.25(1)	C(11)-C(12)	1.39(1)
O(7)-C(6)	1.26(1)	C(13)-O(8)#1	1.28(1)
O(8)-C(13)#2	1.28(1)	C(13)-C(2)#1	1.49(1)
O(10)-C(4)	1.25(1)	C(14)-C(16)	1.42(1)
O(12)-C(4)	1.28(1)	C(15)-C(16)	1.35(2)
O(13)-C(10)	1.21(1)		

Table 0.10 Bond Angles for complex iso2.

Bond	Angle [°]	Bond	Angle [°]	Bond	Angle [°]
O(3)-U(1)-O(6)	174.4(6)	O(4)-U(2)-O(11)	90.6(4)	C(7)-C(2)-C(13)#2	120.3(9)
O(3)-U(1)-O(2)	92.0(5)	O(5)-U(2)-O(11)	90.4(4)	C(15)-C(2)-C(13)#2	119.6(8)
O(6)-U(1)-O(2)	90.6(4)	O(13)#1-U(2)-O(11)	160.5(3)	C(14)-C(3)-C(7)	119.8(8)
O(3)-U(1)-O(8)	85.9(5)	O(14)-U(2)-O(11)	79.7(3)	C(14)-C(3)-C(4)#4	120.6(8)
O(6)-U(1)-O(8)	99.3(7)	O(4)-U(2)-O(12)	89.9(4)	C(7)-C(3)-C(4)#4	119.6(8)
O(2)-U(1)-O(8)	82.3(3)	O(5)-U(2)-O(12)	90.3(5)	O(10)-C(4)-O(12)	119.1(8)
O(3)-U(1)-O(9)	88.8(4)	O(13)#1-U(2)-O(12)	76.9(3)	O(10)-C(4)-C(3)#5	119.8(8)
O(6)-U(1)-O(9)	86.9(6)	O(14)-U(2)-O(12)	158.0(3)	O(12)-C(4)-C(3)#5	121.0(7)
O(2)-U(1)-O(9)	79.1(3)	O(11)-U(2)-O(12)	122.3(2)	O(10)-C(4)-U(2)	60.0(4)
O(8)-U(1)-O(9)	160.4(3)	O(4)-U(2)-O(10)	90.0(4)	O(12)-C(4)-U(2)	59.2(4)
O(3)-U(1)-O(1)	88.7(5)	O(5)-U(2)-O(10)	91.2(4)	C(3)#5-C(4)-U(2)	175.1(8)
O(6)-U(1)-O(1)	90.6(4)	O(13)#1-U(2)-O(10)	129.2(3)	C(8)-C(5)-C(11)	121.6(8)
O(2)-U(1)-O(1)	158.8(2)	O(14)-U(2)-O(10)	149.6(3)	C(8)-C(5)-C(6)	119.1(8)
O(8)-U(1)-O(1)	76.6(3)	O(11)-U(2)-O(10)	69.9(2)	C(11)-C(5)-C(6)	119.3(7)
O(9)-U(1)-O(1)	122.1(2)	O(12)-U(2)-O(10)	52.4(2)	O(1)-C(6)-O(7)	119.5(8)
O(3)-U(1)-O(7)	88.7(4)	O(4)-U(2)-C(4)	90.4(4)	O(1)-C(6)-C(5)	121.1(8)
O(6)-U(1)-O(7)	86.5(5)	O(5)-U(2)-C(4)	90.4(4)	O(7)-C(6)-C(5)	119.4(8)
O(2)-U(1)-O(7)	149.0(3)	O(13)#1-U(2)-C(4)	103.4(3)	O(1)-C(6)-U(1)	59.6(5)
O(8)-U(1)-O(7)	128.7(3)	O(14)-U(2)-C(4)	175.3(3)	O(7)-C(6)-U(1)	59.9(5)

Bond	Angle [°]	Bond	Angle [°]	Bond	Angle [°]
O(9)-U(1)-O(7)	69.9(2)	O(11)-U(2)-C(4)	95.8(2)	C(5)-C(6)-U(1)	176.4(8)
O(1)-U(1)-O(7)	52.2(2)	O(12)-U(2)-C(4)	26.5(2)	C(2)-C(7)-C(3)	119.3(9)
O(3)-U(1)-C(6)	88.1(4)	O(10)-U(2)-C(4)	25.9(2)	C(5)-C(8)-C(1)	118.1(8)
O(6)-U(1)-C(6)	88.8(4)	C(6)-O(1)-U(1)	94.3(5)	C(12)-C(9)-C(1)	120.1(8)
O(2)-U(1)-C(6)	175.2(3)	C(10)-O(2)-U(1)	172.5(7)	O(13)-C(10)-O(2)	122.8(9)
O(8)-U(1)-C(6)	102.6(3)	C(6)-O(7)-U(1)	93.9(6)	O(13)-C(10)-C(1)#6	118.4(8)
O(9)-U(1)-C(6)	96.1(2)	C(13)#2-O(8)-U(1)	146.9(10)	O(2)-C(10)-C(1)#6	118.4(8)
O(1)-U(1)-C(6)	26.0(2)	C(4)-O(10)-U(2)	94.2(5)	C(12)-C(11)-C(5)	118.6(8)
O(7)-U(1)-C(6)	26.2(2)	C(4)-O(12)-U(2)	94.3(5)	C(9)-C(12)-C(11)	121.0(9)
O(4)-U(2)-O(5)	178.7(5)	C(10)-O(13)-U(2)#2	162.5(8)	O(14)-C(13)-O(8)#1	124.4(10)
O(4)-U(2)-O(13)#1	86.0(5)	C(13)-O(14)-U(2)	170.2(10)	O(14)-C(13)-C(2)#1	117.5(10)
O(5)-U(2)-O(13)#1	92.7(5)	C(9)-C(1)-C(8)	120.6(8)	O(8)#1-C(13)-C(2)#1	118.1(8)
O(4)-U(2)-O(14)	90.9(5)	C(9)-C(1)-C(10)#3	121.0(7)	C(3)-C(14)-C(16)	120.5(10)
O(5)-U(2)-O(14)	88.4(5)	C(8)-C(1)-C(10)#3	118.4(8)	C(16)-C(15)-C(2)	121.1(9)
O(13)#1-U(2)-O(14)	81.2(3)	C(7)-C(2)-C(15)	120.0(9)	C(15)-C(16)-C(14)	119.2(11)

Table 0.11 Bond valence calculation for complex iso2.

Atom	Atom bond	Bond length	Bond valence [vu]	Atom valence [vu]
U1	U(1)-O(3)	1,75	1,79	6,19
	U(1)-O(6)	1,76	1,75	
	U(1)-O(2)	2,29	0,63	
	U(1)-O(8)	2,31	0,61	
	U(1)-O(9)	2,39	0,52	
	U(1)-O(1)	2,47	0,45	
	U(1)-O(7)	2,47	0,45	
U2	U(2)-O(4)	1,73	1,86	6,21
	U(2)-O(5)	1,76	1,75	
	U(2)-O(13)	2,31	0,61	
	U(2)-O(14)	2,31	0,61	
	U(2)-O(11)	2,42	0,49	
	U(2)-O(12)	2,46	0,45	
	U(2)-O(10)	2,48	0,44	
O1	U(1)-O(1)	2,47	0,45	1,73
	O(1)-C(6)	1,26	1,28	
O2	U(1)-O(2)	2,29	0,63	1,94
	O(2)-C(10)	1,25	1,31	
O3	U(1)-O(3)	1,75	1,79	1,79
O4	U(2)-O(4)	1,73	1,86	1,86
O5	U(2)-O(5)	1,76	1,75	1,75
O6	U(1)-O(6)	1,76	1,75	1,75
O7	U(1)-O(7)	2,47	0,45	1,73
	O(7)-C(6)	1,26	1,28	
O8	U(1)-O(8)	2,31	0,61	1,84
	O(8)-C(13)	1,28	1,24	
O9	U(1)-O(9)	2,39	0,52	0,52
O10	U(2)-O(10)	2,48	0,44	1,75
	O(10)-C(4)	1,25	1,31	
O11	U(2)-O(11)	2,42	0,49	0,49
O12	U(2)-O(12)	2,46	0,45	1,69
	O(12)-C(4)	1,28	1,24	
O13	U(2)-O(13)	2,31	0,61	2,02
	O(13)-C(10)	1,21	1,41	
O14	U(2)-O(14)	2,31	0,61	1,92
	O(14)-C(13)	1,25	1,31	

Table 0.12 Atomic coordinates (x10⁴) and equivalent isotropic displacement parameters (A²x10³) for complex iso3.

Atom	x	y	z	U(eq)
U(1)	5000	5000	5000	24(1)
O(1)	3609(3)	2291(2)	2745(2)	34(1)
O(2)	3162(4)	1518(3)	5569(2)	43(1)
O(3)	4370(4)	3940(3)	7537(2)	43(1)
O(4)	2514(3)	5187(3)	4882(2)	39(1)
O(5)	2123(4)	-933(3)	3002(2)	42(1)
C(1)	2771(3)	496(3)	2191(2)	25(1)
C(2)	3461(4)	2094(3)	7008(2)	29(1)
C(3)	3067(3)	1217(3)	-410(2)	23(1)
C(4)	2427(3)	-215(3)	524(2)	23(1)
C(5)	2740(3)	573(3)	8016(2)	24(1)
C(6)	1779(4)	-1478(3)	7389(2)	30(1)
C(7)	1490(4)	-2267(3)	-105(2)	35(1)
C(8)	1164(5)	-2898(3)	-1672(3)	39(1)

Table 0.13 Bond lengths for complex iso3.

Bond	Bond lengths [Å]	Bond	Bond lengths [Å]
U(1)-O(4)	1.756(2)	O(3)-C(2)	1.246(3)
U(1)-O(4)#1	1.756(2)	O(5)-C(1)	1.310(2)
U(1)-O(1)#1	2.454(2)	C(1)-C(4)	1.479(3)
U(1)-O(1)	2.454(2)	C(2)-C(5)	1.489(3)
U(1)-O(2)	2.502(2)	C(3)-C(4)	1.390(3)
U(1)-O(2)#1	2.502(2)	C(3)-C(5)#2	1.394(3)
U(1)-O(3)	2.514(2)	C(4)-C(7)	1.392(3)
U(1)-O(3)#1	2.514(2)	C(5)-C(6)	1.391(3)
U(1)-C(2)	2.905(2)	C(5)-C(3)#3	1.394(3)
U(1)-C(2)#1	2.905(2)	C(6)-C(8)#3	1.386(3)
O(1)-C(1)	1.218(3)	C(7)-C(8)	1.387(3)
O(2)-C(2)	1.273(3)	C(8)-C(6)#2	1.386(3)

Table 0.14 Bond Angles for complex iso3.

Bond	Angle [°]	Bond	Angle [°]	Bond	Angle [°]
O(4)-U(1)-O(4)#1	180.000(1)	O(2)#1-U(1)-O(3)	128.86(5)	C(2)-O(3)-U(1)	95.2(1)
O(4)-U(1)-O(1)#1	90.06(7)	O(4)-U(1)-O(3)#1	90.15(8)	O(1)-C(1)-O(5)	123.5(2)
O(4)#1-U(1)-O(1)#1	89.94(7)	O(4)#1-U(1)-O(3)#1	89.85(8)	O(1)-C(1)-C(4)	121.3(2)
O(4)-U(1)-O(1)	89.94(7)	O(1)#1-U(1)-O(3)#1	116.61(5)	O(5)-C(1)-C(4)	115.2(2)
O(4)#1-U(1)-O(1)	90.06(7)	O(1)-U(1)-O(3)#1	63.39(5)	O(3)-C(2)-O(2)	118.5(2)
O(1)#1-U(1)-O(1)	180.0	O(2)-U(1)-O(3)#1	128.86(5)	O(3)-C(2)-C(5)	121.5(2)
O(4)-U(1)-O(2)	90.37(8)	O(2)#1-U(1)-O(3)#1	51.14(5)	O(2)-C(2)-C(5)	120.0(2)
O(4)#1-U(1)-O(2)	89.63(8)	O(3)-U(1)-O(3)#1	180.0	O(3)-C(2)-U(1)	59.5(1)
O(1)#1-U(1)-O(2)	114.53(5)	O(4)-U(1)-C(2)	90.67(8)	O(2)-C(2)-U(1)	59.1(1)
O(1)-U(1)-O(2)	65.47(5)	O(4)#1-U(1)-C(2)	89.33(8)	C(5)-C(2)-U(1)	177.6(2)
O(4)-U(1)-O(2)#1	89.63(8)	O(1)#1-U(1)-C(2)	88.66(5)	C(4)-C(3)-C(5)#2	119.2(2)
O(4)#1-U(1)-O(2)#1	90.37(8)	O(1)-U(1)-C(2)	91.34(5)	C(3)-C(4)-C(7)	120.4(2)
O(1)#1-U(1)-O(2)#1	65.47(5)	O(2)-U(1)-C(2)	25.87(6)	C(3)-C(4)-C(1)	118.4(2)
O(1)-U(1)-O(2)#1	114.53(5)	O(2)#1-U(1)-C(2)	154.13(6)	C(7)-C(4)-C(1)	121.2(2)
O(2)-U(1)-O(2)#1	180.0	O(3)-U(1)-C(2)	25.28(6)	C(6)-C(5)-C(3)#3	120.4(2)
O(4)-U(1)-O(3)	89.85(8)	O(3)#1-U(1)-C(2)	154.72(6)	C(6)-C(5)-C(2)	120.0(2)
O(4)#1-U(1)-O(3)	90.15(8)	O(3)#1-U(1)-C(2)#1	25.28(6)	C(3)#3-C(5)-C(2)	119.6(2)
O(1)#1-U(1)-O(3)	63.39(5)	C(2)-U(1)-C(2)#1	180.0	C(8)#3-C(6)-C(5)	120.1(2)
O(1)-U(1)-O(3)	116.61(5)	C(1)-O(1)-U(1)	149.8(1)	C(8)-C(7)-C(4)	120.2(2)
O(2)-U(1)-O(3)	51.14(5)	C(2)-O(2)-U(1)	95.1(1)	C(6)#2-C(8)-C(7)	119.8(2)

Table 0.15 Bond valence calculation for complex iso3.

Atom	Atom bond	Bond length	Bond valence [vu]	Atom valence [vu]
U1	U(1)-O(4)	1,756	1,77	6,11
	U(1)-O(4)#1	1,756	1,77	
	U(1)-O(1)#1	2,454	0,46	
	U(1)-O(1)	2,454	0,46	
	U(1)-O(2)	2,502	0,42	
	U(1)-O(2)#1	2,502	0,42	
	U(1)-O(3)	2,514	0,41	
	U(1)-O(3)#1	2,514	0,41	
O1	U(1)-O(1)	2,454	0,46	1,85
	O(1)-C(1)	1,218	1,39	
O2	U(1)-O(2)	2,502	0,42	1,67
	O(2)-C(2)	1,273	1,25	
O3	U(1)-O(3)	2,514	0,41	1,73
	O(3)-C(2)	1,246	1,32	
O4	U(1)-O(4)	1,756	1,77	1,77
O5	O(5)-C(1)	1,310	1,17	1,17

Table 0.16 Atomic coordinates (x10^4) and equivalent isotropic displacement parameters (A^2x10^3) for complex iso4.

Atom	x	y	z	U(eq)
U(1)	1212(1)	2014(1)	2904(1)	22(1)
O(1)	2619(6)	1924(4)	5983(4)	38(1)
O(2)	196(1)	3249(4)	4275(9)	37(2)
O(3)	72(1)	3293(4)	1567(9)	37(2)
O(4)	-241(7)	1893(2)	-158(4)	38(1)
O(5)	3732(5)	2014(6)	2772(4)	37(1)
O(6)	-1306(5)	2024(6)	3062(4)	37(1)
O(7)	209(1)	842(4)	4568(8)	33(2)
O(8)	34(1)	833(4)	1297(8)	34(1)
O(9)	3684(8)	-1608(3)	7228(5)	49(1)
O(10)	495(1)	-1736(5)	10019(9)	58(2)
C(1)	2712(8)	1188(3)	5940(7)	27(1)
C(2)	3530(8)	739(3)	7498(7)	27(1)
C(3)	4265(8)	-485(3)	8840(7)	29(1)
C(4)	-1567(9)	-493(4)	-2999(7)	27(1)
C(5)	-285(9)	1165(3)	-105(6)	29(1)
C(6)	-1030(8)	704(3)	-1648(6)	23(1)
C(7)	434(1)	-1342(4)	8760(9)	39(1)
C(8)	1391(7)	3635(3)	2963(6)	25(1)
C(9)	-497(2)	699(7)	45(1)	43(2)
C(10)	-883(8)	-90(3)	-1564(6)	23(1)
C(11)	-2386(9)	-150(3)	-4520(6)	31(1)
C(12)	-257(1)	647(3)	-4602(7)	34(1)
C(13)	-187(1)	1071(3)	-3163(7)	31(1)
C(14)	3553(7)	-48(3)	7391(6)	26(1)
C(15)	500(1)	-123(4)	10383(7)	36(1)
C(16)	-5712(9)	1105(3)	-976(7)	35(1)
OW1	8990(8)	-1990(4)	12180(6)	66(2)
OW2	378(1)	-1861(5)	1311(1)	113(3)
OW3	1107(1)	-619(8)	1303(1)	117(4)
N(1)	-3717(4)	2008(5)	1315(3)	15(1)

Table 0.17 Bond lengths for complex iso4.

Bond	Bond lengths [Å]	Bond	Bond lengths [Å]
U(1)-O(5)	1.768(3)	C(1)-C(2)	1.490(7)
U(1)-O(6)	1.776(3)	C(2)-C(14)	1.381(7)
U(1)-O(2)	2.433(8)	C(2)-C(16)#1	1.393(8)
U(1)-O(8)	2.445(7)	C(3)-C(15)	1.401(8)
U(1)-O(7)	2.456(7)	C(3)-C(14)	1.401(7)

Bond	Bond lengths [Å]	Bond	Bond lengths [Å]
U(1)-O(3)	2.485(7)	C(3)-C(7)	1.502(8)
U(1)-O(4)	2.487(4)	C(4)-C(10)	1.359(8)
U(1)-O(1)	2.495(3)	C(4)-C(11)	1.375(8)
U(1)-C(8)	2.840(5)	C(4)-C(8)#2	1.530(8)
U(1)-C(1)	2.853(5)	C(5)-C(6)	1.488(7)
U(1)-C(5)	2.855(5)	C(6)-C(13)	1.391(7)
O(1)-C(1)	1.291(8)	C(6)-C(10)	1.393(6)
O(2)-C(8)	1.257(9)	C(8)-C(4)#3	1.530(8)
O(3)-C(8)	1.279(8)	C(9)-C(16)	1.36(1)
O(4)-C(5)	1.275(6)	C(9)-C(15)#4	1.44(1)
O(6)-N(1)	1.839(4)	C(11)-C(12)	1.399(7)
O(7)-C(1)	1.265(9)	C(12)-C(13)	1.382(8)
O(8)-C(5)	1.273(8)	C(15)-C(9)#1	1.434(1)
O(9)-C(7)	1.322(8)	C(16)-C(2)#4	1.393(8)
O(10)-C(7)	1.232(9)		

Table 0.18 Bond Angles for complex iso4.

Bond	Angle [°]	Bond	Angle [°]	Bond	Angle [°]
O(5)-U(1)-O(6)	179.1(4)	O(1)-U(1)-C(8)	92.5(2)	C(14)-C(2)-C(1)	118.5(5)
O(5)-U(1)-O(2)	88.3(4)	O(5)-U(1)-C(1)	88.9(2)	C(16)#1-C(2)-C(1)	120.7(5)
O(6)-U(1)-O(2)	90.9(4)	O(6)-U(1)-C(1)	90.8(2)	C(15)-C(3)-C(14)	120.0(5)
O(5)-U(1)-O(8)	91.9(3)	O(2)-U(1)-C(1)	93.1(2)	C(15)-C(3)-C(7)	119.2(6)
O(6)-U(1)-O(8)	88.9(4)	O(8)-U(1)-C(1)	91.9(2)	C(14)-C(3)-C(7)	120.8(5)
O(2)-U(1)-O(8)	175.0(2)	O(7)-U(1)-C(1)	26.2(2)	C(10)-C(4)-C(11)	122.8(6)
O(5)-U(1)-O(7)	88.5(4)	O(3)-U(1)-C(1)	145.9(2)	C(10)-C(4)-C(8)#2	119.8(5)
O(6)-U(1)-O(7)	91.7(3)	O(4)-U(1)-C(1)	144.7(2)	C(11)-C(4)-C(8)#2	117.4(5)
O(2)-U(1)-O(7)	119.3(2)	O(1)-U(1)-C(1)	26.9(2)	O(8)-C(5)-O(4)	119.0(5)
O(8)-U(1)-O(7)	65.7(3)	C(8)-U(1)-C(1)	119.3(1)	O(8)-C(5)-C(6)	120.0(5)
O(5)-U(1)-O(3)	87.8(4)	O(5)-U(1)-C(5)	91.2(2)	O(4)-C(5)-C(6)	121.0(5)
O(6)-U(1)-O(3)	91.9(4)	O(6)-U(1)-C(5)	89.6(2)	O(8)-C(5)-U(1)	58.5(4)
O(2)-U(1)-O(3)	52.9(3)	O(2)-U(1)-C(5)	148.6(2)	O(4)-C(5)-U(1)	60.5(3)
O(8)-U(1)-O(3)	122.1(2)	O(8)-U(1)-C(5)	26.4(2)	C(6)-C(5)-U(1)	178.4(4)
O(7)-U(1)-O(3)	171.5(2)	O(7)-U(1)-C(5)	92.0(2)	C(13)-C(6)-C(10)	120.7(4)
O(5)-U(1)-O(4)	90.3(2)	O(3)-U(1)-C(5)	95.7(2)	C(13)-C(6)-C(5)	119.5(4)
O(6)-U(1)-O(4)	90.4(2)	O(4)-U(1)-C(5)	26.5(1)	C(10)-C(6)-C(5)	119.8(4)
O(2)-U(1)-O(4)	122.1(2)	O(1)-U(1)-C(5)	145.0(2)	O(10)-C(7)-O(9)	125.2(7)
O(8)-U(1)-O(4)	52.9(2)	C(8)-U(1)-C(5)	122.47(14)	O(10)-C(7)-C(3)	121.8(7)
O(7)-U(1)-O(4)	118.5(2)	C(1)-U(1)-C(5)	118.24(16)	O(9)-C(7)-C(3)	113.0(5)
O(3)-U(1)-O(4)	69.2(2)	C(1)-O(1)-U(1)	92.2(3)	O(2)-C(8)-O(3)	119.6(7)
O(5)-U(1)-O(1)	90.5(1)	C(8)-O(2)-U(1)	95.3(5)	O(2)-C(8)-C(4)#3	121.2(5)
O(6)-U(1)-O(1)	88.8(1)	C(8)-O(3)-U(1)	92.3(4)	O(3)-C(8)-C(4)#3	119.2(5)
O(2)-U(1)-O(1)	66.4(2)	C(5)-O(4)-U(1)	93.1(3)	O(2)-C(8)-U(1)	58.6(4)
O(8)-U(1)-O(1)	118.6(2)	U(1)-O(6)-N(1)	125.7(2)	O(3)-C(8)-U(1)	61.0(4)
O(7)-U(1)-O(1)	53.1(2)	C(1)-O(7)-U(1)	94.7(4)	C(4)#3-C(8)-U(1)	178.0(4)
O(3)-U(1)-O(1)	119.3(2)	C(5)-O(8)-U(1)	95.1(4)	C(16)-C(9)-C(15)#4	119.4(7)
O(4)-U(1)-O(1)	171.5(2)	O(7)-C(1)-O(1)	120.0(5)	C(4)-C(10)-C(6)	118.2(5)
O(5)-U(1)-C(8)	87.9(4)	O(7)-C(1)-C(2)	119.4(5)	C(4)-C(11)-C(12)	119.1(5)
O(6)-U(1)-C(8)	91.5(4)	O(1)-C(1)-C(2)	120.6(5)	C(13)-C(12)-C(11)	119.3(5)
O(2)-U(1)-C(8)	26.2(2)	O(7)-C(1)-U(1)	59.1(4)	C(12)-C(13)-C(6)	119.9(5)
O(8)-U(1)-C(8)	148.9(2)	O(1)-C(1)-U(1)	60.9(3)	C(2)-C(14)-C(3)	119.6(5)
O(7)-U(1)-C(8)	145.4(2)	C(2)-C(1)-U(1)	178.0(4)	C(3)-C(15)-C(9)#1	119.1(6)
O(3)-U(1)-C(8)	26.8(2)	C(14)-C(2)-C(16)	120.8(5)	C(9)-C(16)-C(2)#4	121.0(7)
O(4)-U(1)-C(8)	96.0(1)				

Table 0.19 Bond valence calculation for complex iso4.

Atom	Atom bond	Bond length	Bond valence [vu]	Atom valence [vu]
U1	U(1)-O(5)	1,768	1,73	6,12

	U(1)-O(6)	1,776	1,70	
	U(1)-O(2)	2,433	0,48	
	U(1)-O(8)	2,445	0,47	
	U(1)-O(7)	2,456	0,46	
	U(1)-O(3)	2,485	0,43	
	U(1)-O(4)	2,487	0,43	
	U(1)-O(1)	2,495	0,43	
O1	U(1)-O(1)	2,495	0,43	1,64
	O(1)-C(1)	1,291	1,21	
O2	U(1)-O(2)	2,433	0,48	1,77
	O(2)-C(8)	1,257	1,29	
O3	U(1)-O(3)	2,485	0,43	1,67
	O(3)-C(8)	1,279	1,24	
O4	U(1)-O(4)	2,487	0,43	1,68
	O(4)-C(5)	1,275	1,25	
O5	U(1)-O(5)	1,768	1,73	1,73
O6	U(1)-O(6)	1,776	1,70	1,70
O7	U(1)-O(7)	2,456	0,46	1,73
	O(7)-C(1)	1,265	1,27	
O8	U(1)-O(8)	2,445	0,47	1,72
	O(8)-C(5)	1,273	1,25	
O9	O(9)-C(7)	1,322	1,14	1,14
O10	O(10)-C(7)	1,232	1,36	1,36

Table 0.20 Atomic coordinates (x10⁴) and equivalent isotropic displacement parameters (A²x10³) for complex iso5.

Atom	x	y	z	U(eq)
U(1)	5000	0	0	32(1)
U(2)	1290(1)	3191(1)	3730(1)	23(1)
O(1)	464(1)	4112(6)	2229(5)	37(2)
O(2)	2252(9)	4744(6)	5347(5)	31(2)
O(3)	499(9)	1359(6)	2226(5)	31(2)
O(4)	1980(14)	2513(7)	5301(5)	66(3)
O(5)	3351(10)	507(8)	447(6)	46(2)
O(6)	2647(10)	-1773(7)	-1290(5)	49(2)
O(7)	4229(11)	-2400(7)	310(5)	50(2)
O(8)	1191(11)	645(7)	3590(5)	44(2)
O(9)	1339(9)	5667(6)	3599(5)	33(2)
O(10)	3521(9)	3528(7)	3779(6)	42(2)
O(11)	6096(10)	-814(7)	1541(5)	40(2)
O(12)	-943(9)	2803(7)	3672(5)	37(2)
C(1)	778(13)	5376(10)	2676(7)	29(2)
C(2)	712(12)	371(9)	2685(7)	25(2)
C(3)	5248(14)	-2078(10)	1163(7)	32(3)
C(4)	2477(15)	3781(10)	5797(8)	35(3)
C(5)	475(13)	6513(9)	2132(7)	25(2)
C(6)	3365(13)	4037(9)	6844(7)	26(2)
C(7)	5457(14)	-3224(10)	1707(7)	31(3)
C(8)	436(13)	-1069(9)	2127(7)	25(2)
C(9)	6381(13)	-2956(10)	2684(7)	31(3)
C(10)	4022(14)	5435(10)	7376(8)	37(3)
C(11)	676(13)	7849(9)	2632(7)	30(2)
C(12)	-18(15)	-1374(10)	1134(7)	35(3)
C(13)	-48(15)	6210(10)	1121(7)	37(3)
C(14)	4743(15)	-4628(10)	1197(7)	36(3)
C(15)	-275(17)	-2720(10)	633(8)	48(3)
C(16)	5036(15)	-5717(11)	1650(8)	41(3)
N(1)	-3535(12)	2252(9)	4665(7)	41(2)
C(17)	-5000	0	5000	54(5)
C(18)	-4690(30)	1470(20)	5222(15)	31(5)
C(19)	-3670(30)	820(20)	4540(20)	52(7)
OW1	-5373(18)	936(14)	2642(10)	120(4)
OW2	-1560(50)	280(40)	4540(30)	388(19)

Table 0.21 Bond lengths for complex iso5.

Bond	Bond lengths [Å]	Bond	Bond lengths [Å]
U(1)-O(5)#1	1.776(8)	C(1)-C(5)	1.50(1)
U(1)-O(5)	1.776(8)	C(2)-C(8)	1.48(1)
U(1)-O(6)#1	2.455(7)	C(3)-C(7)	1.49(1)
U(1)-O(6)	2.455(7)	C(4)-C(6)	1.47(1)
U(1)-O(7)	2.463(7)	C(5)-C(11)	1.38(1)
U(1)-O(7)#1	2.463(7)	C(5)-C(13)	1.40(1)
U(1)-O(11)	2.510(6)	C(6)-C(9)#2	1.38(1)
U(1)-O(11)#1	2.510(6)	C(6)-C(10)	1.41(1)
U(1)-C(3)	2.86(1)	C(7)-C(9)	1.39(1)
U(1)-C(3)#1	2.86(1)	C(7)-C(14)	1.40(1)
U(2)-O(12)	1.750(7)	C(8)-C(12)	1.38(1)
U(2)-O(10)	1.753(7)	C(8)-C(11)#3	1.41(1)
U(2)-O(4)	2.444(7)	C(9)-C(6)#2	1.38(1)
U(2)-O(2)	2.467(6)	C(10)-C(16)#2	1.39(1)
U(2)-O(1)	2.483(6)	C(11)-C(8)#4	1.41(1)
U(2)-O(9)	2.484(6)	C(12)-C(15)	1.38(1)
U(2)-O(8)	2.489(6)	C(13)-C(15)#4	1.38(1)
U(2)-O(3)	2.491(6)	C(14)-C(16)	1.38(1)
U(2)-C(4)	2.86(1)	C(15)-C(13)#3	1.38(1)
U(2)-C(1)	2.871(9)	C(16)-C(10)#2	1.39(1)
U(2)-C(2)	2.874(9)	N(1)-C(19)	1.38(2)
O(1)-C(1)	1.27(1)	N(1)-C(18)	1.55(2)
O(2)-C(4)	1.25(1)	C(17)-C(18)	1.40(2)
O(3)-C(2)	1.28(1)	C(17)-C(18)#5	1.40(2)
O(4)-C(4)	1.28(1)	C(17)-C(19)#5	1.56(3)
O(7)-C(3)	1.26(1)	C(17)-C(19)	1.56(3)
O(8)-C(2)	1.25(1)	C(18)-C(19)	1.60(3)
O(9)-C(1)	1.28(1)	C(19)-OW2	1.91(4)
O(11)-C(3)	1.26(1)		

Table 0.22 Bond Angles for complex iso5.

Bond	Angle [°]	Bond	Angle [°]	Bond	Angle [°]
O(5)#1-U(1)-O(5)	180.0(7)	O(10)-U(2)-O(9)	90.4(3)	O(9)-C(1)-U(2)	59.7(4)
O(5)#1-U(1)-O(6)#1	88.8(3)	O(4)-U(2)-O(9)	121.4(2)	C(5)-C(1)-U(2)	178.8(7)
O(5)-U(1)-O(6)#1	91.2(3)	O(2)-U(2)-O(9)	69.1(2)	O(8)-C(2)-O(3)	119.5(8)
O(5)#1-U(1)-O(6)	91.2(3)	O(1)-U(2)-O(9)	52.5(2)	O(8)-C(2)-C(8)	121.4(8)
O(5)-U(1)-O(6)	88.8(3)	O(12)-U(2)-O(8)	90.3(3)	O(3)-C(2)-C(8)	119.0(9)
O(6)#1-U(1)-O(6)	180.0(3)	O(10)-U(2)-O(8)	88.1(3)	O(8)-C(2)-U(2)	59.7(5)
O(5)#1-U(1)-O(7)	86.8(3)	O(4)-U(2)-O(8)	67.3(2)	O(3)-C(2)-U(2)	59.9(5)
O(5)-U(1)-O(7)	93.2(3)	O(2)-U(2)-O(8)	119.4(2)	C(8)-C(2)-U(2)	178.5(7)
O(6)#1-U(1)-O(7)	116.5(2)	O(1)-U(2)-O(8)	118.9(2)	O(7)-C(3)-O(11)	120.3(9)
O(6)-U(1)-O(7)	63.5(2)	O(9)-U(2)-O(8)	171.2(2)	O(7)-C(3)-C(7)	118.7(9)
O(5)#1-U(1)-O(7)#1	93.2(3)	O(12)-U(2)-O(3)	89.1(3)	O(11)-C(3)-C(7)	121.0(9)
O(5)-U(1)-O(7)#1	86.8(3)	O(10)-U(2)-O(3)	89.7(3)	O(7)-C(3)-U(1)	59.1(5)
O(6)#1-U(1)-O(7)#1	63.5(2)	O(4)-U(2)-O(3)	119.4(2)	O(11)-C(3)-U(1)	61.3(5)
O(6)-U(1)-O(7)#1	116.5(2)	O(2)-U(2)-O(3)	171.3(2)	C(7)-C(3)-U(1)	174.6(8)
O(7)-U(1)-O(7)#1	180.0(3)	O(1)-U(2)-O(3)	66.8(2)	O(2)-C(4)-O(4)	117.4(9)
O(5)#1-U(1)-O(11)	91.2(3)	O(9)-U(2)-O(3)	119.2(2)	O(2)-C(4)-C(6)	123.7(9)
O(5)-U(1)-O(11)	88.8(3)	O(8)-U(2)-O(3)	52.1(2)	O(4)-C(4)-C(6)	118.8(8)
O(6)#1-U(1)-O(11)	64.8(2)	O(12)-U(2)-C(4)	93.2(3)	O(2)-C(4)-U(2)	59.4(5)
O(6)-U(1)-O(11)	115.2(2)	O(10)-U(2)-C(4)	87.1(3)	O(4)-C(4)-U(2)	58.5(5)
O(7)-U(1)-O(11)	52.0(2)	O(4)-U(2)-C(4)	26.6(2)	C(6)-C(4)-U(2)	170.4(8)
O(7)#1-U(1)-O(11)	128.0(2)	O(2)-U(2)-C(4)	25.9(2)	C(11)-C(5)-C(13)	120.4(8)
O(5)#1-U(1)-O(11)#1	88.8(3)	O(1)-U(2)-C(4)	147.5(2)	C(11)-C(5)-C(1)	119.6(9)
O(5)-U(1)-O(11)#1	91.2(3)	O(9)-U(2)-C(4)	95.0(2)	C(13)-C(5)-C(1)	120.0(8)
O(6)#1-U(1)-O(11)#1	115.2(2)	O(8)-U(2)-C(4)	93.6(2)	C(9)#2-C(6)-C(10)	118.9(9)
O(6)-U(1)-O(11)#1	64.8(2)	O(3)-U(2)-C(4)	145.6(2)	C(9)#2-C(6)-C(4)	122.3(9)
O(7)-U(1)-O(11)#1	128.0(2)	O(12)-U(2)-C(1)	89.1(3)	C(10)-C(6)-C(4)	118.8(8)
O(7)#1-U(1)-O(11)#1	52.0(2)	O(10)-U(2)-C(1)	92.1(3)	C(9)-C(7)-C(14)	119.0(9)

Bond	Angle [°]	Bond	Angle [°]	Bond	Angle [°]
O(11)-U(1)-O(11)#1	180.0(5)	O(4)-U(2)-C(1)	147.6(3)	C(9)-C(7)-C(3)	122.7(9)
O(5)#1-U(1)-C(3)	87.9(3)	O(2)-U(2)-C(1)	95.5(2)	C(14)-C(7)-C(3)	118.3(9)
O(5)-U(1)-C(3)	92.1(3)	O(1)-U(2)-C(1)	26.2(2)	C(12)-C(8)-C(11)#3	119.0(9)
O(6)#1-U(1)-C(3)	90.6(3)	O(9)-U(2)-C(1)	26.3(2)	C(12)-C(8)-C(2)	122.1(8)
O(6)-U(1)-C(3)	89.4(3)	O(8)-U(2)-C(1)	145.1(3)	C(11)#3-C(8)-C(2)	118.9(9)
O(7)-U(1)-C(3)	26.0(2)	O(3)-U(2)-C(1)	93.0(2)	C(6)#2-C(9)-C(7)	121.4(9)
O(7)#1-U(1)-C(3)	154.0(2)	C(4)-U(2)-C(1)	121.4(3)	C(16)#2-C(10)-C(6)	120.2(9)
O(11)-U(1)-C(3)	26.1(2)	O(12)-U(2)-C(2)	89.5(3)	C(5)-C(11)-C(8)#4	119.9(9)
O(11)#1-U(1)-C(3)	153.9(2)	O(10)-U(2)-C(2)	88.9(3)	C(8)-C(12)-C(15)	121.1(9)
O(5)#1-U(1)-C(3)#1	92.1(3)	O(4)-U(2)-C(2)	93.0(3)	C(15)#4-C(13)-C(5)	119.2(9)
O(5)-U(1)-C(3)#1	87.9(3)	O(2)-U(2)-C(2)	145.1(2)	C(16)-C(14)-C(7)	120.3(9)
O(6)#1-U(1)-C(3)#1	89.4(3)	O(1)-U(2)-C(2)	93.2(2)	C(12)-C(15)-C(13)#3	120.5(10)
O(6)-U(1)-C(3)#1	90.6(3)	O(9)-U(2)-C(2)	145.6(2)	C(14)-C(16)-C(10)#2	120.1(10)
O(7)-U(1)-C(3)#1	154.0(2)	O(8)-U(2)-C(2)	25.7(2)	C(19)-N(1)-C(18)	66.0(14)
O(7)#1-U(1)-C(3)#1	26.0(2)	O(3)-U(2)-C(2)	26.4(2)	C(18)-C(17)-C(18)#5	180.000(2)
O(11)-U(1)-C(3)#1	153.9(2)	C(4)-U(2)-C(2)	119.3(3)	C(18)-C(17)-C(19)#5	114.5(12)
O(11)#1-U(1)-C(3)#1	26.1(2)	C(1)-U(2)-C(2)	119.3(3)	C(18)#5-C(17)-C(19)#5	65.5(12)
C(3)-U(1)-C(3)#1	180.0(3)	C(1)-O(1)-U(2)	94.2(6)	C(18)-C(17)-C(19)	65.5(12)
O(12)-U(2)-O(10)	178.4(3)	C(4)-O(2)-U(2)	94.7(6)	C(18)#5-C(17)-C(19)	114.5(12)
O(12)-U(2)-O(4)	89.3(3)	C(2)-O(3)-U(2)	93.8(6)	C(19)#5-C(17)-C(19)	180.000(5)
O(10)-U(2)-O(4)	90.3(4)	C(4)-O(4)-U(2)	95.0(6)	C(17)-C(18)-N(1)	113.6(15)
O(12)-U(2)-O(2)	93.1(3)	C(3)-O(7)-U(1)	94.9(6)	C(17)-C(18)-C(19)	62.1(12)
O(10)-U(2)-O(2)	87.9(3)	C(2)-O(8)-U(2)	94.6(5)	N(1)-C(18)-C(19)	51.9(11)
O(4)-U(2)-O(2)	52.3(2)	C(1)-O(9)-U(2)	94.0(5)	N(1)-C(19)-C(17)	114.1(19)
O(12)-U(2)-O(1)	87.5(3)	C(3)-O(11)-U(1)	92.6(6)	N(1)-C(19)-C(18)	62.1(13)
O(10)-U(2)-O(1)	93.1(3)	O(1)-C(1)-O(9)	119.3(8)	C(17)-C(19)-C(18)	52.4(11)
O(4)-U(2)-O(1)	173.0(3)	O(1)-C(1)-C(5)	120.7(9)	N(1)-C(19)-OW2	116.0(19)
O(2)-U(2)-O(1)	121.6(2)	O(9)-C(1)-C(5)	120.1(8)	C(17)-C(19)-OW2	120.3(17)
O(12)-U(2)-O(9)	91.2(3)	O(1)-C(1)-U(2)	59.6(5)	C(18)-C(19)-OW2	144(2)

Table 0.23 Bond valence calculation for complex iso5.

Atom	Atom bond	Bond length	Bond valence [vu]	Atom valence [vu]
U1	U(1)-O(5)#1	1,776	1,70	6,05
	U(1)-O(5)	1,776	1,70	
	U(1)-O(6)#1	2,455	0,46	
	U(1)-O(6)	2,455	0,46	
	U(1)-O(7)	2,463	0,45	
	U(1)-O(7)#1	2,463	0,45	
	U(1)-O(11)	2,510	0,41	
	U(1)-O(11)#1	2,510	0,41	
U2	U(2)-O(12)	1,750	1,79	6,21
	U(2)-O(10)	1,753	1,78	
	U(2)-O(4)	2,444	0,47	
	U(2)-O(2)	2,467	0,45	
	U(2)-O(1)	2,483	0,44	
	U(2)-O(9)	2,484	0,43	
	U(2)-O(8)	2,489	0,43	
	U(2)-O(3)	2,491	0,43	
O1	U(2)-O(1)	2,483	0,44	1,70
	O(1)-C(1)	1,270	1,26	
O2	U(2)-O(2)	2,467	0,45	1,76
	O(2)-C(4)	1,250	1,31	
O3	U(2)-O(3)	2,491	0,43	1,66
	O(3)-C(2)	1,280	1,24	
O4	U(2)-O(4)	2,444	0,47	1,71
	O(4)-C(4)	1,280	1,24	
O5	U(1)-O(5)	1,776	1,70	1,70
O6	U(1)-O(6)	2,455	0,46	0,46
O7	U(1)-O(7)	2,463	0,45	1,74
	O(7)-C(3)	1,260	1,28	
O8	U(2)-O(8)	2,489	0,43	1,74
	O(8)-C(2)	1,250	1,31	

Atom	Atom bond	Bond length	Bond valence [vu]	Atom valence [vu]
O9	U(2)-O(9)	2,484	0,43	1,67
	O(9)-C(1)	1,280	1,24	
O10	U(2)-O(10)	1,753	1,78	1,78
O11	U(1)-O(11)	2,510	0,41	1,70
	O(11)-C(3)	1,260	1,28	
O12	U(2)-O(12)	1,750	1,79	1,79

Table 0.24 Atomic coordinates (x10⁴) and equivalent isotropic displacement parameters (A²x10³) for complex iso6.

Atom	x	y	z	U(eq)
U(1)	289(1)	995(1)	6289(1)	22(1)
O(1)	1252(5)	820(2)	6981(2)	36(1)
O(2)	-639(5)	1164(2)	5579(2)	34(1)
O(3)	-781(4)	-276(2)	6267(2)	34(1)
O(4)	-2508(4)	949(2)	6731(2)	30(1)
O(5)	1627(4)	2219(2)	6187(2)	37(1)
O(6)	-1170(5)	1988(2)	6767(2)	37(1)
O(7)	3008(5)	1275(2)	5878(2)	32(1)
O(8)	1630(4)	-126(2)	5881(2)	33(1)
C(1)	444(6)	-554(2)	6017(2)	26(1)
C(2)	-2425(6)	1629(3)	6897(2)	27(1)
C(3)	2914(6)	1965(3)	5978(2)	28(1)
C(4)	-3753(6)	1991(3)	7224(2)	26(1)
C(5)	517(6)	-1355(2)	5860(2)	23(1)
C(6)	4291(6)	2445(2)	5840(2)	24(1)
C(7)	-5000	1610(3)	7500	27(2)
C(8)	4206(6)	3196(2)	5975(2)	25(1)
C(9)	1887(6)	-1653(3)	5601(2)	30(1)
C(10)	-3752(7)	2758(3)	7233(2)	32(1)
C(11)	5691(6)	2168(2)	5594(2)	30(1)
C(12)	1998(7)	-2385(3)	5484(3)	32(1)
C(13)	-5000	3133(4)	7500	39(2)
N(1)	-4822(7)	22(3)	6105(2)	55(1)
C(14)	-3959(9)	-51(5)	5539(4)	64(2)
C(15)	5000(10)	0	5000	46(2)
OW1	-4746(9)	-1438(3)	6630(4)	94(2)
OW2	3052(12)	-487(4)	7433(6)	151(4)

Table 0.25 Bond lengths for complex iso6.

Bond	Bond lengths [Å]	Bond	Bond lengths [Å]
U(1)-O(2)	1.779(4)	C(3)-C(6)	1.471(7)
U(1)-O(1)	1.759(4)	C(4)-C(10)	1.387(7)
U(1)-O(6)	2.412(4)	C(4)-C(7)	1.389(6)
U(1)-O(3)	2.467(3)	C(5)-C(8)#1	1.384(7)
U(1)-O(8)	2.486(4)	C(5)-C(9)	1.387(7)
U(1)-O(5)	2.488(3)	C(6)-C(11)	1.381(7)
U(1)-O(7)	2.494(4)	C(6)-C(8)	1.394(6)
U(1)-O(4)	2.529(3)	C(7)-C(4)#2	1.389(6)
U(1)-C(1)	2.868(4)	C(8)-C(5)#3	1.384(7)
U(1)-C(2)	2.870(5)	C(9)-C(12)	1.352(7)
U(1)-C(3)	2.887(5)	C(10)-C(13)	1.376(6)
O(3)-C(1)	1.265(6)	C(11)-C(12)#3	1.379(7)
O(4)-C(2)	1.285(6)	C(12)-C(11)#1	1.379(7)
O(5)-C(3)	1.255(6)	C(13)-C(10)#2	1.376(6)
O(6)-C(2)	1.264(6)	N(1)-C(14)	1.451(9)
O(7)-C(3)	1.271(6)	C(14)-C(15)#4	1.478(9)
O(8)-C(1)	1.289(6)	C(15)-C(14)#5	1.478(9)
C(1)-C(5)	1.492(6)	C(15)-C(14)#6	1.478(9)
C(2)-C(4)	1.476(7)		

Table 0.26 Bond Angles for complex iso6.

Bond	Angle [°]	Bond	Angle [°]	Bond	Angle [°]
O(2)-U(1)-O(1)	178.5(2)	O(5)-U(1)-C(1)	146.0(1)	O(8)-C(1)-U(1)	59.9(2)
O(2)-U(1)-O(6)	92.3(2)	O(7)-U(1)-C(1)	94.6(1)	C(5)-C(1)-U(1)	178.6(3)
O(1)-U(1)-O(6)	89.0(2)	O(4)-U(1)-C(1)	95.2(1)	O(6)-C(2)-O(4)	118.1(5)
O(2)-U(1)-O(3)	89.2(2)	O(2)-U(1)-C(2)	90.2(1)	O(6)-C(2)-C(4)	120.3(5)
O(1)-U(1)-O(3)	90.8(2)	O(1)-U(1)-C(2)	91.3(2)	O(4)-C(2)-C(4)	121.6(4)
O(6)-U(1)-O(3)	121.3(1)	O(6)-U(1)-C(2)	25.9(1)	O(6)-C(2)-U(1)	56.4(3)
O(2)-U(1)-O(8)	90.8(2)	O(3)-U(1)-C(2)	95.5(1)	O(4)-C(2)-U(1)	61.8(3)
O(1)-U(1)-O(8)	88.0(2)	O(8)-U(1)-C(2)	148.2(1)	C(4)-C(2)-U(1)	176.4(4)
O(6)-U(1)-O(8)	173.3(1)	O(5)-U(1)-C(2)	92.4(1)	O(5)-C(3)-O(7)	118.4(5)
O(3)-U(1)-O(8)	52.7(1)	O(7)-U(1)-C(2)	143.8(1)	O(5)-C(3)-C(6)	121.9(4)
O(2)-U(1)-O(5)	87.8(2)	O(4)-U(1)-C(2)	26.6(1)	O(7)-C(3)-C(6)	119.7(5)
O(1)-U(1)-O(5)	92.0(2)	C(1)-U(1)-C(2)	121.6(1)	O(5)-C(3)-U(1)	59.1(2)
O(6)-U(1)-O(5)	66.7(1)	O(2)-U(1)-C(3)	90.8(2)	O(7)-C(3)-U(1)	59.4(3)
O(3)-U(1)-O(5)	171.6(1)	O(1)-U(1)-C(3)	88.4(2)	C(6)-C(3)-U(1)	177.6(4)
O(8)-U(1)-O(5)	119.4(1)	O(6)-U(1)-C(3)	92.0(1)	C(10)-C(4)-C(7)	119.4(5)
O(2)-U(1)-O(7)	92.1(2)	O(3)-U(1)-C(3)	146.7(1)	C(10)-C(4)-C(2)	116.8(5)
O(1)-U(1)-O(7)	86.6(2)	O(8)-U(1)-C(3)	93.9(1)	C(7)-C(4)-C(2)	123.8(5)
O(6)-U(1)-O(7)	117.9(1)	O(5)-U(1)-C(3)	25.6(1)	C(8)#1-C(5)-C(9)	119.9(4)
O(3)-U(1)-O(7)	120.7(1)	O(7)-U(1)-C(3)	26.0(1)	C(8)#1-C(5)-C(1)	119.6(5)
O(8)-U(1)-O(7)	67.9(1)	O(4)-U(1)-C(3)	144.2(1)	C(9)-C(5)-C(1)	120.5(4)
O(5)-U(1)-O(7)	51.6(1)	C(1)-U(1)-C(3)	120.6(2)	C(11)-C(6)-C(8)	118.8(4)
O(2)-U(1)-O(4)	87.0(2)	C(2)-U(1)-C(3)	117.8(1)	C(11)-C(6)-C(3)	121.8(4)
O(1)-U(1)-O(4)	94.4(2)	C(1)-O(3)-U(1)	95.0(3)	C(8)-C(6)-C(3)	119.4(5)
O(6)-U(1)-O(4)	52.5(1)	C(2)-O(4)-U(1)	91.6(3)	C(4)#2-C(7)-C(4)	120.5(6)
O(3)-U(1)-O(4)	69.1(1)	C(3)-O(5)-U(1)	95.3(3)	C(5)#3-C(8)-C(6)	119.4(5)
O(8)-U(1)-O(4)	121.8(1)	C(2)-O(6)-U(1)	97.7(3)	C(12)-C(9)-C(5)	121.0(5)
O(5)-U(1)-O(4)	118.6(1)	C(3)-O(7)-U(1)	94.5(3)	C(13)-C(10)-C(4)	119.9(5)
O(7)-U(1)-O(4)	170.2(1)	C(1)-O(8)-U(1)	93.4(3)	C(6)-C(11)-C(12)#3	121.6(4)
O(2)-U(1)-C(1)	90.1(2)	O(3)-C(1)-O(8)	118.9(4)	C(9)-C(12)-C(11)#1	119.1(5)
O(1)-U(1)-C(1)	89.2(2)	O(3)-C(1)-C(5)	121.3(4)	C(10)#2-C(13)-C(10)	121.0(6)
O(6)-U(1)-C(1)	147.3(1)	O(8)-C(1)-C(5)	119.8(5)	N(1)-C(14)-C(15)#4	113.6(6)
O(3)-U(1)-C(1)	26.1(1)	O(3)-C(1)-U(1)	59.0(2)	C(14)#5-C(15)-C(14)#6	108.1(8)
O(8)-U(1)-C(1)	26.7(1)				

Table 0.27 Bond valence calculation for complex iso6.

Atom	Atom bond	Bond length	Bond valence [vu]	Atom valence [vu]
U1	U(1)-O(2)	1,779	1,69	6,08
	U(1)-O(1)	1,759	1,76	
	U(1)-O(6)	2,412	0,50	
	U(1)-O(3)	2,467	0,45	
	U(1)-O(8)	2,486	0,43	
	U(1)-O(5)	2,488	0,43	
	U(1)-O(7)	2,494	0,43	
	U(1)-O(4)	2,529	0,40	
O1	U(1)-O(1)	1,759	1,76	1,76
O2	U(1)-O(2)	1,779	1,69	1,69
O3	U(1)-O(3)	2,467	0,45	1,72
	O(3)-C(1)	1,265	1,27	
O4	U(1)-O(4)	2,529	0,40	1,62
	O(4)-C(2)	1,285	1,22	
O5	U(1)-O(5)	2,488	0,43	1,73
	O(5)-C(3)	1,255	1,30	
O6	U(1)-O(6)	2,412	0,50	1,77
	O(6)-C(2)	1,264	1,27	
O7	U(1)-O(7)	2,494	0,43	1,68
	O(7)-C(3)	1,271	1,26	
O8	U(1)-O(8)	2,486	0,43	1,65
	O(8)-C(1)	1,289	1,21	

Table 0.28 Atomic coordinates (x10⁴) and equivalent isotropic displacement parameters (A²x10³) for complex iso7.

Atom	x	y	z	U(eq)
U(1)	512(1)	7250(1)	8803(1)	20(1)
U(2)	-2227(1)	7036(1)	8351(1)	26(1)
O(1)	-876(4)	7823(8)	9389(4)	26(1)
O(2)	-865(3)	6442(8)	7671(3)	22(1)
O(3)	547(4)	4858(8)	9150(4)	29(1)
O(4)	955(4)	8361(9)	10350(4)	31(1)
O(5)	461(4)	9632(8)	8473(4)	33(1)
O(6)	2130(4)	7277(10)	9142(5)	41(2)
O(7)	-2950(4)	7702(10)	9656(5)	41(2)
O(8)	-3846(4)	7006(11)	8370(5)	45(2)
O(9)	-2136(4)	4641(9)	8711(4)	37(2)
O(10)	2845(4)	6108(10)	8104(4)	40(2)
O(11)	-2257(4)	9407(9)	7999(5)	42(2)
C(1)	-3757(6)	7386(13)	9202(6)	32(2)
C(2)	2856(6)	6832(12)	8870(6)	30(2)
C(3)	3767(5)	7172(12)	9468(6)	28(2)
C(4)	-4588(6)	7416(12)	9627(6)	31(2)
C(5)	-5435(6)	7071(11)	9093(6)	27(2)
C(6)	3841(6)	7579(13)	10371(6)	33(2)
C(7)	-4520(6)	7795(13)	10532(6)	35(2)
C(8)	4687(7)	7870(14)	10900(7)	41(2)
OW1	-1047(8)	2735(11)	7572(8)	90(3)

Table 0.29 Bond lengths for complex iso7.

Bond	Bond lengths [Å]	Bond	Bond lengths [Å]
U(1)-O(5)	1.752(6)	O(2)-U(1)#1	2.445(5)
U(1)-O(3)	1.768(6)	O(6)-C(2)	1.25(1)
U(1)-O(6)	2.339(6)	O(7)-C(1)	1.28(1)
U(1)-O(1)	2.406(5)	O(8)-C(1)	1.27(1)
U(1)-O(4)	2.435(6)	O(10)-C(2)	1.26(1)
U(1)-O(2)#1	2.445(5)	O(10)-U(2)#1	2.309(6)
U(1)-O(2)	2.459(5)	C(1)-C(4)	1.48(1)
U(1)-U(1)#1	3.9398(6)	C(2)-C(3)	1.49(1)
U(1)-U(2)	3.9608(4)	C(3)-C(6)	1.38(1)
U(2)-O(11)	1.757(7)	C(3)-C(5)#2	1.40(1)
U(2)-O(9)	1.775(6)	C(4)-C(5)	1.37(1)
U(2)-O(10)#1	2.309(6)	C(4)-C(7)	1.38(1)
U(2)-O(1)	2.356(6)	C(5)-C(3)#3	1.40(1)
U(2)-O(8)	2.387(6)	C(6)-C(8)	1.36(1)
U(2)-O(2)	2.452(5)	C(7)-C(8)#3	1.38(1)
U(2)-O(7)	2.452(7)	C(8)-C(7)#2	1.38(1)
U(2)-C(1)	2.804(9)		

Table 0.30 Bond Angles for complex iso7.

Bond	Angle [°]	Bond	Angle [°]	Bond	Angle [°]
O(5)-U(1)-O(3)	178.8(3)	O(2)#1-U(1)-U(2)	102.5(1)	O(10)#1-U(2)-U(1)	112.4(2)
O(5)-U(1)-O(6)	92.4(3)	O(2)-U(1)-U(2)	36.2(1)	O(1)-U(2)-U(1)	34.1(1)
O(3)-U(1)-O(6)	88.3(3)	U(1)#1-U(1)-U(2)	69.002(9)	O(8)-U(2)-U(1)	169.5(2)
O(5)-U(1)-O(1)	87.0(2)	O(11)-U(2)-O(9)	177.2(3)	O(2)-U(2)-U(1)	36.3(1)
O(3)-U(1)-O(1)	91.8(2)	O(11)-U(2)-O(10)#1	90.0(3)	O(7)-U(2)-U(1)	115.7(2)
O(6)-U(1)-O(1)	144.8(2)	O(9)-U(2)-O(10)#1	90.8(3)	C(1)-U(2)-U(1)	142.7(2)
O(5)-U(1)-O(4)	87.2(2)	O(11)-U(2)-O(1)	87.0(3)	U(2)-O(1)-U(1)	112.6(2)
O(3)-U(1)-O(4)	92.1(2)	O(9)-U(2)-O(1)	90.9(3)	U(1)#1-O(2)-U(2)	132.1(2)
O(6)-U(1)-O(4)	73.0(2)	O(10)#1-U(2)-O(1)	146.3(2)	U(1)#1-O(2)-U(1)	106.9(2)
O(1)-U(1)-O(4)	71.8(2)	O(11)-U(2)-O(8)	92.5(3)	U(2)-O(2)-U(1)	107.5(2)
O(5)-U(1)-O(2)#1	88.3(2)	O(9)-U(2)-O(8)	90.3(3)	C(2)-O(6)-U(1)	145.3(6)
O(3)-U(1)-O(2)#1	92.7(2)	O(10)#1-U(2)-O(8)	78.0(2)	C(1)-O(7)-U(2)	92.0(5)
O(6)-U(1)-O(2)#1	79.6(2)	O(1)-U(2)-O(8)	135.6(2)	C(1)-O(8)-U(2)	95.2(5)

Bond	Angle [°]	Bond	Angle [°]	Bond	Angle [°]
O(1)-U(1)-O(2)#1	135.5(2)	O(11)-U(2)-O(2)	90.7(2)	C(2)-O(10)-U(2)#1	133.9(6)
O(4)-U(1)-O(2)#1	152.0(2)	O(9)-U(2)-O(2)	86.8(2)	O(8)-C(1)-O(7)	118.8(8)
O(5)-U(1)-O(2)	92.3(2)	O(10)#1-U(2)-O(2)	76.1(2)	O(8)-C(1)-C(4)	119.4(8)
O(3)-U(1)-O(2)	87.7(2)	O(1)-U(2)-O(2)	70.4(2)	O(7)-C(1)-C(4)	121.8(8)
O(6)-U(1)-O(2)	145.6(2)	O(8)-U(2)-O(2)	153.9(2)	O(8)-C(1)-U(2)	58.0(4)
O(1)-U(1)-O(2)	69.5(2)	O(11)-U(2)-O(7)	94.0(3)	O(7)-C(1)-U(2)	60.9(5)
O(4)-U(1)-O(2)	141.3(2)	O(9)-U(2)-O(7)	87.5(3)	C(4)-C(1)-U(2)	175.4(7)
O(2)#1-U(1)-O(2)	66.5(2)	O(10)#1-U(2)-O(7)	131.8(2)	O(6)-C(2)-O(10)	122.3(9)
O(5)-U(1)-U(1)#1	74.3(2)	O(1)-U(2)-O(7)	81.9(2)	O(6)-C(2)-C(3)	119.2(8)
O(3)-U(1)-U(1)#1	106.3(2)	O(8)-U(2)-O(7)	53.8(2)	O(10)-C(2)-C(3)	118.5(7)
O(6)-U(1)-U(1)#1	113.6(2)	O(2)-U(2)-O(7)	151.6(2)	C(6)-C(3)-C(5)#2	119.6(8)
O(1)-U(1)-U(1)#1	100.1(1)	O(11)-U(2)-C(1)	94.4(3)	C(6)-C(3)-C(2)	122.1(8)
O(4)-U(1)-U(1)#1	160.3(2)	O(9)-U(2)-C(1)	88.0(3)	C(5)#2-C(3)-C(2)	118.3(8)
O(2)#1-U(1)-U(1)#1	36.7(1)	O(10)#1-U(2)-C(1)	104.7(2)	C(5)-C(4)-C(7)	120.7(8)
O(2)-U(1)-U(1)#1	36.4(1)	O(1)-U(2)-C(1)	108.9(2)	C(5)-C(4)-C(1)	118.3(8)
O(5)-U(1)-U(2)	90.0(2)	O(8)-U(2)-C(1)	26.8(2)	C(7)-C(4)-C(1)	121.1(8)
O(3)-U(1)-U(2)	89.3(2)	O(2)-U(2)-C(1)	174.7(2)	C(4)-C(5)-C(3)#3	119.3(8)
O(6)-U(1)-U(2)	176.9(2)	O(7)-U(2)-C(1)	27.1(2)	C(8)-C(6)-C(3)	120.5(8)
O(1)-U(1)-U(2)	33.3(1)	O(11)-U(2)-U(1)	89.1(2)	C(4)-C(7)-C(8)#3	119.6(9)
O(4)-U(1)-U(2)	105.1(1)	O(9)-U(2)-U(1)	88.2(2)	C(6)-C(8)-C(7)#2	120(1)

Table 0.31 Bond valence calculation for complex iso7.

Atom	Atom bond	Bond length	Bond valence [vu]	Atom valence [vu]
U1	U(1)-O(5)	1,752	1,78	5,98
	U(1)-O(3)	1,768	1,73	
	U(1)-O(6)	2,339	0,57	
	U(1)-O(1)	2,406	0,50	
	U(1)-O(4)	2,435	0,48	
	U(1)-O(2)#1	2,445	0,47	
	U(1)-O(2)	2,459	0,46	
U2	U(2)-O(11)	1,757	1,76	6,07
	U(2)-O(9)	1,775	1,70	
	U(2)-O(10)#1	2,309	0,61	
	U(2)-O(1)	2,356	0,56	
	U(2)-O(8)	2,387	0,52	
	U(2)-O(2)	2,452	0,46	
	U(2)-O(7)	2,452	0,46	
O1	U(1)-O(1)	2,406	0,50	1,06
	U(2)-O(1)	2,356	0,56	
O2	U(1)-O(2)#1	2,445	0,47	1,39
	U(1)-O(2)	2,459	0,46	
	U(2)-O(2)	2,452	0,46	
O3	U(1)-O(3)	1,768	1,73	1,73
O4	U(1)-O(4)	2,435	0,48	0,48
O5	U(1)-O(5)	1,752	1,78	1,78
O6	U(1)-O(6)	2,339	0,57	1,88
	O(6)-C(2)	1,250	1,31	
O7	U(2)-O(7)	2,452	0,46	1,70
	O(7)-C(1)	1,280	1,24	
O8	U(2)-O(8)	2,387	0,52	1,78
	O(8)-C(1)	1,270	1,26	
O9	U(2)-O(9)	1,775	1,70	1,70
O10	U(2)-O(10)#1	2,309	0,61	1,89
	O(10)-C(2)	1,260	1,28	

Table 0.32 Atomic coordinates (x10⁴) and equivalent isotropic displacement parameters (A²x10³) for complex iso8.

Atom	x	y	z	U(eq)
U(1)	7855(1)	3018(1)	3336(1)	16(1)
U(2)	10467(1)	2603(1)	3724(1)	15(1)
O(1)	12147(3)	2183(7)	4115(3)	40(1)
O(2)	9103(3)	2278(6)	4454(3)	22(1)

O(3)	10867(2)	3065(6)	2322(3)	21(1)
O(4)	10401(3)	71(6)	3536(3)	25(1)
O(5)	7089(3)	2616(6)	4756(3)	30(1)
O(6)	10598(3)	5106(6)	4014(3)	27(1)
O(7)	12833(2)	3936(6)	3165(2)	24(1)
O(8)	7965(3)	5538(6)	3592(3)	29(1)
O(9)	10933(3)	1763(6)	5355(3)	27(1)
O(10)	6209(3)	3179(7)	3425(3)	32(1)
O(11)	7691(3)	534(6)	3053(3)	28(1)
C(1)	12842(4)	2956(8)	3897(4)	22(1)
C(2)	5428(4)	2675(8)	4705(4)	21(1)
C(3)	13763(4)	2719(7)	4507(4)	19(1)
C(4)	4575(4)	2954(8)	4139(4)	21(1)
C(5)	13803(4)	2222(9)	5426(4)	26(1)
C(6)	5455(4)	2219(9)	5625(4)	28(1)
C(7)	6283(4)	2829(8)	4276(4)	24(1)
C(8)	5356(4)	7988(10)	4014(4)	32(1)
N(1)	8033(5)	2274(8)	6648(5)	43(2)

Table 0.33 Bond lengths for complex iso8.

Bond	Bond lengths [Å]	Bond	Bond lengths [Å]
U(1)-O(11)	1.791(4)	C(2)-C(7)	1.493(8)
U(1)-O(8)	1.802(4)	C(3)-C(5)	1.390(8)
U(1)-O(3)#1	2.241(4)	C(3)-C(4)#2	1.391(8)
U(1)-O(2)	2.310(4)	C(4)-C(3)#3	1.391(8)
U(1)-O(7)#1	2.365(4)	C(5)-C(8)#4	1.373(8)
U(1)-O(10)	2.433(4)	C(6)-C(8)#5	1.382(9)
U(1)-O(5)	2.542(5)	C(8)-C(5)#4	1.373(8)
U(1)-C(7)	2.870(6)	C(8)-C(6)#5	1.382(9)
U(1)-U(2)	3.7790(3)	O(1)-C(1)	1.237(7)
U(2)-O(4)	1.790(4)	O(3)-U(1)#1	2.241(4)
U(2)-O(6)	1.803(4)	O(3)-U(2)#1	2.304(4)
U(2)-O(3)	2.258(4)	O(5)-C(7)	1.280(7)
U(2)-O(3)#1	2.304(4)	O(7)-C(1)	1.276(7)
U(2)-O(2)	2.423(4)	O(7)-U(1)#1	2.365(4)
U(2)-O(1)	2.448(4)	O(10)-C(7)	1.264(7)
U(2)-O(9)	2.460(4)	C(1)-C(3)	1.503(8)
U(2)-U(2)#1	3.6437(4)	C(2)-C(6)	1.386(8)
O(1)-C(1)	1.237(7)	C(2)-C(4)	1.398(8)
O(3)-U(1)#1	2.241(4)	C(2)-C(7)	1.493(8)
O(3)-U(2)#1	2.304(4)	C(3)-C(5)	1.390(8)
O(5)-C(7)	1.280(7)	C(3)-C(4)#2	1.391(8)
O(7)-C(1)	1.276(7)	C(4)-C(3)#3	1.391(8)
O(7)-U(1)#1	2.365(4)	C(5)-C(8)#4	1.373(8)
O(10)-C(7)	1.264(7)	C(6)-C(8)#5	1.382(9)
C(1)-C(3)	1.503(8)	C(8)-C(5)#4	1.373(8)
C(2)-C(6)	1.386(8)	C(8)-C(6)#5	1.382(9)
C(2)-C(4)	1.398(8)		

Table 0.34 Bond Angles for complex iso8.

Bond	Angle [°]	Bond	Angle [°]	Bond	Angle [°]
O(11)-U(1)-O(8)	177.3(2)	O(10)-U(1)-U(2)	168.2(1)	O(6)-U(2)-U(1)	91.6(1)
O(11)-U(1)-O(3)#1	90.2(2)	O(5)-U(1)-U(2)	115.84(9)	O(3)-U(2)-U(1)	104.79(9)
O(8)-U(1)-O(3)#1	91.4(2)	C(7)-U(1)-U(2)	142.3(1)	O(3)#1-U(2)-U(1)	33.21(9)
O(11)-U(1)-O(2)	90.6(2)	O(4)-U(2)-O(6)	174.7(2)	O(2)-U(2)-U(1)	35.99(9)
O(8)-U(1)-O(2)	92.1(2)	O(4)-U(2)-O(3)	90.9(2)	O(1)-U(2)-U(1)	174.52(1)
O(3)#1-U(1)-O(2)	72.2(1)	O(6)-U(2)-O(3)	92.6(2)	O(9)-U(2)-U(1)	106.22(9)
O(11)-U(1)-O(7)#1	91.4(2)	O(4)-U(2)-O(3)#1	90.9(2)	U(1)-O(2)-U(2)	105.9(2)

O(8)-U(1)-O(7)#1	86.6(2)	O(6)-U(2)-O(3)#1	94.0(2)	U(1)#1-O(3)-U(2)	138.7(2)
O(3)#1-U(1)-O(7)#1	81.4(1)	O(3)-U(2)-O(3)#1	71.6(1)	U(1)#1-O(3)-U(2)#1	112.5(2)
O(2)-U(1)-O(7)#1	153.5(1)	O(4)-U(2)-O(2)	87.0(2)	U(2)-O(3)-U(2)#1	106.0(1)
O(11)-U(1)-O(10)	87.8(2)	O(6)-U(2)-O(2)	92.8(2)	C(7)-O(5)-U(1)	91.2(4)
O(8)-U(1)-O(10)	89.9(2)	O(3)-U(2)-O(2)	140.5(1)	C(1)-O(7)-U(1)#1	126.1(4)
O(3)#1-U(1)-O(10)	157.5(1)	O(3)#1-U(2)-O(2)	69.0(1)	C(7)-O(10)-U(1)	96.8(3)
O(2)-U(1)-O(10)	130.3(1)	O(4)-U(2)-O(1)	86.8(2)	O(1)-C(1)-O(7)	123.9(5)
O(7)#1-U(1)-O(10)	76.3(1)	O(6)-U(2)-O(1)	89.8(2)	O(1)-C(1)-C(3)	119.4(5)
O(11)-U(1)-O(5)	91.4(2)	O(3)-U(2)-O(1)	80.4(1)	O(7)-C(1)-C(3)	116.8(5)
O(8)-U(1)-O(5)	88.4(2)	O(3)#1-U(2)-O(1)	151.9(1)	C(6)-C(2)-C(4)	119.7(5)
O(3)#1-U(1)-O(5)	150.1(1)	O(2)-U(2)-O(1)	138.6(1)	C(6)-C(2)-C(7)	122.5(5)
O(2)-U(1)-O(5)	78.0(1)	O(4)-U(2)-O(9)	85.1(2)	C(4)-C(2)-C(7)	117.7(5)
O(7)#1-U(1)-O(5)	128.4(1)	O(6)-U(2)-O(9)	89.9(2)	C(5)-C(3)-C(4)#2	120.3(5)
O(10)-U(1)-O(5)	52.4(1)	O(3)-U(2)-O(9)	148.8(1)	C(5)-C(3)-C(1)	120.2(5)
O(11)-U(1)-C(7)	88.9(2)	O(3)#1-U(2)-O(9)	139.3(1)	C(4)#2-C(3)-C(1)	119.5(5)
O(8)-U(1)-C(7)	89.7(2)	O(2)-U(2)-O(9)	70.3(1)	C(3)#3-C(4)-C(2)	119.1(5)
O(3)#1-U(1)-C(7)	176.4(2)	O(1)-U(2)-O(9)	68.5(2)	C(8)#4-C(5)-C(3)	120.2(6)
O(2)-U(1)-C(7)	104.4(2)	O(4)-U(2)-U(2)#1	81.1(1)	C(8)#5-C(6)-C(2)	120.7(5)
O(7)#1-U(1)-C(7)	102.2(1)	O(6)-U(2)-U(2)#1	104.1(1)	O(10)-C(7)-O(5)	119.6(5)
O(10)-U(1)-C(7)	25.9(2)	O(3)-U(2)-U(2)#1	37.42(9)	O(10)-C(7)-C(2)	119.4(5)
O(5)-U(1)-C(7)	26.5(2)	O(3)#1-U(2)-U(2)#1	36.57(9)	O(5)-C(7)-C(2)	121.0(5)
O(11)-U(1)-U(2)	93.1(1)	O(2)-U(2)-U(2)#1	103.63(9)	O(10)-C(7)-U(1)	57.3(3)
O(8)-U(1)-U(2)	89.4(1)	O(1)-U(2)-U(2)#1	115.7(1)	O(5)-C(7)-U(1)	62.3(3)
O(3)#1-U(1)-U(2)	34.3(1)	O(9)-U(2)-U(2)#1	165.2(1)	C(2)-C(7)-U(1)	176.1(4)
O(2)-U(1)-U(2)	38.1(1)	O(4)-U(2)-U(1)	91.4(1)	C(5)#4-C(8)-C(6)#5	119.9(6)
O(7)#1-U(1)-U(2)	115.4(1)				

Table 0.35 Bond valence calculation for complex iso8.

Atom	Atom bond	Bond length	Bond valence [vu]	Atom valence [vu]
U1	U(1)-O(11)	1,791	1,65	5,98
	U(1)-O(8)	1,802	1,62	
	U(1)-O(3)#1	2,241	0,69	
	U(1)-O(2)	2,310	0,61	
	U(1)-O(7)#1	2,365	0,55	
	U(1)-O(10)	2,433	0,48	
	U(1)-O(5)	2,542	0,39	
U2	U(2)-O(4)	1,790	1,65	5,96
	U(2)-O(6)	1,803	1,61	
	U(2)-O(3)	2,258	0,67	
	U(2)-O(3)#1	2,304	0,61	
	U(2)-O(2)	2,423	0,49	
	U(2)-O(1)	2,448	0,47	
	U(2)-O(9)	2,460	0,45	
O1	U(2)-O(1)	2,448	0,47	1,74
	O(1)-C(1)	1,237	1,27	
O2	U(2)-O(2)	2,423	0,49	1,10
	U(1)-O(2)	2,310	0,61	
O3	U(1)-O(3)#1	2,241	0,69	1,98
	U(2)-O(3)	2,258	0,67	
	U(2)-O(3)#1	2,304	0,61	
O4	U(2)-O(4)	1,790	1,65	1,65
O5	U(1)-O(5)	2,542	0,39	1,62
	O(5)-C(7)	1,280	1,24	
O6	U(2)-O(6)	1,803	1,61	1,61
O7	U(1)-O(7)#1	2,365	0,55	1,79
	O(7)-C(1)	1,276	1,25	
O8	U(1)-O(8)	1,802	1,62	1,62
O9	U(2)-O(9)	2,460	0,45	0,45
O10	U(1)-O(10)	2,433	0,48	1,75
	O(10)-C(7)	1,264	1,27	
O11	U(1)-O(11)	1,791	1,65	1,65

Table 0.36 Atomic coordinates (x10⁴) and equivalent isotropic displacement parameters (A²x10³) for complex iso9.

Atom	x	y	z	U(eq)
U(1)	5389(1)	1072(1)	1135(1)	38(1)
U(2)	2828(1)	514(1)	862(1)	38(1)
O(1)	5872(13)	-70(20)	-211(19)	38(6)
O(2)	7018(13)	1680(20)	1695(19)	40(6)
O(3)	5197(17)	2170(20)	60(30)	65(8)
O(4)	4048(18)	1520(30)	1960(30)	83(10)
O(5)	1141(15)	490(20)	990(20)	53(7)
O(6)	3017(18)	-530(20)	1910(30)	76(10)
O(7)	5630(17)	50(30)	2190(20)	71(9)
O(8)	2032(15)	1590(30)	2260(20)	68(9)
O(9)	2579(19)	1600(40)	-90(30)	99(13)
O(10)	2284(19)	-800(40)	-450(30)	125(17)
O(11)	5710(20)	2610(30)	2720(30)	90(12)
C(1)	2250(30)	-1360(40)	-1400(40)	66(13)
C(2)	1270(30)	1210(40)	1790(40)	62(13)
C(3)	1280(20)	-1750(30)	-2000(30)	39(9)
C(4)	370(20)	1670(30)	2220(40)	60(12)
C(5)	1310(30)	2550(30)	-2820(40)	62(13)
C(6)	-530(30)	1340(30)	1540(40)	60(12)
C(7)	420(30)	2490(40)	3090(30)	64(13)
C(8)	-310(30)	2930(50)	3440(40)	100(20)
N(1)	6760(40)	-1660(50)	2540(60)	150(20)
OW1	5000	5000	0	290(60)

Table 0.37 Bond lengths for complex iso9.

Bond	Bond lengths [Å]	Bond	Bond lengths [Å]
U(1)-O(7)	1.71(3)	O(1)-U(2)#1	2.21(2)
U(1)-O(3)	1.78(3)	O(1)-U(1)#1	2.28(2)
U(1)-O(1)	2.26(2)	O(2)-C(1)#1	1.23(4)
U(1)-O(1)#1	2.28(2)	O(5)-C(2)	1.25(5)
U(1)-O(4)	2.37(3)	O(8)-C(2)	1.22(5)
U(1)-O(2)	2.44(2)	O(10)-C(1)	1.27(5)
U(1)-O(11)	2.56(3)	C(1)-O(2)#1	1.23(4)
U(1)-U(1)#1	3.674(3)	C(1)-C(3)	1.52(5)
U(1)-U(2)	3.732(2)	C(2)-C(4)	1.57(5)
U(2)-O(9)	1.70(4)	C(3)-C(5)	1.34(5)
U(2)-O(6)	1.71(3)	C(3)-C(6)#2	1.38(5)
U(2)-O(1)#1	2.21(2)	C(4)-C(7)	1.40(5)
U(2)-O(10)	2.21(4)	C(4)-C(6)	1.44(5)
U(2)-O(4)	2.31(3)	C(5)-C(8)#2	1.56(6)
U(2)-O(5)	2.48(2)	C(6)-C(3)#2	1.38(5)
U(2)-O(8)	2.49(2)	C(7)-C(8)	1.31(5)
U(2)-C(2)	2.78(3)	C(8)-C(5)#2	1.56(6)

Table 0.38 Bond Angles for complex iso9.

Bond	Angle [°]	Bond	Angle [°]	Bond	Angle [°]
O(7)-U(1)-O(3)	177.0(12)	O(2)-U(1)-U(2)	167.5(5)	O(1)#1-U(2)-U(1)	34.4(5)
O(7)-U(1)-O(1)	89.5(11)	O(11)-U(1)-U(2)	104.1(6)	O(10)-U(2)-U(1)	114.4(7)
O(3)-U(1)-O(1)	90.8(10)	U(1)#1-U(1)-U(2)	68.93(4)	O(4)-U(2)-U(1)	37.7(7)
O(7)-U(1)-O(1)#1	89.5(11)	O(9)-U(2)-O(6)	174.8(15)	O(5)-U(2)-U(1)	167.4(6)
O(3)-U(1)-O(1)#1	93.5(10)	O(9)-U(2)-O(1)#1	93.9(12)	O(8)-U(2)-U(1)	115.0(6)
O(1)-U(1)-O(1)#1	71.9(8)	O(6)-U(2)-O(1)#1	90.8(10)	C(2)-U(2)-U(1)	140.9(11)
O(7)-U(1)-O(4)	87.8(13)	O(9)-U(2)-O(10)	96.3(18)	U(2)#1-O(1)-U(1)	139.5(9)
O(3)-U(1)-O(4)	93.8(12)	O(6)-U(2)-O(10)	86.5(17)	U(2)#1-O(1)-U(1)#1	112.4(10)

O(1)-U(1)-O(4)	141.5(8)	O(1)#1-U(2)-O(10)	80.0(9)	U(1)-O(1)-U(1)#1	108.1(8)
O(1)#1-U(1)-O(4)	69.8(9)	O(9)-U(2)-O(4)	89.8(15)	C(1)#1-O(2)-U(1)	133(2)
O(7)-U(1)-O(2)	87.9(10)	O(6)-U(2)-O(4)	89.7(14)	U(2)-O(4)-U(1)	105.7(12)
O(3)-U(1)-O(2)	89.1(10)	O(1)#1-U(2)-O(4)	72.0(9)	C(2)-O(5)-U(2)	90.7(19)
O(1)-U(1)-O(2)	87.3(7)	O(10)-U(2)-O(4)	151.6(10)	C(2)-O(8)-U(2)	91(2)
O(1)#1-U(1)-O(2)	159.0(8)	O(9)-U(2)-O(5)	86.9(12)	C(1)-O(10)-U(2)	155(3)
O(4)-U(1)-O(2)	130.9(8)	O(6)-U(2)-O(5)	89.4(10)	O(2)#1-C(1)-O(10)	119(3)
O(7)-U(1)-O(11)	92.1(13)	O(1)#1-U(2)-O(5)	158.1(8)	O(2)#1-C(1)-C(3)	124(3)
O(3)-U(1)-O(11)	86.2(13)	O(10)-U(2)-O(5)	78.2(9)	O(10)-C(1)-C(3)	116(3)
O(1)-U(1)-O(11)	150.8(7)	O(4)-U(2)-O(5)	129.9(9)	O(8)-C(2)-O(5)	126(3)
O(1)#1-U(1)-O(11)	137.3(8)	O(9)-U(2)-O(8)	86.5(14)	O(8)-C(2)-C(4)	118(4)
O(4)-U(1)-O(11)	67.6(9)	O(6)-U(2)-O(8)	88.4(12)	O(5)-C(2)-C(4)	116(4)
O(2)-U(1)-O(11)	63.7(8)	O(1)#1-U(2)-O(8)	149.4(8)	O(8)-C(2)-U(2)	63.3(17)
O(7)-U(1)-U(1)#1	89.4(10)	O(10)-U(2)-O(8)	130.5(9)	O(5)-C(2)-U(2)	62.7(16)
O(3)-U(1)-U(1)#1	92.7(9)	O(4)-U(2)-O(8)	77.4(9)	C(4)-C(2)-U(2)	175(3)
O(1)-U(1)-U(1)#1	36.1(5)	O(5)-U(2)-O(8)	52.5(8)	C(5)-C(3)-C(6)#2	130(3)
O(1)#1-U(1)-U(1)#1	35.7(6)	O(9)-U(2)-C(2)	85.2(14)	C(5)-C(3)-C(1)	113(3)
O(4)-U(1)-U(1)#1	105.4(7)	O(6)-U(2)-C(2)	89.9(12)	C(6)#2-C(3)-C(1)	117(3)
O(2)-U(1)-U(1)#1	123.4(5)	O(1)#1-U(2)-C(2)	175.3(12)	C(7)-C(4)-C(6)	120(3)
O(11)-U(1)-U(1)#1	172.9(6)	O(10)-U(2)-C(2)	104.7(13)	C(7)-C(4)-C(2)	122(3)
O(7)-U(1)-U(2)	90.2(8)	O(4)-U(2)-C(2)	103.4(13)	C(6)-C(4)-C(2)	117(4)
O(3)-U(1)-U(2)	92.6(7)	O(5)-U(2)-C(2)	26.6(11)	C(3)-C(5)-C(8)#2	112(3)
O(1)-U(1)-U(2)	105.1(5)	O(8)-U(2)-C(2)	26.0(11)	C(3)#2-C(6)-C(4)	113(4)
O(1)#1-U(1)-U(2)	33.2(6)	O(9)-U(2)-U(1)	90.5(10)	C(8)-C(7)-C(4)	124(4)
O(4)-U(1)-U(2)	36.6(7)	O(6)-U(2)-U(1)	92.3(9)	C(7)-C(8)-C(5)#2	119(4)

Table 0.39 Bond valence calculation for complex iso9.

Atom	Atom bond	Bond length	Bond valence [vu]	Atom valence [vu]
U1	U(1)-O(7)	1,71	1,93	6,31
	U(1)-O(3)	1,78	1,69	
	U(1)-O(1)	2,26	0,67	
	U(1)-O(1)#1	2,28	0,64	
	U(1)-O(4)	2,37	0,54	
	U(1)-O(2)	2,44	0,47	
	U(1)-O(11)	2,56	0,38	
U2	U(2)-O(9)	1,70	1,97	6,84
	U(2)-O(6)	1,71	1,93	
	U(2)-O(1)#1	2,21	0,74	
	U(2)-O(10)	2,21	0,74	
	U(2)-O(4)	2,31	0,61	
	U(2)-O(5)	2,48	0,44	
	U(2)-O(8)	2,49	0,43	
O1	U(1)-O(1)	2,26	0,67	2,05
	U(1)-O(1)#1	2,28	0,64	
	U(2)-O(1)#1	2,21	0,74	
O2	U(1)-O(2)	2,44	0,47	1,83
	O(2)-C(1)#1	1,23	1,36	
O3	U(1)-O(3)	1,78	1,69	2,23
O4	U(1)-O(4)	2,37	0,54	1,15
	U(2)-O(4)	2,31	0,61	
O5	U(2)-O(5)	2,48	0,44	1,75
	O(5)-C(2)	1,25	1,31	
O6	U(1)-O(3)	1,78	1,69	3,61
O7	U(1)-O(7)	1,71	1,93	2,36
O8	U(2)-O(8)	2,49	0,43	1,82
	O(8)-C(2)	1,22	1,39	
O9	U(2)-O(9)	1,70	1,97	1,97
O10	U(2)-O(10)	2,21	0,74	2,00
	O(10)-C(1)	1,27	1,26	
O11	U(1)-O(11)	2,56	0,38	0,38

Table 0.40 Atomic coordinates (x10⁴) and equivalent isotropic displacement parameters (A²x10³) for complex iso10.

Atom	x	y	z	U(eq)
U(1)	8961(1)	8248(1)	4496(1)	12(1)
U(2)	7953(1)	6386(1)	1275(1)	13(1)
U(3)	9722(1)	9524(1)	2567(1)	12(1)
U(4)	6165(1)	8711(1)	647(1)	11(1)
O(1)	7959(4)	7901(2)	2898(2)	13(1)
O(2)	9245(4)	10073(2)	4213(2)	14(1)
O(3)	8269(4)	8100(2)	1253(2)	15(1)
O(4)	4056(4)	8454(2)	-614(2)	18(1)
O(5)	5139(4)	10364(2)	1336(2)	17(1)
O(6)	6581(5)	7125(3)	-584(2)	23(1)
O(7)	8434(5)	6145(3)	-349(2)	20(1)
O(8)	6810(5)	8477(3)	4902(2)	22(1)
O(9)	4221(4)	7953(3)	1031(2)	20(1)
O(10)	7663(4)	9936(3)	2329(2)	19(1)
O(11)	7332(6)	6311(2)	3860(2)	28(1)
O(12)	8029(4)	9536(3)	269(2)	22(1)
O(13)	11319(5)	11418(3)	3125(2)	25(1)
O(14)	11783(4)	9203(3)	2836(2)	21(1)
O(15)	5486(5)	6021(3)	1001(2)	24(1)
O(16)	10409(5)	6687(3)	1532(2)	24(1)
O(17)	7475(8)	5547(3)	2341(3)	44(1)
O(18)	11126(5)	8017(3)	4111(2)	23(1)
O(19)	8020(5)	4410(3)	381(2)	26(1)
O(20)	10543(5)	12577(3)	4414(2)	27(1)
O(21)	11393(5)	9844(4)	1305(3)	31(1)
C(1)	4293(5)	8640(3)	-1350(3)	14(1)
C(2)	7166(6)	5481(3)	3109(3)	18(1)
C(3)	11003(6)	12348(3)	3597(3)	19(1)
C(4)	7700(6)	6532(3)	-861(3)	16(1)
C(5)	6625(6)	4325(3)	3117(3)	15(1)
C(6)	3987(6)	7673(3)	-2268(3)	16(1)
C(7)	11257(6)	13210(3)	3179(3)	15(1)
C(8)	8135(6)	6255(3)	-1855(3)	16(1)
C(9)	6473(6)	3410(3)	2277(3)	16(1)
C(10)	8356(6)	7056(3)	-2246(3)	17(1)
C(11)	6305(7)	4156(4)	3944(3)	22(1)
C(12)	11140(7)	14285(4)	3715(3)	21(1)
C(13)	4249(7)	7842(3)	-3108(3)	22(1)
C(14)	8239(7)	5176(4)	-2400(3)	23(1)
C(15)	8583(8)	4911(4)	-3331(3)	26(1)
C(16)	5886(7)	3081(4)	3943(3)	25(1)
OW1	4217(5)	7731(4)	2870(3)	37(1)
OW2	5681(6)	10170(4)	4136(3)	41(1)

Table 0.41 Bond lengths for complex iso10.

Bond	Bond lengths [Å]	Bond	Bond lengths [Å]
U(1)-O(8)	1.773(3)	O(2)-U(1)#1	2.416(3)
U(1)-O(18)	1.775(3)	O(4)-C(1)	1.256(5)
U(1)-O(11)	2.360(3)	O(5)-C(1)#2	1.277(4)
U(1)-O(20)#1	2.398(3)	O(6)-C(4)	1.259(5)
U(1)-O(1)	2.406(3)	O(7)-C(4)	1.274(5)
U(1)-O(2)#1	2.416(3)	O(11)-C(2)	1.248(5)
U(1)-O(2)	2.586(3)	O(13)-C(3)	1.265(5)
U(1)-U(3)	3.9241(2)	O(17)-C(2)	1.241(5)

U(2)-O(15)	1.765(3)	O(20)-C(3)	1.255(5)
U(2)-O(16)	1.763(3)	O(20)-U(1)#1	2.398(3)
U(2)-O(3)	2.249(3)	C(1)-O(5)#2	1.277(4)
U(2)-O(17)	2.296(3)	C(1)-C(6)	1.485(5)
U(2)-O(7)	2.448(3)	C(2)-C(5)	1.495(5)
U(2)-O(19)	2.491(3)	C(3)-C(7)	1.491(5)
U(2)-O(1)	2.566(3)	C(4)-C(8)	1.499(5)
U(2)-U(3)	3.7553(2)	C(5)-C(9)	1.388(5)
U(2)-U(4)	4.0739(2)	C(5)-C(11)	1.389(5)
U(3)-O(14)	1.770(3)	C(6)-C(9)#3	1.391(5)
U(3)-O(10)	1.823(3)	C(6)-C(13)	1.404(6)
U(3)-O(3)	2.217(3)	C(7)-C(12)	1.388(6)
U(3)-O(13)	2.311(3)	C(7)-C(10)#4	1.402(5)
U(3)-O(2)	2.426(3)	C(8)-C(14)	1.393(6)
U(3)-O(21)	2.432(3)	C(8)-C(10)	1.387(5)
U(3)-O(1)	2.456(3)	C(9)-C(6)#3	1.391(5)
U(3)-U(4)	3.5852(2)	C(10)-C(7)#4	1.402(5)
U(4)-O(9)	1.777(3)	C(11)-C(16)	1.385(6)
U(4)-O(12)	1.780(3)	C(12)-C(15)#4	1.380(6)
U(4)-O(3)	2.267(3)	C(13)-C(16)#3	1.393(6)
U(4)-O(4)	2.346(3)	C(14)-C(15)	1.390(6)
U(4)-O(6)	2.352(3)	C(15)-C(12)#4	1.380(6)
U(4)-O(5)	2.385(3)	C(16)-C(13)#3	1.393(6)
U(4)-O(10)	2.548(3)		

Table 0.42 Bond valence calculation for complex iso10.

Atom	Atom bond	Bond length	Bond valence [vu]	Atom valence [vu]
U1	U(1)-O(8)	1,773	1,71	5,83
	U(1)-O(18)	1,775	1,70	
	U(1)-O(11)	2,360	0,55	
	U(1)-O(20)#1	2,398	0,51	
	U(1)-O(1)	2,406	0,50	
	U(1)-O(2)#1	2,416	0,49	
	U(1)-O(2)	2,586	0,36	
U2	U(2)-O(15)	1,765	1,74	6,05
	U(2)-O(16)	1,763	1,74	
	U(2)-O(3)	2,249	0,68	
	U(2)-O(17)	2,296	0,62	
	U(2)-O(7)	2,448	0,47	
	U(2)-O(19)	2,491	0,43	
	U(2)-O(1)	2,566	0,37	
U3	U(3)-O(14)	1,770	1,72	6,03
	U(3)-O(10)	1,823	1,55	
	U(3)-O(3)	2,217	0,73	
	U(3)-O(13)	2,311	0,61	
	U(3)-O(2)	2,426	0,49	
	U(3)-O(21)	2,432	0,48	
	U(3)-O(1)	2,456	0,46	
U4	U(4)-O(9)	1,777	1,70	6,08
	U(4)-O(12)	1,780	1,69	
	U(4)-O(3)	2,267	0,66	
	U(4)-O(4)	2,346	0,57	
	U(4)-O(6)	2,352	0,56	
	U(4)-O(5)	2,390	0,53	
	U(4)-O(10)	2,550	0,38	
O1	U(1)-O(1)	2,406	0,50	1,33
	U(2)-O(1)	2,566	0,37	
	U(3)-O(1)	2,456	0,46	
O2	U(1)-O(2)	2,586	0,36	1,34
	U(1)-O(2)#1	2,416	0,49	
	U(3)-O(2)	2,426	0,49	

Atom	Atom bond	Bond length	Bond valence [vu]	Atom valence [vu]
O3	U(2)-O(3)	2,249	0,68	2,07
	U(3)-O(3)	2,217	0,73	
	U(4)-O(3)	2,267	0,66	
O4	U(4)-O(4)	2,346	0,57	1,86
	O(4)-C(1)	1,256	1,29	
O5	U(4)-O(5)	2,390	0,53	1,77
	O(5)-C(1)#2	1,277	1,24	
O6	U(4)-O(6)	2,352	0,56	1,85
	O(6)-C(4)	1,259	1,29	
O7	U(2)-O(7)	2,448	0,47	1,72
	O(7)-C(4)	1,274	1,25	
O8	U(1)-O(8)	1,773	1,71	1,71
O9	U(4)-O(9)	1,777	1,70	1,70
O10	U(3)-O(10)	1,823	1,55	1,94
	U(4)-O(10)	2,550	0,38	
O11	U(1)-O(11)	2,36	0,55	1,87
	O(11)-C(2)	1,248	1,31	
O12	U(4)-O(12)	1,780	1,69	1,69
O13	U(3)-O(13)	2,311	0,61	1,88
	O(13)-C(3)	1,265	1,27	
O14	U(3)-O(14)	1,770	1,72	1,72
O15	U(2)-O(15)	1,765	1,74	1,74
O16	U(2)-O(16)	1,763	1,74	1,74
O17	U(2)-O(17)	2,296	0,62	1,96
	O(17)-C(2)	1,241	1,33	
O18	U(1)-O(18)	1,775	1,70	1,70
O19	U(2)-O(19)	2,491	0,43	0,43
O20	U(1)-O(20)#1	2,398	0,51	1,81
	O(20)-C(3)	1,255	1,30	
O21	U(3)-O(21)	2,432	0,48	0,48

Table 0.43 Bond Angles for complex iso10.

Bond	Angle [°]	Bond	Angle [°]	Bond	Angle [°]
O(8)-U(1)-O(18)	178.88(15)	O(14)-U(3)-O(3)	105.30(13)	O(9)-U(4)-U(3)	100.18(10)
O(8)-U(1)-O(11)	86.48(15)	O(10)-U(3)-O(3)	77.63(12)	O(12)-U(4)-U(3)	81.44(10)
O(18)-U(1)-O(11)	93.51(15)	O(14)-U(3)-O(13)	90.74(14)	O(3)-U(4)-U(3)	36.44(7)
O(8)-U(1)-O(20)#1	93.38(14)	O(10)-U(3)-O(13)	86.16(13)	O(4)-U(4)-U(3)	171.13(7)
O(18)-U(1)-O(20)#1	85.57(14)	O(3)-U(3)-O(13)	141.06(11)	O(6)-U(4)-U(3)	108.20(8)
O(11)-U(1)-O(20)#1	70.48(12)	O(14)-U(3)-O(2)	88.26(13)	O(5)-U(4)-U(3)	94.01(7)
O(8)-U(1)-O(1)	93.91(13)	O(10)-U(3)-O(2)	90.49(12)	O(10)-U(4)-U(3)	28.71(6)
O(18)-U(1)-O(1)	87.17(13)	O(3)-U(3)-O(2)	134.50(10)	O(9)-U(4)-U(2)	73.44(10)
O(11)-U(1)-O(1)	76.81(10)	O(13)-U(3)-O(2)	79.99(11)	O(12)-U(4)-U(2)	110.22(10)
O(20)#1-U(1)-O(1)	145.93(11)	O(14)-U(3)-O(21)	83.19(14)	O(3)-U(4)-U(2)	25.45(7)
O(8)-U(1)-O(2)#1	91.22(13)	O(10)-U(3)-O(21)	96.57(13)	O(4)-U(4)-U(2)	129.57(7)
O(18)-U(1)-O(2)#1	88.25(13)	O(3)-U(3)-O(21)	73.96(12)	O(6)-U(4)-U(2)	60.85(8)
O(11)-U(1)-O(2)#1	150.99(10)	O(13)-U(3)-O(21)	73.04(13)	O(5)-U(4)-U(2)	142.64(7)
O(20)#1-U(1)-O(2)#1	80.81(11)	O(2)-U(3)-O(21)	151.53(12)	O(10)-U(4)-U(2)	81.10(7)
O(1)-U(1)-O(2)#1	132.20(9)	O(14)-U(3)-O(1)	86.48(12)	U(3)-U(4)-U(2)	58.304(4)
O(8)-U(1)-O(2)	82.70(12)	O(10)-U(3)-O(1)	95.79(12)	U(1)-O(1)-U(3)	107.65(10)
O(18)-U(1)-O(2)	97.99(13)	O(3)-U(3)-O(1)	69.12(9)	U(1)-O(1)-U(2)	135.90(11)
O(11)-U(1)-O(2)	141.07(11)	O(13)-U(3)-O(1)	148.58(11)	U(3)-O(1)-U(2)	96.77(9)
O(20)#1-U(1)-O(2)	147.21(11)	O(2)-U(3)-O(1)	68.65(9)	U(1)#1-O(2)-U(3)	126.68(12)
O(1)-U(1)-O(2)	66.83(8)	O(21)-U(3)-O(1)	137.30(12)	U(1)#1-O(2)-U(1)	113.20(10)
O(2)#1-U(1)-O(2)	66.80(10)	O(14)-U(3)-U(4)	140.33(11)	U(3)-O(2)-U(1)	103.04(9)
O(8)-U(1)-U(3)	104.21(11)	O(10)-U(3)-U(4)	42.18(9)	U(3)-O(3)-U(2)	114.47(11)
O(18)-U(1)-U(3)	76.83(11)	O(3)-U(3)-U(4)	37.40(7)	U(3)-O(3)-U(4)	106.16(11)
O(11)-U(1)-U(3)	112.32(8)	O(13)-U(3)-U(4)	112.45(9)	U(2)-O(3)-U(4)	128.87(13)
O(20)#1-U(1)-U(3)	162.27(9)	O(2)-U(3)-U(4)	125.99(7)	C(1)-O(4)-U(4)	132.4(3)
O(1)-U(1)-U(3)	36.61(6)	O(21)-U(3)-U(4)	74.22(8)	C(1)#2-O(5)-U(4)	133.6(3)
O(2)#1-U(1)-U(3)	96.29(6)	O(1)-U(3)-U(4)	88.54(6)	C(4)-O(6)-U(4)	143.3(3)
O(2)-U(1)-U(3)	37.03(6)	O(14)-U(3)-U(2)	82.85(11)	C(4)-O(7)-U(2)	127.7(3)
O(15)-U(2)-O(16)	177.45(15)	O(10)-U(3)-U(2)	100.32(10)	U(3)-O(10)-U(4)	109.12(13)

Bond	Angle [°]	Bond	Angle [°]	Bond	Angle [°]
O(15)-U(2)-O(3)	91.06(13)	O(3)-U(3)-U(2)	33.02(7)	C(2)-O(11)-U(1)	137.9(3)
O(16)-U(2)-O(3)	91.37(13)	O(13)-U(3)-U(2)	166.90(9)	C(3)-O(13)-U(3)	137.8(3)
O(15)-U(2)-O(17)	88.86(18)	O(2)-U(3)-U(2)	111.08(6)	C(2)-O(17)-U(2)	156.6(3)
O(16)-U(2)-O(17)	89.87(18)	O(21)-U(3)-U(2)	94.78(10)	C(3)-O(20)-U(1)#1	128.2(3)
O(3)-U(2)-O(17)	138.06(12)	O(1)-U(3)-U(2)	42.73(6)	O(4)-C(1)-O(5)#2	122.3(3)
O(15)-U(2)-O(7)	91.23(14)	U(4)-U(3)-U(2)	67.373(4)	O(4)-C(1)-C(6)	119.2(3)
O(16)-U(2)-O(7)	88.61(14)	O(14)-U(3)-U(1)	69.79(11)	O(5)#2-C(1)-C(6)	118.4(3)
O(3)-U(2)-O(7)	75.47(10)	O(10)-U(3)-U(1)	110.90(10)	O(17)-C(2)-O(11)	124.1(4)
O(17)-U(2)-O(7)	146.47(11)	O(3)-U(3)-U(1)	104.08(7)	O(17)-C(2)-C(5)	116.5(4)
O(15)-U(2)-O(19)	91.86(14)	O(13)-U(3)-U(1)	114.78(9)	O(11)-C(2)-C(5)	119.3(4)
O(16)-U(2)-O(19)	85.68(14)	O(2)-U(3)-U(1)	39.94(6)	O(20)-C(3)-O(13)	122.2(4)
O(3)-U(2)-O(19)	146.74(11)	O(21)-U(3)-U(1)	151.55(9)	O(20)-C(3)-C(7)	119.2(4)
O(17)-U(2)-O(19)	75.14(12)	O(1)-U(3)-U(1)	35.75(6)	O(13)-C(3)-C(7)	118.6(4)
O(7)-U(2)-O(19)	71.34(11)	U(4)-U(3)-U(1)	121.844(5)	O(6)-C(4)-O(7)	123.4(4)
O(15)-U(2)-O(1)	93.58(13)	U(2)-U(3)-U(1)	73.721(4)	O(6)-C(4)-C(8)	117.2(3)
O(16)-U(2)-O(1)	88.11(13)	O(9)-U(4)-O(12)	176.25(14)	O(7)-C(4)-C(8)	119.3(3)
O(3)-U(2)-O(1)	66.63(9)	O(9)-U(4)-O(3)	93.09(12)	C(9)-C(5)-C(11)	120.1(3)
O(17)-U(2)-O(1)	71.52(11)	O(12)-U(4)-O(3)	90.20(12)	C(9)-C(5)-C(2)	118.6(3)
O(7)-U(2)-O(1)	141.85(9)	O(9)-U(4)-O(4)	86.93(13)	C(11)-C(5)-C(2)	121.3(3)
O(19)-U(2)-O(1)	146.07(10)	O(12)-U(4)-O(4)	91.16(13)	C(9)#3-C(6)-C(13)	120.2(4)
O(15)-U(2)-U(3)	108.29(11)	O(3)-U(4)-O(4)	149.39(10)	C(9)#3-C(6)-C(1)	118.5(3)
O(16)-U(2)-U(3)	74.22(11)	O(9)-U(4)-O(6)	95.69(14)	C(13)-C(6)-C(1)	121.2(3)
O(3)-U(2)-U(3)	32.50(7)	O(12)-U(4)-O(6)	86.97(15)	C(12)-C(7)-C(10)#4	119.8(3)
O(17)-U(2)-U(3)	109.30(9)	O(3)-U(4)-O(6)	73.46(10)	C(12)-C(7)-C(3)	120.2(4)
O(7)-U(2)-U(3)	102.47(7)	O(4)-U(4)-O(6)	76.08(10)	C(10)#4-C(7)-C(3)	120.0(4)
O(19)-U(2)-U(3)	159.25(9)	O(9)-U(4)-O(5)	89.38(13)	C(14)-C(8)-C(10)	119.9(4)
O(1)-U(2)-U(3)	40.49(6)	O(12)-U(4)-O(5)	87.12(13)	C(14)-C(8)-C(4)	119.9(3)
O(15)-U(2)-U(4)	66.39(11)	O(3)-U(4)-O(5)	129.94(10)	C(10)-C(8)-C(4)	120.1(3)
O(16)-U(2)-U(4)	115.90(11)	O(4)-U(4)-O(5)	80.67(10)	C(5)-C(9)-C(6)#3	119.8(4)
O(3)-U(2)-U(4)	25.68(7)	O(6)-U(4)-O(5)	155.86(10)	C(8)-C(10)-C(7)#4	119.9(4)
O(17)-U(2)-U(4)	138.26(12)	O(9)-U(4)-O(10)	92.02(13)	C(16)-C(11)-C(5)	120.4(4)
O(7)-U(2)-U(4)	70.57(7)	O(12)-U(4)-O(10)	87.82(13)	C(15)#4-C(12)-C(7)	120.0(4)
O(19)-U(2)-U(4)	135.19(8)	O(3)-U(4)-O(10)	63.66(10)	C(16)#3-C(13)-C(6)	119.3(4)
O(1)-U(2)-U(4)	76.88(6)	O(4)-U(4)-O(10)	146.95(9)	C(8)-C(14)-C(15)	119.7(4)
U(3)-U(2)-U(4)	54.323(4)	O(6)-U(4)-O(10)	136.75(10)	C(12)#4-C(15)-C(14)	120.6(4)
O(14)-U(3)-O(10)	176.83(15)	O(5)-U(4)-O(10)	66.29(10)	C(11)-C(16)-C(13)#3	120.2(4)

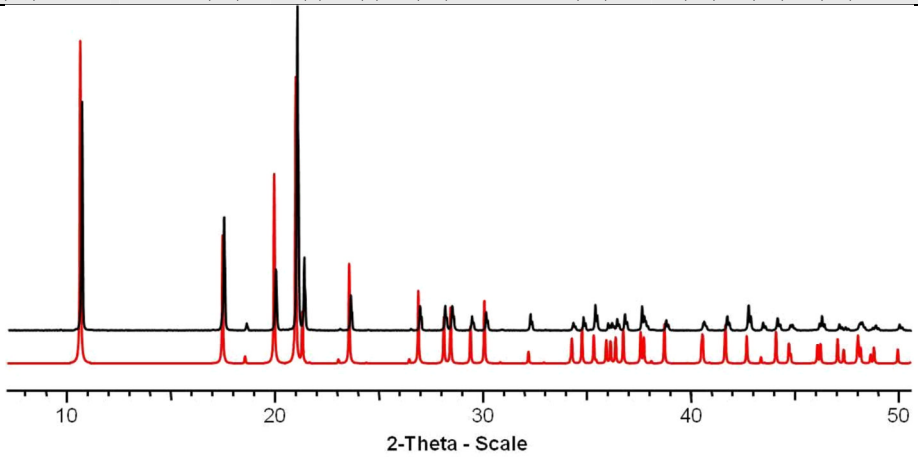

Figure 0.1 Comparison between the experimental (black) and simulated (red) PXRD patterns of the **iso1** phase.

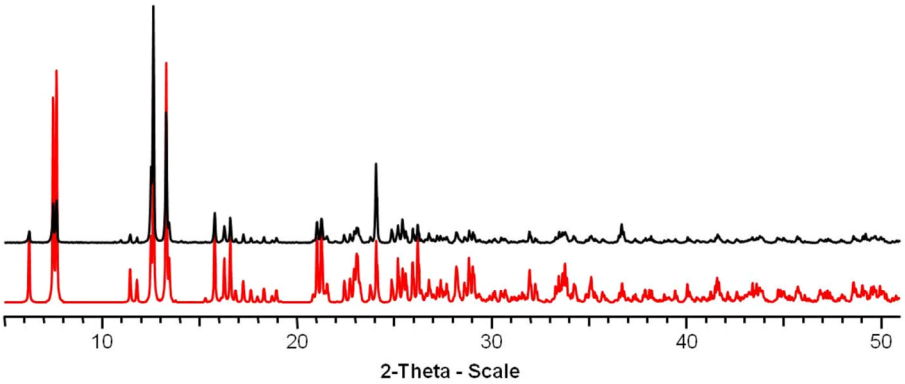

Figure 0.2 Comparison between the experimental (black) and simulated (red) PXRD patterns of the **iso10** phase.

Pyromellitate System

Table 0.1 Structure refinement and crystal data for pyr1 - pyr3 uranyl pyromellitate complexes.

	pyr1	pyr2	pyr3
formula	$C_{10}H_2O_{16}U_2$	$C_{30}H_6N_6O_{48}U_3$	$C_{14}H_{18}N_2O_{16}U$
formula weight	854.18	1836.51	612.3
temperature/K	293(2)	293(2)	293(2)
crystal type	yellow block	yellow block	yellow block
crystal size/mm	0.26 x 0.22 x 0.15	0.18 x 0.16 x 0.15	0.12 x 0.10 x 0.04
crystal system	Orthorhombic	Monoclinic	Monoclinic
space group	*P bcn*	*C* 2/*c*	*P* 2_1/*n*
a/Å	12.8489(2)	55.631(2)	7.2181(6)
b/Å	12.7051(2)	7.1082(3)	13.686(1)
c/Å	9.97360(10)	13.1074(5)	9.2779(7)
α/deg	90	90	90
ß/deg	90	95.831(1)	92.580(2)
γ/deg	90	90	90
volume/Å^3	1628.16(4)	5156.4(4)	915.6(1)
Z, ρ_{calc}/g·cm^{-3}	4, 3.485	4, 2.365	2, 2.2204
μ/mm^{-1}	19.958	9.521	8.920
Θ range/deg	2.25 to 31.50	1.47 to 27.63	2.65 to 26.44
limiting indices	-18 ≤ h ≤ 18 -18 ≤ k ≤ 18 -14 ≤ l ≤ 13	-72 ≤ h ≤ 72 -9 ≤ k ≤ 5 -17 ≤ l ≤ 17	-9<=h<=9 -17<=k<=17 -11<=l<=11
collected reflections	146460	23709	89921
unique reflections	2717 [R(int) = 0.0520]	5994 [R(int) = 0.0339]	5601 [R(int) = 0.0928]
parameters	124	366	60
goodness-of-fit on F^2	0.964	1.310	1.270
final *R* indices [$I > 2\sigma(I)$]	R1 = 0.0164 wR2 = 0.0428	R1 = 0.0277 wR2 = 0.0309	R1 = 0.0484 wR2 = 0.0418
R indices (all data)	R1 = 0.0237 wR2 = 0.0471	R1 = 0.0396 wR2 = 0.0324	R1 = 0.1268 wR2 = 0.0496
largest diff peak and hole/e·Å^{-3}	0.979 and -1.442	1.89 and -1.10	3.96 and -1.85

Table 0.2 Structure refinement and crystal data for pyr4 - pyr6 uranyl pyromellitate complexes.

	pyr4	pyr5	pyr6	pyr7
formula	$C_{10}H_2NO_{16}U_2$	$C_{10}H_2O_{18}U_3$	$C_{14}H_{18}N_2O_{14}U_2$	$C_{15}H_3N_2O_{35}U_3$
formula weight	868,18	1124.21	914.36	2199.3
temperature/K	293(2)	293(2)	293(2)	293(2)
crystal type	yellow needle	yellow block	yellow block	yellow needle
crystal size/mm	0.27 x 0.06 x 0.06	0.15 x 0.11 x 0.07	0.12 x 0.11 x 0.06	0.20 x 0.08 x 0.03
crystal system	Monoclinic	Triclinic	Monoclinic	Orthorhombic
space group	*P* 2_1/n	*P* -1	*P* 2_1/c	*P* nnm
a/Å	9.1844(2)	5.5266(3)	13.5550(5)	13.198(2)
b/Å	21.6150(5)	7.6559(3)	14.6014(4)	14.852(2)
c/Å	11.5401(2)	11.3208(4)	11.7868(4)	23.407(4)
α/deg	90	100.846(2)	90	90
ß/deg	112.701(1)	100.440(2)	110.728(2)	90
γ/deg	90	96.940(2)	90	90
volume/Å^3	2113.5(1)	456.66(3)	2181.9(1)	4588.1(12)
Z, ρ_{calc}/g·cm^{-3}	4, 2.729	1, 4.088	4, 2.784	4, 3.183
μ/mm^{-1}	15.379	26.628	14.899	21.198
Θ range/deg	1.88 to 24.94	1.87 to 30.03	1.61 to 26.02	1.62 to 33.21
limiting indices	-10<=h<=10 -25<=k<=25 -13<=l<=13	-7 ≤ h ≤ 7 -10 ≤ k ≤ 10 -15 ≤ l ≤ 15	-16 ≤ h ≤ 16 -18 ≤ k ≤ 16 -14 ≤ l ≤ 14	-20<=h<=20 -22<=k<=22 -35<=l<=35
collected reflections	89921	70902	111148	135027

	pyr4	pyr5	pyr6	pyr7
unique reflections	3691 [R(int) = 0.0806]	2662 [R(int) = 0.0605]	4305 [R(int) = 0.1201]	8983 [R(int) = 0.0634]
parameters	248	142	259	146
goodness-of-fit on F^2	1.442	0.717	1.180	2.940
final R indices [$I > 2\sigma(I)$]	R1 = 0.0336 wR2 = 0.0947	R1 = 0.0188 wR2 = 0.0683	R1 = 0.0346 wR2 = 0.0727	R1 = 0.0444 wR2 = 0.0733
R indices (all data)	R1 = 0.0459 wR2 = 0.1138	R1 = 0.0244 wR2 = 0.0844	R1 = 0.0600 wR2 = 0.0972	R1 = 0.0634 wR2 = 0.0747
largest diff peak and hole/e·Å^{-3}	3.698 and -1.069	0.909 and -1.552	2.524 and -1.697	4.81 and -5.51

Table 0.3 Atomic coordinates (x10^4) and equivalent isotropic displacement parameters (A^{2}x10^3) for complex pyr1.

Atom	x	y	z	U(eq)
U(1)	7986(1)	8131(1)	4051(1)	15(1)
O(1)	8022(2)	9322(2)	4960(3)	25(1)
O(2)	8005(2)	6943(2)	3150(3)	26(1)
O(3)	6617(2)	8898(2)	2667(2)	23(1)
O(4)	9857(2)	7910(2)	4215(3)	27(1)
O(5)	6376(2)	7552(2)	4996(3)	24(1)
O(6)	8445(2)	7301(2)	6064(2)	26(1)
O(7)	8783(2)	9121(2)	2256(3)	32(1)
C(1)	6304(2)	8583(2)	1547(3)	15(1)
C(2)	10458(2)	7226(2)	4693(3)	15(1)
C(3)	10142(2)	6085(2)	4836(3)	14(1)
C(4)	5602(2)	9287(2)	745(3)	14(1)
C(5)	10732(2)	5369(2)	4102(3)	15(1)

Table 0.4 Bond lengths for complex pyr1.

Bond	Bond lengths [Å]	Bond	Bond lengths [Å]
U(1)-O(2)	1.758(3)	O(6)-C(1)#2	1.264(4)
U(1)-O(1)	1.764(3)	C(1)-O(6)#3	1.264(4)
U(1)-O(6)	2.343(2)	C(1)-C(4)	1.501(4)
U(1)-O(5)	2.390(2)	C(2)-O(5)#4	1.252(4)
U(1)-O(7)	2.415(3)	C(2)-C(3)	1.513(4)
U(1)-O(4)	2.426(2)	C(3)-C(5)	1.391(4)
U(1)-O(3)	2.438(2)	C(3)-C(4)#2	1.401(4)
O(3)-C(1)	1.254(4)	C(4)-C(5)#5	1.393(4)
O(4)-C(2)	1.256(4)	C(4)-C(3)#3	1.401(4)
O(5)-C(2)#1	1.252(4)	C(5)-C(4)#6	1.393(4)

Table 0.5 Bond Angles for complex pyr1.

Bond	Angle [°]	Bond	Angle [°]	Bond	Angle [°]
O(2)-U(1)-O(1)	177.73(11)	O(5)-U(1)-O(4)	142.72(8)	O(3)-C(1)-C(4)	118.5(3)
O(2)-U(1)-O(6)	92.73(11)	O(7)-U(1)-O(4)	71.93(9)	O(6)#3-C(1)-C(4)	118.7(3)
O(1)-U(1)-O(6)	86.54(11)	O(2)-U(1)-O(3)	93.63(10)	O(5)#4-C(2)-O(4)	121.1(3)
O(2)-U(1)-O(5)	87.05(11)	O(1)-U(1)-O(3)	88.11(10)	O(5)#4-C(2)-C(3)	116.4(3)
O(1)-U(1)-O(5)	94.84(10)	O(6)-U(1)-O(3)	147.79(9)	O(4)-C(2)-C(3)	122.3(3)
O(6)-U(1)-O(5)	75.00(10)	O(5)-U(1)-O(3)	73.85(9)	C(5)-C(3)-C(4)#2	119.5(3)
O(2)-U(1)-O(7)	93.58(12)	O(7)-U(1)-O(3)	71.26(9)	C(5)-C(3)-C(2)	115.5(3)
O(1)-U(1)-O(7)	85.60(11)	O(4)-U(1)-O(3)	143.05(9)	C(4)#2-C(3)-C(2)	124.6(3)
O(6)-U(1)-O(7)	139.69(10)	C(1)-O(3)-U(1)	127.5(2)	C(5)#5-C(4)-C(3)#3	119.0(3)
O(5)-U(1)-O(7)	145.07(9)	C(2)-O(4)-U(1)	135.6(2)	C(5)#5-C(4)-C(1)	117.3(3)
O(2)-U(1)-O(4)	85.49(10)	C(2)#1-O(5)-U(1)	147.6(2)	C(3)#3-C(4)-C(1)	123.7(3)
O(1)-U(1)-O(4)	92.24(10)	C(1)#2-O(6)-U(1)	142.3(2)	C(3)-C(5)-C(4)#6	121.5(3)
O(6)-U(1)-O(4)	68.95(9)	O(3)-C(1)-O(6)#3	122.8(3)		

Table 0.6 Bond valence calculation for complex pyr1.

Atom	Atom bond	Bond length	Bond valence [vu]	Atom valence [vu]

U1	U(1)-O(2)	1,758	1,76	6,04
	U(1)-O(1)	1,764	1,74	
	U(1)-O(6)	2,343	0,57	
	U(1)-O(5)	2,390	0,52	
	U(1)-O(7)	2,415	0,50	
	U(1)-O(4)	2,426	0,49	
	U(1)-O(3)	2,438	0,47	
O1	U(1)-O(1)	1,764	1,74	1,74
O2	U(1)-O(2)	1,758	1,76	1,76
O3	U(1)-O(3)	2,438	0,47	1,77
	O(3)-C(1)	1,254	1,30	
O4	U(1)-O(4)	2,426	0,49	1,78
	O(4)-C(2)	1,256	1,29	
O5	U(1)-O(5)	2,390	0,52	1,82
	O(5)-C(2)	1,252	1,30	
O6	U(1)-O(6)	2,343	0,57	1,84
	O(6)-C(1)	1,264	1,27	
O7	U(1)-O(7)	2,415	0,50	0,50

Table 0.7 Atomic coordinates ($x10^4$) and equivalent isotropic displacement parameters (A^2x10^3) for complex pyr2.

Atom	x	y	z	U(eq)
U(1)	6669(1)	7367(1)	4137(1)	12(1)
U(2)	5000	7026(1)	2500	13(1)
O(1)	6931(1)	10060(4)	4331(2)	18(1)
O(2)	6745(1)	7222(5)	2854(3)	23(1)
O(3)	5069(1)	7001(5)	1209(2)	23(1)
O(4)	6594(1)	7502(5)	5417(3)	24(1)
O(5)	6871(1)	4270(4)	4595(3)	25(1)
O(6)	7109(1)	6696(4)	4680(3)	27(1)
O(7)	5255(1)	9788(4)	2673(2)	22(1)
O(8)	6408(1)	4685(4)	3937(2)	20(1)
O(9)	5446(1)	6424(4)	2971(3)	27(1)
O(10)	6229(1)	8034(4)	3616(3)	28(1)
O(11)	6464(1)	10489(4)	3679(3)	29(1)
O(12)	5210(1)	3980(4)	2993(2)	26(1)
O(13)	6957(1)	10688(5)	6008(2)	26(1)
O(14)	6366(1)	4161(5)	2259(2)	29(1)
O(15)	5302(1)	10348(5)	4347(2)	29(1)
C(1)	7033(1)	10798(5)	5152(3)	14(1)
C(2)	7082(1)	4941(5)	4724(3)	16(1)
C(3)	6300(1)	3989(5)	3132(3)	16(1)
C(4)	6254(1)	9799(6)	3562(3)	20(1)
C(5)	5368(1)	10492(5)	3481(3)	18(1)
C(6)	7270(1)	11742(5)	5053(3)	14(1)
C(7)	5420(1)	4672(5)	3065(3)	18(1)
C(8)	6041(1)	11069(5)	3406(3)	15(1)
C(9)	6064(1)	3011(5)	3245(3)	15(1)
C(10)	5606(1)	11442(5)	3364(3)	16(1)
C(11)	7296(1)	13666(5)	4885(3)	16(1)
C(12)	7525(1)	14415(5)	4839(3)	17(1)
C(13)	5632(1)	13378(5)	3213(3)	15(1)
C(14)	5811(1)	10310(6)	3459(3)	18(1)
C(15)	5861(1)	4141(5)	3147(3)	16(1)
N(1)	6844(1)	12298(6)	2451(4)	28(1)
N(2)	6484(1)	7343(6)	836(4)	30(1)
N(3)	5173(1)	7739(6)	5865(4)	29(1)
OW1	5561(1)	5476(7)	5584(3)	55(1)
OW2	5606(1)	11630(8)	6039(3)	49(1)
OW3	6040(1)	3378(8)	536(3)	53(1)
OW4	7283(1)	11575(8)	7729(3)	50(1)
OW5	7238(1)	4544(8)	2274(4)	53(1)

Atom	x	y	z	U(eq)
OW6	6084(1)	9517(7)	1045(3)	53(1)

Table 0.8 Bond lengths for complex pyr2.

Bond	Bond lengths [Å]	Bond	Bond lengths [Å]
U(1)-O(4)	1.775(3)	O(10)-C(4)	1.267(5)
U(1)-O(2)	1.781(3)	O(11)-C(4)	1.265(5)
U(1)-O(8)	2.399(3)	O(12)-C(7)	1.265(4)
U(1)-O(1)	2.406(3)	O(13)-C(1)	1.241(4)
U(1)-O(10)	2.526(3)	O(14)-C(3)	1.246(4)
U(1)-O(5)	2.522(3)	O(15)-C(5)	1.234(4)
U(1)-O(6)	2.528(3)	C(1)-C(6)	1.502(5)
U(1)-O(11)	2.545(3)	C(2)-C(11)#2	1.497(5)
U(1)-C(2)	2.917(4)	C(3)-C(9)	1.509(5)
U(1)-C(4)	2.928(4)	C(4)-C(8)	1.488(5)
U(2)-O(3)#1	1.776(3)	C(5)-C(10)	1.511(5)
U(2)-O(3)	1.776(3)	C(6)-C(11)	1.398(5)
U(2)-O(7)	2.423(3)	C(6)-C(12)#3	1.404(5)
U(2)-O(7)#1	2.423(3)	C(7)-C(13)#2	1.496(5)
U(2)-O(12)#1	2.516(3)	C(8)-C(14)	1.398(5)
U(2)-O(12)	2.516(3)	C(8)-C(9)#4	1.407(5)
U(2)-O(9)#1	2.537(3)	C(9)-C(15)	1.386(5)
U(2)-O(9)	2.537(3)	C(9)-C(8)#2	1.407(5)
U(2)-C(7)#1	2.911(4)	C(10)-C(14)	1.395(5)
U(2)-C(7)	2.911(4)	C(10)-C(13)	1.402(5)
O(1)-C(1)	1.279(4)	C(11)-C(12)	1.390(5)
O(5)-C(2)	1.263(4)	C(11)-C(2)#4	1.497(5)
O(6)-C(2)	1.261(4)	C(12)-C(6)#3	1.404(5)
O(7)-C(5)	1.280(5)	C(13)-C(15)#4	1.396(5)
O(8)-C(3)	1.263(4)	C(13)-C(7)#4	1.496(5)
O(9)-C(7)	1.265(4)	C(15)-C(13)#2	1.396(5)

Table 0.9 Bond Angles for complex pyr2.

Bond	Angle [°]	Bond	Angle [°]	Bond	Angle [°]
O(4)-U(1)-O(2)	179.76(15)	O(3)-U(2)-O(7)#1	95.77(13)	C(7)-O(12)-U(2)	94.9(2)
O(4)-U(1)-O(8)	86.99(13)	O(7)-U(2)-O(7)#1	71.42(14)	O(13)-C(1)-O(1)	125.2(3)
O(2)-U(1)-O(8)	92.85(13)	O(3)#1-U(2)-O(12)#1	95.56(13)	O(13)-C(1)-C(6)	119.2(3)
O(4)-U(1)-O(1)	93.22(13)	O(3)-U(2)-O(12)#1	83.45(13)	O(1)-C(1)-C(6)	115.5(3)
O(2)-U(1)-O(1)	86.94(13)	O(7)-U(2)-O(12)#1	167.40(10)	O(5)-C(2)-O(6)	119.0(3)
O(8)-U(1)-O(1)	179.76(9)	O(7)#1-U(2)-O(12)#1	115.08(10)	O(5)-C(2)-C(11)#2	120.3(3)
O(4)-U(1)-O(10)	85.96(15)	O(3)#1-U(2)-O(12)	83.45(13)	O(6)-C(2)-C(11)#2	120.7(3)
O(2)-U(1)-O(10)	94.13(14)	O(3)-U(2)-O(12)	95.56(13)	O(5)-C(2)-U(1)	59.5(2)
O(8)-U(1)-O(10)	63.81(10)	O(7)-U(2)-O(12)	115.08(10)	O(6)-C(2)-U(1)	59.8(2)
O(1)-U(1)-O(10)	116.10(10)	O(7)#1-U(2)-O(12)	167.40(10)	C(11)#2-C(2)-U(1)	172.8(3)
O(4)-U(1)-O(5)	87.97(14)	O(12)#1-U(2)-O(12)	60.92(13)	O(14)-C(3)-O(8)	124.8(4)
O(2)-U(1)-O(5)	91.81(14)	O(3)#1-U(2)-O(9)#1	85.89(14)	O(14)-C(3)-C(9)	118.6(3)
O(8)-U(1)-O(5)	65.18(10)	O(3)-U(2)-O(9)#1	93.92(14)	O(8)-C(3)-C(9)	116.4(3)
O(1)-U(1)-O(5)	114.94(9)	O(7)-U(2)-O(9)#1	135.25(10)	O(11)-C(4)-O(10)	119.0(4)
O(10)-U(1)-O(5)	128.84(10)	O(7)#1-U(2)-O(9)#1	64.15(10)	O(11)-C(4)-C(8)	119.6(4)
O(4)-U(1)-O(6)	93.40(15)	O(12)#1-U(2)-O(9)#1	51.27(9)	O(10)-C(4)-C(8)	121.4(4)
O(2)-U(1)-O(6)	86.51(14)	O(12)-U(2)-O(9)#1	109.54(10)	O(11)-C(4)-U(1)	60.0(2)
O(8)-U(1)-O(6)	116.09(10)	O(3)#1-U(2)-O(9)	93.92(14)	O(10)-C(4)-U(1)	59.2(2)
O(1)-U(1)-O(6)	64.02(10)	O(3)-U(2)-O(9)	85.89(14)	C(8)-C(4)-U(1)	173.0(3)
O(10)-U(1)-O(6)	179.35(8)	O(7)-U(2)-O(9)	64.15(10)	O(15)-C(5)-O(7)	124.3(4)
O(5)-U(1)-O(6)	51.00(10)	O(7)#1-U(2)-O(9)	135.25(10)	O(15)-C(5)-C(10)	118.6(3)
O(4)-U(1)-O(11)	91.88(14)	O(12)#1-U(2)-O(9)	109.54(10)	O(7)-C(5)-C(10)	117.1(3)
O(2)-U(1)-O(11)	88.35(14)	O(12)-U(2)-O(9)	51.27(9)	C(11)-C(6)-C(12)#3	119.7(3)
O(8)-U(1)-O(11)	114.64(9)	O(9)#1-U(2)-O(9)	160.55(14)	C(11)-C(6)-C(1)	124.0(3)
O(1)-U(1)-O(11)	65.25(9)	O(3)#1-U(2)-C(7)#1	89.47(14)	C(12)#3-C(6)-C(1)	116.3(3)
O(10)-U(1)-O(11)	50.96(9)	O(3)-U(2)-C(7)#1	89.87(13)	O(9)-C(7)-O(12)	119.6(3)
O(5)-U(1)-O(11)	179.76(8)	O(7)-U(2)-C(7)#1	159.90(10)	O(9)-C(7)-C(13)#2	121.4(3)
O(6)-U(1)-O(11)	129.19(10)	O(7)#1-U(2)-C(7)#1	89.78(10)	O(12)-C(7)-C(13)#2	118.9(3)

Bond	Angle [°]	Bond	Angle [°]	Bond	Angle [°]
O(4)-U(1)-C(2)	92.19(14)	O(12)#1-U(2)-C(7)#1	25.66(10)	O(9)-C(7)-U(2)	60.4(2)
O(2)-U(1)-C(2)	87.64(14)	O(12)-U(2)-C(7)#1	84.75(10)	O(12)-C(7)-U(2)	59.5(2)
O(8)-U(1)-C(2)	90.57(10)	O(9)#1-U(2)-C(7)#1	25.68(9)	C(13)#2-C(7)-U(2)	172.5(3)
O(1)-U(1)-C(2)	89.53(10)	O(9)-U(2)-C(7)#1	134.97(11)	C(14)-C(8)-C(9)#4	119.1(3)
O(10)-U(1)-C(2)	154.36(10)	O(3)#1-U(2)-C(7)	89.87(13)	C(14)-C(8)-C(4)	118.6(3)
O(5)-U(1)-C(2)	25.56(10)	O(3)-U(2)-C(7)	89.47(14)	C(9)#4-C(8)-C(4)	122.3(3)
O(6)-U(1)-C(2)	25.52(9)	O(7)-U(2)-C(7)	89.78(10)	C(15)-C(9)-C(8)#2	119.9(3)
O(11)-U(1)-C(2)	154.64(10)	O(7)#1-U(2)-C(7)	159.90(10)	C(15)-C(9)-C(3)	115.9(3)
O(4)-U(1)-C(4)	87.43(14)	O(12)#1-U(2)-C(7)	84.75(10)	C(8)#2-C(9)-C(3)	124.2(3)
O(2)-U(1)-C(4)	92.74(14)	O(12)-U(2)-C(7)	25.66(10)	C(14)-C(10)-C(13)	119.1(3)
O(8)-U(1)-C(4)	89.33(10)	O(9)#1-U(2)-C(7)	134.97(11)	C(14)-C(10)-C(5)	116.9(3)
O(1)-U(1)-C(4)	90.57(10)	O(9)-U(2)-C(7)	25.68(9)	C(13)-C(10)-C(5)	124.0(3)
O(10)-U(1)-C(4)	25.53(10)	C(7)#1-U(2)-C(7)	109.67(15)	C(12)-C(11)-C(6)	119.6(3)
O(5)-U(1)-C(4)	154.29(10)	C(1)-O(1)-U(1)	128.9(2)	C(12)-C(11)-C(2)#4	118.8(3)
O(6)-U(1)-C(4)	154.59(11)	C(2)-O(5)-U(1)	95.0(2)	C(6)-C(11)-C(2)#4	121.5(3)
O(11)-U(1)-C(4)	25.50(10)	C(2)-O(6)-U(1)	94.7(2)	C(11)-C(12)-C(6)#3	120.7(3)
C(2)-U(1)-C(4)	179.61(10)	C(5)-O(7)-U(2)	129.1(2)	C(15)#4-C(13)-C(10)	119.9(3)
O(3)#1-U(2)-O(3)	178.9(2)	C(3)-O(8)-U(1)	129.5(2)	C(15)#4-C(13)-C(7)#4	117.8(3)
O(3)#1-U(2)-O(7)	95.77(13)	C(7)-O(9)-U(2)	93.9(2)	C(10)-C(13)-C(7)#4	122.2(3)
O(3)-U(2)-O(7)	85.16(13)	C(4)-O(10)-U(1)	95.3(2)	C(10)-C(14)-C(8)	121.2(4)
O(3)#1-U(2)-O(7)#1	85.16(13)	C(4)-O(11)-U(1)	94.5(2)	C(9)-C(15)-C(13)#2	120.8(4)

Table 0.10 Bond valence calculation for complex pyr2.

Atom	Atom bond	Bond length	Bond valence [vu]	Atom valence [vu]
U1	U(1)-O(4)	1,775	1,70	5,99
	U(1)-O(2)	1,781	1,68	
	U(1)-O(8)	2,399	0,51	
	U(1)-O(1)	2,406	0,50	
	U(1)-O(10)	2,526	0,40	
	U(1)-O(5)	2,522	0,40	
	U(1)-O(6)	2,528	0,40	
	U(1)-O(11)	2,545	0,39	
U2	U(2)-O(3)	1,776	1,70	5,97
	U(2)-O(3)#1	1,776	1,70	
	U(2)-O(7)	2,423	0,49	
	U(2)-O(7)#1	2,423	0,49	
	U(2)-O(12)	2,516	0,41	
	U(2)-O(12)#1	2,516	0,41	
	U(2)-O(9)	2,537	0,39	
	U(2)-O(9)#1	2,537	0,39	
O1	U(1)-O(1)	2,406	0,50	1,74
	O(1)-C(1)	1,279	1,24	
O2	U(1)-O(2)	1,781	1,68	1,68
O3	U(2)-O(3)	1,776	1,70	1,70
O4	U(1)-O(4)	1,775	1,70	1,70
O5	U(1)-O(5)	2,522	0,40	1,68
	O(5)-C(2)	1,263	1,28	
O6	U(1)-O(6)	2,528	0,40	1,68
	O(6)-C(2)	1,261	1,28	
O7	O(7)-U(2)	2,423	0,49	2,21
	O(7)-U(2)#1	2,423	0,49	
	O(7)-C(5)	1,280	1,24	
O8	U(1)-O(8)	2,399	0,51	1,79
	O(8)-C(3)	1,263	1,28	
O9	O(9)-U(2)	2,537	0,39	2,06
	O(9)-U(2)#1	2,537	0,39	
	O(9)-C(7)	1,265	1,27	
O10	U(1)-O(10)	2,526	0,40	1,67
	O(10)-C(4)	1,267	1,27	
O11	U(1)-O(11)	2,545	0,39	1,66
	O(11)-C(4)	1,265	1,27	

Atom	Atom bond	Bond length	Bond valence [vu]	Atom valence [vu]
O12	U(2)-O(12)	2,516	0,41	2,09
	O(12)-U(2)#1	2,516	0,41	
	C(7)-O(12)	1,265	1,27	
O13	O(13)-C(1)	1,241	1,33	1,33
O14	O(14)-C(3)	1,246	1,32	1,32
O15	O(15)-C(5)	1,234	1,35	1,35

Table 0.11 Atomic coordinates (x10⁴) and equivalent isotropic displacement parameters (A²x10³) for complex pyr3.

Atom	x	y	z	U(eq)
U(1)	0	0	0	21(1)
O(81)	820(6)	-275(3)	2647(4)	24(1)
O(82)	3155(6)	-174(3)	1238(4)	22(1)
C(2)	3837(8)	-142(5)	3785(5)	18(1)
C(8)	2515(8)	-198(4)	2504(6)	18(1)
C(1)	5747(8)	-177(4)	3644(5)	16(1)
C(3)	3096(8)	80(7)	5122(5)	19(1)
O(1u)	219(7)	1243(3)	184(5)	31(1)
O(71)	7463(6)	258(3)	1617(4)	18(1)
O(72)	6665(7)	-1309(4)	1944(5)	35(1)
N(1s)	4832(9)	-1842(5)	-604(6)	43(2)
C(7)	6666(10)	-454(5)	2249(7)	22(2)
C(11s)	3710(14)	-2551(6)	111(10)	65(3)
C(12s)	5762(14)	-2267(6)	-1855(9)	64(3)

Table 0.12 Bond lengths for complex pyr3.

Bond	Bond lengths [Å]	Bond	Bond lengths [Å]
U(1)-O(81)	2.528(4)	O(82)-C(8)	1.282(7)
U(1)-O(81)#1	2.528(4)	C(2)-C(8)	1.492(7)
U(1)-O(82)	2.515(4)	C(2)-C(1)	1.392(8)
U(1)-O(82)#1	2.515(4)	C(2)-C(3)	1.406(7)
U(1)-C(8)	2.896(6)	C(1)-C(3)	1.393(7)
U(1)-C(8)#1	2.896(6)	C(1)-C(7)	1.528(8)
U(1)-O(1u)	1.716(4)	O(71)-C(7)	1.286(8)
U(1)-O(1u)#1	1.716(4)	O(72)-C(7)	1.204(9)
U(1)-O(71)	2.445(4)	N(1s)-C(11s)	1.444(11)
U(1)-O(71)#1	2.445(4)	N(1s)-C(12s)	1.485(11)
O(81)-C(8)	1.241(7)		

Table 0.13 Bond Angles for complex pyr3.

Bond	Angle [°]	Bond	Angle [°]	Bond	Angle [°]
O(81)-U(1)-O(81)#1	180.0(5)	O(81)-C(2)-C(3)#4	177.3(4)	O(71)-C(1)-O(72)	57.02(19)
O(81)-U(1)-O(82)	51.30(13)	O(81)-C(2)-C(7)	118.2(3)	O(71)-C(1)-C(7)	29.5(3)
O(81)-U(1)-O(82)#1	128.70(13)	O(82)-C(2)-C(2)#4	153.4(3)	O(72)-C(1)-C(7)	27.6(3)
O(81)-U(1)-C(8)	25.30(16)	O(82)-C(2)-C(8)	28.0(3)	O(81)-C(3)-C(2)	58.2(3)
O(81)-U(1)-C(8)#1	154.70(16)	O(82)-C(2)-C(1)	93.8(3)	O(81)-C(3)-C(2)#4	148.1(3)
O(81)-U(1)-O(1u)	91.97(18)	O(82)-C(2)-C(1)#4	169.6(4)	O(81)-C(3)-C(8)	26.24(17)
O(81)-U(1)-O(1u)#1	88.03(18)	O(82)-C(2)-C(3)	143.7(4)	O(81)-C(3)-C(1)	87.7(2)
O(81)-U(1)-O(71)#2	64.82(14)	O(82)-C(2)-C(3)#4	124.3(3)	O(81)-C(3)-C(1)#4	175.5(6)
O(81)-U(1)-O(71)#3	115.18(14)	O(82)-C(2)-C(7)	65.4(2)	O(81)-C(3)-C(3)#4	117.7(2)
O(81)#1-U(1)-O(82)	128.70(13)	C(2)#4-C(2)-C(8)	174.4(5)	O(81)-C(3)-C(7)#4	148.1(3)
O(81)#1-U(1)-O(82)#1	51.30(13)	C(2)#4-C(2)-C(1)	61.1(3)	C(2)-C(3)-C(2)#4	90.0(4)
O(81)#1-U(1)-C(8)	154.70(16)	C(2)#4-C(2)-C(1)#4	30.07(18)	C(2)-C(3)-C(8)	32.4(3)
O(81)#1-U(1)-C(8)#1	25.30(16)	C(2)#4-C(2)-C(3)	59.6(3)	C(2)-C(3)-C(1)	29.5(3)
O(81)#1-U(1)-O(1u)	88.03(18)	C(2)#4-C(2)-C(3)#4	30.42(18)	C(2)-C(3)-C(1)#4	120.5(5)
O(81)#1-U(1)-O(1u)#1	91.97(18)	C(2)#4-C(2)-C(7)	90.4(2)	C(2)-C(3)-C(3)#4	59.6(3)
O(81)#1-U(1)-O(71)#2	115.18(14)	C(8)-C(2)-C(1)	121.6(5)	C(2)-C(3)-C(7)#4	153.7(4)
O(81)#1-U(1)-O(71)#3	64.82(14)	C(8)-C(2)-C(1)#4	146.8(4)	C(2)#4-C(3)-C(8)	122.2(3)
O(82)-U(1)-O(82)#1	180.0(5)	C(8)-C(2)-C(3)	117.3(5)	C(2)#4-C(3)-C(1)	60.5(2)

Bond	Angle [°]	Bond	Angle [°]	Bond	Angle [°]
O(82)-U(1)-C(8)	26.22(14)	C(8)-C(2)-C(3)#4	152.2(4)	C(2)#4-C(3)-C(1)#4	30.7(3)
O(82)-U(1)-C(8)#1	153.78(14)	C(8)-C(2)-C(7)	92.6(4)	C(2)#4-C(3)-C(3)#4	30.42(17)
O(82)-U(1)-O(1u)	88.3(2)	C(1)-C(2)-C(1)#4	91.1(3)	C(2)#4-C(3)-C(7)#4	63.7(2)
O(82)-U(1)-O(1u)#1	91.7(2)	C(1)-C(2)-C(3)	120.6(5)	C(8)-C(3)-C(1)	61.8(2)
O(82)-U(1)-O(71)#2	114.92(12)	C(1)-C(2)-C(3)#4	30.7(3)	C(8)-C(3)-C(1)#4	152.9(4)
O(82)-U(1)-O(71)#3	65.08(12)	C(1)-C(2)-C(7)	29.5(3)	C(8)-C(3)-C(3)#4	91.9(2)
O(82)#1-U(1)-C(8)	153.78(14)	C(1)#4-C(2)-C(3)	29.6(3)	C(8)-C(3)-C(7)#4	173.5(4)
O(82)#1-U(1)-C(8)#1	26.22(14)	C(1)#4-C(2)-C(3)#4	60.5(2)	C(1)-C(3)-C(1)#4	91.1(4)
O(82)#1-U(1)-O(1u)	91.7(2)	C(1)#4-C(2)-C(7)	120.4(3)	C(1)-C(3)-C(3)#4	30.10(17)
O(82)#1-U(1)-O(1u)#1	88.3(2)	C(3)-C(2)-C(3)#4	90.0(3)	C(1)-C(3)-C(7)#4	124.2(3)
O(82)#1-U(1)-O(71)#2	65.08(12)	C(3)-C(2)-C(7)	150.0(4)	C(1)#4-C(3)-C(3)#4	61.0(3)
O(82)#1-U(1)-O(71)#3	114.92(12)	C(3)#4-C(2)-C(7)	60.0(2)	C(1)#4-C(3)-C(7)#4	33.2(3)
C(8)-U(1)-C(8)#1	180.0(5)	U(1)-C(8)-O(81)	60.5(3)	C(3)#4-C(3)-C(7)#4	94.1(3)
C(8)-U(1)-O(1u)	87.8(2)	U(1)-C(8)-O(82)	60.1(3)	U(1)-O(1u)-O(71)#2	60.25(16)
C(8)-U(1)-O(1u)#1	92.2(2)	U(1)-C(8)-C(2)	171.7(4)	U(1)#9-O(71)-O(81)#9	59.11(13)
C(8)-U(1)-O(71)#2	88.91(15)	U(1)-C(8)-C(1)	150.6(3)	U(1)#9-O(71)-O(82)#3	58.75(12)
C(8)-U(1)-O(71)#3	91.09(15)	U(1)-C(8)-C(3)	147.7(3)	U(1)#9-O(71)-C(1)	151.9(2)
C(8)#1-U(1)-O(1u)	92.2(2)	O(81)-C(8)-O(82)	119.8(5)	U(1)#9-O(71)-O(1u)#9	37.55(11)
C(8)#1-U(1)-O(1u)#1	87.8(2)	O(81)-C(8)-C(2)	121.2(5)	U(1)#9-O(71)-O(72)	98.58(19)
C(8)#1-U(1)-O(71)#2	91.09(15)	O(81)-C(8)-C(1)	148.8(4)	U(1)#9-O(71)-N(1s)#3	110.27(18)
C(8)#1-U(1)-O(71)#3	88.91(15)	O(81)-C(8)-C(3)	91.9(4)	U(1)#9-O(71)-C(7)	122.2(4)
O(1u)-U(1)-O(1u)#1	180.0(5)	O(82)-C(8)-C(2)	119.0(5)	O(81)#9-O(71)-O(82)#3	116.93(19)
O(1u)-U(1)-O(71)#2	82.21(19)	O(82)-C(8)-C(1)	91.1(4)	O(81)#9-O(71)-C(1)	98.4(2)
O(1u)-U(1)-O(71)#3	97.79(19)	O(82)-C(8)-C(3)	147.5(4)	O(81)#9-O(71)-O(1u)#9	69.31(17)
O(1u)#1-U(1)-O(71)#2	97.79(19)	C(2)-C(8)-C(1)	28.1(3)	O(81)#9-O(71)-O(72)	85.7(2)
O(1u)#1-U(1)-O(71)#3	82.21(19)	C(2)-C(8)-C(3)	30.3(3)	O(81)#9-O(71)-N(1s)#3	145.9(2)
O(71)#2-U(1)-O(71)#3	180.0(5)	C(1)-C(8)-C(3)	58.2(2)	O(81)#9-O(71)-C(7)	92.7(4)
U(1)-O(81)-O(82)	64.06(14)	O(82)-C(1)-C(2)	57.0(3)	O(82)#3-O(71)-C(1)	134.9(2)
U(1)-O(81)-C(2)	126.0(2)	O(82)-C(1)-C(2)#4	144.8(3)	O(82)#3-O(71)-O(1u)#9	68.81(16)
U(1)-O(81)-C(8)	94.2(3)	O(82)-C(1)-C(8)	26.76(16)	O(82)#3-O(71)-O(72)	93.5(2)
U(1)-O(81)-C(3)	150.7(2)	O(82)-C(1)-C(1)#4	115.8(2)	O(82)#3-O(71)-N(1s)#3	68.78(17)
U(1)-O(81)-O(71)#2	56.07(12)	O(82)-C(1)-C(3)	86.3(2)	O(82)#3-O(71)-C(7)	111.2(4)
O(82)-O(81)-C(2)	63.0(2)	O(82)-C(1)-C(3)#4	173.1(5)	C(1)-O(71)-O(1u)#9	155.2(2)
O(82)-O(81)-C(8)	30.6(3)	O(82)-C(1)-O(71)	74.13(18)	C(1)-O(71)-O(72)	60.5(2)
O(82)-O(81)-C(3)	92.3(2)	O(82)-C(1)-O(72)	70.53(19)	C(1)-O(71)-C(7)	35.8(3)
O(82)-O(81)-O(71)#2	118.8(2)	O(82)-C(1)-C(7)	68.4(3)	O(1u)#9-O(71)-O(72)	136.0(2)
C(2)-O(81)-C(8)	32.4(3)	C(2)-C(1)-C(2)#4	88.9(3)	O(1u)#9-O(71)-N(1s)#3	83.80(19)
C(2)-O(81)-C(3)	30.07(17)	C(2)-C(1)-C(8)	30.3(3)	O(1u)#9-O(71)-C(7)	157.9(4)
C(2)-O(81)-O(71)#2	159.3(3)	C(2)-C(1)-C(1)#4	59.4(3)	O(72)-O(71)-N(1s)#3	128.3(3)
C(8)-O(81)-C(3)	61.9(3)	C(2)-C(1)-C(3)	29.9(3)	O(72)-O(71)-C(7)	24.8(3)
C(8)-O(81)-O(71)#2	145.4(4)	C(2)-C(1)-C(3)#4	118.6(5)	N(1s)#3-O(71)-C(7)	117.4(4)
C(3)-O(81)-O(71)#2	137.4(2)	C(2)-C(1)-O(71)	128.4(4)	C(1)-O(72)-O(71)	62.5(2)
U(1)-O(82)-O(81)	64.64(15)	C(2)-C(1)-O(72)	113.6(4)	C(1)-O(72)-N(1s)	128.1(3)
U(1)-O(82)-C(2)	126.2(2)	C(2)-C(1)-C(7)	123.9(5)	C(1)-O(72)-C(7)	36.0(4)
U(1)-O(82)-C(8)	93.7(3)	C(2)#4-C(1)-C(8)	119.0(3)	O(71)-O(72)-N(1s)	104.7(2)
U(1)-O(82)-C(1)	155.16(19)	C(2)#4-C(1)-C(1)#4	29.51(18)	O(71)-O(72)-C(7)	26.6(4)
U(1)-O(82)-O(71)#3	56.17(12)	C(2)#4-C(1)-C(3)	59.0(2)	N(1s)-O(72)-C(7)	117.0(4)
U(1)-O(82)-C(7)	172.8(2)	C(2)#4-C(1)-C(3)#4	29.9(3)	O(71)#3-N(1s)-O(72)	109.2(2)
O(81)-O(82)-C(2)	62.60(19)	C(2)#4-C(1)-O(71)	133.4(3)	O(71)#3-N(1s)-C(11s)	109.4(5)
O(81)-O(82)-C(8)	29.5(3)	C(2)#4-C(1)-O(72)	139.3(3)	O(71)#3-N(1s)-C(12s)	108.4(4)
O(81)-O(82)-C(1)	91.62(19)	C(2)#4-C(1)-C(7)	146.8(4)	O(72)-N(1s)-C(11s)	92.4(5)
O(81)-O(82)-O(71)#3	119.5(2)	C(8)-C(1)-C(1)#4	89.6(2)	O(72)-N(1s)-C(12s)	123.9(5)
O(81)-O(82)-C(7)	121.5(2)	C(8)-C(1)-C(3)	60.0(2)	C(11s)-N(1s)-C(12s)	112.3(7)
C(2)-O(82)-C(8)	33.1(3)	C(8)-C(1)-C(3)#4	148.9(4)	O(82)-C(7)-C(2)	53.98(19)
C(2)-O(82)-C(1)	29.19(18)	C(8)-C(1)-O(71)	100.2(2)	O(82)-C(7)-C(1)	79.7(4)
C(2)-O(82)-O(71)#3	177.4(3)	C(8)-C(1)-O(72)	89.7(2)	O(82)-C(7)-C(3)#4	109.5(3)
C(2)-O(82)-C(7)	60.6(2)	C(8)-C(1)-C(7)	94.1(4)	O(82)-C(7)-O(71)	99.6(4)
C(8)-O(82)-C(1)	62.1(3)	C(1)#4-C(1)-C(3)	29.54(17)	O(82)-C(7)-O(72)	93.7(4)
C(8)-O(82)-O(71)#3	149.0(4)	C(1)#4-C(1)-C(3)#4	59.3(3)	C(2)-C(7)-C(1)	26.6(3)
C(8)-O(82)-C(7)	92.8(3)	C(1)#4-C(1)-O(71)	153.7(3)	C(2)-C(7)-C(3)#4	56.4(2)
C(1)-O(82)-O(71)#3	148.5(2)	C(1)#4-C(1)-O(72)	148.1(3)	C(2)-C(7)-O(71)	120.6(5)
C(1)-O(82)-C(7)	31.88(18)	C(1)#4-C(1)-C(7)	174.2(4)	C(2)-C(7)-O(72)	107.4(5)
O(71)#3-O(82)-C(7)	116.9(2)	C(3)-C(1)-C(3)#4	88.9(3)	C(1)-C(7)-C(3)#4	29.9(3)

Bond	Angle [°]	Bond	Angle [°]	Bond	Angle [°]
O(81)-C(2)-O(82)	54.40(17)	C(3)-C(1)-O(71)	149.7(3)	C(1)-C(7)-O(71)	114.7(5)
O(81)-C(2)-C(2)#4	151.3(3)	C(3)-C(1)-O(72)	137.2(3)	C(1)-C(7)-O(72)	116.4(6)
O(81)-C(2)-C(8)	26.4(3)	C(3)-C(1)-C(7)	153.8(4)	C(3)#4-C(7)-O(71)	106.2(4)
O(81)-C(2)-C(1)	147.6(4)	C(3)#4-C(1)-O(71)	108.2(4)	C(3)#4-C(7)-O(72)	115.4(5)
O(81)-C(2)-C(1)#4	121.2(3)	C(3)#4-C(1)-O(72)	116.2(5)	O(71)-C(7)-O(72)	128.7(6)
O(81)-C(2)-C(3)	91.8(4)	C(3)#4-C(1)-C(7)	116.9(5)	N(1s)-C(12s)-C(11s)	33.3(4)

Table 0.14 Bond valence calculation for complex pyr3.

Atom	Atom bond	Bond length	Bond valence [vu]	Atom valence [vu]
U1	U(1)-O(81)	2,528	0,40	6,37
	U(1)-O(81)#1	2,528	0,40	
	U(1)-O(82)	2,515	0,41	
	U(1)-O(82)#1	2,515	0,41	
	U(1)-O(1u)	1,716	1,91	
	U(1)-O(1u)#1	1,716	1,91	
	U(1)-O(71)	2,445	0,47	
	U(1)-O(71)#1	2,445	0,47	
O1u	U(1)-O(1u)	1,716	1,91	1,91
O71	U(1)-O(71)	2,445	0,47	1,69
	O(71)-C(7)	1,286	1,22	
O72	O(72)-C(7)	1,204	1,43	1,43
O81	U(1)-O(81)	2,528	0,40	1,73
	O(81)-C(8)	1,241	1,33	
O82	U(1)-O(82)	2,515	0,41	1,64
	O(82)-C(8)	1,282	1,23	

Table 0.15 Atomic coordinates ($x10^4$) and equivalent isotropic displacement parameters (A^2x10^3) for complex pyr4.

Atom	x	y	z	U(eq)
U(1)	2926(1)	2463(1)	2792(1)	17(1)
U(2)	-831(1)	4995(1)	1305(1)	22(1)
O(1)	-1903(17)	5006(4)	2999(12)	69(4)
O(2)	1171(9)	3364(3)	2289(7)	20(2)
O(3)	4805(9)	1612(3)	3345(7)	19(2)
O(4)	1274(9)	1967(4)	2290(7)	27(2)
O(5)	4570(9)	2965(3)	3285(7)	25(2)
O(6)	2461(11)	2931(4)	4602(7)	33(2)
O(7)	6821(10)	992(3)	3520(8)	31(2)
O(8)	-809(11)	4001(4)	2087(9)	36(2)
O(9)	2366(10)	2943(4)	689(7)	26(2)
O(10)	-2732(11)	4839(4)	162(9)	39(2)
O(11)	3393(11)	2017(4)	968(7)	31(2)
O(12)	1067(11)	5152(4)	2474(8)	36(2)
O(13)	3495(10)	2006(4)	4921(7)	28(2)
O(14)	332(10)	4403(4)	196(8)	30(2)
C(1)	2878(13)	2501(5)	270(10)	17(2)
C(2)	2998(13)	2469(5)	5296(10)	20(2)
C(3)	-185(13)	3469(5)	2241(10)	18(2)
C(4)	6156(14)	1530(5)	3358(9)	19(2)
C(5)	2901(13)	2503(5)	-1013(10)	18(2)
C(6)	3010(13)	2489(5)	6609(10)	20(2)
C(7)	7097(13)	2037(5)	3097(10)	16(2)
C(8)	-1168(12)	2961(5)	2496(9)	15(2)
C(9)	-1238(13)	2950(5)	3669(10)	18(2)
C(10)	2155(13)	2946(5)	6921(10)	18(2)
N(1)	3720(20)	4258(8)	2072(16)	81(5)
OW1	-2010(30)	4231(11)	5040(20)	183(9)
OW2	-4870(30)	5558(11)	2600(20)	177(9)

Table 0.16 Bond lengths for complex pyr4.

Bond	Bond lengths [Å]	Bond	Bond lengths [Å]

U(1)-O(4)	1.763(8)	O(7)-C(4)	1.293(13)
U(1)-O(5)	1.767(8)	O(7)-U(2)#3	2.378(7)
U(1)-O(3)	2.432(7)	O(8)-C(3)	1.268(13)
U(1)-O(2)	2.450(7)	O(9)-C(1)	1.242(12)
U(1)-O(11)	2.498(8)	O(11)-C(1)	1.293(13)
U(1)-O(6)	2.501(8)	O(13)-C(2)	1.247(13)
U(1)-O(9)	2.504(7)	O(14)-U(2)#1	2.348(7)
U(1)-O(13)	2.509(7)	C(1)-C(5)	1.489(14)
U(1)-C(2)	2.865(10)	C(2)-C(6)	1.511(14)
U(1)-C(1)	2.895(10)	C(3)-C(8)	1.521(14)
U(2)-O(10)	1.767(9)	C(4)-C(7)	1.496(14)
U(2)-O(12)	1.777(9)	C(5)-C(9)#4	1.395(14)
U(2)-O(8)	2.327(8)	C(5)-C(7)#5	1.415(15)
U(2)-O(14)	2.338(7)	C(6)-C(10)	1.394(15)
U(2)-O(14)#1	2.348(7)	C(6)-C(8)#6	1.402(15)
U(2)-O(7)#2	2.378(7)	C(7)-C(10)#4	1.378(14)
U(2)-O(1)	2.506(10)	C(7)-C(5)#6	1.415(15)
U(2)-U(2)#1	3.8655(8)	C(8)-C(9)	1.380(14)
O(2)-C(3)	1.245(13)	C(8)-C(6)#5	1.402(15)
O(3)-C(4)	1.248(13)	C(9)-C(5)#7	1.395(14)
O(6)-C(2)	1.256(13)	C(10)-C(7)#7	1.378(14)

Table 0.17 Bond Angles for complex pyr4.

Bond	Angle [°]	Bond	Angle [°]	Bond	Angle [°]
O(4)-U(1)-O(5)	179.4(4)	O(3)-U(1)-C(1)	91.1(3)	C(4)-O(7)-U(2)#3	130.8(7)
O(4)-U(1)-O(3)	93.5(3)	O(2)-U(1)-C(1)	89.2(3)	C(3)-O(8)-U(2)	145.9(7)
O(5)-U(1)-O(3)	87.0(3)	O(11)-U(1)-C(1)	26.5(3)	C(1)-O(9)-U(1)	95.2(6)
O(4)-U(1)-O(2)	90.1(3)	O(6)-U(1)-C(1)	152.4(3)	C(1)-O(11)-U(1)	94.2(6)
O(5)-U(1)-O(2)	89.4(3)	O(9)-U(1)-C(1)	25.3(3)	C(2)-O(13)-U(1)	93.3(6)
O(3)-U(1)-O(2)	176.5(2)	O(13)-U(1)-C(1)	155.8(3)	U(2)-O(14)-U(2)#1	111.1(3)
O(4)-U(1)-O(11)	84.0(3)	C(2)-U(1)-C(1)	178.0(3)	O(9)-C(1)-O(11)	118.8(9)
O(5)-U(1)-O(11)	96.0(3)	O(10)-U(2)-O(12)	179.0(4)	O(9)-C(1)-C(5)	122.5(9)
O(3)-U(1)-O(11)	66.1(2)	O(10)-U(2)-O(8)	88.4(4)	O(11)-C(1)-C(5)	118.6(9)
O(2)-U(1)-O(11)	114.7(2)	O(12)-U(2)-O(8)	91.3(4)	O(9)-C(1)-U(1)	59.5(5)
O(4)-U(1)-O(6)	96.8(3)	O(10)-U(2)-O(14)	90.9(4)	O(11)-C(1)-U(1)	59.4(5)
O(5)-U(1)-O(6)	83.2(3)	O(12)-U(2)-O(14)	89.9(4)	C(5)-C(1)-U(1)	177.8(7)
O(3)-U(1)-O(6)	114.8(3)	O(8)-U(2)-O(14)	76.7(3)	O(13)-C(2)-O(6)	121.6(9)
O(2)-U(1)-O(6)	64.4(2)	O(10)-U(2)-O(14)#1	88.5(4)	O(13)-C(2)-C(6)	120.6(9)
O(11)-U(1)-O(6)	178.8(2)	O(12)-U(2)-O(14)#1	92.3(4)	O(6)-C(2)-C(6)	117.8(9)
O(4)-U(1)-O(9)	96.0(3)	O(8)-U(2)-O(14)#1	145.3(3)	O(13)-C(2)-U(1)	60.9(5)
O(5)-U(1)-O(9)	83.5(3)	O(14)-U(2)-O(14)#1	68.9(3)	O(6)-C(2)-U(1)	60.6(5)
O(3)-U(1)-O(9)	115.3(2)	O(10)-U(2)-O(7)#2	86.3(4)	C(6)-C(2)-U(1)	178.4(8)
O(2)-U(1)-O(9)	64.6(2)	O(12)-U(2)-O(7)#2	93.3(4)	O(2)-C(3)-O(8)	124.2(10)
O(11)-U(1)-O(9)	51.7(2)	O(8)-U(2)-O(7)#2	138.6(3)	O(2)-C(3)-C(8)	121.1(9)
O(6)-U(1)-O(9)	127.1(2)	O(14)-U(2)-O(7)#2	144.4(3)	O(8)-C(3)-C(8)	114.4(9)
O(4)-U(1)-O(13)	84.8(3)	O(14)#1-U(2)-O(7)#2	75.6(3)	O(3)-C(4)-O(7)	122.8(10)
O(5)-U(1)-O(13)	95.6(3)	O(10)-U(2)-O(1)	90.6(5)	O(3)-C(4)-C(7)	122.9(10)
O(3)-U(1)-O(13)	65.6(2)	O(12)-U(2)-O(1)	88.4(4)	O(7)-C(4)-C(7)	114.2(9)
O(2)-U(1)-O(13)	114.5(2)	O(8)-U(2)-O(1)	69.7(3)	C(9)#4-C(5)-C(7)#5	119.5(9)
O(11)-U(1)-O(13)	129.4(2)	O(14)-U(2)-O(1)	146.3(3)	C(9)#4-C(5)-C(1)	119.1(9)
O(6)-U(1)-O(13)	51.7(3)	O(14)#1-U(2)-O(1)	144.9(3)	C(7)#5-C(5)-C(1)	121.3(9)
O(9)-U(1)-O(13)	178.7(2)	O(7)#2-U(2)-O(1)	69.3(3)	C(10)-C(6)-C(8)#6	120.1(9)
O(4)-U(1)-C(2)	90.9(3)	O(10)-U(2)-U(2)#1	89.6(3)	C(10)-C(6)-C(2)	119.5(9)
O(5)-U(1)-C(2)	89.3(3)	O(12)-U(2)-U(2)#1	91.4(3)	C(8)#6-C(6)-C(2)	120.4(9)
O(3)-U(1)-C(2)	90.1(3)	O(8)-U(2)-U(2)#1	111.1(2)	C(10)#4-C(7)-C(5)#6	119.2(9)
O(2)-U(1)-C(2)	89.5(3)	O(14)-U(2)-U(2)#1	34.5(2)	C(10)#4-C(7)-C(4)	117.5(9)
O(11)-U(1)-C(2)	155.1(3)	O(14)#1-U(2)-U(2)#1	34.3(2)	C(5)#6-C(7)-C(4)	123.2(9)
O(6)-U(1)-C(2)	26.0(3)	O(7)#2-U(2)-U(2)#1	109.9(2)	C(9)-C(8)-C(6)#5	119.3(9)
O(9)-U(1)-C(2)	153.1(3)	O(1)-U(2)-U(2)#1	179.1(2)	C(9)-C(8)-C(3)	117.2(9)
O(13)-U(1)-C(2)	25.7(3)	C(3)-O(2)-U(1)	135.3(7)	C(6)#5-C(8)-C(3)	123.5(9)
O(4)-U(1)-C(1)	90.6(3)	C(4)-O(3)-U(1)	135.4(7)	C(8)-C(9)-C(5)#7	121.0(10)

Table 0.18 Bond valence calculation for complex pyr5.

Atom	Atom bond	Bond length	Bond valence [vu]	Atom valence [vu]

U1	U(1)-O(4)	1,763	1,74	6,09
	U(1)-O(5)	1,767	1,73	
	U(1)-O(3)	2,432	0,48	
	U(1)-O(2)	2,450	0,46	
	U(1)-O(11)	2,498	0,42	
	U(1)-O(6)	2,501	0,42	
	U(1)-O(9)	2,504	0,42	
	U(1)-O(13)	2,509	0,41	
U2	U(2)-O(10)	1,767	1,73	6,52
	U(2)-O(12)	1,777	1,70	
	U(2)-O(8)	2,327	0,59	
	U(2)-O(14)	2,338	0,58	
	U(2)-O(14)#1	2,348	0,56	
	U(2)-O(7)	2,378	0,53	
	U(2)-O(1)	2,506	0,42	
O1	U(2)-O(1)	2,506	0,42	0,42
O2	U(1)-O(2)	2,450	0,46	1,79
	O(2)-C(3)	1,245	1,32	
O3	U(1)-O(3)	2,432	0,48	1,79
	O(3)-C(4)	1,248	1,31	
O4	U(1)-O(4)	1,763	1,74	1,74
O5	U(1)-O(5)	1,767	1,73	1,73
O6	U(1)-O(6)	2,501	0,42	1,71
	O(6)-C(2)	1,256	1,29	
O7	U(2)-O(7)	2,378	0,53	1,74
	O(7)-C(4)	1,293	1,21	
O8	U(2)-O(8)	2,327	0,59	1,85
	O(8)-C(3)	1,268	1,26	
O9	U(1)-O(9)	2,504	0,42	1,75
	O(9)-C(1)	1,242	1,33	
O10	U(2)-O(10)	1,767	1,73	1,73
O11	U(1)-O(11)	2,498	0,42	1,63
	O(11)-C(1)	1,293	1,21	
O12	U(2)-O(12)	1,777	1,70	1,70
O13	U(1)-O(13)	2,509	0,41	1,73
	O(13)-C(2)	1,247	1,32	
O14	O(14)-U(2)	2,338	0,58	1,14
	O(14)-U(2)#1	2,348	0,56	

Table 0.19 Atomic coordinates (x10⁴) and equivalent isotropic displacement parameters (A²x10³) for complex pyr5.

Atom	x	y	z	U(eq)
U(1)	5000	0	0	11(1)
U(2)	5788(1)	-4143(1)	-2610(1)	12(1)
O(1)	4014(8)	-3106(5)	-6041(3)	21(1)
O(2)	3114(8)	-3857(5)	-4354(4)	20(1)
O(3)	7145(7)	-2292(5)	-670(3)	19(1)
O(4)	8699(8)	-5687(6)	-1444(4)	20(1)
O(5)	8107(9)	-613(6)	1701(4)	25(1)
O(6)	2570(8)	-1705(6)	124(4)	21(1)
O(7)	3249(8)	-5236(6)	-2113(4)	22(1)
O(8)	8385(8)	-3150(6)	-3083(4)	24(1)
O(9)	5692(7)	1204(5)	2351(3)	19(1)
C(1)	3058(9)	-2857(6)	-5123(4)	13(1)
C(2)	7489(10)	339(6)	2592(4)	15(1)
C(3)	1623(9)	-1307(6)	-4976(4)	13(1)
C(4)	1241(9)	-294(7)	-3872(4)	14(1)
C(5)	374(10)	-976(7)	-6072(4)	16(1)

Table 0.20 Bond lengths for complex pyr5.

Bond	Bond lengths [Å]	Bond	Bond lengths [Å]
U(1)-O(6)	1.800(4)	U(2)-O(1)#2	2.384(3)

U(1)-O(6)#1	1.800(4)	U(2)-O(4)	2.450(4)
U(1)-O(3)	2.321(3)	U(2)-O(9)#1	2.470(4)
U(1)-O(3)#1	2.321(3)	O(1)-C(1)	1.243(6)
U(1)-O(5)	2.493(4)	O(1)-U(2)#2	2.384(3)
U(1)-O(5)#1	2.493(4)	O(2)-C(1)	1.262(6)
U(1)-O(9)#1	2.589(3)	O(5)-C(2)	1.255(6)
U(1)-O(9)	2.589(3)	O(9)-C(2)	1.275(6)
U(1)-C(2)	2.956(5)	O(9)-U(2)#1	2.470(4)
U(1)-C(2)#1	2.956(5)	C(1)-C(3)	1.505(6)
U(1)-U(2)	4.0313(2)	C(2)-C(4)#1	1.499(6)
U(1)-U(2)#1	4.0313(2)	C(3)-C(5)	1.389(7)
U(2)-O(8)	1.759(4)	C(3)-C(4)	1.407(7)
U(2)-O(7)	1.779(4)	C(4)-C(5)#3	1.400(7)
U(2)-O(2)	2.305(4)	C(4)-C(2)#1	1.499(6)
U(2)-O(3)	2.317(4)	C(5)-C(4)#3	1.400(7)

Table 0.21 Bond Angles for complex pyr5.

Bond	Angle [°]	Bond	Angle [°]	Bond	Angle [°]
O(6)-U(1)-O(6)#1	180.0(3)	O(3)#1-U(1)-C(2)#1	91.94(13)	O(2)-U(2)-O(4)	153.62(14)
O(6)-U(1)-O(3)	88.10(17)	O(5)-U(1)-C(2)#1	155.19(14)	O(3)-U(2)-O(4)	73.86(13)
O(6)#1-U(1)-O(3)	91.90(17)	O(5)#1-U(1)-C(2)#1	24.81(14)	O(1)#2-U(2)-O(4)	73.32(13)
O(6)-U(1)-O(3)#1	91.90(17)	O(9)#1-U(1)-C(2)#1	25.51(12)	O(8)-U(2)-O(9)#1	88.76(17)
O(6)#1-U(1)-O(3)#1	88.10(17)	O(9)-U(1)-C(2)#1	154.49(12)	O(7)-U(2)-O(9)#1	93.99(17)
O(3)-U(1)-O(3)#1	180.00(15)	C(2)-U(1)-C(2)#1	180.00(8)	O(2)-U(2)-O(9)#1	67.75(12)
O(6)-U(1)-O(5)	94.06(19)	O(6)-U(1)-U(2)	79.50(14)	O(3)-U(2)-O(9)#1	64.85(11)
O(6)#1-U(1)-O(5)	85.94(19)	O(6)#1-U(1)-U(2)	100.50(14)	O(1)#2-U(2)-O(9)#1	147.78(12)
O(3)-U(1)-O(5)	67.42(13)	O(3)-U(1)-U(2)	29.60(9)	O(4)-U(2)-O(9)#1	138.41(13)
O(3)#1-U(1)-O(5)	112.58(13)	O(3)#1-U(1)-U(2)	150.40(9)	O(8)-U(2)-U(1)	99.91(14)
O(6)-U(1)-O(5)#1	85.94(19)	O(5)-U(1)-U(2)	96.36(10)	O(7)-U(2)-U(1)	81.69(14)
O(6)#1-U(1)-O(5)#1	94.06(19)	O(5)#1-U(1)-U(2)	83.64(10)	O(2)-U(2)-U(1)	103.85(10)
O(3)-U(1)-O(5)#1	112.58(13)	O(9)#1-U(1)-U(2)	36.17(8)	O(3)-U(2)-U(1)	29.67(9)
O(3)#1-U(1)-O(5)#1	67.42(13)	O(9)-U(1)-U(2)	143.83(8)	O(1)#2-U(2)-U(1)	170.82(9)
O(5)-U(1)-O(5)#1	180.00(14)	C(2)-U(1)-U(2)	120.13(9)	O(4)-U(2)-U(1)	102.38(10)
O(6)-U(1)-O(9)#1	91.66(17)	C(2)#1-U(1)-U(2)	59.87(9)	O(9)#1-U(2)-U(1)	38.20(8)
O(6)#1-U(1)-O(9)#1	88.34(17)	O(6)-U(1)-U(2)#1	100.50(14)	C(1)-O(1)-U(2)#2	129.5(3)
O(3)-U(1)-O(9)#1	62.85(11)	O(6)#1-U(1)-U(2)#1	79.50(14)	C(1)-O(2)-U(2)	137.6(4)
O(3)#1-U(1)-O(9)#1	117.15(11)	O(3)-U(1)-U(2)#1	150.40(9)	U(2)-O(3)-U(1)	120.73(15)
O(5)-U(1)-O(9)#1	129.67(12)	O(3)#1-U(1)-U(2)#1	29.60(9)	C(2)-O(5)-U(1)	98.7(3)
O(5)#1-U(1)-O(9)#1	50.33(12)	O(5)-U(1)-U(2)#1	83.64(10)	C(2)-O(9)-U(2)#1	147.2(3)
O(6)-U(1)-O(9)	88.34(17)	O(5)#1-U(1)-U(2)#1	96.36(10)	C(2)-O(9)-U(1)	93.5(3)
O(6)#1-U(1)-O(9)	91.66(17)	O(9)#1-U(1)-U(2)#1	143.83(8)	U(2)#1-O(9)-U(1)	105.63(12)
O(3)-U(1)-O(9)	117.15(11)	O(9)-U(1)-U(2)#1	36.17(8)	O(1)-C(1)-O(2)	124.6(4)
O(3)#1-U(1)-O(9)	62.85(11)	C(2)-U(1)-U(2)#1	59.87(9)	O(1)-C(1)-C(3)	116.7(4)
O(5)-U(1)-O(9)	50.33(12)	C(2)#1-U(1)-U(2)#1	120.13(9)	O(2)-C(1)-C(3)	118.7(4)
O(5)#1-U(1)-O(9)	129.67(12)	U(2)-U(1)-U(2)#1	180.000(7)	O(5)-C(2)-O(9)	117.4(4)
O(9)#1-U(1)-O(9)	180.0(3)	O(8)-U(2)-O(7)	177.07(17)	O(5)-C(2)-C(4)#1	118.7(4)
O(6)-U(1)-C(2)	91.31(17)	O(8)-U(2)-O(2)	91.75(18)	O(9)-C(2)-C(4)#1	123.8(4)
O(6)#1-U(1)-C(2)	88.69(17)	O(7)-U(2)-O(2)	90.24(18)	O(5)-C(2)-U(1)	56.5(3)
O(3)-U(1)-C(2)	91.94(13)	O(8)-U(2)-O(3)	90.09(18)	O(9)-C(2)-U(1)	61.0(2)
O(3)#1-U(1)-C(2)	88.06(13)	O(7)-U(2)-O(3)	90.15(18)	C(4)#1-C(2)-U(1)	173.7(3)
O(5)-U(1)-C(2)	24.81(14)	O(2)-U(2)-O(3)	132.50(13)	C(5)-C(3)-C(4)	117.7(4)
O(5)#1-U(1)-C(2)	155.19(14)	O(8)-U(2)-O(1)#2	88.03(17)	C(5)-C(3)-C(1)	114.8(4)
O(9)#1-U(1)-C(2)	154.49(12)	O(7)-U(2)-O(1)#2	90.19(17)	C(4)-C(3)-C(1)	127.3(4)
O(9)-U(1)-C(2)	25.51(12)	O(2)-U(2)-O(1)#2	80.31(13)	C(5)#3-C(4)-C(3)	118.9(4)
O(6)-U(1)-C(2)#1	88.69(17)	O(3)-U(2)-O(1)#2	147.18(12)	C(5)#3-C(4)-C(2)#1	114.3(4)
O(6)#1-U(1)-C(2)#1	91.31(17)	O(8)-U(2)-O(4)	86.46(17)	C(3)-C(4)-C(2)#1	126.8(4)
O(3)-U(1)-C(2)#1	88.06(13)	O(7)-U(2)-O(4)	90.80(16)	C(3)-C(5)-C(4)#3	123.5(4)

Table 0.22 Bond valence calculation for complex pyr5.

Atom	Atom bond	Bond length	Bond valence [vu]	Atom valence [vu]
U1	U(1)-O(6)	1,800	1,62	6,00
	U(1)-O(6)#1	1,800	1,62	

	U(1)-O(3)	2,321	0,59	
	U(1)-O(3)#1	2,321	0,59	
	U(1)-O(5)	2,493	0,43	
	U(1)-O(5)#1	2,493	0,43	
	U(1)-O(9)	2,589	0,35	
	U(1)-O(9)#2	2,589	0,35	
U2	U(2)-O(8)	1,759	1,76	6,09
	U(2)-O(7)	1,779	1,69	
	U(2)-O(2)	2,305	0,61	
	U(2)-O(3)	2,317	0,60	
	U(2)-O(1)	2,384	0,53	
	U(2)-O(4)	2,450	0,46	
	U(2)-O(9)	2,470	0,45	
O1	U(2)-O(1)	2,384	0,53	1,85
	O(1)-C(1)	1,243	1,33	
O2	U(2)-O(2)	2,305	0,61	1,89
	O(2)-C(1)	1,262	1,28	
O3	U(1)-O(3)	2,321	0,59	1,19
	U(2)-O(2)	2,317	0,60	
O4	U(2)-O(4)	2,450	0,46	0,46
O5	U(1)-O(5)	2,493	0,43	1,72
	O(5)-C(2)	1,255	1,30	
O6	U(1)-O(6)	1,800	1,62	1,62
O7	U(2)-O(7)	1,779	1,69	1,69
O8	U(2)-O(8)	1,759	1,76	1,76
O9	U(2)-O(9)	2,470	0,45	2,05
	U(1)-O(9)	2,589	0,35	
	O(9)-C(2)	1,275	1,25	

Table 0.23 Atomic coordinates ($x10^4$) and equivalent isotropic displacement parameters (A^2x10^3) for complex pyr6.

Atom	x	y	z	U(eq)
U(1)	5020(1)	198(1)	3472(1)	18(1)
U(2)	2228(1)	197(1)	3915(1)	18(1)
O(1)	1557(7)	51(7)	1611(7)	48(3)
O(2)	375(5)	121(6)	3078(6)	30(2)
O(3)	2172(6)	1407(5)	3885(7)	35(2)
O(4)	2212(6)	-998(7)	3929(7)	39(2)
O(5)	5264(6)	1389(5)	3783(7)	33(2)
O(6)	4765(6)	-968(6)	3061(8)	40(2)
O(7)	1449(5)	299(6)	5572(6)	31(2)
O(8)	4870(5)	518(6)	1421(6)	28(2)
O(9)	3967(5)	134(6)	4593(7)	37(2)
O(10)	6863(6)	-28(6)	3699(7)	33(2)
O(11)	3175(5)	522(6)	2270(6)	35(2)
O(12)	-571(6)	1278(6)	3365(8)	43(2)
O(13)	4241(6)	1902(6)	707(8)	41(2)
C(1)	2359(8)	273(8)	1413(9)	23(2)
C(2)	7715(8)	-165(8)	3530(9)	22(2)
C(3)	-469(8)	555(8)	2905(9)	24(2)
C(4)	4178(8)	1070(8)	758(9)	22(2)
C(5)	-1423(7)	121(7)	1979(8)	13(2)
C(6)	-2283(7)	-206(7)	2264(8)	18(2)
C(7)	2348(8)	259(7)	122(8)	18(2)
C(8)	3197(7)	618(7)	-161(8)	17(2)
C(9)	3143(8)	587(7)	-1356(9)	19(2)
C(10)	-1461(8)	79(8)	799(9)	21(2)
N(1)	557(8)	2242(7)	5334(9)	35(2)
N(2)	6249(8)	2525(7)	1070(9)	38(3)
OW	2740(8)	2663(7)	1726(9)	61(3)
C(11)	3046(12)	-2613(10)	2657(13)	55(4)
C(12)	6431(12)	3132(11)	5231(14)	58(4)
C(13)	289(13)	3101(11)	4643(15)	68(5)

Atom	x	y	z	U(eq)
C(14)	27(13)	2134(12)	6211(15)	74(5)

Table 0.24 Bond lengths for complex pyr6.

Bond	Bond lengths [Å]	Bond	Bond lengths [Å]
U(1)-O(6)	1.770(9)	O(10)-C(2)	1.256(12)
U(1)-O(5)	1.783(8)	O(10)-U(2)#1	2.653(7)
U(1)-O(9)#1	2.260(7)	O(11)-C(1)	1.258(12)
U(1)-O(9)	2.264(8)	O(12)-C(3)	1.217(14)
U(1)-O(8)	2.399(7)	O(13)-C(4)	1.220(13)
U(1)-O(10)	2.439(7)	C(1)-C(7)	1.517(13)
U(1)-O(11)	2.445(7)	C(2)-O(7)#1	1.263(12)
U(1)-U(1)#1	3.6673(7)	C(2)-C(6)#2	1.493(13)
U(1)-U(2)#1	3.9504(5)	C(2)-U(2)#1	2.986(10)
U(1)-U(2)	3.9986(5)	C(3)-C(5)	1.505(13)
U(2)-O(4)	1.745(10)	C(4)-C(8)	1.535(13)
U(2)-O(3)	1.768(8)	C(5)-C(10)	1.375(13)
U(2)-O(9)	2.207(7)	C(5)-C(6)	1.407(14)
U(2)-O(2)	2.354(7)	C(6)-C(9)#3	1.390(13)
U(2)-O(7)	2.532(7)	C(6)-C(2)#4	1.493(13)
U(2)-O(1)	2.549(8)	C(7)-C(10)#3	1.395(14)
U(2)-O(10)#1	2.653(7)	C(7)-C(8)	1.408(14)
U(2)-O(11)	2.719(8)	C(8)-C(9)	1.385(13)
U(2)-C(2)#1	2.986(10)	C(9)-C(6)#3	1.390(13)
U(2)-C(1)	3.018(10)	C(10)-C(7)#3	1.395(14)
U(2)-U(1)#1	3.9504(5)	N(1)-C(14)	1.461(18)
O(1)-C(1)	1.234(13)	N(1)-C(13)	1.468(18)
O(2)-C(3)	1.260(13)	N(2)-C(12)#5	1.461(17)
O(7)-C(2)#1	1.263(12)	N(2)-C(11)#6	1.480(16)
O(8)-C(4)	1.274(13)	C(11)-N(2)#7	1.480(16)
O(9)-U(1)#1	2.260(7)	C(12)-N(2)#8	1.461(17)

Table 0.25 Bond Angles for complex pyr6.

Bond	Angle [°]	Bond	Angle [°]	Bond	Angle [°]
O(6)-U(1)-O(5)	176.2(4)	O(9)-U(2)-O(7)	114.0(2)	O(10)#1-U(2)-U(1)	91.86(15)
O(6)-U(1)-O(9)#1	93.4(4)	O(2)-U(2)-O(7)	69.6(2)	O(11)-U(2)-U(1)	36.83(14)
O(5)-U(1)-O(9)#1	90.0(3)	O(4)-U(2)-O(1)	85.7(3)	C(2)#1-U(2)-U(1)	116.4(2)
O(6)-U(1)-O(9)	91.0(3)	O(3)-U(2)-O(1)	93.8(3)	C(1)-U(2)-U(1)	59.1(2)
O(5)-U(1)-O(9)	91.7(3)	O(9)-U(2)-O(1)	108.4(3)	U(1)#1-U(2)-U(1)	54.946(10)
O(9)#1-U(1)-O(9)	71.7(3)	O(2)-U(2)-O(1)	67.9(3)	C(1)-O(1)-U(2)	100.0(6)
O(6)-U(1)-O(8)	88.4(3)	O(7)-U(2)-O(1)	137.5(2)	C(3)-O(2)-U(2)	144.8(8)
O(5)-U(1)-O(8)	87.8(3)	O(4)-U(2)-O(10)	84.2(3)	C(2)#1-O(7)-U(2)	98.2(6)
O(9)#1-U(1)-O(8)	149.7(2)	O(3)-U(2)-O(10)	96.6(3)	C(4)-O(8)-U(1)	121.6(6)
O(9)-U(1)-O(8)	138.6(2)	O(9)-U(2)-O(10)	64.9(2)	U(2)-O(9)-U(1)#1	124.4(3)
O(6)-U(1)-O(10)	89.6(3)	O(2)-U(2)-O(10)	117.8(2)	U(2)-O(9)-U(1)	126.9(3)
O(5)-U(1)-O(10)	90.1(3)	O(7)-U(2)-O(10)	49.6(2)	U(1)#1-O(9)-U(1)	108.3(3)
O(9)#1-U(1)-O(10)	68.1(3)	O(1)-U(2)-O(10)	168.1(3)	C(2)-O(10)-U(1)	165.5(7)
O(9)-U(1)-O(10)	139.7(2)	O(4)-U(2)-O(11)	101.1(3)	C(2)-O(10)-U(2)#1	92.6(6)
O(8)-U(1)-O(10)	81.7(2)	O(3)-U(2)-O(11)	80.7(3)	U(1)-O(10)-U(2)#1	101.7(3)
O(6)-U(1)-O(11)	88.1(3)	O(9)-U(2)-O(11)	63.4(2)	C(1)-O(11)-U(1)	146.8(8)
O(5)-U(1)-O(11)	90.5(3)	O(2)-U(2)-O(11)	114.3(2)	C(1)-O(11)-U(2)	91.1(6)
O(9)#1-U(1)-O(11)	139.3(3)	O(7)-U(2)-O(11)	166.1(3)	U(1)-O(11)-U(2)	101.4(2)
O(9)-U(1)-O(11)	67.6(2)	O(1)-U(2)-O(11)	48.4(2)	O(1)-C(1)-O(11)	120.5(10)
O(8)-U(1)-O(11)	71.0(2)	O(10)-U(2)-O(11)	127.8(2)	O(1)-C(1)-C(7)	119.3(9)
O(10)-U(1)-O(11)	152.6(3)	O(4)-U(2)-C(2)#1	88.3(3)	O(11)-C(1)-C(7)	120.2(9)
O(6)-U(1)-U(1)#1	92.7(3)	O(3)-U(2)-C(2)#1	91.2(3)	O(1)-C(1)-U(2)	56.3(5)
O(5)-U(1)-U(1)#1	91.0(2)	O(9)-U(2)-C(2)#1	89.5(3)	O(11)-C(1)-U(2)	64.2(6)
O(9)#1-U(1)-U(1)#1	35.88(19)	O(2)-U(2)-C(2)#1	93.7(3)	C(7)-C(1)-U(2)	175.3(7)
O(9)-U(1)-U(1)#1	35.80(17)	O(7)-U(2)-C(2)#1	24.7(3)	O(10)-C(2)-O(7)#1	119.6(9)
O(8)-U(1)-U(1)#1	174.26(17)	O(1)-U(2)-C(2)#1	160.9(3)	O(10)-C(2)-C(6)#2	119.5(9)
O(10)-U(1)-U(1)#1	103.95(18)	O(10)#1-U(2)-C(2)	24.9(3)	O(7)#1-C(2)-C(6)#2	120.9(9)
O(11)-U(1)-U(1)#1	103.43(18)	O(11)-U(2)-C(2)#1	150.7(2)	O(10)-C(2)-U(2)#1	62.5(5)

Bond	Angle [°]	Bond	Angle [°]	Bond	Angle [°]
O(6)-U(1)-U(2)#1	96.4(3)	O(4)-U(2)-C(1)	92.9(3)	O(7)#1-C(2)-U(2)#1	57.1(5)
O(5)-U(1)-U(2)#1	85.8(2)	O(3)-U(2)-C(1)	87.8(3)	C(6)#2-C(2)-U(2)#1	176.5(8)
O(9)#1-U(1)-U(2)#1	27.45(19)	O(9)-U(2)-C(1)	86.0(3)	O(12)-C(3)-O(2)	127.2(10)
O(9)-U(1)-U(2)#1	98.93(17)	O(2)-U(2)-C(1)	90.9(3)	O(12)-C(3)-C(5)	119.0(10)
O(8)-U(1)-U(2)#1	122.26(16)	O(7)-U(2)-C(1)	159.4(3)	O(2)-C(3)-C(5)	113.8(10)
O(10)-U(1)-U(2)#1	41.12(17)	O(1)-U(2)-C(1)	23.8(3)	O(13)-C(4)-O(8)	127.7(10)
O(11)-U(1)-U(2)#1	165.98(17)	O(10)#1-U(2)-C(1)	150.8(3)	O(13)-C(4)-C(8)	116.9(9)
U(1)#1-U(1)-U(2)#1	63.195(11)	O(11)-U(2)-C(1)	24.6(2)	O(8)-C(4)-C(8)	115.2(10)
O(6)-U(1)-U(2)	86.2(3)	C(2)#1-U(2)-C(1)	175.3(3)	C(10)-C(5)-C(6)	119.3(8)
O(5)-U(1)-U(2)	95.1(3)	O(4)-U(2)-U(1)#1	81.8(2)	C(10)-C(5)-C(3)	117.9(9)
O(9)#1-U(1)-U(2)	97.68(19)	O(3)-U(2)-U(1)#1	100.6(3)	C(6)-C(5)-C(3)	122.8(8)
O(9)-U(1)-U(2)	26.20(17)	O(9)-U(2)-U(1)#1	28.18(19)	C(9)#3-C(6)-C(5)	119.5(9)
O(8)-U(1)-U(2)	112.66(16)	O(2)-U(2)-U(1)#1	153.27(18)	C(9)#3-C(6)-C(2)#4	119.2(9)
O(10)-U(1)-U(2)	164.90(18)	O(7)-U(2)-U(1)#1	86.78(16)	C(5)-C(6)-C(2)#4	121.3(8)
O(11)-U(1)-U(2)	41.80(18)	O(1)-U(2)-U(1)#1	134.5(2)	C(10)#3-C(7)-C(8)	119.9(9)
U(1)#1-U(1)-U(2)	61.8(1)	O(10)#1-U(2)-U(1)	37.21(15)	C(10)#3-C(7)-C(1)	119.1(9)
U(2)#1-U(1)-U(2)	125.05(1)	O(11)-U(2)-U(1)#1	91.59(14)	C(8)-C(7)-C(1)	120.9(9)
O(4)-U(2)-O(3)	177.0(3)	C(2)#1-U(2)-U(1)	62.0(2)	C(9)-C(8)-C(7)	118.4(9)
O(4)-U(2)-O(9)	88.3(3)	C(1)-U(2)-U(1)#1	113.7(2)	C(9)-C(8)-C(4)	116.9(9)
O(3)-U(2)-O(9)	94.7(4)	O(4)-U(2)-U(1)	91.0(2)	C(7)-C(8)-C(4)	124.7(9)
O(4)-U(2)-O(2)	86.7(3)	O(3)-U(2)-U(1)	91.9(3)	C(8)-C(9)-C(6)#3	121.6(9)
O(3)-U(2)-O(2)	90.4(3)	O(9)-U(2)-U(1)	26.94(19)	C(5)-C(10)-C(7)#3	121.1(9)
O(9)-U(2)-O(2)	174.0(3)	O(2)-U(2)-U(1)	149.77(17)	C(14)-N(1)-C(13)	113.4(12)
O(4)-U(2)-O(7)	92.4(3)	O(7)-U(2)-U(1)	140.62(16)	C(12)#5-N(2)-C(11)#6	113.2(11)
O(3)-U(2)-O(7)	86.0(3)	O(1)-U(2)-U(1)	81.87(19)		

Table 0.26 Bond valence calculation for complex pyr6.

Atom	Atom bond	Bond length	Bond valence [vu]	Atom valence [vu]
U1	U(1)-O(6)	1,770	1,72	6,18
	U(1)-O(5)	1,783	1,68	
	U(1)-O(9)	2,260	0,67	
	U(1)-O(9)#1	2,264	0,66	
	U(1)-O(8)	2,399	0,51	
	U(1)-O(10)	2,439	0,47	
	U(1)-O(11)	2,445	0,47	
U2	U(2)-O(4)	1,745	1,80	6,19
	U(2)-O(3)	1,768	1,73	
	U(2)-O(9)	2,207	0,74	
	U(2)-O(2)	2,354	0,56	
	U(2)-O(7)	2,532	0,40	
	U(2)-O(1)	2,549	0,38	
	U(2)-O(10)	2,653	0,31	
	U(2)-O(11)	2,719	0,28	
O1	U(2)-O(1)	2,549	0,38	1,73
	O(1)-C(1)	1,234	1,35	
O2	U(2)-O(2)	2,354	0,56	1,84
	O(2)-C(3)	1,260	1,28	
O3	U(2)-O(3)	1,768	1,73	1,73
O4	U(2)-O(4)	1,745	1,80	1,80
O5	U(1)-O(5)	1,783	1,68	1,68
O6	U(1)-O(6)	1,770	1,72	1,72
O7	U(2)-O(7)	2,532	0,40	1,67
	O(7)-C(2)	1,263	1,28	
O8	U(1)-O(8)	2,399	0,51	1,76
	O(8)-C(4)	1,274	1,25	
O9	U(1)-O(9)	2,260	0,67	2,07
	U(1)-O(9)#1	2,264	0,66	
	U(2)-O(9)	2,207	0,74	
O10	U(1)-O(10)	2,439	0,47	2,08
	U(2)-O(10)	2,653	0,31	
	O(10)-C(2)	1,256	1,29	

Atom	Atom bond	Bond length	Bond valence [vu]	Atom valence [vu]
O11	U(1)-O(11)	2,445	0,47	2,03
	U(2)-O(11)	2,719	0,28	
	O(11)-C(1)	1,258	1,29	
O12	O(12)-C(3)	1,217	1,40	1,40
O13	O(13)-C(4)	1,220	1,39	1,39

Table 0.27 Atomic coordinates (x10⁴) and equivalent isotropic displacement parameters (A²x10³) for complex pyr7.

Atom	x	y	z	U(eq)
U(1)	3524(1)	2005(1)	1916(1)	15(1)
U(2)	120(1)	1935(1)	1929(1)	15(1)
U(3)	1685(1)	3146(1)	3043(1)	14(1)
O(1h)	1801(4)	1935(3)	2346(2)	16(1)
O(81b)	812(5)	-1546(4)	1081(2)	19(1)
O(71a)	5698(5)	772(3)	1426(2)	19(1)
O(71b)	1081(5)	866(4)	1391(3)	23(1)
O(82b)	2209(5)	-900(3)	1437(2)	21(1)
O(1)	5119(4)	2209(4)	2263(3)	18(1)
O(11u)	3428(5)	3136(4)	1694(3)	22(1)
O(12u)	3594(5)	877(4)	2125(3)	23(1)
O(21u)	483(5)	2882(4)	1524(3)	25(1)
O(31u)	1798(5)	3907(4)	2463(2)	21(1)
O(22u)	-263(5)	983(4)	2336(3)	23(1)
O(72b)	2459(5)	1628(4)	1123(3)	22(1)
O(72a)	4532(5)	1712(4)	1084(3)	21(1)
O(2h)	3429(4)	2493(4)	2909(2)	16(1)
O(32u)	1615(5)	2388(4)	3629(3)	23(1)
C(7b)	1808(7)	996(5)	1057(4)	17(2)
C(6b)	1968(9)	925(7)	0	15(2)
C(7a)	5081(7)	998(5)	1056(4)	17(2)
C(1a)	4990(6)	480(5)	519(4)	15(2)
C(1b)	1843(6)	463(5)	514(3)	15(2)
C(3b)	1532(8)	-913(7)	0	13(2)
C(2b)	1630(6)	-454(5)	517(3)	16(2)
C(8b)	1527(7)	-975(5)	1053(4)	16(2)
C(3a)	4998(8)	949(7)	0	14(2)
O(1w)	1970(20)	3756(19)	692(12)	129(10)
O(2w)	5090(20)	3630(18)	679(12)	130(11)
O(3w)	0	5000	2072(7)	74(5)
O(4w)	1688(6)	269(5)	2824(4)	39(2)
N(1)	3479(8)	986(6)	3582(4)	48(3)

Table 0.28 Bond lengths for complex pyr7.

Bond	Bond lengths [Å]	Bond	Bond lengths [Å]
U(1)-O(1h)	2.490(6)	O(1)-O(12u)	2.840(8)
U(1)-O(1)	2.276(6)	O(1)-O(21u)#6	2.884(9)
U(1)-O(11u)	1.763(6)	O(1)-O(31u)#6	2.841(8)
U(1)-O(12u)	1.748(6)	O(1)-O(22u)#6	2.890(8)
U(1)-O(72b)	2.394(6)	O(1)-O(72a)	2.960(9)
U(1)-O(72a)	2.399(6)	O(1)-O(2h)	2.728(8)
U(1)-O(2h)	2.439(6)	O(1)-O(32u)#6	2.935(9)
U(2)-O(1h)	2.423(6)	O(11u)-O(72b)	2.905(8)
U(2)-O(81b)#1	2.406(6)	O(11u)-O(72a)	2.940(8)
U(2)-O(71b)	2.390(6)	O(12u)-O(72b)	2.997(9)
U(2)-O(1)#2	2.279(6)	O(12u)-O(3w)#4	2.946(12)
U(2)-O(21u)	1.762(6)	O(31u)-O(4w)#3	2.922(10)
U(2)-O(22u)	1.778(6)	O(22u)-O(2h)#2	2.904(8)
U(2)-O(2h)#2	2.418(6)	O(22u)-O(4w)#1	2.881(10)
U(3)-O(1h)	2.432(5)	O(72b)-O(72a)	2.741(9)
U(3)-O(71a)#2	2.414(6)	O(72b)-C(7b)	1.281(10)
U(3)-O(82b)#3	2.370(6)	O(72b)-C(6b)	2.902(7)

Bond	Bond lengths [Å]	Bond	Bond lengths [Å]
U(3)-O(1)#2	2.251(6)	O(72b)-C(1b)	2.384(10)
U(3)-O(31u)	1.774(6)	O(72a)-C(7a)	1.285(10)
U(3)-O(2h)	2.516(6)	O(72a)-C(1a)	2.337(10)
U(3)-O(32u)	1.776(6)	O(72a)-C(3a)	2.846(8)
O(1h)-O(71b)	2.902(8)	O(2h)-O(32u)	2.931(8)
O(1h)-O(1)#2	2.717(8)	O(2h)-N(1)	2.739(11)
O(1h)-O(12u)	2.888(8)	O(32u)-O(2w)#2	2.99(3)
O(1h)-O(21u)	2.950(8)	C(7b)-C(6b)	2.486(9)
O(1h)-O(31u)	2.941(8)	C(7b)-C(1b)	1.498(11)
O(1h)-O(2h)	2.653(8)	C(7b)-C(2b)	2.508(11)
O(1h)-O(4w)	2.720(9)	C(7b)-C(8b)	2.951(11)
O(81b)-O(71b)#1	2.792(9)	C(6b)-C(1b)	1.395(9)
O(81b)-O(82b)	2.239(9)	C(6b)-C(1b)#7	1.395(9)
O(81b)-O(21u)#1	2.816(8)	C(6b)-C(3b)	2.789(14)
O(81b)-O(2h)#4	2.937(8)	C(6b)-C(2b)	2.420(12)
O(81b)-C(3b)	2.862(8)	C(6b)-C(2b)#7	2.420(12)
O(81b)-C(2b)	2.354(10)	C(7a)-C(7a)#5	2.972(11)
O(81b)-C(8b)	1.270(10)	C(7a)-C(1a)	1.479(12)
O(71a)-O(71a)#5	2.940(8)	C(7a)-C(1a)#5	2.530(11)
O(71a)-O(82b)#5	2.769(9)	C(7a)-C(3a)	2.475(9)
O(71a)-O(1)	2.996(8)	C(1a)-C(1a)#5	1.425(11)
O(71a)-O(72a)	2.226(8)	C(1a)-C(1a)#8	2.816(11)
O(71a)-O(32u)#6	2.993(8)	C(1a)-C(1a)#7	2.429(12)
O(71a)-C(7a)	1.235(10)	C(1a)-C(3a)	1.400(10)
O(71a)-C(7a)#5	2.952(10)	C(1a)-C(3a)#5	2.444(12)
O(71a)-C(1a)	2.359(10)	C(1b)-C(1b)#7	2.407(11)
O(71a)-C(1a)#5	2.963(10)	C(1b)-C(3b)	2.407(12)
O(71b)-O(22u)	2.840(9)	C(1b)-C(2b)	1.390(11)
O(71b)-O(72b)	2.231(9)	C(1b)-C(2b)#7	2.785(11)
O(71b)-C(7b)	1.252(11)	C(1b)-C(8b)	2.515(11)
O(71b)-C(1b)	2.363(10)	C(3b)-C(2b)	1.395(10)
O(71b)-C(2b)	2.925(10)	C(3b)-C(2b)#7	1.395(10)
O(71b)-C(8b)	2.908(10)	C(3b)-C(8b)	2.466(8)
O(82b)-O(31u)#4	2.904(8)	C(3b)-C(8b)#7	2.466(8)
O(82b)-O(2h)#4	2.957(8)	C(2b)-C(2b)#7	2.421(12)
O(82b)-O(32u)#4	2.983(8)	C(2b)-C(8b)	1.480(11)
O(82b)-C(1b)	2.999(10)	C(3a)-C(3a)#5	2.817(15)
O(82b)-C(2b)	2.379(10)	O(3w)-N(1)#3	2.918(13)
O(82b)-C(8b)	1.277(10)	O(3w)-N(1)#2	2.918(13)
O(1)-O(11u)	2.941(9)		

Table 0.29 Bond Angles for complex pyr7.

Bond	Angle [°]	Bond	Angle [°]	Bond	Angle [°]
O(1h)-U(1)-O(1)	134.9(2)	O(71b)-U(2)-O(2h)#2	143.7(2)	U(1)-O(1h)-O(2h)	56.50(17)
O(1h)-U(1)-O(11u)	95.3(2)	O(1)#2-U(2)-O(21u)	90.1(2)	U(2)-O(1h)-U(3)	102.3(2)
O(1h)-U(1)-O(12u)	84.0(2)	O(1)#2-U(2)-O(22u)	90.0(2)	U(2)-O(1h)-O(71b)	52.41(17)
O(1h)-U(1)-O(72b)	76.6(2)	O(1)#2-U(2)-O(2h)#2	70.9(2)	U(2)-O(1h)-O(1)#2	52.27(17)
O(1h)-U(1)-O(72a)	145.9(2)	O(21u)-U(2)-O(22u)	179.3(3)	U(2)-O(1h)-O(12u)	132.7(2)
O(1h)-U(1)-O(2h)	65.13(19)	O(21u)-U(2)-O(2h)#2	93.2(3)	U(2)-O(1h)-O(21u)	36.66(15)
O(1)-U(1)-O(11u)	92.6(2)	O(22u)-U(2)-O(2h)#2	86.2(2)	U(2)-O(1h)-O(31u)	92.1(2)
O(1)-U(1)-O(12u)	88.8(3)	O(1h)-U(3)-O(71a)#2	150.6(2)	U(2)-O(1h)-O(2h)	160.3(3)
O(1)-U(1)-O(72b)	148.3(2)	O(1h)-U(3)-O(82b)#3	138.4(2)	U(3)-O(1h)-O(71b)	154.2(3)
O(1)-U(1)-O(72a)	78.5(2)	O(1h)-U(3)-O(1)#2	70.8(2)	U(3)-O(1h)-O(1)#2	51.48(16)
O(1)-U(1)-O(2h)	70.6(2)	O(1h)-U(3)-O(31u)	87.3(2)	U(3)-O(1h)-O(12u)	125.0(3)
O(11u)-U(1)-O(12u)	178.6(3)	O(1h)-U(3)-O(2h)	64.82(19)	U(3)-O(1h)-O(21u)	92.8(2)
O(11u)-U(1)-O(72b)	87.3(2)	O(1h)-U(3)-O(32u)	93.0(2)	U(3)-O(1h)-O(31u)	37.05(13)
O(11u)-U(1)-O(72a)	88.5(2)	O(71a)-U(3)-O(82b)	70.7(2)	U(3)-O(1h)-O(2h)	59.12(17)
O(11u)-U(1)-O(2h)	89.6(2)	O(71a)-U(3)-O(1)	79.8(2)	O(71b)-O(1h)-O(1)#2	104.4(3)
O(12u)-U(1)-O(72b)	91.4(2)	O(71a)-U(3)-O(31u)	90.9(2)	O(71b)-O(1h)-O(12u)	80.3(2)
O(12u)-U(1)-O(72a)	91.4(2)	O(71a)#2-U(3)-O(2h)	144.52(19)	O(71b)-O(1h)-O(21u)	64.2(2)
O(12u)-U(1)-O(2h)	91.2(2)	O(71a)-U(3)-O(32u)	89.8(2)	O(71b)-O(1h)-O(31u)	128.0(3)
O(72b)-U(1)-O(72a)	69.8(2)	O(82b)-U(3)-O(1)#2	150.3(2)	O(71b)-O(1h)-O(2h)	144.9(3)

Bond	Angle [°]	Bond	Angle [°]	Bond	Angle [°]
O(72b)-U(1)-O(2h)	141.1(2)	O(82b)-U(3)-O(31u)	87.7(2)	O(1)#2-O(1h)-O(12u)	169.9(3)
O(72a)-U(1)-O(2h)	148.9(2)	O(82b)-U(3)-O(2h)	74.42(19)	O(1)#2-O(1h)-O(21u)	61.0(2)
O(1h)-U(2)-O(81b)#1	143.2(2)	O(82b)-U(3)-O(32u)	90.8(2)	O(1)#2-O(1h)-O(31u)	60.1(2)
O(1h)-U(2)-O(71b)	74.1(2)	O(1)#2-U(3)-O(31u)	89.0(2)	O(1)#2-O(1h)-O(2h)	110.4(3)
O(1h)-U(2)-O(1)#2	70.5(2)	O(1)#2-U(3)-O(2h)	135.25(19)	O(12u)-O(1h)-O(21u)	128.7(3)
O(1h)-U(2)-O(21u)	88.1(3)	O(1)#2-U(3)-O(32u)	92.8(3)	O(12u)-O(1h)-O(31u)	124.0(3)
O(1h)-U(2)-O(22u)	92.6(2)	O(31u)-U(3)-O(2h)	94.2(2)	O(12u)-O(1h)-O(2h)	66.1(2)
O(1h)-U(2)-O(2h)#2	141.42(19)	O(31u)-U(3)-O(32u)	178.1(3)	O(21u)-O(1h)-O(31u)	65.5(2)
O(81b)#1-U(2)-O(71b)	71.2(2)	O(2h)-U(3)-O(32u)	84.2(2)	O(21u)-O(1h)-O(2h)	130.7(3)
O(81b)#1-U(2)-O(1)#2	144.9(2)	U(1)-O(1h)-U(2)	132.3(2)	O(31u)-O(1h)-O(2h)	69.1(2)
O(81b)#1-U(2)-O(21u)	83.5(2)	U(1)-O(1h)-U(3)	107.3(2)	U(2)-O(81b)-O(71b)	54.15(17)
O(81b)#1-U(2)-O(22u)	96.0(2)	U(1)-O(1h)-O(71b)	90.6(2)	U(2)#1-O(81b)-O(82b)	102.5(3)
O(81b)#1-U(2)-O(2h)	75.0(2)	U(1)-O(1h)-O(1)#2	149.7(2)	U(2)-O(81b)-O(21u)	38.44(15)
O(71b)-U(2)-O(1)#2	143.9(2)	U(1)-O(1h)-O(12u)	37.01(14)	U(2)#1-O(81b)-O(2h)	52.69(16)
O(71b)-U(2)-O(21u)	95.8(2)	U(1)-O(1h)-O(21u)	104.7(2)	U(2)#1-O(81b)-C(3b)	168.0(3)
O(71b)-U(2)-O(22u)	84.5(2)	U(1)-O(1h)-O(31u)	89.8(2)	U(2)#1-O(81b)-C(2b)	149.6(3)

Table 0.30 Bond valence calculation for complex pyr7.

Atom	Atom bond	Bond length	Bond valence [vu]	Atom valence [vu]
U1	U(1)-O(1h)	2,490	0,43	6,11
	U(1)-O(1)	2,276	0,65	
	U(1)-O(11u)	1,763	1,74	
	U(1)-O(12u)	1,748	1,79	
	U(1)-O(72b)	2,394	0,52	
	U(1)-O(72a)	2,399	0,51	
	U(1)-O(2h)	2,439	0,47	
U2	U(2)-O(1h)	2,423	0,49	6,09
	U(2)-O(81b)	2,406	0,50	
	U(2)-O(71b)	2,390	0,52	
	U(2)-O(1)	2,279	0,64	
	U(2)-O(21u)	1,762	1,75	
	U(2)-O(22u)	1,778	1,69	
	U(2)-O(2h)	2,418	0,49	
U3	U(3)-O(1h)	2,432	0,48	6,01
	U(3)-O(71a)	2,414	0,50	
	U(3)-O(82b)	2,370	0,54	
	U(3)-O(1)	2,251	0,68	
	U(3)-O(31u)	1,774	1,71	
	U(3)-O(2h)	2,516	0,41	
	U(3)-O(32u)	1,776	1,70	
O1	U(1)-O(1)	2,276	0,65	1,97
	U(2)-O(1)	2,279	0,64	
	U(3)-O(1)	2,251	0,68	
O1h	U(1)-O(1h)	2,490	0,43	1,40
	U(2)-O(1h)	2,423	0,49	
	U(3)-O(1h)	2,432	0,48	
O2h	U(1)-O(2h)	2,439	0,47	1,37
	U(2)-O(2h)	2,418	0,49	
	U(3)-O(2h)	2,516	0,41	
O11u	U(1)-O(11u)	1,763	1,74	1,74
O12u	U(1)-O(12u)	1,748	1,79	1,79
O21u	U(2)-O(21u)	1,762	1,75	1,75
O22u	U(2)-O(22u)	1,778	1,69	1,69
O31u	U(3)-O(31u)	1,774	1,71	1,71
O32u	U(3)-O(32u)	1,776	1,70	1,70
O71a	U(3)-O(71a)	2,414	0,50	1,84
	O(71a)-C(7a)	1,235	1,35	
O71b	U(2)-O(71b)	2,390	0,52	1,82
	O(71b)-C(7b)	1,252	1,30	
O72a	U(1)-O(72a)	2,399	0,51	1,74
	O(72a)-C(7a)	1,285	1,22	

Atom	Atom bond	Bond length	Bond valence [vu]	Atom valence [vu]
O72b	U(1)-O(72b)	2,394	0,52	1,75
	O(72b)-C(7b)	1,281	1,23	
O81b	U(2)-O(81b)	2,406	0,50	1,76
	O(81b)-C(8b)	1,27	1,26	
O82b	U(3)-O(82b)	2,370	0,54	1,78
	O(82b)-C(8b)	1,277	1,24	

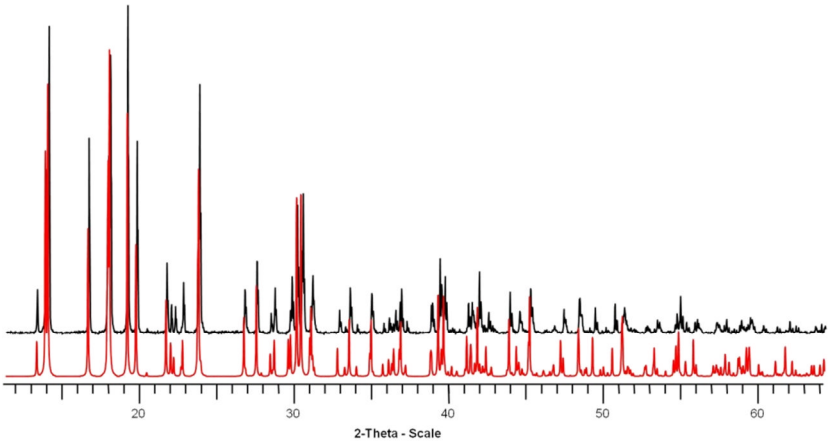

Figure 0.1 Comparison between the experimental (black) and simulated (red) PXRD patterns of the **pyr1** phase.

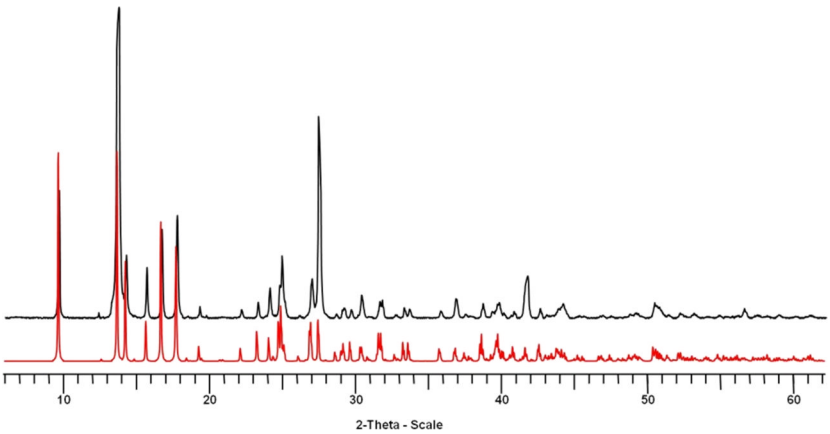

Figure 0.2 Comparison between the experimental (black) and simulated (red) PXRD patterns of the **pyr2** phase.

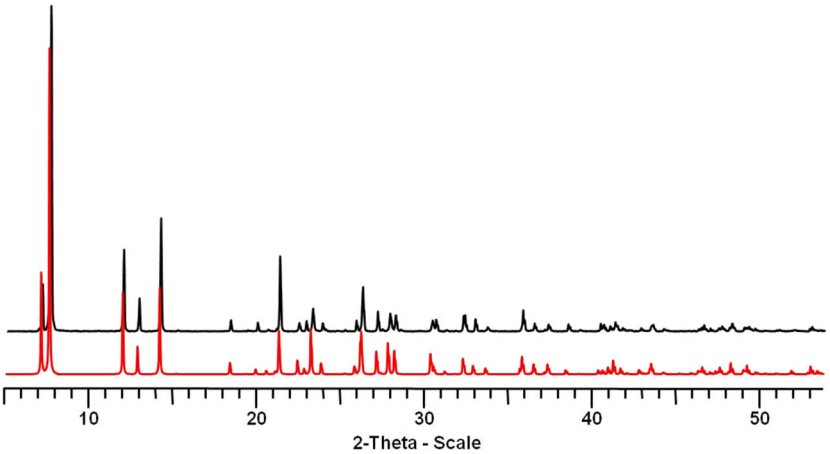

Figure 0.3 Comparison between the experimental (black) and simulated (red) PXRD patterns of the **pyr7** phase.

Six fold coordinated uranyl centers in aromatic carboxylate frameworks

Table 0.1 Crystal data and structure refinement for six fold coordinated uranyl complexes.

	ter1	bpd1	adc1
formula	$C_8H_4O_6U$	$C_{14}H_8O_6U$	$C_{14}H_8N_2O_6U$
formula weight	434.14	510.23	538.25
temperature/K	293(2)	293(2)	293(2)
crystal type	yellow block	yellow block	yellow block
crystal size/mm	0.10 × 0.06 × 0.06	0.25 × 0.19 × 0.06	0.07 × 0.07 × 0.04
crystal system	triclinic	monoclinic	triclinic
space group	*P*-1	*C*2/*m*	*P*-1
a/Å	5.1144(2)	9.0105(2)	5.137(1)
b/Å	5.5731(2)	14.4741(3)	5.611(1)
c/Å	8.4717(3)	5.3067(1)	12.944(2)
α/deg	90.004(2)	90	95.95(1)
ß/deg	94.397(2)	103.364(1)	90.63(1)
γ/deg	107.984(2)	90	107.04(1)
volume/Å^3	228.92(2)	673.35(2)	354.4(1)
Z, ρ_{calc}/g·cm^{-3}	1, 3.149	2, 2.517	1, 2.522
μ/mm^{-1}	17.731	12.077	11.483
Θ range/deg	3.85–37.53	2.72–31.26	3.82–25.80
limiting indices	$-8 \le h \le 8$ $-9 \le k \le 9$ $-13 \le l \le 13$	$-13 \le h \le 13$ $-20 \le k \le 21$ $-7 \le l \le 7$	$-6 \le h \le 6$ $-6 \le k \le 6$ $-14 \le l \le 15$
collected reflections	24681	11277	8780
unique reflections	2259 [R(int) = 0.0375]	1143 [R(int) = 0.0476]	1341 [R(int) = 0.0438]
parameters	70	53	106
goodness-of-fit on F^2	1.012	1.056	1.060
final *R* indices [$I > 2\sigma(I)$]	R1 = 0.0147 wR2 = 0.0276	R1 = 0.0219 wR2 = 0.0461	R1 = 0.0188 wR2 = 0.0450
R indices (all data)	R1 = 0.0148 wR2 = 0.0277	R1 = 0.0231 wR2 = 0.0466	R1 = 0.0188 wR2 = 0.0450
largest diff peak and hole/e·Å^{-3}	0.962 and -1.469	1.408 and -0.634	1.140 and -0.949

Table 0.2 Atomic coordinates (x10^4) and equivalent isotropic displacement parameters (A^{2}x10^3) for complex ter1.

Atom	x	y	z	U(eq)
U(1)	0	0	0	16(1)
O(1)	2564(3)	-1273(3)	2031(2)	28(1)
O(2)	157(3)	2645(3)	1194(2)	31(1)
O(3)	3952(3)	2251(3)	-1095(2)	29(1)
C(1)	4422(3)	-2318(3)	2160(2)	20(1)
C(2)	4734(3)	-3693(3)	3635(2)	19(1)
C(3)	3398(4)	-3375(3)	4956(2)	23(1)
C(4)	6341(4)	-5319(4)	3679(2)	23(1)

Table 0.3 Bond lengths for complex ter1.

Bond	Bond lengths [Å]	Bond	Bond lengths [Å]
U(1)-O(2)#1	1.765(1)	O(3)-C(1)#2	1.266(2)
U(1)-O(2)	1.765(1)	C(1)-O(3)#2	1.266(2)
U(1)-O(3)#1	2.289(1)	C(1)-C(2)	1.489(2)
U(1)-O(3)	2.289(1)	C(2)-C(3)	1.394(2)
U(1)-O(1)#1	2.326(1)	C(2)-C(4)	1.398(2)
U(1)-O(1)	2.326(1)	C(3)-C(4)#3	1.386(2)
O(1)-C(1)	1.257(2)	C(4)-C(3)#3	1.386(2)

Table 0.4 Bond Angles for complex ter1.

Bond	Angle [°]	Bond	Angle [°]
O(2)#1-U(1)-O(2)	180.0(1)	O(3)-U(1)-O(1)	90.79(5)
O(2)#1-U(1)-O(3)#1	90.41(7)	O(1)#1-U(1)-O(1)	180.0(1)
O(2)-U(1)-O(3)#1	89.59(7)	C(1)-O(1)-U(1)	137.5(1)
O(2)#1-U(1)-O(3)	89.59(7)	C(1)#2-O(3)-U(1)	146.6(1)
O(2)-U(1)-O(3)	90.41(7)	O(1)-C(1)-O(3)#2	123.0(2)
O(3)#1-U(1)-O(3)	180.0(1)	O(1)-C(1)-C(2)	118.7(2)
O(2)#1-U(1)-O(1)#1	88.51(6)	O(3)#2-C(1)-C(2)	118.4(2)
O(2)-U(1)-O(1)#1	91.49(6)	C(3)-C(2)-C(4)	120.4(2)
O(3)#1-U(1)-O(1)#1	90.79(5)	C(3)-C(2)-C(1)	119.9(2)
O(3)-U(1)-O(1)#1	89.21(5)	C(4)-C(2)-C(1)	119.7(2)
O(2)#1-U(1)-O(1)	91.49(6)	C(4)#3-C(3)-C(2)	119.9(2)
O(2)-U(1)-O(1)	88.51(6)	C(3)#3-C(4)-C(2)	119.8(2)
O(3)#1-U(1)-O(1)	89.21(5)		

Table 0.5 Bond valence calculation for complex ter1.

Atom	Atom bond	Bond length	Bond valence [vu]	Atom valence [vu]
U1	U(1)-O(2)	1,765	1,74	6,50
	U(1)-O(2)#1	1,765	1,74	
	U(1)-O(3)	2,289	0,63	
	U(1)-O(3)#1	2,289	0,63	
	U(1)-O(1)	2,326	0,59	
	U(1)-O(1)#1	2,326	0,59	
O1	U(1)-O(1)	2,326	0,59	1,88
	O(1)-C(1)	1,257	1,29	
O2	U(1)-O(2)	1,765	1,74	1,74
O3	U(1)-O(3)	2,289	0,63	1,90
	O(3)-C(1)	1,266	1,27	

Table 0.6 Atomic coordinates ($x10^4$) and equivalent isotropic displacement parameters (A^2x10^3) for complex bpd1.

Atom	x	y	z	U(eq)
U(1)	0	5000	0	23(1)
O(1)	330(5)	3896(2)	3162(6)	58(1)
O(2)	1963(5)	5000	176(9)	56(1)
C(1)	0	2449(3)	5000	27(1)
C(2)	0	512(3)	5000	26(1)
C(3)	0	3476(3)	5000	28(1)
C(4)	708(7)	1010(3)	3409(10)	63(2)
C(5)	695(7)	1966(3)	3382(10)	63(2)

Table 0.7 Bond lengths for complex bpd1.

Bond	Bond lengths [Å]	Bond	Bond lengths [Å]
U(1)-O(2)	1.749(4)	C(1)-C(5)#4	1.366(4)
U(1)-O(2)#1	1.749(4)	C(1)-C(3)	1.486(6)
U(1)-O(1)#2	2.287(3)	C(2)-C(4)#4	1.374(5)
U(1)-O(1)#3	2.287(3)	C(2)-C(4)	1.374(5)
U(1)-O(1)	2.287(3)	C(2)-C(2)#5	1.483(9)
U(1)-O(1)#1	2.287(3)	C(3)-O(1)#4	1.242(3)
O(1)-C(3)	1.242(3)	C(4)-C(5)	1.384(6)
C(1)-C(5)	1.366(4)		

Table 0.8 Bond Angles for complex bpd1.

Bond	Angle [°]	Bond	Angle [°]
O(2)-U(1)-O(2)#1	180.0	O(1)-U(1)-O(1)#1	180.0(2)
O(2)-U(1)-O(1)#2	89.9(2)	C(3)-O(1)-U(1)	154.7(3)
O(2)#1-U(1)-O(1)#2	90.1(2)	C(5)-C(1)-C(5)#4	118.5(5)
O(2)-U(1)-O(1)#3	90.1(2)	C(5)-C(1)-C(3)	120.8(2)
O(2)#1-U(1)-O(1)#3	89.9(2)	C(5)#4-C(1)-C(3)	120.8(2)
O(1)#2-U(1)-O(1)#3	180.0(1)	C(4)#4-C(2)-C(4)	116.7(5)
O(2)-U(1)-O(1)	90.1(2)	C(4)#4-C(2)-C(2)#5	121.6(2)
O(2)#1-U(1)-O(1)	89.9(2)	C(4)-C(2)-C(2)#5	121.6(2)
O(1)#2-U(1)-O(1)	91.3(2)	O(1)#4-C(3)-O(1)	121.4(4)
O(1)#3-U(1)-O(1)	88.7(2)	O(1)#4-C(3)-C(1)	119.3(2)
O(2)-U(1)-O(1)#1	89.9(2)	O(1)-C(3)-C(1)	119.3(2)
O(2)#1-U(1)-O(1)#1	90.1(2)	C(2)-C(4)-C(5)	121.8(4)
O(1)#2-U(1)-O(1)#1	88.7(2)	C(1)-C(5)-C(4)	120.6(4)
O(1)#3-U(1)-O(1)#1	91.3(2)		

Table 0.9 Bond valence calculation for complex bpd1.

Atom	Atom bond	Bond length	Bond valence [vu]	Atom valence [vu]
U1	U(1)-O(2)	1,749	1,79	6,12
	U(1)-O(2)#1	1,749	1,79	
	U(1)-O(1)	2,287	0,63	
	U(1)-O(1)#1	2,287	0,63	
	U(1)-O(1)#2	2,287	0,63	
	U(1)-O(1)#3	2,287	0,63	
O1	U(1)-O(1)	2,287	0,63	1,96
	O(1)-C(3)	1,242	1,33	
O2	U(1)-O(2)	1,749	1,79	1,79

Table 0.10 Atomic coordinates ($x10^4$) and equivalent isotropic displacement parameters (A^2x10^3) for complex adc1.

Atom	x	y	z	U(eq)
U(1)	5000	5000	5000	22(1)
O(1)	5045(7)	2626(6)	5773(3)	37(1)
O(2)	2931(7)	6788(6)	6335(3)	33(1)
O(3)	827(7)	2647(6)	4301(3)	37(1)
C(1)	1034(9)	7777(8)	6404(3)	26(1)
C(2)	-970(9)	489(8)	2660(3)	24(1)
C(3)	832(10)	2845(8)	9059(4)	31(1)
C(4)	2545(10)	9624(9)	8223(4)	33(1)
C(5)	-741(10)	2746(9)	8173(4)	35(1)
C(6)	-675(10)	1101(9)	7316(4)	33(1)
C(7)	2478(11)	1281(10)	9083(4)	38(1)
N(1)	896(9)	4457(8)	9989(3)	39(1)

Table 0.11 Bond lengths for complex adc1.

Bond	Bond lengths [Å]	Bond	Bond lengths [Å]
U(1)-O(1)#1	1.752(3)	C(2)-C(6)#3	1.399(6)
U(1)-O(1)	1.752(3)	C(2)-C(1)#2	1.479(6)
U(1)-O(3)	2.282(3)	C(3)-C(5)	1.382(7)
U(1)-O(3)#1	2.282(3)	C(3)-C(7)	1.388(7)
U(1)-O(2)#1	2.330(3)	C(3)-N(1)	1.424(6)
U(1)-O(2)	2.330(3)	C(4)-C(2)#2	1.379(7)
O(2)-C(1)	1.254(5)	C(4)-C(7)#4	1.382(7)
O(3)-C(1)#2	1.268(6)	C(5)-C(6)	1.375(7)
C(1)-O(3)#2	1.268(6)	C(6)-C(2)#3	1.399(6)
C(1)-C(2)#2	1.479(6)	C(7)-C(4)#5	1.382(7)
C(2)-C(4)#2	1.379(7)	N(1)-N(1)#6	1.243(8)

Table 0.12 Bond Angles for complex adc1.

Bond	Angle [°]	Bond	Angle [°]
O(1)#1-U(1)-O(1)	180.000(1)	C(1)#2-O(3)-U(1)	149.5(3)
O(1)#1-U(1)-O(3)	90.2(2)	O(2)-C(1)-O(3)#2	122.4(4)
O(1)-U(1)-O(3)	89.8(2)	O(2)-C(1)-C(2)#2	118.9(4)
O(1)#1-U(1)-O(3)#1	89.8(2)	O(3)#2-C(1)-C(2)#2	118.7(4)
O(1)-U(1)-O(3)#1	90.2(2)	C(4)#2-C(2)-C(6)#3	119.6(4)
O(3)-U(1)-O(3)#1	180.0	C(4)#2-C(2)-C(1)#2	121.2(4)
O(1)#1-U(1)-O(2)#1	88.7(1)	C(6)#3-C(2)-C(1)#2	119.2(4)
O(1)-U(1)-O(2)#1	91.3(1)	C(5)-C(3)-C(7)	120.0(4)
O(3)-U(1)-O(2)#1	89.7(1)	C(5)-C(3)-N(1)	124.6(4)
O(3)#1-U(1)-O(2)#1	90.3(1)	C(7)-C(3)-N(1)	115.4(4)
O(1)#1-U(1)-O(2)	91.3(1)	C(2)#2-C(4)-C(7)#4	120.2(4)
O(1)-U(1)-O(2)	88.7(1)	C(6)-C(5)-C(3)	120.1(4)
O(3)-U(1)-O(2)	90.3(1)	C(5)-C(6)-C(2)#3	120.2(4)
O(3)#1-U(1)-O(2)	89.7(1)	C(4)#5-C(7)-C(3)	120.1(4)
O(2)#1-U(1)-O(2)	180.000(1)	N(1)#6-N(1)-C(3)	114.2(5)
C(1)-O(2)-U(1)	136.4(3)		

Table 0.13 Bond valence calculation for complex adc1.

Atom	Atom bond	Bond length	Bond valence [vu]	Atom valence [vu]
U1	U(1)-O(1)	1,752	1,78	6,01
	U(1)-O(1)#1	1,752	1,78	
	U(1)-O(3)	2,282	0,64	
	U(1)-O(3)#1	2,282	0,64	
	U(1)-O(2)	2,330	0,58	
	U(1)-O(2)#1	2,330	0,58	
O1	U(1)-O(1)	1,752	1,78	1,78
O2	U(1)-O(2)	2,330	0,58	1,88
	O(2)-C(1)	1,254	1,30	
O3	U(1)-O(3)	2,282	0,64	1,91
	O(3)-C(1)	1,268	1,26	

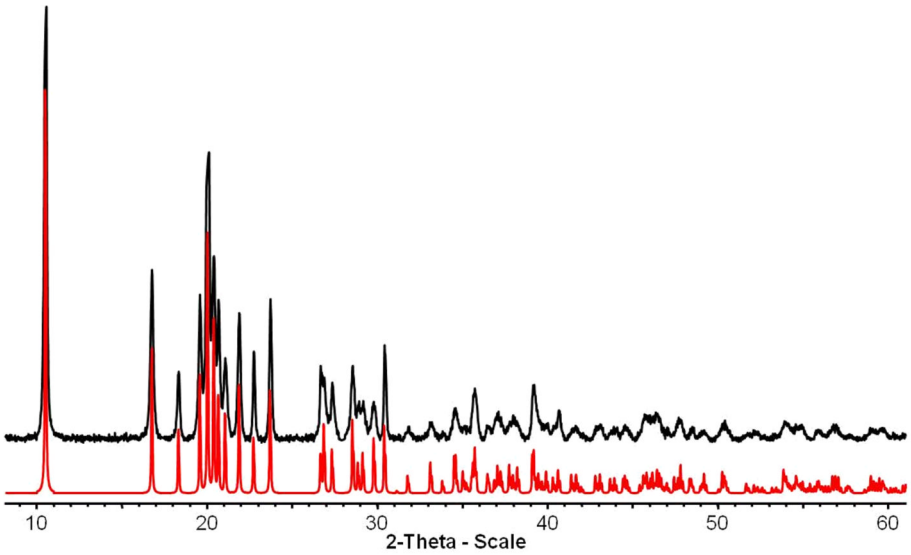

Figure 0.1 Comparison between the experimental (black) and simulated (red) PXRD patterns of the **ter1** phase.

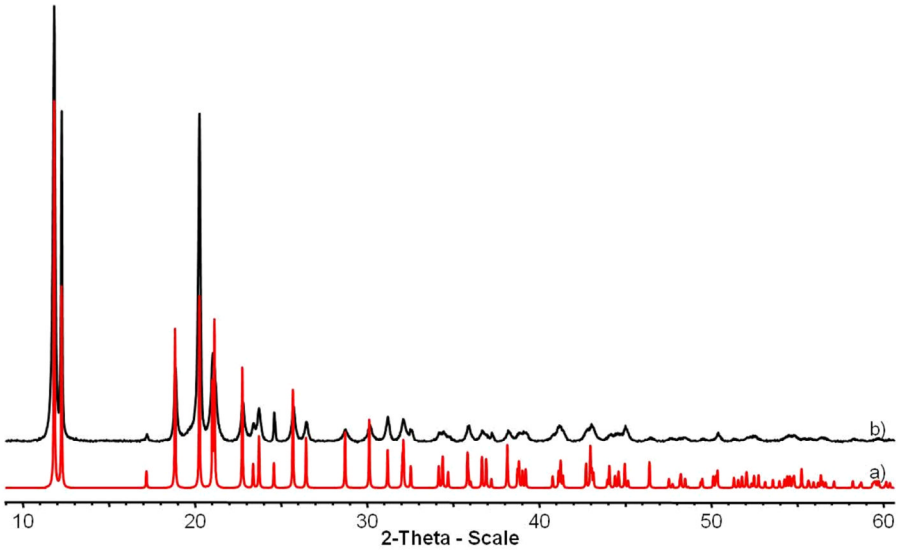

Figure 0.2 Comparison between the experimental (black) and simulated (red) PXRD patterns of the **bpd1** phase.

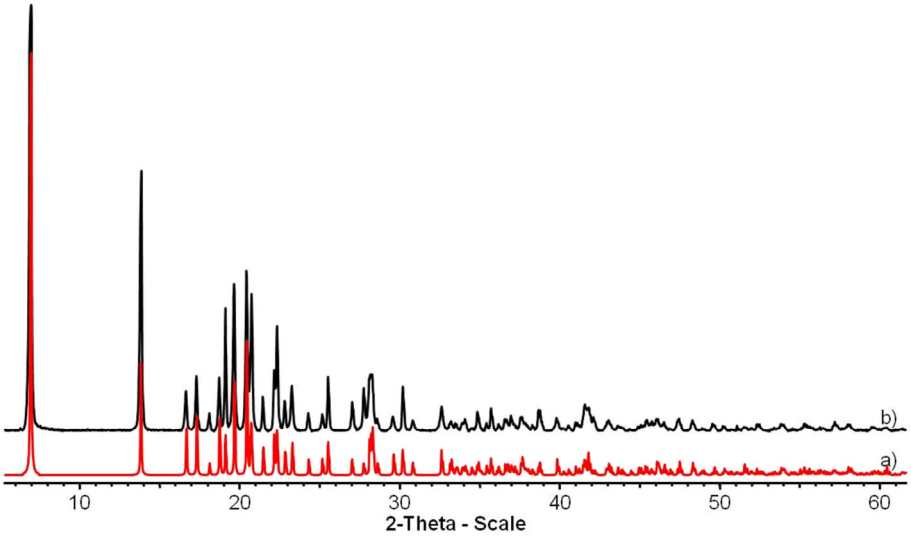

Figure 0.3 Comparison between the experimental (black) and simulated (red) PXRD patterns of the **adc1** phase.

Mixed U^{VI}/Ln^{III} metal centers in aromatic carboxylate frameworks.

Table 0.1 Crystal data and structure refinement data for CeUpht, NdUpht and CeUpyr mixed cation complexes.

	CeUpht	NdUpht	CeUpyr
formula	$C_{32}H_{16}CeNO_{34}U_4$	$C_{32}H_{16}NNdO_{33}U_4$	$C_{30}H_6Ce_2O_{47}U_3$
formula weight	2050.7	2038.8	2112.7
temperature/K	293(2)	293(2)	293(2)
crystal type	yellow block	yellow block	purple block
crystal size/mm	0.12 × 0.08 × 0.05	0.17 × 0.07 × 0.06	0.15 × 0.11 × 0.07
crystal system	monoclinic	monoclinic	triclinic
space group	*P*2/*n*	*P*2/*n*	*P*-1
a/Å	15.9635(2)	15.9634(6)	10.9229(2)
b/Å	19.9741(3)	19.9848(8)	11.5371(3)
c/Å	7.2160(1)	7.1993(3)	13.4516(3)
α/deg	90	90	69.5020(5)
ß/deg	95.3854(7)	95.430(2)	80.0490(6)
γ/deg	90	90	62.2530(5)
volume/Å^3	2289.63(5)	2286.5(2)	1405.14(6)
Z, ρ_{calc}/g·cm^{-3}	2, 2.974	2, 2.960	1, 2.496
μ/mm^{-1}	15.182	15.34	10.318
Θ range/deg	1.02 – 26.52	1.64 – 26.4	1.62 – 30.98
limiting indices	–19 ≤ h ≤ 19 –24 ≤ k ≤ 24 –9 ≤ l ≤ 9	–19 ≤ h ≤ 19 –24 ≤ k ≤ 24 –9 ≤ l ≤ 8	–15 ≤ h ≤ 15 –16 ≤ k ≤ 16 –19 ≤ l ≤ 19
collected reflections	31635	52752	37593
unique reflections	4673 [R(int) = 0.0356]	22816 [R(int) = 0.079]	8899 [R(int) = 0.0352]
parameters	310	306	364
goodness-of-fit on F^2	3.80	1.35	2.38
final *R* indices [$I > 2\sigma(I)$]	R1 = 0.0594 wR2 = 0.0793	R1 = 0.0561 wR2 = 0.0562	R1 = 0.0332 wR2 = 0.0500
R indices (all data)	R1 = 0.0694 wR2 = 0.0799	R1 = 0.1507 wR2 = 0.0789	R1 = 0.0380 wR2 = 0.0505
largest diff peak and hole/e·Å^{-3}	6.37 and −5.93	3.21 and −1.92	5.77 and −4.00

Table 0.2 Crystal data and structure refinement data for NdUpyr, CeUmel and NdUmel mixed cation complexes.

	NdUpyr	CeUmel	NdUmel
formula	$C_{30}H_6Nd_2O_{47}U_3$	$C_{12}CeO_{29}U_2$	$C_{12}NdO_{29}U_2$
formula weight	2120.9	1224.3	1228.4
temperature/K	293(2)	293(2)	293(2)
crystal type	purple block	yellow platelet	yellow needle
crystal size/mm	0.15 × 0.13 × 0.03	0.13 × 0.08 × 0.02	0.21 × 0.20 × 0.08
crystal system	triclinic	orthorhombic	orthorhombic
space group	*P*-1	*Pna*2$_1$	*Pna*2$_1$
a/Å	10.8981(13)	15.8523(8)	15.8367(8)
b/Å	11.5452(14)	8.3188(5)	8.3203(6)
c/Å	13.4086(16)	21.5884(12)	21.5047(3)
α/deg	69.399(3)	90	90
ß/deg	79.959(3)	90	90
γ/deg	62.242(2)	90	90
volume/Å^3	1397.4(3)	2846.9(3)	2833.6(3)
Z, ρ_{calc}/g·cm^{-3}	1, 2.520	4, 2.856	4, 2.879
μ/mm^{-1}	10.604	13.036	13.323
Θ range/deg	1.62 – 32.58	1.89 - 33.72	2.57 - 30.56

	NdUpyr	CeUmel	NdUmel
limiting indices	$-16 \le h \le 16$ $-17 \le k \le 17$ $-20 \le l \le 20$	$-24 \le h \le 24$ $-12 \le k \le 12$ $-33 \le l \le 31$	$-20 \le h \le 22$ $-11 \le k \le 11$ $-28 \le l \le 30$
collected reflections	47359	58532	26709
unique reflections	10168 [R(int) = 0.0485]	10922 [R(int) = 0.0687]	8088 [R(int) = 0.0517]
parameters	365	337	191
goodness-of-fit on F^2	1.62	1.25	1.00
final R indices [$I > 2\sigma(I)$]	R1 = 0.0304 wR2 = 0.0418	R1 = 0.0365 wR2 = 0.0375	R1 = 0.0313 wR2 = 0.0351
R indices (all data)	R1 = 0.0456 wR2 = 0.0430	R1 = 0.0612 wR2 = 0.0400	R1 = 0.0443 wR2 = 0.0375
largest diff peak and hole/e·Å^{-3}	2.10 and −1.98	2.91 and −2.23	1.50 and −1.35

Table 0.3 Atomic coordinates (x10^4) and equivalent isotropic displacement parameters (A^{2}x10^3) for complex CeUpht.

Atom	x	y	z	U(eq)
U(1)	7500	8408(1)	2500	17(1)
U(2)	7500	6523(1)	2500	18(1)
U(3)	5339(1)	7459(1)	2168(1)	19(1)
Ce(1)	2500	8069(1)	-2500	17(1)
O(31u)	5384(8)	7508(5)	4639(2)	39(3)
O(12b)	4209(6)	8231(5)	2213(14)	24(3)
O(82a)	6633(6)	5451(5)	2324(16)	31(4)
O(82b)	6618(6)	9494(5)	2475(14)	25(3)
O(11a)	4245(7)	6689(5)	1918(17)	38(4)
O(1w)	2500	9366(8)	-2500	42(4)
C(2a)	4364(8)	5555(7)	2942(17)	17(4)
C(3b)	3632(9)	9840(7)	1700(20)	30(5)
O(81a)	5898(6)	6359(5)	2532(15)	30(4)
O(1u)	7537(6)	8471(4)	114(13)	17(3)
O(32u)	5254(6)	7480(4)	-302(13)	21(3)
O(81b)	5860(6)	8586(5)	1915(15)	29(4)
C(7b)	5117(9)	9637(7)	2202(19)	19(4)
O(2u)	7456(6)	6538(5)	110(13)	22(3)
O(1)	6719(7)	7474(4)	2298(17)	31(4)
O(11b)	3703(7)	8618(5)	-526(15)	36(4)
C(4b)	3761(10)	10483(8)	2360(20)	33(6)
C(5b)	4538(11)	10715(8)	2930(20)	35(6)
C(2b)	4313(8)	9394(6)	1692(18)	16(4)
C(7a)	5160(9)	5305(6)	2492(19)	18(4)
C(4a)	3841(11)	4399(7)	2715(19)	33(6)
C(6a)	5244(10)	4644(7)	2253(19)	27(5)
C(6b)	5206(10)	10297(7)	2870(20)	32(5)
C(3a)	3741(10)	5080(7)	3030(20)	31(5)
C(8b)	5884(9)	9221(7)	2225(19)	22(5)
C(8a)	5926(9)	5720(6)	2440(20)	25(5)
C(5a)	4589(11)	4164(8)	2270(20)	40(6)
O(2w)	1140(20)	7579(13)	-1800(40)	66(6)
N(1)	7500	4108(18)	2500	125(13)
C(1b)	4070(8)	8706(6)	1000(20)	23(5)
O(12a)	3702(10)	6378(6)	4550(20)	79(6)
C(1a)	4098(10)	6262(7)	3140(30)	37(6)
O(3w)	2282(13)	7017(11)	-4520(30)	40(4)
O(4w)	2319(19)	8270(15)	1080(40)	72(6)
O(3w')	2371(15)	7387(11)	-5610(30)	40(4)
O(2w')	1561(17)	7128(14)	-2740(40)	66(6)
O(4w')	1806(19)	8550(15)	230(40)	72(6)
O(5w)	6831(18)	7474(11)	-2570(40)	56(7)

Table 0.4 Bond lengths for complex CeUpht.

Bond	Bond length	Bond	Bond length
U(1)-U(2)	3.765(1)	Ce(1)-O(3w)	2.56(2)
U(1)-U(3)	3.9244(6)	Ce(1)-O(3w)#2	2.56(2)
U(1)-U(3)#1	3.9244(6)	Ce(1)-O(4w)	2.66(3)
U(1)-O(82b)	2.58(1)	Ce(1)-O(4w)#2	2.66(3)
U(1)-O(82b)#1	2.58(1)	Ce(1)-O(3w')	2.62(2)
U(1)-O(1u)	1.73(1)	Ce(1)-O(3w')#2	2.62(2)
U(1)-O(1u)#1	1.73(1)	Ce(1)-O(2w')	2.40(3)
U(1)-O(81b)	2.64(1)	Ce(1)-O(2w')#2	2.40(3)
U(1)-O(81b)#1	2.64(1)	Ce(1)-O(4w')	2.54(3)
U(1)-O(1)	2.24(1)	Ce(1)-O(4w')#2	2.54(3)
U(1)-O(1)#1	2.24(1)	O(12b)-C(1b)	1.30(2)
U(1)-C(8b)	3.04(1)	O(82a)-C(8a)	1.26(2)
U(1)-C(8b)#1	3.04(1)	O(82b)-C(8b)	1.29(2)
U(2)-U(3)	3.911(1)	O(11a)-C(1a)	1.26(2)
U(2)-U(3)#1	3.911(1)	C(2a)-C(7a)	1.43(2)
U(2)-O(82a)	2.55(1)	C(2a)-C(3a)	1.38(2)
U(2)-O(82a)#1	2.55(1)	C(2a)-C(1a)	1.48(2)
U(2)-O(81a)	2.58(1)	C(3b)-C(4b)	1.38(2)
U(2)-O(81a)#1	2.58(1)	C(3b)-C(2b)	1.41(2)
U(2)-O(2u)	1.72(1)	O(81a)-C(8a)	1.28(2)
U(2)-O(2u)#1	1.72(1)	O(81b)-C(8b)	1.29(2)
U(2)-O(1)	2.27(1)	C(7b)-C(2b)	1.39(2)
U(2)-O(1)#1	2.27(1)	C(7b)-C(6b)	1.41(2)
U(2)-C(8a)	2.98(1)	C(7b)-C(8b)	1.48(2)
U(2)-C(8a)#1	2.98(1)	O(11b)-C(1b)	1.21(2)
U(3)-O(31u)	1.779(2)	C(4b)-C(5b)	1.35(2)
U(3)-O(12b)	2.38(1)	C(5b)-C(6b)	1.36(2)
U(3)-O(11a)	2.32(1)	C(2b)-C(1b)	1.50(2)
U(3)-O(81a)	2.38(1)	C(7a)-C(6a)	1.34(2)
U(3)-O(32u)	1.77(1)	C(7a)-C(8a)	1.48(2)
U(3)-O(81b)	2.41(1)	C(4a)-C(3a)	1.39(2)
U(3)-O(1)	2.20(1)	C(4a)-C(5a)	1.35(2)
U(3)-C(1b)	3.27(1)	C(6a)-C(5a)	1.42(2)
U(3)-C(1a)	3.22(2)	O(2w)-O(2w')	1.35(4)
Ce(1)-O(1w)	2.59(2)	O(12a)-C(1a)	1.27(2)
Ce(1)-O(11b)	2.53(1)	O(3w)-O(3w')	1.10(3)
Ce(1)-O(11b)#2	2.53(1)	O(3w)-O(2w')	1.81(4)
Ce(1)-O(2w)	2.48(3)	O(4w)-O(4w)#3	2.07(4)
Ce(1)-O(2w)#2	2.48(3)	O(4w)-O(3w')#2	1.87(4)
Ce(1)-C(1b)	3.62(1)	O(4w)-O(4w')	1.12(4)
Ce(1)-C(1b)#2	3.62(1)	O(5w)-O(5w)#4	2.13(4)

Table 0.5 Bond Angles for complex CeUpht.

Bond	Angle [°]	Bond	Angle [°]	Bond	Angle [°]
U(2)-U(1)-U(3)	61.10(1)	O(2u)-U(2)-O(1)	87.2(4)	C(1b)-Ce(1)-O(4w)	53.1(7)
U(2)-U(1)-U(3)#1	61.10(1)	O(2u)-U(2)-O(1)#1	91.2(4)	C(1b)-Ce(1)-O(4w)#2	119.6(7)
U(2)-U(1)-O(82b)	147.0(2)	O(2u)-U(2)-C(8a)	92.2(4)	C(1b)-Ce(1)-O(3w')	140.8(6)
U(2)-U(1)-O(82b)#1	147.0(2)	O(2u)-U(2)-C(8a)#1	88.8(4)	C(1b)-Ce(1)-O(3w')#2	65.8(5)
U(2)-U(1)-O(1u)	94.1(3)	O(2u)#1-U(2)-O(1)	91.2(4)	C(1b)-Ce(1)-O(2w')	135.5(7)
U(2)-U(1)-O(1u)#1	94.1(3)	O(2u)#1-U(2)-O(1)#1	87.2(4)	C(1b)-Ce(1)-O(2w')#2	80.6(7)
U(2)-U(1)-O(81b)	97.7(2)	O(2u)#1-U(2)-C(8a)	88.8(4)	C(1b)-Ce(1)-O(4w')	69.5(7)
U(2)-U(1)-O(81b)#1	97.7(2)	O(2u)#1-U(2)-C(8a)#1	92.2(4)	C(1b)-Ce(1)-O(4w')#2	94.8(7)
U(2)-U(1)-O(1)	33.7(3)	O(1)-U(2)-O(1)#1	66.4(4)	C(1b)#2-Ce(1)-O(3w)	81.0(5)
U(2)-U(1)-O(1)#1	33.7(3)	O(1)-U(2)-C(8a)	89.5(4)	C(1b)#2-Ce(1)-O(3w)#2	137.2(5)
U(2)-U(1)-C(8b)	122.3(3)	O(1)-U(2)-C(8a)#1	155.5(4)	C(1b)#2-Ce(1)-O(4w)	119.6(7)
U(2)-U(1)-C(8b)#1	122.3(3)	O(1)#1-U(2)-C(8a)	155.5(4)	C(1b)#2-Ce(1)-O(4w)#2	53.1(7)
U(3)-U(1)-U(3)#1	122.19(2)	O(1)#1-U(2)-C(8a)#1	89.5(4)	C(1b)#2-Ce(1)-O(3w')	65.8(5)
U(3)-U(1)-O(82b)	86.0(2)	C(8a)-U(2)-C(8a)#1	114.8(4)	C(1b)-Ce(1)-O(3w')	140.8(6)
U(3)-U(1)-O(82b)#1	151.8(2)	U(1)-U(3)-U(2)	57.44(1)	C(1b)#2-Ce(1)-O(2w')	80.6(7)
U(3)-U(1)-O(1u)	94.9(3)	U(1)-U(3)-O(31u)	87.7(4)	C(1b)-Ce(1)-O(2w')	135.5(7)
U(3)-U(1)-O(1u)#1	89.1(3)	U(1)-U(3)-O(12b)	110.5(2)	C(1b)#2-Ce(1)-O(4w')	94.8(7)

Bond	Angle [°]	Bond	Angle [°]	Bond	Angle [°]
U(3)-U(1)-O(81b)	37.0(2)	U(1)-U(3)-O(11a)	167.3(3)	C(1b)#2-Ce(1)-O(4w')	69.5(7)
U(3)-U(1)-O(81b)#1	158.3(2)	U(1)-U(3)-O(81a)	97.0(2)	O(3w)-Ce(1)-O(3w)#2	69.7(7)
U(3)-U(1)-O(1)	27.5(3)	U(1)-U(3)-O(32u)	91.9(3)	O(3w)-Ce(1)-O(4w)	130.9(8)
U(3)-U(1)-O(1)#1	94.7(3)	U(1)-U(3)-O(81b)	41.1(2)	O(3w)-Ce(1)-O(4w)#2	66.0(8)
U(3)-U(1)-C(8b)	61.2(3)	U(1)-U(3)-O(1)	28.1(2)	O(3w)-Ce(1)-O(3w')	24.5(7)
U(3)-U(1)-C(8b)#1	176.6(3)	U(1)-U(3)-C(1b)	99.6(2)	O(3w)-Ce(1)-O(3w')#2	93.2(7)
U(3)#1-U(1)-O(82b)	151.8(2)	U(1)-U(3)-C(1a)	154.1(3)	O(3w)-Ce(1)-O(2w')	42.7(8)
U(3)#1-U(1)-O(82b)#1	86.0(2)	U(2)-U(3)-O(31u)	90.7(4)	O(3w)-Ce(1)-O(2w')#2	56.6(8)
U(3)#1-U(1)-O(1u)	89.1(3)	U(2)-U(3)-O(12b)	167.4(2)	O(3w)-Ce(1)-O(4w')	134.9(8)
U(3)#1-U(1)-O(1u)#1	94.9(3)	U(2)-U(3)-O(11a)	109.9(3)	O(3w)-Ce(1)-O(4w')#2	85.1(8)
U(3)#1-U(1)-O(81b)	158.3(2)	U(2)-U(3)-O(81a)	39.8(2)	O(3w)#2-Ce(1)-O(4w)	66.0(8)
U(3)#1-U(1)-O(81b)#1	37.0(2)	U(2)-U(3)-O(32u)	93.2(3)	O(3w)-Ce(1)-O(4w)	130.9(8)
U(3)#1-U(1)-O(1)	94.7(3)	U(2)-U(3)-O(81b)	98.2(2)	O(3w)#2-Ce(1)-O(3w')	93.2(7)
U(3)#1-U(1)-O(1)#1	27.5(3)	U(2)-U(3)-O(1)	29.4(2)	O(3w)-Ce(1)-O(3w')	24.5(7)
U(3)#1-U(1)-C(8b)	176.6(3)	U(2)-U(3)-C(1b)	154.3(2)	O(3w)#2-Ce(1)-O(2w')	56.6(8)
U(3)#1-U(1)-C(8b)#1	61.2(3)	U(2)-U(3)-C(1a)	100.9(3)	O(3w)-Ce(1)-O(2w')	42.7(8)
O(82b)-U(1)-O(82b)#1	65.9(3)	O(31u)-U(3)-O(12b)	84.8(4)	O(3w)#2-Ce(1)-O(4w')	85.1(8)
O(82b)-U(1)-O(1u)	90.1(4)	O(31u)-U(3)-O(11a)	94.2(5)	O(3w)-Ce(1)-O(4w')	134.9(8)
O(82b)-U(1)-O(1u)#1	83.0(4)	O(31u)-U(3)-O(81a)	87.8(4)	O(4w)-Ce(1)-O(4w)#2	162.6(9)
O(82b)-U(1)-O(81b)	49.7(3)	O(31u)-U(3)-O(32u)	175.0(4)	O(4w)-Ce(1)-O(3w')	154.9(8)
O(82b)-U(1)-O(81b)#1	114.9(3)	O(31u)-U(3)-O(81b)	92.4(4)	O(4w)-Ce(1)-O(3w')#2	41.5(8)
O(82b)-U(1)-O(1)	113.5(3)	O(31u)-U(3)-O(1)	90.6(5)	O(4w)-Ce(1)-O(2w')	93.7(9)
O(82b)-U(1)-O(1)#1	176.6(4)	O(31u)-U(3)-C(1b)	100.5(5)	O(4w)-Ce(1)-O(2w')#2	99.8(9)
O(82b)-U(1)-C(8b)	24.9(3)	O(31u)-U(3)-C(1a)	78.0(5)	O(4w)-Ce(1)-O(4w')	24.9(9)
O(82b)-U(1)-C(8b)#1	90.6(3)	O(12b)-U(3)-O(11a)	82.2(3)	O(4w)-Ce(1)-O(4w')#2	142.5(9)
O(82b)#1-U(1)-O(1u)	83.0(4)	O(12b)-U(3)-O(81a)	151.2(3)	O(4w)#2-Ce(1)-O(3w')	41.5(8)
O(82b)-U(1)-O(1u)	90.1(4)	O(12b)-U(3)-O(32u)	90.7(4)	O(4w)-Ce(1)-O(3w')	154.9(8)
O(82b)#1-U(1)-O(81b)	114.9(3)	O(12b)-U(3)-O(81b)	70.3(3)	O(4w)#2-Ce(1)-O(2w')	99.8(9)
O(82b)-U(1)-O(81b)	49.7(3)	O(12b)-U(3)-O(1)	138.6(3)	O(4w)-Ce(1)-O(2w')	93.7(9)
O(82b)#1-U(1)-O(1)	176.6(4)	O(12b)-U(3)-C(1b)	19.4(4)	O(4w)#2-Ce(1)-O(4w')	142.5(9)
O(82b)#1-U(1)-O(1)#1	113.5(3)	O(12b)-U(3)-C(1a)	89.7(4)	O(4w)-Ce(1)-O(4w')	24.9(9)
O(82b)#1-U(1)-C(8b)	90.6(3)	O(11a)-U(3)-O(81a)	70.6(3)	O(3w')-Ce(1)-O(3w')#2	117.3(7)
O(82b)-U(1)-C(8b)	24.9(3)	O(11a)-U(3)-O(32u)	87.2(4)	O(3w')-Ce(1)-O(2w')	62.0(9)
O(1u)-U(1)-O(1u)#1	171.8(4)	O(11a)-U(3)-O(81b)	151.0(3)	O(3w')-Ce(1)-O(2w')#2	69.7(8)
O(1u)-U(1)-O(81b)	87.5(4)	O(11a)-U(3)-O(1)	139.2(3)	O(3w')-Ce(1)-O(4w')	149.1(9)
O(1u)-U(1)-O(81b)#1	91.4(4)	O(11a)-U(3)-C(1b)	92.4(3)	O(3w')-Ce(1)-O(4w')#2	62.4(8)
O(1u)-U(1)-O(1)	93.8(4)	O(11a)-U(3)-C(1a)	18.6(4)	O(3w')#2-Ce(1)-O(2w')	69.7(8)
O(1u)-U(1)-O(1)#1	93.1(4)	O(81a)-U(3)-O(32u)	97.2(4)	O(3w')-Ce(1)-O(2w')	62.0(9)
O(1u)-U(1)-C(8b)	90.2(4)	O(81a)-U(3)-O(81b)	137.9(3)	O(3w')#2-Ce(1)-O(4w')	62.4(8)
O(1u)-U(1)-C(8b)#1	85.4(4)	O(81a)-U(3)-O(1)	69.1(3)	O(3w')-Ce(1)-O(4w')	149.1(9)
O(1u)#1-U(1)-O(81b)	91.4(4)	O(81a)-U(3)-C(1b)	161.7(3)	O(2w')-Ce(1)-O(2w')#2	76.9(9)
O(1u)-U(1)-O(81b)	87.5(4)	O(81a)-U(3)-C(1a)	61.5(4)	O(2w')-Ce(1)-O(4w')	92.2(10)
O(1u)#1-U(1)-O(1)	93.1(4)	O(32u)-U(3)-O(81b)	84.1(4)	O(2w')-Ce(1)-O(4w')#2	123.7(9)
O(1u)#1-U(1)-O(1)#1	93.8(4)	O(32u)-U(3)-O(1)	91.4(5)	O(2w')#2-Ce(1)-O(4w')	123.7(9)
O(1u)#1-U(1)-C(8b)	85.4(4)	O(32u)-U(3)-C(1b)	74.7(4)	O(2w')-Ce(1)-O(4w')	92.2(10)
O(1u)#1-U(1)-C(8b)#1	90.2(4)	O(32u)-U(3)-C(1a)	104.2(4)	O(4w')-Ce(1)-O(4w')#2	135.5(10)
O(81b)-U(1)-O(81b)#1	164.5(3)	O(81b)-U(3)-O(1)	68.8(3)	U(3)-O(12b)-C(1b)	123.2(9)
O(81b)-U(1)-O(1)	64.1(3)	O(81b)-U(3)-C(1b)	58.6(3)	U(2)-O(82a)-C(8a)	97.1(8)
O(81b)-U(1)-O(1)#1	131.4(3)	O(81b)-U(3)-C(1a)	158.7(4)	U(1)-O(82b)-C(8b)	97.7(8)
O(81b)-U(1)-C(8b)	25.0(3)	O(1)-U(3)-C(1b)	126.5(3)	U(3)-O(11a)-C(1a)	125.5(10)
O(81b)-U(1)-C(8b)#1	139.7(3)	O(1)-U(3)-C(1a)	129.5(3)	C(7a)-C(2a)-C(3a)	115.5(12)
O(81b)#1-U(1)-O(1)	131.4(3)	C(1b)-U(3)-C(1a)	104.0(4)	C(7a)-C(2a)-C(1a)	128.5(12)
O(81b)#1-U(1)-O(1)#1	64.1(3)	O(1w)-Ce(1)-O(11b)	64.3(2)	C(3a)-C(2a)-C(1a)	115.8(12)
O(81b)#1-U(1)-C(8b)	139.7(3)	O(1w)-Ce(1)-O(11b)#2	64.3(2)	C(4b)-C(3b)-C(2b)	120.0(13)
O(81b)-U(1)-C(8b)	25.0(3)	O(1w)-Ce(1)-O(2w)	113.3(6)	U(2)-O(81a)-U(3)	104.1(3)
O(1)-U(1)-O(1)#1	67.3(4)	O(1w)-Ce(1)-O(2w)#2	113.3(6)	U(2)-O(81a)-C(8a)	95.0(8)
O(1)-U(1)-C(8b)	88.7(4)	O(1w)-Ce(1)-C(1b)	69.4(2)	U(3)-O(81a)-C(8a)	158.6(9)
O(1)-U(1)-C(8b)#1	155.9(4)	O(1w)-Ce(1)-C(1b)#2	69.4(2)	U(1)-O(81b)-U(3)	101.9(3)
O(1)#1-U(1)-C(8b)	155.9(4)	O(1w)-Ce(1)-O(3w)	145.1(5)	U(1)-O(81b)-C(8b)	95.3(8)
O(1)#1-U(1)-C(8b)#1	88.7(4)	O(1w)-Ce(1)-O(3w)#2	145.1(5)	U(3)-O(81b)-C(8b)	155.6(10)
C(8b)-U(1)-C(8b)#1	115.4(4)	O(1w)-Ce(1)-O(4w)	81.3(6)	C(2b)-C(7b)-C(6b)	118.6(13)
U(1)-U(2)-U(3)	61.46(1)	O(1w)-Ce(1)-O(4w)#2	81.3(6)	C(2b)-C(7b)-C(8b)	123.4(12)
U(1)-U(2)-U(3)#1	61.46(1)	O(1w)-Ce(1)-O(3w')	121.4(5)	C(6b)-C(7b)-C(8b)	117.8(12)

Bond	Angle [°]	Bond	Angle [°]	Bond	Angle [°]
U(1)-U(2)-O(82a)	147.2(2)	O(1w)-Ce(1)-O(3w')#2	121.4(5)	U(1)-O(1)-U(2)	113.2(4)
U(1)-U(2)-O(82a)#1	147.2(2)	O(1w)-Ce(1)-O(2w')	141.5(7)	U(1)-O(1)-U(3)	124.4(4)
U(1)-U(2)-O(81a)	97.3(2)	O(1w)-Ce(1)-O(2w')#2	141.5(7)	U(2)-O(1)-U(3)	122.3(4)
U(1)-U(2)-O(81a)#1	97.3(2)	O(1w)-Ce(1)-O(4w')	67.8(7)	Ce(1)-O(11b)-C(1b)	148.4(10)
U(1)-U(2)-O(2u)	89.0(3)	O(1w)-Ce(1)-O(4w')#2	67.8(7)	C(3b)-C(4b)-C(5b)	121.8(15)
U(1)-U(2)-O(2u)#1	89.0(3)	O(11b)-Ce(1)-O(11b)#2	128.7(3)	C(4b)-C(5b)-C(6b)	118.7(14)
U(1)-U(2)-O(1)	33.2(3)	O(11b)-Ce(1)-O(2w)	133.7(7)	C(3b)-C(2b)-C(7b)	118.2(12)
U(1)-U(2)-O(1)#1	33.2(3)	O(11b)-Ce(1)-O(2w)#2	69.6(7)	C(3b)-C(2b)-C(1b)	113.9(11)
U(1)-U(2)-C(8a)	122.6(3)	O(11b)-Ce(1)-C(1b)	10.1(4)	C(7b)-C(2b)-C(1b)	127.7(12)
U(1)-U(2)-C(8a)#1	122.6(3)	O(11b)-Ce(1)-C(1b)#2	132.8(3)	C(2a)-C(7a)-C(6a)	118.4(13)
U(3)-U(2)-U(3)#1	122.92(2)	O(11b)-Ce(1)-O(3w)	136.9(5)	C(2a)-C(7a)-C(8a)	124.3(11)
U(3)-U(2)-O(82a)	85.8(2)	O(11b)-Ce(1)-O(3w)#2	88.9(5)	C(6a)-C(7a)-C(8a)	117.1(13)
U(3)-U(2)-O(82a)#1	151.3(2)	O(11b)-Ce(1)-O(4w)	62.2(7)	C(3a)-C(4a)-C(5a)	119.9(15)
U(3)-U(2)-O(81a)	36.1(2)	O(11b)-Ce(1)-O(4w)#2	109.6(7)	C(7a)-C(6a)-C(5a)	125.6(15)
U(3)-U(2)-O(81a)#1	158.4(2)	O(11b)-Ce(1)-O(3w')	134.6(6)	C(7b)-C(6b)-C(5b)	122.3(14)
U(3)-U(2)-O(2u)	88.7(3)	O(11b)-Ce(1)-O(3w')#2	75.4(6)	C(2a)-C(3a)-C(4a)	124.7(14)
U(3)-U(2)-O(2u)#1	90.3(3)	O(11b)-Ce(1)-O(2w')	144.7(7)	U(1)-C(8b)-O(82b)	57.4(7)
U(3)-U(2)-O(1)	28.4(3)	O(11b)-Ce(1)-O(2w')#2	82.1(7)	U(1)-C(8b)-O(81b)	59.8(7)
U(3)-U(2)-O(1)#1	94.6(3)	O(11b)-Ce(1)-O(4w')	76.3(7)	U(1)-C(8b)-C(7b)	176.4(9)
U(3)-U(2)-C(8a)	61.2(3)	O(11b)-Ce(1)-O(4w')#2	84.8(7)	O(82b)-C(8b)-O(81b)	116.9(12)
U(3)-U(2)-C(8a)#1	175.2(3)	O(11b)#2-Ce(1)-O(2w)	69.6(7)	O(82b)-C(8b)-C(7b)	120.4(12)
U(3)#1-U(2)-O(82a)	151.3(2)	O(11b)-Ce(1)-O(2w)	133.7(7)	O(81b)-C(8b)-C(7b)	122.7(12)
U(3)#1-U(2)-O(82a)#1	85.8(2)	O(11b)#2-Ce(1)-C(1b)	132.8(3)	U(2)-C(8a)-O(82a)	58.1(7)
U(3)#1-U(2)-O(81a)	158.4(2)	O(11b)-Ce(1)-C(1b)	10.1(4)	U(2)-C(8a)-O(81a)	59.7(7)
U(3)#1-U(2)-O(81a)#1	36.1(2)	O(11b)#2-Ce(1)-O(3w)	88.9(5)	U(2)-C(8a)-C(7a)	177.2(10)
U(3)#1-U(2)-O(2u)	90.3(3)	O(11b)-Ce(1)-O(3w)	136.9(5)	O(82a)-C(8a)-O(81a)	117.7(12)
U(3)#1-U(2)-O(2u)#1	88.7(3)	O(11b)#2-Ce(1)-O(4w)	109.6(7)	O(82a)-C(8a)-C(7a)	120.6(12)
U(3)#1-U(2)-O(1)	94.6(3)	O(11b)-Ce(1)-O(4w)	62.2(7)	O(81a)-C(8a)-C(7a)	121.7(12)
U(3)#1-U(2)-O(1)#1	28.4(3)	O(11b)#2-Ce(1)-O(3w')	75.4(6)	C(4a)-C(5a)-C(6a)	115.8(14)
U(3)#1-U(2)-C(8a)	175.2(3)	O(11b)-Ce(1)-O(3w')	134.6(6)	Ce(1)-O(2w)-O(2w')	70.8(18)
U(3)#1-U(2)-C(8a)#1	61.2(3)	O(11b)#2-Ce(1)-O(2w')	82.1(7)	U(3)-C(1b)-Ce(1)	106.5(4)
O(82a)-U(2)-O(82a)#1	65.5(3)	O(11b)-Ce(1)-O(2w')	144.7(7)	U(3)-C(1b)-O(12b)	37.5(6)
O(82a)-U(2)-O(81a)	50.1(3)	O(11b)#2-Ce(1)-O(4w')	84.8(7)	U(3)-C(1b)-O(11b)	111.1(9)
O(82a)-U(2)-O(81a)#1	115.3(3)	O(11b)-Ce(1)-O(4w')	76.3(7)	U(3)-C(1b)-C(2b)	118.5(8)
O(82a)-U(2)-O(2u)	89.6(4)	O(2w)-Ce(1)-O(2w)#2	133.5(9)	Ce(1)-C(1b)-O(12b)	106.1(8)
O(82a)-U(2)-O(2u)#1	92.0(4)	O(2w)-Ce(1)-C(1b)	124.1(7)	Ce(1)-C(1b)-O(11b)	21.5(7)
O(82a)-U(2)-O(1)	114.1(3)	O(2w)-Ce(1)-C(1b)#2	73.6(7)	Ce(1)-C(1b)-C(2b)	134.0(8)
O(82a)-U(2)-O(1)#1	179.1(4)	O(2w)-Ce(1)-O(3w)	73.5(8)	O(12b)-C(1b)-O(11b)	123.1(12)
O(82a)-U(2)-C(8a)	24.8(3)	O(2w)-Ce(1)-O(3w)#2	68.6(8)	O(12b)-C(1b)-C(2b)	115.0(13)
O(82a)-U(2)-C(8a)#1	90.1(3)	O(2w)-Ce(1)-O(4w)	71.6(9)	O(11b)-C(1b)-C(2b)	121.6(12)
O(82a)#1-U(2)-O(81a)	115.3(3)	O(2w)-Ce(1)-O(4w)#2	115.8(9)	U(3)-C(1a)-O(11a)	35.9(7)
O(82a)-U(2)-O(81a)	50.1(3)	O(2w)-Ce(1)-O(3w')	88.2(9)	U(3)-C(1a)-C(2a)	119.8(10)
O(82a)#1-U(2)-O(2u)	92.0(4)	O(2w)-Ce(1)-O(3w')#2	67.7(9)	U(3)-C(1a)-O(12a)	113.6(10)
O(82a)-U(2)-O(2u)	89.6(4)	O(2w)-Ce(1)-O(2w')	32.0(9)	O(11a)-C(1a)-C(2a)	120.2(15)
O(82a)#1-U(2)-O(1)	179.1(4)	O(2w)-Ce(1)-O(2w')#2	103.3(9)	O(11a)-C(1a)-O(12a)	125.0(14)
O(82a)#1-U(2)-O(1)#1	114.1(3)	O(2w)-Ce(1)-O(4w')	62.4(9)	C(2a)-C(1a)-O(12a)	114.8(14)
O(82a)#1-U(2)-C(8a)	90.1(3)	O(2w)-Ce(1)-O(4w')#2	139.6(10)	Ce(1)-O(3w)-O(3w')	80.6(17)
O(82a)-U(2)-C(8a)	24.8(3)	O(2w)#2-Ce(1)-C(1b)	73.6(7)	Ce(1)-O(3w)-O(2w')	63.8(11)
O(81a)-U(2)-O(81a)#1	165.4(3)	O(2w)-Ce(1)-C(1b)	124.1(7)	O(3w')-O(3w)-O(2w')	124(2)
O(81a)-U(2)-O(2u)	93.7(4)	O(2w)#2-Ce(1)-O(3w)	68.6(8)	Ce(1)-O(4w)-O(4w)#3	156.0(17)
O(81a)-U(2)-O(2u)#1	86.6(4)	O(2w)-Ce(1)-O(3w)	73.5(8)	Ce(1)-O(4w)-O(3w')#2	68.1(12)
O(81a)-U(2)-O(1)	64.4(3)	O(2w)#2-Ce(1)-O(4w)	115.8(9)	Ce(1)-O(4w)-O(4w')	72(2)
O(81a)-U(2)-O(1)#1	130.2(3)	O(2w)-Ce(1)-O(4w)	71.6(9)	O(4w)-O(4w)-O(3w')	97.1(17)
O(81a)-U(2)-C(8a)	25.3(3)	O(2w)#2-Ce(1)-O(3w')	67.7(9)	O(4w)#3-O(4w)-O(4w')	131(3)
O(81a)-U(2)-C(8a)#1	140.1(3)	O(2w)-Ce(1)-O(3w')	88.2(9)	O(3w')#2-O(4w)-O(4w')	124(3)
O(81a)#1-U(2)-O(2u)	86.6(4)	O(2w)#2-Ce(1)-O(2w')	103.3(9)	Ce(1)-O(3w')-O(3w)	74.9(17)
O(81a)-U(2)-O(2u)	93.7(4)	O(2w)-Ce(1)-O(2w')	32.0(9)	Ce(1)-O(3w')-O(4w)#2	70.3(11)
O(81a)#1-U(2)-O(1)	130.2(3)	O(2w)#2-Ce(1)-O(4w')	139.6(10)	O(3w)-O(3w')-O(4w)#2	145(2)
O(81a)#1-U(2)-O(1)#1	64.4(3)	O(2w)-Ce(1)-O(4w')	62.4(9)	Ce(1)-O(2w')-O(2w)	77.2(17)
O(81a)#1-U(2)-C(8a)	140.1(3)	C(1b)-Ce(1)-C(1b)#2	138.8(3)	Ce(1)-O(2w')-O(3w)	73.5(12)
O(81a)-U(2)-C(8a)	25.3(3)	C(1b)-Ce(1)-O(3w)	137.2(5)	O(2w)-O(2w')-O(3w)	145(2)
O(2u)-U(2)-O(2u)#1	178.0(4)	C(1b)-Ce(1)-O(3w)#2	81.0(5)	Ce(1)-O(4w')-O(4w)	84(2)

Table 0.6 Bond valence calculation for complex CeUpht.

Atom	Atom bond	Bond length	Bond valence [vu]	Atom valence [vu]
U1	U(1)-O(82b)	2,58	0,36	6,47
	U(1)-O(82b)#1	2,58	0,36	
	U(1)-O(1u)	1,73	1,86	
	U(1)-O(1u)#1	1,73	1,86	
	U(1)-O(81b)	2,64	0,32	
	U(1)-O(81b)#1	2,64	0,32	
	U(1)-O(1)	2,24	0,69	
	U(1)-O(1)#1	2,24	0,69	
U2	U(2)-O(82a)	2,55	0,38	6,58
	U(2)-O(82a)#1	2,55	0,38	
	U(2)-O(81a)	2,58	0,36	
	U(2)-O(81a)#1	2,58	0,36	
	U(2)-O(2u)	1,72	1,89	
	U(2)-O(2u)#1	1,72	1,89	
	U(2)-O(1)	2,27	0,66	
	U(2)-O(1)#1	2,27	0,66	
U3	U(3)-O(31u)	1,78	1,69	6,32
	U(3)-O(12b)	2,38	0,53	
	U(3)-O(11a)	2,32	0,60	
	U(3)-O(81a)	2,38	0,53	
	U(3)-O(32u)	1,77	1,72	
	U(3)-O(81b)	2,41	0,50	
	U(3)-O(1)	2,20	0,75	
Ce1	Ce(1)-O(1w)	2,59	0,27	2,66
	Ce(1)-O(11b)	2,53	0,32	
	Ce(1)-O(11b)#2	2,53	0,32	
	Ce(1)-O(2w)	2,48	0,36	
	Ce(1)-O(2w)#2	2,48	0,36	
	Ce(1)-O(3w)	2,56	0,29	
	Ce(1)-O(3w)#2	2,56	0,29	
	Ce(1)-O(4w)	2,66	0,22	
	Ce(1)-O(4w)#2	2,66	0,22	
O1	U(1)-O(1)	2,24	0,69	2,10
	U(2)-O(1)	2,27	0,66	
	U(3)-O(1)	2,20	0,75	
O11a	U(3)-O(11a)	2,32	0,60	2,02
	O(11a)-C(1a)	1,26	1,42	
O11b	Ce(1)-O(11b)	2,53	0,44	2,07
	O(11b)-C(1b)	1,21	1,63	
O12a	O(12a)-C(1a)	1,27	1,26	1,26
O12b	U(3)-O(12b)	2,38	0,53	1,81
	O(12b)-C(1b)	1,30	1,28	
O1u	U(1)-O(1u)	1,73	1,86	1,86
O1w	Ce(1)-O(1w)	2,59	0,27	0,27
O2u	U(2)-O(2u)	1,72	1,89	1,89
O2w	Ce(1)-O(2w)	2,48	0,36	0,36
O31u	U(3)-O(31u)	1,78	1,69	1,69
O32u	U(3)-O(32u)	1,77	1,72	1,72
O3w	Ce(1)-O(3w)	2,56	0,29	0,29
O4w	Ce(1)-O(4w)	2,66	0,22	0,22
O81a	U(2)-O(81a)	2,58	0,36	2,24
	U(3)-O(81a)	2,38	0,53	
	O(81a)-C(8a)	1,28	1,35	
O81b	U(1)-O(81b)	2,64	0,32	2,13
	U(3)-O(81b)	2,41	0,50	
	O(81b)-C(8b)	1,29	1,31	
O82a	U(2)-O(82a)	2,55	0,38	1,80
	O(82a)-C(8a)	1,26	1,42	
O82b	U(1)-O(82b)	2,58	0,36	1,67
	O(82b)-C(8b)	1,29	1,31	

Table 0.7 Atomic coordinates (x10⁴) and equivalent isotropic displacement parameters (A²x10³) for complex NdUpht.

Atom	x	y	z	U(eq)
U(1)	7500	8413(1)	2500	20(1)
U(2)	7500	6526(1)	2500	19(1)
U(3)	5335(1)	7463(1)	2175(1)	21(1)
Nd(1)	2500	8076(1)	-2500	22(1)
O(31u)	5370(4)	7488(3)	4629(9)	37(2)
O(12b)	4202(4)	8235(3)	2203(9)	28(3)
O(82a)	6630(5)	5451(3)	2383(11)	33(2)
O(82b)	6606(4)	9500(3)	2446(9)	22(2)
O(11a)	4246(4)	6685(3)	1987(10)	37(3)
O(1w)	2500	9350(5)	-2500	58(5)
C(2a)	4339(6)	5526(4)	2865(14)	22(3)
C(3b)	3636(6)	9856(5)	1737(13)	29(4)
O(12a)	3698(6)	6387(4)	4522(14)	72(4)
O(81a)	5902(4)	6367(3)	2507(10)	28(3)
O(1u)	7553(4)	8454(3)	66(9)	30(3)
O(32u)	5225(4)	7452(3)	-322(8)	29(2)
O(81b)	5864(4)	8590(3)	1929(8)	26(2)
C(7b)	5126(6)	9635(4)	2219(13)	18(3)
O(2u)	7451(4)	6500(3)	49(9)	31(3)
O(1)	6711(4)	7484(3)	2266(10)	31(2)
O(11b)	3707(4)	8633(3)	-551(10)	38(3)
C(4b)	3730(8)	0460(5)	2359(15)	37(4)
C(5b)	4538(7)	0699(5)	2982(15)	39(5)
C(2b)	4290(6)	9417(4)	1653(13)	20(3)
C(7a)	5153(6)	5311(4)	2519(12)	17(3)
C(4a)	3821(7)	4431(5)	2725(15)	37(4)
C(6a)	5238(6)	4654(4)	2227(14)	29(4)
C(6b)	5203(7)	0269(4)	2928(14)	31(4)
C(1a)	4107(6)	6257(5)	3219(18)	39(5)
C(3a)	3709(6)	5085(4)	3046(13)	30(4)
C(8b)	5889(6)	9243(4)	2195(12)	19(3)
C(8a)	5932(7)	5704(4)	2485(14)	25(4)
C(5a)	4586(7)	4194(5)	2350(14)	35(4)
O(2w)	1134(10)	7615(7)	-1770(20)	57(3)
O(2w')	1445(10)	7190(8)	-2660(20)	57(3)
N(1)	7500	4109(9)	2500	102(6)
O(3w)	2185(9)	7088(7)	-4530(20)	45(3)
O(3w')	2387(9)	7392(7)	-5540(20)	45(3)
C(1b)	4074(6)	8716(5)	1036(14)	24(3)
O(4w)	2220(12)	8345(9)	880(30)	72(4)
O(4w')	1732(12)	8610(9)	130(30)	72(4)

Table 0.8 Bond lengths for complex NdUpht.

Bond	Bond length	Bond	Bond length
U(1)-U(2)	3.772(1)	O(82a)-O(81a)	2.18(1)
U(1)-U(3)	3.9315(4)	O(82a)-C(7a)	2.39(1)
U(1)-U(3)#1	3.9315(4)	O(82a)-C(8a)	1.23(1)
U(1)-O(82b)	2.60(1)	O(82b)-O(81b)	2.18(1)
U(1)-O(82b)#1	2.60(1)	O(82b)-C(7b)	2.37(1)
U(1)-O(1u)	1.76(1)	O(82b)-C(8b)	1.25(1)
U(1)-O(1u)#1	1.76 (1)	O(11a)-C(2a)	2.40(1)
U(1)-O(81b)	2.63(1)	O(11a)-O(12a)	2.18(1)
U(1)-O(81b)#1	2.63(1)	O(11a)-C(1a)	1.27(1)
U(1)-O(1)	2.24(1)	C(2a)-O(12a)	2.38(1)
U(1)-O(1)#1	2.24(1)	C(2a)-C(7a)	1.41(1)
U(1)-C(8b)	3.05(1)	C(2a)-C(4a)	2.34(1)
U(1)-C(8b)#1	3.05(1)	C(2a)-C(6a)	2.33(1)
U(2)-U(3)	3.9186(4)	C(2a)-C(1a)	1.53(1)
U(2)-U(3)#1	3.9186(4)	C(2a)-C(3a)	1.35(1)
U(2)-O(82a)	2.56(1)	C(3b)-C(7b)	2.41(1)

Bond	Bond length	Bond	Bond length
U(2)-O(82a)#1	2.56(1)	C(3b)-C(4b)	1.29(1)
U(2)-O(81a)	2.57(1)	C(3b)-C(5b)	2.34(1)
U(2)-O(81a)#1	2.57(1)	C(3b)-C(2b)	1.37(1)
U(2)-O(2u)	1.76(1)	C(3b)-C(1b)	2.45(1)
U(2)-O(2u)#1	1.76(1)	O(12a)-C(1a)	1.22(2)
U(2)-O(1)	2.29 (1)	O(81a)-C(7a)	2.43(1)
U(2)-O(1)#1	2.29 (1)	O(81a)-C(8a)	1.33(1)
U(2)-C(8a)	2.99(1)	O(81b)-C(7b)	2.42(1)
U(2)-C(8a)#1	2.99(1)	O(81b)-C(8b)	1.32(1)
U(3)-Nd(1)	5.516(1)	C(7b)-C(5b)	2.41(1)
U(3)-O(31u)	1.76(1)	C(7b)-C(2b)	1.43(1)
U(3)-O(12b)	2.38(1)	C(7b)-C(6b)	1.37(1)
U(3)-O(11a)	2.33(1)	C(7b)-C(8b)	1.45(1)
U(3)-O(81a)	2.37(1)	O(11b)-C(2b)	2.36(1)
U(3)-O(32u)	1.79(1)	O(11b)-C(1b)	1.25(1)
U(3)-O(81b)	2.42(1)	C(4b)-C(5b)	1.41(2)
U(3)-O(1)	2.19(1)	C(4b)-C(2b)	2.34(1)
U(3)-C(1a)	3.24(1)	C(4b)-C(6b)	2.38(2)
U(3)-C(8b)	3.67(1)	C(5b)-C(6b)	1.37(2)
U(3)-C(8a)	3.64 (1)	C(2b)-C(6b)	2.37(1)
U(3)-C(1b)	3.27(1)	C(2b)-C(1b)	1.50(1)
Nd(1)-O(1w)	2.55(1)	C(7a)-C(6a)	1.34(1)
Nd(1)-O(11b)	2.53(1)	C(7a)-C(3a)	2.41(1)
Nd(1)-O(11b)#2	2.53(1)	C(7a)-C(8a)	1.47(1)
Nd(1)-O(2w)	2.47(2)	C(7a)-C(5a)	2.41(1)
Nd(1)-O(2w)#2	2.47(2)	C(4a)-C(6a)	2.37(2)
Nd(1)-O(3w)	2.48(1)	C(4a)-C(3a)	1.34(1)
Nd(1)-O(3w)#2	2.48(1)	C(4a)-C(5a)	1.36(2)
Nd(1)-C(1b)	3.64(1)	C(6a)-C(8a)	2.37(1)
Nd(1)-C(1b)#2	3.64(1)	C(6a)-C(5a)	1.40(1)
Nd(1)-O(4w)	2.57(2)	C(6b)-C(8b)	2.41(1)
Nd(1)-O(4w)#2	2.57(2)	C(1a)-C(3a)	2.43(1)
O(12b)-O(11b)	2.21(1)	C(3a)-C(5a)	2.35(1)
O(12b)-C(2b)	2.40(1)	O(4w)-O(4w)#3	2.42(3)
O(12b)-C(1b)	1.28(1)		

Table 0.9 Bond Angles for complex NdUpht.

Bond	Angle [°]	Bond	Angle [°]	Bond	Angle [°]
U(2)-U(1)-U(3)	61.19(1)	O(31u)-U(3)-O(32u)	176.1(3)	O(82a)-O(81a)-C(7a)	62.2(3)
U(2)-U(1)-U(3)#1	61.19(1)	O(31u)-U(3)-O(81b)	93.9(2)	O(82a)-O(81a)-C(8a)	30.5(5)
U(2)-U(1)-O(82b)	146.8(1)	O(31u)-U(3)-O(1)	91.9(3)	C(7a)-O(81a)-C(8a)	31.7(6)
U(2)-U(1)-O(82b)#1	146.8(1)	O(31u)-U(3)-C(1a)	75.6(3)	U(1)-O(81b)-U(3)	102.2(2)
U(2)-U(1)-O(1u)	92.6(2)	O(31u)-U(3)-C(8b)	89.1(2)	U(1)-O(81b)-O(82b)	64.6(2)
U(2)-U(1)-O(1u)#1	92.6(2)	O(31u)-U(3)-C(8a)	89.0(3)	U(1)-O(81b)-C(7b)	126.0(3)
U(2)-U(1)-O(81b)	97.7(1)	O(31u)-U(3)-C(1b)	100.9(3)	U(1)-O(81b)-C(8b)	95.4(5)
U(2)-U(1)-O(81b)#1	97.7(1)	O(12b)-U(3)-O(11a)	82.5(2)	U(3)-O(81b)-O(82b)	162.0(3)
U(2)-U(1)-O(1)	34.1(2)	O(12b)-U(3)-O(81a)	151.8(2)	U(3)-O(81b)-C(7b)	128.5(4)
U(2)-U(1)-O(1)#1	34.1(2)	O(12b)-U(3)-O(32u)	90.8(3)	U(3)-O(81b)-C(8b)	156.5(6)
U(2)-U(1)-C(8b)	122.9(2)	O(12b)-U(3)-O(81b)	70.6(2)	O(82b)-O(81b)-C(7b)	61.7(3)
U(2)-U(1)-C(8b)#1	122.9(2)	O(12b)-U(3)-O(1)	138.4(2)	O(82b)-O(81b)-C(8b)	31.0(5)
U(3)-U(1)-U(3)#1	122.22(1)	O(12b)-U(3)-C(1a)	90.2(2)	C(7b)-O(81b)-C(8b)	30.8(5)
U(3)-U(1)-O(82b)	85.7(1)	O(12b)-U(3)-C(8b)	63.5(2)	O(82b)-C(7b)-C(3b)	174.1(5)
U(3)-U(1)-O(82b)#1	152.1(1)	O(12b)-U(3)-C(8a)	145.1(2)	O(82b)-C(7b)-O(81b)	54.3(3)
U(3)-U(1)-O(1u)	95.0(2)	O(12b)-U(3)-C(1b)	19.0(2)	O(82b)-C(7b)-C(5b)	119.5(5)
U(3)-U(1)-O(1u)#1	87.5(2)	O(11a)-U(3)-O(81a)	70.4(2)	O(82b)-C(7b)-C(2b)	152.3(7)
U(3)-U(1)-O(81b)	37.0(1)	O(11a)-U(3)-O(32u)	86.1(3)	O(82b)-C(7b)-C(6b)	91.5(7)
U(3)-U(1)-O(81b)#1	158.3(1)	O(11a)-U(3)-O(81b)	151.9(2)	O(82b)-C(7b)-C(8b)	26.5(4)
U(3)-U(1)-O(1)	27.2(2)	O(11a)-U(3)-O(1)	139.1(2)	C(3b)-C(7b)-O(81b)	128.9(5)
U(3)-U(1)-O(1)#1	95.1(2)	O(11a)-U(3)-C(1a)	18.4(3)	C(3b)-C(7b)-C(5b)	58.1(4)
U(3)-U(1)-C(8b)	61.8(2)	O(11a)-U(3)-C(8b)	145.8(2)	C(3b)-C(7b)-C(2b)	29.7(5)
U(3)-U(1)-C(8b)#1	175.9(2)	O(11a)-U(3)-C(8a)	63.2(2)	C(3b)-C(7b)-C(6b)	86.4(7)
U(3)#1-U(1)-O(82b)	152.1(1)	O(11a)-U(3)-C(1b)	93.4(2)	C(3b)-C(7b)-C(8b)	156.3(7)

Bond	Angle [°]	Bond	Angle [°]	Bond	Angle [°]
U(3)#1-U(1)-O(82b)#1	85.7(1)	O(81a)-U(3)-O(32u)	95.2(3)	O(81b)-C(7b)-C(5b)	170.5(5)
U(3)#1-U(1)-O(1u)	87.5(2)	O(81a)-U(3)-O(81b)	137.3(2)	O(81b)-C(7b)-C(2b)	99.3(5)
U(3)#1-U(1)-O(1u)#1	95.0(2)	O(81a)-U(3)-O(1)	69.1(2)	O(81b)-C(7b)-C(6b)	143.7(7)
U(3)#1-U(1)-O(81b)	158.38(1)	O(81a)-U(3)-C(1a)	61.6(2)	O(81b)-C(7b)-C(8b)	27.7(4)
U(3)#1-U(1)-O(81b)#1	37.0(1)	O(81a)-U(3)-C(8b)	143.7(2)	C(5b)-C(7b)-C(2b)	87.7(6)
U(3)#1-U(1)-O(1)	95.1(2)	O(81a)-U(3)-C(8a)	7.4(2)	C(5b)-C(7b)-C(6b)	28.3(6)
U(3)#1-U(1)-O(1)#1	27.2(2)	O(81a)-U(3)-C(1b)	162.2(2)	C(5b)-C(7b)-C(8b)	145.7(7)
U(3)#1-U(1)-C(8b)	175.9(2)	O(32u)-U(3)-O(81b)	86.5(2)	C(2b)-C(7b)-C(6b)	116.0(9)
U(3)#1-U(1)-C(8b)#1	61.8(2)	O(32u)-U(3)-O(1)	91.9(3)	C(2b)-C(7b)-C(8b)	126.6(7)
O(82b)-U(1)-O(82b)#1	66.5(2)	O(32u)-U(3)-C(1a)	102.7(3)	C(6b)-C(7b)-C(8b)	117.3(9)
O(82b)-U(1)-O(1u)	91.4(2)	O(32u)-U(3)-C(8b)	90.9(2)	U(1)-O(1)-U(2)	112.7(3)
O(82b)-U(1)-O(1u)#1	84.2(2)	O(32u)-U(3)-C(8a)	92.9(2)	U(1)-O(1)-U(3)	124.9(3)
O(82b)-U(1)-O(81b)	49.4(2)	O(32u)-U(3)-C(1b)	76.0(3)	U(2)-O(1)-U(3)	121.9(3)
O(82b)-U(1)-O(81b)#1	115.3(2)	O(81b)-U(3)-O(1)	68.2(2)	Nd(1)-O(11b)-O(12b)	121.8(3)
O(82b)-U(1)-O(1)	112.8(2)	O(81b)-U(3)-C(1a)	158.9(2)	Nd(1)-O(11b)-C(2b)	153.7(4)
O(82b)-U(1)-O(1)#1	176.5(2)	O(81b)-U(3)-C(8b)	8.3(2)	Nd(1)-O(11b)-C(1b)	146.6(6)
O(82b)-U(1)-C(8b)	23.9(2)	O(81b)-U(3)-C(8a)	144.3(2)	O(12b)-O(11b)-C(2b)	63.3(3)
O(82b)-U(1)-C(8b)#1	90.3(2)	O(81b)-U(3)-C(1b)	58.6(2)	O(12b)-O(11b)-C(1b)	29.3(5)
O(82b)#1-U(1)-O(1u)	84.2(2)	O(1)-U(3)-C(1a)	129.4(2)	C(2b)-O(11b)-C(1b)	34.1(5)
O(82b)#1-U(1)-O(1u)#1	91.4(2)	O(1)-U(3)-C(8b)	74.9(2)	C(3b)-C(4b)-C(5b)	120.0(11)
O(82b)#1-U(1)-O(81b)	115.2(2)	O(1)-U(3)-C(8a)	76.2(2)	C(3b)-C(4b)-C(2b)	29.2(6)
O(82b)#1-U(1)-O(81b)#1	49.4(2)	O(1)-U(3)-C(1b)	125.7(2)	C(3b)-C(4b)-C(6b)	89.4(8)
O(82b)#1-U(1)-O(1)	176.5(2)	C(1a)-U(3)-C(8b)	150.7(2)	C(5b)-C(4b)-C(2b)	90.8(7)
O(82b)#1-U(1)-O(1)#1	112.8(2)	C(1a)-U(3)-C(8a)	55.2(2)	C(5b)-C(4b)-C(6b)	30.6(5)
O(82b)#1-U(1)-C(8b)	90.3(2)	C(1a)-U(3)-C(1b)	104.9(2)	C(2b)-C(4b)-C(6b)	60.2(4)
O(82b)#1-U(1)-C(8b)#1	23.9(2)	C(8b)-U(3)-C(8a)	151.0(2)	C(3b)-C(5b)-C(7b)	61.0(4)
O(1u)-U(1)-O(1u)#1	174.7(3)	C(8b)-U(3)-C(1b)	53.1(2)	C(3b)-C(5b)-C(4b)	28.6(5)
O(1u)-U(1)-O(81b)	88.8(2)	C(8a)-U(3)-C(1b)	155.0(2)	C(3b)-C(5b)-C(6b)	89.3(7)
O(1u)-U(1)-O(81b)#1	90.5(2)	U(3)-Nd(1)-U(3)#2	154.32(2)	C(7b)-C(5b)-C(4b)	89.6(7)
O(1u)-U(1)-O(1)	92.5(3)	U(3)-Nd(1)-O(1w)	102.84(1)	C(7b)-C(5b)-C(6b)	28.3(5)
O(1u)-U(1)-O(1)#1	91.9(3)	U(3)-Nd(1)-O(11b)	38.9(1)	C(4b)-C(5b)-C(6b)	117.9(9)
O(1u)-U(1)-C(8b)	91.3(3)	U(3)-Nd(1)-O(11b)#2	166.8(1)	O(12b)-C(2b)-C(3b)	124.5(7)
O(1u)-U(1)-C(8b)#1	85.8(3)	U(3)-Nd(1)-O(2w)	118.5(3)	O(12b)-C(2b)-C(7b)	108.7(6)
O(1u)#1-U(1)-O(81b)	90.5(2)	U(3)-Nd(1)-O(2w)#2	50.0(3)	O(12b)-C(2b)-O(11b)	55.4(3)
O(1u)#1-U(1)-O(81b)#1	88.8(2)	U(3)-Nd(1)-O(3w)	106.9(3)	O(12b)-C(2b)-C(4b)	144.1(6)
O(1u)#1-U(1)-O(1)	91.9(3)	U(3)-Nd(1)-O(3w)#2	49.8(3)	O(12b)-C(2b)-C(6b)	133.4(5)
O(1u)#1-U(1)-O(1)#1	92.5(3)	U(3)-Nd(1)-C(1b)	34.7(2)	O(12b)-C(2b)-C(1b)	27.7(4)
O(1u)#1-U(1)-C(8b)	85.8(3)	U(3)-Nd(1)-C(1b)#2	168.0(2)	C(3b)-C(2b)-C(7b)	119.2(8)
O(1u)#1-U(1)-C(8b)#1	91.3(3)	U(3)-Nd(1)-O(4w)	71.0(4)	C(3b)-C(2b)-O(11b)	101.6(6)
O(81b)-U(1)-O(81b)#1	164.6(2)	U(3)-Nd(1)-O(4w)#2	114.7(4)	C(3b)-C(2b)-C(4b)	27.4(5)
O(81b)-U(1)-O(1)	63.7(2)	U(3)#2-Nd(1)-O(1w)	102.84(1)	C(3b)-C(2b)-C(6b)	88.1(6)
O(81b)-U(1)-O(1)#1	131.8(2)	U(3)#2-Nd(1)-O(11b)	166.8(1)	C(3b)-C(2b)-C(1b)	117.2(8)
O(81b)-U(1)-C(8b)	25.5(2)	U(3)#2-Nd(1)-O(11b)#2	38.9(1)	C(7b)-C(2b)-O(11b)	134.0(7)
O(81b)-U(1)-C(8b)#1	139.2(2)	U(3)#2-Nd(1)-O(2w)	50.0(3)	C(7b)-C(2b)-C(4b)	91.8(6)
O(81b)#1-U(1)-O(1)	131.8(2)	U(3)#2-Nd(1)-O(2w)#2	118.5(3)	C(7b)-C(2b)-C(6b)	31.2(5)
O(81b)#1-U(1)-O(1)#1	63.7(2)	U(3)#2-Nd(1)-O(3w)	49.8(3)	C(7b)-C(2b)-C(1b)	123.5(8)
O(81b)#1-U(1)-C(8b)	139.2(2)	U(3)#2-Nd(1)-O(3w)#2	106.9(3)	O(11b)-C(2b)-C(4b)	127.1(5)
O(81b)#1-U(1)-C(8b)#1	25.5(2)	U(3)#2-Nd(1)-C(1b)	168.0(2)	O(11b)-C(2b)-C(6b)	158.0(6)
O(1)-U(1)-O(1)#1	68.1(2)	U(3)#2-Nd(1)-C(1b)#2	34.7(1)	O(11b)-C(2b)-C(1b)	27.8(4)
O(1)-U(1)-C(8b)	88.9(2)	U(3)#2-Nd(1)-O(4w)	114.7(4)	C(4b)-C(2b)-C(6b)	60.7(4)
O(1)-U(1)-C(8b)#1	156.9(2)	U(3)#2-Nd(1)-O(4w)#2	71.0(4)	C(4b)-C(2b)-C(1b)	144.4(7)
O(1)#1-U(1)-C(8b)	156.9(2)	O(1w)-Nd(1)-O(11b)	63.9(1)	C(6b)-C(2b)-C(1b)	154.4(7)
O(1)#1-U(1)-C(8b)#1	88.9(2)	O(1w)-Nd(1)-O(11b)#2	63.9(1)	O(82a)-C(7a)-C(2a)	154.2(6)
C(8b)-U(1)-C(8b)#1	114.1(2)	O(1w)-Nd(1)-O(2w)	111.9(3)	O(82a)-C(7a)-O(81a)	53.7(3)
U(1)-U(2)-U(3)	61.45(1)	O(1w)-Nd(1)-O(2w)#2	111.9(3)	O(82a)-C(7a)-C(6a)	89.6(6)
U(1)-U(2)-U(3)#1	61.45(1)	O(1w)-Nd(1)-O(3w)	142.8(3)	O(82a)-C(7a)-C(3a)	172.1(5)
U(1)-U(2)-O(82a)	147.2(2)	O(1w)-Nd(1)-O(3w)#2	142.8(3)	O(82a)-C(7a)-C(8a)	25.5(4)
U(1)-U(2)-O(82a)#1	147.2(2)	O(1w)-Nd(1)-C(1b)	69.4(2)	O(82a)-C(7a)-C(5a)	118.4(5)
U(1)-U(2)-O(81a)	97.1(1)	O(1w)-Nd(1)-C(1b)#2	69.4(2)	C(2a)-C(7a)-O(81a)	101.4(5)
U(1)-U(2)-O(81a)#1	97.1(1)	O(1w)-Nd(1)-O(4w)	77.9(4)	C(2a)-C(7a)-C(6a)	115.8(8)
U(1)-U(2)-O(2u)	91.7(2)	O(1w)-Nd(1)-O(4w)#2	77.9(4)	C(2a)-C(7a)-C(3a)	28.5(4)
U(1)-U(2)-O(2u)#1	91.7(2)	O(11b)-Nd(1)-O(11b)#2	127.8(2)	C(2a)-C(7a)-C(8a)	129.3(8)
U(1)-U(2)-O(1)	33.2(2)	O(11b)-Nd(1)-O(2w)	133.4(4)	C(2a)-C(7a)-C(5a)	86.7(6)

Bond	Angle [°]	Bond	Angle [°]	Bond	Angle [°]
U(1)-U(2)-O(1)#1	33.2(2)	O(11b)-Nd(1)-O(2w)#2	69.0(4)	O(81a)-C(7a)-C(6a)	142.7(8)
U(1)-U(2)-C(8a)	123.3(2)	O(11b)-Nd(1)-O(3w)	141.1(4)	O(81a)-C(7a)-C(3a)	129.9(4)
U(1)-U(2)-C(8a)#1	123.3(2)	O(11b)-Nd(1)-O(3w)#2	85.5(3)	O(81a)-C(7a)-C(8a)	28.2(4)
U(3)-U(2)-U(3)#1	122.90(1)	O(11b)-Nd(1)-C(1b)	10.9(2)	O(81a)-C(7a)-C(5a)	171.7(5)
U(3)-U(2)-O(82a)	85.8(2)	O(11b)-Nd(1)-C(1b)#2	132.3(2)	C(6a)-C(7a)-C(3a)	87.3(6)
U(3)-U(2)-O(82a)#1	151.3(2)	O(11b)-Nd(1)-O(4w)	64.9(4)	C(6a)-C(7a)-C(8a)	115.0(9)
U(3)-U(2)-O(81a)	35.8(1)	O(11b)-Nd(1)-O(4w)#2	104.0(4)	C(6a)-C(7a)-C(5a)	29.1(5)
U(3)-U(2)-O(81a)#1	158.2(1)	O(11b)#2-Nd(1)-O(2w)	69.0(4)	C(3a)-C(7a)-C(8a)	157.3(7)
U(3)-U(2)-O(2u)	89.9(2)	O(11b)#2-Nd(1)-O(2w)#2	133.4(4)	C(3a)-C(7a)-C(5a)	58.3(4)
U(3)-U(2)-O(2u)#1	91.7(2)	O(11b)#2-Nd(1)-O(3w)	85.5(3)	C(8a)-C(7a)-C(5a)	143.9(7)
U(3)-U(2)-O(1)	28.4(2)	O(11b)#2-Nd(1)-O(3w)#2	141.1(4)	C(2a)-C(4a)-C(6a)	59.4(4)
U(3)-U(2)-O(1)#1	94.6(2)	O(11b)#2-Nd(1)-C(1b)	132.3(2)	C(2a)-C(4a)-C(3a)	29.9(5)
U(3)-U(2)-C(8a)	61.9(2)	O(11b)#2-Nd(1)-C(1b)#2	10.9(2)	C(2a)-C(4a)-C(5a)	90.8(7)
U(3)-U(2)-C(8a)#1	174.3(2)	O(11b)#2-Nd(1)-O(4w)	104.0(4)	C(6a)-C(4a)-C(3a)	89.3(7)
U(3)#1-U(2)-O(82a)	151.3(2)	O(11b)#2-Nd(1)-O(4w)#2	64.9(4)	C(6a)-C(4a)-C(5a)	31.4(5)
U(3)#1-U(2)-O(82a)#1	85.8(2)	O(2w)-Nd(1)-O(2w)#2	136.2(5)	C(3a)-C(4a)-C(5a)	120.7(10)
U(3)#1-U(2)-O(81a)	158.2(1)	O(2w)-Nd(1)-O(3w)	72.2(5)	C(2a)-C(6a)-C(7a)	33.1(5)
U(3)#1-U(2)-O(81a)#1	35.8(1)	O(2w)-Nd(1)-O(3w)#2	73.2(5)	C(2a)-C(6a)-C(4a)	59.7(4)
U(3)#1-U(2)-O(2u)	91.7(2)	O(2w)-Nd(1)-C(1b)	123.2(4)	C(2a)-C(6a)-C(8a)	67.3(4)
U(3)#1-U(2)-O(2u)#1	89.9(2)	O(2w)-Nd(1)-C(1b)#2	73.4(4)	C(2a)-C(6a)-C(5a)	90.2(7)
U(3)#1-U(2)-O(1)	94.6(2)	O(2w)-Nd(1)-O(4w)	68.9(5)	C(7a)-C(6a)-C(4a)	92.8(7)
U(3)#1-U(2)-O(1)#1	28.4(2)	O(2w)-Nd(1)-O(4w)#2	121.0(5)	C(7a)-C(6a)-C(8a)	34.3(5)
U(3)#1-U(2)-C(8a)	174.3(2)	O(2w)#2-Nd(1)-O(3w)	73.2(5)	C(7a)-C(6a)-C(5a)	123.2(9)
U(3)#1-U(2)-C(8a)#1	61.9(2)	O(2w)#2-Nd(1)-O(3w)#2	72.2(5)	C(4a)-C(6a)-C(8a)	126.9(5)
O(82a)-U(2)-O(82a)#1	65.6(2)	O(2w)#2-Nd(1)-C(1b)	73.4(4)	C(4a)-C(6a)-C(5a)	30.5(5)
O(82a)-U(2)-O(81a)	50.2(2)	O(2w)#2-Nd(1)-C(1b)#2	123.2(4)	C(8a)-C(6a)-C(5a)	157.2(8)
O(82a)-U(2)-O(81a)#1	115.6(2)	O(2w)#2-Nd(1)-O(4w)	121.0(5)	C(7b)-C(6b)-C(4b)	91.8(7)
O(82a)-U(2)-O(2u)	88.3(3)	O(2w)#2-Nd(1)-O(4w)#2	68.9(5)	C(7b)-C(6b)-C(5b)	123.3(10)
O(82a)-U(2)-O(2u)#1	88.9(3)	O(3w)-Nd(1)-O(3w)#2	74.4(5)	C(7b)-C(6b)-C(2b)	32.8(5)
O(82a)-U(2)-O(1)	114.0(2)	O(3w)-Nd(1)-C(1b)	141.3(4)	C(7b)-C(6b)-C(8b)	32.3(5)
O(82a)-U(2)-O(1)#1	177.7(2)	O(3w)-Nd(1)-C(1b)#2	77.2(4)	C(4b)-C(6b)-C(5b)	31.6(6)
O(82a)-U(2)-C(8a)	24.0(2)	O(3w)-Nd(1)-O(4w)	132.9(5)	C(4b)-C(6b)-C(2b)	59.1(4)
O(82a)-U(2)-C(8a)#1	89.5(2)	O(3w)-Nd(1)-O(4w)#2	69.7(5)	C(4b)-C(6b)-C(8b)	124.2(5)
O(82a)#1-U(2)-O(81a)	115.6(2)	O(3w)#2-Nd(1)-C(1b)	77.2(4)	C(5b)-C(6b)-C(2b)	90.7(7)
O(82a)#1-U(2)-O(81a)#1	50.2(2)	O(3w)#2-Nd(1)-C(1b)#2	141.3(4)	C(5b)-C(6b)-C(8b)	155.7(8)
O(82a)#1-U(2)-O(2u)	88.9(3)	O(3w)#2-Nd(1)-O(4w)	69.7(5)	C(2b)-C(6b)-C(8b)	65.1(4)
O(82a)#1-U(2)-O(2u)#1	88.3(3)	O(3w)#2-Nd(1)-O(4w)#2	132.9(5)	U(3)-C(1a)-O(11a)	35.4(4)
O(82a)#1-U(2)-O(1)	177.7(2)	C(1b)-Nd(1)-C(1b)#2	138.8(2)	U(3)-C(1a)-C(2a)	120.6(6)
O(82a)#1-U(2)-O(1)#1	114.0(2)	C(1b)-Nd(1)-O(4w)	55.6(4)	U(3)-C(1a)-O(12a)	113.5(7)
O(82a)#1-U(2)-C(8a)	89.5(2)	C(1b)-Nd(1)-O(4w)#2	114.7(4)	U(3)-C(1a)-C(3a)	150.1(5)
O(82a)#1-U(2)-C(8a)#1	24.0(2)	C(1b)#2-Nd(1)-O(4w)	114.7(4)	O(11a)-C(1a)-C(2a)	117.7(10)
O(81a)-U(2)-O(81a)#1	165.8(2)	C(1b)#2-Nd(1)-O(4w)#2	55.6(4)	O(11a)-C(1a)-O(12a)	122.4(9)
O(81a)-U(2)-O(2u)	92.8(3)	O(4w)-Nd(1)-O(4w)#2	155.9(6)	O(11a)-C(1a)-C(3a)	132.7(9)
O(81a)-U(2)-O(2u)#1	86.8(3)	U(3)-O(12b)-O(11b)	115.7(3)	C(2a)-C(1a)-O(12a)	119.0(10)
O(81a)-U(2)-O(1)	64.2(2)	U(3)-O(12b)-C(2b)	125.5(4)	C(2a)-C(1a)-C(3a)	30.5(5)
O(81a)-U(2)-O(1)#1	129.9(2)	U(3)-O(12b)-C(1b)	123.8(6)	O(12a)-C(1a)-C(3a)	95.1(7)
O(81a)-U(2)-C(8a)	26.2(2)	O(11b)-O(12b)-C(2b)	61.3(3)	C(2a)-C(3a)-C(7a)	29.9(5)
O(81a)-U(2)-C(8a)#1	139.6(2)	O(11b)-O(12b)-C(1b)	28.4(5)	C(2a)-C(3a)-C(4a)	120.4(9)
O(81a)#1-U(2)-O(2u)	86.8(3)	C(2b)-O(12b)-C(1b)	33.0(5)	C(2a)-C(3a)-C(1a)	35.2(5)
O(81a)#1-U(2)-O(2u)#1	92.8(3)	U(2)-O(82a)-O(81a)	65.3(2)	C(2a)-C(3a)-C(5a)	90.6(7)
O(81a)#1-U(2)-O(1)	129.9(2)	U(2)-O(82a)-C(7a)	129.3(3)	C(7a)-C(3a)-C(4a)	90.6(7)
O(81a)#1-U(2)-O(1)#1	64.2(2)	U(2)-O(82a)-C(8a)	98.3(5)	C(7a)-C(3a)-C(1a)	65.1(4)
O(81a)#1-U(2)-C(8a)	139.6(2)	O(81a)-O(82a)-C(7a)	64.1(3)	C(7a)-C(3a)-C(5a)	60.7(4)
O(81a)#1-U(2)-C(8a)#1	26.2(2)	O(81a)-O(82a)-C(8a)	33.1(5)	C(4a)-C(3a)-C(1a)	155.5(8)
O(2u)-U(2)-O(2u)#1	176.7(3)	C(7a)-O(82a)-C(8a)	31.0(5)	C(4a)-C(3a)-C(5a)	29.9(6)
O(2u)-U(2)-O(1)	88.8(3)	U(1)-O(82b)-O(81b)	66.1(2)	C(1a)-C(3a)-C(5a)	125.8(5)
O(2u)-U(2)-O(1)#1	94.0(3)	U(1)-O(82b)-C(7b)	129.8(3)	U(1)-C(8b)-U(3)	70.98(16)
O(2u)-U(2)-C(8a)	91.3(3)	U(1)-O(82b)-C(8b)	98.8(5)	U(1)-C(8b)-O(82b)	57.3(4)
O(2u)-U(2)-C(8a)#1	86.9(3)	O(81b)-O(82b)-C(7b)	64.0(3)	U(1)-C(8b)-O(81b)	59.1(4)
O(2u)#1-U(2)-O(1)	94.0(3)	O(81b)-O(82b)-C(8b)	32.8(4)	U(1)-C(8b)-C(7b)	175.2(6)
O(2u)#1-U(2)-O(1)#1	88.8(3)	C(7b)-O(82b)-C(8b)	31.2(5)	U(1)-C(8b)-C(6b)	147.7(4)
O(2u)#1-U(2)-C(8a)	86.9(3)	U(3)-O(11a)-C(2a)	127.0(4)	U(3)-C(8b)-O(82b)	128.0(6)
O(2u)#1-U(2)-C(8a)#1	91.3(3)	U(3)-O(11a)-O(12a)	119.4(4)	U(3)-C(8b)-O(81b)	15.3(4)

Bond	Angle [°]	Bond	Angle [°]	Bond	Angle [°]
O(1)-U(2)-O(1)#1	66.5(2)	U(3)-O(11a)-C(1a)	126.1(6)	U(3)-C(8b)-C(7b)	108.8(5)
O(1)-U(2)-C(8a)	90.3(2)	C(2a)-O(11a)-O(12a)	62.4(4)	U(3)-C(8b)-C(6b)	135.5(4)
O(1)-U(2)-C(8a)#1	156.0(2)	C(2a)-O(11a)-C(1a)	34.4(6)	O(82b)-C(8b)-O(81b)	116.2(8)
O(1)#1-U(2)-C(8a)	156.0(2)	O(12a)-O(11a)-C(1a)	28.2(6)	O(82b)-C(8b)-C(7b)	122.3(7)
O(1)#1-U(2)-C(8a)#1	90.3(2)	O(11a)-C(2a)-O(12a)	54.3(3)	O(82b)-C(8b)-C(6b)	92.7(6)
C(8a)-U(2)-C(8a)#1	113.5(2)	O(11a)-C(2a)-C(7a)	106.4(6)	O(81b)-C(8b)-C(7b)	121.5(8)
U(1)-U(3)-U(2)	57.44(1)	O(11a)-C(2a)-C(4a)	151.5(5)	O(81b)-C(8b)-C(6b)	150.1(7)
U(1)-U(3)-Nd(1)	126.50(1)	O(11a)-C(2a)-C(6a)	133.9(5)	C(7b)-C(8b)-C(6b)	30.3(5)
U(1)-U(3)-O(31u)	89.0(2)	O(11a)-C(2a)-C(1a)	27.8(5)	U(2)-C(8a)-U(3)	71.63(17)
U(1)-U(3)-O(12b)	110.5(2)	O(11a)-C(2a)-C(3a)	128.7(7)	U(2)-C(8a)-O(82a)	57.6(5)
U(1)-U(3)-O(11a)	167.0(2)	O(12a)-C(2a)-C(7a)	139.0(7)	U(2)-C(8a)-O(81a)	58.9(5)
U(1)-U(3)-O(81a)	96.6(2)	O(12a)-C(2a)-C(4a)	122.1(6)	U(2)-C(8a)-C(7a)	178.4(7)
U(1)-U(3)-O(32u)	93.9(2)	O(12a)-C(2a)-C(6a)	160.3(6)	U(2)-C(8a)-C(6a)	150.5(5)
U(1)-U(3)-O(81b)	40.8(2)	O(12a)-C(2a)-C(1a)	26.6(5)	U(3)-C(8a)-O(82a)	128.7(6)
U(1)-U(3)-O(1)	27.9(2)	O(12a)-C(2a)-C(3a)	93.7(7)	U(3)-C(8a)-O(81a)	13.4(4)
U(1)-U(3)-C(1a)	153.3(2)	C(7a)-C(2a)-C(4a)	92.0(6)	U(3)-C(8a)-C(7a)	107.4(6)
U(1)-U(3)-C(8b)	47.2(2)	C(7a)-C(2a)-C(6a)	31.2(4)	U(3)-C(8a)-C(6a)	137.0(5)
U(1)-U(3)-C(8a)	103.8(2)	C(7a)-C(2a)-C(1a)	124.0(8)	O(82a)-C(8a)-O(81a)	116.4(9)
U(1)-U(3)-C(1b)	99.3(2)	C(7a)-C(2a)-C(3a)	121.6(8)	O(82a)-C(8a)-C(7a)	123.5(7)
U(2)-U(3)-Nd(1)	144.17(1)	C(4a)-C(2a)-C(6a)	60.9(4)	O(82a)-C(8a)-C(6a)	92.9(6)
U(2)-U(3)-O(31u)	90.5(2)	C(4a)-C(2a)-C(1a)	143.9(7)	O(81a)-C(8a)-C(7a)	120.1(9)
U(2)-U(3)-O(12b)	167.5(2)	C(4a)-C(2a)-C(3a)	29.7(5)	O(81a)-C(8a)-C(6a)	150.2(8)
U(2)-U(3)-O(11a)	109.5(2)	C(6a)-C(2a)-C(1a)	155.2(7)	C(7a)-C(8a)-C(6a)	30.8(4)
U(2)-U(3)-O(81a)	39.4(2)	C(6a)-C(2a)-C(3a)	90.5(6)	C(7a)-C(5a)-C(4a)	90.4(7)
U(2)-U(3)-O(32u)	93.2(2)	C(1a)-C(2a)-C(3a)	114.3(8)	C(7a)-C(5a)-C(6a)	27.7(5)
U(2)-U(3)-O(81b)	97.9(2)	C(7b)-C(3b)-C(4b)	92.3(8)	C(7a)-C(5a)-C(3a)	61.0(4)
U(2)-U(3)-O(1)	29.7(2)	C(7b)-C(3b)-C(5b)	60.9(4)	C(4a)-C(5a)-C(6a)	118.1(9)
U(2)-U(3)-C(1a)	100.4(2)	C(7b)-C(3b)-C(2b)	31.1(5)	C(4a)-C(5a)-C(3a)	29.5(5)
U(2)-U(3)-C(8b)	104.6(2)	C(7b)-C(3b)-C(1b)	64.1(4)	C(6a)-C(5a)-C(3a)	88.7(6)
U(2)-U(3)-C(8a)	46.5(2)	C(4b)-C(3b)-C(5b)	31.4(7)	U(3)-C(1b)-Nd(1)	105.9(3)
U(2)-U(3)-C(1b)	154.1(2)	C(4b)-C(3b)-C(2b)	123.4(10)	U(3)-C(1b)-O(12b)	37.2(4)
Nd(1)-U(3)-O(31u)	123.5(2)	C(4b)-C(3b)-C(1b)	156.2(9)	U(3)-C(1b)-C(3b)	147.3(4)
Nd(1)-U(3)-O(12b)	44.0(2)	C(5b)-C(3b)-C(2b)	92.0(6)	U(3)-C(1b)-O(11b)	110.7(6)
Nd(1)-U(3)-O(11a)	63.1(2)	C(5b)-C(3b)-C(1b)	124.9(5)	U(3)-C(1b)-C(2b)	121.5(6)
Nd(1)-U(3)-O(81a)	123.4(2)	C(2b)-C(3b)-C(1b)	33.0(5)	Nd(1)-C(1b)-O(12b)	104.6(6)
Nd(1)-U(3)-O(32u)	52.6(2)	O(11a)-O(12a)-C(2a)	63.4(4)	Nd(1)-C(1b)-C(3b)	106.2(4)
Nd(1)-U(3)-O(81b)	91.2(1)	O(11a)-O(12a)-C(1a)	29.4(6)	Nd(1)-C(1b)-O(11b)	22.5(4)
Nd(1)-U(3)-O(1)	140.9(2)	C(2a)-O(12a)-C(1a)	34.3(6)	Nd(1)-C(1b)-C(2b)	131.3(6)
Nd(1)-U(3)-C(1a)	80.1(2)	U(2)-O(81a)-U(3)	104.8(2)	O(12b)-C(1b)-C(3b)	126.4(7)
Nd(1)-U(3)-C(8b)	88.3(1)	U(2)-O(81a)-O(82a)	64.5(3)	O(12b)-C(1b)-O(11b)	122.3(9)
Nd(1)-U(3)-C(8a)	116.5(2)	U(2)-O(81a)-C(7a)	126.6(3)	O(12b)-C(1b)-C(2b)	119.3(8)
Nd(1)-U(3)-C(1b)	39.3(2)	U(2)-O(81a)-C(8a)	94.9(6)	C(3b)-C(1b)-O(11b)	101.2(6)
O(31u)-U(3)-O(12b)	85.7(3)	U(3)-O(81a)-O(82a)	166.6(4)	C(3b)-C(1b)-C(2b)	29.8(5)
O(31u)-U(3)-O(11a)	91.7(3)	U(3)-O(81a)-C(7a)	128.3(3)	O(11b)-C(1b)-C(2b)	118.1(8)
O(31u)-U(3)-O(81a)	87.1(3)	U(3)-O(81a)-C(8a)	159.2(6)	Nd(1)-O(4w)-O(4w)#3	146.2(10)

Table 0.10 Bond valence calculation for complex NdUpht.

Atom	Atom bond	Bond length	Bond valence[vu]	Atom valence[vu]
U1	U(1)-O(82b)	2,60	0,35	6,24
	U(1)-O(82b)#1	2,60	0,35	
	U(1)-O(1u)	1,76	1,75	
	U(1)-O(1u)#1	1,76	1,75	
	U(1)-O(81b)	2,63	0,33	
	U(1)-O(81b)#1	2,63	0,33	
	U(1)-O(1)	2,24	0,69	
	U(1)-O(1)#1	2,24	0,69	
U2	U(2)-O(82a)	2,56	0,38	6,25
	U(2)-O(82a)#1	2,56	0,38	
	U(2)-O(81a)	2,57	0,37	
	U(2)-O(81a)#1	2,57	0,37	
	U(2)-O(2u)	1,76	1,75	
	U(2)-O(2u)#1	1,76	1,75	
	U(2)-O(1)	2,29	0,63	
	U(2)-O(1)#1	2,29	0,63	
U3	U(3)-O(31u)	1,76	1,75	6,62
	U(3)-O(12b)	2,38	0,53	
	U(3)-O(11a)	2,33	0,58	
	U(3)-O(81a)	2,37	0,54	
	U(3)-O(32u)	1,79	1,65	
	U(3)-O(81b)	2,42	0,49	
	U(3)-O(1)	2,19	0,77	
Nd1	Nd(1)-O(1w)	2,55	0,30	2,98
	Nd(1)-O(11b)	2,53	0,32	
	Nd(1)-O(11b)#2	2,53	0,32	
	Nd(1)-O(2w)	2,47	0,37	
	Nd(1)-O(2w)#2	2,47	0,37	
	Nd(1)-O(3w)	2,48	0,36	
	Nd(1)-O(3w)#2	2,48	0,36	
	Nd(1)-O(4w)	2,57	0,28	
	Nd(1)-O(4w)#2	2,57	0,28	
O1	U(1)-O(1)	2,24	0,69	2,09
	U(2)-O(1)	2,29	0,63	
	U(3)-O(1)	2,19	0,77	
O11a	U(3)-O(11a)	2,33	0,58	1,97
	O(11a)-C(1a)	1,27	1,38	
O11b	Nd(1)-O(11b)	2,53	0,32	1,78
	O(11b)-C(1b)	1,25	1,46	
O12a	O(12a)-C(1a)	1,22	1,58	1,58
O12b	U(3)-O(12b)	2,38	0,53	1,88
	O(12b)-C(1b)	1,28	1,35	
O1u	U(1)-O(1u)	1,76	1,75	1,75
O1w	Nd(1)-O(1w)	2,55	0,30	0,30
O2u	U(2)-O(2u)	1,76	1,75	1,75
O2w	Nd(1)-O(2w)	2,47	0,37	0,37
O31u	U(3)-O(31u)	1,76	1,75	1,75
O32u	U(3)-O(32u)	1,79	1,65	1,65
O3w	Nd(1)-O(3w)	2,48	0,36	0,36
O4w	Nd(1)-O(4w)	2,57	0,28	0,28
O81a	U(2)-O(81a)	2,57	0,37	2,08
	U(3)-O(81a)	2,37	0,54	
	O(81a)-C(8a)	1,33	1,18	
O81b	U(1)-O(81b)	2,63	0,33	2,03
	U(3)-O(81b)	2,42	0,49	
	O(81b)-C(8b)	1,32	1,21	
O82a	U(2)-O(82a)	2,56	0,38	1,92
	O(82a)-C(8a)	1,23	1,54	
O82b	U(1)-O(82b)	2,60	0,35	1,81
	O(82b)-C(8b)	1,25	1,46	

Table 0.11 Atomic coordinates (x10⁴) and equivalent isotropic displacement parameters (A²x10³) for complex CeUpyr.

Atom	x	y	z	U(eq)
U(1)	10000	-5000	5000	15(1)
U(2)	6320(1)	-2981(1)	-1667(1)	16(1)
Ce(1a)	3779(1)	-2148(1)	2247(1)	17(1)
Ce(1b)	3455(3)	-1603(3)	2100(2)	17(1)
O(81)	10995(3)	-3567(3)	3774(3)	19(1)
O(82b)	5065(4)	-3079(3)	-2867(3)	21(2)
O(101)	6896(4)	-2167(3)	-537(3)	23(2)
O(92)	5720(4)	912(3)	1729(3)	23(1)
O(71)	12260(4)	-4827(4)	2042(4)	31(2)
O(22u)	5497(4)	-3819(3)	-611(3)	26(2)
O(11u)	9398(4)	-5023(4)	3875(3)	27(2)
O(21u)	7146(4)	-2163(4)	-2705(3)	28(2)
O(72b)	7389(4)	-3683(4)	-4686(4)	38(2)
O(82)	11429(4)	-2062(3)	2399(3)	24(2)
O(71b)	8570(4)	-2496(4)	-5224(4)	29(2)
O(91)	4833(4)	-600(4)	2260(4)	33(2)
O(72)	11417(4)	-5281(4)	945(4)	39(2)
O(4w)	3730(4)	-4128(4)	3820(4)	36(2)
O(1w)	2004(5)	308(5)	1631(5)	51(2)
O(5w)	5026(6)	-4354(5)	1723(4)	49(2)
O(2w)	6105(5)	-3613(5)	3228(5)	59(3)
O(6w)	2866(6)	-1722(7)	405(5)	62(3)
O(81b)	4238(5)	-2968(4)	-4300(4)	34(2)
C(9)	5806(5)	-276(4)	1905(4)	18(2)
C(8)	10791(4)	-2766(4)	2832(4)	14(2)
C(2)	9650(5)	-2574(4)	2205(4)	14(2)
C(4)	7219(5)	-1343(4)	1716(4)	15(2)
C(1)	9901(5)	-3373(4)	1549(4)	16(2)
C(5)	7486(5)	-2138(4)	1042(4)	16(2)
C(3)	8305(5)	-1546(4)	2266(4)	17(2)
C(7b)	7444(5)	-2545(5)	-4960(4)	21(2)
C(8b)	4748(5)	-2536(4)	-3851(4)	19(2)
C(7)	11264(5)	-4550(5)	1505(5)	22(2)
C(10)	6431(5)	-1981(4)	376(4)	18(2)
C(3b)	3786(5)	2(4)	-4522(4)	19(2)
C(1b)	6155(5)	-1246(4)	-4966(4)	17(2)
C(2b)	4925(5)	-1256(4)	-4463(4)	18(2)
C(6)	8818(5)	-3111(4)	960(4)	20(2)
O(7w)	2168(11)	6178(10)	6851(8)	122(3)
O(9w)	-617(15)	8690(14)	5932(12)	79(4)
O(8w)	509(16)	9022(15)	9246(13)	86(4)
O(10w)	650(20)	-90(20)	6329(17)	120(6)
O(102)	5238(4)	-1728(5)	673(4)	34(2)
O(3w)	2880(5)	-1341(4)	3848(4)	42(2)

Table 0.12 Bond lengths for complex CeUpyr.

Bond	Bond length	Bond	Bond length
U(1)-O(81)	2.404(3)	O(92)-C(4)	2.346(5)
U(1)-O(81)#1	2.404(3)	O(71)-O(72)	2.182(9)
U(1)-O(11u)	1.764(5)	O(71)-C(1)	2.383(6)
U(1)-O(11u)#1	1.764(5)	O(71)-C(7)	1.262(8)
U(1)-O(72b)#2	2.573(4)	O(72b)-O(71b)	2.166(7)
U(1)-O(72b)#3	2.573(4)	O(72b)-C(7b)	1.261(8)
U(1)-O(71b)#2	2.496(4)	O(72b)-C(1b)	2.402(6)
U(1)-O(71b)#3	2.496(4)	O(82)-C(8)	1.241(7)
U(1)-C(8)	3.440(4)	O(82)-C(2)	2.355(8)
U(1)-C(8)#1	3.440(4)	O(71b)-C(7b)	1.242(7)
U(1)-C(2)	3.774(4)	O(71b)-C(1b)	2.377(6)
U(1)-C(2)#1	3.774(4)	O(91)-C(9)	1.252(7)
U(1)-C(7b)#2	2.917(4)	O(91)-C(4)	2.401(6)

Bond	Bond length	Bond	Bond length
U(1)-C(7b)#3	2.917(4)	O(72)-C(1)	2.375(6)
U(2)-O(82b)	2.352(5)	O(72)-C(7)	1.256(9)
U(2)-O(101)	2.339(5)	O(81b)-C(8b)	1.228(9)
U(2)-O(92)#4	2.376(3)	O(81b)-C(2b)	2.352(8)
U(2)-O(71)#3	2.455(5)	C(9)-C(4)	1.509(6)
U(2)-O(22u)	1.780(4)	C(9)-C(3)	2.464(7)
U(2)-O(21u)	1.757(4)	C(8)-C(2)	1.513(8)
U(2)-O(72)#3	2.434(4)	C(2)-C(4)	2.437(7)
U(2)-C(9)#4	3.302(4)	C(2)-C(1)	1.398(8)
U(2)-C(8b)	3.421(6)	C(2)-C(3)	1.406(6)
U(2)-C(7)#3	2.809(4)	C(2)-C(6)	2.407(9)
U(2)-C(10)	3.372(6)	C(4)-C(5)	1.411(8)
U(2)-C(2b)	3.787(5)	C(4)-C(3)	1.390(9)
Ce(1a)-O(82)#5	2.497(5)	C(4)-C(6)	2.401(7)
Ce(1a)-O(91)	2.541(6)	C(1)-C(5)	2.428(7)
Ce(1a)-O(4w)	2.528(4)	C(1)-C(3)	2.415(7)
Ce(1a)-O(1w)	2.504(4)	C(1)-C(7)	1.486(6)
Ce(1a)-O(5w)	2.555(6)	C(1)-C(6)	1.393(9)
Ce(1a)-O(2w)	2.579(5)	C(5)-C(3)	2.417(9)
Ce(1a)-O(6w)	2.630(7)	C(5)-C(10)	1.487(9)
Ce(1a)-C(9)	3.631(6)	C(5)-C(6)	1.378(6)
Ce(1a)-C(8)#5	3.559(5)	C(5)-O(102)	2.382(8)
Ce(1a)-C(4)	4.165(6)	C(3)-H(1c3)	0.959(6)
Ce(1a)-C(5)	4.097(5)	C(7b)-C(3b)#6	2.474(6)
Ce(1a)-C(10)	3.524(5)	C(7b)-C(1b)	1.503(6)
Ce(1a)-O(102)	2.468(5)	C(8b)-C(3b)	2.471(6)
Ce(1a)-O(3w)	2.508(5)	C(8b)-C(2b)	1.502(7)
O(81)-O(82)	2.208(5)	C(10)-C(6)	2.437(7)
O(81)-C(8)	1.263(6)	C(10)-O(102)	1.221(7)
O(81)-C(2)	2.395(7)	C(3b)-C(1b)	2.393(6)
O(82b)-O(81b)	2.207(8)	C(3b)-C(1b)#6	1.385(7)
O(82b)-C(8b)	1.281(6)	C(3b)-C(2b)	1.390(5)
O(82b)-C(2b)	2.389(5)	C(3b)-C(2b)#6	2.406(8)
O(101)-C(5)	2.339(8)	C(3b)-H(1c3b)	0.960(5)
O(101)-C(10)	1.296(7)	C(1b)-C(2b)	1.399(7)
O(101)-O(102)	2.211(6)	C(1b)-C(2b)#6	2.430(6)
O(92)-O(91)	2.226(7)	C(6)-H(1c6)	0.960(6)
O(92)-C(9)	1.266(6)		

Table 0.13 Bond Angles for complex CeUpyr.

Bond	Angle [°]	Bond	Angle [°]	Bond	Angle [°]
O(81)-U(1)-O(81)#1	180.0(5)	O(22u)-U(2)-C(10)	76.62(19)	U(2)-O(82b)-C(8b)	138.8(4)
O(81)-U(1)-O(11u)	86.50(18)	O(21u)-U(2)-O(72)#3	88.93(15)	U(2)-O(101)-C(10)	134.1(4)
O(81)-U(1)-O(11u)#1	93.50(18)	O(21u)-U(2)-C(9)#4	79.84(15)	U(2)#4-O(92)-C(9)	127.4(3)
O(81)-U(1)-O(72b)#2	113.35(11)	O(21u)-U(2)-C(7)#3	87.55(15)	U(2)#3-O(71)-C(7)	92.5(4)
O(81)-U(1)-O(72b)#3	66.65(11)	O(21u)-U(2)-C(10)	103.2(2)	U(1)#7-O(72b)-C(7b)	92.7(3)
O(81)-U(1)-O(71b)#2	66.61(12)	O(72)#3-U(2)-C(9)#4	139.53(18)	Ce(1a)#8-O(82)-C(8)	142.1(3)
O(81)-U(1)-O(71b)#3	113.39(12)	O(72)#3-U(2)-C(7)#3	26.5(2)	U(1)#7-O(71b)-C(7b)	96.9(3)
O(81)-U(1)-C(7b)#2	89.63(13)	O(72)#3-U(2)-C(10)	79.26(15)	Ce(1a)-O(91)-C(9)	144.2(4)
O(81)-U(1)-C(7b)#3	90.37(13)	C(9)#4-U(2)-C(7)#3	162.22(17)	U(2)#3-O(72)-C(7)	93.7(3)
O(81)#1-U(1)-O(11u)	93.50(18)	C(9)#4-U(2)-C(10)	66.04(12)	U(2)#4-C(9)-Ce(1a)	108.85(13)
O(81)#1-U(1)-O(11u)#1	86.50(18)	C(7)#3-U(2)-C(10)	105.34(16)	U(2)#4-C(9)-O(92)	34.8(2)
O(81)#1-U(1)-O(72b)#2	66.65(11)	O(82)#5-Ce(1a)-O(91)	137.72(12)	U(2)#4-C(9)-O(91)	90.1(3)
O(81)#1-U(1)-O(72b)#3	113.35(11)	O(82)#5-Ce(1a)-O(4w)	71.12(13)	U(2)#4-C(9)-C(4)	149.1(4)
O(81)#1-U(1)-O(71b)#2	113.39(12)	O(82)#5-Ce(1a)-O(1w)	70.53(16)	Ce(1a)-C(9)-O(92)	143.5(3)
O(81)#1-U(1)-O(71b)#3	66.61(12)	O(82)#5-Ce(1a)-O(5w)	95.69(18)	Ce(1a)-C(9)-O(91)	24.2(3)
O(81)#1-U(1)-C(7b)#2	90.37(13)	O(82)#5-Ce(1a)-O(2w)	138.86(15)	Ce(1a)-C(9)-C(4)	100.0(3)
O(81)#1-U(1)-C(7b)#3	89.63(13)	O(82)#5-Ce(1a)-O(6w)	67.81(17)	O(92)-C(9)-O(91)	124.2(4)
O(11u)-U(1)-O(11u)#1	180.0(5)	O(82)#5-Ce(1a)-C(9)	147.20(10)	O(92)-C(9)-C(4)	115.1(5)
O(11u)-U(1)-O(72b)#2	81.70(18)	O(82)#5-Ce(1a)-C(8)#5	12.36(9)	O(91)-C(9)-C(4)	120.6(5)
O(11u)-U(1)-O(72b)#3	98.30(18)	O(82)#5-Ce(1a)-C(10)	141.46(14)	Ce(1a)#8-C(8)-O(81)	102.9(3)
O(11u)-U(1)-O(71b)#2	97.09(16)	O(82)#5-Ce(1a)-O(102)	130.79(16)	Ce(1a)#8-C(8)-O(82)	25.51(19)

Bond	Angle [°]	Bond	Angle [°]	Bond	Angle [°]
O(11u)-U(1)-O(71b)#3	82.91(16)	O(82)#5-Ce(1a)-O(3w)	80.36(18)	Ce(1a)#8-C(8)-C(2)	136.4(3)
O(11u)-U(1)-C(7b)#2	89.22(17)	O(91)-Ce(1a)-O(4w)	124.54(17)	O(81)-C(8)-O(82)	123.7(6)
O(11u)-U(1)-C(7b)#3	90.78(17)	O(91)-Ce(1a)-O(1w)	71.23(17)	O(81)-C(8)-C(2)	119.0(5)
O(11u)#1-U(1)-O(72b)#2	98.30(18)	O(91)-Ce(1a)-O(5w)	125.98(17)	O(82)-C(8)-C(2)	117.2(4)
O(11u)#1-U(1)-O(72b)#3	81.70(18)	O(91)-Ce(1a)-O(2w)	70.19(16)	C(8)-C(2)-C(1)	121.8(4)
O(11u)#1-U(1)-O(71b)#2	82.91(16)	O(91)-Ce(1a)-O(6w)	115.9(2)	C(8)-C(2)-C(3)	119.2(5)
O(11u)#1-U(1)-O(71b)#3	97.09(16)	O(91)-Ce(1a)-C(9)	11.64(13)	C(1)-C(2)-C(3)	119.0(5)
O(11u)#1-U(1)-C(7b)#2	90.78(17)	O(91)-Ce(1a)-C(8)#5	145.79(12)	C(9)-C(4)-C(5)	124.3(5)
O(11u)#1-U(1)-C(7b)#3	89.22(17)	O(91)-Ce(1a)-C(10)	62.88(15)	C(9)-C(4)-C(3)	116.4(5)
O(72b)#2-U(1)-O(72b)#3	180.0(5)	O(91)-Ce(1a)-O(102)	66.40(18)	C(5)-C(4)-C(3)	119.3(4)
O(72b)#2-U(1)-O(71b)#2	50.58(15)	O(91)-Ce(1a)-O(3w)	71.44(18)	C(2)-C(1)-C(7)	122.3(5)
O(72b)#2-U(1)-O(71b)#3	129.42(15)	O(4w)-Ce(1a)-O(1w)	130.02(15)	C(2)-C(1)-C(6)	119.1(4)
O(72b)#2-U(1)-C(7b)#2	25.58(16)	O(4w)-Ce(1a)-O(5w)	71.50(16)	C(7)-C(1)-C(6)	118.5(5)
O(72b)#2-U(1)-C(7b)#3	154.42(16)	O(4w)-Ce(1a)-O(2w)	67.75(17)	C(4)-C(5)-C(10)	124.6(4)
O(72b)#3-U(1)-O(71b)#2	129.42(15)	O(4w)-Ce(1a)-O(6w)	119.3(2)	C(4)-C(5)-C(6)	118.9(5)
O(72b)#3-U(1)-O(71b)#3	50.58(15)	O(4w)-Ce(1a)-C(9)	128.01(15)	C(10)-C(5)-C(6)	116.5(5)
O(72b)#3-U(1)-C(7b)#2	154.42(16)	O(4w)-Ce(1a)-C(8)#5	59.25(13)	C(2)-C(3)-C(4)	121.3(5)
O(72b)#3-U(1)-C(7b)#3	25.58(16)	O(4w)-Ce(1a)-C(10)	130.36(11)	C(2)-C(3)-H(1c3)	119.3433
O(71b)#2-U(1)-O(71b)#3	180.0(5)	O(4w)-Ce(1a)-O(102)	139.24(13)	C(4)-C(3)-H(1c3)	119.3443
O(71b)#2-U(1)-C(7b)#2	25.00(16)	O(4w)-Ce(1a)-O(3w)	70.71(16)	U(1)#7-C(7b)-O(72b)	61.8(2)
O(71b)#2-U(1)-C(7b)#3	155.00(16)	O(1w)-Ce(1a)-O(5w)	142.8(2)	U(1)#7-C(7b)-O(71b)	58.1(2)
O(71b)#3-U(1)-C(7b)#2	155.00(16)	O(1w)-Ce(1a)-O(2w)	139.9(2)	U(1)#7-C(7b)-C(1b)	177.7(4)
O(71b)#3-U(1)-C(7b)#3	25.00(16)	O(1w)-Ce(1a)-O(6w)	72.4(2)	O(72b)-C(7b)-O(71b)	119.9(4)
C(7b)#2-U(1)-C(7b)#3	180.0(5)	O(1w)-Ce(1a)-C(9)	77.72(16)	O(72b)-C(7b)-C(1b)	120.4(5)
O(82b)-U(2)-O(101)	160.35(10)	O(1w)-Ce(1a)-C(8)#5	82.37(15)	O(71b)-C(7b)-C(1b)	119.7(5)
O(82b)-U(2)-O(92)#4	81.68(15)	O(1w)-Ce(1a)-C(10)	99.53(14)	O(82b)-C(8b)-O(81b)	123.1(5)
O(82b)-U(2)-O(71)#3	73.48(14)	O(1w)-Ce(1a)-O(102)	90.53(15)	O(82b)-C(8b)-C(2b)	118.2(6)
O(82b)-U(2)-O(22u)	88.40(19)	O(1w)-Ce(1a)-O(3w)	72.32(17)	O(81b)-C(8b)-C(2b)	118.6(5)
O(82b)-U(2)-O(21u)	91.9(2)	O(5w)-Ce(1a)-O(2w)	72.4(2)	U(2)#3-C(7)-O(71)	60.8(3)
O(82b)-U(2)-O(72)#3	126.51(16)	O(5w)-Ce(1a)-O(6w)	70.39(19)	U(2)#3-C(7)-O(72)	59.8(2)
O(82b)-U(2)-C(9)#4	92.88(13)	O(5w)-Ce(1a)-C(9)	114.96(17)	U(2)#3-C(7)-C(1)	171.3(4)
O(82b)-U(2)-C(7)#3	100.08(17)	O(5w)-Ce(1a)-C(8)#5	88.16(17)	O(71)-C(7)-O(72)	120.1(4)
O(82b)-U(2)-C(10)	150.77(11)	O(5w)-Ce(1a)-C(10)	69.42(16)	O(71)-C(7)-C(1)	120.0(6)
O(101)-U(2)-O(92)#4	78.71(14)	O(5w)-Ce(1a)-O(102)	72.27(18)	O(72)-C(7)-C(1)	119.9(6)
O(101)-U(2)-O(71)#3	126.17(14)	O(5w)-Ce(1a)-O(3w)	141.17(14)	U(2)-C(10)-Ce(1a)	111.14(18)
O(101)-U(2)-O(22u)	91.6(2)	O(2w)-Ce(1a)-O(6w)	136.12(19)	U(2)-C(10)-O(101)	29.9(3)
O(101)-U(2)-O(21u)	88.2(2)	O(2w)-Ce(1a)-C(9)	66.38(15)	U(2)-C(10)-C(5)	138.5(3)
O(101)-U(2)-O(72)#3	73.15(16)	O(2w)-Ce(1a)-C(8)#5	126.93(14)	U(2)-C(10)-O(102)	96.0(4)
O(101)-U(2)-C(9)#4	67.79(13)	O(2w)-Ce(1a)-C(10)	72.10(15)	Ce(1a)-C(10)-O(101)	141.0(4)
O(101)-U(2)-C(7)#3	99.56(17)	O(2w)-Ce(1a)-O(102)	84.00(16)	Ce(1a)-C(10)-C(5)	101.8(3)
O(101)-U(2)-C(10)	16.03(13)	O(2w)-Ce(1a)-O(3w)	85.35(19)	Ce(1a)-C(10)-O(102)	24.6(3)
O(92)#4-U(2)-O(71)#3	154.88(17)	O(6w)-Ce(1a)-C(9)	110.39(19)	O(101)-C(10)-C(5)	114.2(4)
O(92)#4-U(2)-O(22u)	86.44(14)	O(6w)-Ce(1a)-C(8)#5	74.15(17)	O(101)-C(10)-O(102)	123.0(6)
O(92)#4-U(2)-O(21u)	93.96(14)	O(6w)-Ce(1a)-C(10)	73.68(17)	C(5)-C(10)-O(102)	122.9(5)
O(92)#4-U(2)-O(72)#3	151.60(18)	O(6w)-Ce(1a)-O(102)	63.18(19)	C(1b)#6-C(3b)-C(2b)	122.2(5)
O(92)#4-U(2)-C(9)#4	17.74(15)	O(6w)-Ce(1a)-O(3w)	138.53(16)	C(1b)#6-C(3b)-H(1c3b)	118.8839
O(92)#4-U(2)-C(7)#3	177.65(17)	C(9)-Ce(1a)-C(8)#5	156.78(10)	C(2b)-C(3b)-H(1c3b)	118.8839
O(92)#4-U(2)-C(10)	72.57(14)	C(9)-Ce(1a)-C(10)	51.47(14)	C(7b)-C(1b)-C(3b)#6	117.9(5)
O(71)#3-U(2)-O(22u)	89.11(16)	C(9)-Ce(1a)-O(102)	55.80(17)	C(7b)-C(1b)-C(2b)	122.5(4)
O(71)#3-U(2)-O(21u)	90.64(17)	C(9)-Ce(1a)-O(3w)	82.44(17)	C(3b)#6-C(1b)-C(2b)	119.6(4)
O(71)#3-U(2)-O(72)#3	53.02(18)	C(8)#5-Ce(1a)-C(10)	145.45(14)	C(8b)-C(2b)-C(3b)	117.3(4)
O(71)#3-U(2)-C(9)#4	163.20(14)	C(8)#5-Ce(1a)-O(102)	136.83(16)	C(8b)-C(2b)-C(1b)	124.5(4)
O(71)#3-U(2)-C(7)#3	26.69(19)	C(8)#5-Ce(1a)-O(3w)	80.21(18)	C(3b)-C(2b)-C(1b)	118.2(4)
O(71)#3-U(2)-C(10)	130.16(13)	C(10)-Ce(1a)-O(102)	11.90(12)	C(1)-C(6)-C(5)	122.4(6)
O(22u)-U(2)-O(21u)	179.53(17)	C(10)-Ce(1a)-O(3w)	133.53(19)	C(1)-C(6)-H(1c6)	118.8187
O(22u)-U(2)-O(72)#3	90.61(16)	O(102)-Ce(1a)-O(3w)	137.7(2)	C(5)-C(6)-H(1c6)	118.8182
O(22u)-U(2)-C(9)#4	100.50(14)	U(1)-O(81)-C(8)	137.2(4)	Ce(1a)-O(102)-C(10)	143.5(4)
O(22u)-U(2)-C(7)#3	92.05(15)				

Table 0.14 Bond valence calculation for complex CeUpyr.

Atom	Atom bond	Bond length	Bond valence[vu]	Atom valence[vu]
U1	U(1)-O(81)	2,404	0,51	6,07
	U(1)-O(81)#1	2,404	0,51	
	U(1)-O(11u)	1,764	1,74	
	U(1)-O(11u)#1	1,764	1,74	
	U(1)-O(72b)#2	2,573	0,37	
	U(1)-O(72b)#3	2,573	0,37	
	U(1)-O(71b)#2	2,496	0,42	
	U(1)-O(71b)#3	2,496	0,42	
U2	U(2)-O(82b)	2,352	0,56	6,05
	U(2)-O(101)	2,339	0,57	
	U(2)-O(92)#4	2,376	0,53	
	U(2)-O(71)#3	2,455	0,46	
	U(2)-O(22u)	1,78	1,69	
	U(2)-O(21u)	1,757	1,76	
	U(2)-O(72)#3	2,434	0,48	
Ce1a	Ce(1a)-O(82)#5	2,497	0,35	2,84
	Ce(1a)-O(91)	2,541	0,31	
	Ce(1a)-O(4w)	2,528	0,32	
	Ce(1a)-O(1w)	2,504	0,34	
	Ce(1a)-O(5w)	2,555	0,30	
	Ce(1a)-O(2w)	2,579	0,28	
	Ce(1a)-O(6w)	2,63	0,24	
	Ce(1a)-O(102)	2,468	0,37	
	Ce(1a)-O(3w)	2,508	0,34	
O101	U(2)-O(101)	2,339	0,57	1,86
	O(101)-C(10)	1,296	1,29	
O102	Ce(1a)-O(102)	2,468	0,37	1,95
	O(102)-C(10)	1,221	1,58	
O11u	U(1)-O(11u)	1,764	1,74	1,74
O1w	Ce(1a)-O(1w)	2,504	0,34	0,34
O21u	U(2)-O(21u)	1,757	1,76	1,76
O22u	U(2)-O(22u)	1,78	1,69	1,69
O2w	Ce(1a)-O(2w)	2,579	0,28	0,28
O3w	Ce(1a)-O(3w)	2,508	0,34	0,34
O4w	Ce(1a)-O(4w)	2,528	0,32	0,32
O5w	Ce(1a)-O(5w)	2,555	0,30	0,30
O6w	Ce(1a)-O(6w)	2,63	0,24	0,24
O71	U(2)-O(71)#3	2,455	0,46	1,87
	O(71)-C(7)	1,262	1,41	
O71b	U(1)-O(71b)	2,496	0,42	1,92
	O(71b)-C(7b)	1,242	1,49	
O72	U(2)-O(72)#3	2,434	0,48	1,91
	O(72)-C(7)	1,256	1,44	
O72b	U(1)-O(72b)#2	2,573	0,37	1,78
	O(72b)-C(7b)	1,261	1,42	
O81	U(1)-O(81)	2,404	0,51	1,92
	O(81)-C(8)	1,263	1,41	
O81b	O(81b)-C(8b)	1,228	1,55	1,55
O82	Ce(1a)-O(82)#5	2,497	0,35	1,84
	O(82)-C(8)	1,241	1,50	
O82b	U(2)-O(82b)	2,352	0,56	1,90
	O(82b)-C(8b)	1,281	1,34	
O91	Ce(1a)-O(91)	2,541	0,31	1,76
	O(91)-C(9)	1,252	1,45	
O92	U(2)-O(92)#4	2,376	0,53	1,93
	O(92)-C(9)	1,266	1,40	

Table 0.15 Atomic coordinates (x10⁴) and equivalent isotropic displacement parameters (A²x10³) for complex NdUpyr.

Atom	x	y	z	U(eq)
U(1)	10000	5000	5000	14(1)
U(2)	6308(1)	7040(1)	8325(1)	14(1)
Nd(1)	6203(1)	12163(1)	7759(1)	18(1)
O(81)	10995(3)	6432(3)	3775(3)	16(1)
O(82b)	5053(3)	6930(3)	7125(3)	19(1)
O(101)	6893(3)	7850(4)	9455(3)	19(2)
O(92)	4272(3)	9098(3)	8277(3)	20(2)
O(71)	7738(4)	4864(4)	7937(3)	26(2)
O(22u)	5490(4)	6209(4)	9381(3)	24(2)
O(11u)	9408(4)	4972(4)	3879(3)	25(2)
O(21u)	7145(4)	7859(4)	7274(3)	27(2)
O(72b)	7350(4)	6322(4)	5297(4)	36(2)
O(82)	11463(4)	7915(4)	2388(3)	22(2)
O(71b)	8565(4)	7497(4)	4752(3)	28(2)
O(91)	5170(4)	10598(4)	7787(4)	29(2)
O(72)	8566(4)	5304(4)	9040(3)	33(2)
O(102)	5252(4)	8209(5)	10682(3)	31(2)
O(4w)	6250(4)	14121(4)	6194(3)	29(2)
O(3w)	7069(5)	11372(4)	6179(3)	37(2)
O(1w)	7953(4)	9735(4)	8371(4)	41(2)
O(5w)	4980(5)	14343(4)	8263(4)	40(2)
O(2w)	3912(4)	13570(5)	6779(4)	43(2)
O(6w)	7144(5)	11725(6)	9556(4)	55(3)
O(81b)	4230(5)	7028(4)	5704(3)	32(2)
C(9)	4191(5)	10290(5)	8104(4)	16(2)
C(8)	10807(4)	7226(4)	2830(4)	12(2)
C(2)	9668(4)	7420(4)	2193(4)	13(2)
C(4)	2780(4)	11357(5)	8290(4)	15(2)
C(1)	9915(4)	6622(5)	1541(4)	16(2)
C(5)	2501(5)	12156(4)	8961(4)	14(2)
C(3)	8323(5)	8454(5)	2254(4)	15(2)
C(7b)	7425(5)	7444(5)	5033(4)	21(2)
C(8b)	4745(5)	7474(5)	6141(4)	17(2)
C(7)	8732(5)	4570(5)	8479(4)	20(2)
C(10)	6451(5)	7992(5)	10367(4)	15(2)
C(3b)	3781(5)	10005(5)	5491(4)	17(2)
C(1b)	6154(5)	8754(5)	5024(4)	15(2)
C(2b)	4912(5)	8756(4)	5527(4)	14(2)
C(6)	1160(5)	13123(5)	9049(4)	18(2)
O(7w)	2186(8)	6155(8)	6862(7)	98(2)
O(9w)	9345(12)	8612(12)	6040(9)	60(3)
O(8w)	474(12)	9014(11)	9256(9)	59(3)
O(10w)	602(16)	9876(16)	6459(13)	99(5)

Table 0.16 Bond lengths for complex NdUpyr.

Bond	Bond length	Bond	Bond length
U(1)-O(81)	2.396(4)	Nd(1)-C(8)#2	3.548(5)
U(1)-O(81)#1	2.396(4)	Nd(1)-C(10)#3	3.513(5)
U(1)-O(11u)	1.751(5)	O(81)-C(8)	1.260(5)
U(1)-O(11u)#1	1.751(5)	O(82b)-C(8b)	1.273(6)
U(1)-O(72b)	2.598(4)	O(101)-C(10)	1.272(6)
U(1)-O(72b)#1	2.598(4)	O(92)-C(9)	1.274(7)
U(1)-O(71b)	2.485(4)	O(71)-C(7)	1.256(8)
U(1)-O(71b)#1	2.485(4)	O(72b)-C(7b)	1.256(8)
U(1)-C(7b)	2.917(4)	O(82)-C(8)	1.243(7)
U(1)-C(7b)#1	2.917(4)	O(71b)-C(7b)	1.257(7)
U(2)-O(82b)	2.356(5)	O(91)-C(9)	1.239(7)
U(2)-O(101)	2.338(5)	O(72)-C(7)	1.256(9)
U(2)-O(92)	2.367(3)	O(102)-C(10)	1.236(6)
U(2)-O(71)	2.450(4)	O(81b)-C(8b)	1.234(9)

Bond	Bond length	Bond	Bond length
U(2)-O(22u)	1.767(4)	C(9)-C(4)	1.505(6)
U(2)-O(21u)	1.770(4)	C(8)-C(2)	1.515(8)
U(2)-O(72)	2.422(3)	C(2)-C(1)	1.392(8)
U(2)-C(9)	3.298(5)	C(2)-C(3)	1.406(5)
U(2)-C(7)	2.813(4)	C(4)-C(5)	1.406(8)
U(2)-C(10)	3.341(6)	C(4)-C(3)#4	1.406(8)
Nd(1)-O(82)#2	2.478(4)	C(1)-C(7)#1	1.480(6)
Nd(1)-O(91)	2.523(5)	C(1)-C(6)#4	1.387(8)
Nd(1)-O(102)#3	2.432(4)	C(5)-C(10)#3	1.487(8)
Nd(1)-O(4w)	2.499(4)	C(5)-C(6)	1.382(6)
Nd(1)-O(3w)	2.465(5)	C(7b)-C(1b)	1.499(6)
Nd(1)-O(1w)	2.473(4)	C(8b)-C(2b)	1.497(7)
Nd(1)-O(5w)	2.515(5)	C(3b)-C(1b)#4	1.385(7)
Nd(1)-O(2w)	2.543(4)	C(3b)-C(2b)	1.384(6)
Nd(1)-O(6w)	2.576(6)	C(1b)-C(2b)	1.402(7)
Nd(1)-C(9)	3.614(6)		

Table 0.17 Bond Angles for complex NdUpyr.

Bond	Angle [°]	Bond	Angle [°]	Bond	Angle [°]
O(81)-U(1)-O(81)#1	180.0(5)	O(22u)-U(2)-C(9)	100.33(14)	C(9)-Nd(1)-C(8)#2	156.48(10)
O(81)-U(1)-O(11u)	86.62(18)	O(22u)-U(2)-C(7)	92.23(15)	C(9)-Nd(1)-C(10)#3	51.78(13)
O(81)-U(1)-O(11u)#1	93.38(18)	O(22u)-U(2)-C(10)	76.36(19)	C(8)#2-Nd(1)-C(10)#3	145.40(14)
O(81)-U(1)-O(72b)	113.32(11)	O(21u)-U(2)-O(72)	88.77(15)	U(1)-O(81)-C(8)	137.7(4)
O(81)-U(1)-O(72b)#1	66.68(11)	O(21u)-U(2)-C(9)	80.14(15)	U(2)-O(82b)-C(8b)	138.1(4)
O(81)-U(1)-O(71b)	66.31(12)	O(21u)-U(2)-C(7)	87.21(15)	U(2)-O(101)-C(10)	133.2(4)
O(81)-U(1)-O(71b)#1	113.69(12)	O(21u)-U(2)-C(10)	103.5(2)	U(2)-O(92)-C(9)	127.3(3)
O(81)-U(1)-C(7b)	89.83(13)	O(72)-U(2)-C(9)	139.37(18)	U(2)-O(71)-C(7)	93.1(4)
O(81)-U(1)-C(7b)#1	90.17(13)	O(72)-U(2)-C(7)	26.43(19)	U(1)-O(72b)-C(7b)	91.6(3)
O(81)#1-U(1)-O(11u)	93.38(18)	O(72)-U(2)-C(10)	78.86(14)	Nd(1)#2-O(82)-C(8)	142.8(3)
O(81)#1-U(1)-O(11u)#1	86.62(18)	C(9)-U(2)-C(7)	162.00(18)	U(1)-O(71b)-C(7b)	96.9(3)
O(81)#1-U(1)-O(72b)	66.68(11)	C(9)-U(2)-C(10)	66.27(12)	Nd(1)-O(91)-C(9)	145.6(4)
O(81)#1-U(1)-O(72b)#1	113.32(11)	C(7)-U(2)-C(10)	104.87(15)	U(2)-O(72)-C(7)	94.4(3)
O(81)#1-U(1)-O(71b)	113.69(12)	O(82)#2-Nd(1)-O(91)	137.68(12)	Nd(1)#3-O(102)-C(10)	144.7(3)
O(81)#1-U(1)-O(71b)#1	66.31(12)	O(82)#2-Nd(1)-O(102)#3	130.37(15)	U(2)-C(9)-Nd(1)	109.29(13)
O(81)#1-U(1)-C(7b)	90.17(13)	O(82)#2-Nd(1)-O(4w)	71.22(12)	U(2)-C(9)-O(92)	34.8(2)
O(81)#1-U(1)-C(7b)#1	89.83(13)	O(82)#2-Nd(1)-O(3w)	81.18(17)	U(2)-C(9)-O(91)	90.0(3)
O(11u)-U(1)-O(11u)#1	180.0(5)	O(82)#2-Nd(1)-O(1w)	70.88(15)	U(2)-C(9)-C(4)	149.3(4)
O(11u)-U(1)-O(72b)	81.16(17)	O(82)#2-Nd(1)-O(5w)	95.18(17)	Nd(1)-C(9)-O(92)	143.9(3)
O(11u)-U(1)-O(72b)#1	98.84(17)	O(82)#2-Nd(1)-O(2w)	139.30(13)	Nd(1)-C(9)-O(91)	23.2(3)
O(11u)-U(1)-O(71b)	96.62(16)	O(82)#2-Nd(1)-O(6w)	66.67(15)	Nd(1)-C(9)-C(4)	99.6(4)
O(11u)-U(1)-O(71b)#1	83.38(16)	O(82)#2-Nd(1)-C(9)	147.21(11)	O(92)-C(9)-O(91)	124.4(4)
O(11u)-U(1)-C(7b)	89.06(17)	O(82)#2-Nd(1)-C(8)#2	12.24(9)	O(92)-C(9)-C(4)	115.2(5)
O(11u)-U(1)-C(7b)#1	90.94(17)	O(82)#2-Nd(1)-C(10)#3	141.17(13)	O(91)-C(9)-C(4)	120.4(5)
O(11u)#1-U(1)-O(72b)	98.84(17)	O(91)-Nd(1)-O(102)#3	66.52(18)	Nd(1)#2-C(8)-O(81)	103.5(3)
O(11u)#1-U(1)-O(72b)#1	81.16(17)	O(91)-Nd(1)-O(4w)	125.63(16)	Nd(1)#2-C(8)-O(82)	24.99(18)
O(11u)#1-U(1)-O(71b)	83.38(16)	O(91)-Nd(1)-O(3w)	71.73(17)	Nd(1)#2-C(8)-C(2)	136.0(3)
O(11u)#1-U(1)-O(71b)#1	96.62(16)	O(91)-Nd(1)-O(1w)	70.27(16)	O(81)-C(8)-O(82)	124.2(5)
O(11u)#1-U(1)-C(7b)	90.94(17)	O(91)-Nd(1)-O(5w)	126.30(16)	O(81)-C(8)-C(2)	118.8(5)
O(11u)#1-U(1)-C(7b)#1	89.06(17)	O(91)-Nd(1)-O(2w)	70.17(15)	O(82)-C(8)-C(2)	116.9(4)
O(72b)-U(1)-O(72b)#1	180.0(5)	O(91)-Nd(1)-O(6w)	115.06(19)	C(8)-C(2)-C(1)	122.2(4)
O(72b)-U(1)-O(71b)	50.81(14)	O(91)-Nd(1)-C(9)	11.15(12)	C(8)-C(2)-C(3)	118.7(5)
O(72b)-U(1)-O(71b)#1	129.19(14)	O(91)-Nd(1)-C(8)#2	145.72(11)	C(1)-C(2)-C(3)	119.1(5)
O(72b)-U(1)-C(7b)	25.49(16)	O(91)-Nd(1)-C(10)#3	62.50(14)	C(9)-C(4)-C(5)	124.9(5)
O(72b)-U(1)-C(7b)#1	154.51(16)	O(102)#3-Nd(1)-O(4w)	138.31(12)	C(9)-C(4)-C(3)#4	116.2(5)
O(72b)#1-U(1)-O(71b)	129.19(14)	O(102)#3-Nd(1)-O(3w)	138.2(2)	C(5)-C(4)-C(3)#4	118.9(4)
O(72b)#1-U(1)-O(71b)#1	50.81(14)	O(102)#3-Nd(1)-O(1w)	91.27(14)	C(2)-C(1)-C(7)#1	121.9(5)
O(72b)#1-U(1)-C(7b)	154.51(16)	O(102)#3-Nd(1)-O(5w)	71.63(17)	C(2)-C(1)-C(6)#4	119.6(4)
O(72b)#1-U(1)-C(7b)#1	25.49(16)	O(102)#3-Nd(1)-O(2w)	83.87(14)	C(7)#1-C(1)-C(6)#4	118.3(6)
O(71b)-U(1)-O(71b)#1	180.0(5)	O(102)#3-Nd(1)-O(6w)	63.77(17)	C(4)-C(5)-C(10)#3	124.7(4)
O(71b)-U(1)-C(7b)	25.32(16)	O(102)#3-Nd(1)-C(9)	56.74(17)	C(4)-C(5)-C(6)	119.3(5)
O(71b)-U(1)-C(7b)#1	154.68(16)	O(102)#3-Nd(1)-C(8)#2	136.40(16)	C(10)#3-C(5)-C(6)	116.0(5)
O(71b)#1-U(1)-C(7b)	154.68(16)	O(102)#3-Nd(1)-C(10)#3	11.74(12)	C(2)-C(3)-C(4)#4	120.9(5)

Bond	Angle [°]	Bond	Angle [°]	Bond	Angle [°]
O(71b)#1-U(1)-C(7b)#1	25.32(16)	O(4w)-Nd(1)-O(3w)	70.81(15)	U(1)-C(7b)-O(72b)	62.9(2)
C(7b)-U(1)-C(7b)#1	180.0(5)	O(4w)-Nd(1)-O(1w)	130.17(13)	U(1)-C(7b)-O(71b)	57.7(2)
O(82b)-U(2)-O(101)	160.77(10)	O(4w)-Nd(1)-O(5w)	71.12(14)	U(1)-C(7b)-C(1b)	176.3(4)
O(82b)-U(2)-O(92)	82.29(14)	O(4w)-Nd(1)-O(2w)	68.12(15)	O(72b)-C(7b)-O(71b)	120.6(4)
O(82b)-U(2)-O(71)	73.22(13)	O(4w)-Nd(1)-O(6w)	119.2(2)	O(72b)-C(7b)-C(1b)	120.8(5)
O(82b)-U(2)-O(22u)	88.36(19)	O(4w)-Nd(1)-C(9)	128.00(14)	O(71b)-C(7b)-C(1b)	118.6(5)
O(82b)-U(2)-O(21u)	92.05(19)	O(4w)-Nd(1)-C(8)#2	59.37(12)	O(82b)-C(8b)-O(81b)	121.7(5)
O(82b)-U(2)-O(72)	125.96(15)	O(4w)-Nd(1)-C(10)#3	130.17(10)	O(82b)-C(8b)-C(2b)	118.7(6)
O(82b)-U(2)-C(9)	93.62(13)	O(3w)-Nd(1)-O(1w)	72.47(15)	O(81b)-C(8b)-C(2b)	119.4(4)
O(82b)-U(2)-C(7)	99.62(16)	O(3w)-Nd(1)-O(5w)	140.80(13)	U(2)-C(7)-O(71)	60.4(3)
O(82b)-U(2)-C(10)	151.44(11)	O(3w)-Nd(1)-O(2w)	84.14(16)	U(2)-C(7)-O(72)	59.1(2)
O(101)-U(2)-O(92)	78.52(14)	O(3w)-Nd(1)-O(6w)	137.95(14)	U(2)-C(7)-C(1)#1	172.8(4)
O(101)-U(2)-O(71)	126.01(13)	O(3w)-Nd(1)-C(9)	81.87(16)	O(71)-C(7)-O(72)	119.1(4)
O(101)-U(2)-O(22u)	91.65(19)	O(3w)-Nd(1)-C(8)#2	80.64(17)	O(71)-C(7)-C(1)#1	120.7(6)
O(101)-U(2)-O(21u)	88.1(2)	O(3w)-Nd(1)-C(10)#3	133.19(18)	O(72)-C(7)-C(1)#1	120.2(5)
O(101)-U(2)-O(72)	73.28(15)	O(1w)-Nd(1)-O(5w)	143.10(18)	U(2)-C(10)-Nd(1)#3	111.08(17)
O(101)-U(2)-C(9)	67.45(13)	O(1w)-Nd(1)-O(2w)	138.6(2)	U(2)-C(10)-O(101)	30.6(3)
O(101)-U(2)-C(7)	99.59(16)	O(1w)-Nd(1)-O(6w)	71.83(19)	U(2)-C(10)-O(102)	95.1(4)
O(101)-U(2)-C(10)	16.11(13)	O(1w)-Nd(1)-C(9)	77.32(15)	U(2)-C(10)-C(5)#3	139.6(3)
O(92)-U(2)-O(71)	155.28(16)	O(1w)-Nd(1)-C(8)#2	82.49(14)	Nd(1)#3-C(10)-O(101)	141.5(4)
O(92)-U(2)-O(22u)	86.19(14)	O(1w)-Nd(1)-C(10)#3	99.56(13)	Nd(1)#3-C(10)-O(102)	23.6(2)
O(92)-U(2)-O(21u)	94.36(14)	O(5w)-Nd(1)-O(2w)	73.40(19)	Nd(1)#3-C(10)-C(5)#3	101.4(3)
O(92)-U(2)-O(72)	151.51(18)	O(5w)-Nd(1)-O(6w)	71.29(17)	O(101)-C(10)-O(102)	122.7(6)
O(92)-U(2)-C(9)	17.89(15)	O(5w)-Nd(1)-C(9)	115.46(15)	O(101)-C(10)-C(5)#3	114.9(4)
O(92)-U(2)-C(7)	177.49(15)	O(5w)-Nd(1)-C(8)#2	87.97(16)	O(102)-C(10)-C(5)#3	122.4(5)
O(92)-U(2)-C(10)	72.86(13)	O(5w)-Nd(1)-C(10)#3	69.62(15)	C(1b)#4-C(3b)-C(2b)	121.8(5)
O(71)-U(2)-O(22u)	89.73(16)	O(2w)-Nd(1)-O(6w)	137.88(16)	C(7b)-C(1b)-C(3b)#4	118.6(4)
O(71)-U(2)-O(21u)	89.91(17)	O(2w)-Nd(1)-C(9)	65.73(14)	C(7b)-C(1b)-C(2b)	122.0(5)
O(71)-U(2)-O(72)	52.74(17)	O(2w)-Nd(1)-C(8)#2	127.47(13)	C(3b)#4-C(1b)-C(2b)	119.3(4)
O(71)-U(2)-C(9)	163.30(13)	O(2w)-Nd(1)-C(10)#3	72.15(13)	C(8b)-C(2b)-C(3b)	117.4(4)
O(71)-U(2)-C(7)	26.46(18)	O(6w)-Nd(1)-C(9)	110.84(17)	C(8b)-C(2b)-C(1b)	123.6(4)
O(71)-U(2)-C(10)	129.64(12)	O(6w)-Nd(1)-C(8)#2	73.37(16)	C(3b)-C(2b)-C(1b)	118.9(5)
O(22u)-U(2)-O(21u)	179.36(16)	O(6w)-Nd(1)-C(10)#3	74.56(15)	C(1)#4-C(6)-C(5)	122.0(6)
O(22u)-U(2)-O(72)	90.59(15)				

Table 0.18 Bond valence calculation for complex NdUpyr.

Atom	Atom bond	Bond length	Bond valence[vu]	Atom valence[vu]
U1	U(1)-O(81)	2,396	0,51	6,16
	U(1)-O(81)#1	2,396	0,51	
	U(1)-O(11u)	1,751	1,78	
	U(1)-O(11u)#1	1,751	1,78	
	U(1)-O(72b)	2,598	0,35	
	U(1)-O(72b)#1	2,598	0,35	
	U(1)-O(71b)	2,485	0,43	
	U(1)-O(71b)#1	2,485	0,43	
U2	U(2)-O(82b)	2,356	0,56	6,07
	U(2)-O(101)	2,338	0,58	
	U(2)-O(92)	2,367	0,54	
	U(2)-O(71)	2,450	0,46	
	U(2)-O(22u)	1,767	1,73	
	U(2)-O(21u)	1,770	1,72	
	U(2)-O(72)	2,422	0,49	
Nd1	Nd(1)-O(82)	2,478	0,36	3,11
	Nd(1)-O(91)	2,523	0,32	
	Nd(1)-O(102)	2,432	0,41	
	Nd(1)-O(4w)	2,499	0,34	
	Nd(1)-O(3w)	2,465	0,38	
	Nd(1)-O(1w)	2,473	0,37	
	Nd(1)-O(5w)	2,515	0,33	
	Nd(1)-O(2w)	2,543	0,31	
	Nd(1)-O(6w)	2,576	0,28	

Atom	Atom bond	Bond length	Bond valence[vu]	Atom valence[vu]
O101	U(2)-O(101)	2,338	0,58	1,95
	O(101)-C(10)	1,272	1,38	
O102	Nd(1)-O(102)	2,432	0,41	1,93
	O(102)-C(10)	1,236	1,52	
O11u	U(1)-O(11u)	1,751	1,78	1,78
O1w	Nd(1)-O(1w)	2,473	0,37	0,37
O21u	U(2)-O(21u)	1,770	1,72	1,72
O22u	U(2)-O(22u)	1,767	1,73	1,73
O2w	Nd(1)-O(2w)	2,543	0,31	0,31
O3w	Nd(1)-O(3w)	2,465	0,38	0,38
O4w	Nd(1)-O(4w)	2,499	0,34	0,34
O5w	Nd(1)-O(5w)	2,515	0,33	0,33
O6w	Nd(1)-O(6w)	2,576	0,28	0,28
O71	U(2)-O(71)	2,450	0,46	1,90
	O(71)-C(7)	1,256	1,44	
O71b	U(1)-O(71b)	2,485	0,43	1,87
	O(71b)-C(7b)	1,257	1,43	
O72	U(2)-O(72)	2,422	0,49	1,93
	O(72)-C(7)	1,256	1,44	
O72b	U(1)-O(72b)	2,598	0,35	1,78
	O(72b)-C(7b)	1,256	1,44	
O81	U(1)-O(81)	2,396	0,51	1,94
	O(81)-C(8)	1,260	1,42	
O81b	O(81b)-C(8b)	1,234	1,52	1,52
O82	Nd(1)-O(82)	2,478	0,36	1,85
	O(82)-C(8)	1,243	1,49	
O82b	U(2)-O(82b)	2,356	0,56	1,93
	O(82b)-C(8b)	1,273	1,37	
O91	Nd(1)-O(91)	2,523	0,32	1,83
	O(91)-C(9)	1,239	1,50	
O92	U(2)-O(92)	2,367	0,54	1,91
	O(92)-C(9)	1,274	1,37	

Table 0.19 Atomic coordinates ($x10^4$) and equivalent isotropic displacement parameters (A^2x10^3) for complex CeUmel.

Atom	x	y	z	U(eq)
U(1)	3560(1)	10223(1)	238	14(1)
U(2)	1341(1)	4847(1)	282(1)	14(1)
Ce(1)	3432(1)	6452(1)	2725(1)	22(1)
C(10a)	3126(4)	5179(7)	218(6)	15(2)
C(4a)	4077(4)	5200(7)	183(4)	10(2)
O(102)	2727(3)	4550(7)	-229(3)	25(2)
O(101)	2747(3)	5770(7)	665(3)	21(2)
C(1a)	836(4)	9854(8)	210(6)	20(2)
C(7a)	1785(4)	9898(7)	183(5)	15(2)
O(72a)	2165(3)	10592(7)	-241(3)	23(2)
C(8a)	870(4)	8110(9)	1161(4)	14(2)
O(81a)	1055(3)	6660(6)	1095(3)	16(2)
O(82a)	991(3)	8884(7)	1658(3)	22(2)
C(9)	4090(4)	6996(10)	1152(4)	14(2)
O(92)	3830(4)	8423(7)	1061(3)	17(2)
O(91)	4069(4)	6322(7)	1667(3)	23(2)
O(12u)	3797(3)	8626(8)	-284(3)	23(2)
O(22u)	1551(3)	3239(7)	792(3)	23(2)
O(122)	4080(3)	6178(7)	3746(3)	21(2)
O(5w)	2786(4)	8595(8)	3446(4)	38(2)
O(4w)	2609(4)	8437(8)	2042(3)	38(2)
O(121)	1080(3)	3169(6)	-581(3)	19(2)
O(1)	-49(3)	4223(6)	473(3)	21(2)
O(111)	3840(3)	11907(7)	-625(3)	22(2)
O(13u)	3356(3)	11859(6)	748(3)	22(2)
O(21u)	1121(3)	6446(7)	-230(3)	21(2)

Atom	x	y	z	U(eq)
O(112)	3918(3)	13986(7)	-1248(3)	21(2)
C(11a)	4047(4)	13348(9)	-753(4)	13(2)
O(3w)	4259(4)	9012(8)	2720(5)	53(2)
O(2w)	5012(4)	5659(8)	2712(4)	45(2)
O(1w)	2569(6)	4793(11)	1956(5)	76(3)
O(71a)	2186(3)	9194(7)	614(3)	23(2)
C(2a)	403(4)	8990(8)	648(4)	10(2)
C(6a)	393(4)	10766(8)	-244(3)	11(2)
C(3a)	-469(4)	8932(8)	642(3)	10(2)
C(5a)	4504(4)	4295(8)	-245(4)	11(2)
C(12a)	843(4)	1756(9)	-726(4)	15(2)
O(11w)	5682(6)	106(10)	2203(5)	70(3)
O(8w)	5010(5)	2793(10)	1577(4)	58(2)
O(7w)	3543(6)	3521(14)	2949(5)	102(4)
O(10w)	4581(7)	1668(14)	3544(6)	110(4)
O(6w)	1972(7)	5645(13)	3155(5)	103(4)
O(12w)	3714(8)	7192(16)	8432(7)	133(5)
O(9w)	2230(8)	1744(16)	2358(6)	137(5)

Table 0.20 Bond lengths for complex CeUmel.

Bond	Bond length	Bond	Bond length
U(1)-U(2)#1	4.409(1)	C(4a)-C(5a)	1.37(1)
U(1)-C(7a)	2.830(6)	O(102)-O(101)	2.18(1)
U(1)-O(72a)	2.461(5)	C(1a)-C(7a)	1.51(1)
U(1)-C(9)	3.436(8)	C(1a)-O(72a)	2.40(1)
U(1)-O(92)	2.362(6)	C(1a)-O(71a)	2.38(1)
U(1)-O(12u)	1.782(7)	C(1a)-C(2a)	1.37(1)
U(1)-O(1)#1	2.309(5)	C(1a)-C(6a)	1.43(1)
U(1)-O(111)	2.373(6)	C(1a)-C(3a)	2.40(1)
U(1)-O(13u)	1.781(6)	C(1a)-C(5a)#3	2.43(1)
U(1)-C(11a)	3.454(8)	C(7a)-O(72a)	1.24(1)
U(1)-O(71a)	2.477(5)	C(7a)-O(71a)	1.27(1)
U(2)-C(10a)	2.847(6)	O(72a)-O(71a)	2.18(1)
U(2)-O(102)	2.471(5)	C(8a)-O(81a)	1.25(1)
U(2)-O(101)	2.499(5)	C(8a)-O(82a)	1.27(1)
U(2)-C(8a)	3.396(8)	C(8a)-C(2a)	1.52(1)
U(2)-O(81a)	2.359(6)	O(81a)-O(82a)	2.22(1)
U(2)-O(22u)	1.764(6)	O(81a)-C(2a)	2.40(1)
U(2)-O(121)	2.364(6)	O(82a)-C(2a)	2.37(1)
U(2)-O(1)	2.301(5)	C(9)-O(92)	1.27(1)
U(2)-O(21u)	1.764(6)	C(9)-O(91)	1.25(1)
U(2)-C(2a)	3.836(7)	C(9)-C(3a)#1	1.52(1)
U(2)-C(12a)	3.459(8)	O(92)-O(91)	2.22(1)
Ce(1)-C(9)	3.580(9)	O(92)-C(3a)#1	2.43(1)
Ce(1)-O(91)	2.499(7)	O(91)-C(3a)#1	2.34(1)
Ce(1)-O(122)	2.443(6)	O(122)-O(121)#2	2.22(1)
Ce(1)-O(5w)	2.579(7)	O(122)-C(6a)#4	2.36(1)
Ce(1)-O(4w)	2.570(7)	O(122)-C(12a)#2	1.24(1)
Ce(1)-O(3w)	2.501(7)	O(121)-C(6a)#5	2.39(1)
Ce(1)-O(2w)	2.590(6)	O(121)-C(12a)	1.27(1)
Ce(1)-O(1w)	2.56(1)	O(111)-O(112)	2.19(1)
Ce(1)-C(12a)#2	3.546(8)	O(111)-C(11a)	1.27(1)
Ce(1)-O(7w)	2.50(1)	O(111)-C(5a)#6	2.39(1)
Ce(1)-O(6w)	2.58(1)	O(112)-C(11a)	1.21(1)
C(10a)-C(4a)	1.510(9)	O(112)-C(5a)#6	2.37(1)
C(10a)-O(102)	1.27(1)	C(11a)-C(5a)#6	1.53(1)
C(10a)-O(101)	1.24(1)	C(2a)-C(6a)	2.43(1)
C(4a)-O(102)	2.380(8)	C(2a)-C(3a)	1.38(1)
C(4a)-O(101)	2.398(9)	C(6a)-C(5a)#3	1.41(1)
C(4a)-C(2a)#1	2.43(1)	C(6a)-C(12a)#6	1.51(1)
C(4a)-C(6a)#1	2.418(9)	C(3a)-C(5a)#3	2.42(1)
C(4a)-C(3a)#1	1.42(1)		

Table 0.21 Bond Angles for complex CeUmel.

Bond	Angle [°]	Bond	Angle [°]	Bond	Angle [°]
U(2)#1-U(1)-C(7a)	173.7(1)	O(81a)-U(2)-O(22u)	93.2(2)	C(12a)#2-Ce(1)-O(7w)	82.1(3)
U(2)#1-U(1)-O(72a)	155.4(1)	O(81a)-U(2)-O(121)	158.5(2)	C(12a)#2-Ce(1)-O(6w)	88.2(3)
U(2)#1-U(1)-O(92)	78.2(1)	O(81a)-U(2)-O(1h)	80.0(2)	O(7w)-Ce(1)-O(6w)	74.9(3)
U(2)#1-U(1)-O(12u)	78.1(1)	O(81a)-U(2)-O(21u)	86.9(2)	U(2)-C(10a)-C(4a)	175.1(4)
U(2)#1-U(1)-O(1)#1	16.9(1)	O(22u)-U(2)-O(121)	94.5(2)	U(2)-C(10a)-O(102)	60.0(3)
U(2)#1-U(1)-O(111)	80.7(1)	O(22u)-U(2)-O(1h)	84.1(2)	U(2)-C(10a)-O(101)	61.3(3)
U(2)#1-U(1)-O(13u)	100.3(2)	O(22u)-U(2)-O(21u)	179.4(2)	C(4a)-C(10a)-O(102)	117.7(9)
U(2)#1-U(1)-O(71a)	150.2(1)	O(121)-U(2)-O(1h)	80.8(2)	C(4a)-C(10a)-O(101)	121.2(8)
C(7a)-U(1)-O(72a)	25.9(3)	O(121)-U(2)-O(21u)	85.3(2)	O(102)-C(10a)-O(101)	121.0(6)
C(7a)-U(1)-O(92)	98.7(2)	O(1)-U(2)-O(21u)	95.3(2)	C(10a)-C(4a)-C(3a)#1	118.5(7)
C(7a)-U(1)-O(12u)	96.4(2)	C(9)-Ce(1)-O(91)	11.9(2)	C(10a)-C(4a)-C(5a)	121.4(7)
C(7a)-U(1)-O(1h)#1	167.9(2)	C(9)-Ce(1)-O(122)	138.2(2)	C(3a)#1-C(4a)-C(5a)	119.9(6)
C(7a)-U(1)-O(111)	102.1(2)	C(9)-Ce(1)-O(5w)	126.9(2)	U(2)-O(102)-C(10a)	93.6(5)
C(7a)-U(1)-O(13u)	85.3(2)	C(9)-Ce(1)-O(4w)	61.5(2)	U(2)-O(101)-C(10a)	93.0(5)
C(7a)-U(1)-O(71a)	26.7(2)	C(9)-Ce(1)-O(3w)	74.7(3)	C(7a)-C(1a)-C(2a)	122.7(8)
O(72a)-U(1)-O(92)	123.9(2)	C(9)-Ce(1)-O(2w)	74.9(2)	C(7a)-C(1a)-C(6a)	116.9(8)
O(72a)-U(1)-O(12u)	90.9(2)	C(9)-Ce(1)-O(1w)	67.0(2)	C(2a)-C(1a)-C(6a)	120.4(6)
O(72a)-U(1)-O(1h)#1	157.8(2)	C(9)-Ce(1)-C(12a)#2	142.3(2)	U(1)-C(7a)-C(1a)	173.8(7)
O(72a)-U(1)-O(111)	76.4(2)	C(9)-Ce(1)-O(7w)	106.7(3)	U(1)-C(7a)-O(72a)	60.1(4)
O(72a)-U(1)-O(13u)	90.0(2)	C(9)-Ce(1)-O(6w)	129.4(3)	U(1)-C(7a)-O(71a)	61.0(3)
O(72a)-U(1)-O(71a)	52.4(2)	O(91)-Ce(1)-O(122)	130.6(2)	C(1a)-C(7a)-O(72a)	121.8(8)
O(92)-U(1)-O(12u)	88.0(2)	O(91)-Ce(1)-O(5w)	137.9(2)	C(1a)-C(7a)-O(71a)	117.3(8)
O(92)-U(1)-O(1h)#1	77.8(2)	O(91)-Ce(1)-O(4w)	73.0(2)	O(72a)-C(7a)-O(71a)	120.8(6)
O(92)-U(1)-O(111)	158.6(2)	O(91)-Ce(1)-O(3w)	79.7(3)	U(1)-O(72a)-C(7a)	94.0(5)
O(92)-U(1)-O(13u)	93.0(2)	O(91)-Ce(1)-O(2w)	65.7(2)	O(81a)-C(8a)-O(82a)	123.6(8)
O(92)-U(1)-O(71a)	72.2(2)	O(91)-Ce(1)-O(1w)	66.4(3)	O(81a)-C(8a)-C(2a)	119.7(7)
O(12u)-U(1)-O(1h)#1	95.0(2)	O(91)-Ce(1)-C(12a)#2	137.3(3)	O(82a)-C(8a)-C(2a)	116.5(7)
O(12u)-U(1)-O(111)	84.5(2)	O(91)-Ce(1)-O(7w)	96.2(3)	U(2)-O(81a)-C(8a)	138.4(6)
O(12u)-U(1)-O(13u)	177.9(3)	O(91)-Ce(1)-O(6w)	132.8(3)	Ce(1)-C(9)-O(92)	99.7(5)
O(12u)-U(1)-O(71a)	97.8(2)	O(122)-Ce(1)-O(5w)	71.8(2)	Ce(1)-C(9)-O(91)	24.3(4)
O(1h)#1-U(1)-O(111)	82.9(2)	O(122)-Ce(1)-O(4w)	142.3(2)	Ce(1)-C(9)-C(3a)#1	139.4(5)
O(1h)#1-U(1)-O(13u)	83.4(2)	O(122)-Ce(1)-O(3w)	82.1(3)	O(92)-C(9)-O(91)	123.2(7)
O(1h)#1-U(1)-O(71a)	146.8(2)	O(122)-Ce(1)-O(2w)	65.1(2)	O(92)-C(9)-C(3a)#1	120.9(7)
O(111)-U(1)-O(13u)	93.9(2)	O(122)-Ce(1)-O(1w)	139.5(2)	O(91)-C(9)-C(3a)#1	115.6(7)
O(111)-U(1)-O(71a)	128.7(2)	O(122)-Ce(1)-C(12a)#2	11.2(2)	U(1)-O(92)-C(9)	139.9(5)
O(13u)-U(1)-O(71a)	84.3(2)	O(122)-Ce(1)-O(7w)	72.7(3)	Ce(1)-O(91)-C(9)	143.8(5)
U(1)#3-U(2)-C(10a)	173.7(2)	O(122)-Ce(1)-O(6w)	91.6(3)	Ce(1)-O(122)-C(12a)#2	146.4(5)
U(1)#3-U(2)-O(102)	151.4(1)	O(5w)-Ce(1)-O(4w)	72.6(2)	U(2)-O(121)-C(12a)	142.2(6)
U(1)#3-U(2)-O(101)	154.5(1)	O(5w)-Ce(1)-O(3w)	67.8(2)	U(1)#3-O(1)-U(2)	146.1(3)
U(1)#3-U(2)-O(81a)	80.3(1)	O(5w)-Ce(1)-O(2w)	124.5(2)	U(1)-O(111)-C(11a)	140.7(6)
U(1)#3-U(2)-O(22u)	101.1(2)	O(5w)-Ce(1)-O(1w)	123.5(3)	O(111)-C(11a)-O(112)	124.1(7)
U(1)#3-U(2)-O(121)	78.5(1)	O(5w)-Ce(1)-C(12a)#2	60.7(2)	O(111)-C(11a)-C(5a)#6	116.9(7)
U(1)#3-U(2)-O(1h)	17.0(1)	O(5w)-Ce(1)-O(7w)	125.9(3)	O(112)-C(11a)-C(5a)#6	119.1(7)
U(1)#3-U(2)-O(21u)	78.4(2)	O(5w)-Ce(1)-O(6w)	66.8(3)	U(1)-O(71a)-C(7a)	92.3(4)
C(10a)-U(2)-O(102)	26.4(3)	O(4w)-Ce(1)-O(3w)	73.5(2)	C(1a)-C(2a)-C(8a)	120.7(6)
C(10a)-U(2)-O(101)	25.8(3)	O(4w)-Ce(1)-O(2w)	130.4(2)	C(1a)-C(2a)-C(3a)	120.7(7)
C(10a)-U(2)-O(81a)	99.5(2)	O(4w)-Ce(1)-O(1w)	72.7(3)	C(8a)-C(2a)-C(3a)	118.6(6)
C(10a)-U(2)-O(22u)	85.2(2)	O(4w)-Ce(1)-C(12a)#2	131.3(2)	C(1a)-C(6a)-C(5a)#3	118.4(6)
C(10a)-U(2)-O(121)	101.2(3)	O(4w)-Ce(1)-O(7w)	140.9(3)	C(1a)-C(6a)-C(12a)#6	122.1(6)
C(10a)-U(2)-O(1h)	169.2(2)	O(4w)-Ce(1)-O(6w)	85.3(3)	C(5a)#3-C(6a)-C(12a)#6	119.5(6)
C(10a)-U(2)-O(21u)	95.4(3)	O(3w)-Ce(1)-O(2w)	73.2(2)	C(4a)#3-C(3a)-C(9)#3	122.1(5)
O(102)-U(2)-O(101)	52.1(2)	O(3w)-Ce(1)-O(1w)	137.6(3)	C(4a)#3-C(3a)-C(2a)	119.7(6)
O(102)-U(2)-O(81a)	124.6(2)	O(3w)-Ce(1)-C(12a)#2	76.9(3)	C(9)#3-C(3a)-C(2a)	118.1(6)
O(102)-U(2)-O(22u)	92.0(2)	O(3w)-Ce(1)-O(7w)	142.9(3)	C(4a)-C(5a)-C(11a)#5	122.1(6)
O(102)-U(2)-O(121)	75.2(2)	O(3w)-Ce(1)-O(6w)	133.8(3)	C(4a)-C(5a)-C(6a)#1	120.8(7)
O(102)-U(2)-O(1h)	155.4(2)	O(2w)-Ce(1)-O(1w)	111.9(3)	C(11a)#5-C(5a)-C(6a)#1	117.2(6)
O(102)-U(2)-O(21u)	88.4(2)	O(2w)-Ce(1)-C(12a)#2	73.5(2)	Ce(1)#7-C(12a)-O(122)#7	22.4(3)
O(101)-U(2)-O(81a)	74.2(2)	O(2w)-Ce(1)-O(7w)	71.6(3)	Ce(1)#7-C(12a)-O(121)	101.6(5)
O(101)-U(2)-O(22u)	81.8(2)	O(2w)-Ce(1)-O(6w)	143.6(3)	Ce(1)#7-C(12a)-C(6a)#5	140.0(5)
O(101)-U(2)-O(121)	126.8(2)	O(1w)-Ce(1)-C(12a)#2	145.5(2)	O(122)#7-C(12a)-O(121)	123.6(7)
O(101)-U(2)-O(1h)	149.8(2)	O(1w)-Ce(1)-O(7w)	68.6(3)	O(122)#7-C(12a)-C(6a)#5	117.9(7)
O(101)-U(2)-O(21u)	98.8(2)	O(1w)-Ce(1)-O(6w)	67.2(3)	O(121)-C(12a)-C(6a)#5	118.4(7)

Table 0.22 Bond valence calculation for complex CeUmel.

Atom	Atom bond	Bond length	Bond valence[vu]	Atom valence[vu]
U1	U(1)-O(72a)	2,46	0,45	5,96
	U(1)-O(92)	2,36	0,55	
	U(1)-O(12u)	1,78	1,69	
	U(1)-O(1)#1	2,31	0,61	
	U(1)-O(111)	2,37	0,54	
	U(1)-O(13u)	1,78	1,69	
	U(1)-O(71a)	2,48	0,44	
U2	U(2)-O(102)	2,47	0,45	6,09
	U(2)-O(101)	2,50	0,42	
	U(2)-O(81a)	2,36	0,55	
	U(2)-O(22u)	1,76	1,75	
	U(2)-O(121)	2,36	0,55	
	U(2)-O(1)	2,30	0,62	
	U(2)-O(21u)	1,76	1,75	
Ce1	Ce(1)-O(91)	2,50	0,34	2,84
	Ce(1)-O(122)	2,44	0,40	
	Ce(1)-O(5w)	2,58	0,28	
	Ce(1)-O(4w)	2,57	0,28	
	Ce(1)-O(3w)	2,50	0,34	
	Ce(1)-O(2w)	2,59	0,27	
	Ce(1)-O(1w)	2,56	0,29	
	Ce(1)-O(7w)	2,50	0,34	
	Ce(1)-O(6w)	2,58	0,28	
O1	U(1)-O(1)#1	2,31	0,61	1,23
	U(2)-O(1)	2,30	0,62	
O101	U(2)-O(101)	2,50	0,42	1,92
	C(10a)-O(101)	1,24	1,50	
O102	U(2)-O(102)	2,47	0,45	1,83
	C(10a)-O(102)	1,27	1,38	
O111	U(1)-O(111)	2,37	0,54	1,92
	O(111)-C(11a)	1,27	1,38	
O112	O(112)-C(11a)	1,21	1,63	1,63
O121	U(2)-O(121)	2,36	0,55	1,93
	O(121)-C(12a)	1,27	1,38	
O122	Ce(1)-O(122)	2,44	0,40	1,90
	O(122)-C(12a)#2	1,24	1,50	
O12u	U(1)-O(12u)	1,78	1,69	1,69
O13u	U(1)-O(13u)	1,78	1,69	1,69
O1w	Ce(1)-O(1w)	2,56	0,29	0,29
O21u	U(2)-O(21u)	1,76	1,75	1,75
O22u	U(2)-O(22u)	1,76	1,75	1,75
O2w	Ce(1)-O(2w)	2,59	0,27	0,27
O3w	Ce(1)-O(3w)	2,50	0,34	0,34
O4w	Ce(1)-O(4w)	2,57	0,28	0,28
O5w	Ce(1)-O(5w)	2,58	0,28	0,28
O6w	Ce(1)-O(6w)	2,58	0,28	0,28
O71a	U(1)-O(71a)	2,48	0,44	1,82
	C(7a)-O(71a)	1,27	1,38	
O72a	U(1)-O(72a)	2,46	0,45	1,95
	C(7a)-O(72a)	1,24	1,50	
O7w	Ce(1)-O(7w)	2,50	0,34	0,34
O81a	U(2)-O(81a)	2,36	0,55	2,01
	C(8a)-O(81a)	1,25	1,46	
O82a	C(8a)-O(82a)	1,27	1,38	1,38
O91	Ce(1)-O(91)	2,50	0,34	1,80
	C(9)-O(91)	1,25	1,46	
O92	U(1)-O(92)	2,36	0,55	1,93
	C(9)-O(92)	1,27	1,38	

Table 0.23 Atomic coordinates (x10⁴) and equivalent isotropic displacement parameters (A²x10³) for complex NdUmel.

Atom	x	y	z	U(eq)
U(1)	3558(1)	10230(1)	239	12(1)
U(2)	1337(1)	4841(1)	281(1)	12(1)
Nd(1)	3435(1)	6455(1)	2723(1)	18(1)
C(10a)	3131(4)	5178(6)	219(4)	13(1)
C(4a)	4072(4)	5215(7)	194(3)	12(1)
O(102)	2720(3)	4575(6)	-238(3)	19(1)
O(101)	2739(3)	5776(6)	666(2)	18(1)
C(1a)	840(4)	9855(6)	207(4)	13(1)
C(7a)	1782(4)	9884(6)	188(3)	14(1)
O(72a)	2166(4)	10605(7)	-242(3)	23(1)
C(8a)	875(4)	8099(8)	1171(3)	13(1)
O(81a)	1044(3)	6654(6)	1110(2)	16(1)
O(82a)	996(3)	8885(6)	1659(3)	21(1)
C(9)	4074(4)	6987(8)	1163(3)	10(1)
O(92)	3824(3)	8418(6)	1064(3)	18(1)
O(91)	4063(3)	6330(6)	1680(3)	22(1)
O(12u)	3790(3)	8630(7)	-281(3)	22(1)
O(22u)	1549(3)	3226(6)	793(2)	20(1)
O(122)	4075(3)	6160(6)	3750(3)	19(1)
O(5w)	2795(4)	8576(7)	3430(3)	30(1)
O(4w)	2617(4)	8435(8)	2047(3)	37(2)
O(121)	1073(3)	3154(6)	-583(3)	18(1)
O(1h)	-51(3)	4236(7)	473(2)	20(1)
O(111)	3836(3)	11893(6)	-622(3)	18(1)
O(13u)	3347(3)	11838(6)	752(2)	22(1)
O(21u)	1105(3)	6448(6)	-244(3)	22(1)
O(112)	3916(3)	14001(7)	-1258(3)	22(1)
C(11a)	4046(4)	13341(8)	-752(3)	11(1)
O(3w)	4255(4)	8988(8)	2716(4)	45(2)
O(2w)	4987(3)	5672(8)	2708(4)	39(2)
O(1w)	2552(6)	4849(10)	1956(5)	66(2)
O(71a)	2185(3)	9167(7)	609(3)	22(1)
C(2a)	403(4)	8997(8)	649(3)	10(1)
C(6a)	381(4)	10761(8)	-240(3)	10(1)
C(3a)	-478(4)	8926(7)	653(3)	9(1)
C(5a)	4506(4)	4284(8)	-253(3)	10(1)
C(12a)	841(4)	1757(8)	-729(3)	13(1)
O(11w)	5700(6)	105(10)	2211(4)	58(2)
O(8w)	5016(5)	2811(11)	1582(4)	58(2)
O(7w)	3567(7)	3552(15)	2889(6)	105(4)
O(10w)	4571(7)	1650(12)	3527(5)	84(3)
O(6w)	2012(7)	5638(14)	3147(5)	94(3)
O(12w)	3757(8)	7196(18)	8461(7)	123(5)
O(9w)	2248(9)	1802(17)	2387(6)	128(5)

Table 0.24 Bond lengths for complex NdUmel.

Bond	Bond length	Bond	Bond length
U(1)-U(2)#1	4.403(1)	Nd(1)-O(7w)	2.45(1)
U(1)-C(7a)	2.830(6)	Nd(1)-O(6w)	2.52(1)
U(1)-O(72a)	2.455(6)	C(10a)-C(4a)	1.49(1)
U(1)-O(92)	2.365(6)	C(10a)-O(102)	1.28(1)
U(1)-O(12u)	1.777(6)	C(10a)-O(101)	1.25(1)
U(1)-O(1h)#1	2.303(5)	C(4a)-C(3a)#1	1.41(1)
U(1)-O(111)	2.354(6)	C(4a)-C(5a)	1.41(1)
U(1)-O(13u)	1.766(5)	C(1a)-C(7a)	1.49(1)
U(1)-O(71a)	2.478(5)	C(1a)-C(2a)	1.38(1)
U(2)-C(10a)	2.857(6)	C(1a)-C(6a)	1.42(1)
U(2)-O(102)	2.468(5)	C(7a)-O(72a)	1.26(1)
U(2)-O(101)	2.493(5)	C(7a)-O(71a)	1.26(1)
U(2)-O(81a)	2.381(5)	C(8a)-O(81a)	1.24(1)

Bond	Bond length	Bond	Bond length
U(2)-O(22u)	1.769(5)	C(8a)-O(82a)	1.25(1)
U(2)-O(121)	2.366(6)	C(8a)-C(2a)	1.54(1)
U(2)-O(1h)	2.293(5)	C(9)-O(92)	1.27(1)
U(2)-O(21u)	1.789(6)	C(9)-O(91)	1.24(1)
Nd(1)-C(9)	3.532(6)	C(9)-C(3a)#1	1.51(1)
Nd(1)-O(91)	2.455(6)	O(122)-C(12a)#2	1.23(1)
Nd(1)-O(122)	2.443(6)	O(121)-C(12a)	1.26(1)
Nd(1)-O(5w)	2.541(6)	O(111)-C(11a)	1.28(1)
Nd(1)-O(4w)	2.550(7)	O(112)-C(11a)	1.24(1)
Nd(1)-O(3w)	2.476(7)	C(11a)-C(5a)#3	1.52(1)
Nd(1)-O(2w)	2.543(5)	C(2a)-C(3a)	1.40(1)
Nd(1)-O(1w)	2.54(1)	C(6a)-C(5a)#4	1.39(1)
Nd(1)-C(12a)#2	3.53(1)	C(6a)-C(12a)#3	1.52(1)

Table 0.25 Bond Angles for complex NdUmel.

Bond	Angle [°]	Bond	Angle [°]	Bond	Angle [°]
O(2w)-Nd(1)-O(7w)	70.5(3)	C(8a)#1-C(9)-C(3a)#1	61.5(3)	O(92)-O(71a)-C(2a)	152.9(3)
O(2w)-Nd(1)-O(6w)	143.0(3)	O(92)-C(9)-O(91)	124.1(6)	O(13u)-O(71a)-C(2a)	131.9(3)
O(1w)-Nd(1)-O(7w)	67.9(4)	O(92)-C(9)-C(2a)#1	119.4(5)	C(4a)#4-C(2a)-C(1a)	91.0(4)
O(1w)-Nd(1)-O(6w)	66.5(3)	O(92)-C(9)-C(3a)#1	119.6(6)	C(4a)#4-C(2a)-C(7a)	121.3(3)
O(7w)-Nd(1)-O(6w)	76.0(4)	O(91)-C(9)-C(2a)#1	105.2(5)	C(4a)#4-C(2a)-C(8a)	148.2(5)
U(2)-C(10a)-C(4a)	175.5(4)	O(91)-C(9)-C(3a)#1	115.8(6)	C(4a)#4-C(2a)-O(81a)	138.9(3)
U(2)-C(10a)-O(102)	59.5(3)	C(2a)#1-C(9)-C(3a)#1	28.8(3)	C(4a)#4-C(2a)-O(82a)	136.8(4)
U(2)-C(10a)-O(101)	60.5(3)	U(1)-O(92)-O(101)	98.9(2)	C(4a)#4-C(2a)-C(9)#4	62.4(3)
U(2)-C(10a)-C(9)	121.5(3)	U(1)-O(92)-C(9)	141.1(5)	C(4a)#4-C(2a)-O(71a)	147.7(3)
U(2)-C(10a)-C(11a)#5	117.9(3)	U(1)-O(92)-O(91)	167.9(3)	C(4a)#4-C(2a)-C(6a)	60.1(3)
U(2)-C(10a)-C(3a)#1	152.3(3)	U(1)-O(92)-O(12u)	37.8(1)	C(4a)#4-C(2a)-C(3a)	30.9(3)
U(2)-C(10a)-C(5a)	148.3(3)	U(1)-O(92)-O(4w)	115.7(2)	C(4a)#4-C(2a)-C(5a)#4	30.4(2)
C(4a)-C(10a)-O(102)	119.3(6)	U(1)-O(92)-O(1h)#1	50.6(1)	C(1a)-C(2a)-C(7a)	30.3(3)
C(4a)-C(10a)-O(101)	121.1(6)	U(1)-O(92)-O(71a)	55.9(2)	C(1a)-C(2a)-C(8a)	120.7(6)
C(4a)-C(10a)-C(9)	60.4(4)	U(1)-O(92)-C(3a)#1	108.8(3)	C(1a)-C(2a)-O(81a)	119.5(5)
C(4a)-C(10a)-C(11a)#5	59.9(4)	O(101)-O(92)-C(9)	61.8(4)	C(1a)-C(2a)-O(82a)	117.1(5)
C(4a)-C(10a)-C(3a)#1	29.4(3)	O(101)-O(92)-O(91)	71.7(2)	C(1a)-C(2a)-C(9)#4	153.4(5)
C(4a)-C(10a)-C(5a)	29.2(3)	O(101)-O(92)-O(12u)	75.1(2)	C(1a)-C(2a)-O(71a)	56.7(4)
O(102)-C(10a)-O(101)	119.6(6)	O(101)-O(92)-O(4w)	80.0(2)	C(1a)-C(2a)-C(6a)	31.0(3)
O(102)-C(10a)-C(9)	171.8(5)	O(101)-O(92)-O(1h)#1	137.1(2)	C(1a)-C(2a)-C(3a)	121.9(6)
O(102)-C(10a)-C(11a)	60.4(4)	O(101)-O(92)-O(71a)	61.8(2)	C(1a)-C(2a)-C(5a)#4	60.7(4)
O(102)-C(10a)-C(3a)#1	148.1(5)	O(101)-O(92)-C(3a)#1	63.5(2)	C(7a)-C(2a)-C(8a)	90.4(4)
O(102)-C(10a)-C(5a)	90.8(5)	C(9)-O(92)-O(91)	27.5(4)	C(7a)-C(2a)-O(81a)	91.9(3)
O(101)-C(10a)-C(9)	61.0(4)	C(9)-O(92)-O(12u)	103.4(4)	C(7a)-C(2a)-O(82a)	91.6(3)
O(101)-C(10a)-C(11a)	172.3(5)	C(9)-O(92)-O(4w)	95.1(4)	C(7a)-C(2a)-C(9)#4	176.3(4)
O(101)-C(10a)-C(3a)#1	91.8(5)	C(9)-O(92)-O(1h)#1	120.4(4)	C(7a)-C(2a)-O(71a)	26.4(2)
O(101)-C(10a)-C(5a)	149.3(5)	C(9)-O(92)-O(71a)	123.2(4)	C(7a)-C(2a)-C(6a)	61.3(3)
C(9)-C(10a)-C(11a)#5	120.2(3)	C(9)-O(92)-C(3a)#1	33.1(4)	C(7a)-C(2a)-C(3a)	152.1(5)
C(9)-C(10a)-C(3a)#1	31.0(2)	O(91)-O(92)-O(12u)	130.3(3)	C(7a)-C(2a)-C(5a)#4	91.0(3)
C(9)-C(10a)-C(5a)	89.5(3)	O(91)-O(92)-O(4w)	71.1(2)	C(8a)-C(2a)-O(81a)	26.4(3)
C(11a)-C(10a)-C(3a)	89.2(3)	O(91)-O(92)-O(1h)#1	132.6(3)	C(8a)-C(2a)-O(82a)	28.5(3)
C(11a)#5-C(10a)-C(5a)	30.7(2)	O(91)-O(92)-O(71a)	122.2(3)	C(8a)-C(2a)-C(9)#4	85.9(4)
C(3a)#1-C(10a)-C(5a)	58.5(2)	O(91)-O(92)-C(3a)#1	60.4(2)	C(8a)-C(2a)-O(71a)	64.0(3)
C(10a)-C(4a)-O(102)	27.8(3)	O(12u)-O(92)-O(4w)	136.7(3)	C(8a)-C(2a)-C(6a)	151.6(5)
C(10a)-C(4a)-O(101)	26.6(3)	O(12u)-O(92)-O(1h)#1	62.5(2)	C(8a)-C(2a)-C(3a)	117.4(6)
C(10a)-C(4a)-C(1a)#1	176.5(5)	O(12u)-O(92)-O(71a)	68.0(2)	C(8a)-C(2a)-C(5a)#4	177.2(5)
C(10a)-C(4a)-C(9)	89.1(4)	O(12u)-O(92)-C(3a)#1	72.1(2)	O(81a)-C(2a)-O(82a)	54.8(2)
C(10a)-C(4a)-C(11a)#5	90.0(4)	O(4w)-O(92)-O(1h)#1	136.5(3)	O(81a)-C(2a)-C(9)#4	84.7(3)
C(10a)-C(4a)-C(2a)#1	149.7(5)	O(4w)-O(92)-O(71a)	69.0(2)	O(81a)-C(2a)-O(71a)	68.4(2)
C(10a)-C(4a)-C(6a)#1	149.8(5)	O(4w)-O(92)-C(3a)#1	125.7(3)	O(81a)-C(2a)-C(6a)	145.5(4)
C(10a)-C(4a)-C(3a)#1	119.4(6)	O(1h)#1-O(92)-O(71a)	105.1(2)	O(81a)-C(2a)-C(3a)	112.6(4)
C(10a)-C(4a)-C(5a)	119.9(6)	O(1h)#1-O(92)-C(3a)#1	95.8(3)	O(81a)-C(2a)-C(5a)#4	155.8(3)
O(102)-C(4a)-O(101)	54.4(2)	O(71a)-O(92)-C(3a)#1	118.1(3)	O(82a)-C(2a)-C(9)#4	85.2(3)
O(102)-C(4a)-C(1a)#1	153.2(4)	Nd(1)-O(91)-C(9)	143.7(5)	O(82a)-C(2a)-O(71a)	68.5(2)
O(102)-C(4a)-C(9)	116.6(3)	Nd(1)-O(91)-O(92)	116.3(3)	O(82a)-C(2a)-C(6a)	139.2(4)
O(102)-C(4a)-C(11a)#5	62.7(3)	Nd(1)-O(91)-O(4w)	54.8(2)	O(82a)-C(2a)-C(3a)	113.0(5)

Bond	Angle [°]	Bond	Angle [°]	Bond	Angle [°]
O(102)-C(4a)-C(2a)#1	176.8(3)	Nd(1)-O(91)-O(2w)	58.8(2)	O(82a)-C(2a)-C(5a)#4	149.1(3)
O(102)-C(4a)-C(6a)#1	122.9(3)	Nd(1)-O(91)-O(1w)	58.0(2)	C(9)#4-C(2a)-O(71a)	149.9(3)
O(102)-C(4a)-C(3a)#1	146.7(5)	Nd(1)-O(91)-C(3a)#1	173.7(3)	C(9)#4-C(2a)-C(6a)	122.4(3)
O(102)-C(4a)-C(5a)	92.8(4)	C(9)-O(91)-O(92)	28.4(4)	C(9)#4-C(2a)-C(3a)	31.5(3)
O(101)-C(4a)-C(1a)#1	152.1(4)	C(9)-O(91)-O(4w)	89.3(4)	C(9)#4-C(2a)-C(5a)#4	92.7(3)
O(101)-C(4a)-C(9)	62.7(3)	C(9)-O(91)-O(2w)	144.6(5)	O(71a)-C(2a)-C(6a)	87.7(3)
O(101)-C(4a)-C(11a)#5	116.2(3)	C(9)-O(91)-O(1w)	113.7(5)	O(71a)-C(2a)-C(3a)	178.5(5)
O(101)-C(4a)-C(2a)#1	123.1(4)	C(9)-O(91)-C(3a)#1	35.7(4)	O(71a)-C(2a)-C(5a)#4	117.4(3)
O(101)-C(4a)-C(6a)#1	171.5(3)	O(92)-O(91)-O(4w)	64.4(2)	C(6a)-C(2a)-C(3a)	90.9(4)
O(101)-C(4a)-C(3a)#1	92.9(4)	O(92)-O(91)-O(2w)	137.6(3)	C(6a)-C(2a)-C(5a)#4	29.7(2)
O(101)-C(4a)-C(5a)	145.7(5)	O(92)-O(91)-O(1w)	109.3(3)	C(3a)-C(2a)-C(5a)#4	61.2(4)
C(1a)#1-C(4a)-C(9)	90.2(3)	O(92)-O(91)-C(3a)#1	63.9(3)	C(4a)#4-C(6a)-C(1a)	90.0(4)
C(1a)-C(4a)-C(11a)	90.6(3)	O(4w)-O(91)-O(2w)	108.5(3)	C(4a)#4-C(6a)-C(7a)	121.3(3)
C(1a)#1-C(4a)-C(2a)#1	29.4(2)	O(4w)-O(91)-O(1w)	62.6(2)	C(4a)#4-C(6a)-O(72a)	147.5(3)
C(1a)#1-C(4a)-C(6a)#1	30.5(2)	O(4w)-O(91)-C(3a)#1	122.8(3)	C(4a)#4-C(6a)-O(122)#6	135.8(4)
C(1a)#1-C(4a)-C(3a)#1	59.9(4)	O(2w)-O(91)-O(1w)	101.7(3)	C(4a)#4-C(6a)-O(121)#3	142.5(3)
C(1a)#1-C(4a)-C(5a)	60.5(4)	O(2w)-O(91)-C(3a)#1	125.9(3)	C(4a)#4-C(6a)-C(11a)#15	62.9(3)
C(9)-C(4a)-C(11a)#5	177.7(3)	O(1w)-O(91)-C(3a)#1	115.7(3)	C(4a)#4-C(6a)-C(2a)	60.1(3)
C(9)-C(4a)-C(2a)#1	60.7(3)	U(1)-O(12u)-O(92)	54.6(2)	C(4a)#4-C(6a)-C(3a)	30.2(2)
C(9)-C(4a)-C(6a)#1	120.6(3)	U(1)-O(12u)-O(111)	56.4(2)	C(4a)#4-C(6a)-C(5a)#4	30.7(4)
C(9)-C(4a)-C(3a)#1	30.3(3)	U(1)-O(12u)-O(12w)#8	151.0(4)	C(4a)#4-C(6a)-C(12a)#3	149.3(5)
C(9)-C(4a)-C(5a)	150.6(5)	O(92)-O(12u)-O(111)	108.6(2)	C(1a)-C(6a)-C(7a)	31.3(3)
C(11a)-C(4a)-C(2a)	120.0(3)	O(92)-O(12u)-O(12w)#8	152.7(4)	C(1a)-C(6a)-O(72a)	57.7(4)
C(11a)-C(4a)-C(6a)	60.1(3)	O(111)-O(12u)-O(12w)#8	98.7(4)	C(1a)-C(6a)-O(122)#6	120.7(5)
C(11a)-C(4a)-C(3a)	150.5(5)	U(2)-O(22u)-O(101)	60.0(2)	C(1a)-C(6a)-O(121)#3	114.6(4)
C(11a)#5-C(4a)-C(5a)	30.1(3)	U(2)-O(22u)-O(1h)	55.9(2)	C(1a)-C(6a)-C(11a)#15	152.8(5)
C(2a)#1-C(4a)-C(6a)#1	59.9(3)	O(101)-O(22u)-O(1h)	110.9(2)	C(1a)-C(6a)-C(2a)	30.0(3)
C(2a)#1-C(4a)-C(3a)#1	30.5(3)	Nd(1)-O(122)-O(72a)#9	113.7(2)	C(1a)-C(6a)-C(3a)	59.8(4)
C(2a)#1-C(4a)-C(5a)	90.0(4)	Nd(1)-O(122)-O(5w)	55.5(2)	C(1a)-C(6a)-C(5a)#4	120.7(6)
C(6a)#1-C(4a)-C(3a)#1	90.4(4)	Nd(1)-O(122)-O(121)#2	118.0(3)	C(1a)-C(6a)-C(12a)#3	120.7(6)
C(6a)#1-C(4a)-C(5a)	30.1(3)	Nd(1)-O(122)-O(2w)	59.1(2)	C(7a)-C(6a)-O(72a)	26.4(2)
C(3a)#1-C(4a)-C(5a)	120.4(6)	Nd(1)-O(122)-C(6a)#9	176.2(3)	C(7a)-C(6a)-O(122)#6	93.2(3)
U(2)-O(102)-C(10a)	93.9(4)	Nd(1)-O(122)-C(12a)#2	145.7(5)	C(7a)-C(6a)-O(121)#3	87.1(3)
U(2)-O(102)-C(4a)	126.7(3)	Nd(1)-O(122)-O(7w)	52.9(3)	C(7a)-C(6a)-C(11a)#15	175.2(4)
U(2)-O(102)-O(101)	64.4(2)	O(72a)#9-O(122)-O(5w)	79.6(2)	C(7a)-C(6a)-C(2a)	61.3(3)
U(2)-O(102)-O(121)	50.7(1)	O(72a)-O(122)-O(121)	64.6(2)	C(7a)-C(6a)-C(3a)	91.1(3)
U(2)-O(102)-O(111)#5	136.3(2)	O(72a)#9-O(122)-O(2w)	160.0(3)	C(7a)-C(6a)-C(5a)#4	152.0(5)
U(2)-O(102)-O(21u)	36.7(1)	O(72a)#9-O(122)-C(6a)#9	63.0(2)	C(7a)-C(6a)-C(12a)#3	89.3(4)
U(2)-O(102)-O(112)#5	157.6(2)	O(72a)-O(122)-C(12a)	57.9(4)	O(72a)-C(6a)-O(122)#6	68.9(2)
U(2)-O(102)-C(11a)#5	161.7(3)	O(72a)#9-O(122)-O(7w)	99.3(3)	O(72a)-C(6a)-O(121)#3	65.1(2)
U(2)-O(102)-C(5a)	153.7(3)	O(5w)-O(122)-O(121)#2	64.2(2)	O(72a)-C(6a)-C(11a)#15	149.1(3)
C(10a)-O(102)-C(4a)	32.9(4)	O(5w)-O(122)-O(2w)	106.2(3)	O(72a)-C(6a)-C(2a)	87.7(3)
C(10a)-O(102)-O(101)	29.8(3)	O(5w)-O(122)-C(6a)#9	124.3(3)	O(72a)-C(6a)-C(3a)	117.4(3)
C(10a)-O(102)-O(121)	142.8(5)	O(5w)-O(122)-C(12a)#2	90.6(4)	O(72a)-C(6a)-C(5a)#4	175.6(5)
C(10a)-O(102)-O(111)	101.9(4)	O(5w)-O(122)-O(7w)	99.6(3)	O(72a)-C(6a)-C(12a)#3	63.0(4)
C(10a)-O(102)-O(21u)	103.5(4)	O(121)#2-O(122)-O(2w)	135.3(3)	O(122)#6-C(6a)-O(121)#3	55.3(2)
C(10a)-O(102)-O(112)	108.0(4)	O(121)#2-O(122)-C(6a)#9	63.0(3)	O(122)#6-C(6a)-C(11a)	82.0(3)
C(10a)-O(102)-C(11a)	94.0(4)	O(121)-O(122)-C(12a)	28.0(4)	O(122)#6-C(6a)-C(2a)	144.2(4)
C(10a)-O(102)-C(5a)	62.3(4)	O(121)#2-O(122)-O(7w)	158.1(3)	O(122)#6-C(6a)-C(3a)	152.1(3)
C(4a)-O(102)-O(101)	62.6(3)	O(2w)-O(122)-C(6a)#9	123.2(3)	O(122)#6-C(6a)-C(5a)#4	110.5(5)
C(4a)-O(102)-O(121)	167.1(3)	O(2w)-O(122)-C(12a)#2	139.3(5)	O(122)#6-C(6a)-C(12a)#3	27.6(3)
C(4a)-O(102)-O(111)	75.1(2)	O(2w)-O(122)-O(7w)	61.1(3)	O(121)#3-C(6a)-C(11a)	90.2(3)
C(4a)-O(102)-O(21u)	130.5(3)	C(6a)#9-O(122)-C(12a)#2	35.0(4)	O(121)#3-C(6a)-C(2a)	138.2(4)
C(4a)-O(102)-O(112)#5	75.5(2)	C(6a)#9-O(122)-O(7w)	124.8(4)	O(121)#3-C(6a)-C(3a)	152.5(3)
C(4a)-O(102)-C(11a)#5	61.8(2)	C(12a)#2-O(122)-O(7w)	153.1(5)	O(121)#3-C(6a)-C(5a)#4	118.3(5)
C(4a)-O(102)-C(5a)	29.8(2)	Nd(1)-O(5w)-O(122)	52.4(2)	O(121)#3-C(6a)-C(12a)#3	27.7(3)
O(101)-O(102)-O(121)	114.7(3)	Nd(1)-O(5w)-O(4w)	54.2(2)	C(11a)#15-C(6a)-C(2a)	122.9(3)
O(101)-O(102)-O(111)	125.7(3)	Nd(1)-O(5w)-O(121)#2	96.4(2)	C(11a)#15-C(6a)-C(3a)	93.1(3)
O(101)-O(102)-O(21u)	77.1(2)	Nd(1)-O(5w)-O(112)#9	127.9(3)	C(11a)#15-C(6a)-C(5a)#4	32.1(4)
O(101)-O(102)-O(112)	136.8(3)	Nd(1)-O(5w)-O(3w)	55.0(2)	C(11a)#15-C(6a)-C(12a)	86.4(4)
O(101)-O(102)-C(11a)	123.4(3)	Nd(1)-O(5w)-O(6w)	56.1(3)	C(2a)-C(6a)-C(3a)	29.8(2)
O(101)-O(102)-C(5a)	92.0(3)	O(122)-O(5w)-O(4w)	105.7(3)	C(2a)-C(6a)-C(5a)#4	90.8(4)
O(121)-O(102)-O(111)	98.9(2)	O(122)-O(5w)-O(121)#2	45.1(2)	C(2a)-C(6a)-C(12a)#3	150.6(5)

Bond	Angle [°]	Bond	Angle [°]	Bond	Angle [°]
O(121)-O(102)-O(21u)	56.9(2)	O(122)-O(5w)-O(112)#9	134.0(3)	C(3a)-C(6a)-C(5a)#4	61.0(4)
O(121)-O(102)-O(112)	108.5(2)	O(122)-O(5w)-O(3w)	69.0(2)	C(3a)-C(6a)-C(12a)#3	179.5(5)
O(121)-O(102)-C(11a)	116.8(3)	O(122)-O(5w)-O(6w)	76.1(3)	C(5a)#4-C(6a)-C(12a)#3	118.6(6)
O(121)-O(102)-C(5a)	147.3(3)	O(4w)-O(5w)-O(121)#2	144.0(3)	C(10a)#4-C(3a)-C(4a)#4	31.2(3)
O(111)-O(102)-O(21u)	154.1(2)	O(4w)-O(5w)-O(112)#9	98.7(3)	C(10a)#4-C(3a)-O(101)#4	26.1(2)
O(111)-O(102)-O(112)	44.4(2)	O(4w)-O(5w)-O(3w)	62.4(3)	C(10a)#4-C(3a)-C(1a)	121.0(3)
O(111)-O(102)-C(11a)	25.5(2)	O(4w)-O(5w)-O(6w)	73.1(3)	C(10a)#4-C(3a)-C(8a)	175.5(4)
O(111)#5-O(102)-C(5a)	48.6(2)	O(121)-O(5w)-O(112)	116.8(3)	C(10a)#4-C(3a)-C(9)#4	90.4(4)
O(21u)-O(102)-O(112)	129.2(2)	O(121)#2-O(5w)-O(3w)	84.4(3)	C(10a)#4-C(3a)-O(92)#4	88.5(3)
O(21u)-O(102)-C(11a)	154.0(3)	O(121)#2-O(5w)-O(6w)	109.7(3)	C(10a)#4-C(3a)-O(91)#4	96.1(3)
O(21u)-O(102)-C(5a)	153.5(3)	O(112)#9-O(5w)-O(3w)	155.7(3)	C(10a)#4-C(3a)-C(2a)	149.7(5)
O(112)-O(102)-C(11a)	24.9(2)	O(112)#9-O(5w)-O(6w)	74.7(3)	C(10a)#4-C(3a)-C(6a)	90.5(3)
O(112)#5-O(102)-C(5a)	48.4(2)	O(3w)-O(5w)-O(6w)	110.7(3)	C(10a)#4-C(3a)-C(5a)#4	60.9(3)
C(11a)#5-O(102)-C(5a)	32.0(2)	Nd(1)-O(4w)-O(82a)	137.9(3)	C(4a)#4-C(3a)-O(101)#4	57.2(3)
U(2)-O(101)-C(10a)	93.6(4)	Nd(1)-O(4w)-O(92)	94.5(2)	C(4a)#4-C(3a)-C(1a)	89.8(4)
U(2)-O(101)-C(4a)	125.8(3)	Nd(1)-O(4w)-O(91)	51.9(2)	C(4a)#4-C(3a)-C(8a)	151.7(5)
U(2)-O(101)-O(102)	63.3(2)	Nd(1)-O(4w)-O(5w)	53.9(2)	C(4a)#4-C(3a)-C(9)#4	121.6(6)
U(2)-O(101)-O(81a)	51.2(1)	Nd(1)-O(4w)-O(1w)	53.9(2)	C(4a)#4-C(3a)-O(92)#4	115.7(4)
U(2)-O(101)-C(9)	172.3(3)	Nd(1)-O(4w)-O(9w)#3	124.9(4)	C(4a)#4-C(3a)-O(91)#4	123.3(5)
U(2)-O(101)-O(92)	148.9(2)	O(82a)-O(4w)-O(92)	113.9(3)	C(4a)#4-C(3a)-C(2a)	118.7(6)
U(2)-O(101)-O(22u)	37.9(1)	O(82a)-O(4w)-O(91)	136.2(3)	C(4a)#4-C(3a)-C(6a)	59.4(4)
U(2)-O(101)-O(1w)	98.2(2)	O(82a)-O(4w)-O(5w)	112.8(3)	C(4a)#4-C(3a)-C(5a)#4	29.8(3)
U(2)-O(101)-O(71a)	91.2(2)	O(82a)-O(4w)-O(1w)	94.8(3)	O(101)#4-C(3a)-C(1a)	146.5(3)
U(2)-O(101)-C(3a)#1	155.6(3)	O(82a)-O(4w)-O(9w)#3	76.1(3)	O(101)#4-C(3a)-C(8a)	150.4(3)
C(10a)-O(101)-C(4a)	32.3(4)	O(92)-O(4w)-O(91)	44.6(2)	O(101)#4-C(3a)-C(9)#4	64.5(3)
C(10a)-O(101)-O(102)	30.6(4)	O(92)-O(4w)-O(5w)	132.5(3)	O(101)#4-C(3a)-O(92)#4	67.0(2)
C(10a)-O(101)-O(81a)	143.5(5)	O(92)-O(4w)-O(1w)	88.3(3)	O(101)#4-C(3a)-O(91)#4	71.9(2)
C(10a)-O(101)-C(9)	93.9(4)	O(92)-O(4w)-O(9w)#3	108.8(4)	O(101)#4-C(3a)-C(2a)	172.6(5)
C(10a)-O(101)-O(92)	103.5(4)	O(91)-O(4w)-O(5w)	102.3(3)	O(101)#4-C(3a)-C(6a)	116.2(3)
C(10a)-O(101)-O(22u)	96.1(4)	O(91)-O(4w)-O(1w)	54.9(2)	O(101)#4-C(3a)-C(5a)#4	86.8(3)
C(10a)-O(101)-O(1w)	133.1(5)	O(91)-O(4w)-O(9w)#3	140.6(4)	C(1a)-C(3a)-C(8a)	61.9(3)
C(10a)-O(101)-O(71a)	119.8(4)	O(5w)-O(4w)-O(1w)	96.2(3)	C(1a)-C(3a)-C(9)#4	148.4(5)
C(10a)-O(101)-C(3a)#1	62.1(4)	O(5w)-O(4w)-O(9w)#3	74.6(3)	C(1a)-C(3a)-O(92)#4	143.0(3)
C(4a)-O(101)-O(102)	62.9(3)	O(1w)-O(4w)-O(9w)#3	162.8(4)	C(1a)-C(3a)-O(91)#4	132.2(4)
C(4a)-O(101)-O(81a)	173.3(3)	U(2)-O(121)-O(102)	53.9(2)	C(1a)-C(3a)-C(2a)	28.8(3)
C(4a)-O(101)-C(9)	61.8(2)	U(2)-O(121)-O(72a)#5	97.7(2)	C(1a)-C(3a)-C(6a)	30.4(2)
C(4a)-O(101)-O(92)	75.6(2)	U(2)-O(121)-O(122)#10	167.4(3)	C(1a)-C(3a)-C(5a)#4	60.0(3)
C(4a)-O(101)-O(22u)	118.6(3)	U(2)-O(121)-O(5w)#10	114.1(2)	C(8a)-C(3a)-C(9)#4	86.6(4)
C(4a)-O(101)-O(1w)	116.4(3)	U(2)-O(121)-O(21u)	38.9(1)	C(8a)-C(3a)-O(92)#4	90.4(3)
C(4a)-O(101)-O(71a)	115.6(3)	U(2)-O(121)-C(6a)#5	109.5(3)	C(8a)-C(3a)-O(91)#4	79.7(3)
C(4a)-O(101)-C(3a)#1	29.8(2)	U(2)-O(121)-C(12a)	142.7(5)	C(8a)-C(3a)-C(2a)	33.0(3)
O(102)-O(101)-O(81a)	113.0(3)	O(102)-O(121)-O(72a)#5	72.3(2)	C(8a)-C(3a)-C(6a)	92.3(3)
O(102)-O(101)-C(9)	124.1(3)	O(102)-O(121)-O(122)	123.9(3)	C(8a)-C(3a)-C(5a)#4	121.9(3)
O(102)-O(101)-O(92)	127.8(3)	O(102)-O(121)-O(5w)#10	64.9(2)	C(9)#4-C(3a)-O(92)#4	27.3(3)
O(102)-O(101)-O(22u)	74.7(2)	O(102)-O(121)-O(21u)	62.2(2)	C(9)#4-C(3a)-O(91)#4	28.5(3)
O(102)-O(101)-O(1w)	136.8(3)	O(102)-O(121)-C(6a)#5	131.3(3)	C(9)#4-C(3a)-C(2a)	119.6(6)
O(102)-O(101)-O(71a)	113.3(3)	O(102)-O(121)-C(12a)	133.5(4)	C(9)#4-C(3a)-C(6a)	176.5(5)
O(102)-O(101)-C(3a)#1	92.6(3)	O(72a)-O(121)-O(122)	70.8(2)	C(9)#4-C(3a)-C(5a)#4	151.3(5)
O(81a)-O(101)-C(9)	121.1(3)	O(72a)-O(121)-O(5w)	84.2(2)	O(92)#4-C(3a)-O(91)#4	55.7(2)
O(81a)-O(101)-O(92)	104.8(2)	O(72a)#5-O(121)-O(21u)	130.3(2)	O(92)#4-C(3a)-C(2a)	119.6(5)
O(81a)-O(101)-O(22u)	63.3(2)	O(72a)#5-O(121)-C(6a)#5	65.0(2)	O(92)#4-C(3a)-C(6a)	156.1(3)
O(81a)-O(101)-O(1w)	70.2(2)	O(72a)#5-O(121)-C(12a)	63.4(4)	O(92)#4-C(3a)-C(5a)#4	141.1(3)
O(81a)-O(101)-O(71a)	60.4(2)	O(122) -O(121)-O(5w)	70.7(2)	O(91)#4-C(3a)-C(2a)	108.7(5)
O(81a)-O(101)-C(3a)#1	152.9(3)	O(122)-O(121)-O(21u)	153.6(3)	O(91)#4-C(3a)-C(6a)	148.0(3)
C(9)-O(101)-O(92)	25.8(2)	O(122)-O(121)-C(6a)	61.7(2)	O(91)#4-C(3a)-C(5a)#4	143.5(3)
C(9)-O(101)-O(22u)	142.6(3)	O(122)#10-O(121)-C(12a)	27.4(4)	C(2a)-C(3a)-C(6a)	59.3(4)
C(9)-O(101)-O(1w)	77.9(3)	O(5w)#10-O(121)-O(21u)	93.5(2)	C(2a)-C(3a)-C(5a)#4	88.9(4)
C(9)-O(101)-O(71a)	83.5(2)	O(5w)-O(121)-C(6a)	129.2(3)	C(6a)-C(3a)-C(5a)#4	29.6(2)
C(9)-O(101)-C(3a)#1	32.0(2)	O(5w)#10-O(121)-C(12a)	96.5(4)	C(10a)-C(5a)-C(4a)	30.9(3)
O(92)-O(101)-O(22u)	157.2(3)	O(21u)-O(121)-C(6a)#5	137.2(3)	C(10a)-C(5a)-O(102)	26.8(2)
O(92)-O(101)-O(1w)	88.8(3)	O(21u)-O(121)-C(12a)	164.1(5)	C(10a)-C(5a)-C(1a)#1	120.0(3)
O(92)-O(101)-O(71a)	57.9(2)	C(6a)#5-O(121)-C(12a)	34.3(4)	C(10a)-C(5a)-O(111)#5	89.7(3)
O(92)-O(101)-C(3a)#1	49.5(2)	U(1)#4-O(1h)-U(2)	146.7(3)	C(10a)-C(5a)-O(112)#5	93.2(3)

Bond	Angle [°]	Bond	Angle [°]	Bond	Angle [°]
O(22u)-O(101)-O(1w)	69.0(2)	U(1)#4-O(1h)-O(81a)	121.7(2)	C(10a)-C(5a)-C(11a)#5	91.3(4)
O(22u)-O(101)-O(71a)	121.2(2)	U(1)#4-O(1h)-O(92)#4	52.0(2)	C(10a)-C(5a)-C(2a)#1	90.5(3)
O(22u)-O(101)-C(3a)	136.4(3)	U(1)#4-O(1h)-O(22u)	173.0(3)	C(10a)-C(5a)-C(6a)#1	149.9(5)
O(1w)-O(101)-O(71a)	105.3(3)	U(1)#4-O(1h)-O(13u)#4	39.6(1)	C(10a)-C(5a)-C(3a)#1	60.6(3)
O(1w)-O(101)-C(3a)#1	97.7(3)	U(1)#4-O(1h)-O(8w)#7	108.9(2)	C(10a)-C(5a)-C(12a)#16	176.8(4)
O(71a)-O(101)-C(3a)#1	102.2(2)	U(2)-O(1h)-O(81a)	51.6(1)	C(4a)-C(5a)-O(102)	57.4(3)
C(4a)#4-C(1a)-C(7a)	177.9(5)	U(2)-O(1h)-O(92)#4	121.0(2)	C(4a)-C(5a)-C(1a)#1	89.1(4)
C(4a)#4-C(1a)-O(72a)	151.5(4)	U(2)-O(1h)-O(22u)	39.7(1)	C(4a)-C(5a)-O(111)#5	117.8(4)
C(4a)#4-C(1a)-C(8a)	91.0(3)	U(2)-O(1h)-O(13u)#4	173.3(3)	C(4a)-C(5a)-O(112)#5	118.9(5)
C(4a)#4-C(1a)-O(71a)	153.8(4)	U(2)-O(1h)-O(8w)#7	103.9(2)	C(4a)-C(5a)-C(11a)#5	122.1(6)
C(4a)#4-C(1a)-C(2a)	59.5(4)	O(81a)-O(1h)-O(92)#4	72.9(2)	C(4a)-C(5a)-C(2a)#1	59.7(4)
C(4a)#4-C(1a)-C(6a)	59.6(4)	O(81a)-O(1h)-O(22u)	63.8(2)	C(4a)-C(5a)-C(6a)#1	119.2(6)
C(4a)#4-C(1a)-C(3a)	30.3(2)	O(81a)-O(1h)-O(13u)#4	130.8(2)	C(4a)-C(5a)-C(3a)#1	29.8(3)
C(4a)#4-C(1a)-C(5a)#4	30.3(2)	O(81a)-O(1h)-O(8w)#7	89.9(2)	C(4a)-C(5a)-C(12a)#16	151.5(5)
C(4a)#4-C(1a)-C(12a)	90.4(3)	O(92)#4-O(1h)-O(22u)	130.8(2)	O(102)-C(5a)-C(1a)#1	146.4(3)
C(7a)-C(1a)-O(72a)	26.9(3)	O(92)#4-O(1h)-O(13u)#4	64.0(2)	O(102)-C(5a)-O(111)#5	68.4(2)
C(7a)-C(1a)-C(8a)	90.5(4)	O(92)#4-O(1h)-O(8w)#7	93.2(2)	O(102)-C(5a)-O(112)#5	68.0(2)
C(7a)-C(1a)-O(71a)	27.7(3)	O(22u)-O(1h)-O(13u)#4	133.9(3)	O(102)-C(5a)-C(11a)#5	64.7(4)
C(7a)-C(1a)-C(2a)	122.0(6)	O(22u)-O(1h)-O(8w)#7	65.6(2)	O(102)-C(5a)-C(2a)#1	117.0(3)
C(7a)-C(1a)-C(6a)	119.0(6)	O(13u)#4-O(1h)-O(8w)#7	70.6(2)	O(102)-C(5a)-C(6a)#1	176.2(5)
C(7a)-C(1a)-C(3a)	151.2(5)	U(1)-O(111)-O(102)#3	96.4(2)	O(102)-C(5a)-C(3a)#1	87.1(3)
C(7a)-C(1a)-C(5a)#4	148.2(5)	U(1)-O(111)-O(72a)	53.5(2)	O(102)-C(5a)-C(12a)#16	151.1(3)
C(7a)-C(1a)-C(12a)#3	88.2(4)	U(1)-O(111)-O(12u)	39.0(1)	C(1a)#1-C(5a)-O(111)#5	139.8(3)
O(72a)-C(1a)-C(8a)	117.4(3)	U(1)-O(111)-O(112)	163.1(3)	C(1a)#1-C(5a)-O(112)#5	137.8(4)
O(72a)-C(1a)-O(71a)	54.7(2)	U(1)-O(111)-C(11a)	140.6(5)	C(1a)#1-C(5a)-C(11a)#5	148.8(5)
O(72a)-C(1a)-C(2a)	148.8(5)	U(1)-O(111)-C(5a)#3	108.1(3)	C(1a)#1-C(5a)-C(2a)#1	29.5(2)
O(72a)-C(1a)-C(6a)	92.2(4)	O(102)#3-O(111)-O(72a)	70.4(2)	C(1a)#1-C(5a)-C(6a)#1	30.0(3)
O(72a)-C(1a)-C(3a)	176.5(3)	O(102)#3-O(111)-O(12u)	129.7(2)	C(1a)#1-C(5a)-C(3a)#1	59.4(3)
O(72a)-C(1a)-C(5a)#4	121.3(4)	O(102)#3-O(111)-O(112)	67.2(2)	C(1a)#1-C(5a)-C(12a)#16	62.4(3)
O(72a)-C(1a)-C(12a)#3	61.4(3)	O(102)#3-O(111)-C(11a)	60.5(4)	O(111)#5-C(5a)-O(112)#5	55.8(2)
C(8a)-C(1a)-O(71a)	62.8(3)	O(102)#3-O(111)-C(5a)#3	63.0(2)	O(111)#5-C(5a)-C(11a)#5	28.4(3)
C(8a)-C(1a)-C(2a)	31.5(4)	O(72a)-O(111)-O(12u)	63.(2)	O(111)#5-C(5a)-C(2a)#1	151.8(3)
C(8a)-C(1a)-C(6a)	150.4(5)	O(72a)-O(111)-O(112)	120.3(3)	O(111)#5-C(5a)-C(6a)#1	115.3(5)
C(8a)-C(1a)-C(3a)	60.8(3)	O(72a)-O(111)-C(11a)	129.1(4)	O(111)#5-C(5a)-C(3a)#1	140.7(3)
C(8a)-C(1a)-C(5a)#4	121.3(3)	O(72a)-O(111)-C(5a)#3	127.2(3)	O(111)#5-C(5a)-C(12a)	87.2(3)
C(8a)-C(1a)-C(12a)#3	176.7(4)	O(12u)-O(111)-O(112)	157.1(3)	O(112)#5-C(5a)-C(11a)#5	27.4(3)
O(71a)-C(1a)-C(2a)	94.3(4)	O(12u)-O(111)-C(11a)	166.3(5)	O(112)#5-C(5a)-C(2a)#1	152.2(3)
O(71a)-C(1a)-C(6a)	146.6(5)	O(12u)-O(111)-C(5a)#3	136.7(3)	O(112)#5-C(5a)-C(6a)#1	114.3(5)
O(71a)-C(1a)-C(3a)	123.5(4)	O(112)-O(111)-C(11a)	27.2(4)	O(112)#5-C(5a)-C(3a)#1	142.2(4)
O(71a)-C(1a)-C(5a)#4	175.8(4)	O(112)-O(111)-C(5a)#3	61.5(3)	O(112)#5-C(5a)-C(12a)	85.7(3)
O(71a)-C(1a)-C(12a)#3	115.8(3)	C(11a)-O(111)-C(5a)#3	34.3(4)	C(11a)#5-C(5a)-C(2a)#1	178.2(5)
C(2a)-C(1a)-C(6a)	119.0(6)	U(1)-O(13u)-O(1h)#1	56.2(2)	C(11a)#5-C(5a)-C(6a)#1	118.7(6)
C(2a)-C(1a)-C(3a)	29.3(3)	U(1)-O(13u)-O(71a)	58.2(2)	C(11a)#5-C(5a)-C(3a)#1	151.8(5)
C(2a)-C(1a)-C(5a)#4	89.8(4)	O(1h)#1-O(13u)-O(71a)	108.2(2)	C(11a)#5-C(5a)-C(12a)	86.4(4)
C(2a)-C(1a)-C(12a)#3	149.9(5)	U(2)-O(21u)-O(102)	55.5(2)	C(2a)#1-C(5a)-C(6a)#1	59.5(4)
C(6a)-C(1a)-C(3a)	89.8(4)	U(2)-O(21u)-O(81a)	54.6(2)	C(2a)#1-C(5a)-C(3a)#1	29.9(2)
C(6a)-C(1a)-C(5a)#4	29.3(3)	U(2)-O(21u)-O(121)	56.2(2)	C(2a)#1-C(5a)-C(12a)#16	91.8(3)
C(6a)-C(1a)-C(12a)#3	30.8(3)	U(2)-O(21u)-O(10w)#6	134.9(3)	C(6a)#1-C(5a)-C(3a)#1	89.4(4)
C(3a)-C(1a)-C(5a)#4	60.6(3)	O(102)-O(21u)-O(81a)	93.1(2)	C(6a)#1-C(5a)-C(12a)#16	32.3(4)
C(3a)-C(1a)-C(12a)#3	120.6(3)	O(102)-O(21u)-O(121)	60.9(2)	C(3a)#1-C(5a)-C(12a)#16	121.8(3)
C(5a)#4-C(1a)-C(12a)	60.1(3)	O(102)-O(21u)-O(10w)#6	110.8(3)	C(1a)#5-C(12a)-C(7a)#5	30.7(2)
U(1)-C(7a)-C(1a)	173.8(4)	O(81a)-O(21u)-O(121)	108.2(2)	C(1a)#5-C(12a)-O(72a)#5	56.1(2)
U(1)-C(7a)-O(72a)	60.0(4)	O(81a)-O(21u)-O(10w)#6	155.1(3)	C(1a)#5-C(12a)-O(122)	117.8(5)
U(1)-C(7a)-C(8a)	120.4(3)	O(121)-O(21u)-O(10w)#6	79.2(3)	C(1a)#5-C(12a)-O(121)	112.0(5)
U(1)-C(7a)-O(71a)	61.0(3)	O(102)-O(112)-O(5w)	65.0(2)	C(1a)#5-C(12a)-C(11a)#4	89.7(3)
U(1)-C(7a)-C(2a)	151.6(3)	O(102)#3-O(112)-O(111)	68.5(2)	C(1a)#5-C(12a)-C(6a)#5	28.5(3)
U(1)-C(7a)-C(6a)	149.7(3)	O(102)#3-O(112)-C(11a)	61.5(4)	C(1a)#5-C(12a)-C(5a)#7	57.6(2)
U(1)-C(7a)-C(12a)#3	118.6(3)	O(102)O(112)-O(2w)	164.9(3)	C(7a)#5-C(12a)-O(72a)#5	25.4(2)
C(1a)-C(7a)-O(72a)	120.6(6)	O(102)#3-O(112)-C(5a)#3	63.7(2)	C(7a)#5-C(12a)-O(122)	110.1(5)
C(1a)-C(7a)-C(8a)	59.2(4)	O(102)-O(112)-O(12w)	87.0(4)	C(7a)#5-C(12a)-O(121)	100.0(5)
C(1a)-C(7a)-O(71a)	118.8(6)	O(5w)#6-O(112)-O(111)	89.6(3)	C(7a)#5-C(12a)-C(11a)#4	120.4(3)
C(1a)-C(7a)-C(2a)	27.7(3)	O(5w)#6-O(112)-C(11a)	108.3(5)	C(7a)#5-C(12a)-C(6a)#5	59.2(4)
C(1a)-C(7a)-C(6a)	29.7(3)	O(5w)-O(112)-O(2w)	114.5(3)	C(7a)#5-C(12a)-C(5a)#7	88.3(3)

Bond	Angle [°]	Bond	Angle [°]	Bond	Angle [°]
C(1a)-C(7a)-C(12a)#3	61.1(4)	O(5w)#6-O(112)-C(5a)#3	127.6(3)	O(72a)-C(12a)-O(122)	97.7(5)
O(72a)-C(7a)-C(8a)	178.1(5)	O(5w)-O(112)-O(12w)	88.9(3)	O(72a)#5-C(12a)-O(121)	90.3(4)
O(72a)-C(7a)-O(71a)	120.6(6)	O(111)-O(112)-C(11a)	28.3(4)	O(72a)#5-C(12a)-C(11a)	145.5(3)
O(72a)-C(7a)-C(2a)	148.2(5)	O(111)-O(112)-O(2w)#11	126.3(3)	O(72a)#5-C(12a)-C(6a)#5	84.5(4)
O(72a)-C(7a)-C(6a)	91.1(4)	O(111)-O(112)-C(5a)#3	62.6(3)	O(72a)#5-C(12a)-C(5a)#7	113.5(3)
O(72a)-C(7a)-C(12a)#3	59.7(4)	O(111)-O(112)-O(12w)	153.5(4)	O(122)#10-C(12a)-O(121)	124.6(7)
C(8a)-C(7a)-O(71a)	59.6(4)	C(11a)-O(112)-O(2w)#11	129.1(5)	O(122)#10-C(12a)-C(11a)	94.6(5)
C(8a)-C(7a)-C(2a)	31.4(2)	C(11a)-O(112)-C(5a)#3	34.4(4)	O(122)#10-C(12a)-C(6a)	117.3(6)
C(8a)-C(7a)-C(6a)	88.8(3)	C(11a)-O(112)-O(12w)	129.9(6)	O(122)#10-C(12a)-C(5a)	108.8(5)
C(8a)-C(7a)-C(12a)#3	120.2(3)	O(2w)#11-O(112)-C(5a)	117.7(3)	O(121)-C(12a)-C(11a)#4	108.8(5)
O(71a)-C(7a)-C(2a)	91.1(4)	O(2w)-O(112)-O(12w)#12	77.9(4)	O(121)-C(12a)-C(6a)#5	117.9(6)
O(71a)-C(7a)-C(6a)	148.3(5)	C(5a)-O(112)-O(12w)#	98.1(4)	O(121)-C(12a)-C(5a)#7	117.6(5)
O(71a)-C(7a)-C(12a)#3	175.8(5)	C(10a)#3-C(11a)-C(4a)#3	30.2(2)	C(11a)#4-C(12a)-C(6a)#5	61.2(4)
C(2a)-C(7a)-C(6a)	57.4(2)	C(10a)#3-C(11a)-O(102)	25.5(2)	C(11a)#4-C(12a)-C(5a)#7	32.1(2)
C(2a)-C(7a)-C(12a)#3	88.9(3)	C(10a)#3-C(11a)-O(111)	101.8(4)	C(6a)#5-C(12a)-C(5a)#7	29.1(3)
C(6a)-C(7a)-C(12a)#3	31.5(2)	C(10a)#3-C(11a)-O(112)	108.0(5)	O(81a)#16-O(11w)-O(3w)	108.7(3)
U(1)-O(72a)-C(1a)	125.8(3)	C(10a)-C(11a)-C(6a)	87.1(3)	O(81a)-O(11w)-O(1w)	70.4(3)
U(1)-O(72a)-C(7a)	93.6(4)	C(10a)#3-C(11a)-C(5a)#3	58.0(3)	O(81a)#16-O(11w)-O(8w)	94.8(3)
U(1)-O(72a)-O(122)#6	157.5(3)	C(10a)-C(11a)-C(12a)	119.4(3)	O(81a)6-O(11w)-O(6w)	109.0(4)
U(1)-O(72a)-O(121)#3	138.8(3)	C(4a)#3-C(11a)-O(102)#3	55.4(2)	O(3w)#5-O(11w)-O(1w)	155.8(4)
U(1)-O(72a)-O(111)	50.4(2)	C(4a)#3-C(11a)-O(111)	113.8(5)	O(3w)#5-O(11w)-O(8w)	98.1(3)
U(1)-O(72a)-O(71a)	64.2(2)	C(4a)#3-C(11a)-O(112)	115.5(5)	O(3w)#5-O(11w)-O(6w)	104.5(4)
U(1)-O(72a)-C(6a)	154.4(3)	C(4a)#3-C(11a)-C(6a)#13	57.0(2)	O(1w)#16-O(11w)-O(8w)	106.1(4)
U(1)-O(72a)-C(12a)#3	165.0(3)	C(4a)#3-C(11a)-C(5a)#3	27.9(3)	O(1w)-O(11w)-O(6w)	55.8(3)
C(1a)-O(72a)-C(7a)	32.5(4)	C(4a)#3-C(11a)-C(12a)#1	89.3(3)	O(8w)-O(11w)-O(6w)#16	139.2(4)
C(1a)-O(72a)-O(122)#6	75.8(3)	O(102)#3-C(11a)-O(111)	94.0(4)	O(1h)#16-O(8w)-O(11w)	86.6(3)
C(1a)-O(72a)-O(121)#3	76.3(2)	O(102)#3-C(11a)-O(112)	93.7(4)	Nd(1)-O(7w)-O(122)	52.6(3)
C(1a)-O(72a)-O(111)	170.6(3)	O(102)-C(11a)-C(6a)	112.4(3)	Nd(1)-O(7w)-O(2w)	56.2(3)
C(1a)-O(72a)-O(71a)	62.1(3)	O(102)#3-C(11a)-C(5a)#3	83.3(4)	Nd(1)-O(7w)-O(1w)	57.6(3)
C(1a)-O(72a)-C(6a)	30.1(2)	O(102)-C(11a)-C(12a)	144.7(3)	Nd(1)-O(7w)-O(10w)	136.1(6)
C(1a)-O(72a)-C(12a)#3	62.6(3)	O(111)-C(11a)-O(112)	124.5(6)	Nd(1)-O(7w)-O(9w)	113.4(5)
C(7a)-O(72a)-O(122)#6	107.0(4)	O(111)-C(11a)-C(6a)#13	113.9(5)	O(122)-O(7w)-O(2w)	54.9(3)
C(7a)-O(72a)-O(121)#3	104.6(4)	O(111)-C(11a)-C(5a)#3	117.3(6)	O(122)-O(7w)-O(1w)	108.8(5)
C(7a)-O(72a)-O(111)	143.5(5)	O(111)-C(11a)-C(12a)#1	103.2(4)	O(122)-O(7w)-O(10w)	87.2(4)
C(7a)-O(72a)-O(71a)	29.7(4)	O(112)-C(11a)-C(6a)#13	113.3(5)	O(122)-O(7w)-O(9w)	146.6(5)
C(7a)-O(72a)-C(6a)	62.5(4)	O(112)-C(11a)-C(5a)#3	118.2(6)	O(2w)-O(7w)-O(1w)	96.6(5)
C(7a)-O(72a)-C(12a)#3	94.9(4)	O(112)-C(11a)-C(12a)#1	101.2(5)	O(2w)-O(7w)-O(10w)	88.1(4)
O(122)-O(72a)-O(121)	44.7(2)	C(6a)-C(11a)-C(5a)	29.1(3)	O(2w)-O(7w)-O(9w)	149.1(6)
O(122)-O(72a)-O(111)	109.5(2)	C(6a)-C(11a)-C(12a)	32.4(2)	O(1w)-O(7w)-O(10w)	163.1(6)
O(122)-O(72a)-O(71a)	135.0(3)	C(5a)#3-C(11a)-C(12a)#1	61.5(4)	O(1w)-O(7w)-O(9w)	59.2(4)
O(122)#6-O(72a)-C(6a)	48.1(2)	Nd(1)-O(3w)-O(5w)	57.2(2)	O(10w)-O(7w)-O(9w)	110.1(6)
O(122)-O(72a)-C(12a)	24.4(2)	Nd(1)-O(3w)-O(2w)	54.4(2)	O(21u)#9-O(10w)-O(3w)	116.9(4)
O(121)-O(72a)-O(111)	101.7(2)	Nd(1)-O(3w)-O(11w)#3	137.8(4)	O(21u)#9-O(10w)-O(7w)	106.9(5)
O(121)-O(72a)-O(71a)	129.4(3)	Nd(1)-O(3w)-O(10w)#3	138.3(4)	O(21u)-O(10w)-O(12w)	114.7(5)
O(121)#3-O(72a)-C(6a)	49.9(2)	O(5w)-O(3w)-O(2w)	102.1(3)	O(3w)#5-O(10w)-O(7w)	92.4(5)
O(121)-O(72a)-C(12a)	26.4(2)	O(5w)-O(3w)-O(11w)#3	164.7(4)	O(3w)-O(10w)-O(12w)	113.4(5)
O(111)-O(72a)-O(71a)	114.5(3)	O(5w)-O(3w)-O(10w)#3	84.5(3)	O(7w)-O(10w)-O(12w)#17	109.7(5)
O(111)-O(72a)-C(6a)	150.9(3)	O(2w)-O(3w)-O(11w)#3	89.3(3)	Nd(1)-O(6w)-O(5w)	56.6(3)
O(111)-O(72a)-C(12a)	119.2(3)	O(2w)-O(3w)-O(10w)#3	130.4(4)	Nd(1)-O(6w)-O(1w)	57.0(3)
O(71a)-O(72a)-C(6a)	92.2(3)	O(11w)-O(3w)-O(10w)	80.2(3)	Nd(1)-O(6w)-O(11w)#7	115.9(4)
O(71a)-O(72a)-C(12a)	124.4(3)	Nd(1)-O(2w)-O(82a)#1	122.0(3)	O(5w)-O(6w)-O(1w)	105.6(4)
C(6a)-O(72a)-C(12a)#3	32.5(2)	Nd(1)-O(2w)-O(91)	55.7(2)	O(5w)-O(6w)-O(11w)#7	129.8(5)
C(1a)-C(8a)-C(7a)	30.3(2)	Nd(1)-O(2w)-O(122)	55.5(2)	O(1w)-O(6w)-O(11w)#7	62.6(3)
C(1a)-C(8a)-O(81a)	118.5(5)	Nd(1)-O(2w)-O(112)#14	123.9(3)	O(12u)-O(12w)-O(112)	100.9(5)
C(1a)-C(8a)-O(82a)	112.8(5)	Nd(1)-O(2w)-O(3w)	52.4(2)	O(12u)-O(12w)-O(10w)	78.5(4)
C(1a)-C(8a)-C(9)#4	89.3(3)	Nd(1)-O(2w)-O(7w)	53.2(3)	O(12u)-O(12w)-O(9w)	143.6(6)
C(1a)-C(8a)-O(71a)	55.4(2)	O(82a)#1-O(2w)-O(91)	67.8(2)	O(112)-O(12w)-O(10w)	103.5(5)
C(1a)-C(8a)-C(2a)	27.8(3)	O(82a)#1-O(2w)-O(122)	163.5(3)	O(112)#19-O(12w)-O(9w)	96.9(6)
C(1a)-C(8a)-C(3a)	57.4(2)	O(82a)-O(2w)-O(112)	105.7(2)	O(10w)-O(12w)-O(9w)	127.6(6)
C(7a)-C(8a)-O(81a)	107.9(5)	O(82a)#1-O(2w)-O(3w)	96.0(3)	O(4w)#5-O(9w)-O(1w)	139.3(6)
C(7a)-C(8a)-O(82a)	105.2(5)	O(82a)#1-O(2w)-O(7w)	129.5(4)	O(4w)#5-O(9w)-O(7w)	116.5(6)
C(7a)-C(8a)-C(9)#4	119.6(3)	O(91)-O(2w)-O(122)	111.0(3)	O(4w)#5-O(9w)-O(12w)	115.1(6)
C(7a)-C(8a)-O(71a)	25.08(18)	O(91)-O(2w)-O(112)#14	162.2(3)	O(1w)-O(9w)-O(7w)	60.8(5)

Table 0.26 valence calculation for complex NdUmel.

Atom	Atom bond	Bond length	Bond valence [vu]	Atom valence [vu]
U1	U(1)-O(72a)	2,46	0,45	6,02
	U(1)-O(92)	2,37	0,54	
	U(1)-O(12u)	1,78	1,69	
	U(1)-O(1h)#1	2,30	0,62	
	U(1)-O(111)	2,35	0,56	
	U(1)-O(13u)	1,77	1,72	
	U(1)-O(71a)	2,48	0,44	
U2	U(2)-O(102)	2,47	0,45	5,95
	U(2)-O(101)	2,49	0,43	
	U(2)-O(81a)	2,38	0,53	
	U(2)-O(22u)	1,77	1,72	
	U(2)-O(121)	2,37	0,54	
	U(2)-O(1h)	2,29	0,63	
	U(2)-O(21u)	1,79	1,65	
Nd1	Nd(1)-O(91)	2,46	0,38	3,10
	Nd(1)-O(122)	2,44	0,40	
	Nd(1)-O(5w)	2,54	0,31	
	Nd(1)-O(4w)	2,55	0,30	
	Nd(1)-O(3w)	2,48	0,36	
	Nd(1)-O(2w)	2,54	0,31	
	Nd(1)-O(1w)	2,54	0,31	
	Nd(1)-O(7w)	2,45	0,39	
	Nd(1)-O(6w)	2,52	0,33	
O101	U(2)-O(101)	2,49	0,43	1,89
	C(10a)-O(101)	1,25	1,46	
O102	U(2)-O(102)	2,47	0,45	1,79
	C(10a)-O(102)	1,28	1,35	
O111	U(1)-O(111)	2,35	0,56	1,91
	O(111)-C(11a)	1,28	1,35	
O112	O(112)-C(11a)	1,24	1,50	1,50
O121	U(2)-O(121)	2,37	0,54	1,96
	O(121)-C(12a)	1,26	1,42	
O122	Nd(1)-O(122)	2,44	0,40	1,95
	O(122)-C(12a)#2	1,23	1,54	
O12u	U(1)-O(12u)	1,78	1,69	1,69
O13u	U(1)-O(13u)	1,77	1,72	1,72
O1h	U(1)-O(1h)	2,30	0,62	1,25
	U(2)-O(1h)	2,29	0,63	
O1w	Nd(1)-O(1w)	2,54	0,31	0,31
O21u	U(2)-O(21u)	1,79	1,65	1,65
O22u	U(2)-O(22u)	1,77	1,72	1,72
O2w	Nd(1)-O(2w)	2,54	0,31	0,31
O3w	Nd(1)-O(3w)	2,48	0,36	0,36
O4w	Nd(1)-O(4w)	2,55	0,30	0,30
O5w	Nd(1)-O(5w)	2,54	0,31	0,31
O6w	Nd(1)-O(6w)	2,52	0,33	0,33
O71a	U(1)-O(71a)	2,48	0,44	1,86
	C(7a)-O(71a)	1,26	1,42	
O72a	U(1)-O(72a)	2,46	0,45	1,88
	C(7a)-O(72a)	1,26	1,42	
O7w	Nd(1)-O(7w)	2,45	0,39	0,39
O81a	U(2)-O(81a)	2,38	0,53	2,03
	C(8a)-O(81a)	1,24	1,50	
O82a	C(8a)-O(82a)	1,25	1,46	1,46
O91	Nd(1)-O(91)	2,46	0,38	1,88
	C(9)-O(91)	1,24	1,50	
O92	U(1)-O(92)	2,37	0,54	1,92
	C(9)-O(92)	1,27	1,38	

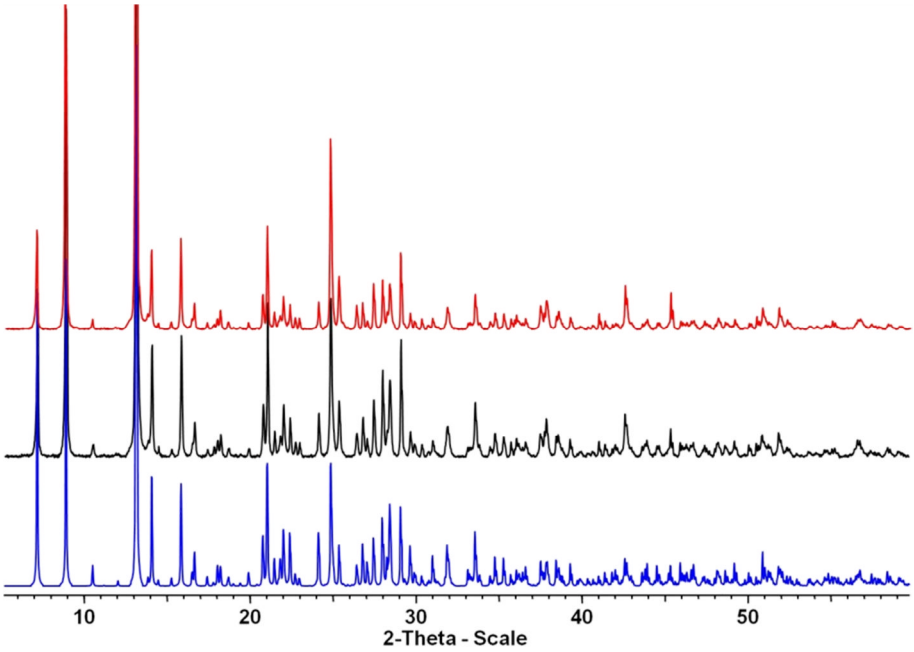

Figure 0.1 Comparison between the simulated (blue) PXRD pattern of **LnUpht** and the experimental ones of the **CeUpht** (black) and **NdUpht** (red) phases.

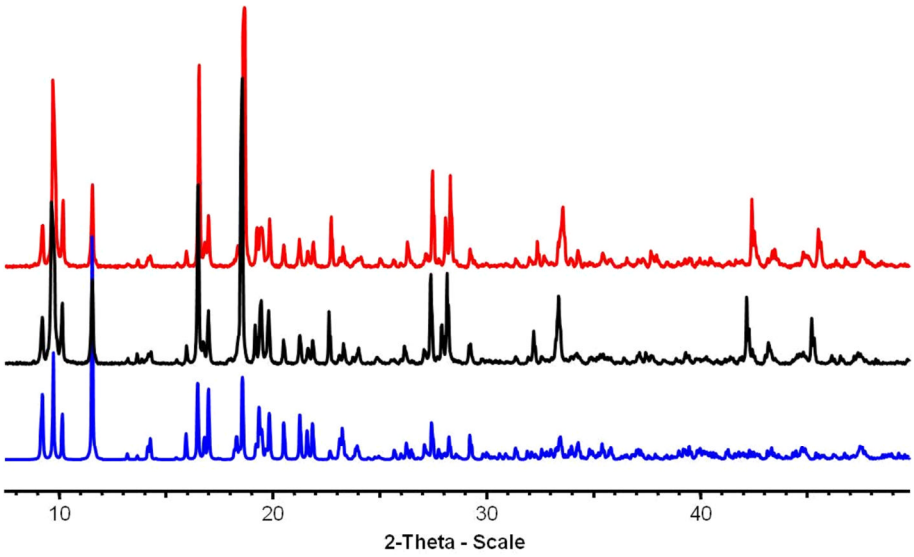

Figure 0.2 Comparison between the simulated (blue) PXRD pattern of **LnUpyr** and the experimental ones of the **CeUpyr** (black) and **NdUpyr** (red) phases.

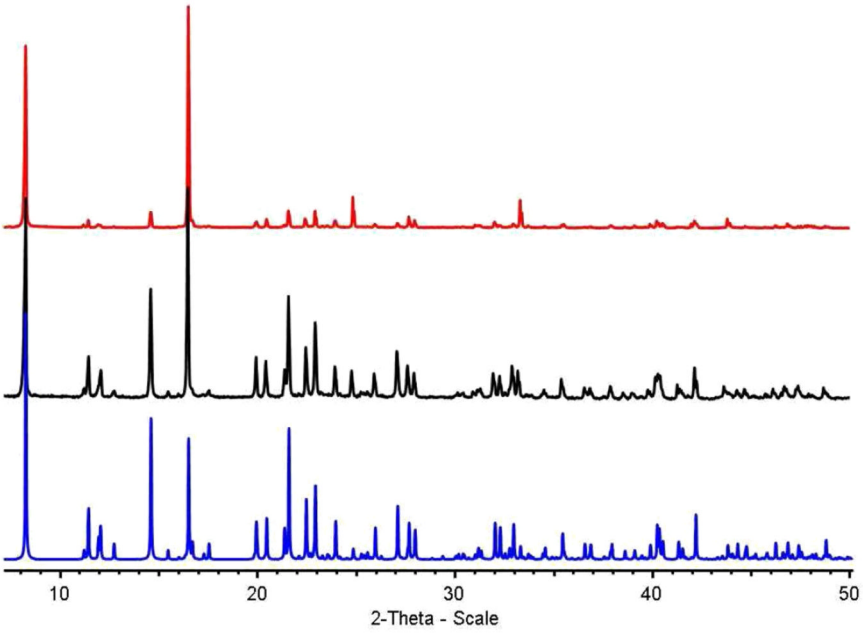

Figure 0.3 Comparison between the simulated (blue) PXRD pattern of **LnUmel** and the experimental ones of the **CeUmel** (black) and **NdUmel**(red) phases.

Annex C

Secondary Research Areas

Inorganic Chemistry

Communication

pubs.acs.org/IC

Metal–Organic-Framework-Type 1D-Channel Open Network of a Tetravalent Uranium Trimesate

Christophe Volkringer, Ionut Mihalcea, Jean-François Vigier, Arnaud Beaurain, Marc Visseaux, and Thierry Loiseau*

Unité de Catalyse et Chimie du Solide (UCCS), UMR CNRS 8181, Université de Lille Nord de France, USTL-ENSCL, Bat. C7, BP 90108, 59652 Villeneuve d'Ascq, France

Supporting Information

ABSTRACT: An uranium trimesate open framework is built up from trinuclear building blocks (μ_3-OU_3) connected to each other by tricarboxylate linkers to generate honeycomb-like 3D topology. This compound was solvothermally synthesized from low-valent uranium in an *N*,*N*-dimethylformamide solvent under an inert atmosphere, favoring stabilization of the tetravalent oxidation state, which is confirmed by X-ray photoelectron spectroscopy analysis.

For the past decade, the number of synthesis reports of metallic carboxylates has grown exponentially because of their implication in the construction of metal–organic frameworks (MOFs), exhibiting highly porous and fascinating atomic architectures.[1] Transition d or 4f block elements are the most used metals for the construction of such compounds, but actinide cations were also involved in the elaboration of a large variety of hybrid organic–inorganic assemblies. Since the use of the oxalate ligand in the industrial process for actinide extraction and separation, a significant effort has been focused on the reactivity of different organic polycarboxylate anions,[2] mainly with uranyl cations, UO_2^{2+}, either at room temperature or under mild hydrothermal conditions, resulting in multi-dimensional (1D, 2D, and 3D) extended uranyl–organic frameworks (UOFs).[3] Reduced oxidation states of uranium (V or IV) have been less investigated for this class of solids. Pentavalent uranium is known to rapidly undergo redox disproportionation to U^{IV} and U^{VI} cations in aqueous solution, and its isolation is very difficult in coordination complexes,[4] despite recent successes in the crystallization of large stable polynuclear species.[5] Although tetravalent uranium carboxylates have been identified for more than 50 years,[6] only a very few reports described the different varieties of its coordination complexes involved in low-dimensional networks.[7] In some cases, systems involving phthalic acid have been investigated in order to study polydentate interactions with U^{IV} in biological processes inducing redox reactions.[8]

Here we show that reactivity of the 1,3,5-benzenetricarboxylate (or trimesate, noted btc hereafter) linker with a source of uranium trichoride under solvothermal conditions gave rise to the formation of an unprecedented 3D framework, $U_3O(btc)_3(OH)(H_2O)_2\cdot 2.5DMF\cdot 1.5H_2O$ (**1**), involving μ_3-O trinuclear building blocks containing U^{IV}.

Green crystals (Figure S1 in the Supporting Information, SI) of **1** were prepared by using the solvothermal route under an inert atmosphere from the reaction of UCl_3 and trimesic acid in an anhydrous *N*,*N*-dimethylformamide (DMF) solvent at 150 °C for 24 h. Its single-crystal X-ray diffraction (XRD) analysis revealed an original extended open network with honeycomb-like topology. In a first approximation, uranium is 8-fold coordinated with six carboxyl O_c atoms, one terminal O atom, and one bridging O atom (Figure 1), defining a distorted

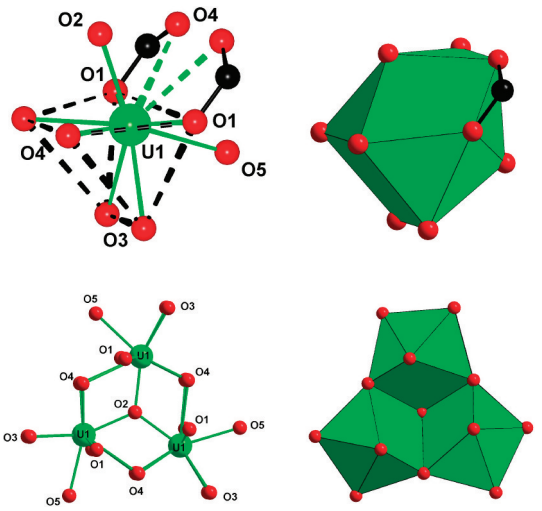

Figure 1. (top) Coordination environment around the center U1 in **1**. (U1–O1 = 2.465(11), Å, U1–O3 = 2.438(10) Å, U1–O4 = 2.419(10) Å. Dotted black lines indicate a trigonal prism with the two atoms O2 [μ_3-O; U1–O2 = 2.2254(7) Å] and O5 [terminal aquo group; U1–O5 = 2.474(15) Å] capping two of its square faces. The dotted green lines show two additional long U1–O4 bondings [2.918(10) Å]. (bottom) Trinuclear building motif with the specific μ_3-O group bridging the three U atoms.

trigonal-prismatic polyhedron. One of its square faces is capped by an O atom in the terminal position [U–O5 = 2.474(15) Å]. This bond length fits well with the existence of terminal H_2O species, in good agreement with the bond-valence-sum calculations (0.44).[9] The hypothetical presence of Cl^- anions (coming from the uranium source) is ruled out because the

Received: October 11, 2011
Published: October 28, 2011

usual U−Cl distance is much longer (U−Cl > 2.6 Å).[10] Another oxo species (O2) also caps a second square face of the U-centered trigonal prism with a relatively short U−O2 distance of 2.2254(7) Å. It is shared between three U cations, in a strict trigonal plane (U1−O2−U1 angle of 120°), and this specific connection mode results in a μ_3-O-centered trinuclear core $U_3(\mu_3\text{-}O(O_c)_{18}(H_2O)_3$ (Figure 1).

A similar motif was previously mentioned in tetravalent uranium compounds,[10a,b,11] in which the bond lengths μ_3-O−U are in the range 2.20−2.28 Å. Each U-centered polyhedron is additionally linked to each other through two carboxylate arms of two distinct trimesate groups. One observes two long U1−O4 distances of 2.918(10) Å, which contribute to the coordination sphere around the U atom. In fact, the position of the U1 atom is slightly affected by these two neighboring carboxyl O atoms and shifted from the center of previously defined trigonal prisms toward the two additional O atoms with a deviation of ≈+0.4 Å. The trimeric units are then connected to each other through nine trimesate ligands. Two of the carboxylate arms adopt a syn−anti bidentate mode bridging two distinct U atoms. This induces the formation of rods developed along the *c* axis (Figure 2), with alternation of the

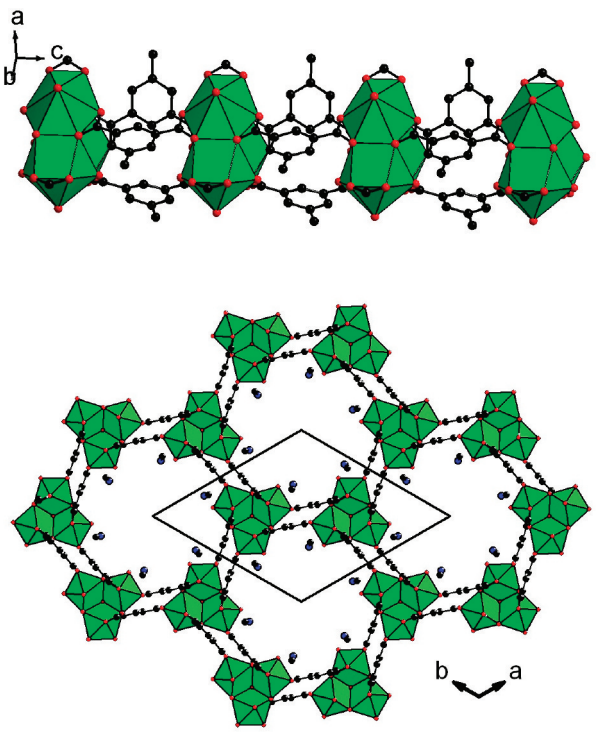

Figure 2. (top) View of rods from the connection mode of the trinuclear units with two of the carboxylate arms of the trimesate ligands along the *c* axis. (bottom) View of structure **1** perpendicular to the *c* axis, showing a honeycomb-like network of 1D channels of 11.2 Å. Fragments of DMF trapped within the channels are also indicated (blue/black circles).

trimers and part of three different organic ligands (1 and 3 positions of carboxylate groups). The latter connect two distinct trinuclear units to each other. The third carboxylate function (5 position) is bonded to one U atom belonging to a third trimer, in a symmetric chelating fashion, and ensures network tridimensionality in the *ab* plane.

The resulting framework (Figure 2) is reminiscent of a honeycomb-like net and delimits 1D channels extending along the *c* axis, with a free opening diameter of close to 11 Å (based on the ionic radius of 1.35 Å for oxygen) The tunnels are bound by the trimeric cores with terminal water species pointing toward their center and benzene planes of trimesates parallel to the channel axis. Interestingly, the atomic arrangement observed in **1** clearly shows that the driving force for crystal assembly is not given by the ternary symmetry of the trimesate ligand but rather by the symmetry of the inorganic building block itself. A similar structural feature was previously illustrated in the thorium trimesate TOF-2[12] or aluminum trimesate MIL-110.[13]

Only fragments of organic solvent are revealed from XRD analysis. DMF and H_2O molecules are assumed to fill the structure channels with a ratio of U_3/DMF/H_2O = 1/2.5/1.5 (from chemical and thermogravimetric analyses; Figure S4 in the SI). The presence of DMF is observed by ^{1}H NMR of the liquid resulting from the dissolution of phase **1** (Figure S3 in the SI). The occurrence of the oxygen ligand (oxo, hydroxo, or aquo) could be due to partial dehydration of the acid, which is known to lead to the production of anhydride and water. The latter reaction would be favored by the presence of Lewis acid (U^{III}) or Bronsted acid (HCl, from deprotonation of trimesic acid and chloride anions).

The chemical formula deduced from XRD analysis led to $U_3O(btc)_3(H_2O)_3$, with 11 negative charges for the network, which should be balanced by the charge from the three U cations. With a formal positive charge of 3.67 for a neutral framework, this should correspond to a mixed U^{III}/U^{IV} valence for uranium. The bond-valence-sum calculations from the parameters developed by Burns et al.[9] gave a value of 3.99 (or 4.37 with the two long U−O4 bonds), which is close to the formal valence 4+ for uranium. The tetravalent state was further confirmed by X-ray photoelectron spectroscopy (XPS) analysis. The U 4f XPS spectrum (Figures 3 and S6 in the SI) shows the

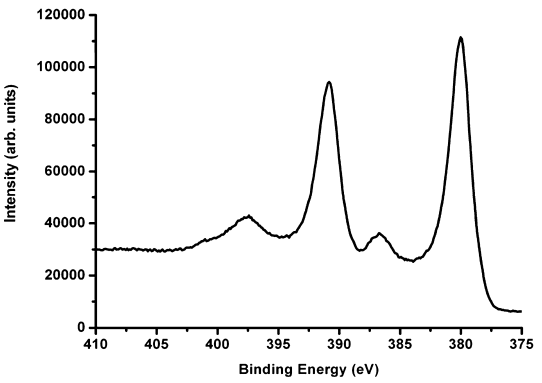

Figure 3. U 4f XPS spectrum of **1** (after 60 s of Ar^+ etching).

binding energies located at 379.9 eV (fwhm =1.94) and 390.8 eV (fwhm =1.94) for the main U $4f_{7/2}$ and U $4f_{5/2}$ components, respectively. These binding energy values are comparable to those observed in U^{IV}-based compounds previously reported in the literature.[14]

This analysis is consistent with the presence of U^{IV} only, and there is a need for additional negative charges for ensuring the electroneutrality of the structure. Cl^- anions could be present within the structure channels, but Castaing microprobe analysis indicated only a trace (U_3/Cl ≈ 24). Therefore, a partial OH/H_2O occupancy (with a OH/H_2O ratio of 1/2) is considered for the terminal U−O bonding. Such a statistical distribution

dx.doi.org/10.1021/ic2021963 | *Inorg. Chem.* 2011, 50, 11865−11867

was previously reported in other MOF compounds containing closely related μ_3-O trinuclear units.[15] It is noticeable that compound **1** is obtained from a trivalent uranium source. Oxidation into U^{IV} of the latter thus occurs during the hydrothermal treatment and could come from the presence of traces of O in the different starting reactants. This would give rise to the in situ conversion of U^{III} into U^{IV}, which favors the formation of the final structure (attempts using UCl_4 did not lead to the formation of the present phase). An oxidation of U^{III} in the presence of controlled amount of water was also described in literature and led to the crystallization of different U^{IV} and/or U^{V}-bearing complexes.[16]

The phase persists up to 240 °C under air and then transforms into α-U_3O_8 from 340 °C (Figures S4 and S5 in the SI). Moreover, slow oxidation is perceptible after long exposition (several days) in an air atmosphere. Attempts of Brunauer–Emmett–Teller surface area measurements were carried out from N_2 sorption with different degassing temperatures (100, 150, and 200 °C, under a primary vacuum), but no N_2 sorption capacity was observed. This result is quite unexpected regarding the potential porosity of the atomic structure, which would be compatible with N_2 diffusion within the tunnels. A similar behavior was previously reported in thorium trimesate (TOF-2[12]) with a closely related open framework. One explanation would be that the removal of encapsulated solvent molecules (DMF) is not efficient enough for the releasing porosity of this material.

This MOF phase opens the way to the construction of new extended architectures based on tetravalent uranium associated with carboxylate linkers. New crystal chemistry with low-valence-state uranium could thus be envisaged with O-donor ligands, also possibly offering novel opportunities toward the utilization of U-based compounds in catalysis.[17]

■ ASSOCIATED CONTENT

Supporting Information

Synthesis procedures and analytical data, crystallographic data for **1** (CIF), SEM images, powder XRD patterns, IR spectrum, and detailed figures of the XPS spectrum (Figures S1–S7). This material is available free of charge via the Internet at http://pubs.acs.org. The file CCDC 832042 contains the supplementary crystallographic data. These data can also be obtained free of charge from The Cambridge Crystallographic Data Centre via www.ccdc.cam.ac.uk/data_request/cif.

■ AUTHOR INFORMATION

Corresponding Author

*E-mail: thierry.loiseau@ensc-lille.fr.

■ ACKNOWLEDGMENTS

This work was supported by the GNR MATINEX of PACEN program and by the French ANR Project ANR-08-BLAN-0216-01. The authors thank Prof. Francis Abraham for helpful discussions and Nora Djelal, Laurence Burylo, and Catherine Melliet for technical assistance (UCCS).

■ DEDICATION

Dedicated to Prof. Gérard Férey on the occasion of his 70th birthday.

■ REFERENCES

(1) See themed issue Metal–Organic Frameworks: Long, J. R.; Yaghi, O. M. *Chem. Soc. Rev.* **2009**, *38*, 1201.
(2) Leciejewicz, J.; Alcock, N. W.; Kemp, T. J. *Struct. Bonding (Berlin)* **1995**, *82*, 43.
(3) (a) Kim, J.-Y.; Norquist, A. J.; O'Hare, D. *Dalton Trans.* **2003**, 2813. (b) Cahill, C. L.; de Lill, D. T.; Frisch, M. *CrystEngComm* **2007**, *9*, 15. (c) Thuéry, P. *CrystEngComm* **2009**, *11*, 1081.
(4) (a) Arnold, P. L.; Love, J. B.; Patel, D. *Coord. Chem. Rev.* **2009**, *253*, 1973. (b) Graves, C. R.; Kiplinger, J. L. *Chem. Commun.* **2009**, 3831.
(5) (a) Mougel, V.; Horeglad, P.; Nocton, G.; Pécaut, J.; Mazzanti, M. *Angew. Chem., Int. Ed.* **2009**, *48*, 8477. (b) Mougel, V.; Horeglad, P.; Nocton, G.; Pécaut, J.; Mazzanti, M. *Chem.—Eur. J.* **2010**, *16*, 14365.
(6) Paul, R. C.; Ghotra, J. S.; Bains, M. S. J. *Inorg. Nucl. Chem.* **1965**, *27*, 265.
(7) (a) Jelenic, I.; Grdenic, D.; Bezjak, A. *Acta Crystallogr.* **1964**, *17*, 758. (b) Takao, S.; Takao, K.; Kraus, W.; Emmerling, F.; Scheinost, A. C.; Bernhard, G.; Hennig, C. *Eur. J. Inorg. Chem.* **2009**, 4771. (c) Biswas, B.; Mougel, V.; Pécaut, J.; Mazzanti, M. *Angew. Chem., Int. Ed.* **2011**, *50*, 5745. (d) Zhang, Y.-J.; Collison, D.; Livens, F. R.; Powell, A. K.; Wocadlo, S.; Eccles, H. *Polyhedron* **2000**, *19*, 1757. (e) Duvieubourg-Garela, L.; Vigier, N.; Abraham, F.; Grandjean, S. J. *Solid State Chem.* **2008**, *181*, 2008.
(8) Vazquez, G. J.; Dodge, C. J.; Francis, A. J. *Inorg. Chem.* **2009**, *48*, 9485.
(9) Burns, P. C.; Ewing, R. C.; Hawthorne, F. C. *Can. Mineral.* **1997**, *35*, 1551.
(10) (a) Salmon, L.; Thuéry, P.; Ephritikine, M. *Polyhedron* **2006**, *25*, 1537. (b) Leverd, P. C.; Nierlich, M. *Eur. J. Inorg. Chem.* **2000**, 1733. (c) Salmon, L.; Thuéry, P.; Asfari, Z.; Ephritikine, M. *Dalton Trans.* **2006**, 3006. (d) Cotton, F. A.; Marler, D. O.; Schwotzer, W. *Acta Crystallogr., Sect. C* **1984**, *40*, 1186. (e) Van den Bossche, G.; Rebizant, J.; Spirlet, M. R.; Goffart, J. *Acta Crystallogr., Sect. C* **1986**, *42*, 1478. (f) Moisan, L.; Le Borgne, T.; Thuéry, P.; Ephritikine, M. *Acta Crystallogr., Sect. C* **2002**, *58*, m98. (g) Salmon, L.; Thuéry, P.; Ephritikine, M. *Polyhedron* **2004**, *23*, 623. (h) Salmon, L.; Thuéry, P.; Ephritikine, M. *Dalton Trans.* **2004**, 4139.
(11) Cotton, F. A.; Marler, D. O.; Schwotzer, W. *Inorg. Chim. Acta* **1984**, *95*, 207.
(12) Ok, K. M.; Sung, J.; Hu, G.; Jacobs, R. M. J.; O'Hare, D. *J. Am. Chem. Soc.* **2008**, *130*, 3762.
(13) Volkringer, C.; Popov, D.; Loiseau, T.; Guillou, N.; Férey, G.; Haouas, M.; Taulelle, F.; Mellot-Draznieks, C.; Burghammer, M.; Riekel, C. *Nat. Mater.* **2007**, *6*, 760.
(14) (a) Liu, J.-H.; Van den Berghe, S.; Konstantinovic, M. J. *J. Solid State Chem.* **2009**, *182*, 1105. (b) Lee, C.-S.; Wang, S.-L.; Lii, K.-H. J. *Am. Chem. Soc.* **2009**, *131*, 15116. (c) Liu, H.-K.; Lii, K.-H. *Inorg. Chem.* **2011**, *50*, 5870.
(15) Volkringer, C.; Popov, D.; Loiseau, T.; Férey, G.; Burghammer, M.; Riekel, C.; Haouas, M.; Taulelle, F. *Chem. Mater.* **2009**, *21*, 5695.
(16) Nocton, G.; Burdet, F.; Pecaut, J.; Mazzanti, M. *Angew. Chem., Int. Ed.* **2007**, *46*, 7574.
(17) Fox, A. R.; Bart, S. C.; Meyer, K.; Cummins, C. C. *Nature* **2008**, *455*, 341.

■ NOTE ADDED AFTER ASAP PUBLICATION

This paper was published on the Web on October 28, 2011, with reference 17 not cited in the paper. The corrected version was reposted on October 31, 2011.

Inorganic Chemistry

Article

pubs.acs.org/IC

Water-Free Neodymium 2,6-Naphthalenedicarboxylates Coordination Complexes and Their Application as Catalysts for Isoprene Polymerization

Inês Rodrigues, Ionut Mihalcea, Christophe Volkringer, Thierry Loiseau,* and Marc Visseaux

Unité de Catalyse et Chimie du Solide (UCCS)—UMR CNRS 8181, Université de Lille Nord de France, USTL-ENSCL, Bat C7, BP 90108, 59652 Villeneuve d'Ascq, France

Supporting Information

ABSTRACT: A series of four coordination polymers based on neodymium have been hydrothermally synthesized with different carboxylic acids as a linker. The structures of the compounds $Nd_2(2,6\text{-ndc})_3(H_2O)_3{\cdot}H_2O$ (**1**), $Nd_2(2,6\text{-ndc})_2(ox)(H_2O)_2$ (**2**), and Nd(2,6-ndc)(form) (**3**) (2,6-ndc = 2,6-naphthalenedicarboxylate; ox = oxalate; and form = formate) have been determined by single-crystal X-ray diffraction analysis. They exhibit rather dense networks built up from infinite chains of NdO polyhedra connected to each other through the 2,6-ndc ligand. Terminal and bridging aquo species are present in the coordination sphere of Nd for **1**, whereas some of them are partially replaced by oxalate groups in **2** and fully substituted by formate groups in **3**. The water-free phase **3** as well as the compound $Nd(form)_3$ (**4**) were considered for catalytic reaction for polymerization of isoprene in the presence of Al-based cocatalyst, affording *cis*-polyisoprene with good conversions. Residual Nd material with unchanged structure was found in the polymeric material. The neodymium luminescence of compounds **3** and **4** was also measured.

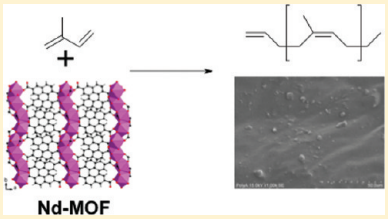

INTRODUCTION

The interest for the new class of porous coordination polymers (PCPs) or metal−organic frameworks (MOFs) has grown exponentially for the past decade, and many potential applications have been discovered in the area of molecular storage and separation, drug delivery, etc.[1−6] These crystalline materials have attracted special attention since their well-defined atomic architectures delimit large cavities or channels systems (micro- and mesoscale), which are generated by the three-dimensional connection of metallic nodes through organic N- or O-donor ligands. Aromatic molecules are usually employed to form rigid extended networks, which remain stable enough upon the removal of solvent species trapped within the pores. The association of metallic cores together with organic linkers gives rise to a wide variety of arrangements, due to the richness of organic chemistry for the elaboration of functionalized molecules and also the diversity of metal candidates from the periodic table. In this context, the choice of metal will be governed by following the chemical or physical targeted properties. This aspect is especially a key point in the field of catalysis, for which the nature of metallic cations is known to play a significant role for enhancing a chemical reaction. In this domain, the porous networks of PCP or MOF solids have been recently considered as heterogeneous catalysts, which combine the occurrence of active metal sites together with confined nanoreactors related to the shape and size of the structure pores. Several reviews have reported these emerging catalysis applications in MOF type materials.[7−11] One of this field concerns the synthetic polyisoprene, which is found in the rubber and tires industry. A family of very efficient coordination catalysts for this purpose is based on the rare earths, particularly neodymium,[12−15] and continuous effort is made to improve catalytic systems with the aim to get better activity and higher selectivities. Lanthanide carboxylates, associated with aluminum cocatalysts, have been widely used in the industry in this frame since the last two decades after the pioneering investigation in the early 1970s.[16] It was shown only recently that neodymium-based carboxylate MOF type materials can be efficiently used for polymerization of isoprene.[17] We therefore are continuing to investigate the study of the reactivity of such compounds as potential Ziegler−Natta catalysts in conjugated diene polymerization. One prerequisite is the absence of any aquo or hydroxo ligands bonded to the metal in the coordination polymer, which makes the catalytic reaction unproductive. This consideration would limit the number of potential solids since they should be stable enough upon dehydration or dehydroxylation processes or do not contain any of these species. The aspect could be critical since most of the lanthanide-based MOF compounds have aquo ligands within their coordination sphere and synthesis strategies must be oriented to avoid such ancillary OH_n coordinating ligands. One solution could be the use of nonaqueous solvent (*N*,*N*-dimethylformamide, methanol, etc.) for the crystallization, but solvent molecules usually belong to the metal environment in the final crystalline solid.

In this contribution, we propose an alternative approach with the association of two types of ligands, with different steric hindrances. We selected the 2,6-naphthalenedicarboxylate (noted 2,6-ndc), a linear rigid ditopic linker that we combine with oxalate (noted ox) or formate (noted form) species. This

Received: September 2, 2011
Published: December 14, 2011

   dx.doi.org/10.1021/ic2019346 | *Inorg. Chem.* 2012, 51, 483−490

naphthalene-based ligand has been previously used for the formation of various porous compounds such as the isoreticular solids IRMOF-8[18] or MOF-69[19] or solids based on trivalent *p* (Al[20,21]) or *f* elements (rare earths[22]). With the lanthanide cations, different coordination polymers already have been reported, for which ancillary solvent water[23−28] or *N*,*N*-dimethylformamide[29] species are present in the surrounding cations. In our study, the oxalate or formate linkers were used as a substituent of aquo ligands to generate carboxylate network with oxo bridges only. The combination of oxalate or formate ligands with other carboxylate linkers has been previously described in the literature.[30−40]

The present work deals with the description of the different phases obtained from the chemical system Nd/2,6-ndc/H_2O in mild hydrothermal conditions (autogenous pressure) and examines the structural effect of the addition of oxalate or formate species in the reaction medium. Three coordination polymers thus have been isolated $Nd_2(2,6\text{-ndc})_3(H_2O)_3{\cdot}H_2O$ (**1**), $Nd_2(2,6\text{-ndc})_2(ox)(H_2O)_2$ (**2**), and Nd(2,6-ndc)(form) (**3**). Only the mixed formate-naphthalenedicarboxylate phase has no coordinated water. During our investigations, a fourth phase, consisting of an anhydrous neodymium formate network,[41] $Nd(form)_3$ (**4**), also has been prepared. The crystal structures of the compounds **1**, **2**, and **3** have been analyzed by means of single-crystal X-ray diffraction. The water-free compounds **3** and **4** have been further considered as precatalysts for the polymerization of isoprene in the presence of methylaluminoxane (MAO) or modified methylaluminoxane (MMAO). Both compounds were found efficient, with mixed ligand complex **3** giving rise to a more *cis*-selective catalyst, up to 88%.

EXPERIMENTAL SECTION

Materials. Neodymium chloride hexahydrate ($NdCl_3{\cdot}6H_2O$, Aldrich, 99.9%), 2,6-naphthalenedicarboxylic acid ($HO_2C{-}C_{10}H_6{-}CO_2H$, noted 2,6-$H_2$ndc, Aldrich, 99%), oxalic acid dihydrate ($C_2O_4H_2{\cdot}2H_2O$, noted $H_2ox{\cdot}2H_2O$, Aldrich, 99%), formic acid (HCO_2H, noted Hform, Aldrich, ≥95%), potassium hydroxide (KOH, Prolabo), ammonium hydroxide (Prolabo, 28%), *N*,*N*-dimethylformamide (Aldrich, ≥99.8%), and deionized water have been used without any further purification. MAO (Aldrich, toluene solution, 10% Al, 1.48 M), MMAO (Akzo Nobel, heptane solution, 7% Al, 18% MMAO, 1.84 M), Al(i-Bu)$_3$ (Aldrich, 99%), and $AlEt_2Cl$ (Aldrich, 1.8 M toluene solution) were used as received. Isoprene (Aldrich, 99.9%) was distilled twice over CaH_2 and molecular sieves (3 A) and then stored at −20 °C in a glovebox. Toluene was purified through alumina column (Mbraun SPS).

Synthesis. The compounds have been hydrothermally synthesized under autogenous pressure using Teflon-lined Parr type autoclaves.

*$Nd_2(2,6\text{-ndc})_3(H_2O)_3{\cdot}H_2O$ (**1**).* A mixture of 0.359 g (1 mmol) of $NdCl_3{\cdot}6H_2O$, 0.109 g (0.5 mmol) of 2,6-naphthalenedicarboxylic acid, 0.6 mL (0.6 mmol) of 1 M KOH, and 4.4 mL (240 mmol) of H_2O was placed in a Parr bomb and then heated statically at 180 °C for 24 h. The solution pH was 2.4 at the end of the reaction. The resulting pink product was then filtered off, washed with water, and dried at room temperature. After the hydrothermal reaction, a mixture of **1** and unreacted 2,6-H_2ndc crystallites was obtained. The latter could be easily removed by further washing with *N*,*N*-dimethylformamide. Elemental analysis, observed (calculated): C, 46.2% (43.1%); H, 2.5% (2.6%).

*$Nd_2(2,6\text{-ndc})_2(ox)(H_2O)_2$ (**2**).* A mixture of 0.360 g (1 mmol) of $NdCl_3{\cdot}6H_2O$, 0.055 g (0.25 mmol) of 2,6-naphthalenedicarboxylic acid, 0.032 g (0.25 mmol) of oxalic acid dihydrate, 1.5 mL (3 mmol) of 2 M NH_3 in water, and 3.5 mL (194 mmol) of H_2O was placed in a Parr bomb and then heated statically at 180 °C for 24 h. The solution pH was 4.8 at the end of the reaction. The resulting pink product was then filtered off, washed with water, and dried at room temperature. After the hydrothermal treatment, a mixture of compounds **1** and **2** was obtained.

*Nd(2,6-ndc)(form) (**3**).* A mixture of 0.180 g (0.5 mmol) of $NdCl_3{\cdot}6H_2O$, 0.032 g (0.9 mmol) of 2,6-naphthalenedicarboxylic acid, 0.5 mL (13 mmol) of formic acid, 1.8 mL (23 mmol) of *N*,*N*-dimethylformamide, and 2.2 mL (120 mmol) of H_2O was placed in a Parr bomb and then heated statically at 180 °C for 24 h. The resulting yellow product was then filtered off, washed with water, and dried at room temperature. Elemental analysis, observed (calculated): C, 35.7% (35.8%); H, 1.0% (1.6%).

*$Nd(form)_3$ (**4**).* The preparation of **4** was recently described in literature.[42] We used a closely related protocol for its synthesis: A mixture of 0.360 g (1 mmol) of $NdCl_3{\cdot}6H_2O$, 3 mL (79 mmol) of formic acid, and 2 mL (2 mmol) of 1 M KOH was placed in a Parr bomb and then heated statically at 180 °C for 24 h. The solution pH was 1.45 at the end of the reaction. The resulting pink product was then filtered off, washed with water, and dried at room temperature. Elemental analysis, observed (calculated): C, 12.6% (12.9%); H, 0.2% (1.1%).

Single-Crystal X-ray Diffraction. Crystals were selected under polarizing optical microscope and glued on a glass fiber for a single-crystal X-ray diffraction experiment. X-ray intensity data were collected on a Bruker X8-APEX2 CCD area detector diffractometer using Mo Kα radiation (λ = 0.71073 Å) with an optical fiber as collimator. Several sets of narrow data frames (20 s per frame) were collected at different values of θ for 2 and 2 initial values of ϕ and ω, respectively, using 0.3° increments of ϕ or ω. Data reduction was accomplished using SAINT V7.53a.[43] The substantial redundancy in data allowed a semiempirical absorption correction (SADABS V2.10[44]) to be applied, on the basis of multiple measurements of equivalent reflections. The structure was solved by direct methods, developed by successive difference Fourier syntheses, and refined by full-matrix least-squares on all F^2 data using SHELX[45] program suite with the WINGX[46] interface. Hydrogen atoms of the benzene ring were included in calculated positions and allowed to ride on their parent atoms. The final refinements include anisotropic thermal parameters of all nonhydrogen atoms and were performed using the SHELX program on the basis of F^2. The crystal data are given in Table 1. The Supporting Information is available in CIF format.

Isoprene Polymerization. All preliminary operations were carried out in a glovebox (Jacomex). In a typical polymerization, a flask was charged with the MOF precatalyst. The solvent (toluene, 1 mL) and the cocatalyst (MAO or MMAO) were added with syringes. In all attempts, the mixture was magnetically stirred for 20 min at room temperature before adding the monomer (isoprene, 0.68 g, 1 mL, 10 mmol). The polymerization was conducted outside the glovebox, under an inert atmosphere, at a given monitored temperature and running time. The viscous mixture was quenched with methanol containing 2,6-di-*tert*-butyl-4-methylphenol (1.0 wt %) as a stabilizer. The resulting isolated polymeric material was dried under vacuum at room temperature to a constant weight. The yield was determined by gravimetry.

Polymer Characterization. The selectivity was determined by ^{1}H NMR and ^{13}C NMR according to published methods.[47] The NMR spectra were recorded on an AC 300 Bruker at 300 MHz, in chloroform-D solutions. Approximately 5 and 40 mg of sample were directly dissolved into the NMR tube in 0.6 mL of solvent for ^{1}H and ^{13}C NMR, respectively. The chemical shifts were calibrated using the residual resonances of the solvent. Quantitative ^{13}C NMR was realized using the *zgig* sequence (Bruker library). The relaxation time d1 was set to 2, 5, and 8 s, and it was found that a relaxation time of 5 s is necessary to allow the relaxation of all carbon nuclei. Size-exclusion chromatography (SEC) was performed in tetrahydrofuran (THF) as an eluent at 20 °C using a Waters 410 refractometer and a Waters Styragel column (HR2, HR3, HR4, and HR5E) calibrated with polystyrene standards.

Luminescence Spectroscopy. Raman spectra were recorded on a FT-Raman Bruker spectrometer, model RSF 100, at room temperature. The excitation source was a YAG:Nd laser ($\lambda_{Exc.}$ =

dx.doi.org/10.1021/ic2019346 | *Inorg. Chem.* 2012, 51, 483−490

Table 1. Crystal Data and Structure Refinement for Different Neodymium 2,6-Napthalenedicarboxylates

	1	2	3
formula	$C_{18}H_9NdO_8$	$C_{13}H_6NdO_7$	$C_{13}H_7NdO_6$
formula weight	497.49	418.42	403.43
temperature (K)	293(2)	293(2)	293(2)
crystal type	pink	pink	pink
crystal size (mm^3)	0.51 × 0.43 × 0.11	0.46 × 0.08 × 0.04	0.18 × 0.16 × 0.09
crystal system	monoclinic	orthorhombic	monoclinic
space group	$P2_1/n$	$Pbca$	$P2_1/c$
a (Å)	17.1900(3)	10.7908(11)	13.0575(9)
b (Å)	15.1901(3)	8.6951(9)	13.0531(9)
c (Å)	25.3382(5)	25.475(2)	6.9251(4)
α (°)	90	90	90
β (°)	106.581(1)	90	94.070(3)
γ (°)	90	90	90
volume ($Å^3$)	6341.1(2)	2390.3(4)	1177.34(1)
Z, ρ_{calcd}($g\ cm^{-3}$)	16, 2.084	8, 2.325	4, 2.276
μ (mm^{-1})	3.324	4.378	4.433
Θ range (°)	1.28−37.62	1.60−30.78	1.56−33.78
limiting indices	$-29 \le h \le 29$	$-15 \le h \le 15$	$-20 \le h \le 20$
	$-26 \le k \le 25$	$-9 \le k \le 12$	$-20 \le k \le 20$
	$-43 \le l \le 41$	$-36 \le l \le 34$	$-10 \le l \le 10$
collected reflections	194453	45287	73399
unique reflections	33503	3738	4714
	[R(int) = 0.0423]	[R(int) = 0.0557]	[R(int) = 0.0562]
parameters	974	191	181
goodness-of-fit on F^2	1.103	1.362	1.172
final R indices [$I > 2\sigma(I)$]	$R1$ = 0.0358	$R1$ = 0.0308	$R1$ = 0.0246
	$wR2$ = 0.0902	$wR2$ = 0.0690	$wR2$ = 0.0614
R indices (all data)	$R1$ = 0.0588	$R1$ = 0.0492	$R1$ = 0.0388
	$wR2$ = 0.1105	$wR2$ = 0.0981	$wR2$ = 0.0832
largest diff. peak and hole (e $Å^{-3}$)	5.746 and −1.367	1.891 and −0.960	1.066 and −1.258

1064 nm) (excitation power 100 mW and an optical aperture of 1.1). The energy values from Raman shift (cm^{-1}), E_R, were converted into emission energy (cm^{-1}), E_E, using the expression: $E_E = E_{laser} - E_R$, where E_{laser} = 9398.5 cm^{-1}. Subsequently, the E_E values were converted in wavelengths (nm).

RESULTS

Structure Descriptions. *Crystal Structure of $Nd_2(2,6\text{-}ndc)_3(H_2O)_3{\cdot}H_2O$ (1).* Compound **1** has a parent structure with other hydrated rare-earth naphthalenedicarboxylates containing Pr,[25] Eu,[25] Tb,[48] and Ho,[26] crystallizing in a similar monoclinic cell ($P2_1/n$, $a \approx 17.0$, $b \approx 15.1$, $c \approx 25.0$ Å, $\beta \approx 106.4°$). Its structure is built up from four crystallographically independent neodymium centers in 9-fold coordination (Figure 1). Each inorganic cation is surrounded by six carboxyl oxygen atoms with Nd−O distances ranging from 2.367(2) up to 2.533(2) Å. Longer Nd−O bonds [2.863(2)−2.906(2) Å] also occur and correspond to a μ_3 connection mode for one carboxyl oxygen atom, which bridges two adjacent neodymium cations and one carbon atom from a carboxylate arm of the organic linker. Water species are found in terminal position with Nd−Ow distances of 2.495(2)−2.595(2) Å range (O27, O29, O25, and O30; Ow stands for water oxygen) and in bridging fashion [Nd−Ow = 2.699(2)−2.830(2) Å; O20 and O28] between two neighboring neodymium cations. The assignment to such μ_2- or η_1-aquo groups is in good agreement with the bond valence

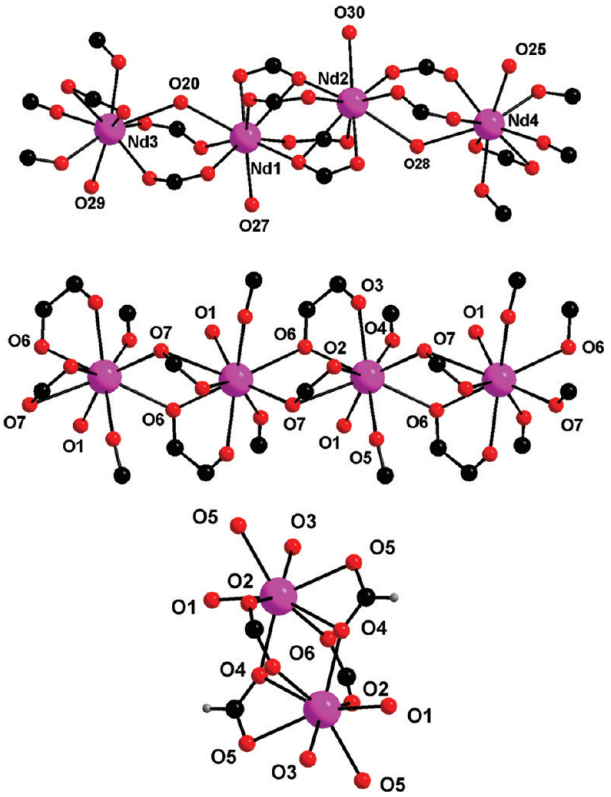

Figure 1. Details of the coordination environments of the four independent neodymium cations forming infinite ribbons in $Nd_2(2,6\text{-}ndc)_3(H_2O)_3{\cdot}H_2O$ (**1**). O25, O27, O29, and O30 correspond to terminal water species, whereas O20 and O28 are μ_2-bridging water species. Only carbon atoms of the carboxylate groups are shown for clarity (top). Details of the 9-fold coordinated neodymium environments forming infinite ribbons in $Nd_2(2,6\text{-ndc})_2(ox)(H_2O)_2$ (**2**). O1 corresponds to terminal water molecule. O6 and O7 belong to oxalate and naphthalenedicarboxylate, respectively, and are μ_3-oxo bridges between two neighboring neodymium centers (middle). View of the dinuclear unit containing 2-fold-coordinated neodymium centers in Nd(2,6-ndc)(form) (**3**) (bottom).

calculations[49] (0.33−0.38 and 0.27−0.36, respectively). The resulting environment (6 μ_2-Oc + 1 μ_3-Oc + η_1-H_2O + μ_2-H_2O; Oc stands for carboxyl oxygen) for neodymium gives rise to the formation of infinite chains of distorted monocapped antiprism polyhedra $NdO_7(H_2O)_2$, running along the a-axis. Within the inorganic ribbons, pairs of edge-sharing neodymium-centered polyhedra [Nd1···Nd2 = 4.112(1) Å and Nd3···Nd4 = 4.114(1) Å] strictly alternate with corner-sharing ones (Nd1···Nd3 and Nd2···Nd4). The chains are linked to each other via the carboxylate arms of the six crystallographically independent naphthalenedicarboxylate ligands, which adopt either a μ_4-$\eta_1{:}\eta_1{:}\eta_1{:}\eta_1$ (each carboxylate group is *syn*−*syn* bidentate) or μ_5-$\eta_2{:}\eta_1{:}\eta_1{:}\eta_1$ connection mode. For the latter, the carboxylate groups are either *syn*−*syn* bidentate or both asymmetric chelating and *syn*−*anti* bidentate. It results in the formation of three-dimensional neutral framework delimiting closely packed channels developing along the a-axis, parallel to the direction of the inorganic chains (Figure 2). Within the tunnels are located two independent water molecules in strong hydrogen bond interactions to each other [2.859(9) Å] and also with the terminal water molecules O29 attached to Nd3 [2.997(6) Å] and O30 attached to Nd2 [2.869(8) Å]. This topological feature is reminiscent of that occurring in the

dx.doi.org/10.1021/ic2019346 | *Inorg. Chem.* 2012, 51, 483−490

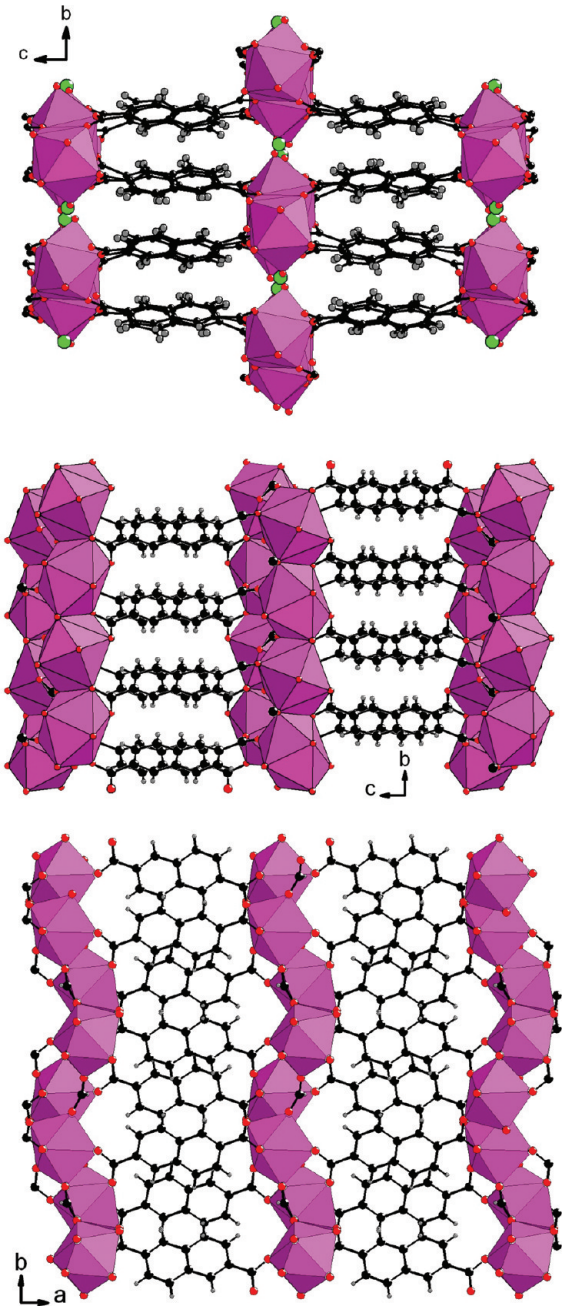

Figure 2. View of the 3D structure of $Nd_2(2,6\text{-ndc})_3(H_2O)_3{\cdot}H_2O$ (**1**) along the *a*-axis, showing the free water species (green circles) encapsulated within channels (top). View of the 3D structure of **2** along the *a*-axis, showing the connection of mixed organic−inorganic layer $Nd_2(2,6\text{-ndc})_2(ox)(H_2O)_2$ through the 2,6-ndc ligand (middle). View of the 3D structure of **3** along the *c*-axis, showing the connection of the mixed organic−inorganic layer Nd(2,6-ndc)(form) through the 2,6-ndc ligand (bottom).

trivalent aluminum naphthalenedicarboxylate (MIL-69[20,21]), which also possesses a lozenge-shape channels like network based on the chains of octahedral units intercrossing with the organic spacer. Other variants of this structure type are reported with different rare earths and concern the content of water bonded to the cations (Ho,[26] Yb[24]). X-ray thermodiffraction experiment (see the Supporting Information) indicates that Bragg peaks are clearly visible up to 180 °C, which then persist up to 440 °C but with lower intensities. Above this

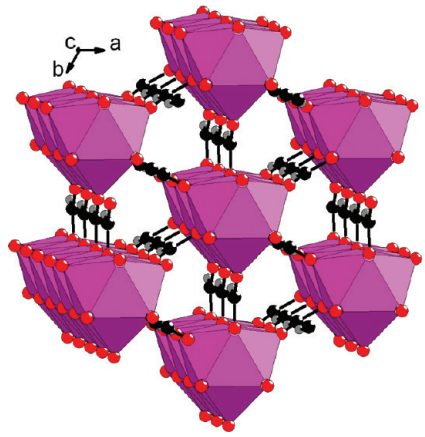

Figure 3. Perspective view of the structure of $Nd(form)_3$ (**4**) along the *c*-axis, showing the connection of the isolated neodymium-centered tricapped trigonal prisms NdO_9 via the formate ligands.

temperature, the decomposed phase is transformed into the cubic form Nd_2O_3 (500−740 °C), and then, the hexagonal form Nd_2O_3 appears.[50]

*Crystal Structure of $Nd_2(2,6\text{-ndc})_2(ox)(H_2O)_2$ (**2**).* The compound **2** still displays a hydrated network but with a lower content as compared to that of **1**. Its structure consists of one crystallographically independent 9-fold coordination defining a distorted monocapped square antiprism. It is surrounded by eight carboxyl oxygen atoms (Figure 1). Four of them (O2, O3, O4, and O5) have a μ_2 connection fashion with Nd−O distances in the range 2.419(4)−2.496(3) Å. Four (2 × O6 and 2 × O7) of them a μ_3 connection fashion with longer Nd−O bonds [2.608(3) and 2.792(4) Å] since they are involved in a bridging mode between two neighboring rare-earth cations and a carboxylate group of the organic part (either ox or 2,6-ndc). The remaining nonbonded oxygen (O1) is a terminal water molecule with Nd−O distance of 2.459(4) Å, in good agreement with bond valence[49] calculations (0.40). Because of the occurrence of μ_3-oxo groups, chains of edge-sharing neodymium centered monocapped square antiprismatic polyhedra $NdO_8(H_2O)$ are generated along the *b*-axis, with Nd···Nd distance of 4.349(1) Å. The oxalate group is connected to four neodymium cations as a hexadentate bridging linker between two adjacent inorganic ribbons, with the μ_4-η_2:η_1:η_2:η_1 configuration. The naphthalenedicarboxylate molecules also contribute as bridging linker between two chains through one of its carboxylate arm (*syn*−*syn* bidentate connection mode). The remaining carboxylate group acts as both an asymmetric chelating and a bidentate (*syn*−*anti*) bridging linker with neodymium centers of a given inorganic chain. The connection mode is μ_4-η_2:η_1:η_1:η_1. It results in the formation of a neutral mixed organic−inorganic layer $Nd_2(2,6\text{-ndc})_2(ox)(H_2O)_2$ developing in the (*a*,*b*) plane. The naphthalenedicarboxylate linker perpendicularly connects the hybrid sheets along the *c*-axis to form a rather compact three-dimensional edifice without any void (Figure 2).

*Crystal Structure of Nd(2,6-ndc)(form) (**3**).* When replacing the oxalate linker by the formate ones, an anhydrous phase (**3**) is revealed from X-ray diffraction analysis. Its structure is built up from one crystallographically independent neodymium center with an 8-fold coordination, which differs from the previous hydrated compounds, which have terminal η_1-aquo ligands and, therefore, a higher coordination state. The geometric polyhedron surrounding the rare-earth atom is a

dx.doi.org/10.1021/ic2019346 | *Inorg. Chem.* 2012, 51, 483−490

Table 2. Isoprene Polymerization with Nd(2,6-ndc)(form) (3) and Nd(form)$_3$ (4) as Precatalysts

run[a]	precatalyst	cocatalyst	T (°C)	time (h)	yield (%)	Mn_{exp} (PDI)[b]	Mn_{th}[c]	selectivity (%)[d] *cis-/trans-*/3,4- (%)
1	**4**	100 MMAO	50	96	33.4	38000 (3.40)	12600	80.5/6.9/12.6
2	**4**	100 MMAO	80	24	29.0	148000/10900 (multimodal)	11000	69.0/17.6/13.4
3	**4**	100 MMAO	80	96	54.5	61000/5700 (bimodal)	20600	57.2/26.6/16.2
4	**4**	300 MMAO	80	24	27.0	39600/5600 (bimodal)	10200	71.8/13.8/14.4
5	**4**	100 MAO	50	24	28.8	15300 (2.84)	10900	61.7/29.0/9.3
6	**4**	50 MAO	80	96	83.6	24100 (2.55)	31600	48.0/40.3/11.7
7	**4**	100 MAO	80	96	77.0	20000 (2.69)	29100	53.6/37.0/9.2
8	**4**	300 MAO	80	96	76.5	5700 (3.68)	28900	55.2/30.4/14.4
9	**4**	10 $AliBu_3$/2 $AlEt_2Cl$	80	24	0			
10	**3**	100 MMAO	50	24	32.2	139000 (1.80)	10900	84.5/7.7/7.8
11	**3**	100 MMAO	50	72	48.2	69000 (4.15)	16400	88.7/4.9/6.4
12	**3**[e]	100 MMAO	50	24	64.3	172000/17000 (bimodal)	21900	83.5/7.9/8.6

[a] $V_{toluene} = V_{isoprene}$ = 1 mL; precatalyst **4**: 18 μmol, [isoprene]/[Nd] = 556; precatalyst **3**: 20 μmol, [isoprene]/[Nd] = 500. [b] Determined by SEC with reference to polystyrene standards; PDI = M_w/M_n. [c] Calculated from yield × [isoprene]/[Nd] × 68 (one polymer chain per Nd). [d] From ^{1}H and ^{13}C NMR. [e] The solid was ground in a mortar for 10 min and subsequently dried in an oven at 100 °C overnight.

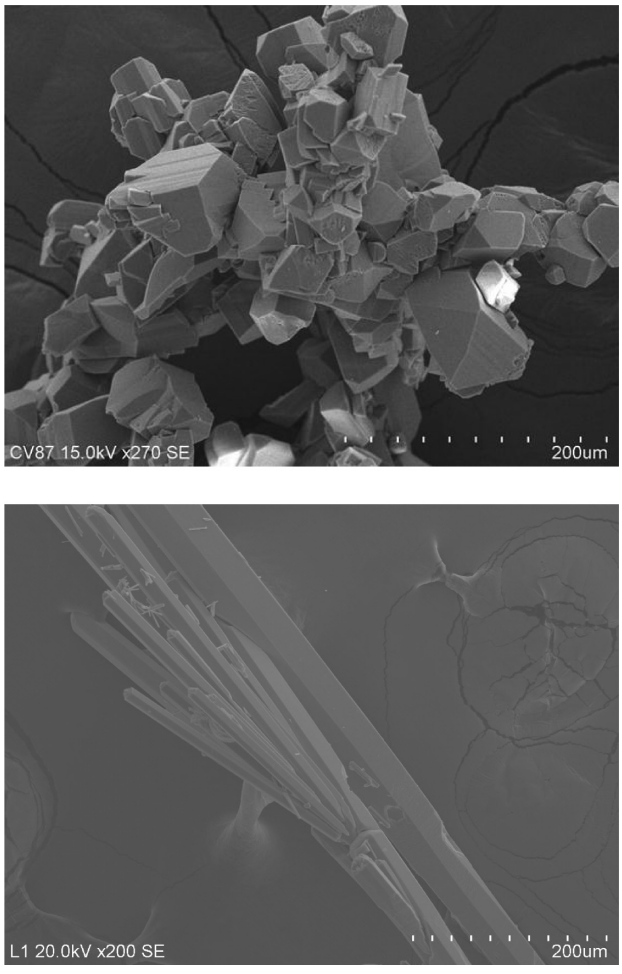

Figure 4. SEM images of Nd(2,6-ndc)(form) (**3**, top) and Nd(form)$_3$ (**4**, bottom).

distorted square antiprism NdO_8, with Nd−O distances ranging from 2.330(2) up to 2.654(2) Å, which can be divided into two groups. Four of the oxygen atoms (O1, O2, O3, and O6) belong to carboxylate groups of the 2,6-ndc linker with Nd−O distances of 2.330(2)−2.400(2) Å range. The four others (O4 and O5) coordinate two neighboring neodymium atoms and also belong to formate groups. Longer Nd−O bondings [2.443(2)−2.654(2) Å] reflect this μ_3-connection fashion. Two of this μ_3-oxo groups bridge two neodymium via a common corner whereas the two others bridge the inorganic cations via a common edge, resulting in a dinuclear motif with a relatively short Nd···Nd distance of 4.0564(3) Å (Figure 1). The formate anions are thus linked to two neodymium atoms in both symmetric chelating and *syn*−*anti* bidentate bridging modes (μ_2-η_2:η_1). The carboxylate arms of the naphthalenedicarboxylate groups bridge two inorganic cations through a *syn*−*syn* and *syn*−*anti* bidentate fashion (μ_4-η_1:η_1:η_1:η_1). This generates a neutral two-dimensional network with the pavement of the connection of dinuclear building blocks adopting two orientations in the (*b*,*c*) plane. It represents a distorted hexagonal net with the Schläfli symbol 6^3 if one considers the neodymium centers as nodes. In this organic−inorganic sheet, the hydrogen atoms of formate are pointing toward the center of the hexagonal ring of the 6^3 net, parallel to the (*b*,*c*) plane, whereas the carboxylate groups of the 2,6-ndc are pointing upward and downward the layer in the [100] direction. The three-dimensional cohesion of the structure is ensured by the ditopic 2,6-ndc ligands, which connect the organic−inorganic sheets to each other, along the *a*-axis (Figure 2). It is also noted that coordination polymers involving both carboxylate and formate linkers are rarely described in literature. Only a few examples reported such structural feature,[37−40] for which formate ligands are generated in situ during the hydrothermal reaction from the decomposition of an organic solvent such as *N*,*N*-dimethylformamide. X-ray thermodiffraction experiment (see the Supporting Information) shows that the phase is stable up to 420 °C, and it is then decomposed and recrystallizes into the cubic form Nd_2O_3 (540−680 °C) followed by the transformation into the hexagonal phase Nd_2O_3.[50]

Crystal Structure of Nd(form)$_3$ (4). Its three-dimensional structure type was previously reported by many authors with different trivalent lanthanide cations (La, Ce, Pr, Nd, Sm, Gd, Tb, Ho, Er, and Tm).[41,42,51−56] The structure of the neodymium formate was recently redetermined from single-crystal analysis in a rhombohedral symmetry.[41,42] It is based on the connection of infinite ribbons of tricapped trigonal prismatic polyhedra NdO_9, linked to each other via the formate groups, which adopt the bidentate bridging mode μ_3-η_2:η_1 (Figure 3). The linkage of the NdO_9 polyhedra occurs through trigonal faces with three μ_3-oxo species. X-ray thermodiffraction

dx.doi.org/10.1021/ic2019346 | *Inorg. Chem.* 2012, 51, 483−490

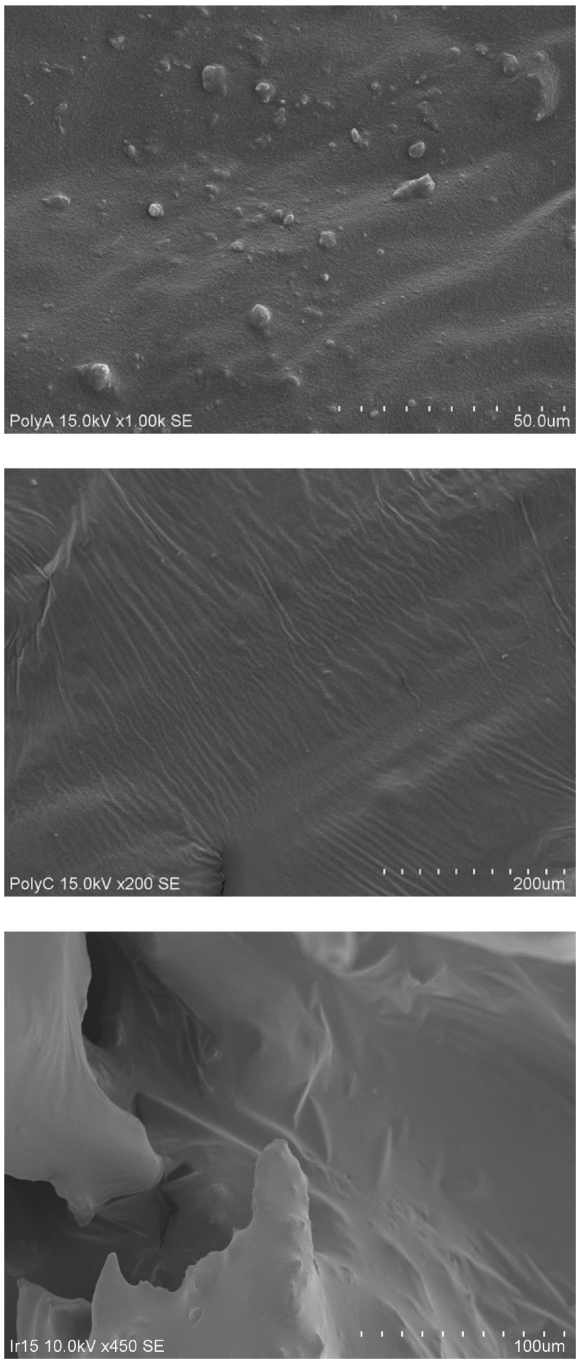

Figure 5. SEM images of the polyisoprene surface produced with Nd(2,6-ndc)(form) (**3**), which was used under two different forms: as-synthesized crystalline powder (top) and manually grinded powder (middle). SEM image of the polyisoprene surface produced with $Nd(form)_3$ (**4**) (bottom).

experiment (see the Supporting Information) indicate that this phase is stable up to 300 °C and then transformed into $Nd_2O_2CO_3$ (pdf file 25-0567) between 380 and 640 °C. Above this temperature, a mixture of the cubic and hexagonal is observed.[50]

Production of Polyisoprene. *Polymerization Catalysis.* As water-free, homoleptic $Nd(form)_3$ (**4**) and mixed ligand Nd(2,6-ndc)(form) (**3**) compounds were assessed as precatalysts toward isoprene polymerization. Because they are built from neodymium carboxylate, the polymerization activity could

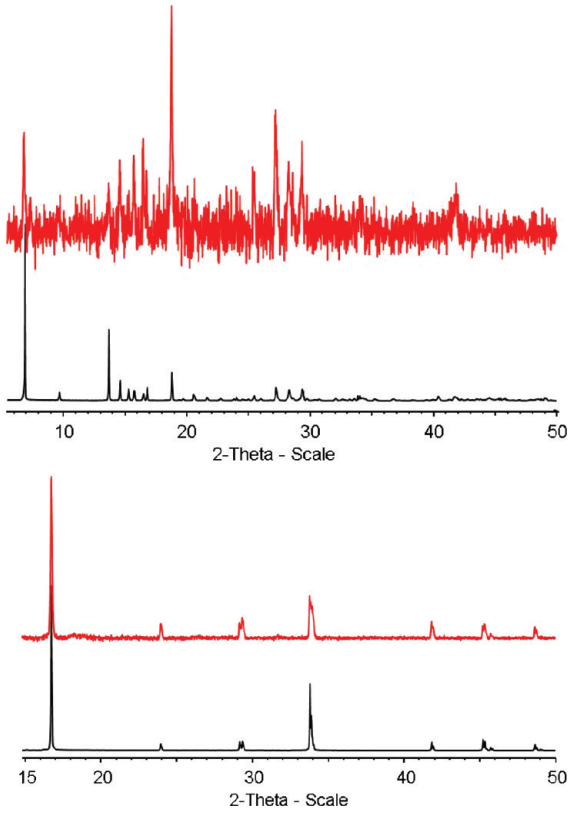

Figure 6. Comparison of XRD patterns of Nd(2,6-ndc)(form) (**3**, top) and $Nd(form)_3$ (**4**, bottom) as synthesized (black) and dispersed in isoprene (red).

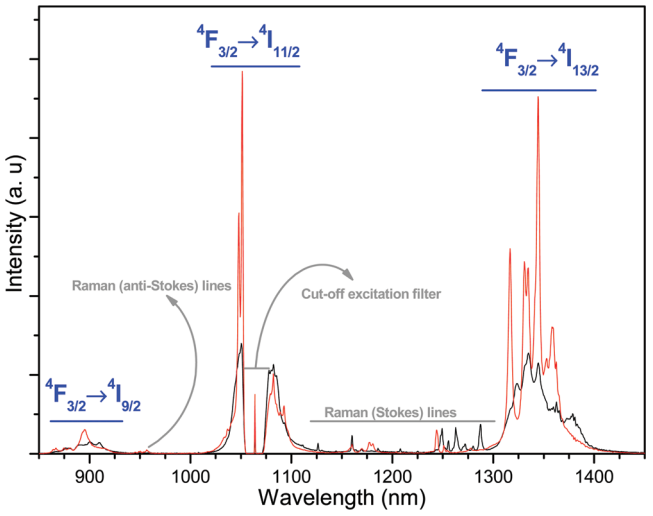

Figure 7. FT-Raman spectra of Nd(2,6-ndc)(form) (**3**, black line) and $Nd(form)_3$ (**4**, red line) samples recorded at room temperature. The excitation source was a YAG:Nd laser ($\lambda_{Exc.}$ = 1064 nm) with an excitation power of 100 mW.

be expected so far as several reports based on related complexes have been published since the last two decades.[13,16] We found that both coordination compounds are efficient when combined with aluminoxanes cocatalysts; selected results are gathered in Table 2. However, as already observed for other neodymium carboxylate-based MOFs, heating (at least 50 °C) and long reaction times (>20 h) are necessary to isolate some

dx.doi.org/10.1021/ic2019346 | *Inorg. Chem.* 2012, 51, 483−490

polymer material. This moderate reactivity is probably related to the heterogeneous nature of the catalytic system.[17]

Experiments were first carried out with **4** combined to MMAO and MAO. It is noteworthy that the latter cocatalyst gives higher conversions (ca. 70−80% at 80 °C, runs 6−8), whereas the selectivity is better with MMAO: polyisoprene 81% *cis*-regular was obtained at low temperature (run 1) with **4**/MMAO and nearly 72% *cis* with larger amounts of cocatalyst (run 4) as already reported with MIL-n compounds. These results prompted us to study the behavior of compound **3** in the same conditions. Associated to MMAO, coordination compound **3** was found more active than **4**, since satisfactory polymer yield is obtained at only 50 °C (64% in 28 h, run 12). Moreover, much higher *cis*-selectivity is reached (88.7% *cis*-regular, run 12). Raising the temperature from 50 to 80 °C causes higher conversion but is detrimental to the selectivity of the process. As a comparison, the polymer yield with MIL-103,[17] for comparable *cis*-selectivities (ca. 90%), never exceeded 30% polymer yield at 50 °C. The impact of grinding of the MOF precatalyst toward the catalytic performances was also assessed. We observed a positive effect in terms of polymer productivity (64 vs 32%, runs 12 vs 10, respectively), while keeping high *cis*-selectivity. Surprisingly, replacing the aluminoxane by $Al(i\text{-}Bu)_3/AlEt_2Cl$, as alternatively proposed for Nd carboxylate-based polymerizations,[16] was ineffective in our case (run 9).

Regarding macromolecular data, when activated with MMAO, precatalysts **3** (runs 10−12) and **4** (runs 1−4) give polymer with broad molecular weight distribution, all having a bimodal character. Several kinds of active species can thus be considered. In general, one high Mn population is present, which likely corresponds to slow initiation rate, possibly due to the heterogeneous character of the polymerization, as already observed previously with MOFs but also with classical Ziegler−Natta heterogeneous catalysts. This might be connected as well with neodymium compound, which is only partially active, and correlates well with the associated structure of the precatalyst (for one polymer chain per metal, without taking account of possible Nd−Al transfer[13]), as also considered with lanthanide carboxylate-based catalysts.[57] One may note that the bimodal character of macromolecular populations in terms of M_n can usually be seen as an advantage with respect to mechanical properties.[58] In contrast, when associated with MAO, precatalyst **4** (runs 5−8) affords polyisoprene, which displays quite monomodal SEC curves, although the PDI (polydispersity index, i.e., M_w/M_n) is rather broad. The molecular weights in the latter case (Mn_{exp}) are in the expected range (Mn_{th}) if one considers that all of the metal is involved in the polymerization process to produce polyisoprene (one polymer chain per Nd, Table 2). From this Mn_{exp}/Mn_{th} ratio, it is obvious in the case of the use of MMAO that all Nd compound is not activated to produce polyisoprene, as postulated above from the bimodal character of the SEC curves. Consequently, and as expected, crystalline residues with the typical related shape of the parent crystalline precatalyst can clearly be observed in the isolated material (see below).

Scanning Electron Microscopy (SEM) Macroscopic Examination. Compounds **3** and **4** have been analyzed by SEM by using the Hitachi S-3400N apparatus (Figure 4). After the hydrothermal treatment, as-synthesized crystallites of **3** with prismatic parallelepiped-like shapes of 20−120 μm size are observed. The phase **4** crystallized with specific needle shape of 200−1000 μm size. The SEM image (Figure 5) of the polyisoprene obtained with the as-synthesized precatalyst **3** clearly revealed some aggregates with 2−20 μm size randomly encapsulated at the surface of the polymer. The sizes of these blocks attributed to the residual solid **3** are smaller than those observed for the as-synthesized crystallites. A partial fragmentation of the precatalyst particles during the polymerization process could explain such a size difference as encountered in Ziegler−Natta heterogeneous catalysis.[59] The X-ray diffraction pattern still showed the signature of the crystalline precatalysts (Figure 6), which is heterogeneously mixed with the polyisoprene matrix. Similar observations are obtained with the precatalyst **4**, for which needle-shape crystallites with shorter lengths (30−100 μm) are visible at the surface of the polymer (Figure 5). For **3**, we also manually ground the as-synthesized crystallites in a mortar for 10 min. In this case, SEM image shows a smooth surface for the polymer, which is an indication of a better dissemination of the MOF in the polymer matrix. The X-ray diffraction patterns (Figure 6) of the polymeric material revealed some traces of the residual MOF phases. The observation of Bragg peaks shows that a part of the precatalysts is still crystalline, but the MOF content embedded within the polymer is quite low as indicated by the weak signal/noise ratio of the X-ray diffraction intensities.

Photoluminescence Properties. FT-Raman spectra were recorded to demonstrate the infrared (IR) photoluminescence capability of Nd(2,6-ndc)(form) (**3**) and $Nd(form)_3$ (**4**) materials (Figure 7); see the corresponding Experimental Section for details. To allow a comparison between the emission intensities of the two samples, all of the experimental setups were fixed (including grain size and packing of the samples); as a result, the two spectra have very similar base lines. The two compounds show the characteristic emission lines of the Nd^{3+} in the IR region, which are assigned to the $^4F_{3/2} \rightarrow {}^4I_{9/2}$, $^4F_{3/2} \rightarrow {}^4I_{11/2}$, and $^4F_{3/2} \rightarrow {}^4I_{13/2}$, intra $4f^3$ transitions between the first excited ($^4F_{3/2}$ state) and the Nd^{3+}ground multiplet levels ($^4I_{9/2}$, $^4I_{11/2}$, and $^4I_{13/2}$). Among them, the $^4F_{3/2} \rightarrow {}^4I_{11/2}$ transition, usually applicable to laser emission, is partially deleted due to the excitation cutoff filter but even though is expected to be dominant in both spectra. The distinct structure of the two compounds results in differentiable spectra, namely, by distinct emission intensities and Stark components distribution (Figure 7). Also, as expected, the vibronic transitions appearing in the Raman shift range 150−1200 cm^{-1} show a completely different profile (Figure 7). Unfortunately, no luminescence signal was detected for the Nd-based coordination polymers embedded into the polyisoprene material. This would be due to the very low concentration of the precatalyst present in the final polymer.

CONCLUSION

In this paper, we have described the synthesis and structural characterization of a series of neodymium-based MOFs, using the 2,6-naphthalenedicarboxylate or formate as organic linkers. The addition of other carboxylates such as oxalate or formate allows us to control the content of bonded water to the rare-earth center at the molecular level. Thanks to the absence of any aquo or hydroxo ligands bonded to the metal in the coordination polymer, the compounds were successfully used as precatalysts for the polymerization of isoprene. Combined with aluminoxanes, they afforded polymer in reasonable yield, up to 88.7% *cis*-regular.

dx.doi.org/10.1021/ic2019346 | *Inorg. Chem.* 2012, 51, 483−490

■ ASSOCIATED CONTENT

Supporting Information

CIF files for phases 1, 2, and 3. Infrared spectra, powder X-ray diffraction patterns, and X-ray thermodiffraction for phases 1, 3, and 4. This material is available free of charge via the Internet at http://pubs.acs.org.

■ AUTHOR INFORMATION

Corresponding Author

*E-mail: thierry.loiseau@ensc-lille.fr.

■ ACKNOWLEDGMENTS

We thank the Region Nord-Pas-De-Calais-Picardie for financial support (MULTI-NANO-MOF project) and T. Jarry & C. Renard (ISP Master Students) for their participation to this work, Nora Djelal, Laurence Burylo, and Catherine Meliet for their technical assistance. Prof. L. Carlos and J. Rocha (University of Aveiro, Portugal) are also acknowledged for measurement of the Nd luminescence spectra.

■ REFERENCES

(1) Yaghi, O. M.; O'Keeffe, M.; Ockwig, N. W.; Chae, H. K.; Eddaoudi, M.; Kim, J. *Nature* **2003**, *423*, 705.
(2) Kitagawa, S.; Kitaura, R.; Noro, S.-I. *Angew. Chem., Int. Ed.* **2004**, *43*, 2334.
(3) Férey, G. *Chem. Soc. Rev.* **2008**, *37*, 191.
(4) Janiak, C.; Vieth, J. K. *New J. Chem.* **2010**, *34*, 2366.
(5) Jiang, H.-L.; Xu, Q. *Chem. Commun.* **2011**, *47*, 3351.
(6) Zhao, D.; Timmons, D. J.; Yuan, D.; Zhou, H.-C. *Acc. Chem. Res.* **2011**, *44*, 123.
(7) Corma, A.; Garcia, H.; Llabres i Xamena, F. X. *Chem. Rev.* **2010**, *110*, 4606.
(8) Farrusseng, D.; Aguado, S.; Pinel, C. *Angew. Chem., Int. Ed.* **2009**, *48*, 7502.
(9) Isaeva, V. I.; Kustov, L. M. *Pet. Chem.* **2010**, *50*, 167.
(10) Lee, J. Y.; Farha, O. K.; Roberts, J.; Scheidt, K. A.; Nguyen, S. T.; Hupp, J. T. *Chem. Soc. Rev.* **2009**, *38*, 1450.
(11) Liu, Y.; Xuan, W.; Cui, Y. *Adv. Mater.* **2010**, *22*, 4112.
(12) Zhang, Z.; Cui, D.; Wang, B.; Liu, B.; Yang, Y. *Struct. Bonding (Berlin, Ger.)* **2010**, *137*, 49.
(13) Friebe, L.; Nuyken, O.; Obrecht, W. *Adv. Polym. Sci.* **2006**, *204*, 1.
(14) Visseaux, M.; Bonnet, F. *Coord. Chem. Rev.* **2011**, *255*, 374.
(15) Shen, Z. *Inorg. Chim. Acta* **1987**, *140*, 7.
(16) Fischbach, A.; Anwander, R. *Adv. Polym. Sci.* **2006**, *204*, 155.
(17) Vitorino, M. J.; Devic, T.; Tromp, M.; Férey, G.; Visseaux, M. *Macromol. Chem. Phys.* **2009**, *210*, 1923.
(18) Rosi, N. L.; Eddaoudi, M.; Kim, J.; O'Keeffe, M.; Yaghi, O. M. *CrystEngComm* **2002**, *4*, 401.
(19) Rosi, N. L.; Kim, J.; Eddaoudi, M.; Chen, B.; O'Keeffe, M.; Yaghi, O. M. *J. Am. Chem. Soc.* **2005**, *127*, 1504.
(20) Loiseau, T.; Mellot-Draznieks, C.; Muguerra, H.; Férey, G.; Haouas, M.; Taulelle, F. *C. R. Chim.* **2005**, *8*, 765.
(21) Senkovska, I.; Hoffmann, F.; Fröba, M.; Getzschmann, J.; Böhlmann, W.; Kaskel, S. *Microporous Mesoporous Mater.* **2009**, *122*, 93.
(22) Zhang, J.-Y.; Bu, J. T.; Chen, S.; Wu, T.; Zheng, S.; Chen, Y.; Nieto, R. A.; Feng, P.; Bu, X. *Angew. Chem., Int. Ed.* **2010**, *49*, 8876.
(23) Min, D.; Lee, S. W. *Bull. Korean Chem. Soc.* **2002**, *23*, 948.
(24) Almeida Paz, F. A.; Klinowski, J. *Chem. Commun.* **2003**, 1484.
(25) Zheng, X.; Sun, C.; Lu, S.; Liao, F.; Gao, S.; Jin, L. *Eur. J. Inorg. Chem.* **2004**, 3262.
(26) Almeida Paz, F. A.; Klinowski, J. *Acta Crystallogr. E* **2008**, *64*, m336.
(27) Almeida Paz, F. A.; Klinowski, J. *Acta Crystallogr. E* **2008**, *64*, m140.
(28) Deluzet, A.; Maudez, W.; Daiguebonne, C.; Guillou, O. *Cryst. Growth Des.* **2003**, *3*, 475.
(29) Wang, Z.; Jin, C.-M.; Shao, T.; Li, Y.-Z.; Zhang, K.-L.; Zhang, H.-T.; You, X.-Z. *Inorg. Chem. Commun.* **2002**, *5*, 642.
(30) Thomas, P.; Trombe, J. C. *J. Chem. Cryst.* **2000**, *30*, 633.
(31) Vaidhyanathan, R.; Narajan, S.; Rao, C. N. R. *J. Solid State Chem.* **2004**, *177*, 1444.
(32) Si, S.; Li, C.; Wang, R.; Li, Y. *J. Mol. Struct.* **2004**, *703*, 11.
(33) Dan, M.; Cottereau, G.; Rao, C. N. R. *Solid State Sci.* **2005**, *7*, 437.
(34) Xiao, F.; Lu, J.; Guo, Z.; Li, T.; Li, Y.; Cao, R. *Inorg. Chem. Commun.* **2008**, *11*, 105.
(35) Yang, Q.-F.; Yu, Y.; Song, T.-Y.; Yu, J.-H.; Zhang, X.; xu, J.-Q.; Wang, T.-G. *CrystEngComm* **2009**, *11*, 1642.
(36) Wang, Z.; Xing, Y.-H.; Wang, C.-G.; Sun, L.-X.; Zhang, J.; Ge, M.-F.; Niu, S.-Y. *CrystEngComm* **2010**, *12*, 762.
(37) Sun, Q.; Zhang, J.-Y.; Tian, H.; Wang, Y.-Q.; Gao, E.-Q. *Inorg. Chem. Commun.* **2009**, *12*, 426.
(38) Dai, F.; Cui, P.; Ye, F.; Sun, D. *Cryst. Growth Des.* **2010**, *10*, 1474.
(39) Deng, Z.-P.; Huo, L.-H.; Wang, H.-Y.; Gao, S.; Zhao, H. *CrystEngComm* **2010**, *12*, 1526.
(40) Han, Y.-F.; Zhou, X.-H.; Zheng, Y.-X.; Shen, Z.; Song, Y.; You, X.-Z. *CrystEngComm* **2008**, *10*, 1237.
(41) Deng, S.; Zhang, N.; Xiao, W.; Chen, C. *Z. Kristallogr. NCS* **2009**, *224*, 275.
(42) Lin, J.-M.; Guan, Y.-F.; Wang, D.-Y.; Dong, W.; Wang, X.-T.; Gao, S. *Dalton Trans.* **2008**, 6165.
(43) *SAINT Plus* Version 7.53a; Bruker Analytical X-ray Systems: Madison, WI, 2008.
(44) Sheldrick, G. M. *SADABS, Bruker-Siemens Area Detector Absorption and Other Correction*, Version 2008/1, 2008.
(45) Sheldrick, G. M. *Acta Crystallogr. A* **2008**, *64*, 112.
(46) Farrugia, L. J. *J. Appl. Crystallogr.* **1999**, *32*, 837.
(47) Terrier, M.; Visseaux, M.; Chenal, T.; Mortreux, A. *J. Polym. Sci., Part A: Polym. Chem.* **2007**, *45*, 2400.
(48) Lee, Y. K.; Lee, S. W. *Bull. Korean Chem. Soc.* **2003**, *24*, 948.
(49) Brese, N. E.; O'Keeffe, M. *Acta Crystallogr. B* **1991**, *47*, 192.
(50) Hirosaki, N.; Ogata, S.; Kocer, C. *J. Alloys Compd.* **2003**, *351*, 31.
(51) Mayer, I.; Steinberg, M.; Feigenblatt, F.; Glasner, A. *J. Phys. Chem.* **1962**, *66*, 1737.
(52) Pabst, A. *Can. Mineral.* **1978**, *16*, 437.
(53) Kistaiah, P.; Murthy, K. S.; Iyengar, L.; Rao, K. V. K. *J. Mater. Sci.* **1981**, *16*, 2321.
(54) Bolotovsky, R. L.; Bulkin, A. P.; Krutov, G. A.; Kudryashev, V. A.; Trunov, V. A.; Ul'yanov, V. A.; Antson, O.; Hiismäki, P.; Pöyry, H.; Tiita, A.; Loshmanov, A. A.; Furmanova, N. G. *Solid State Commun.* **1990**, *76*, 1045.
(55) Xu, Y.; Ding, S.-H.; Zhou, G.-P.; Liu, Y.-G. *Acta Crystallogr. E* **2006**, *62*, m1749.
(56) Go, Y.-B.; Jacobson, A. J. *Chem. Mater.* **2007**, *19*, 4702.
(57) Ferreira, L. C. Jr.; de Santa Maria, L. C.; Costa, M. A. S.; Tochetto Pires, N. M.; Nele, M.; Pinto, J. C. *Polym. Eng. Sci.* **2011**, *51*, 712.
(58) Bohm, L. L. *Angew. Chem., Int. Ed.* **2003**, *42*, 5010.
(59) Fink, G.; Steinmetz, B.; Zechlin, J.; Przybyla, C.; Tesche, B. *Chem. Rev.* **2000**, *100*, 1377.